

USBM Contract No. HO122026

**SURVEY OF ELECTROMAGNETIC AND SEISMIC NOISE
RELATED TO MINE RESCUE COMMUNICATIONS**

**VOLUME I
EMERGENCY AND OPERATIONAL
MINE COMMUNICATIONS**

Robert L. Lagace — Project Leader
Dwain A. Aidala Martyn F. Roetter
Alfred G. Emslie Richard H. Spencer
John J. Ginty Albert W. Welz

ARTHUR D. LITTLE, INC.
C-73912

USBM CONTRACT FINAL REPORT (Contract No. HO122026)
JANUARY 1974

DEPARTMENT OF THE INTERIOR
BUREAU OF MINES
WASHINGTON, D. C.

Arthur D. Little, Inc.

USBM Contract No. HO122026

SURVEY OF ELECTROMAGNETIC AND SEISMIC NOISE
RELATED TO MINE RESCUE COMMUNICATIONS

VOLUME I

EMERGENCY AND OPERATIONAL MINE COMMUNICATIONS

Robert L. Lagace - Project Leader
Dwain A. Aidala Martyn F. Roetter
Alfred G. Emslie Richard H. Spencer
John J. Ginty Albert W. Welz

ARTHUR D. LITTLE, INC.
C-73912

The views and conclusions contained in this document are those of the authors and should not be interpreted as necessarily representing the official policies or recommendations of the Interior Department's Bureau of Mines of the U.S. Government.

USBM CONTRACT FINAL REPORT (Contract No. HO122026)
JANUARY 1974

DEPARTMENT OF THE INTERIOR
BUREAU OF MINES
WASHINGTON, D. C.

FOREWORD

This report was prepared by Arthur D. Little, Inc., Cambridge, Massachusetts under USBM Contract No. H0122026. The contract was initiated under the Coal Mine Health and Safety Research Program. It was administered under the technical direction of the Pittsburgh Mining and Safety Research Center with Mr. Howard E. Parkinson acting as the technical project officer. Mr. Francis M. Naughton was the contract administrator for the Bureau of Mines.

This report is a summary of the work recently completed as part of this contract during the period August 1971 to December 1973. This report was submitted by the authors in January 1974.

VOLUME I

EMERGENCY AND OPERATIONAL MINE COMMUNICATIONS

TABLE OF CONTENTS

	<u>Page</u>
INTRODUCTION	v
PART ONE ASSESSMENT OF ELECTROMAGNETIC NOISE DATA AND DEFINITION OF A NEW MEASUREMENT PROGRAM	1.i
PART TWO ELECTROMAGNETIC THROUGH-THE-EARTH MINE COMMUNICATIONS	2.i
PART THREE LEAKY COAXIAL CABLE FOR GUIDED WIRELESS MINE COMMUNICATION SYSTEMS	3.i
PART FOUR THEORY OF WIRELESS PROPAGATION OF UHF RADIO WAVES IN COAL MINE TUNNELS	4.i
PART FIVE HOIST SHAFT MINE COMMUNICATIONS	5.i
PART SIX TROLLEY WIRE MINE COMMUNICATIONS	6.i
PART SEVEN MINE PAGER PHONE TO PUBLIC TELEPHONE INTERCONNECT SYSTEM	7.i
PART EIGHT TECHNOLOGY TRANSFER SEMINARS ON MINE COMMUNICATIONS AND THROUGH-THE-EARTH ELECTROMAGNETIC WORKSHOP	8.i
PART NINE ADDITIONAL TECHNICAL SUPPORT AND CONSULTING SERVICES RELATED TO MINE COMMUNICATIONS AND MINER LOCATION	9.i

VOLUME II

SEISMIC DETECTION AND LOCATION OF ISOLATED MINERS

TABLE OF CONTENTS

	<u>Page</u>
INTRODUCTION	v
PART ONE EXECUTIVE SUMMARY	1.i
PART TWO DETECTION RANGE AND ARRIVAL TIME ESTIMATES	2.i
PART THREE ESTIMATES OF MINER LOCATION ACCURACY: ERROR ANALYSIS IN SEISMIC LOCATION PROCEDURES FOR TRAPPED MINERS	3.i
PART FOUR ESTIMATES OF MINER LOCATION ACCURACY: WESTINGHOUSE LOCATION PROGRAM "MINER"	4.i
PART FIVE THE REFERENCE EVENT METHOD OF SEISMIC LOCATION FOR MINE RESCUE SYSTEMS	5.i
PART SIX FIELD UTILIZATION OF SEISMIC SYSTEMS	6.i
PART SEVEN THEORETICAL SIGNAL SOURCE AND TRANSMISSION CHARACTERISTICS	7.i
PART EIGHT EARTH MODELS	8.i
PART NINE SEISMIC NOISE CHARACTERISTICS	9.i
PART TEN SIGNAL-TO-NOISE RATIO IMPROVEMENT TECHNIQUES	10.i
PART ELEVEN SEISMIC DETECTION/LOCATION INSTRUMENTATION	11.i
PART TWELVE BRIEFING CHARTS	12.i

INTRODUCTION

This final report documents the work done by Arthur D. Little, Inc. (ADL) on behalf of the U.S. Bureau of Mines, Pittsburgh Mining and Safety Research Center (PMSRC), on Contract HO122026 (which began in August of 1971). Under this contract ADL provided technical assistance to the Bureau on a task basis on virtually all aspects of the Bureau's programs related to present and planned emergency and operational communications and miner location systems for underground coal mines. The work consisted of independent investigations, analyses, experiments, breadboard and prototype hardware development, workshops and technology transfer seminars on mine communications, and on-going evaluations and guidance related to the Bureau's contracted programs on electromagnetic noise, mine communications systems, and trapped miner location. This final report documents the work in two volumes, Volume I, "Emergency and Operational Mine Communications," and Volume II, "Seismic Detection and Location of Isolated Miners." The Tables of Contents of both Volumes are included in each Volume.

Phase I of the contract was devoted to performing an in-depth assessment of electromagnetic noise measurements taken by several contractors and other investigators, and then defining a new noise measurement program and instrumentation system tailored to obtain the necessary but missing noise data. These data are required for use in the design of new emergency and operational communication systems. This work, and the follow-on coordination and guidance activities of ADL on this noise measurement program in subsequent phases of the contract, are treated in Part One of Volume I.

The latter part of Phase I and part of Phase II included preliminary performance predictions related to through-the-earth electromagnetic communication systems. These predictions were based on available theoretical signal propagation results and on recently acquired noise data at several coal mines. This work is treated in Part Two of Volume I.

In Phases II, IV and V, investigations were conducted related to wire, guided-wireless and wireless communications systems for communicating with roving vehicles and personnel underground. This work is documented as follows. Part Three of Volume I treats guided wireless communications via leaky coaxial cable; Part Four treats wireless communications in mine tunnels at UHF frequencies; Part Five treats guided wireless communications down deep hoist shafts; Part Six treats aspects of trolley wire communications; and Part Seven treats a new mine pager telephone to public telephone interconnect system.

Another aspect of Phase V included tasks for providing assistance related to technology transfer seminars on mine communications and to a workshop on through-the-earth electromagnetics. Part Eight of Volume I treats this work. Under Phases II, IV, and V, ADL also provided a wide variety of short-term technical support and consulting services not discussed in the above mentioned Parts. This short-term work is treated in Part Nine of Volume I.

In Phase III of the contract, ADL performed another in-depth assessment on a compressed time schedule, to provide PMSRC with independent technical judgments regarding the potentials and limitations of seismic methods and systems for detecting and locating isolated miners. Volume II of this report is devoted entirely to the treatment of this work.

During the course of this contract we prepared over forty working memoranda, technical reports, seminar papers, and workshop summary reports, in addition to many informal memoranda and the monthly technical reports, to keep PMSRC informed of the progress and findings of our work as they developed. This final report is based on these previous memoranda and reports.

PART ONE

ASSESSMENT OF ELECTROMAGNETIC NOISE
DATA AND DEFINITION OF A NEW
MEASUREMENT PROGRAM

PART ONE

ASSESSMENT OF ELECTROMAGNETIC NOISE
DATA AND DEFINITION OF A NEW
MEASUREMENT PROGRAM

TABLE OF CONTENTS

	<u>Page</u>
List of Tables	1.v
List of Figures	1.vi
INTRODUCTION	1.1
I. SUMMARY - ELECTROMAGNETIC NOISE ASSESSMENT AND RECOMMENDED MEASUREMENT PROGRAM	1.3
II. CONFERENCE PARTICIPANTS AND TENTATIVE PROGRAM ASSIGNMENTS	1.8
III. MEASUREMENT PROGRAM OUTLINE	1.11
A. DATA NEEDED	1.11
B. NOISE CHARACTERISTICS	1.11
C. DATA ACQUISITION AND ANALYSIS	1.12
IV. INSTRUMENTATION AND DATA PROCESSING SYSTEM	1.13
A. BLOCK DIAGRAM	1.13
B. SYSTEM COMPONENTS	1.18
C. REAL AND SYNTHETIC CALIBRATIONS	1.20
D. PLAYBACK AND PROCESSING	1.21
E. EQUIPMENT LIST	1.23
F. SHAPING OF NOISE SPECTRUM SIGNATURE PRIOR TO RECORDING	1.23
G. LOGARITHMIC COMPRESSION	1.24
V. OPERATIONAL CONSIDERATIONS	1.24
A. EQUIPMENT PROOFING	1.24

PART ONE

ASSESSMENT OF ELECTROMAGNETIC NOISE
DATA AND DEFINITION OF A NEW
MEASUREMENT PROGRAM

TABLE OF CONTENTS
(Continued)

	<u>Page</u>
B. RECORD KEEPING	1.24
C. TEST PLANS	1.25
VI. SOME QUESTIONS AND ITEMS TO BE RESOLVED	1.25
A. TAPE RECORDER SUITABILITY	1.25
B. SYSTEM ORGANIZATION	1.26
C. DYNAMIC RANGE CONSIDERATIONS	1.26
D. TRANSMISSION MEASUREMENTS	1.26
E. CONDUCTED NOISE MEASUREMENTS	1.27
F. TAPE RECORDER CROSS TALK AND NON-LINEARITY	1.27
G. COMPUTER-GENERATED POWER SPECTRA	1.27
H. CHOICE OF MINES FOR MEASUREMENTS	1.28
I. EXPERIMENT DESIGN	1.28
VII. BIBLIOGRAPHY	1.30
APPENDIX - SUMMARY REPORTS OF ELECTROMAGNETIC (EM) NOISE MEASUREMENT PROGRAM REVIEW MEETINGS	1.32
I. INTRODUCTION	1.32
II. EM NOISE MEASUREMENT PROGRAM MEETING AT NBS, BOULDER, COLORADO ON 24 MAY 1972	1.33
A. TEST DESIGN AND PLANNING	1.33
B. EQUIPMENT	1.36

PART ONE

ASSESSMENT OF ELECTROMAGNETIC NOISE
DATA AND DEFINITION OF A NEW
MEASUREMENT PROGRAM

TABLE OF CONTENTS
(Continued)

	<u>Page</u>
C. ANALYSIS	1.38
D. MISCELLANEOUS	1.39
III. EM NOISE MEASUREMENT PROGRAM MEETING AT NBS, BOULDER, COLORADO ON 17 AUGUST 1972	1.40
A. TEST DESIGN AND PLANNING	1.40
B. EQUIPMENT	1.44
C. ANALYSIS	1.45
IV. EM NOISE MEASUREMENT PROGRAM MEETINGS AT COLLINS RADIO, NBS, AND PMSRC	1.46
A. MEETING AT COLLINS RADIO., CEDAR RAPIDS, IOWA ON 21, 22 FEBRUARY 1973	1.46
B. MEETING AT NBS, BOULDER, COLORADO ON 22 MAY 1973	1.48
C. MEETING AT PMSRC, BRUCETON, PA., ON 10 OCTOBER 1973	1.49

PART ONE
ASSESSMENT OF ELECTROMAGNETIC NOISE
DATA AND DEFINITION OF A NEW
MEASUREMENT PROGRAM

LIST OF TABLES

<u>Table No.</u>	<u>Title</u>	<u>Page</u>
1	General Summary of Past Measurements, Frequencies, and Data Gaps	1.1
2	Summary of Past Measurement Locations, Conditions, and Data Gaps	1.5
3	Summary of Past Measurements, Processing Methods, and Results	1.3
4	Planned Electromagnetic Noise Measurement Program (Scouting Party)	1.9
5	Outline of Scouting Party Noise Measurement Needs for the 0-10kHz Band	1.10
A1	Summary of NBS EM Noise Measurements (Results of the Planned EM Noise Measurement Program)	1.50

PART ONE

ASSESSMENT OF ELECTROMAGNETIC NOISE
DATA AND DEFINITION OF A NEW
MEASUREMENT PROGRAM

LIST OF FIGURES

<u>Figure No.</u>	<u>Title</u>	<u>Page</u>
1	Simplified Block Diagram Option I - In-Mine Magnetic Fields	1.15
2	Simplified Block Diagram Option II - In-Mine Conducted Noise	1.16
3	Simplified Block Diagram Option III - Surface Magnetic Fields	1.17

PART ONE

ASSESSMENT OF ELECTROMAGNETIC NOISE DATA AND DEFINITION OF A NEW MEASUREMENT PROGRAM

INTRODUCTION

The first phase of our work for PMSRC on this contract was devoted to a comprehensive and in-depth assessment of electromagnetic (EM) noise measurements and data taken by several contractors for use in the design of operational and emergency mine communications. Pertinent measurements and data of other selected investigators were also included in the evaluation. This assessment treated the measurements and instrumentation used, the data analysis and presentation methods, and the utility of the final results. This phase concluded with the identification of the most useful results and methods, the remaining data gaps, the contractor most qualified to fill these data gaps, and the definition (with PMSRC and this contractor — NBS, National Bureau of Standards) of a follow-on noise measurement program, instrumentation system, and data processing methods tailored to obtain the necessary but missing noise data. A partial bibliography of references related to electromagnetic and seismic noise and propagation in the frequency bands of interest was also compiled during this first phase. The body of this Part of the final report presents a summary of the findings of our EM noise assessment, together with detailed recommendations regarding the new noise measurements to be taken and the instrumentation and data processing methods to be used. This work was done during the latter part of 1971 and the early part of 1972.

During subsequent phases of the contract ADL was asked to perform on-going evaluations of the continuing program of electromagnetic (EM) noise and propagation measurements made by Bureau contractors, and to utilize pertinent data from these measurements to make performance estimates for

candidate operational/emergency EM mine communication and location systems. In this advisory and coordinating capacity, ADL participated in program status and system review meetings with the NBS noise measurement team and others, kept in close touch with this team between meetings, and utilized selected portions of the data as they became available. The principal findings, and conclusions of these meetings have been included in the Appendix to this Part. They serve as a convenient reference to the historical development of the follow-on noise measurement program and associated instrumentation. As of the Fall of 1973 this measurement program has been largely completed, and the instrumentation system and noise data are being documented by NBS.

The material summarized in this Part and its Appendix is based on several technical reports and working memoranda created during the first and subsequent phases of this contract. Performance estimates related to candidate electromagnetic through-the-earth mine communication and location systems are treated in Part Two of this final report.

I. SUMMARY — ELECTROMAGNETIC NOISE ASSESSMENT AND RECOMMENDED MEASUREMENT PROGRAM

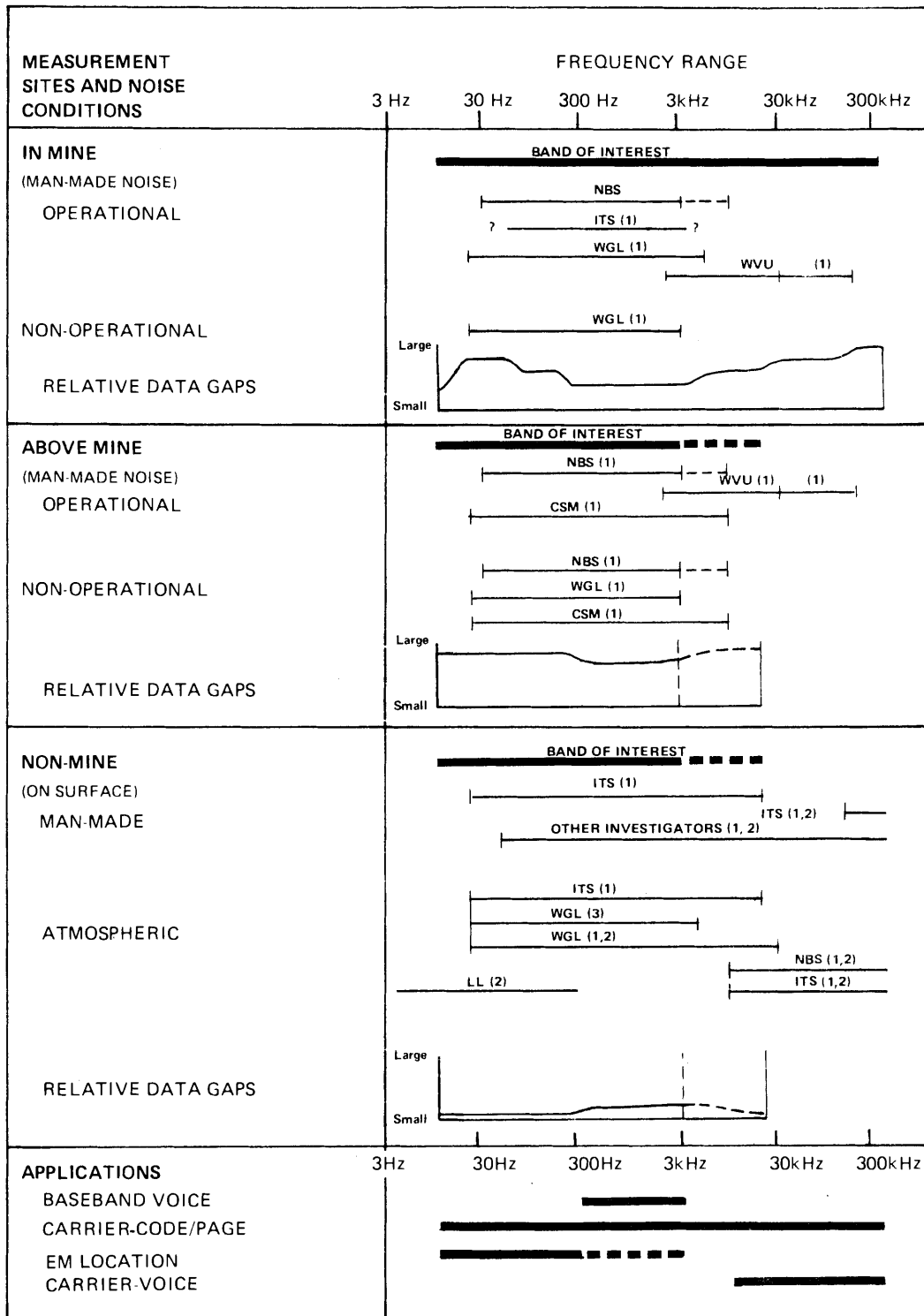
Five conclusions that emerged from ADL's Contractor Noise Measurements Assessment done in the winter of 1971-72, and the 7 December 1971 Bureau of Mines Contractors' Round Table Meeting in Boulder, Colorado were:

- a limited amount of good data has been obtained for characterizing the noise environment for electromagnetic (EM) coal mine operational/emergency communications systems;
- significant noise data gaps still exist;
- suitable instrumentation and data analysis methods are available for filling these data gaps;
- the immediate and most important data gaps should be filled by means of a timely field measurement effort that is purposely limited in scope and duration;
- this field measurement effort should preferably be carried out by a team knowledgeable and experienced in coal mine EM noise measurements.

Tables 1, 2, and 3* summarize some of our findings and conclusions with regard to the EM noise measurements, processing techniques, and results for each of the Bureau of Mines contractors and for some other investigators. Table 1 depicts the noise measurements made by each of the contractors and investigators with respect to frequency bands covered, mine versus non-mine, and operational versus non-operational conditions; together with a graphical indication of the size of the data gaps remaining in each of the frequency bands of interest. Table 2 is a more detailed listing of specific coal mine locations and noise sources of interest, and an identification of those treated in each investigator's measurements, again with an appropriate rating of the size of the data gaps remaining. Table 3 presents a listing of investigators, an identification of their measurement and data processing

* References to Figures, Tables, and Equations apply to those in this Part unless otherwise noted.

TABLE 1
GENERAL SUMMARY OF PAST MEASUREMENTS, FREQUENCIES, AND DATA GAPS



CSM COLORADO SCHOOL OF MINES
 ITS INSTITUTE FOR TELECOMMUNICATION SCIENCES
 NBS NATIONAL BUREAU OF STANDARDS
 WGL WESTINGHOUSE GEORESEARCH LABORATORY
 WVU WEST VIRGINIA UNIVERSITY
 LL MIT LINCOLN LABORATORY

(1) DATA LIMITED IN AMOUNT OR UTILITY
 (2) PAST WORK – NOT FOR BU MINES
 (3) PLANNED BUT NOT STARTED
 ALL MEASUREMENTS WITHOUT A (2)
 NOTE WERE DONE FOR BU MINES

TABLE 2
SUMMARY OF PAST MEASUREMENT LOCATIONS, CONDITIONS, AND DATA GAPS

MEASUREMENT SITES AND NOISE CONDITIONS	INVESTIGATORS							
	CSM	ITS	NBS	WGL	WVU	LL	OTHER	DATA GAPS
IN MINE								
OPERATIONAL		(1)	X	(1)	X(1)			
PWR BOREHOLES			X		X			M
AC & DC POWER CENTERS		?	X		X			M
DC TROLLEY LINES		X	X	?	X			M
AC POWER LINES			X		X			M
HAULAGE TRAINS		X	X		X			M
MINE MACHINERY		?	X		X			L
QUIET PLACES/TIMES		?	X		X			L
WORKING FACES								L
NON-OPERATIONAL				(1)				
PWR BOREHOLES				X				L
OTHER PLACES				X				L
ABOVE MINE								
OPERATIONAL	(1)		(1)		X(1)			
PWR BOREHOLES	X		X					L
POWER LINES	?		X		?			L
PWR SUBSTATIONS								L
MINE MOUTH PWR STATIONS								L
OVER WORKING FACES	X							L
OVER OTHER SECTIONS	X		X					M
NON-OPERATIONAL	(1)		(1)	(1)				
PWR BOREHOLES	X		X	X				L
PWR SUBSTATIONS								L
MINE MOUTH PWR STATIONS								L
POWER LINES			X	X				L
NON-MINE								
MAN-MADE		(1)(1,2)				(2)	(1,2)	S
ATMOSPHERIC		(1)(1,2)	(1,2)	(3)(1,2)		(2)	(1,2)	S/M

CSM COLORADO SCHOOL OF MINES
ITS INSTITUTE FOR TELECOMMUNICATION SCIENCES
NBS NATIONAL BUREAU OF STANDARDS
WGL WESTINGHOUSE GEORESEARCH LABORATORY
WVU WEST VIRGINIA UNIVERSITY
LL MIT LINCOLN LABORATORY

NOTES () INDICATED AT MAJOR HEADINGS OPERATIONAL AND NON-OPERATIONAL ALSO APPLY TO THE CORRESPONDING SUBHEADINGS

- (1) DATA LIMITED IN AMOUNT OR UTILITY
- (2) PAST WORK – NOT FOR BU MINES
- (3) PLANNED BUT NOT STARTED

DATA GAPS: LARGE – L
 MODERATE – M
 SMALL – S

TABLE 3
SUMMARY OF PAST MEASUREMENTS, PROCESSING METHODS, AND RESULTS

EM NOISE MEASUREMENTS, PROCESSING METHODS, AND RESULTS	INVESTIGATORS						
	FOR BU MINES (EXC. AS NOTED)					FOR OTHERS	
	CSM	ITS (2)	NBS	WGL (2)	WVU	LL ATMOS ⁽²⁾	OTHER MAN-MADE ⁽²⁾
METHODS							
ANALOG TAPE RECORD		x (X)	(X)			(X) ⁽⁴⁾	
TUNABLE RCVR/WAVE ANALYZER	x	x (X)		x x	x		x
DIGITAL PROCESSING	x	x	(X)	(X)	x	(X)	
FFT POWER SPECTRUM			(X)	(X)		(X)	
STATISTICAL (AMP./TIME)	x	(X)	x	x		(X)	
ON-SITE ANALYSIS	x	x x		(X)	x x		x
POST-SITE ANALYSIS		x x	(X)	x x	x	(X)	
WIDE BAND (>100 Hz)	x	x (X)	(X)	(X)	x	(X)	x
NARROW BAND (<100 Hz)		x		x x			x
TIME AVERAGED (LONG)		x x		⁽³⁾ x x	x		
SIMULTANEOUS							
FREQUENCIES		(X)	(X)	(X)		(X)	
SENSORS						(X)	
SEQUENTIAL							
FREQUENCIES	x	x x		x x	x		x
SENSORS	x	x	x	x x	x		x
LONG TERM		x (X)		⁽³⁾ x x		(X)	
SHORT TERM	x	x (X)	(X)	(X)	x	(X)	x
CALIBRATIONS		(X)	(X)	x x		(X)	
RESULTS	(1)	(1) (1)		(1) (1)	(1)		(1)
ANALOG NOISE RECORDINGS		x (X)	(X)			(X) ⁽⁴⁾	
CONTINUOUS POWER SPECTRA (HARMONICS & BROADBAND NOISE)			(X)	(X)		(X)	
HI-RESOLUTION			(X)			(X)	
MOD-RESOLUTION			x	x			
DISCRETE PWR SPECTRUM SAMPLES		(X)		x x	x		x
HARMONICS				x	x		
SELECT FREQUENCIES		(X)		⁽³⁾ x x	x		x
SWEPT PWR SPECTRA		x					x
NOISE SOURCE SIGNATURES			(X)				x
AMPLITUDE STATISTICS	x	(X)	x	⁽³⁾ x x	x	(X)	
TIME STATISTICS		x		⁽³⁾ x x	x	(X)	
SPATIAL VARIATIONS				⁽⁵⁾ x	(X)	x ⁽⁵⁾	x
TIME VARIATIONS	x	x x	(X)	⁽³⁾ x x	x	(X)	x
ELECTRIC FIELD	x	x x		⁽³⁾ x x		x	x
MAGNETIC FIELD	x	x	(X)	x x	x	(X)	x

CSM COLORADO SCHOOL OF MINES
ITS INSTITUTE FOR TELECOMMUNICATION SCIENCES
NBS NATIONAL BUREAU OF STANDARDS
WGL WESTINGHOUSE GEORESEARCH LABORATORY
WVU WEST VIRGINIA UNIVERSITY
LL MIT LINCOLN LABORATORY

- (1) DATA LIMITED IN AMOUNT OR UTILITY
(2) PAST WORK – NOT FOR BU MINES
(3) PLANNED BUT NOT STARTED
(4) DIRECT DIGITAL RECORDING ALSO
(5) GEOGRAPHICAL
(X) INDICATE THE MOST PREFERRED METHODS
AND RESULTS TO CHOOSE FROM FOR
FUTURE MEASUREMENTS

methods and noise results, together with an indication of which methods and results should be most suited for future measurement efforts.

Recommendations for the implementation of the next phase* of the Bureau of Mines noise measurement programs are presented in this Part. This next phase will be aimed at filling the most critical data gaps. The following recommendations are based on the above findings and on the conclusions reached during a two-day conference between key staff of the Bureau of Mines, NBS, ITS and ADL in Boulder, Colorado on 13 and 14 March 1972- a conference convened for the express purpose of determining the most efficient and practical means for obtaining the required data.

In brief, a limited noise measurement effort, called a scouting-party expedition, is recommended. Measurements should be concentrated in the frequency band from about 40Hz to 400kHz, with perhaps some limited examination of lower frequencies and of higher frequencies up to about 30mHz. The effort should be one centered around short-term measurements of EM man-made noise, at locations of practical and strategic interest, in and above one or two representative coal mines as summarized in Tables 4 and 5. The main emphasis will be on simultaneous wideband magnetic tape recordings of the noise magnetic field components. Field strength meters modified to measure noise power will be used to a more limited extent, and mainly at the higher frequencies. Highly portable, battery powered, compact equipment will be used to minimize time and confusion in the mines. Data processing and analysis of the noise tapes will be conducted back at the laboratory utilizing available and reliable digital methods and computer software, and some conventional analog methods. High- and moderate-resolution noise power spectra will be obtained, and when appropriate, noise amplitude and time statistics. The noise measurements will be made primarily in locations, and under conditions, where the data gaps are presently moderate-to-large and of high priority; such as in and above working sections, where there is a need to provide wireless communications to supervisory, maintenance, and safety personnel. Long-term measurements of atmospheric noise on the surface are presently not of

* As of the spring of 1972.

high priority; because man-made noise is expected to dominate on the surface above coal mines, and because existing atmospheric noise data, through sparse in some frequency bands, appear to be adequate for making first-order system performance estimates and comparisons. Heavy dependence is placed on the prior demonstrated capabilities of NBS and ITS in recording and analyzing electromagnetic noise.

The "scouting-party" field measurement effort is purposely being designed to be of limited scope and duration in order to: obtain a rapid and better indication of the nature and severity of the coal mine EM noise environment; identify the most critical conditions and parameters; and help identify the most favorable frequencies for mine operational/emergency communications. The remainder of this Part presents an abbreviated description of, and questions related to, the instrumentation and data processing methods that were discussed at the March meeting in Boulder. This Part includes a partial equipment list and block diagrams for the instrumentation to the extent that they are presently defined and in addition documents the main findings and conclusion of the March Boulder meeting, and serves as a framework from which the field measurement instrumentation, data processing, and test plan details can be finalized by the joint NBS/ITS team that will perform the measurements under the guidance of the Bureau of Mines.*

II. CONFERENCE PARTICIPANTS AND TENTATIVE PROGRAM ASSIGNMENTS

The March, 1972, Boulder conference participants were Howard Parkinson of the Bureau of Mines; John Adams, William Bensema and Harold Taggart of NBS; A.D. Spaulding and Robert Matheson of ITS; and Robert Lagace and Richard Spencer of ADL. The following tentative measurement program assignments were agreed upon for a joint NBS/ITS team effort under the guidance and direction of Howard Parkinson of the Bureau of Mines. NBS/ITS program coordinator will be John Adams of NBS; William Bensema will serve as the NBS leader and A. D. Spaulding as the ITS leader; with Robert Matheson of ITS and Harold Taggart of NBS completing the NBS/ITS core team.

* ADL's subsequent participation in the noise measurement program was in an advisory and coordinating capacity in behalf of the Bureau. Principal activities of this ADL effort consisted of periodic communications and participation in status and system review meetings with the NBS/ITS team and the Bureau, as described in the Appendix in this Part.

E-M THRU EARTH VOICE TRANSMISSION-----Blackboard Outline of Limited Measurements Suggested to Characterize Noise Environment -- 7 December Boulder Meeting

Wireless Communications Desired to Supervisors, Foremen, and Safety Man in Each Working Section, which Includes the Faces and Loading Centers

DOWNLINK - In-Mine Radiated Noise - Highest Priority

- Frequency Range: Below 10kHz
- Under Operational Conditions
- Harmonic and Impulsive Noise - Short-Term Measurements
- FIRST MEASUREMENTS - Should Be of a Limited Scouting Party Type

By Visiting Maybe 2-4 D.C. Mines for Some Quick and Simple Measurements at Some Strategic Locations in the Mines: To Build up Confidence in Applicability of Present Results: (i.e., that of Bensema--NBS, and some of WGL's)

● STRATEGIC LOCATIONS IN A D.C. MINE - (Choose High Vs. Low Coal Mines for Convenience of Tests)

- Alongside D.C. Haulageway Track
- On Locomotives
- Near Equipment at the Face
- Near Power Lines Going to the Face
- Near Specific Machinery
- Near Underground Power Substations

- Make Measurements with Air Core Loop, Size of NBS' and with A Small Ferrite Antenna for Comparison
- Behavior Versus Distance from Sources Should Be Examined

UPLINK - Surface Radiated Noise - Lower Priority

- Frequency Range: Below 10kHz
- Under Operational Conditions
- Harmonic and Impulsive Noise - Short-Term Measurements (No Long-Term Atmospherics)
- First Measurements as Above - Limited to Strategic Locations
- Strategic Locations
 - Near Power Boreholes and
 - Near Surface Power Lines and "Mine Mouth" Power Stations
- Again Versus Distance From Sources

TABLE 5

OUTLINE OF SCOUTING PARTY NOISE MEASUREMENT NEEDS FOR THE 0-10kHz BAND
(December 7, 1971-Bureau of Mines Contractors' Round Table Meeting-Boulder, Colorado)

III. MEASUREMENT PROGRAM OUTLINE

A. Data Needed

The Bureau of Mines noise measurement programs to date* have developed considerable data on the character of electromagnetic noise in mining environments. Despite this assembly of data, there still exist substantial gaps in the characterization of the mine noise environment (as shown in Tables 1 and 2). The magnetic field components of the noise are of principal interest. In the mines, there is no EM noise data near the working faces, and only little data of merit near particular equipments, power centers and transmission facilities, and as a function of operating conditions and distance. There is a dearth of noise data in quiet regions of mines. In addition, the modest amount of good data taken to date in mines falls largely in the band from 0-5kHz, thereby creating an even larger gap in the frequency band from 5kHz to 400kHz. In addition, there is the need for obtaining information on the propagation of electromagnetic signals in the regions near working faces, in particular from the working faces to a typical loading point, this distance encompassing about 600 feet. On the surface there is a lack of data in regions directly over the working faces and near power lines and bore holes, again as a function of distance and operating conditions as in the mines. There is also a need for providing data on the correlation of surface noise behavior with in-mine noise behavior. An indication of the data to be obtained by the scouting-party noise measurement program together with an indication of their priorities is shown in Table 4.

B. Noise Characteristics

Measurements made to date* in the mining environment reveal that the noise in the low frequency region from a few Hertz to 5kHz is dominated by 60Hz and its harmonics. Impulsive noise is seldom dominant in this band, assuming high levels only when loaded locomotives with arcing trolley pole contacts pass close by. From the 10kHz region upward the noise, although influenced by harmonic content, does not appear to have power line harmonics that can be separated and isolated as such. Limited data suggest that the noise spectrum levels fall off with frequency in this region

*As of the Spring of 1972.

up to about 100kHz, beyond which the detailed character is unknown. The impulsiveness, dynamic range, and statistics of the noise in the region above 10kHz are unknown at the present time. An objective of the measurement program will be to remove the major uncertainties with regard to these noise characteristics and levels.*

C. Data Acquisition and Analysis

It was the conclusion of the conference participants that the missing noise data could best be obtained by analog tape recording magnetic field noise picked up by loop antennas, and to a more limited extent conducted trolley and telephone line noise by direct pickup. The data on these magnetic tapes could then be reduced to useful forms such as power spectrum plots by digital methods using a computer, for the frequency range below about 20kHz, and by analog or a combination of analog and digital methods, for the higher frequencies. The realization of such a magnetic field noise measurement program can be broken down into several parts:

1. design of the noise measurement system;
2. procurement of the needed parts and components;
3. modification and/or test of components of the system;
4. in-laboratory tests of the completely assembled system;
5. system proof testing by an early field experiment to verify the performance of the system in the mining environment;
6. system modifications based on the findings of this early field trip, if necessary;
7. field trips to specified mines for data acquisition;
8. analysis of the data obtained on these field trips;
9. documentation of the findings of the noise measurement program.

* As of the fall of 1973 this measurement program has been largely completed by NBS. The instrumentation system and noise data are being documented by NBS under its noise measurement program Contract H0133005 with the Bureau of Mines.

IV. INSTRUMENTATION AND DATA PROCESSING SYSTEM

A. Block Diagram

Figures 1, 2, and 3 illustrate block diagrams of alternative system configurations as now conceived. It will be apparent in the discussion that follows that certain options indicated on the diagrams may or may not be used dependent on the findings of an early proofing field trip. However, for the sake of completeness, the elements of the block diagram are discussed. It will be apparent in this discussion that details of component selection have not been made at this time, since these must be made after a study of the detailed requirements and available performance of the various elements which comprise the measurement system.

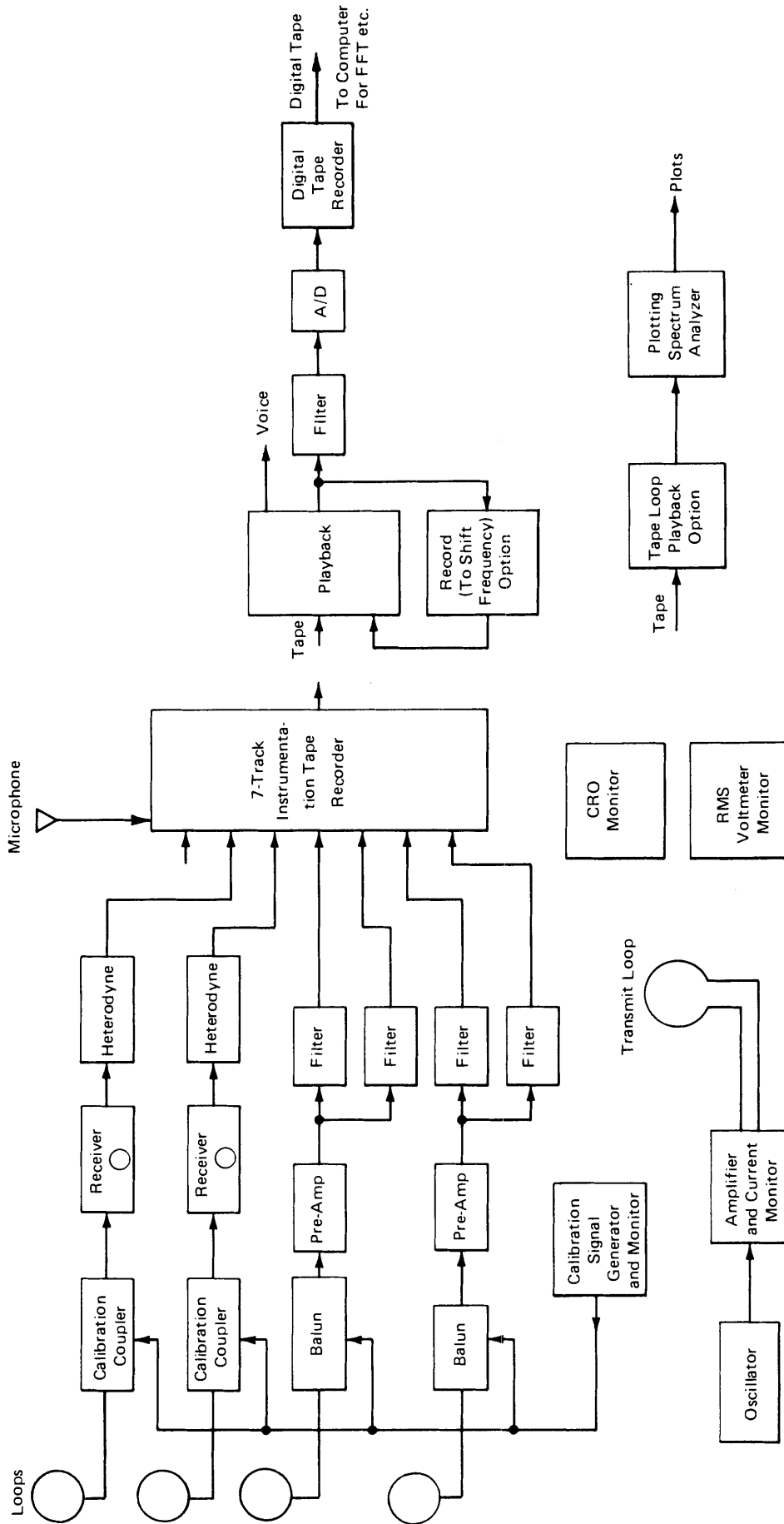
As shown on the block diagram, the sensors for picking up electrical signals related to the noise are loop antennas for the magnetic field components, and direct pickups for currents or voltages on trolley or phone lines. Two loops appears to be a practical compromise for an in-mine system to simultaneously record and examine the behavior of orthogonal magnetic field components. The signals after having been picked up are in most cases passed through preamplifiers, because of the need to operate the recording equipment at a distance from the region in which the noise is being measured. Also shown between the preamplifiers and the pickup loops are the balance to unbalance transitions (baluns) that may be required. A further point of interest in the block diagrams is the injection of calibration signals at the front end of the pre-amplifiers. After the preamplifiers, the signals are fed to a variety of devices.

Starting from the top of Figure 1, it is seen that two loops are indicated as feeding modified Stoddart NM-25T receivers. These receivers convert the broadband noise picked up by loop antennas to relatively narrow band (3.5-5kHz) outputs around a selected center frequency in the ranges of 150kHz to 32mHz. It is further indicated that this narrow band around the carrier is translated to a baseband frequency by the use of a block identified as Heterodyne. This process provides the capability for

recording noise centered around a high frequency on analog tape recorders which do not have baseband responses adequate to reach these higher frequencies. Below the receivers in Figure 1, it is seen that noise waveforms are also picked up by two other loops and fed through their preamplifiers to a pair of filters. After filtering, the waveforms enter separate channels of an analog magnetic tape recorder. In this way, for example, a frequency band from a few Hertz to 375kHz would be split at 100kHz, so that the lower frequency part is recorded FM and the upper part direct. Modified Stoddart NM-12AT receivers with bandwidth (100Hz or 2.5kHz) will also be available for examination of the frequency range 10-250kHz as a backup to the wideband analog recording.

The analog tapes that result from the application of the system are played back in the laboratory. Several modes of operation of this playback are illustrated by the block diagram. In one mode the signals resulting from playback pass through a filter, then to an analog-to-digital (A/D) converter, and hence on to a digital tape. This digital tape contains representations of the waveforms being sampled and is then processed digitally with a computer to yield items such as power spectrum level versus frequency by means of a Fast Fourier Transform computational algorithm. Examples of this type of data processing may be found in the Bensema NBS report and in the Evans Lincoln Lab report, which are cited in the bibliography at the end of this report.

In another processing mode the playback results in the creation of another analog tape. The intent of this processing mode is to enable a scaling of the frequency band of the original recorded waveforms to a lower frequency band, which will in turn enable available analog-to-digital converters to process a correspondingly wider range of real frequencies. As an alternative to this kind of processing, it is indicated that analog processing for a quick look and possibly analog spectrum plotting should be available. The recorded voice channel on the original tape is also shown as being played out through a speaker, and provision is made to monitor any channel by a cathode-ray oscilloscope. Individual



1.15

FIGURE 1 SIMPLIFIED BLOCK DIAGRAM
OPTION I - IN-MINE MAGNETIC FIELDS

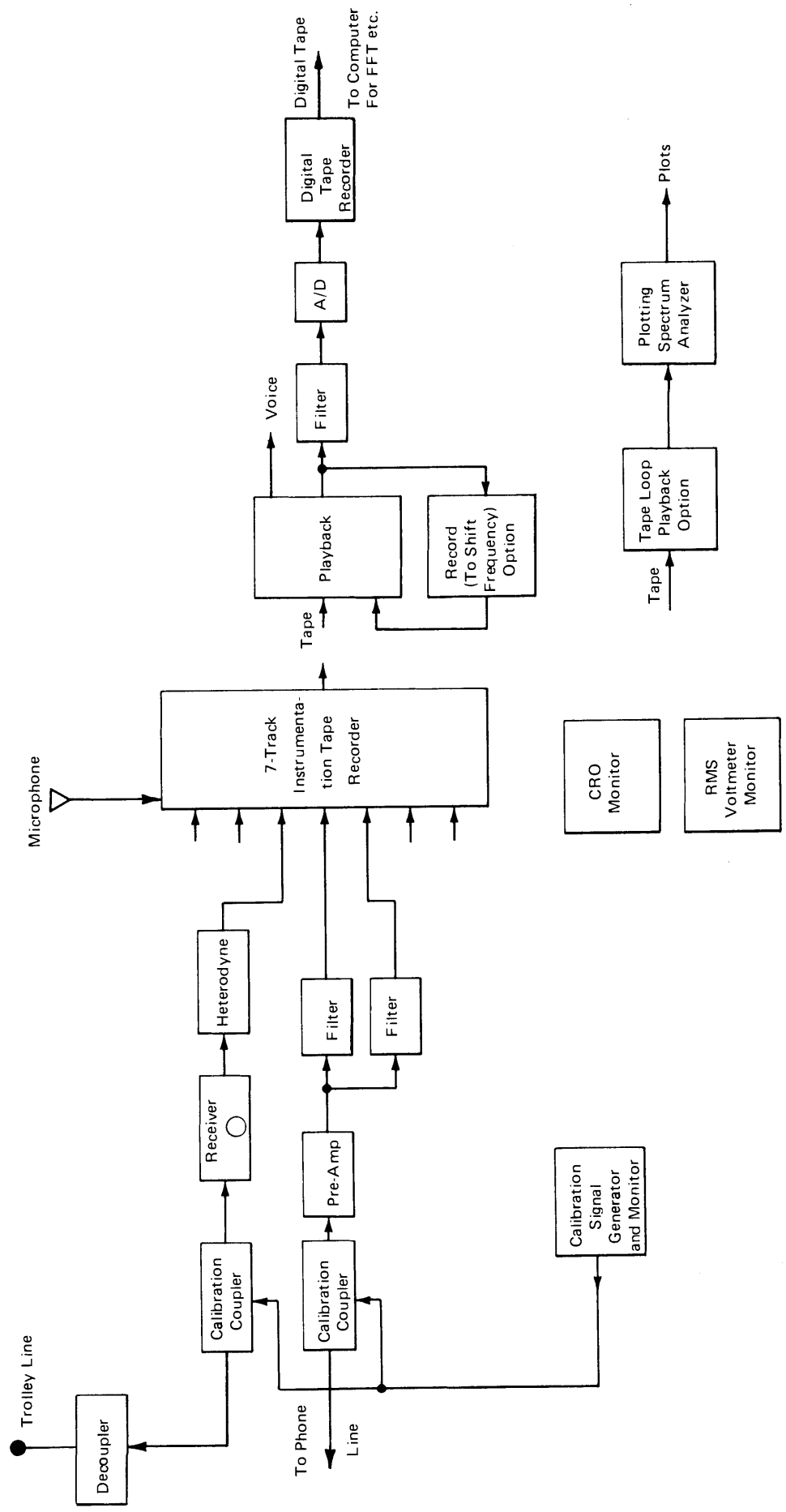


FIGURE 2 SIMPLIFIED BLOCK DIAGRAM
OPTION II - IN-MINE CONDUCTED NOISE

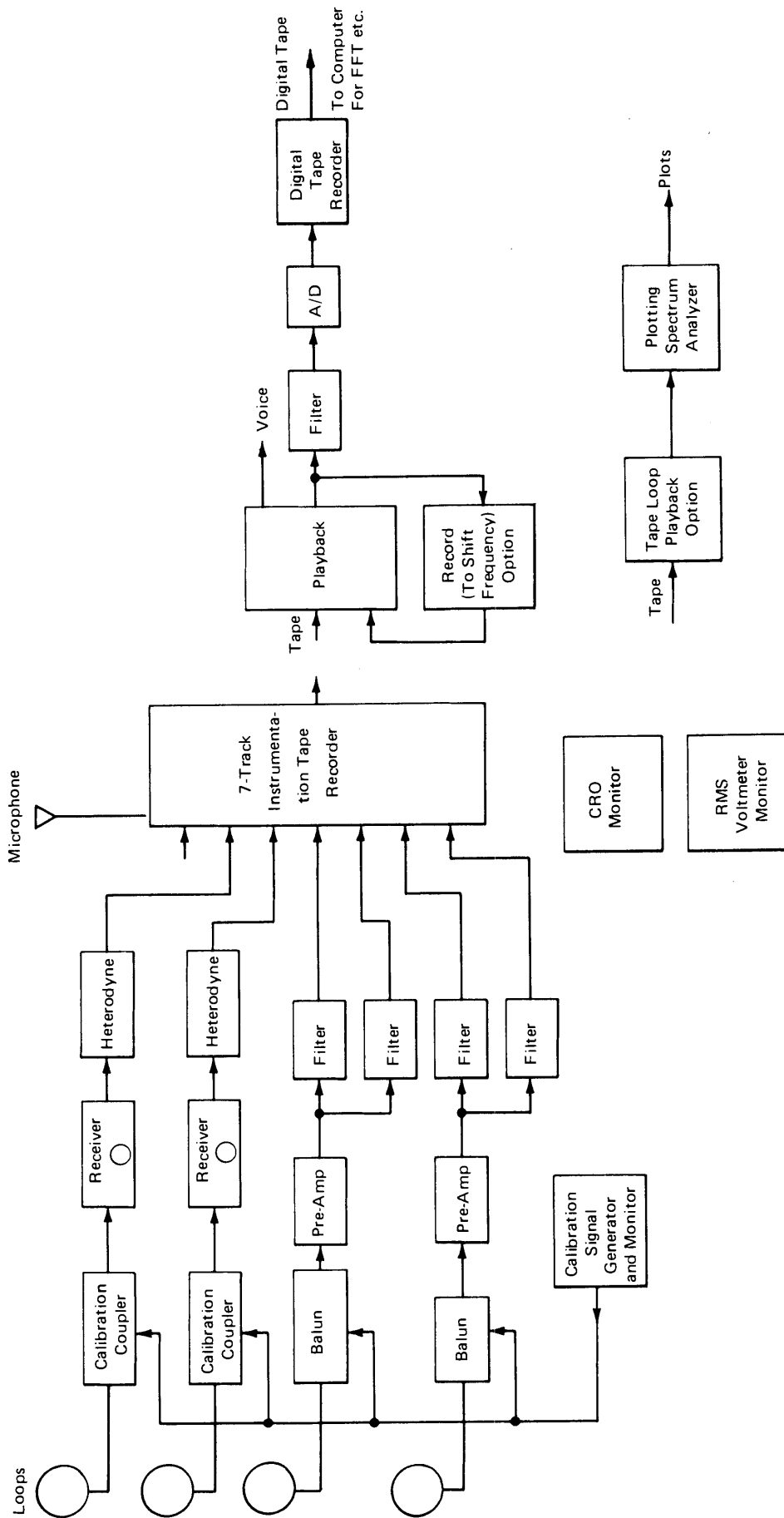


FIGURE 3 SIMPLIFIED BLOCK DIAGRAM
OPTION III - SURFACE MAGNETIC FIELDS

elements that enter this block diagram are discussed below.

B. System Components

1. Loops

It was the consensus that the pickup loops for the measurements should be commercial units of a balanced, shielded nature. Ferrite or other loaded loops were discarded as being subject to significant errors. It was agreed that Stoddart loops of the type used previously by NBS and ITS are acceptable for this use.

2. Preamplifiers

Preamplifiers should be battery-operated units functioning at intrinsically safe voltage and current capacities. This intrinsic safety is needed because these preamplifiers will be used at the working face areas of mines. It is expected that most of the semiconductor-based amplifiers will be operated at low enough voltage levels to meet the requirements, but that care must be used in battery selection to assure that the intrinsically safe limit is not exceeded in terms of battery current capability.

3. Filters

Filters are shown in both the recording and playback parts of the block diagram. The requirements are more severe on filters for recording because these must be battery-operated and should be small in size. The function of the filters is to restrict the bandwidth of the recordings so as to provide maximum use of the available dynamic range of the recorders. The generally required function is that of bandpass with selectable upper and lower band limits. Filter roll-off outside the passband should be at least 48 db per octave. Krohn-Hite Models 3323 or 3343 would be good candidates for this use. A problem arises in the frequency region above 100kHz, because these filters are limited to 100kHz. It may be necessary to add some fixed-frequency passive filters for some particular measurements. Such filters are commercially available from several sources. For operation in the playback mode, where the magnetic tapes

are played back at a fraction of the original recording speed, the Krohn-Hite filters are entirely adequate, and are used primarily to prevent aliasing errors in the subsequent sampling and A/D conversion.

4. Receivers

Two receivers are illustrated in the block diagram. It was agreed that these receivers would be Stoddart NM25T receiver units, modified as ITS has previously modified similar receivers to enable them to indicate several measures of noise, in particular, V_d and V_{rms} , as discussed in Matheson's paper. These modifications will permit manual collection of data over a frequency range much greater than can be accommodated with the analog magnetic tape recording system. These receivers can provide important measures of noise properties without the resort to recording.

In addition to this modification of the receivers, it is planned to shift the IF signal (prior to detection) from the IF center frequency to base-band so that analog recordings can be made of a band about 3.5-5kHz wide, centered at any frequency in the receiver range. Thus, recordings of the noise found at various select frequencies beyond the nominal frequency response of the tape recorders can be obtained. These recordings can then be subjected to the same computer-based analysis that Bensema used in the prior NBS noise measurements below 10kHz. On the block diagram this frequency shifting is noted separately as a heterodyne process, while in actual practice this function would be accomplished within the modified receivers.

5. Tape Recorders

It was agreed that the Lockheed 417WB instrumentation recorder is a prime candidate for recording the analog signals. There is still some uncertainty regarding the ability of this recorder to operate in the expected mine environment. There is a considerable body of experience with the Lockheed 417 recorder, and this recorder will be used if the 417WB is found to be deficient in performance. These recorders are well suited to the needs of the measurement program. Both are compact, battery-

operated, 7-channel instrumentation recorders that use 1/2 inch wide magnetic tape. The 417 has FM capability from 0-10kHz and a direct capability to 100kHz at 30 IPS. The 417WB is the new wideband version, has FM capability from 0-100kHz and a direct capability to 375kHz at 30 IPS. The use of either of these recorders would avoid the substantial difficulties that Bensema faced in the earlier NBS program, due to the need for a power inverter and large battery supply. The 417WB is preferable because of the wide frequency range accommodated in the FM mode for which high accuracy recording can be relied on.

6. Sources

It was agreed that part of the noise measurement program would include measurements of signal propagation characteristics from the face area to the loading point in a representative mine or mines. For this purpose a portable signal drive system and transmitting loop are required. It is estimated that approximately 10 watts of drive power will suffice for the measurements planned. It is not expected that a good commercial, intrinsically safe 10 watt amplifier of capability to 100kHz can be found, and therefore it may be necessary to develop a portable battery-operated system for this purpose.

C. Real and Synthetic Calibrations

It was agreed that two kinds of calibrations are needed for the noise measurement system: 1) a true calibration for which the pickup loops of the measuring system are immersed in known fields and the measuring system output is related to these known values of field; and 2) an artificial calibration to be used in the field. In the second type of calibration, known signal voltage levels are introduced into the system as near the front end as possible. Such a calibration assures that system drifts and gain changes are monitored and known. Usually such calibrations are not able to verify sensor sensitivity, but verify the performance of the remainder of the measuring system. The true calibrations can be accomplished in the NBS calibration facility at Boulder; the synthetic calibration equipment can be made up of commercially available parts.

D. Playback and Processing

The block diagram illustrates different ways in which the tape can be processed to yield the desired measures of noise. As shown on the block diagram, one of the ways of processing is to play back the tape through a filter and an analog-to-digital converter to generate a digital tape representative of the analog signals from the recorder. This procedure follows directly that of Bensema in his noise measurements for the Bureau of Mines. The playback may be at several different speeds to accommodate the bandwidth of the noise waveforms to the sampling rate of the A/D converter. The filter is to remove noise waveform components beyond a prescribed frequency in order to prevent aliasing in the sampled version of the waveform.

A second processing mode illustrated in the block diagram shows rerecording, or dubbing, of the original tapes. It is intended that this dubbing translate an original frequency range to a lower frequency range, thus making the playback of the dub compatible with the limited 16kHz sampling rate of the A/D converter used by Bensema previously. For example, if the 417WB recorder is found to be acceptable for recording, FM recordings with a bandwidth from 0-100kHz can be made. It appears desirable to be able to process recordings of such an original frequency band using computer FFT techniques. Thus, because the present A/D converter limits waveform analysis to a band of about 0-5kHz, a 20:1 reduction of playback speed is required. This range of speed reduction is not likely from one tape playback unit, and, hence a dubbing process is used to overcome this limitation. The two-step process extends the speed range from a maximum of 8:1 in a single playback unit to 64:1 using the dubbing process, and thus encompasses the range required for reduction of 0 to 100kHz to 0 to 5kHz. The use of playbacks of original and dubbed tapes will provide for the ability to generate in the frequency range 0 to 100kHz the kind of spectrum plots produced by Bensema.

An optional type of processing scheme is also illustrated on the block diagram. This option relates to what is done with the recordings made on the direct channels of the tape recorder, for which analog signals up to 375kHz can be analyzed (if the 417WB recorder is used). It is felt that computer-based reduction would be costly for such extended bandwidth signals, and that the merits of the narrowband analysis will be less applicable to the broadband data, particularly in the upper frequency range of such recordings. For these regions we believe that analog spectrum analysis techniques may suffice to determine the nature of noise. In particular, it is suggested that conventional sweeping spectrum analyzers be used for this purpose in conjunction with a tape/loop playback method. The loop is recommended because it permits analysis of a single time period of the original recorded noise, rather than the use of a long time sequence where time variations could be confused with spectral variations.

The key presentation of noise data will be in the form of power spectrum plots similar to those shown in the NBS Bensema report and the Evans Lincoln Lab report, in which the magnetic field noise components are plotted in db relative to 1 ampere per meter, or db relative to 1 ampere per meter per $\sqrt{\text{Hz}}$ versus frequency. Computer-generated FFT outputs are compatible with either presentation, while spectrum analyzer outputs are more suited to the former. These plots can be very useful in revealing characteristic spectrum signatures of specific noise sources. A problem with analog spectrum analyzers is that they are responsive to voltage and thus the spectrum plots become related to voltage, thereby requiring an appropriate calibration. This fact does not trouble analysis of conducted noise, but does pose a problem for magnetic fields for which the generally accepted form of presentation is db relative to 1 ampere per meter in the bandwidth of interest, not voltage out of a loop. Proper system design and calibration will ensure reliable results. Statistical presentations of amplitude and time probability distributions may be desired if the dominant noise in certain frequency bands is found to be impulsive in character. Analysis and presentation methods similar those used by ITS and/or Lincoln Lab can be used if necessary.

E. Equipment List

It was agreed that the following equipment is required in addition to equipment already available at NBS/ITS:

<u>Item</u>	<u>No. Required</u>	<u>Unit Cost</u>	<u>Total Cost</u>	<u>Notes</u>
Lockheed 417WB tape recorder	2	\$19,000	\$38,000	Estimated costs for fully equipped units
Stoddart receivers (NM-25T & NM-12AT)	4 (2 each)	7,000	28,000	Units supplied with accessories
Stoddart receiv- ing loops (90117-3)	3	333	1,000	These loops are in addition to the ones supplied with the receivers
Filters Krohn-Hite 3323	3	1,225	3,675	
Model 323 Tektronix Scope	2	950	1,900	Or similar
PAR Model 113 Preamplifier	3	795	2,385	
Other equipment (calibrators, oscillators, power source, transmit system, etc.)			3,000	Details to be determined

F. Shaping of Noise Spectrum Signature prior to Recording

There is little data on the character of magnetic field noise within mines in the region from 10kHz to 100kHz. It is expected that early proofing tests will reveal the general nature of this noise, and it may become necessary to shape the spectra of the noise in that region so as to assure equal recording signal-to-noise ratio over the band 10kHz to 100kHz. Whether this shaping is necessary or not will be known only after one of these early trips has been made.

G. Logarithmic Compression

The Boulder conference did include the discussion of the possible application of logarithmic compression upon recording and expansion upon replay as a means of accommodating a wider dynamic range of noise than could otherwise be accommodated by the recording equipment. It seemed to be the feeling in the meeting that for the expected types of noise, specifically the harmonically dominated noise, compression-expansion would raise possible severe difficulties in accurately recovering the noise character from such recordings. It was left that only under the most pressing need would such compression and expansion be planned. Again, the utility of this technique, or the need for this technique, will be clarified by early proofing tests in an operating mine.

V. OPERATIONAL CONSIDERATIONS

A. Equipment Proofing

It was agreed that it is desirable to provide several levels of tests for a complex instrumentation system of this type. The first tests constitute tests of the individual components to assure that they perform according to specifications. The second level of tests are laboratory tests wherein the total system is subject to controlled exercises, revealing any possible shortcomings of the total system itself. These two initial testing phases will be followed by an operating test of the system wherein the equipment is taken to a mine where access is easy and does not interfere with the operations. It has been reported that NBS/ITS have an arrangement with the Lincoln Mine to permit this kind of operation. This test will reveal if there are any operational and environmental problems with the existing system. After such proofing and any modifications brought about by these various levels of testing, the equipment would be ready for use in mines selected by the Bureau of Mines for evaluation.

B. Record Keeping

It is important that a program of this nature provide accurate records from which it may be determined at later dates the exact conditions under which various data were taken. For this purpose it is essential to keep

a log-type notebook that clearly identifies times, places, conditions, etc. for future use.

C. Test Plans

It has been recognized by the Bureau of Mines and by NBS/ITS that any field trip into a mine constitutes an interference with the normal mining operations. For this reason it is essential that the field crew be thoroughly schooled in efficient, effective use of time within the mines. This means that the role of each of the field crew must be well-defined and known to him prior to entry into the mines. As an aid to this, it is important that documented test plans be prepared to assure not only that minimum interference with mining operations is had, but that a timely and effective collection of the data necessary is made. These test plans would, therefore, identify the specific purpose of each planned trip to a mine, and include the data gaps which are expected to be filled either fully or partially by such a field trip.

VI. SOME QUESTIONS AND ITEMS TO BE RESOLVED

The Boulder meeting did reveal some areas of concern to the design of the instrumentation system. These questions and items are repeated here for the sake of record. They are not meant to be all-inclusive.*

A. Tape Recorder Suitability

Is the candidate tape recorder (the Lockheed 417WB) suitable for the use intended? a) What is the absolute value of the noise floor in the FM wideband recording mode? b) What is the absolute value of the direct recording mode noise floor? c) Is it expected that the recorder will be sufficiently reliable for use in the mining environment? NBS/ITS will obtain the answers to a,b, and c by means of measurements on a candidate recorder and by means of queries to users of that recorder. If the 417WB is not suitable, the 417 will be used instead.

* These and other questions were subsequently addressed and resolved as the instrumentation system was assembled and tested during the remainder of 1972. (See Appendix to this Part.)

B. System Organization

What is the best system organization for recording the data needed? It is expected that the system organization will be pretty much as shown in the block diagrams and in the options thereto. Specific modifications of this may result from early proofing tests of the equipment in an operating mine and may reveal characteristics of the noise as yet unknown, which could result in a need to modify the noise measurement system.

C. Dynamic Range Considerations

There seems no doubt that the dynamic range of the noise voltages that appear at the output terminals of the loop antennas will be such as to challenge the ability to record the voltages with acceptable fidelity. The work of Bensema shows the seriousness of this problem.

Even if the noise were stationary, a very substantial dynamic range of recording capability is required to simultaneously obtain the level of lines (60 & 360Hz harmonics) and simultaneously the base level of noise between the lines. When the time variability of the noise is added, it compounds the problem. Bensema solved this problem by using skilled operators to adjust recording gain to conform to the noise being received. Such skill will be required in the proposed program.

A second problem related to dynamic range, and more particularly to the noise floor, is the effect of the number of bits used for A/D conversion on the computer-generated FFT noise power spectra. The questions to be answered are: How is the quantizing noise measured? How does quantizing noise appear as a noise floor in the FFT spectra? Which A/D converter should be used, the moderate sampling rate 12-bit model used previously by Bensema or the higher sampling rate 8-bit model that may also be available?

D. Transmission Measurements

The high priority attached to developing wireless communication from the face area to the loading points, places emphasis on obtaining measures of EM transmission in this area. It is expected that the measurement program will include loop-to-loop transmission measurements. For

example, a receive loop could be set up near the loading point, and the transmitting loop then could be moved progressively further away from the receive loop down entries and through cross-cuts. Selected frequencies covering the range to 100kHz could be examined.

E. Conducted Noise Measurements

Data on the conducted noise carried by phone lines and by trolley lines is desired. To obtain such measurements coupling to these lines is desired. Two problems need be resolved in such a program: 1) limiting of the expected powerful voltage transients known to be present on both kinds of lines, and 2) decoupling of the d-c voltage present on the trolley lines.

F. Tape Recorder Cross Talk and Non-linearity

The proposed use of most of the channels of a 7-track recorder imposes a problem associated with cross talk between channels. Measurements need to be made to determine the degree to which this cross talk occurs and how it affects the measurements. There are preferred ways of setting up the channels to minimize such effects, and these should be used.

The non-linearity of the recording process can contribute artifacts to certain types of recordings. In particular, where a single frequency dominates the recorded data it can be expected that the record-playback process will generate harmonics of this frequency. The degree to which the recording system is susceptible to this harmonic generation needs to be determined.

G. Computer-Generated Power Spectra

In order to better estimate the broadband noise floor levels between the harmonics of 60Hz and 360Hz, finer resolution on the computer analysis bandwidths and/or better out-of-band response is desired, particularly for analyzing data below about 5kHz. At the meeting we agreed that these improvements are desired only if they can be realized without major software modifications to existing computer programs at NBS/NOAA. The

present out-of-band response apparently includes improvement features already. Analysis resolution can still be improved (made narrower) by a factor of two, with only minor software adjustments according to Bensema. So this may be worth getting. However, the resultant resolution will also be a function of the degree of frequency scaling used to analyze the tapes.

It would also be desirable to be able to increase the number of time segments used to generate the power spectrum estimates, above the 20 used for the previous NBS measurements; again, if this can be done without major changes and expense. In this way the spectrum estimates could be based on longer and perhaps more representative time intervals for assessing the noise impact on voice communications, particularly if the coal mine noise environments are non-stationary. The ability to vary the number of segments above 20 would also allow some coarse assessment of the degree of noise stationarity. Considerations such as the above should be examined in more detail, in order to get maximum utilization of the instrumentation and data processing potential in the most efficient and economical manner.

H. Choice of Mines for Measurements

Tentative criteria have been expressed on which to base the choice of mines for conducting the scouting-party measurements. Some of these are: that they be large bituminous mines in the East, with high roofs, and in Pennsylvania or West Virginia for convenience; with a DC trolley haulage system, conventional and continuously mined faces, and 3-phase rectified power centers. The criteria need to be spelled out in more detail, expanded, and finalized to conform with the measurement program objectives and the requirements of the Bureau of Mines, which also are to be finalized.

I. Experiment Design

It was agreed that long-term measurements over several consecutive weeks or months in a mine were not warranted for the scouting-party measurement

program. The mine noise characteristics and levels are likely to be quite similar from work-shift to work-shift and repeated many times during a work-shift. Therefore, measurements need be made in a few different mines, at several representative locations and times throughout a work-shift, over a few consecutive days, in the vicinity of important electrical equipment and facilities, under different operational conditions and loads. Such measurements are expected to provide sufficient data for generating statistically significant power spectrum and amplitude and time distribution estimates that can then be used for making first-order system performance estimates and decisions regarding the candidate mine communication techniques. Detailed plans regarding the locations, equipments, conditions, time durations, etc., of specific measurements have yet to be formulated and integrated into a noise measurement program designed to yield the desired results in an efficient and economical manner.

VII. BIBLIOGRAPHY

Bensema, W. D.

COAL MINE ELF ELECTROMAGNETIC NOISE MEASUREMENTS

National Bureau of Standards (December 1971) (Preliminary)

Disney, R. T., R. J. Matheson, and A. D. Spaulding

RADIO NOISE MEASURING AND ANALYSIS FACILITY

Institute for Telecommunication Sciences, Boulder, Colorado (U.S. Dept. of Commerce Publication)*

Evans, James E.

ATMOSPHERIC NOISE (ELF)

MIT Lincoln Laboratory Data and Computer Programs (1968-69)

Including:

Additional information regarding the first package of 10 digital tapes.

Description of Recording System and Digital Tape Format for "LASA" format tapes (Florida data).

Description of Read Package "IOPAK" for "LASA" format tapes.

Description of Recording System and Digital Tape Format for "NAVCOM" format tapes (Norway and Malta data).

Description of Read Package "CAROLE" for "NAVCOM" format tapes.

Description of Fast Fourier Transform program "FOURT".

Description of Spectral Analysis Program "COH 10".

Description of Digital Filtering Program "FILT 9".

Description of Probability Distribution Program "SAN 3".

Subroutines used by G, H and I that may not be available at other installations.

Listing of Lincoln Lab Digital Wideband Data Tapes from Florida, Malta and Norway.

Evans, James E.

PRELIMINARY ANALYSIS OF ELF NOISE

MIT Lincoln Laboratory Technical Report, TN 1969-18 (March 1969).

Little, Arthur D., Inc.

ELECTROMAGNETIC AND SEISMIC NOISE AND PROPAGATION

A Bibliography for U.S. Bureau of Mines, Pittsburgh Mining and Safety
Research Center, March, 1972.

Matheson, Robert J.

INSTRUMENTATION PROBLEMS ENCOUNTERED MAKING MAN-MADE ELECTROMAGNETIC
NOISE MEASUREMENTS FOR PREDICTING COMMUNICATION SYSTEM PERFORMANCE

IEEE Trans. on Electromagnetic Compatibility EMC-12 (4), 151-8

(November 1970).

Spaulding, A. D., W. H. Ahlbeck, and L. R. Espeland

URBAN RESIDENTIAL MAN-MADE RADIO NOISE ANALYSIS AND PREDICTIONS

Telecommunications Research and Engineering Report OT/TRER 14,

Institute for Telecommunication Sciences, Boulder, Colorado (June 1971)

(U.S. Dept. of Commerce Publication).

Taggart, Harold E. and John L. Workman

CALIBRATION PRINCIPLES AND PROCEDURES FOR FIELD STRENGTH METERS

(30Hz to 1GHZ

National Bureau of Standards, Technical Note 370, (March 1969) 151pp.

APPENDIX

SUMMARY REPORTS OF ELECTROMAGNETIC (EM) NOISE MEASUREMENT PROGRAM REVIEW MEETINGS

I. INTRODUCTION

From May of 1972 through October 1973 ADL staff served PMSRC in an advisory and coordinating capacity with respect to the Bureau's measurement program for obtaining quantitative noise data to characterize the EM noise environments of underground coal mines. In this capacity ADL staff kept in close touch with the NBS measurement team, and participated in periodic status report and system review meetings with this team and PMSRC, during both the system implementation phase and the subsequent noise data acquisition and reduction phases. This Appendix presents for historical reference a collection of memoranda prepared by ADL for PMSRC to record the principal findings and decisions of these meetings.

II. EM NOISE MEASUREMENT PROGRAM MEETING AT NBS, BOULDER, COLORADO ON
24 MAY 1972

The EM Noise Measurement Program status report meeting at NBS, Boulder, Colorado, on 24 May 1972, was attended by H. Parkinson of Bureau of Mines; R. Lagace and R. Spencer of ADL; J. Adams, W. Bensema and H. Taggart of NBS; W. Stout and H. Kuchera of Collins Radio; and D. Spaulding of ITS (only for a short time). The principal findings and decisions are summarized below.

A. TEST DESIGN AND PLANNING

Program Schedule

BuMines prefers that tests in mines be started by August, but NBS estimates it will be at least four months before it will be ready to do in-mine tests. At very latest, BuMines wants in-mine work started well before November because of the problems of snow and adverse weather after that time.

The long lead time equipment has been ordered by NBS with negotiations still in progress with Stoddart regarding receiver modifications. Though the program has moved forward, several equipment related details and many planning and test design items have to be resolved. Previous commitments of NBS and ITS staff are expected to taper off by July, at which time substantial effort will be devoted to the BuMines noise instrumentation and measurement program.

Coal Mines for Tests and Their Electrical Environments

Tests are being planned for three big Eastern mines:

- a. U.S. Steel - Robena Mine in Uniontown, Pennsylvania
 - Continuous mining with 600V DC rail haulage
 - Depth - 1,000 feet

- b. Island Creek - North Branch Mine, Charleston, W. Virginia
 - Continuous mining with 300V DC rail personnel haulage and 440V AC belt haulage
 - Depth - 400-500 feet

c. Island Creek - Alpine Mine, Charleston, W. Virginia

- Conventional mining with 300V DC rail personnel haulage and 440V AC belt haulage
- Depth - 400-500 feet

Frequencies present in many mines are given below:

Telephone Frequencies: in Hz:

300Hz to 3000Hz Voiceband

Trolley Line Frequencies: in kHz:

(MSA) (FEMCO)	<u>FM Carrier Deviation</u>
61, 72, 85, 88, 100	+3% Carrier
116, 113, 114, 163, 190	+ 3kHz

(Trolley phones usually on for 10-15 second bursts)

Fan Signaling and Pump Control Frequencies: in kHz:

24.5, 28, 33, 39, 47, 61

(Sent over surface AC power lines by pulsing carrier 15 seconds on, 5 seconds off)

Hoist Frequencies: in kHz:

163 typical, though some use trolley phone frequency of 88, 100.

Noise measurements should be made realizing that mine communication transmissions on these frequencies, and also some from surface transmitters, will be picked up by the noise measurement equipment, so that appropriate precautions must be taken to ensure the collection of unambiguous noise data.

Test Site Communications

BuMines wants a communication link for test coordination between the surface and underground teams. This link should not monopolize the baseband mine telephone. Instead it should make use of a carrier on the mine telephone line. This will be coupled to an independent base station which will relay the messages via radio to mobile units of the surface team. Motorola gear is being purchased by BuMines to provide this coordination.

Noise Data Desired

In reference to the noise characteristics of interest listed in Table 4 of the ADL April 1972 Noise Program Report, the Collins Radio people were asked to comment on what noise parameters were most important for their work. They responded that the high resolution power spectra were most important. With regard to APD's, they are not interested in the 3-D short-term ones in the NBS report, but want longer term statistics that can be used to identify good, average, and worst case noise conditions. Time statistics on the duration between noise bursts and burst duration are also of interest, but considered to be of secondary importance relative to the power spectra and APD's. The question of what will constitute long enough time samples for specifying "long term" APD's that exhibit the important characteristic variations found in coal mines has still to be resolved. NBS also recommends such long-term APD statistics, but with about an equal emphasis on time distribution statistics (TPD's) if low data rate code systems are of interest.

Conducted Noise Measurements

It was agreed that very little thought has been given to this topic, with regard to exactly what data are required, what equipment is needed, and where, when, and under what conditions are the data to be taken. Conducted noise on both the DC trolley lines and the telephone lines (and perhaps power lines) are of interest to BuMines. Concerns were expressed regarding the effects of moving loads, such as locomotives and jeeps on the measured data, and what locations on the lines make most sense to make the measurements. Much more consideration must be given to these measurements, but this task was not specifically assigned to anyone.

Transmission Measurements

Very little thought had been given to this topic, so BuMines assigned the task of devising meaningful transmission measurements over the frequency band of interest to Collins Radio. As a minimum, BuMines wants measurements of transmission loss between section loading points and locations throughout a working section, including the face area; and between working sections and the surface above. These measurements should be coordinated with the noise measurements. In particular, BuMines expressed a desire for a surface loop for transmitting to the face area during the acquisition of noise data. The section-to-surface measurements are expected to assist in the design of a low bandwidth digital through-the-earth parameter monitoring link that Collins is working on for BuMines. Collins is to coordinate its transmission measurement test plans closely with the NBS noise measurement efforts.

A transmitter-power amplifier is still required for these measurements. Two potential sources were cited to be checked: two amplifiers owned by BuMines, one owned by D. Aldridge of WVU. A power amplifier capable of 10 watts CW output over the 300Hz to 400kHz band is desired for these experiments.

B. EQUIPMENT

Tape Recorders

A battery-powered Lockheed 417WB recorder has been ordered for use in the mines as planned. However, a somewhat larger Honeywell Series 5600 unit with a 0-40kHz FM and a 0-300kHz Direct record capability has been substituted for the second Lockheed 417WB planned for use on the surface. The Honeywell unit was chosen for the surface because better reduced-speed tape dubs could be generated by the Honeywell unit, since it offered the capability of getting rid of wow and flutter by servo-controlling the playback to a CW tone recorded on the tape with the measured noise.

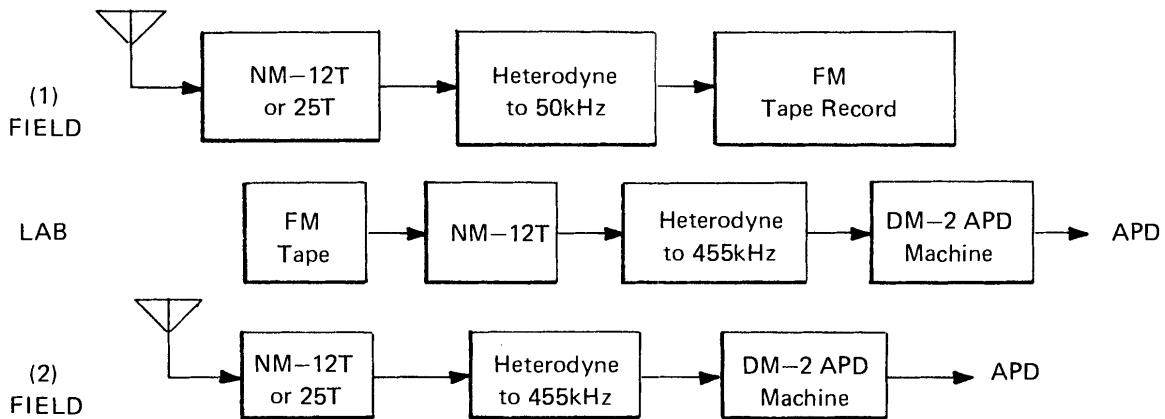
The plan is to playback the Lockheed 0-100kHz FM recordings on the Honeywell at 1/2 speed, thereby compressing the noise spectrum into the band from 0-50kHz. The means for obtaining further reductions to enable processing by the A/D converter were not discussed. NBS is still not sure how the noise spectra will be affected when the Lockheed 0-375kHz Direct recordings are played back into the Honeywell 0-100kHz Direct at reduced speed.

NBS was concerned about potential dynamic range problems if recordings were made across the total 0-100kHz FM on 0-375kHz frequency ranges. It was decided that single frequency CW dynamic range calibrations could be made on H. Taggart's loop calibration facility. There is still a question regarding how seven record-level settings can expeditiously be made in the field.

As a result of (a) the above discussion, (b) questions concerning sensor response and system noise limitations imposed on dynamic range versus frequency, (c) 300Hz being the lower cutoff frequency normally used for voice communications, and (d) the availability of Lincoln Lab surface noise data to frequencies down to 3Hz; it was decided that (1) the lower frequency limit of the noise measurement system would be raised from 40Hz up to 300Hz, (2) the 60Hz noise component would be filtered out before recording, (3) consideration would be given to filtering out the 360Hz component too, but perhaps to lesser degree than the 60Hz, and (4) W. Bensema would choose the appropriate signal conditioning electronics to produce the desired favorable noise recordings. To accomplish (4) the 300Hz to 400kHz band may have to be split up into a high and a low band. The tape recorders had not been received and tested as of this visit.

Stoddart Receivers

The NM-12T and NM-25T receivers, and associated (6) 30-inch loops and (2) 12-inch loops have been ordered, but the question of who, ITS or Stoddart, is going to make the required modifications (rms power and V_d outputs, and heterodyning to baseband) had not yet been resolved. R. Matheson of ITS (not present) is to follow this up. In Matheson's absence, J. Adams gave a thumbnail sketch of developments to date. Two possible configurations for field use of the receivers have been proposed by ITS.



The provisions for generating the indicated noise APD's within the receiver passband at specific carrier frequencies of interest look sound. But the system as shown deviates in one major respect from that originally proposed. Namely, the receiver IF output is being heterodyned down to 50kHz instead of to baseband prior to being recorded. The original system specification to use baseband, would allow for direct compatible processing of the recorded Stoddart waveforms by the NBS spectrum analysis system. Since this change to a 50kHz carrier does not allow such convenient analysis, reasons for the change were requested. In the absence of all ITS personnel, the answer was not available, so J. Adams agreed to check this out later with R. Matheson.

Field Components and Sensors

NBS recommended some simultaneous measurements of all six field components, three magnetic and three electric, as opposed to just magnetic fields as originally planned. Six 30" and two 12" shielded Stoddart loops have been purchased for the magnetic field. The 30" loops are self-resonant at approximately 390kHz, which may be far enough removed from the highest frequency to be recorded. Special electric field sensor antennas are to be made for the electric field. ADL expressed concern about the difficulties normally

associated with taking calibrated E-field "near-field" noise measurements in adverse environments, such as mines. Such closed environments that contain many conducting structures can easily change the response characteristics of whip antennas and distort the electric fields to be measured, thereby making the results difficult to interpret. The limited number of available tape channels may also impose dynamic range limitations for such measurements. NBS acknowledged these difficulties and therefore plans to limit the measurements of all six field components to a small number of the tests. Great care will have to be taken in choosing, calibrating, and using an appropriate E-field sensor antenna. NBS feels that these E-field measurements may help determine the relationships between the strengths of the E- and H-fields in near-field coal mine environments. ADL has reservations concerning the value of these E-field measurements, and feels that the subject should be discussed in more detail.

Permissibility Considerations

NBS would like to bring all its measurement gear, instead of just the loops and preamps, into working sections, including face areas. The topic was discussed, with a tentative agreement that it may be possible. However, to be sure NBS should send equipment descriptions and circuit diagrams to Bob Wolfe at PMSRC, who is the BuMines man concerned with the requirements for safe electrical circuits.

C. ANALYSIS

Noise Power Spectra

ITS commented on that part of the second paragraph on Page 20 of the ADL Instrumentation System Technical Memorandum of April 1972, regarding the outputs of spectrum analyzers relative to those of computer-generated power spectra. Namely, when referring to conventional spectrum analyzers that utilize successive logarithmic detection of the envelope of the input waveform, the analyzer can be calibrated for CW signals, such as harmonics, but not for broadband noise. Therefore the output of the analyzer will agree with the computer spectra only for the CW harmonic noise levels, but not for the broadband noise spectrum levels between the harmonics. ADL agreed with ITS's comments.

NBS reported that it had not yet examined how the number of bits in the A/D quantization process affected the FFT generated broadband noise spectra. But NBS suggested a good experiment to get the answer; namely, take the present tapes of quantized noise data, and look for changes in the computed FFT spectra as the least significant bits in the data are deleted one at a time. ADL agreed to ask Evans of Lincoln Lab for his judgment on the matter. It appears that Evans did not have to face this problem, because his large A/D dynamic range was dictated not by harmonic versus broadband noise spectrum level dynamic range, but by the large dynamic range required to produce APD's to the accuracy desired by Lincoln Lab.

D. MISCELLANEOUS

H. Parkinson heard that additional noise data has been recently released by Lincoln Lab--and that ADL should verify this with J. Evans of Lincoln.

According to Keller's experiments and studies, an overburden conductivity of $\sigma \leq 10^{-2}$ mho/meter is a good value to assume for coal mines ≤ 1000 feet in depth. Values as high as $\sigma = 10^{-1}$ mho/meter are seldom found except perhaps in small pockets.

H. Crary of ITS suggests that frequencies around 1.5GHz may be suitable for wireless point-to-point transmission in mine entries, haulageways, etc., as a result of higher-order waveguide propagation modes.

Radio communication ranges in excess of 2000 feet were obtained by a Sunshine Mine rescue team using 1 watt Motorola walkie talkies at a frequency of 460MHz, with the assistance of a #12 wire deployed on the mine floor as the team advanced into the mine.

H. Parkinson has experienced very favorable wireless along-the-roof communication on working sections on several occasions to ranges of several hundred feet. This was accomplished by connecting a trolley phone 25-watt 88kHz transmitter output to two roof bolts and receiving with a Reach pocket pager. The impedance between two roof bolts stayed pretty constant at about 20-25 ohms* when the separation between them exceeded about 30 feet in the Pittsburgh coal seam. Roof bolts range from 3 to 7 feet in length, 3/4 to 1 inch in diameter, with a 9-inch square roof plate, and a 4 to 5 inch diameter expansion section near the upper end. They are typically spaced 4 feet and greater apart, depending on roof conditions.

* Data taken since then indicate that the total termination impedance for roof bolt pairs separated by 50-200 feet falls mainly in the range of 50-120 ohms.

III. EM NOISE MEASUREMENT PROGRAM MEETING AT NBS, BOULDER, COLORADO ON
17 AUGUST 1972

On 17 August 1972 the EM Noise Measurement Program status report meeting at NBS in Boulder, Colorado was attended by Howard Parkinson of the Bureau of Mines; R. Lagace and R. Spencer of ADL, John Adams and William Bensema of NBS, Don Spaulding and Bob Matheson of ITS; and Bill Stout and Dean Anderson of Collins Radio. The principal findings and decisions are summarized below.

A. TEST DESIGN AND PLANNING

Schedule and Test Plans

The present schedule calls for making system proof-test noise measurements in the Lincoln mine during the last week in September 1972, and noise measurements in Eastern mines starting at the end of October 1972.

It was agreed that NBS would prepare test plans for their visits to the Eastern mines, and these test plans would be submitted to the Bureau of Mines and to Arthur D. Little, Inc. A copy of the test plan for the Lincoln mine preliminary proof-tests would also be forwarded to Arthur D. Little, Inc.

Objectives of Noise Measurement Program

It was agreed that the objectives of the present measurement program are to obtain as output presentations the following items, listed according to their priorities:

- | | |
|--|----------------|
| 1) Noise Power Spectra | |
| 2) Noise Amplitude Probability Distributions (APD's) | |
| 3) Signal Attenuation Curves | <u>Primary</u> |
| ----- | |
| 4) Noise Pulse Duration Distributions (PDD's) | Secondary |
| 5) Noise Correlations | |

Communications Gear for In-Mine Experiments

Howard Parkinson asked Collins Radio to provide ideas, lists of equipment, and utilization details for interfacing surface hand-held radio sets with the mine telephone system, such that experimenters on the surface can talk to experimenters in the mine. The Collins effort is to give PMSRC an alternative to some of Motorola's suggestions. The intent is to provide an independent phone line-to-radio interface at the surface end of the mine telephone line, and quick-connect loud speaking type phones for temporary connection to telephone lines in the

immediate vicinity of EM noise measurement areas. Radio units in the 27 MHz or 416 MHz bands are preferred on the surface. Cabling on the order of 1000 feet may be required to run from the surface telephone line termination to a local high spot to provide adequate radio coverage on the surface. The voice signals sent over this communications link should be translated to a carrier frequency that the phone line will pass without interfering with normal base band voice mine communications.

NBS/ITS requested the use of equipment now held by the Bureau of Mines to help conduct the noise measurement experiments. This equipment consists of the Motorola 416 MHz walkie-talkie radio sets. Howard Parkinson agreed to provide this equipment to NBS/ITS in time for the Lincoln mine tests.

Long Term Statistics of Noise Within Mines

NBS commented that they expect to progress through a learning curve as the experiments proceed in terms of their judgment of recording times required at specific locations and equipment in the mine. They expect to sample the noise from different equipment under various load conditions, and to sample separate units of each equipment type. Howard Parkinson noted that 15 minutes represents a typical cycle-time of the equipment, and that lunch breaks and shift changes also represent times of major changes in mine activity to be examined. It was also decided that leaving the noise equipment in a mine for a continuous 24 hour monitoring period, to ensure that nothing important noise-wise was missed, was neither desirable nor necessary.

Conducted Noise Measurements

A considerable discussion of conducted noise and its measurement took place with mention of the work of WVU (Sierra RF Voltmeter) and Lee Engineering (GR Microvolter) in coal mines as possible guides. It was decided that for the phone lines, appropriate measurements would result if line #1 to ground, line #2 to ground, and line #1 to line #2 conducted noise voltage measurements are made. Concerning trolley lines, it was agreed that the trolley line to ground noise voltage is to be used. It was also agreed that some noise measurements be made on roof bolts, in particular these will be voltage measurements roof bolt to roof bolt as a function of roof bolt separation. The need for measurement of noise current remained unresolved. NBS agreed to develop a plan for obtaining conducted noise measurements. This plan will include treatment of problems of calibration, methods of location of attachments, problems associated with impedances of the sources, and the utility of current probe or nearby magnetic field measurements.

Impedance Measurements

After considerable discussion, it was agreed that the noise measurement program of NBS/ITS will not be required at this time to make telephone or trolley line impedance measurements. ADL was asked to devise practical means for taking trolley line impedance measurements for separate tests to be performed at a later date.

Transmission Measurements

A considerable discussion ensued concerning transmission measurements. It was first agreed that NBS/ITS would design and conduct the specific measurements, and welcome any and all suggestions. It was agreed that one surface loop would be used to transmit to the receiving equipment in the mine, and that this would be at an audio frequency. It is possible that this surface loop could first be used to provide a single sweep of frequency over a wide operating range, and then left to transmit at a single low frequency near 450 Hz for the remainder of the measurements.

It was agreed that if an in-mine transmitter is used, it will be operated at a single high frequency, and used only for in-mine face-area lateral transmission measurements, in order to keep the measurement program within both manageable and safe limits. The in-mine frequency should be either just above or below the trolley phone frequencies of 88 and 100 kHz found in mines. Howard Parkinson suggested that 116 kHz might be most suitable, with an alternative being between 92 - 95 kHz. A stable transmitter of 20 watt capacity should be used for these tests since it approximates that of present trolley phone equipment.

The main objective of these in-mine experiments is to provide firm signal strength experimental data in those section areas where noise measurements are being taken, in order to help establish transmitter power requirements for wireless communications in the face area at trolley phone frequencies. Howard Parkinson suggested that NBS/ITS examine the mine transmission data of Dayne Aldridge of WVU taken in six mines and reported in the WVU 2nd annual report to PMSRC, since they may be able to profit from WVU's experience.

Manning

NBS/ITS confirmed that no manning problems are anticipated, and that three full time technicians will be used in the manning of this measurement program in addition to the required engineering staff.

Discussion of Collins Memorandum of 15 August 1972

The comments and recommendations offered by Collins Radio were discussed at length and the following agreements were reached on each topic.

1) "Power-Down Measurements" - It was agreed that mine power-down measurements are not essential to the noise measurement program. In addition, power shutdowns create a major inconvenience to mine operators, which the Bureau does not want to impose. Therefore, the sampling of "quiet" EM noise conditions will be restricted to finding relatively "quiet" spots, EM-wise, in out-of-the-way places in the mine or measuring during between-shift periods, maintenance shifts, or other operationally "quiet" times.

2) "Concurrent Signal Attenuation Measurements" - It was agreed that there is no need of performing extensive surface-to-mine attenuation measurements at present; in view of the acceptance of conductivity values obtained for generalized mining areas from similar measurements by other Bureau contractors, and the acceptance as adequate, the theory developed so far by Wait for vertical, coaxial loop-to-loop coupling. Only some limited loop-to-loop measurements from surface-to-mine, and laterally from face areas to section loading points are viewed as desirable and appropriate to the present NBS/ITS effort, as described above under Transmission Measurements.

3) "Noise Pick-up from Earth Probes" - It was agreed that noise pick-up from roof bolt earth probes within mines as a function of roof bolt separation is worth measuring by the NBS/ITS team, as discussed above under Conducted Noise Measurements. Surface probe noise measurements are not necessary.

4) "Earth-Probe Signal Attenuation and Related Measurements" - It was agreed that these probe measurements would not be undertaken by the NBS/ITS team on this present noise measurement effort. Much of this data has already been generated by the Bureau and its contractors (PMSRC, CSM, WGL), and such well-experienced teams will be enlisted to acquire additional data that may be required in the future. Howard Parkinson also stated that Bureau experience to date had shown surface probe transmitters used with in-mine loop receivers to be easier and more practical than surface probe transmitters used with in-mine probe receivers.

5) "Theoretical Investigations" - It was agreed that Wait's present work assignment for the Bureau on finite length earth probe transmitters should provide adequate coverage of this topic.

B. EQUIPMENT

Tape Recorders

NBS reported that everything is presently under control with the tape recorders. The delay in delivery of the Lockheed recorders, not received as of the meeting, was not viewed as serious. Filters have been bought to cure any recorder-aliasing problems caused by poor out-of-band response above the desired recording band. A bandwidth compression capability of 128 to 1 is available from the Honeywell-Lockheed tape recorder set. This will be adequate to cover all of the noise recording manipulations envisioned. NBS also noted that in terms of recording time, the equipment to be taken into the mines is capable of recording 14 minutes at the highest tape speed and 56 minutes at the lowest tape speed, per reel of tape.

It is the hope of the NBS/ITS team to be able to record the full frequency band (300 Hz to 375 kHz Direct, 300 Hz to 100 kHz FM) on a single track of the tape recorder, for each sensor. However, if it is found that this is not possible, two channels per sensor will be used to cover the frequency range. The capability of achieving single track operation will be determined by experiments in the Lincoln mine. Recordings of the noise will be made simultaneously wideband (up to 300 kHz) and narrowband (in 3 kHz slices). The output noise distributions of each will be compared to obtain a measure of the impulsiveness of the noise, and therefore, the dynamic range requirements. The narrowband 3 kHz spectrum slices will be produced by passing the noise, picked up by loop sensors, through a modified Stoddart receiver before recording.

It was agreed that the noise measurements need not be made to frequencies below 300 Hz. NBS would still like to reserve the option to go below 300 Hz, if it can be done without introducing system complexity or deterioration of the noise recordings in the required frequency bands (300 Hz to 375 kHz Direct, 300 Hz to 100 kHz FM).

Stoddart Receivers

After considerable discussion, it was agreed, pending a possible change of heart by Bill Bensema of NBS, that 50 kHz is an acceptable center frequency to heterodyne the Stoddart receiver IF output down to, prior to recording the narrowband (3 kHz) slices of high frequency noise to be obtained from the modified Stoddart receivers. Noise recorded in this manner will be utilized to generate APD's using equipment now available at ITS, and to generate some spot spectra, approximately 3 kHz wide and centered at frequencies of interest, using the NBS playback and processing equipment. ITS noted that the modifications to the Stoddart receivers were underway, and expected that all the required modifications will be completed and instruments checked out within five weeks.

Field Components and Sensors

It was agreed that NBS would probably need to measure at most, two magnetic components simultaneously, the vertical component and the horizontal component perpendicular to the entry direction. In some cases it may be adequate to orient the loop for maximum output and just measure that field strength. The Lincoln mine tests with three loops are expected to settle this question. ADL recommended that the loops not be laid on the floor, but centered about half-way between floor and roof as a realistic standard position for the measurements, if possible.

It was agreed that electric field measurements, if made, will be at frequencies above the baseband response of the recording system, namely above 375 kHz. Loops will be used for the tape recorded noise measurements below 375 kHz. NBS noted that some manually recorded E-field measurements could be made, at least in the early trips into the Lincoln mine, to help determine performance of systems operating at frequencies beyond those presently envisioned for the noise tape recordings.

NBS will utilize the modified NM-25T Stoddart receivers to examine frequencies up to 32 MHz, and an available battery powered EMC-25 field strength meter to examine frequencies up to 1 GHz. Interest in this upper frequency range has increased in view of the highly favorable transmission performance obtained by PMSRC with 416 MHz walkie talkies in coal mines. The EMC-25 noise measurements are not intended to give accurate noise measures, because of the instrument's design for CW signals, but are expected to give a quick approximate picture of the noise activity at these higher frequencies.

Permissibility Considerations

NBS/ITS has decided that all the noise measuring equipment should be brought into the face area, thus precluding the use of pre-amps and sensors at the end of long cables separating them from the recording system. Therefore all the equipment must be integrated in a permissible manner for use in the face area, and approved by Bob Wolfe in Pittsburgh. It was agreed that Howard Parkinson would help NBS expedite this permissibility design and approval process.

C. ANALYSIS

Noise Power Spectra

NBS reported on the results of its experiment to determine the effects, on the FFT generated broadband noise spectra, of discarding the least significant bits in the A/D conversion that precedes the noise spectrum computations. The results agree with the classical theory, which predicts an increase in the spectrum level with the deletion of each bit. So it has been determined that all 12 bits of the present A/D converter are required to make adequate power spectrum computations for this program.

Noise Pulse Duration Distributions and Correlations

The methods have not yet been defined for obtaining these two lowest-priority secondary items from the planned noise recordings.

IV. EM NOISE MEASUREMENT PROGRAM MEETINGS AT COLLINS RADIO, NBS, AND PMSRC

Three additional meetings were held in 1973, during and after the period in which the NBS EM noise measurements were conducted, to discuss preliminary findings and the implications of these findings on the instrumentation system and future measurements. The major findings and decisions of these meetings, primarily as they relate to the measurement instrumentation, are briefly summarized below.

A. Meeting at Collins Radio Co., Cedar Rapids, Iowa on 21, 22 February 1973

This meeting was held to discuss the results of the NBS noise measurements in the first major Eastern coal mine (Robena No. 4). Representatives of NBS, PMSRC, Collins Radio Co., Spectra Associates, West Virginia University, and ADL were present.

The meeting and subsequent telephone conversations led to the following principal findings and decisions regarding the instrumentation and future measurements.

- The underground wideband Lockheed FM recording system became system noise limited above about 10 kHz in the Robena mine as a result of the gain settings required to prevent the unexpectedly high levels of harmonic-type noise below 10 kHz from saturating the recorder. To overcome this potential problem at other mines, it was decided to high pass filter the noise waveforms, prior to recording, for two of the three FM channels, while retaining the full bandwidth as before on the third channel. A filter cut off around 10 kHz was chosen. Therefore, the following recordings would be made on the three FM channels of the Lockheed recorder:

<u>Field Component</u>	<u>Noise Bandwidth</u>
Vertical	100 Hz to 100 kHz (as before)
Vertical	10 kHz to 100 kHz
Horizontal (Max.)	10 kHz to 100 kHz

instead of the originally planned recordings below.

Vertical	100 Hz to 100 kHz
Horizontal (x)	100 Hz to 100 kHz
Horizontal (y)	100 Hz to 100 kHz

The 3 kHz to 300 kHz wideband recording of the vertical component on the direct channel would also still be made as originally planned.

- To obtain more noise data close to the working face area of mine sections, it was decided to make the narrowband direct recording system permissible, and to increase the number of frequencies at which measurements would be made with this system which utilized the NM-12 and NM-25 receivers and a different Lockheed recorder. The number of frequencies would be increased, without increasing the total measurement time, by taking readings of two field components (vertical and the maximum horizontal) at six pairs of frequencies, instead of three orthogonal field components at four pairs of frequencies;

<u>Namely</u>		<u>Instead of</u>	
10 kHz	500 kHz	10 kHz	500 kHz
19	1.15 MHz	30	2 MHz
36	2.64	70	8
69	6.0	130	32
131	13.9		
250	32.0		

It was also decided that a 20-minute duration would be used for each of these recordings, unless a particular mine situation or operating condition was clearly more suited to a shorter duration. The 20-minute duration appeared to be the most practical choice, at this point in the program, for generating most of the desired APD and rms level statistics.

- The Robena results indicated that simultaneous surface and underground measurements were not as important as obtaining additional underground noise data covering different locations and operating conditions. Therefore, it was decided that the surface wideband recording system (using the Honeywell recorder) would be modified to allow wideband recording from 10 kHz to 150 kHz on the direct channel and 100 Hz to 20 kHz on FM, at a speed of 30 ips, for use underground. Since this system would still not satisfy permissibility requirements, its underground use would have to be restricted to fresh-air ways.

Detailed information regarding the instrumentation used at the Robena mine and the noise data obtained is available in an NBS report covering the Robena noise measurements.

B. Meeting at NBS, Boulder, Colorado on 22 May 1973

This meeting was held to discuss preliminary results of the additional noise measurements made in March and April of 1973 at one Western mine (Lincoln) and three more Eastern mines, (McElroy, Itmann, and Grace) with the modified instrumentation system prescribed as a result of the above meeting at Collins Radio. Representatives of NBS, ITS, Collins Radio, PMSRC, and ADL were present.

Discussions covered some additional reduced data from the Robena mine, hoist shaft signal and noise measurements made at the Grace iron mine, descriptions of the types and locations of measurements made at each of the three additional Eastern mines, general observations regarding the EM noise environments at these mines, and plans for measurements at the Lucky Friday hardrock mine in Idaho. Reduced data such as wideband spectra were not yet available for examination for the latest mines visited because of unanticipated delays caused by problems with the data processing equipment. The Grace mine hoist shaft data had been manually reduced, so it was available for use by Collins Radio on its hoist shaft communication system project. No problems with, or additional changes to, the instrumentation were reported or recommended at this time.

The following priorities were set for reducing the remaining data; 1) Robena, 2) McElroy, 3) Itmann, and 4) Grace. In addition, the following chart was drawn up to indicate the kind of processed noise data expected for each of these four mines.

Robena Mine

	<u>Wideband</u>		<u>Narrowband</u>	
	<u>Power Spectra</u>	<u>Correlation</u>	<u>APD's</u>	<u>0.1%, RMS, Ave., and 99% Levels</u>
<u>Loops</u>				
In-Mine (Hi-Freq.)	Yes	Yes	Yes	Yes
Surface (Lo-Freq.)	Yes	Yes	Yes	Yes
<u>Roof Bolts</u>	Yes	NA	No	No
<u>Telephone Lines</u>				
Voltage	Yes	NA	No	No
Current	Yes	NA	No	No
<u>Trolley Lines</u>				
Voltage	Yes	NA	No	No
Current	No	NA	No	No

NA-Not Applicable

McElroy, Itman, and Grace Mines

	<u>Wideband</u>		<u>Narrowband</u>	
	<u>Power Spectra</u>	<u>Correlation</u>	<u>APD's</u>	<u>% RMS Ave. 99% Levels</u>
<u>Loops</u>				
In-Mine (Hi-Freq.)	Yes	No	Yes	Yes
Surface (Lo & Hi-Freq.)	Yes (McElroy Only)		No	No
<u>Roof Bolts</u>	Yes	NA	Yes (Itmann Only)	Yes
<u>Telephone Lines</u>	No	NA	No	No
<u>Trolley Lines</u>	Yes (Itmann Only)	NA	No	No

NA-Not Applicable

C. Meeting at PMSRC, Bruceton, Pa., on 10 October 1973

This meeting was held after noise measurements were made late in the summer of 1973 at the last two scheduled mines (Lucky Friday and Geneva) to examine and disseminate additional reduced noise data, review and summarize the overall noise measurement program to date, and define what yet needs to be done. Representatives of NBS, Collins Radio, Westinghouse Georesearch Laboratory (WGL), PMSRC, and ADL were present.

Considerable amounts of reduced data in the form of noise spectra, APD's and other plots for the Robena, McElroy, Itmann, and Grace miners were presented by NBS and discussed by the attendees. All of this data is or soon will be documented in NBS reports. A large chart was drawn up to summarize the EM noise measurements made in mines to date -- as an aid to potential users in identifying data of interest to them, and as an aid to the process of assimilating and correlating this data for characterizing representative noise environments. This chart is included as Table A1.

Several conclusions were also reached regarding what needs to be done. Namely:

- Additional EM noise measurements in mines are not required at this time. One possible exception to this might be an AC-type coal mine, but even this is not certain.

TABLE A1

SUMMARY OF NBS EM NOISE MEASUREMENTS*
(Results of the Planned EM Noise Measurement Program)

Name & Type of Mine	Types of Equipment	Mine Voltage		Type of Haulage	Noise Parameter					Spectra Recorded Freq Mode	Frequencies of APD's	Spectra Processed to What Freq	Additional Information Available	
		AC Volts	DC Volts		U	H	E	I	Voltage					Roof Bolt
Mid Continent Colo. (coal)	AC	?	--	Belt	Y	N	Y	N	N	N	10 kHz	FM	750 Hz	no
Lincoln Colo. (coal)	AC & DC (Motor Generator)	440	250	Belt & Rail	Y	Y	Y	N	N	N	10 kHz	FM	750 Hz	no
Allen Colo. (coal)	AC & DC (Rectifier)	4160	310	Belt & Rail	Y	Y	Y	N	N	N	10 kHz	FM	750 Hz	no
Robena #4 Penn. (coal)	DC (with one AC section (Surface face rect))	--	600	Rail & Belt on Surface	Y	Y	Y	N	Y	Y	100 kHz	FM	100 kHz	yes
McElroy W. Va. (coal)	AC & DC (Rectifier, underground)	7200	300	Belt & Rail	Y	Y	Y	N	N	N	100 kHz	FM	100 kHz	yes
Itmann #3 W. Va. (coal)	AC & DC Longwall	1000	250	Belt & Rail	N	Y	Y	N	N	N	10 kHz	FM	750 Hz	yes
Grace Penn. (iron)	AC & Diesel	4160	--	Belt & Hoist	N	Y	Y	N	N	N	10 kHz	FM	750 Hz	yes
Geneva Utah (coal)	AC & DC	2500	300	Rail & Incline Slope	Y	N	Y	N	N	N	3 kHz	FM	3 kHz	yes
Lucky Friday Idaho (Pb, Zn, Ag)	AC & DC Battery locomotive	2400	600	Battery loc, Hoist & DC Hoist	Y	Y	Y	N	N	N	10 kHz	FM	10 kHz	yes

Y-Yes, N-No

* Drawn up at the 10 October 1973 meeting between NBS, PMSRC, Collins Radio, and ADL staff at Brucecon, Pa.

- Highest priority has been assigned to completing the processing of the present noise data, writing reports associated with these data, and disseminating these reports and data to system designers.
- System designers and other users who need access to or interpretation of these data, particularly before they have been published, should contact NBS directly. In this matter, dubs of select NBS noise recordings may also be obtainable for testing breadboards, prototypes, etc. However, special arrangements will probably have to be made with NBS to generate these tape dubs.
- Finally, the data must now be assembled, analyzed, interpreted, and correlated in a comprehensive manner to determine and understand the important relationships, parameters, sources, etc., that best characterize mine EM noise environments under different operating conditions. This can, and should, also be done on a somewhat less-complete and piece-meal basis to solve certain specific, localized problems, or ones that cannot wait for the more comprehensive approach.

PART TWO

ELECTROMAGNETIC THROUGH-THE-EARTH MINE COMMUNICATIONS

PART TWO
ELECTROMAGNETIC THROUGH-THE-EARTH MINE COMMUNICATIONS

TABLE OF CONTENTS

	<u>Page</u>
List of Tables	2.iv
List of Figures	2.v
INTRODUCTION	2.1
I. SIGNAL POWER ESTIMATES FOR DOWNLINK THROUGH-THE-EARTH BASEBAND VOICE COMMUNICATIONS	2.2
A. METHOD OF CALCULATION - DOWNLINK, HORIZONTAL WIRE ANTENNA	2.2
B. NOISE IN MINES	2.7
1. NOISE PRIMARILY DUE TO 60HZ AND 360HZ HARMONIC PEAKS	2.7
2. NOISE PRIMARILY BROADBAND IMPULSIVE	2.7
3. SIGNAL CURRENT AND POWER ESTIMATES	2.11
II. SIGNAL POWER ESTIMATES FOR UPLINK THROUGH-THE-EARTH BASEBAND VOICE COMMUNICATIONS	2.18
A. METHOD OF CALCULATION - UPLINK, LOOP ANTENNA	2.18
B. NOISE ON THE SURFACE OVER MINES	2.21
C. SIGNAL CURRENT AND POWER ESTIMATES	2.21
III. SPOT S/N RATIO ESTIMATES FOR UPLINK AND DOWNLINK THROUGH-THE-EARTH NARROWBAND CODE COMMUNICATIONS	2.32
A. SIGNAL AND NOISE PLOTS	2.32
B. SPOT SIGNAL-TO-NOISE RATIOS	2.46
C. CONCLUDING REMARKS	2.51

PART TWO

ELECTROMAGNETIC THROUGH-THE-EARTH MINE COMMUNICATIONS

TABLE OF CONTENTS
(Continued)

	<u>Page</u>
IV. EFFECTS OF DIFFERENTIATION ON BASEBAND VOICE SIGNALS TRANSMITTED THROUGH THE EARTH FROM THE SURFACE TO MINES	2.53
A. RECEIVE LOOP OUTPUT	2.53
1. SIGNALS	2.53
2. NOISE	2.55
B. RECEIVE LOOP OUTPUT DIFFERENTIATED	2.56
1. SIGNAL AND NOISE	2.56
C. SIGNAL-TO-NOISE RATIO CALCULATIONS	2.56
D. DISCUSSION	2.60
V. INTELLIGIBILITY OF THROUGH-THE-EARTH ELECTROMAGNETIC COMMUNICATIONS TO MINES (DOWNLINK)	2.61
A. BACKGROUND	2.61
B. ARTICULATION INDEX: METHOD OF COMPUTATION	2.63
C. ARTICULATION INDEX: SPECIFIC CALCULATIONS	2.64
D. SPEECH PEAK CLIPPING	2.68
E. DISCUSSION	2.70
VI. A MEANS FOR OVERCOMING POWER LINE INTERFERENCE	2.72
A. METHODS TO OVERCOME HARMONICS	2.72
B. CIRCUIT IMPLEMENTATION	2.77
C. TESTS AND RESULTS	2.79
D. EXTENSIONS OF WORK	2.82
E. CONCLUSIONS	2.82

PART TWO

ELECTROMAGNETIC THROUGH-THE-EARTH MINE COMMUNICATIONS

LIST OF TABLES

<u>Table No.</u>	<u>Title</u>	<u>Page</u>
1-1	RMS Antenna Current and Power Dissipated for Long-Wire 50-Ohm Antenna	2.16
2-1	Required Loop Magnetic Moment, AMP-Meter ²	2.27
2-2	Average Power Dissipation and RMS Voltage and Current in Uplink Circular Loop Antenna	2.28
2-3	Average Power Dissipated and RMS Voltage in Uplink Circular Loop Antenna	2.29
4-4	Voice Band Signal-to-Noise Ratios in db for Several Sifferentiation Conditions	2.57
5-1	Twenty Frequency Bands of Equal Contribution to Speech Intelligibility	2.63
5-2	High-Frequency Part of Masking Spectrum-- Upward Spread of Masking	2.65
5-3	The Effects on Speech Intelligibility of Peak Clipping with Equal Post-Clipping Amplification	2.70

LIST OF FIGURES

<u>Figure No.</u>	<u>Title</u>	<u>Page</u>
1-1	Average Speech Spectra	2.3
1-2	Downlink Signal, For Horizontal Wire Antenna - 1 AMP Current	2.5
1-3	Horizontal Wire Antenna, Coupling Relationship	2.6
1-4	Horizontal Component of Subsurface EM Noise Magnetic Field, Hy Gunn Quearly Mine, Rock Springs Wyoming (Westinghouse data)	2.8
1-5	Allen Mine, Underground, 3000 Hz BW, 01-14; Antenna Sensitive Axis Pointed Vertical	2.9
1-6	Allen Mine, Underground, 3000 Hz BW, 07-14; Antenna Axis Vertical; Electric Locomotive Pulling Out with Loaded Coal Cars	2.10
1-7	Lincoln Mine, Underground, 3000 Hz BW, 03-23; in Control Room; Severe Trolley Impulsive Noise (Vertical)	2.12
1-8	Allen Mine, Surface, 3000 Hz BW, 03-17; Antenna Sensitive Axis Pointed Vertical	2.13
1-9	Downlink Average Power and RMS Antenna Current for 12 dB S/N Ratio Over the Voice Band	2.15
1-10	Shapes of Voice, Signal Attenuation, and Impulse Noise Spectra	2.17
2-1	Loop Antenna, Coupling Relationship	2.19
2-2	Uplink Signal for Loop Antenna, Unit Magnetic Moment	2.20
2-3	Allen Mine, Surface, 03-17; Antenna Sensitive Axis Pointed Vertical	2.22
2-4	EM Background Noise on Surface-Vertical Component, H_z Gunn Quearly Mine, Rock Springs, Wyoming	2.23

<u>Figure No.</u>	<u>Title</u>	<u>Page</u>
2-5	Lincoln Mine, Surface, 3000 Hz BW, 07-22	2.24
2-6	Transmitter Magnetic Moment (RMS) Required for 12db S/N Ratio Over Voice Bandwidth (500 Hz-3kHz) for Vertical Field Components of Noise and Signal ($\sigma = 10^{-2}$ mhos/meter)	2.25
2-7	Relative Shapes of Signal Attenuation Factor and Voice Spectrum (from 1000 ft depth)	2.26
2-8	Average Power Dissipated in Loop for 12db S/N Over Voice Bandwidth at Surface (uplink transmission)	2.31
3-1	Downlink Signal for Horizontal Wire Antenna - 1 AMP Current	2.33
3-2	Uplink Signal for Loop Antenna - Magnetic Moment = 1460 AMP-Meter ²	2.34
3-3	In-Mine Broadband Noise Densities for Downlink Communications	2.35
3-4	Surface Broadband Noise Densities for Uplink Communications	2.36
3-5	Lincoln Mine, Underground, 3000 Hz BW, 03-23; in Control Room, Severe Trolley Impulsive Noise (Vertical)	2.37
3-6	Lincoln Mine, Underground, 750 Hz BW, 03-20; in Control Room, Severe Trolley Impulsive Noise (Vertical)	2.38
3-7	Allen Mine, Underground, 750 Hz BW, 07-13; Antenna Axis Vertical; Electric Locomotive Pulling Out with Loaded Coal Cars	2.39
3-8	Allen Mine, Underground, 750 Hz BW, 01-13; Antenna Sensitive Axis Pointed Vertical	2.40
3-9	Horizontal Component of Subsurface EM Noise Magnetic Field, Hy, Gunn Quealy Mine, Rock Springs, Wyoming (Westinghouse data)	2.41
3-10	Allen Mine, Surface, 750 Hz Bandwidth (BW), 03-16 Antenna Sensitive Axis Pointed Vertical	2.42

<u>Figure No.</u>	<u>Title</u>	<u>Page</u>
3-11	Lincoln Mine, Surface, 750 Hz BW, 07-21, Antenna Sensitive Axis Pointed Vertical	2.43
3-12	EM Background Noise on Surface-Vertical Component, H_z , Gunn Quealy Mine, Rock Springs, Wyoming	2.44
3-13	Wideband Power Density Spectrum for Florida Data (Feb., May, June, July 1968) Magnetic Field Horizontal Components	2.45
3-14	Downlink (in mine) Signal-to-Noise Ratio for Horizontal Wire Antenna, 1 AMP Current (50 Watts for 50 ohm Resistance), Overburden Conductivity, $\sigma = 10^{-2}$ mho/meter	2.47
3-15	Downlink (in mine) Singal to Noise Ratio for Horizontal Wire Antenna, 1 AMP Current, $\sigma = 10^{-1}$ mho/meter	2.48
3-16	Uplink (surface) Signal-to-Noise Ratio for Loop Antenna, Overburden Conductivity $\sigma = 10^{-2}$ mho/meter, Loop Moment NAI = 1460 AMP-Meter ²	2.49
3-17	Uplink (surface) Signal-to-Noise Ratio for Loop Antenna, Overburden Conductivity $\sigma = 10^{-1}$ mho/meter, Loop Moment NAI = AMP-Meter ²	2.50
4-1	Effects of Receive Loop Differentiation on Earth Attenuation Response and on a Broad- band Noise Spectrum	2.58
4-2	Shapes of Original and Transmitted Voice Spectra, Downlink: Wire Antenna, $\sigma = 10^{-2}$ mho/meter	2.59
5-1	Relationship Between A1 and Various Measures of Speech Intelligibility	2.62
5-2	Received Magnetic Field Spectra	2.66
5-3	Receive Loop Voltage Spectra	2.67
5-4	Increase in RMS Speech Power As A Function of Clipping When Clipped Level Is Raised To Clipping Reference Level	2.69

<u>Figure No.</u>	<u>Title</u>	<u>Page</u>
5-5	Correction to AI The ordinate shows a correction to be applied to the articulation index computed on the assumption that a masking noise is steady-state for various noise-time fractions. The corrected AI cannot exceed 1.0	2.71
5-6	Effective AI Showing the effective AI as a function of the frequency with which a masking noise is interrupted. A parameter of the curves is the corrected AI calculated on the assumption that the masking noise is steady-state and then adjusted according to Fig. 5-5 for the fraction of the time the noise is on.	2.71
6-1	Allen Mine, Underground, 3000 Hz BW, 01-14 Antenna Sensitive Axis Pointed Vertically	2.73
6-2	Functional Representation of Hybrid Filter	2.74
6-3	Filter Frequency Response	2.75
6-4	Signal Waveform and Stored Samples	2.76
6-5	Forty Section Hybrid Filter	2.78
6-6	Block Diagram of Test Configuration	2.80
6-7	Harmonic Rejection 40 Segment Hybrid Filter	2.81
6-8	Rejection of Fourth Harmonic	2.83
6-9	100 Segment Digital Harmonic Filter	2.84

PART TWO
ELECTROMAGNETIC THROUGH-THE-EARTH MINE COMMUNICATIONS
INTRODUCTION

Part Two of this report is based upon six working memoranda prepared during the first half of 1972 at an early stage in our work for the Bureau of Mines. This work presents preliminary performance estimates of baseband voice and narrowband through-the-earth electromagnetic communications systems of principal interest to the Bureau for operational/emergency mine communications applications. The calculations were prepared to obtain early indications of the feasibility and governing parameters of such communications systems. They are based on limited, but pertinent, coal mine electromagnetic noise data acquired to-date by Bureau of Mines contractors; on theoretical signal-attenuation characteristics for two transmitter antenna types of present interest to the Bureau and on semi-empirical models which describe the intelligibility of voice communications as a function of the frequency variations of the signal-to-noise ratio across the voiceband.

This work examines the cases of baseband voice and narrowband communications for uplink and downlink transmissions, for frequencies up to 3kHz. Downlink transmissions are via a horizontal wire antenna, and uplink transmissions via a vertical-axis loop antenna, for typical mine depths of 300, 600, and 1000 feet. Representative coal-mine overburden conductivities of 10^{-2} mhos/meter (moderate and common) and 10^{-1} mhos/meter (high) were used; the former figure for both voice and narrowband calculations and the latter for narrowband calculations only. Examples of high, moderate, and low, surface and subsurface, harmonic and broadband-impulsive noise conditions were taken from NBS and Westinghouse (WGL) mine noise data, together with examples of high- and low-levels of ELF atmospheric noise taken from M.I.T. Lincoln Laboratory data. The effects of simple voice spectrum shaping techniques on the intelligibility of through-the-earth voice communications are examined, and indexes of intelligibility more broadly based than signal-to-noise ratio are discussed. Finally, a means of overcoming the affects of 60 Hz noise and its harmonics which are the largest contributors to typical audio frequency in-mine noise, is suggested.

These feasibility calculations are not intended to serve as definitive and complete treatments, but as a starting point: to establish first-order estimates of the magnitude and variability of transmitter power requirements under different noise, overburden conductivity, and mine depth conditions; to identify relationships, conditions, or frequencies that are likely to limit or enhance system performance; to reveal items requiring further investigation and data still required; and to suggest practical methods for optimizing system performance. These objectives were met by the calculations. Simple experiments to support these calculations can and should be carried out; together with more detailed investigations of specific modulation, coding, noise-suppression, voice-compression and signal-conditioning techniques, aimed at producing through-the-earth operational/emergency mine-communication systems that are not only effective, but practical and economically sound.

I. SIGNAL POWER ESTIMATES FOR DOWNLINK THROUGH-THE-EARTH
BASEBAND VOICE COMMUNICATIONS

Preliminary calculations were performed to determine the feasibility of communications systems using baseband voice signals transmitted through the earth and received in the presence of various types and levels of electromagnetic noise in mines. Even without attempts to remove the major line components of the noise upon reception, or to give the optimum pre-emphasis and peak clipping to the initial transmitted voice spectrum, it appears that intelligible voice signals may be received for an appreciable fraction of the time in mines, using a horizontal wire antenna for the downlink. Of course, to design an effective operational communications system, techniques such as those just mentioned would have to be used, to improve signal-to-noise ratios by perhaps 12-20db. The implementation of these techniques poses no fundamental problems of great difficulty.

A. METHOD OF CALCULATION - DOWNLINK, HORIZONTAL WIRE ANTENNA

We have considered a situation in which voice is baseband transmitted (500Hz to 3kHz) through the earth by a horizontal wire antenna, terminated in a grounded electrode at each end.

The voice spectrum over this bandwidth may be crudely represented by S_o/f as shown in Figure 1-1: where f is frequency in Hertz and S_o is an amplitude gain factor with a value that depends on the signal-to-noise ratio desired at the receiver. Hence the RMS current is

$$I_{\text{rms}} = \left[\int_{500}^{3000} S_o^2 / f^2 df \right]^{1/2} = \frac{S_o}{\sqrt{600}} \quad (\text{amperes}) \quad (1)^*$$

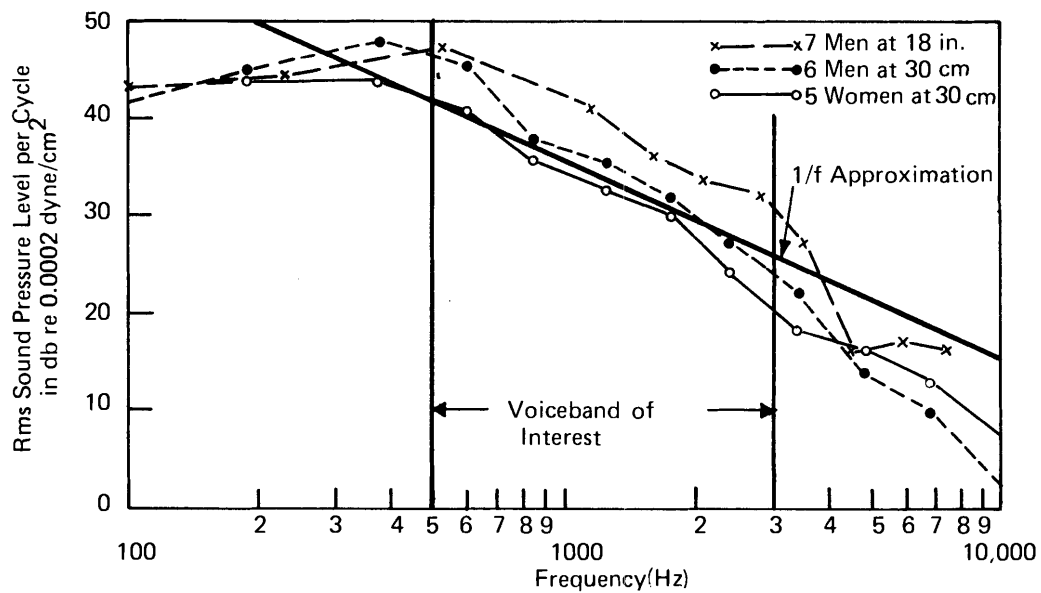
If the series resistance of the antenna electrode/earth contact is assumed equal to 50 ohms (values between 50 Ω and 200 Ω are typical), the transmitter power required may be estimated as

$$P = RI_{\text{rms}}^2 \approx 50 I_{\text{rms}}^2 = S_o^2 / 12 \text{ watts} \quad (2)$$

A horizontal wire antenna produces a magnetic field

$$|H| = \frac{I |A|}{2\pi D} \quad (\text{amperes/meter}) \quad (3)$$

* References to Figures, Tables and Equations apply to those in this Chapter unless otherwise noted.



Source: Handbook of Experimental Psychology, S.S. Stevens (ed.), Wiley, Chapter 26, Licklider, J.C.R. and Miller, G.A., Figure 2, pg. 1042

FIGURE 1-1 AVERAGE SPEECH SPECTRA

where D is the depth of the mine, and |A| is a dimensionless quantity.

In Figure 1-2 plots are shown of the shape of the attenuation as a function of frequency ($|A|/2\pi D$) for the three depths D = 300, 600, 1000 feet, using values for overburden conductivity of $\sigma = 10^{-2}$ and 10^{-1} mhos/meter. These plots were derived using the Westinghouse |A| curve in Figure 1-3.

The RMS magnetic field at the receiver in the mine can then be written

$$H_{\text{rms}} = \frac{S_o}{2\pi D} \left[\int_{500}^{3000} \frac{|A|^2}{f^2} df \right]^{1/2} \text{ Amperes/meter} \quad (4)$$

where |A| is a function of frequency. (The following calculations were done only for the more favorable $\sigma = 10^{-2}$ mho/meter conductivity situation, commonly found over coal mines.)

At D = 300 feet, we approximate

$$\frac{|A|}{2\pi D} = 1.6 \times 10^{-3} (\text{meter}^{-1}) \quad (5)$$

At D = 600 feet, we approximate

$$\frac{|A|}{2\pi D} = 9.13 \times 10^{-4} e^{-.00029f} (\text{meter}^{-1}) \quad (6)$$

At D = 1000 feet, we approximate

$$\frac{|A|}{2\pi D} = 4.97 \times 10^{-4} e^{-.000617f} (\text{meter}^{-1}) \quad (7)$$

In the latter two cases, where $\frac{|A|}{2\pi D}$ is of the form $\alpha e^{-\beta f}$

the received magnetic field is

$$H_{\text{rms}} = \alpha S_o \left[\int_{500}^{3000} \frac{e^{-2\beta f}}{f^2} df \right]^{1/2} \quad (8)$$

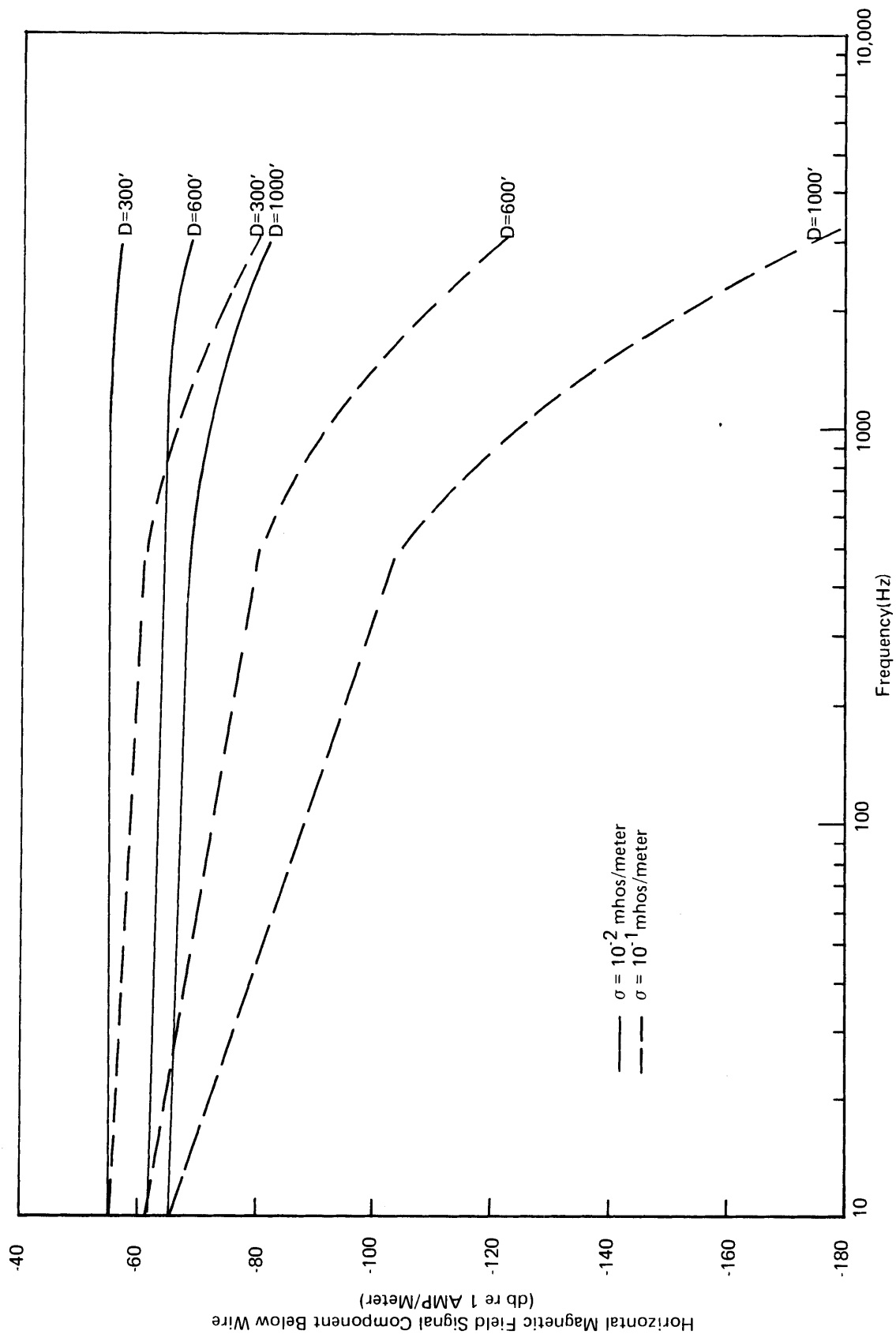
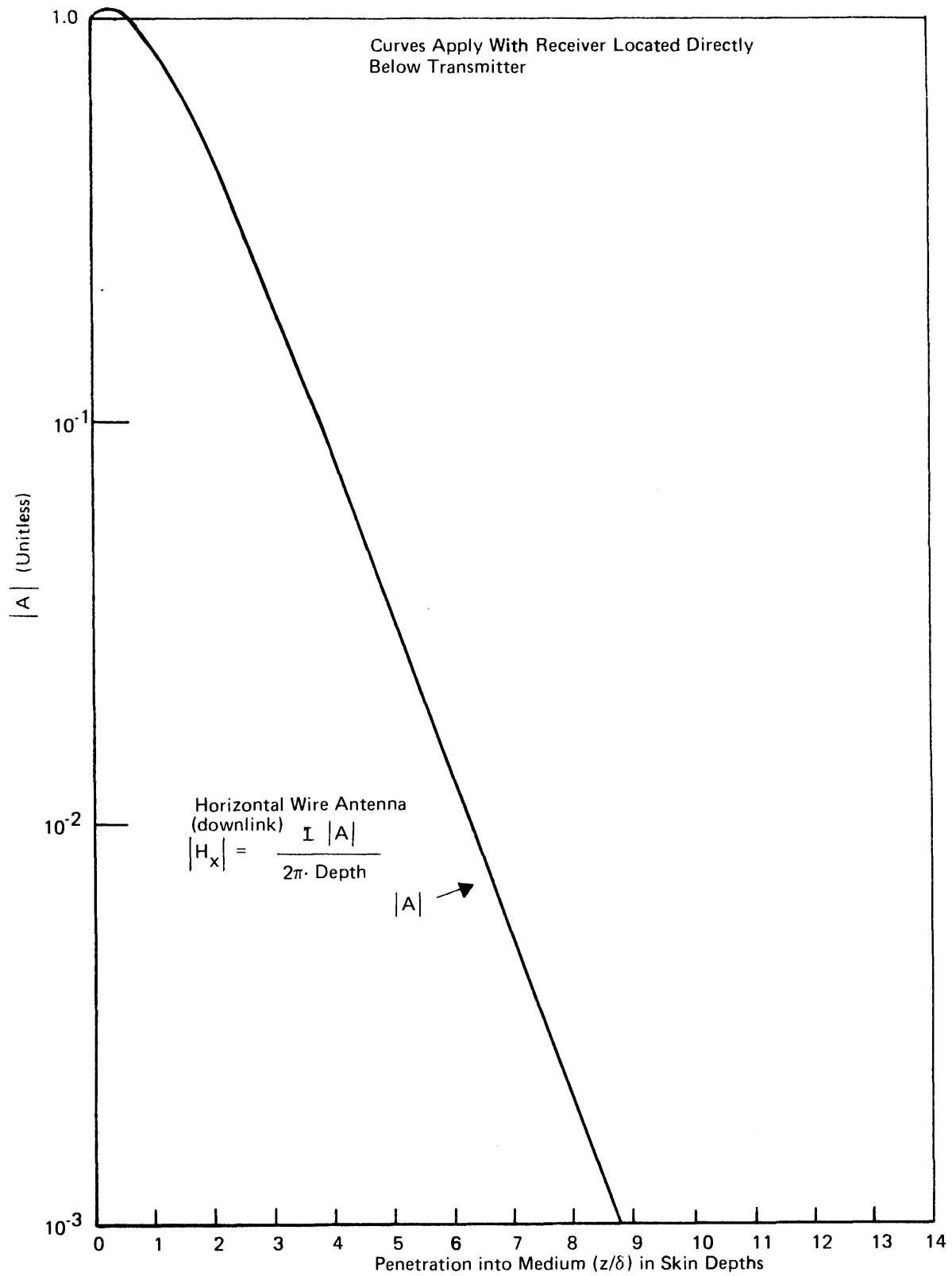


FIGURE 1-2 DOWNLINK SIGNAL, FOR HORIZONTAL WIRE ANTENNA - 1 AMP CURRENT



Source: Westinghouse Georesearch Laboratory (WGL)

FIGURE 1-3 HORIZONTAL WIRE ANTENNA, COUPLING RELATIONSHIP

B. NOISE IN MINES

Two different types of noise situations were considered:

1. Noise Primarily Due to 60Hz and 360Hz Harmonic Peaks

The noise magnetic field can be written

$$N_{\text{rms}} = \sqrt{\sum_i h_i^2} \quad (9)$$

where h_i are the noise peaks in A/M at all 60Hz and 360Hz harmonics lying between 500 and 3000Hz. While there are 42 of these in all, in practice 95% or more of the noise power is often contributed by only 2 or 3 harmonics.

Three cases were calculated:

Gunn Quealy Mine, Rock Springs, Wyoming - Figure 1-4 measurements with mine shut down, horizontal component (Westinghouse data)

$$N_{\text{rms}} = 2.96 \times 10^{-5} \text{ A/M (low noise)}$$

Allen Mine, Colorado - W. D. Bensema⁽¹⁾ (NBS) measurements

(Figure 1-5, Bensema NBS report) power line 60Hz and 360Hz harmonics primarily, vertical component

$$N_{\text{rms}} = 7.7 \times 10^{-5} \text{ A/M (low harmonic noise)}$$

(Figure 1-6, Bensema NBS report) electric locomotive pulling out - 60Hz and 360Hz harmonics primarily, vertical component

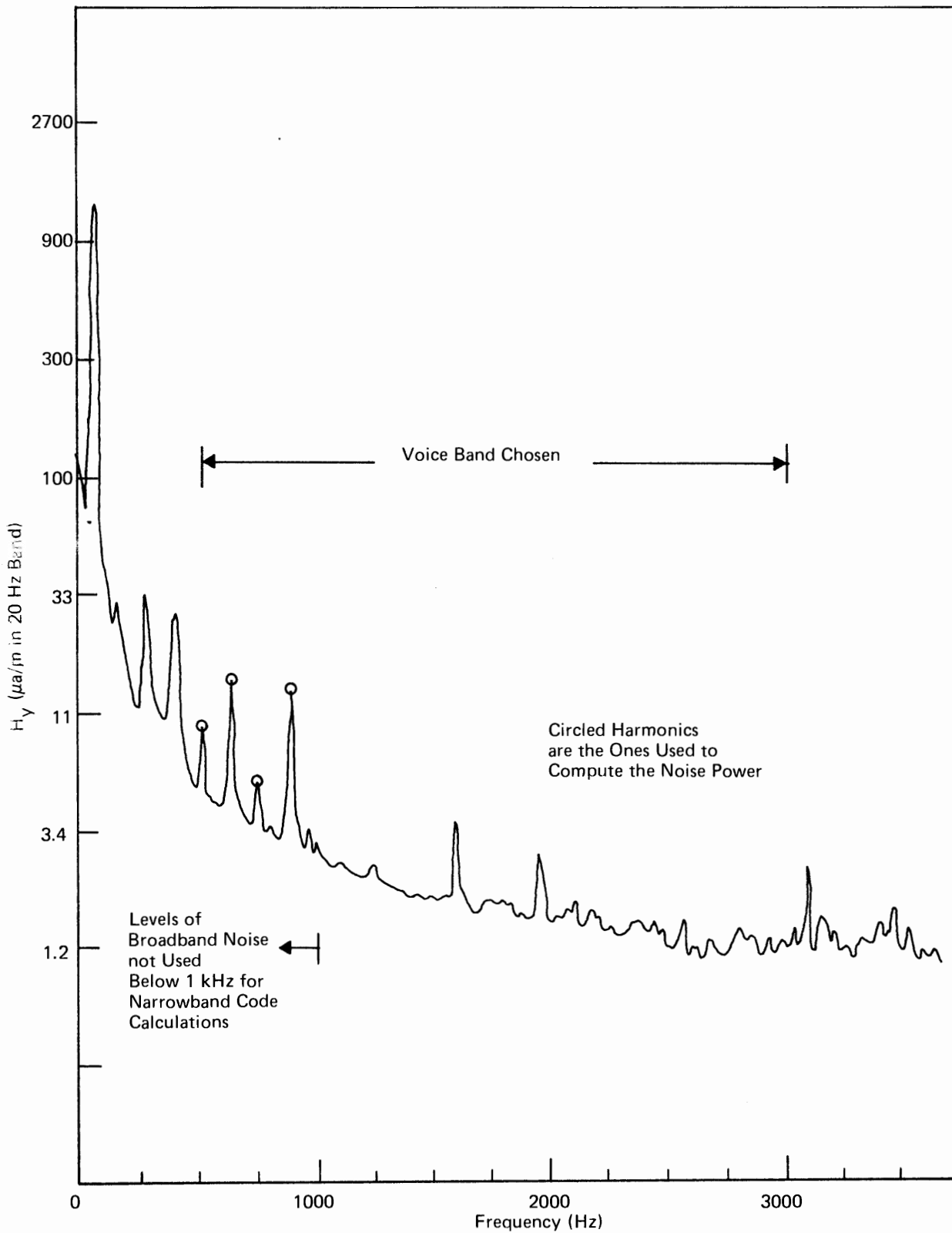
$$N_{\text{rms}} = 1.03 \times 10^{-3} \text{ A/M (high harmonic noise)}$$

2. Noise Primarily Broadband Impulsive

The noise density plots of NBS and WGL data can be approximated, either over the whole bandwidth or individually over several segments of it, by relations of the form

$$N = N_1 e^{-N_2 f} \text{ A/M}/\sqrt{\text{Hz}} \quad (10)$$

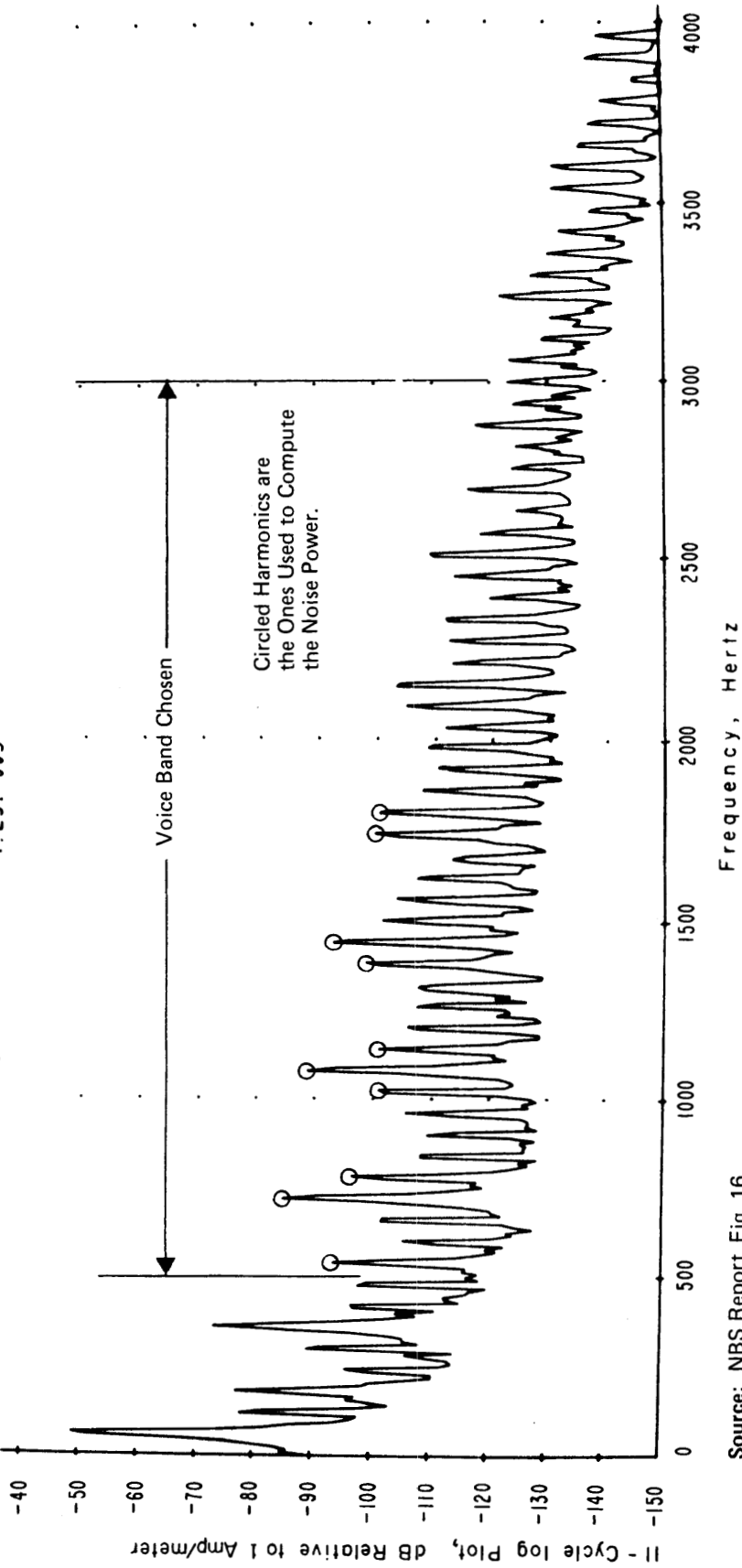
(1) W. D. Bensema, Coal Mine ELF Electromagnetic Noise Measurements, NBS Report 10-739 (1972) - sponsored by U.S. Bureau of Mines, Working Fund Agreement H0111019.



Source: Westinghouse Georesearch Laboratory (WGL)

FIGURE 1-4 HORIZONTAL COMPONENT OF SUBSURFACE EM NOISE MAGNETIC FIELD, H_y
 GUNN QUEALY MINE, ROCK SPRINGS WYOMING (Westinghouse Data)

11 0 0 2048 20 2.56+000 7.81+000 11/22/71 19:50:17 2
 3.91-003 1.05+001 0.00+000 20 49320 49320
 0114220771 Rec. gain corr. = -20 Total const corr. = -78.3
 1.000-004 0.2236 1.231-005



Source: NBS Report Fig. 16

FIGURE 1-5 ALLEN MINE, UNDERGROUND, 3000 Hz BW, 01-14;
 ANTENNA SENSITIVE AXIS POINTED VERTICAL

11 0 0 2048 20 2.56+000 7.81+000 11/22/71 19:53:39 0
 3.91-003 -2.71+001 0.00+000 20 40320 40320
 0714220771 Rec. gain corr. = -20 Total const corr. = -78.3
 1.000-004 0.2236 1.936-005

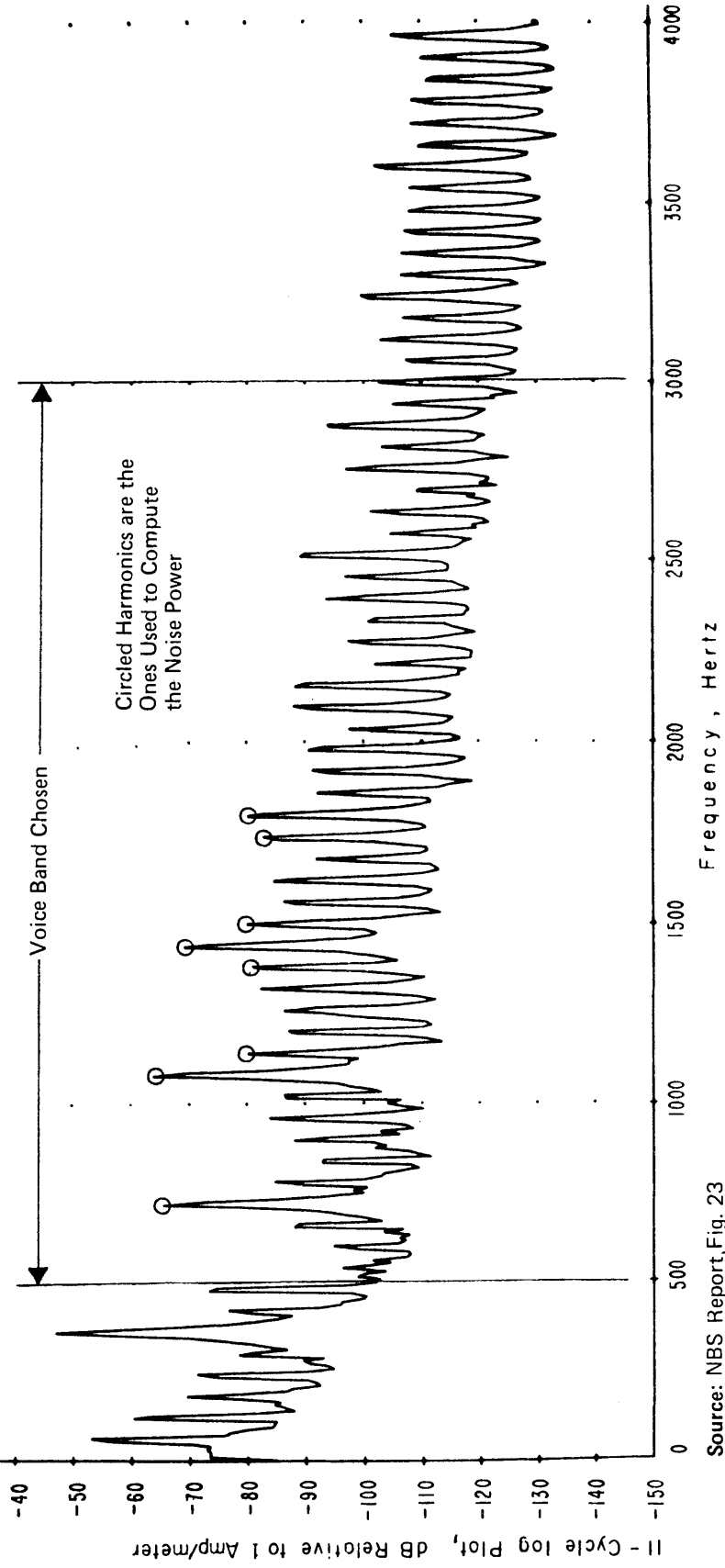


FIGURE 1-6 ALLEN MINE, UNDERGROUND, 3000 Hz BW, 07-14:
 ANTENNA AXIS VERTICAL; ELECTRIC LOCOMOTIVE
 PULLING OUT WITH LOADED COAL CARS

Then the noise magnetic field can be written

$$N_{\text{rms}} = N_1 \left[\int_{500}^{3000} e^{-2N_2 f} df \right]^{1/2} \quad (11)$$

One example studied was severe trolley impulsive noise, vertical component in the Lincoln Mine in Colorado, as shown in Figure 1-7 (Bensema NBS report).

A correction of -9db was applied to his data to take account of the 7.8Hz bandwidth he used.

$$N_{\text{rms}} = 3.71 \times 10^{-3} \text{ A/M (high impulsive noise)}$$

By way of comparison with the above noise values, it is worth noting that the harmonic noise in the same bandwidth on the surface at the Allen Mine shown in Figure 1-8 (Bensema NBS report) gives a value of

$$N_{\text{rms}} = 5 \times 10^{-4} \text{ A/M (harmonic noise on the surface).}$$

3. Signal Current and Power Estimates

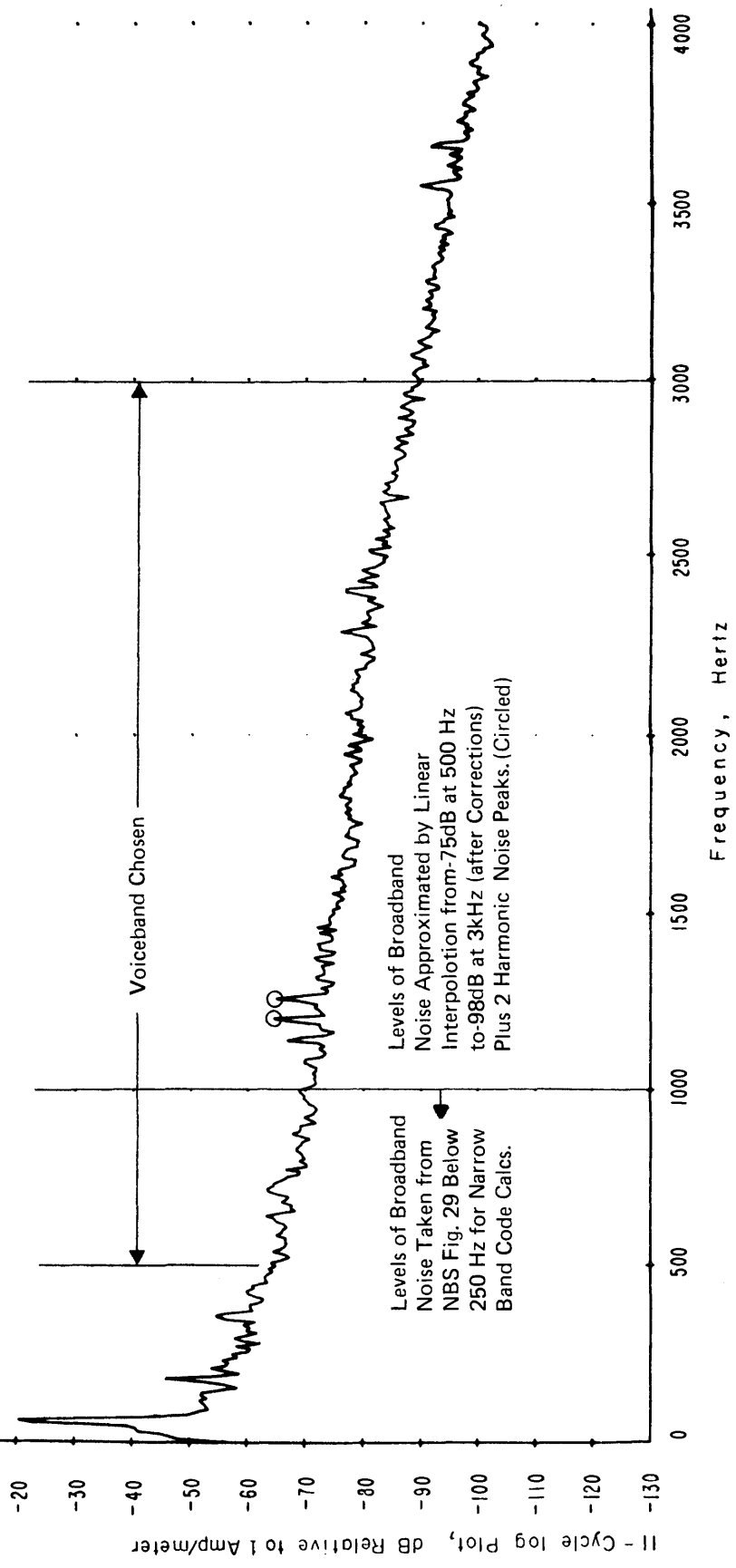
For intelligible voice communications, a criterion of a signal-to-noise ratio equal to or greater than 12db is used. Computing this ratio for the signal-to-noise field quantities, without regard for specific field sensors, we get

$$\frac{H_{\text{rms}}}{N_{\text{rms}}} \geq 4 \quad \text{which represents a reasonable bound on the desired grade of service for voice communications.}$$

(In A3 telephony, a 6db audio S/N ratio produces just-usable-quality reception, and is reserved for operator-to-operator communications. Good commercial quality reception requires an audio S/N ratio on the order of 30db.)

By using this criterion, and combining Eqs. (11) or (9) with (4) or (8), it is possible to determine the corresponding RMS current (or the power) required to achieve a 12db S/N ratio for voice communication through

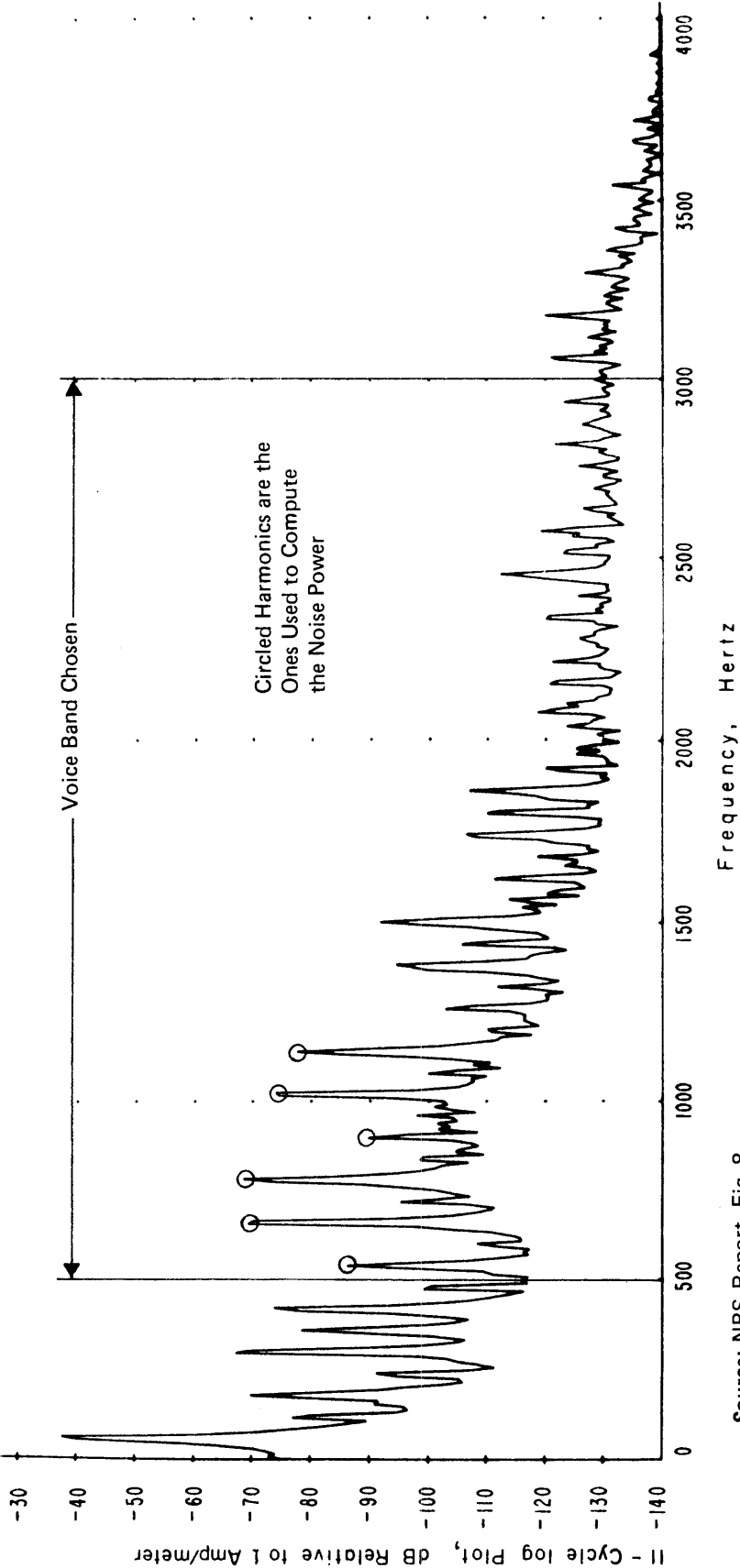
11 0 0 2048 20 2.56+000 7.81+000 11/24/71 08:56:29 3
 3.91-003 -1.00+002 0.00+000 20 40320 40320
 0323250871 Rec. gain corr. = 0 Total const corr. = -54.5
 1.000-002 0.2236 9.224-003



Source: NBS Report Fig. 30

FIGURE 1-7 LINCOLN MINE, UNDERGROUND, 3000 Hz BW, 03-23; IN CONTROL ROOM; SEVERE TROLLEY IMPULSIVE NOISE (Vertical)

11 3 2048 20 2.56+000 7.8+000 12/22/71 12 25 29 7
 3.91-029 -3.89+001 0.00+000 20 40320 40320
 0317210771 Rec. gain corr. = -12 Total const corr. = -70.3
 1.000-003 0.2236 1.675-004



Source: NBS Report, Fig. 8

FIGURE 1-8 ALLEN MINE SURFACE, 3000 Hz BW, 03-17;
 ANTENNA SENSITIVE AXIS POINTED VERTICAL

the earth, to mines under a variety of circumstances. These results can only be rough estimates, given the simplified nature of the assumptions made in the above analysis. However, they are in an important sense "worst case" estimates, since we know that by tailoring the initial voice spectrum and shaping the received noise spectrum, or reducing its few major harmonic components, we can achieve large gains in the final signal-to-noise ratio. Note that the power calculations represent the average power delivered to a 50 ohm load. To deliver the required levels of average power - with linear amplifiers - requires approximately 10-15db more amplifier power handling capability, because of the dynamic range of normal speech.

The results, in terms of the RMS antenna current required, are shown in Figure 1-9 and Table 1-1 for the mine noise cases discussed above at the three depths of 300, 600, and 1000 feet. Vertical components of the noise fields have been compared with the horizontal signal field components produced by a horizontal wire antenna, because NBS published primarily vertical component graphs of in-mine noise. Though the degree of variability between vertical and horizontal components must still be ascertained, it will probably fall well within the wide variation experienced in the vertical field alone. The highest noise level (Lincoln Mine, severe trolley impulsive noise) requires on the order of 100 kilowatts for intelligible voice communication at a depth of 1000 feet, and 23 kilowatts even at 600 feet, for a 50 Ω long-wire antenna impedance. These power levels may mean that voice communication to someone on a moving trolley will not be possible through the earth.

In addition, both the trolley impulsive noise and voice spectra fall off with increasing frequency, as shown in Figure 1-10, as opposed to just the voice spectrum as in typical voice communications systems; so that a S/N ratio greater than 12db, and correspondingly higher transmitter powers may be required to ensure intelligibility under such noise conditions. Signal pre-emphasis before transmission, and noise and signal-spectrum shaping upon reception, can probably be used to advantage here. However, the dominance of this noise type and level is relatively infrequent at any given point in a mine, because harmonic interference is the most prevalent. Hence, by using techniques, such as harmonic rejection filters on reception and signal pre-emphasis and peak clipping on transmission, it appears that intelligible through-the-earth voice communications to mines may be possible at reasonable power levels for the great majority of the time. Calculations of the effects of simple voice spectrum shaping techniques and peak clipping are presented in the subsequent Chapters IV and V of this Part of Volume I. A proposed design of a harmonic rejection filter is described in Chapter VI. The results of these investigations, as will be seen, are sufficiently encouraging to warrant further pursuit of these topics.

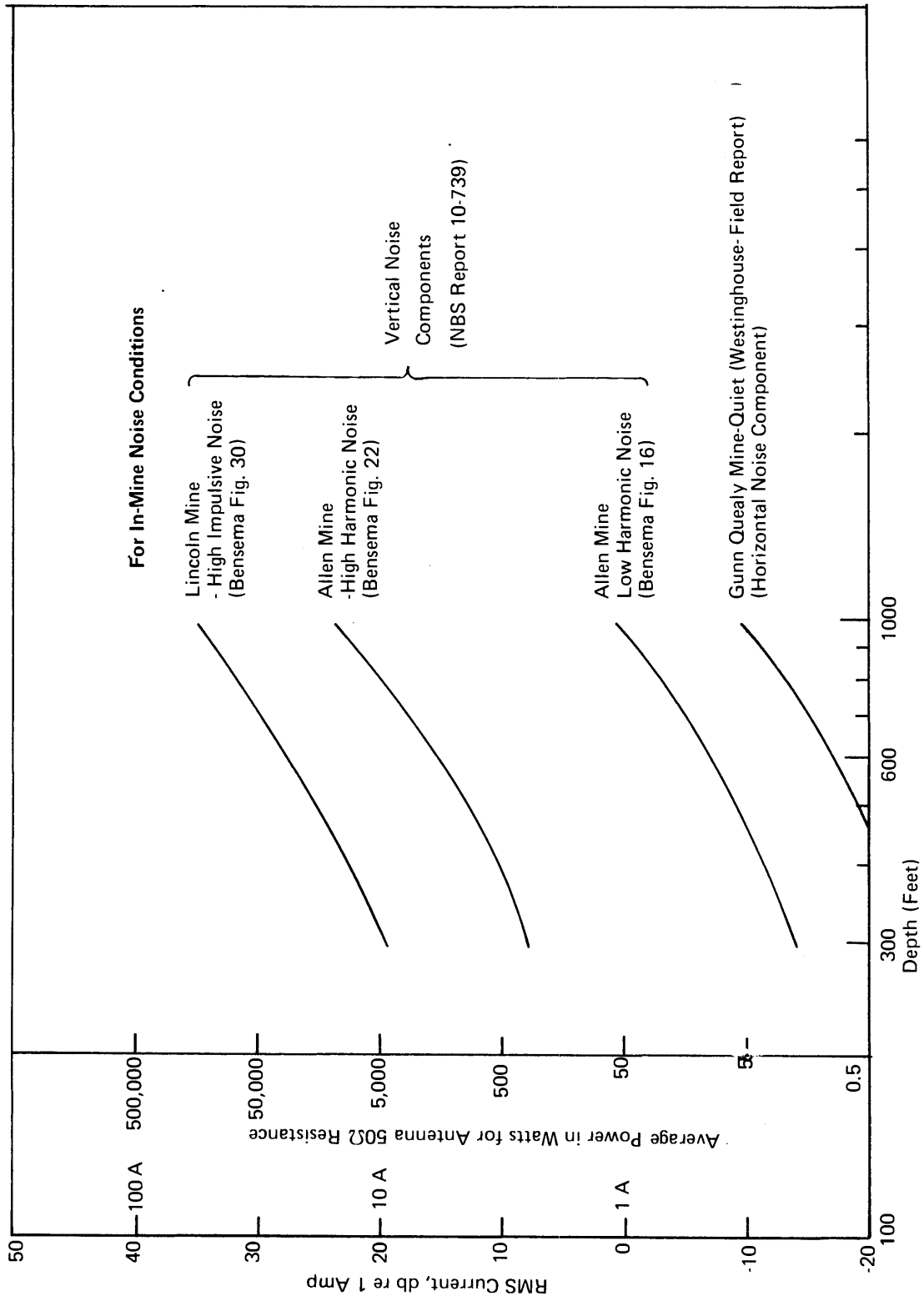


FIGURE 1-9 DOWNLINK AVERAGE POWER AND RMS ANTENNA CURRENT FOR 12db S/N RATIO OVER THE VOICE BAND 500 - 3000 Hz for $\sigma = 10^{-2}$ mhos/meter and Long Wire Transmit Antenna

TABLE 1-1

RMS ANTENNA CURRENT AND AVERAGE POWER DISSIPATED
 FOR LONG-WIRE 50-OHM ANTENNA
 (for $\sigma = 10^{-2}$ mho/meter)

	Depth of Mine, Feet					
	300		600		1000	
	I_{rms} (A)	P(watts)	I_{rms} (A)	P(watts)	I_{rms} (A)	P(watts)
Gunn Quealy Mine (low noise)	.074	0.27	.17	1.4	.42	8.8
Allen Mine (low noise)	.19	1.8	.45	10	1.1	61
Allen Mine (high harmonic noise)	2.6	340	6.0	1800	14.7	11000
Lincoln Mine (high impulsive noise)	9.1	4100	21.6	23000	52.6	140000

These transmitter powers produce a signal-to-noise ratio of 12db over the voice band upon reception under the specified noise conditions. A power handling capability of 10-15db more than the average power dissipated is required if linear amplifiers are used for voice transmission (see text, p. 1-13).

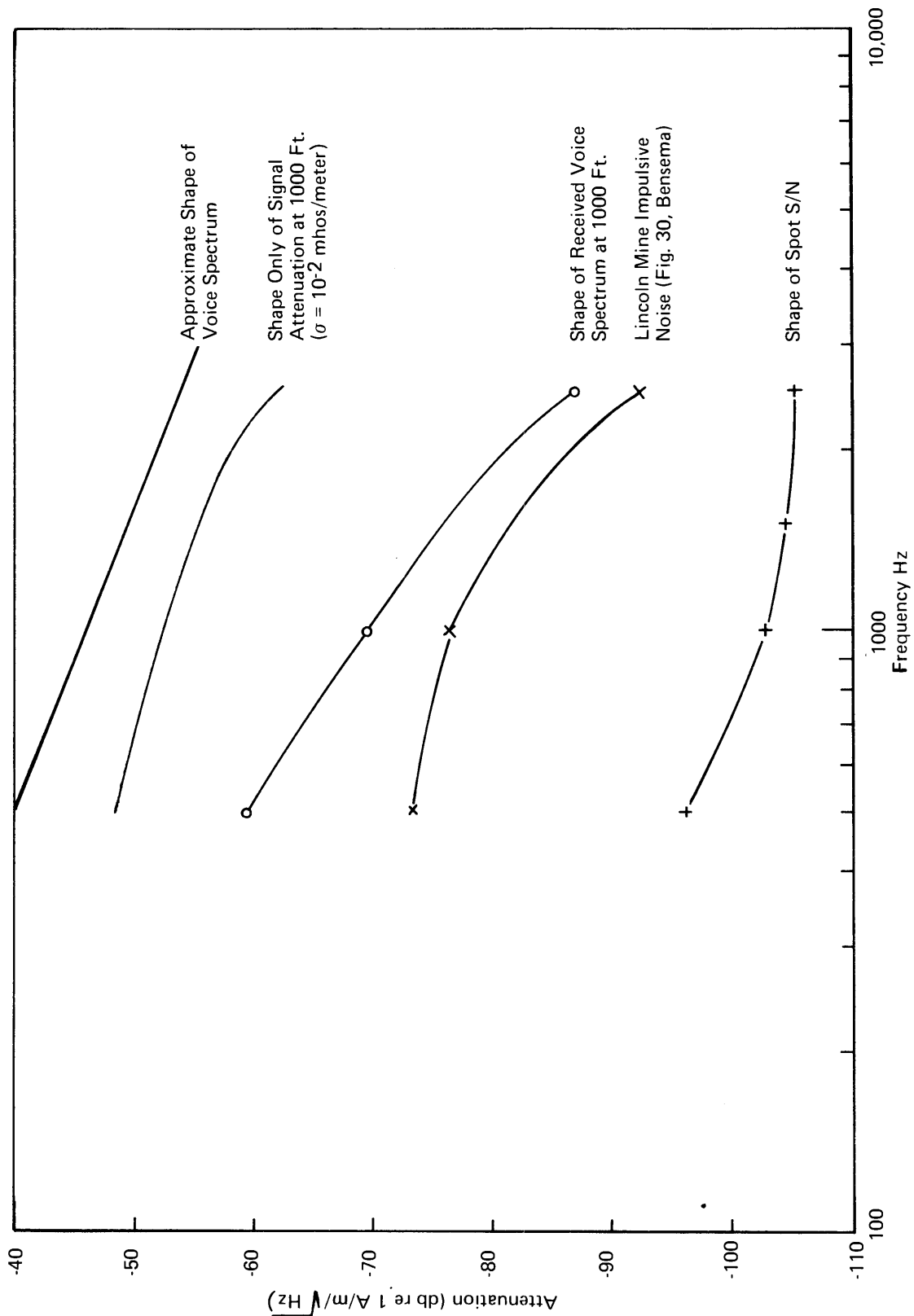


FIGURE 1-10 SHAPES OF VOICE, SIGNAL ATTENUATION, AND IMPULSIVE NOISE SPECTRA

II. SIGNAL POWER ESTIMATES FOR UPLINK THROUGH-THE-EARTH BASEBAND VOICE COMMUNICATIONS

Companion calculations to those described in the preceding Chapter I on downlink through-the-earth communications were performed on the uplink voice channel, using a vertical loop transmitter.

A. METHOD OF CALCULATION - UPLINK, LOOP ANTENNA

The magnetic field at the surface is given by

$$|H_z| = \frac{INA |G|}{2\pi D^3}, \text{ vertical component, where } |G|, \text{ as derived} \quad (1) *$$

by Westinghouse, is plotted in Figure 2-1. Using Figure 2-1 curves of $|G|/2\pi D^3$ versus frequency for three mine depths, with earth conductivities of 10^{-2} and 10^{-1} mhos/meter, were plotted in Figure 2-2.

The value of the RMS magnetic moment ($M_{rms} = NAI_{rms}$), required for a signal-to-noise ratio of 12db between the vertical components of signal and noise magnetic fields at the surface, under a variety of surface noise conditions, was calculated for these three depths. The same $1/f$ voice spectrum, and the methods of signal-to-noise computation described previously were used. A current source for the loop was assumed, so that the spectrum level of $NAI \sim 1/f$. As for the horizontal-wire antenna downlink case, calculations were performed only for the more favorable $\sigma=10^{-2}$ mhow/meter conductivity situation, commonly found over coal mines.

At $D = 300$ feet, we approximate

$$\frac{|G|}{2\pi D^3} = 2.09 \times 10^{-7} e^{-.0000479f} \quad (\text{meter}^{-3}) \quad (2)$$

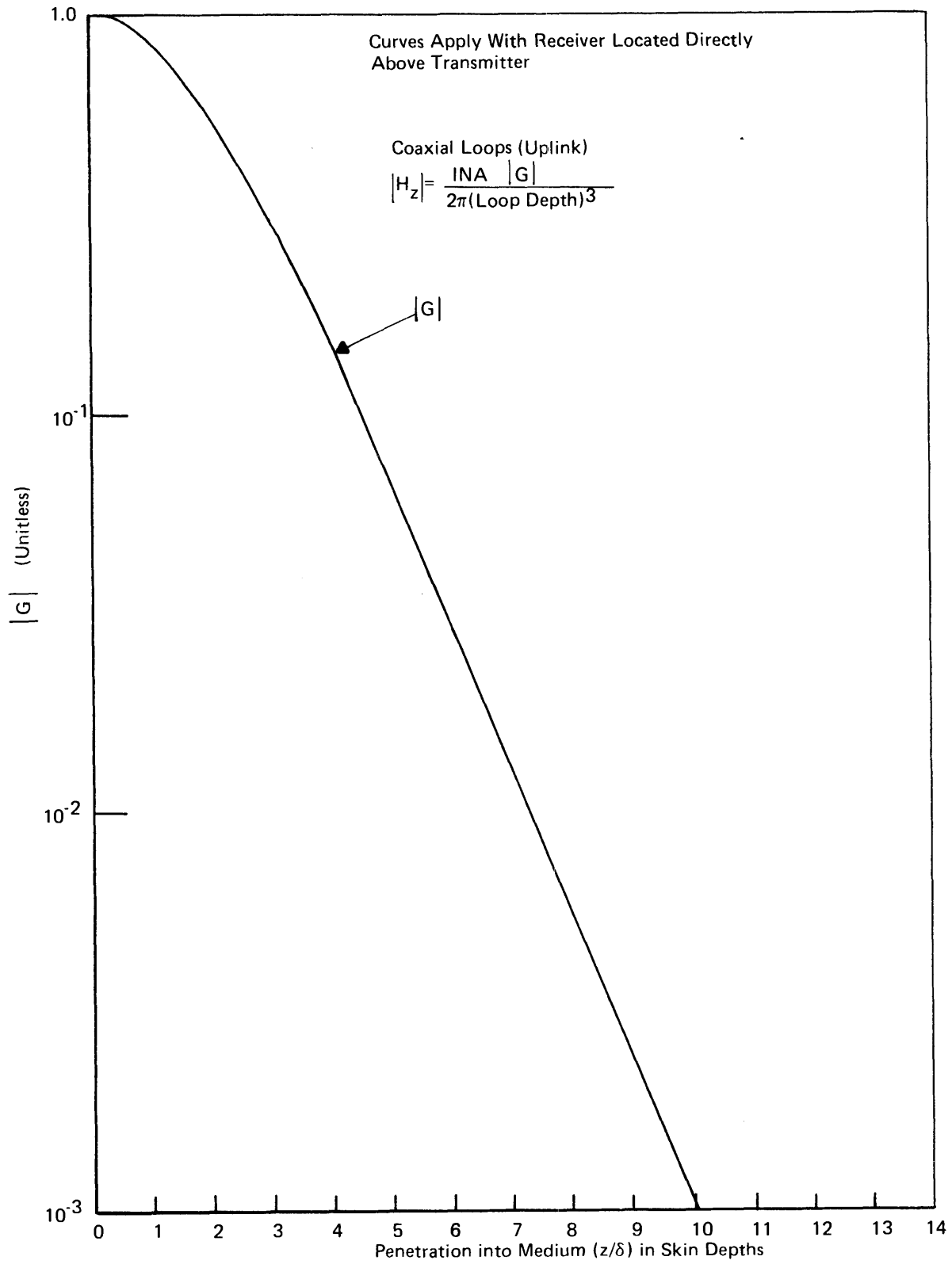
At $D = 600$ feet we approximate

$$\frac{|G|}{2\pi D^3} = 2.58 \times 10^{-8} e^{-.000197f} \quad (\text{meter}^{-3}) \quad (3)$$

At $D = 1000$ feet, we approximate

$$\frac{|G|}{2\pi D^3} = 5.35 \times 10^{-9} e^{-.000454f} \quad (\text{meter}^{-3}) \quad (4)$$

* References to Figures, Tables, and Equations apply to those in this Chapter unless otherwise noted.



Source: Westinghouse Georesearch Laboratory (WGL)

FIGURE 2-1 LOOP ANTENNA, COUPLING RELATIONSHIP

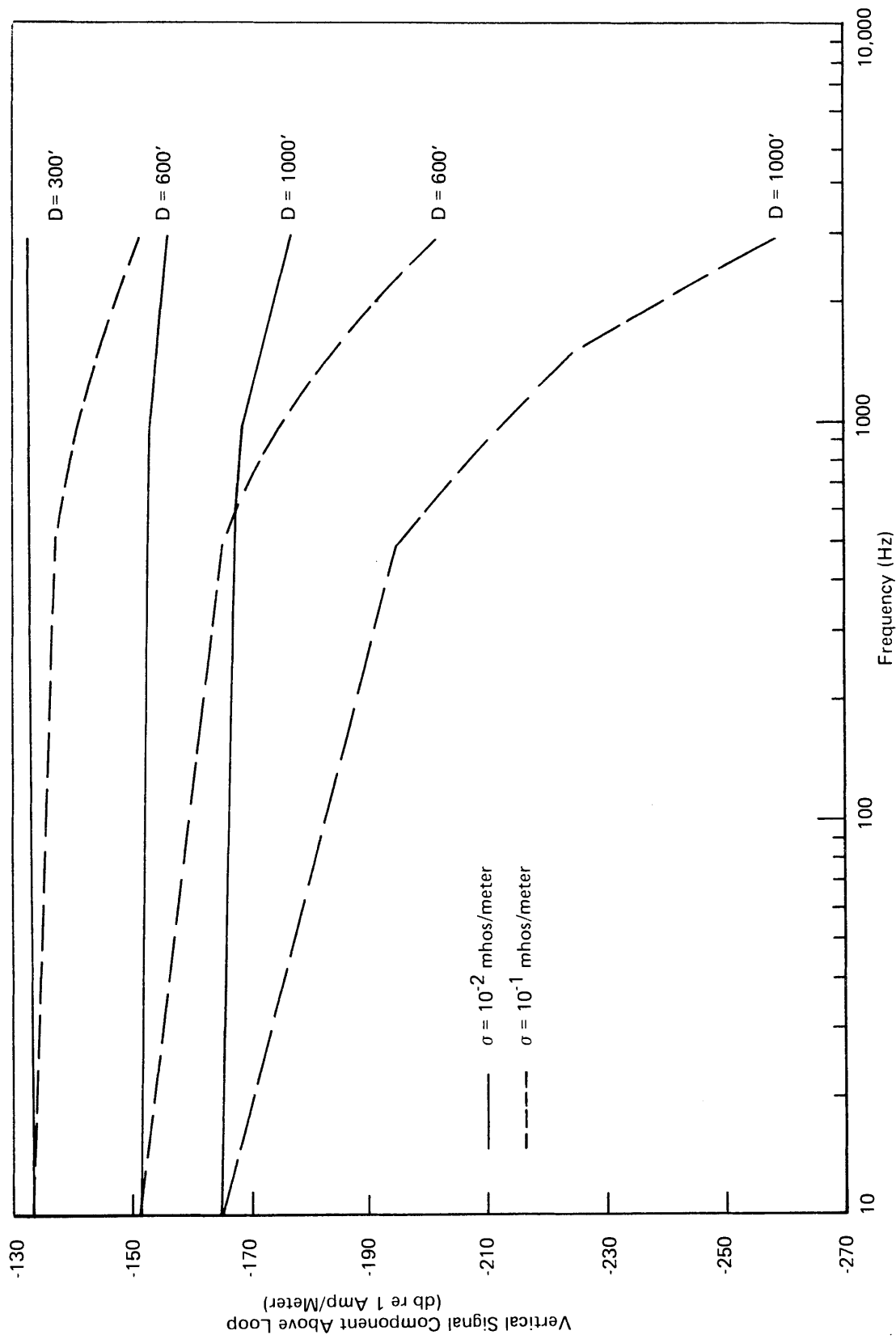


FIGURE 2-2 UPLINK SIGNAL FOR LOOP ANTENNA, UNIT MAGNETIC MOMENT

Since $\frac{|G|}{2\pi D^3}$ is of the form $\alpha e^{-\beta f}$, the received field can be

written in the form

$$H_{\text{rms}} = \alpha S_o \left[\int_{500}^{3000} \frac{e^{-2\beta f}}{f^2} df \right]^{1/2} \quad \text{A/M} \quad (5)$$

as in Equation (8) of Chapter I.

B. NOISE ON THE SURFACE OVER MINES

Surface Noise Conditions:

- (a) Allen Mine (Figure 2-3, Bensema NBS report)* 60 Hz and 360Hz harmonics primarily, vertical component.

$$N_{\text{rms}} = 5 \times 10^{-4} \text{ A/M (high noise)}$$

- (b) Gunn Quealy Mine Figure 2-4, 60 Hz harmonics and broadband background noise, vertical component (Westinghouse data)

$$N_{\text{rms}} = 2.34 \times 10^{-4} \text{ A/M (medium noise)}$$

- (c) Lincoln Mine (Figure 2-5, Bensema NBS report) 60 Hz harmonics primarily, vertical component

$$N_{\text{rms}} = 1.33 \times 10^{-4} \text{ A/M (low noise)}$$

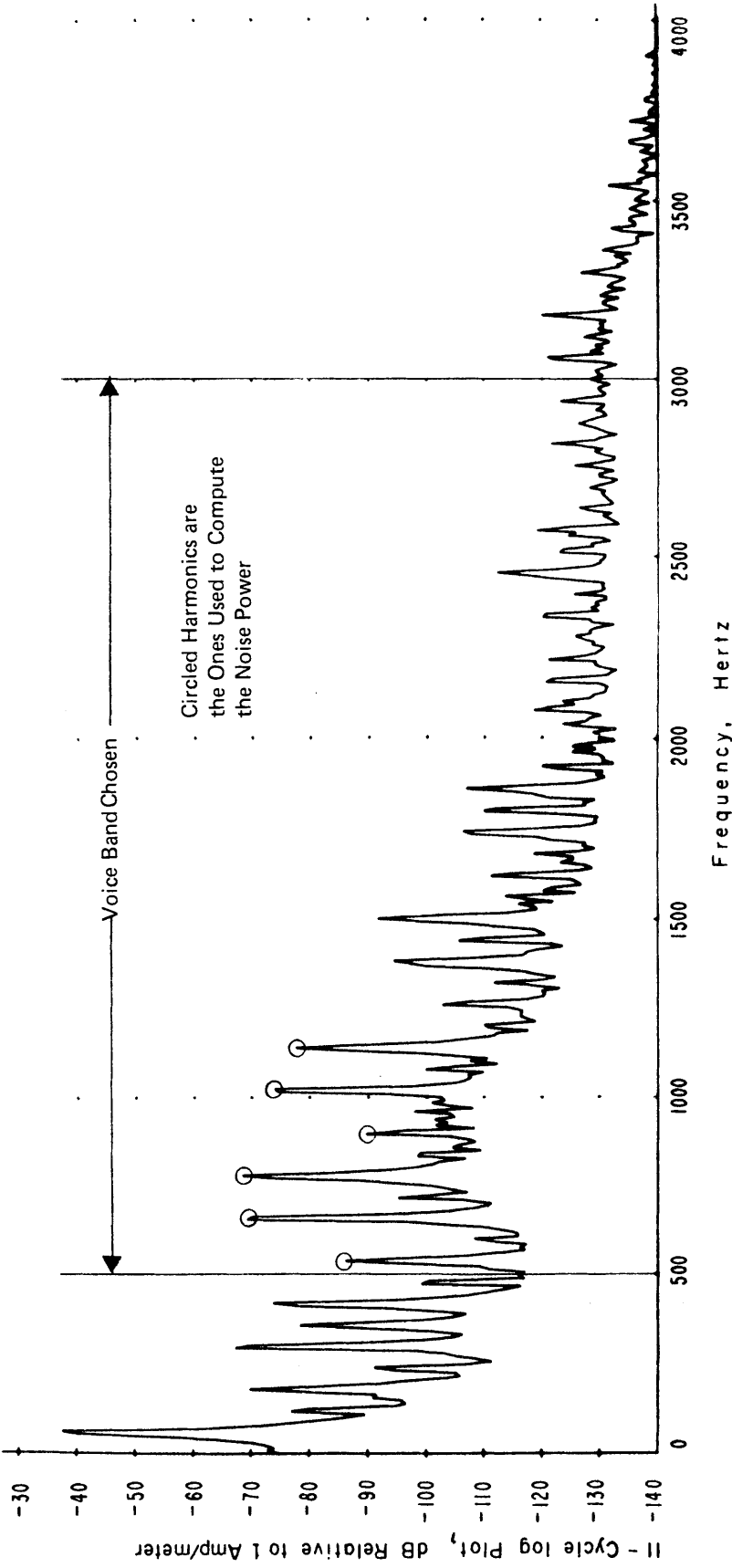
Broadband noise levels were neglected in the noise power calculations, whenever the spectrum level as seen by a 1Hz bandwidth filter was (over the individual 500 or 1000Hz wide segments used to sum noise contributions) more than 40db below the highest harmonic peak lying between 500 and 3000Hz. In cases (a) and (c), this criterion is satisfied over the whole of the voice bandwidth, whereas in case (b) the background noise does not drop more than 30db below the 660Hz peak, and hence has been included in the noise computation.

C. SIGNAL NOISE AND POWER ESTIMATES

A plot of the loop magnetic moment required for voice transmission with a 12db S/N ratio as a function of depth is shown in Figure 2-6. Shapes of the signal attenuation factor and voice spectrum, as functions of frequency, are shown in Figure 2-7. The magnetic moment results are presented in Table 2-1. In Tables 2-2 and 2-3 the power dissipated in

* Ref. I-1, NBS Report 10-739

11 0 0 2048 20 2.56+000 7.81+000 12/22/71 12 25 29 3
 3.91-003 -3.09+001 0.00+000 0.00+000 20 43320 43320
 0317210771 Rec. gain corr. = -12 Total const corr. = -70.3
 1.000-003 0.2236 1.675-004



Source: NBS Report, Fig. 8

FIGURE 2-3 ALLEN MINE, SURFACE, 03-17
ANTENNA SENSITIVE AXIS POINTED VERTICAL

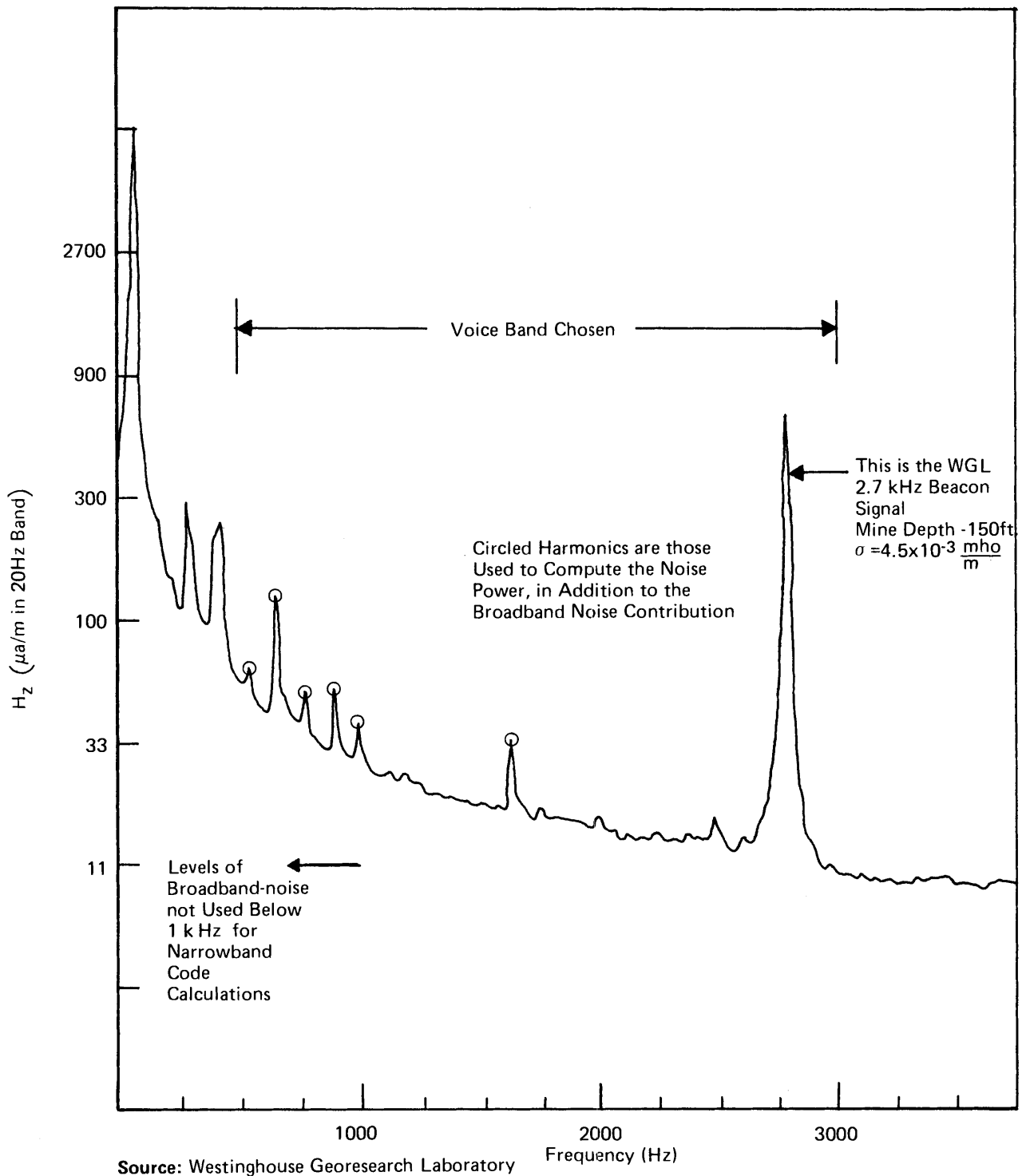
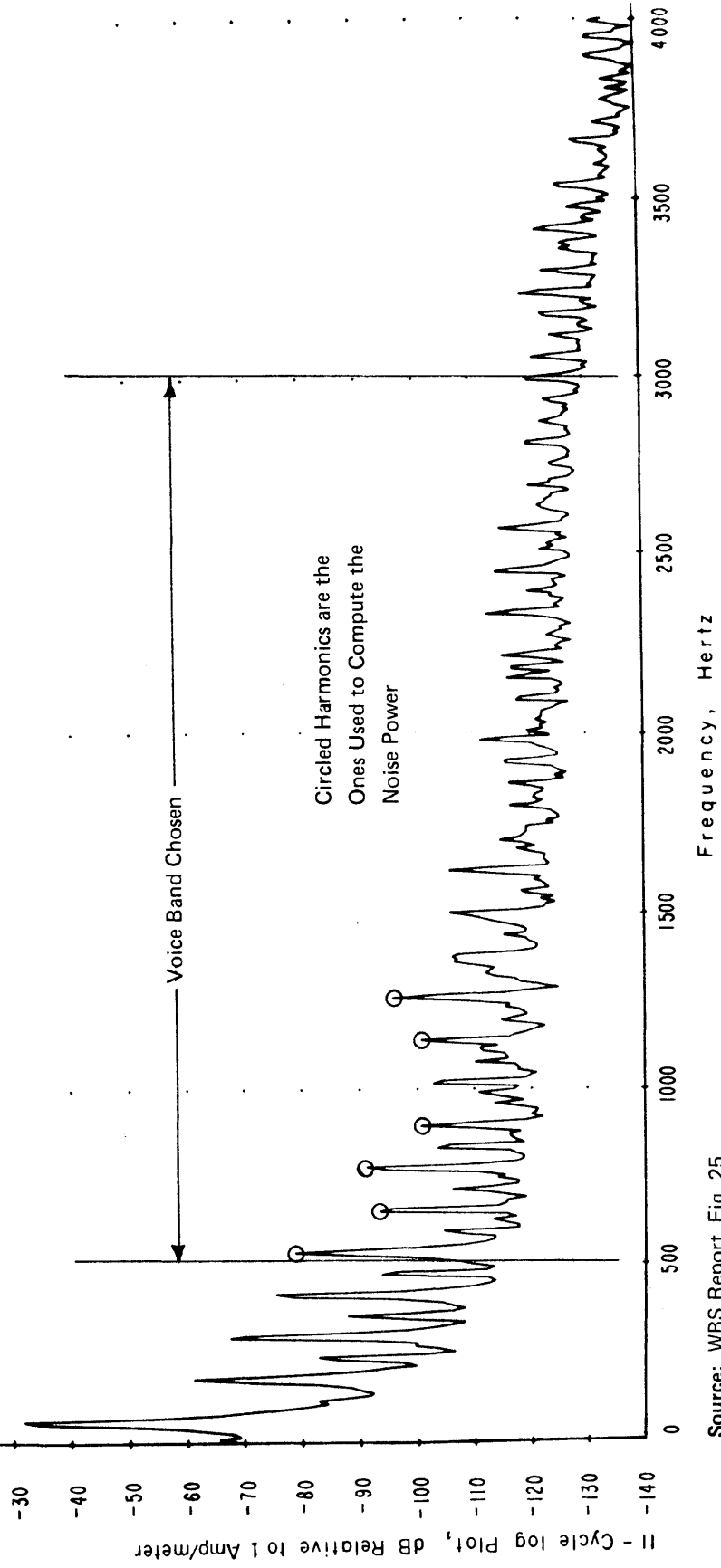


FIGURE 2-4 EM BACKGROUND NOISE ON SURFACE-VERTICAL COMPONENT, H_z , GUNN QUEALY MINE, ROCK SPRINGS, WYOMING

11 0 0 2048 20 2.56+000 7.81+000 11/23/71 14:41:52 7
 3.91-003 -4.04+001 0.00+000 20 40320 40320
 0722250871 Rec. gain corr. = -6 Total const corr. = -60.5
 1.000-003 0.2236 6.514-004



Source: WBS Report Fig. 25

FIGURE 2-5 LINCOLN MINE, SURFACE, 3000 Hz BW, 07-22

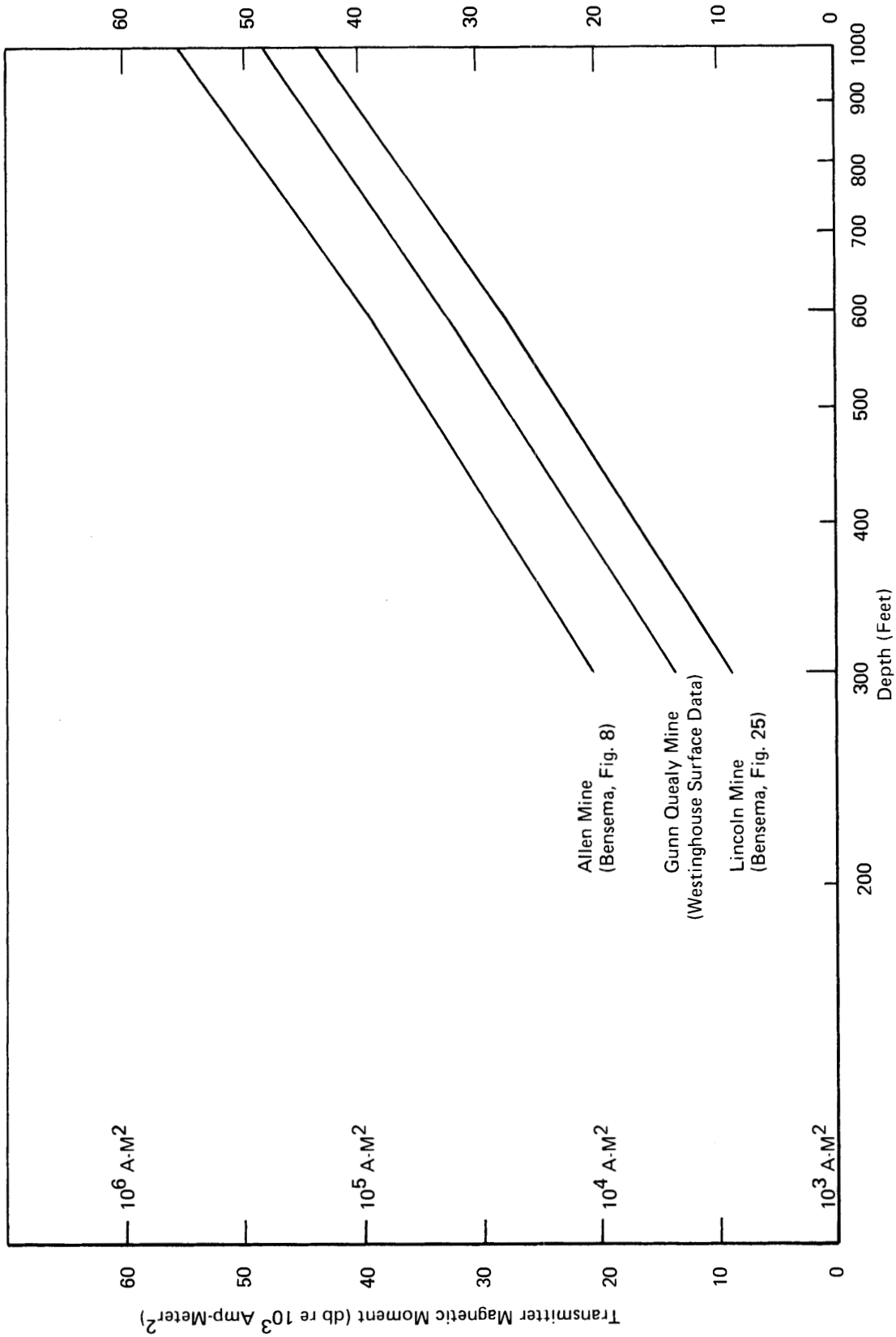


FIGURE 2-8 TRANSMITTER MAGNETIC MOMENT (RMS) REQUIRED FOR 12db S/N RATIO OVER VOICE BANDWIDTH (500 Hz - 3kHz) FOR VERTICAL FIELD COMPONENTS OF NOISE AND SIGNAL ($\sigma = 10^{-2}$ mhos/meter)

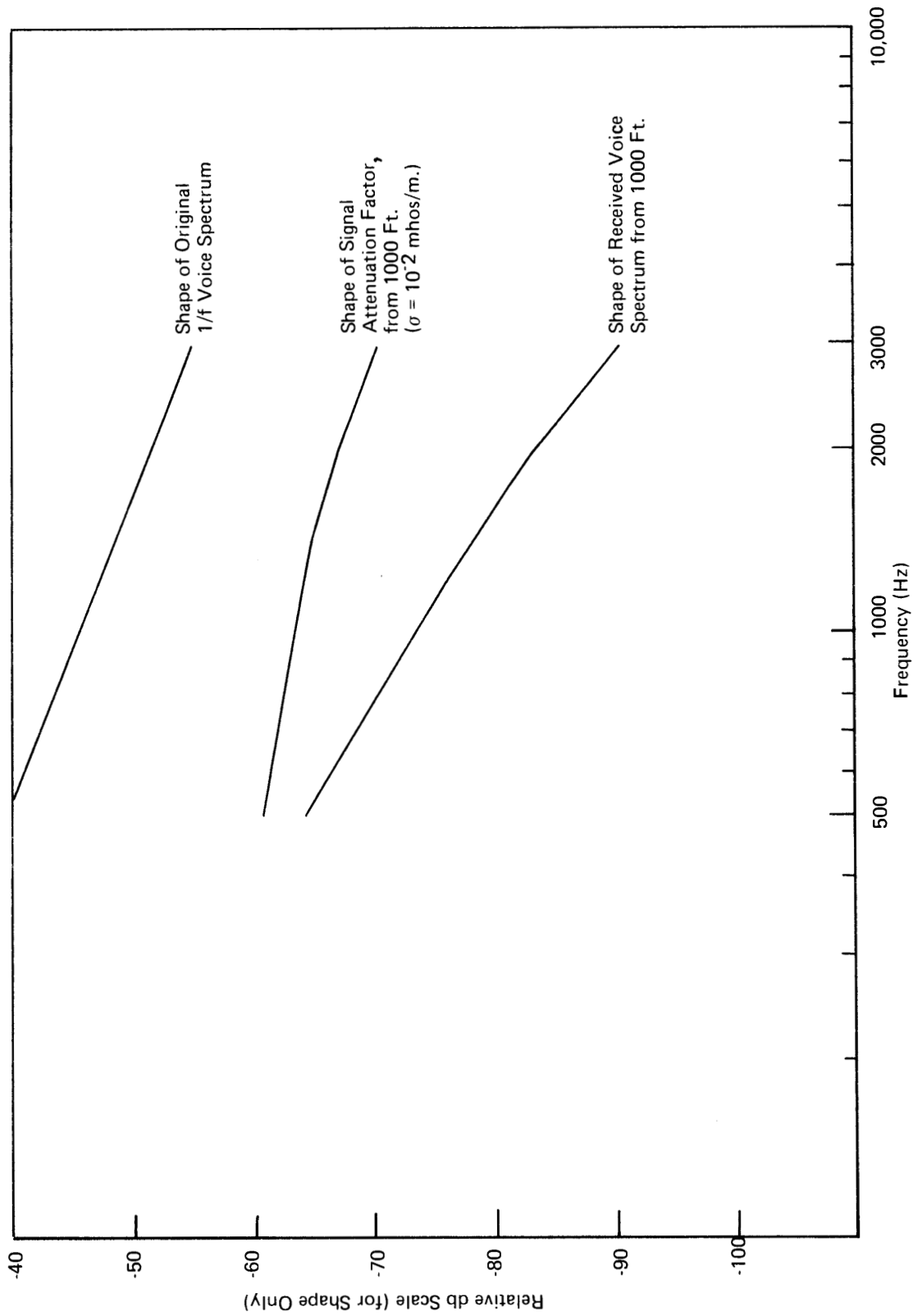


FIGURE 2-7 RELATIVE SHAPES OF SIGNAL ATTENUATION FACTOR AND VOICE SPECTRUM (from 1000 Ft. Depth)

TABLE 2-1

REQUIRED LOOP MAGNETIC MOMENT, AMP-METER²
 for $\sigma = 10^{-2}$ mho/meter*

<u>Surface Noise at:</u>	<u>Depth of Mine (Feet)</u>		
	<u>300</u>	<u>600</u>	<u>1000</u>
Allen Mine (harmonics only)	10,500	94,700	547,000
Gunn Quealy Mine (harmonics and broadband)	4,910	44,300	269,000
Lincoln Mine (harmonics only)	2,790	25,200	153,000

*For a signal-to-noise ratio of 12db over the voice band upon reception.

TABLE 2-2

AVERAGE POWER DISSIPATION AND RMS VOLTAGE AND CURRENT
 IN UPLINK CIRCULAR LOOP ANTENNA
 for $\sigma = 10^{-2}$ mho/meter*

Loop: 100 feet periphery, 20 turns of No. 8 gauge wire (.1285 in. diameter)

Resistance R = 1.3 ohms;
 Inductance L = 27 millihenries;
 NA = 1460 meter²

Surface Noise Condition	Depth of Mine (Feet)								
	300			600			1000		
	I _{rms} (A)	V _{rms} (V)	P(Watts)	I _{rms} (A)	V _{rms} (V)	P(W)	I _{rms} (A)	V _{rms} (V)	P(W)
Allen Mine (high)	7.2	1,500	67	65	13,000	5500	390	82,000	200,000
Gunn Quealy Mine (medium)	3.4	690	14.7	30	6,300	1200	180	38,000	44,000
Lincoln Mine (low)	1.9	400	4.7	17	3,500	390	100	22,000	14,000

*For a 12db signal-to-noise ratio across the voice band upon reception.

TABLE 2-3

AVERAGE POWER DISSIPATED AND RMS VOLTAGE AND CURRENT

IN UPLINK CIRCULAR LOOP ANTENNA

for $\sigma = 10^{-2}$ mho/meter*

Loop: 100 feet periphery, 10 turns of No. 2 gauge wire (.2576 in. diameter)

Resistance R = 0.12 ohms;
 Inductance L = 6.1 millihenries;
 NA = 730 meter²

Surface Noise Condition

	<u>Depth of Mine (Feet)</u>								
	<u>300</u>			<u>600</u>			<u>1000</u>		
	I _{rms} (A)	V _{rms} (V)	P (Watts)	I _{rms} (A)	V _{rms} (V)	P (W)	I _{rms} (A)	V _{rms} (V)	P (W)
Allen Mine (high)	14	690	25	130	6,100	2000	790	37,000	74,000
Gunn Quealy Mine (medium)	6.7	320	5.4	61	2,800	440	370	17,000	16,000
Lincoln Mine (low)	3.8	180	1.8	35	1,600	140	210	9,800	5,300

*For a 12db signal-to-noise ratio across the voice band upon reception.

the loop antenna, and the RMS current and voltage under these transmission conditions, are presented for two alternative loop configurations of reasonable size. The RMS voltage has been calculated for the case where the loop signal current spectrum level varies as $1/f$, so that

$$V_{\text{rms}} \approx I_{\text{rms}} (L^2 \omega_i \omega_f)^{1/2} \quad (6)$$

where L is the inductance of the loop, and ω_i , ω_f are the initial and final edges of the voice bandwidth (i.e., 500 and 3000Hz). These data are also presented in Figure 2-8. Throughout, a value of 10^{-2} mhos/meter has been assumed for the overburden conductivity.

Figure 2-8 shows that the power required varies, under the noise conditions encountered, from easily realizable levels of up to around 100 watts for mine depths in the range of 300 to 600 feet, to the very high values of several hundred kilowatts for the deepest mines (1000 feet) under the worst noise conditions.

Two transmitter loop configurations were chosen with a view to keeping the diameter of the conductor "bundle" roughly constant. The weight increased appreciably from 100 lbs in loop (a), to 150 lbs in loop (b). It is clear that sizable reductions in power can be achieved by careful design of the loop antenna, but a more thorough investigation is needed with proper weighting given to factors such as weight, volume, area, and cost. These gains may, however, not be sufficient to achieve satisfactory voice transmission from the deepest mines under the worst surface-noise conditions, because of the practical limitations imposed on a subsurface system compared with a surface installation. But as in the downlink case, significant gains may be possible by selectively rejecting the worst harmonic contributions by a series of notch filters, and the use of pre-emphasis and peak-clipping techniques on transmission. Further discussion of these techniques may be found in Chapters IV, V, and VI of this Part.

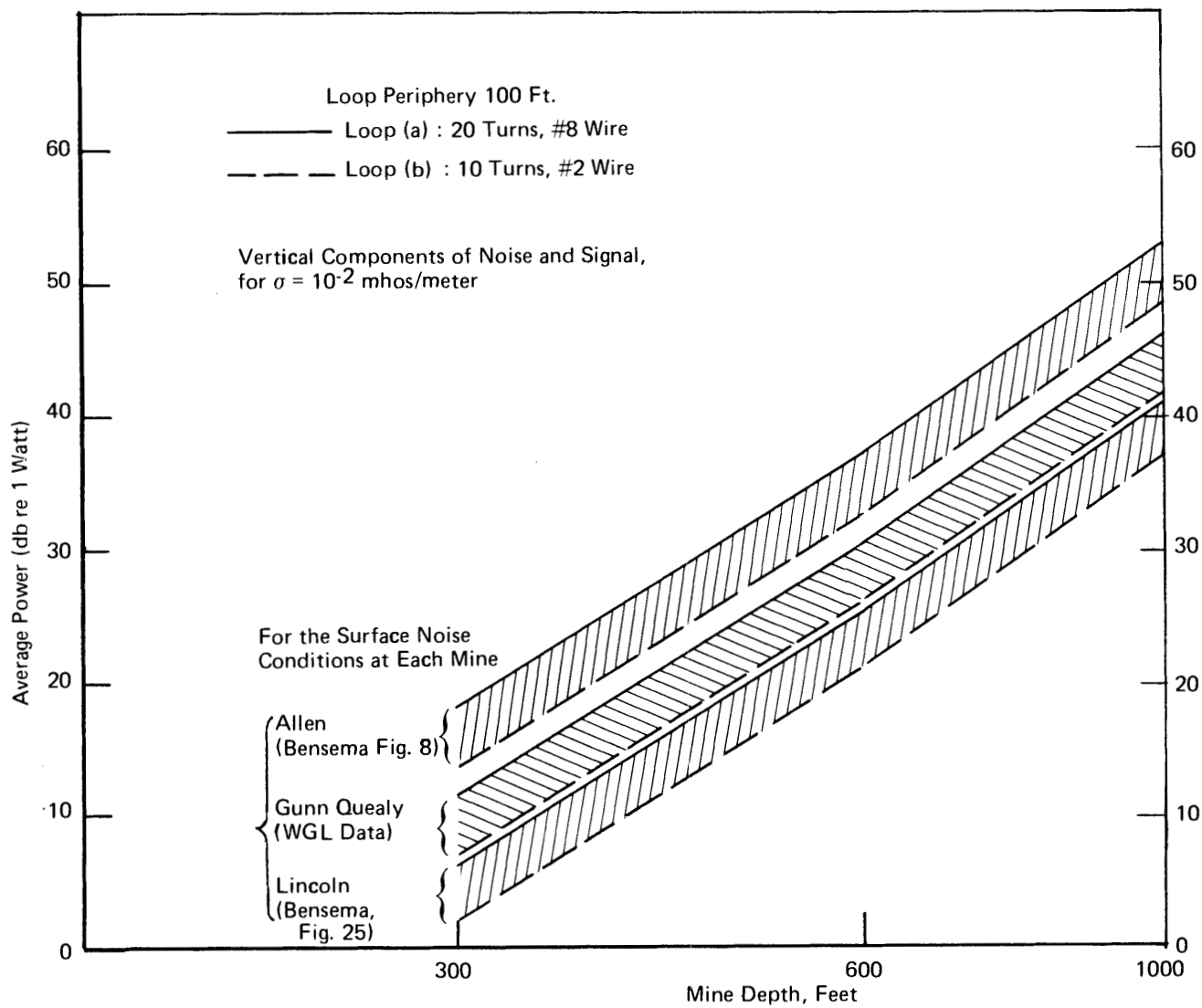


FIGURE 2-8 AVERAGE POWER DISSIPATED IN LOOP FOR 12db S/N OVER VOICE BANDWIDTH AT SURFACE (Uplink Transmission)

III. SPOT S/N RATIO ESTIMATES FOR UPLINK AND DOWNLINK THROUGH-THE-EARTH NARROWBAND CODE COMMUNICATIONS

Estimates of the spot signal-to-noise ratio (S/N) were made as a function of frequency for a variety of in-mine and surface noise conditions likely to be encountered by narrowband code communications systems between mines and the surface. Both uplink and downlink through-the-earth channels were treated. The spot S/N ratio is defined as

$$\left(\frac{S}{N}\right)_{\text{spot}} = \left(\frac{\text{Signal Power}}{\text{Noise Power Density}}\right) \quad (1)*$$

where the signal (S) is expressed in units of amp/meter, and the broadband noise density (N) in units of amp/meter per $\sqrt{\text{Hz}}$. These calculations have been carried out with the limited available noise data, to provide preliminary estimates of performance trends and limitations to be expected for low-frequency narrowband code communications systems, and to help identify related data gaps or limitations. Narrowband systems are of interest to the Bureau of Mines because of the possibility of obtaining code communication under circumstances where voiceband communication may be ineffective (e.g., in high noise and/or high signal-attenuation conditions).

A. SIGNAL AND NOISE PLOTS

Figures 3-1 and 3-2 show, respectively, the signal field strengths at the receiver for a downlink horizontal-wire antenna with a current of 1 ampere (50 watts for the 50-ohm antenna of Chapter I, and an uplink loop antenna with a current of 1 ampere and a magnetic moment of 1460 amp-meter² (1.3 watts for the 20-turn loop of Chapter II). The signals (i.e., the vertical and horizontal magnetic-field components, directly above the loop or below the wire antenna, respectively) are plotted at three mine depths (300, 600, and 1000 feet) for representative overburden conductivities (10^{-2} and 10^{-1} mhos/meter). Figures 3-3 and 3-4 are plots of the broadband noise density both in the mine and on the surface respectively, for a variety of conditions. These data** are taken from W.D. Bensema's NBS report, WGL measurements, and some atmospheric noise measurements on the surface in Florida (unrelated to any mining activity) reported by J. E. Evans in M.I.T. Lincoln Laboratory Technical Note 1969-18, March 1969. Figures 3-5, 3-6, 3-7, 3-8, 3-9, 3-10, 3-11, 3-12, and 3-13 present the original data plots. In a majority of the at-mine cases, vertical noise components are shown, since most measurements have been taken of these. Some in-mine measurements of broadband horizontal noise components (Figures 17 and 18 of Bensema's NBS report)[†] give results not very different from the low vertical broadband noise component plotted from Figure 14 of Bensema's work, in Figure 3-8 of this Chapter. It is reasonable to suppose that broadband horizontal noise is likely to be no higher than the worst broadband vertical noise in the mine.

* References to Figures, Tables, and Equations apply to those in this Chapter unless otherwise noted.

** Adjusted to a 1 Hz bandwidth.

† Ref. I-1, NBS Report 10-739.

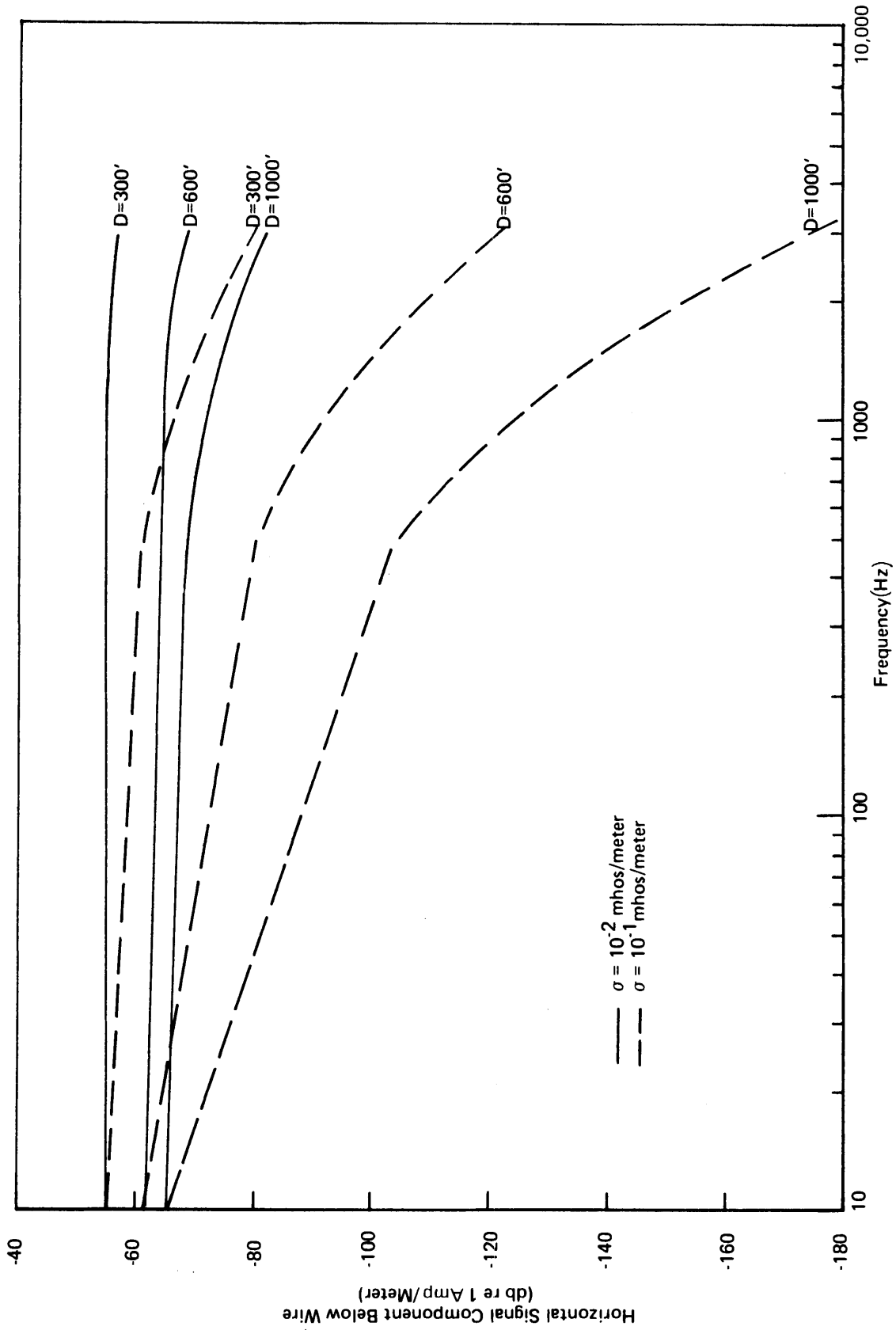


FIGURE 3-1 DOWNLINK SIGNAL FOR HORIZONTAL WIRE ANTENNA - 1 AMP CURRENT

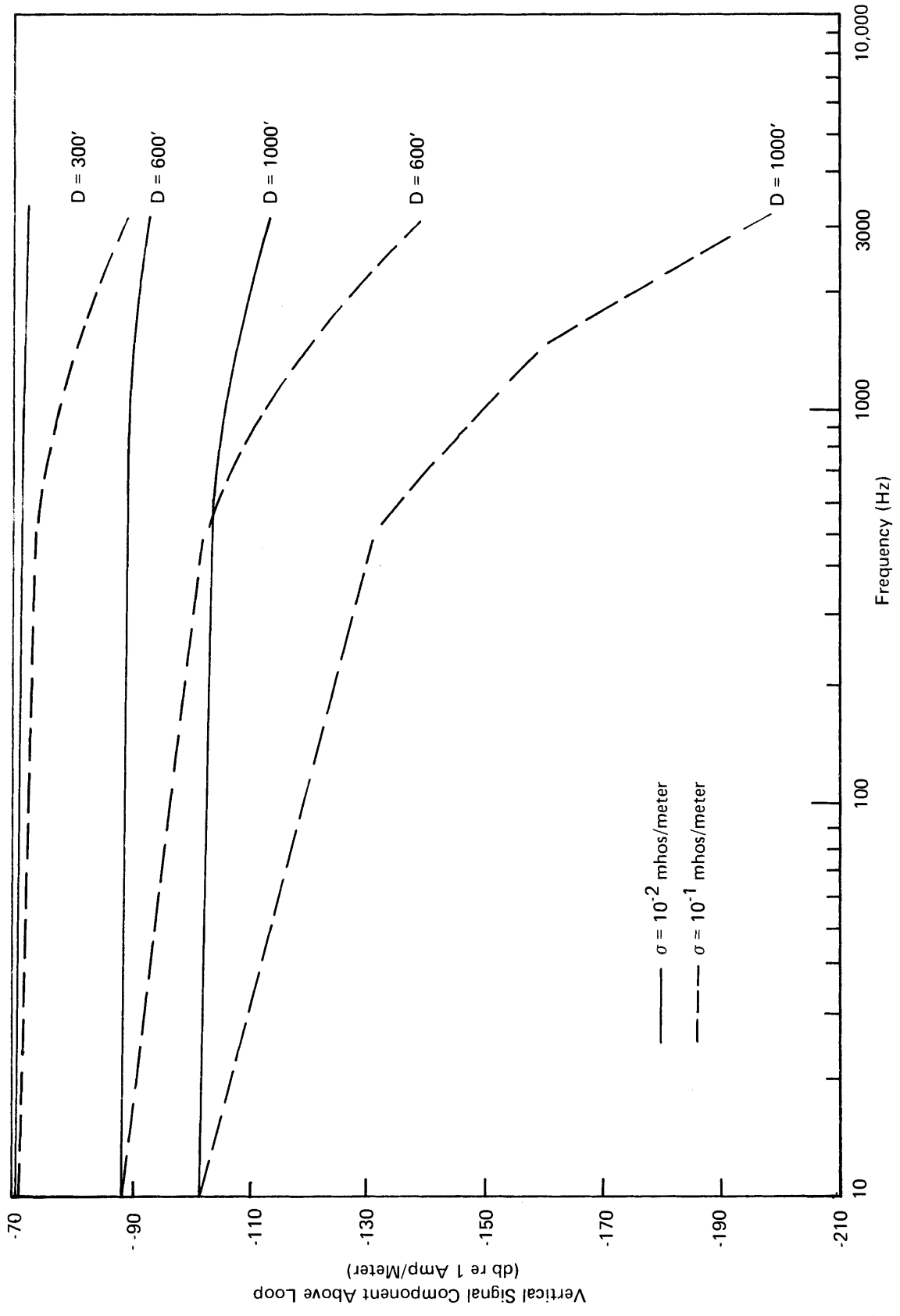


FIGURE 3-2 UPLINK SIGNAL FOR LOOP ANTENNA - MAGNETIC MOMENT = 1460 AMP-METER²

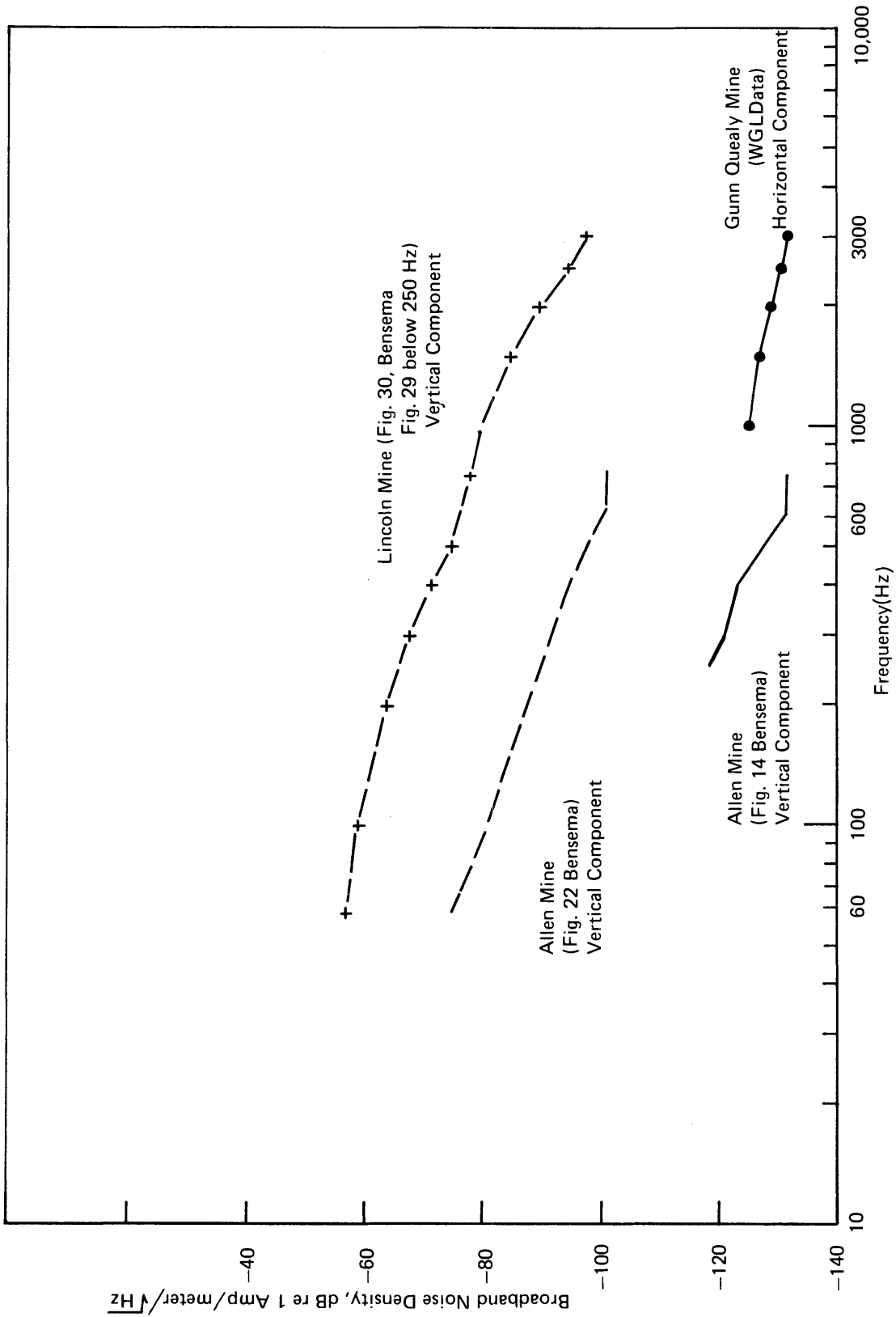


FIGURE 3-3 IN-MINE BROADBAND NOISE DENSITIES FOR DOWNLINK COMMUNICATIONS

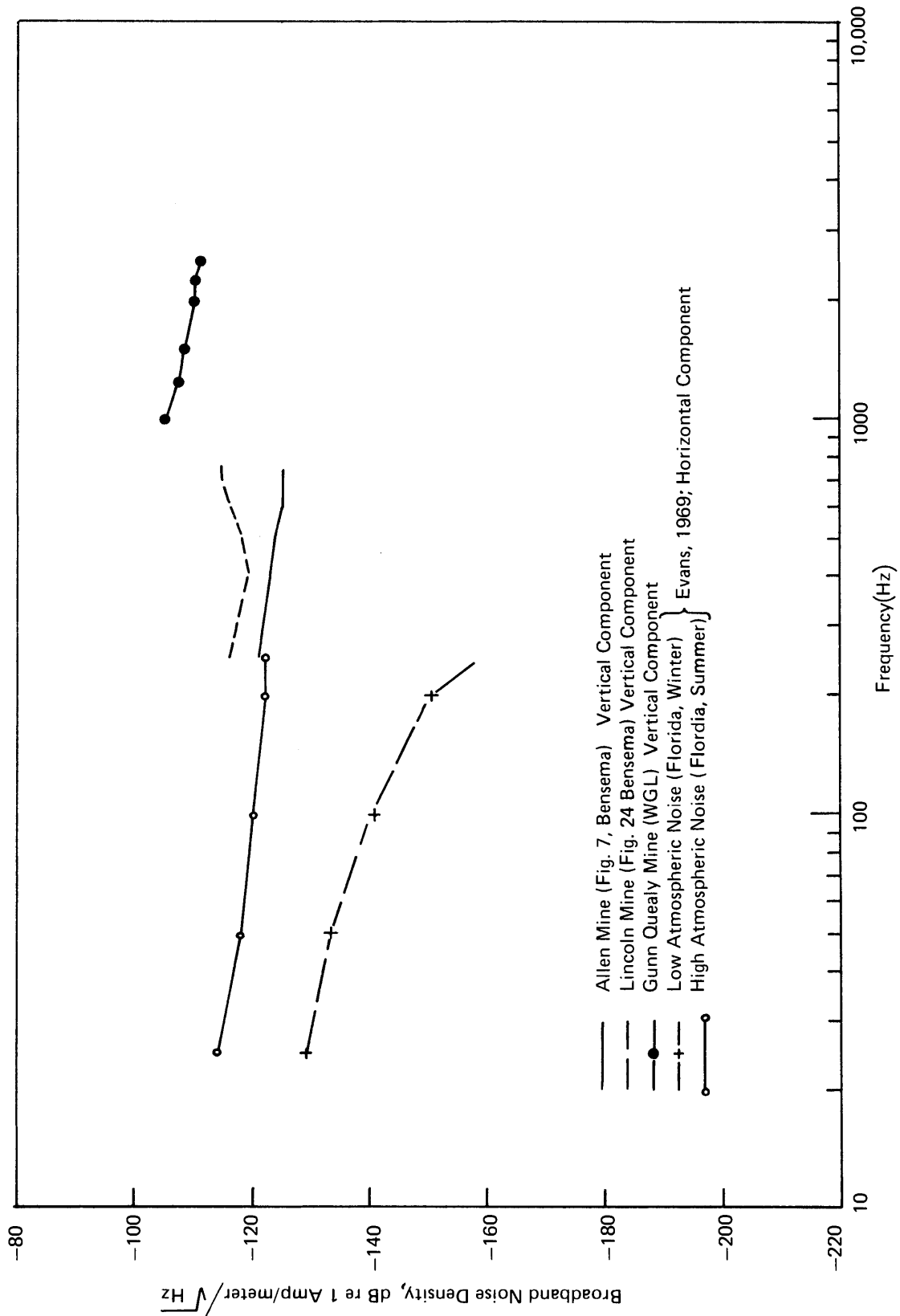
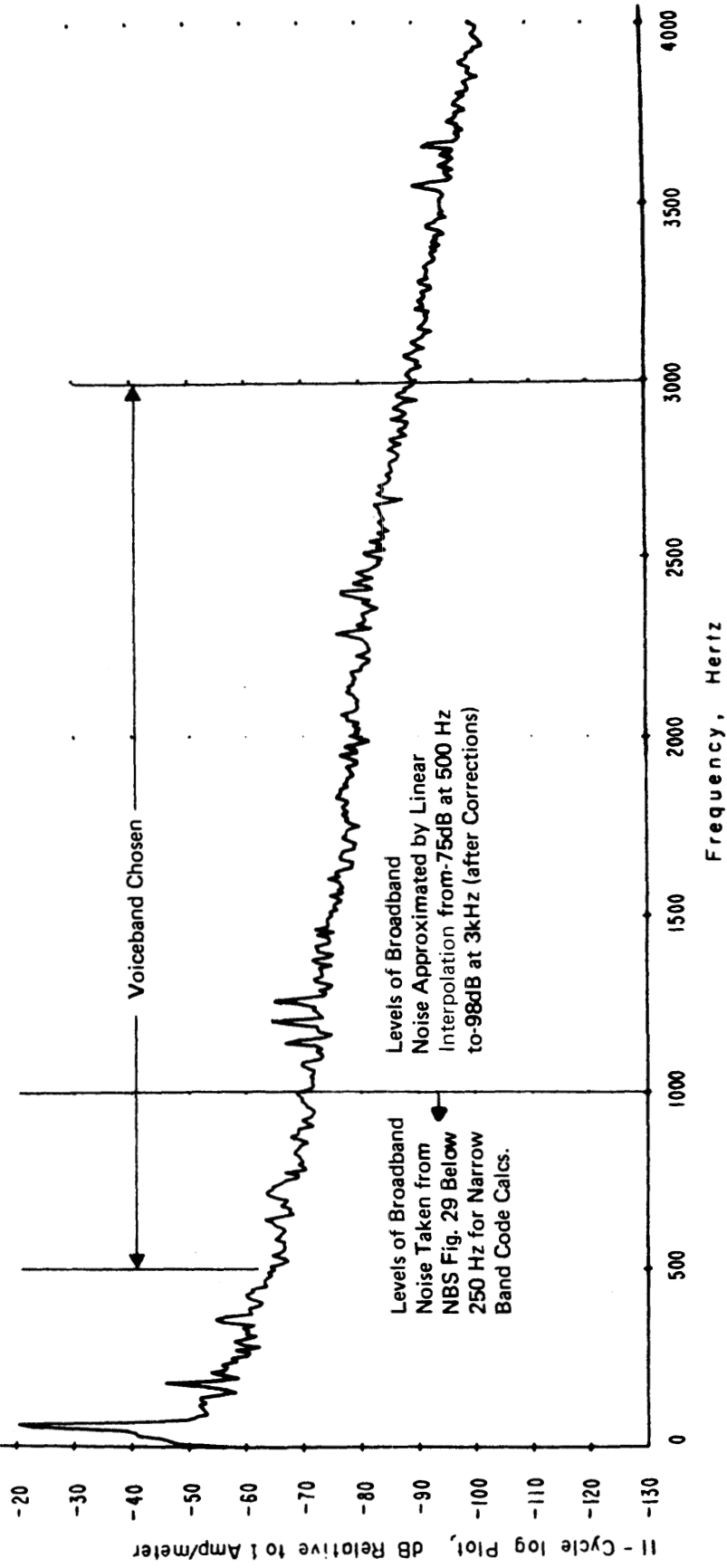


FIGURE 3-4 SURFACE BROADBAND NOISE DENSITIES FOR UPLINK COMMUNICATIONS

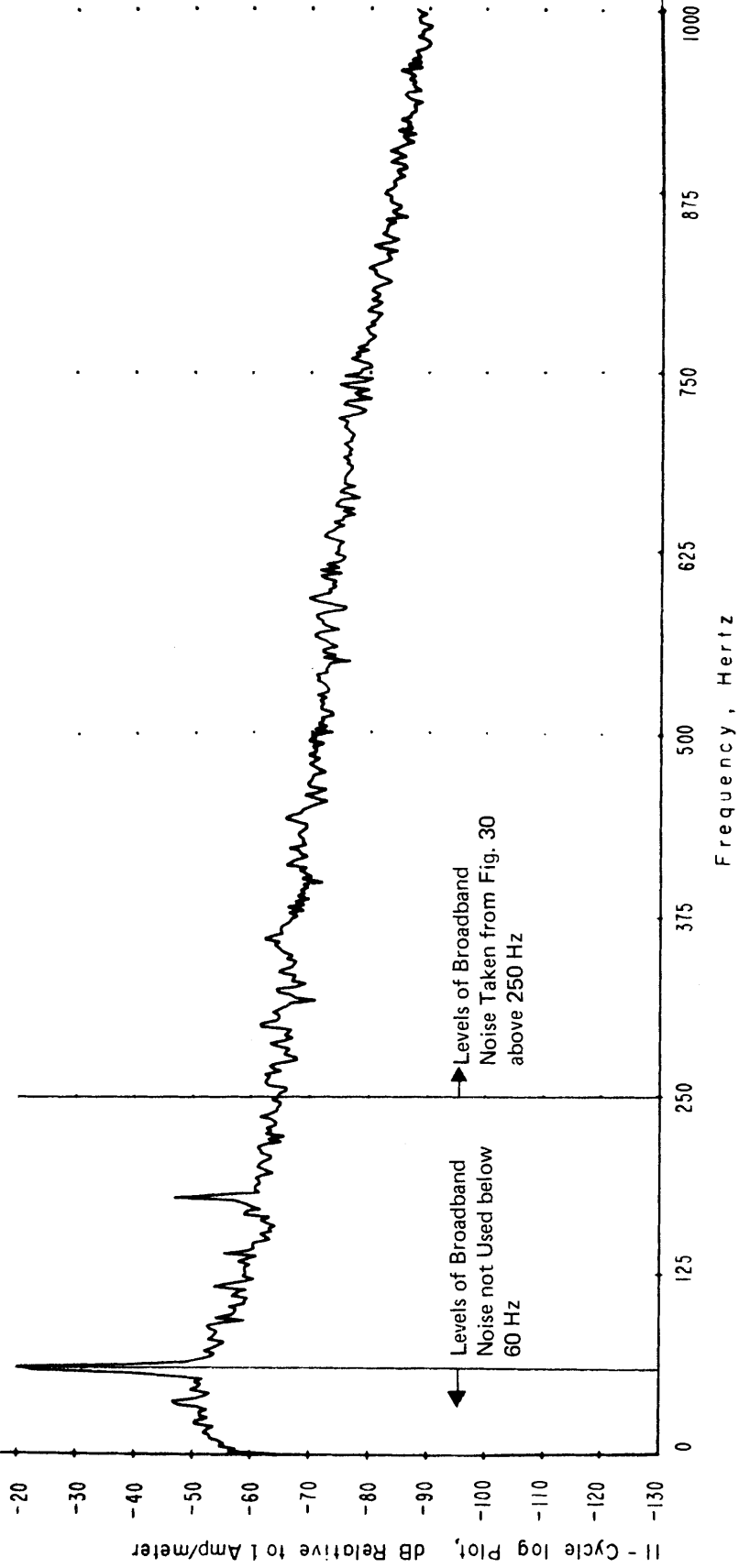
11 0 0 2040 20 2.56+000 7.01+000 11/24/71 00:56:29 3
 3.91-003 -1.00+002 0.00+000 0.00+000 20 40320 40320
 0323250871 Rec. gain corr. = 0 Total const corr. = -54.5
 1.000-002 0.2236 9.224-003



Source: NBS Report, Fig 30

FIGURE 3-5 LINCOLN MINE, UNDERGROUND, 3000 Hz BW, 03-23; IN CONTROL ROOM
 SEVERE TROLLEY IMPULSIVE NOISE (Vertical)

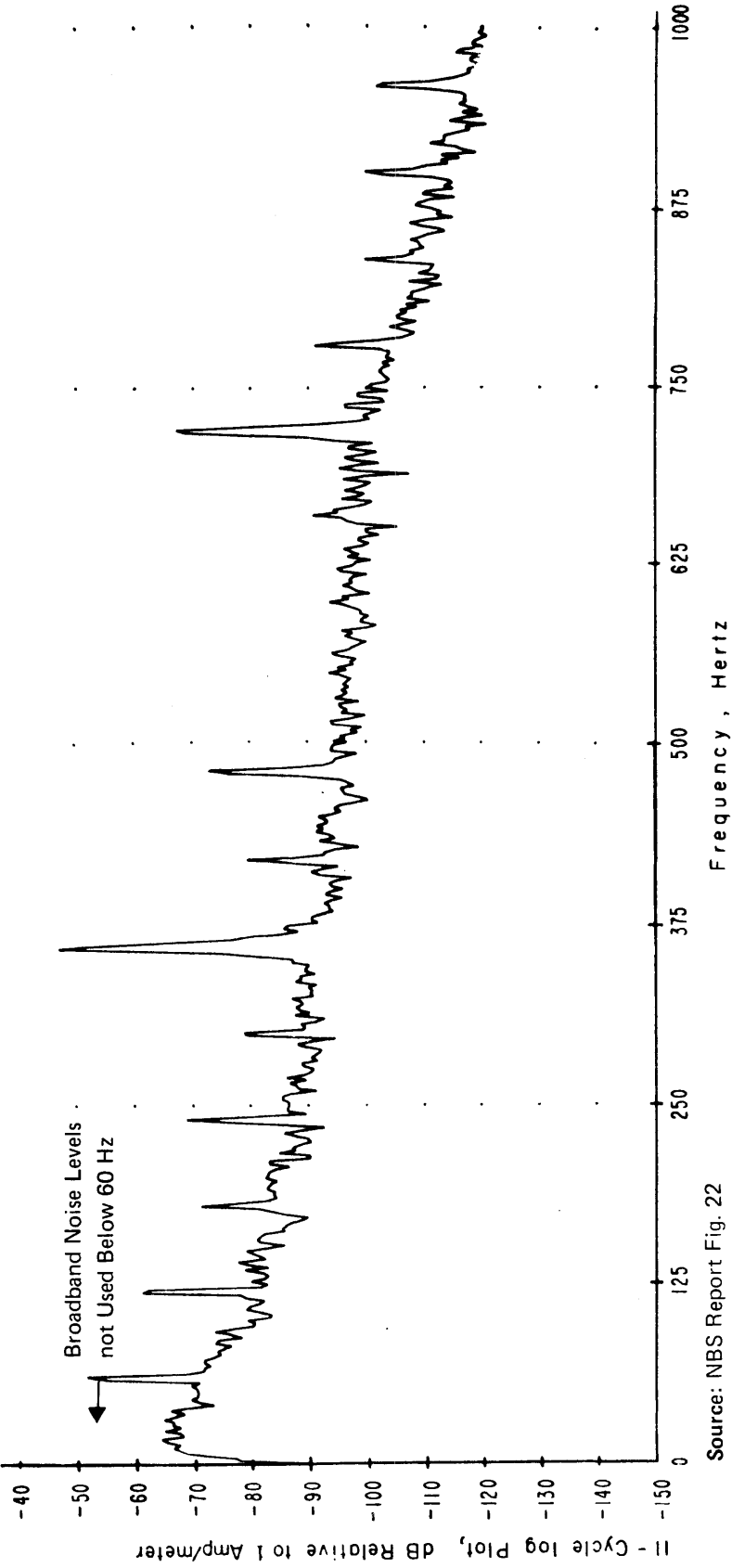
11 0 0 2048 20 1.02+001 1.95+000 11/23/71 08:59:53 3
 3.91-003 -4.17+001 0.00+000 0.00+000 20 40320 40320
 0320250871 Rec. gain corr. = 0 Total const corr. = -60.5
 1.000-002 0.2236 9.798-003



Source: NBS Report Fig 29

FIGURE 3-6 LINCOLN MINE, UNDERGROUND, 750 Hz BW, 03-20. IN CONTROL ROOM. SEVERE TROLLEY IMPULSIVE NOISE (Vertical)

11 11 2.48 20 1.02400 1.95400 11/21/77 15:08.49 9
 3 8.0003 1.00000 1.00000 20 4.332 4.332
 0.322077 Rec. gain corr. = -20 Total const corr. = -84.3
 0.000-004 0.2236 1.900-005



Source: NBS Report Fig. 22

FIGURE 3-7 ALLEN MINE, UNDERGROUND, 750 Hz BW, 07-13;
 ANTENNA AXIS VERTICAL; ELECTRIC LOCOMOTIVE
 PULLING OUT WITH LOADED COAL CARS

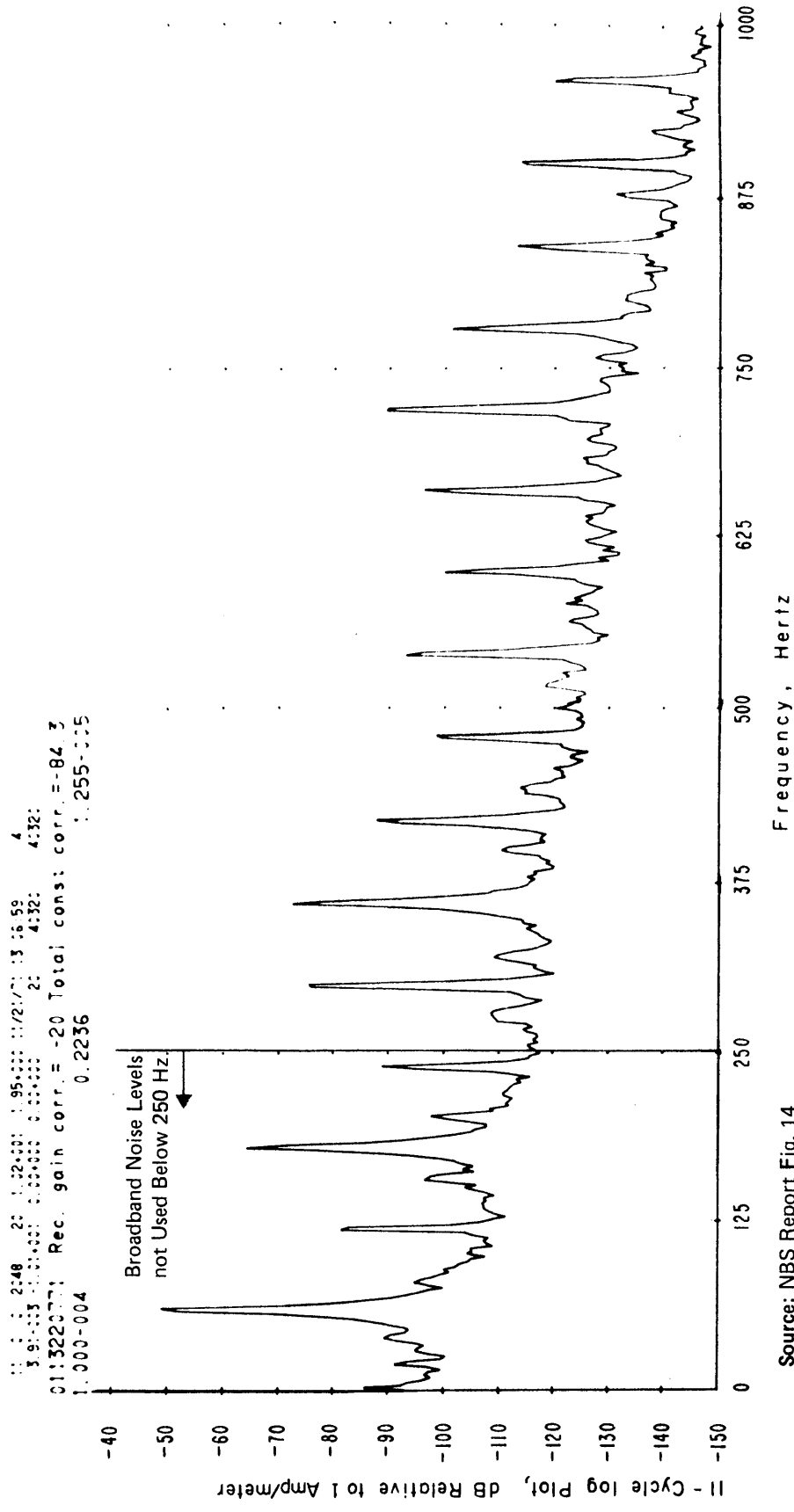
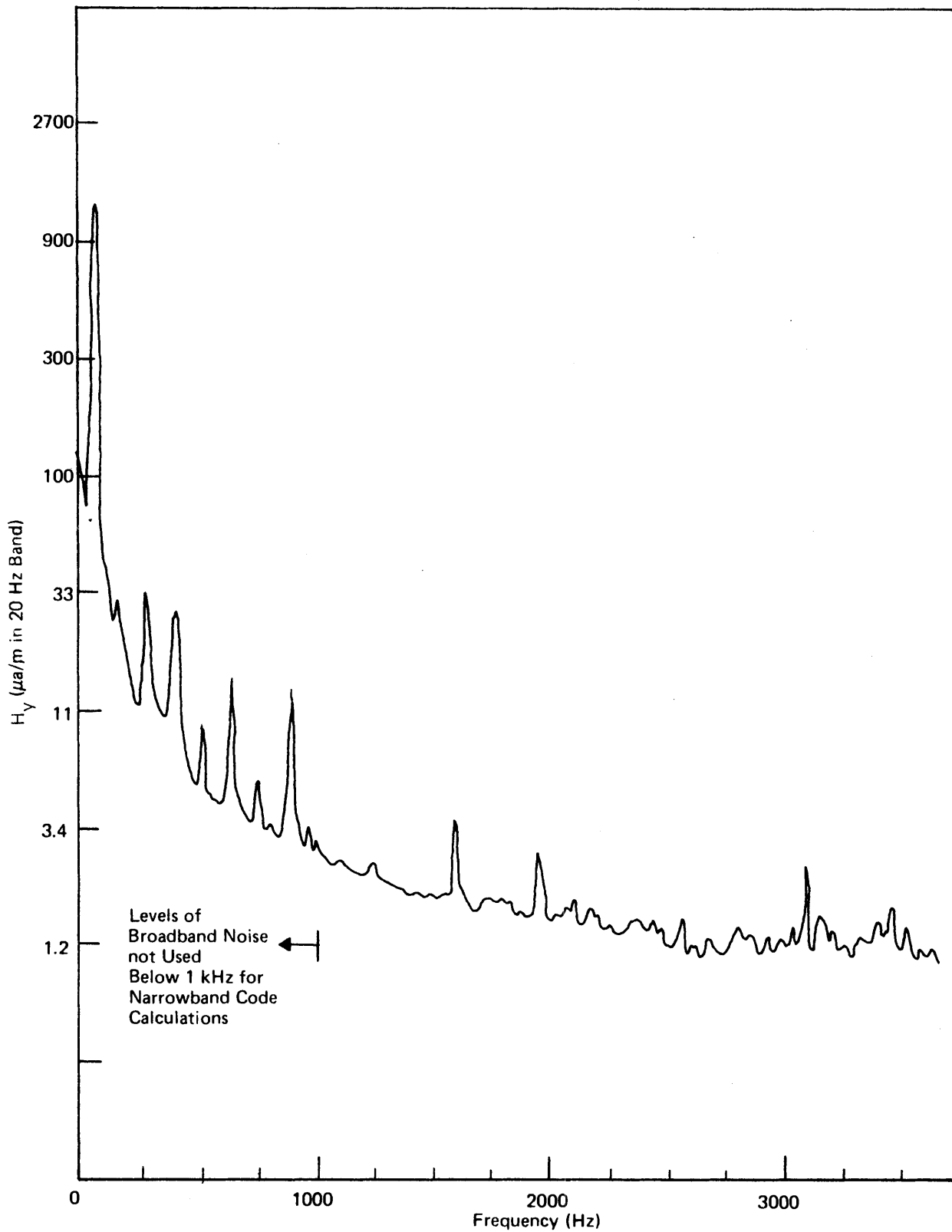


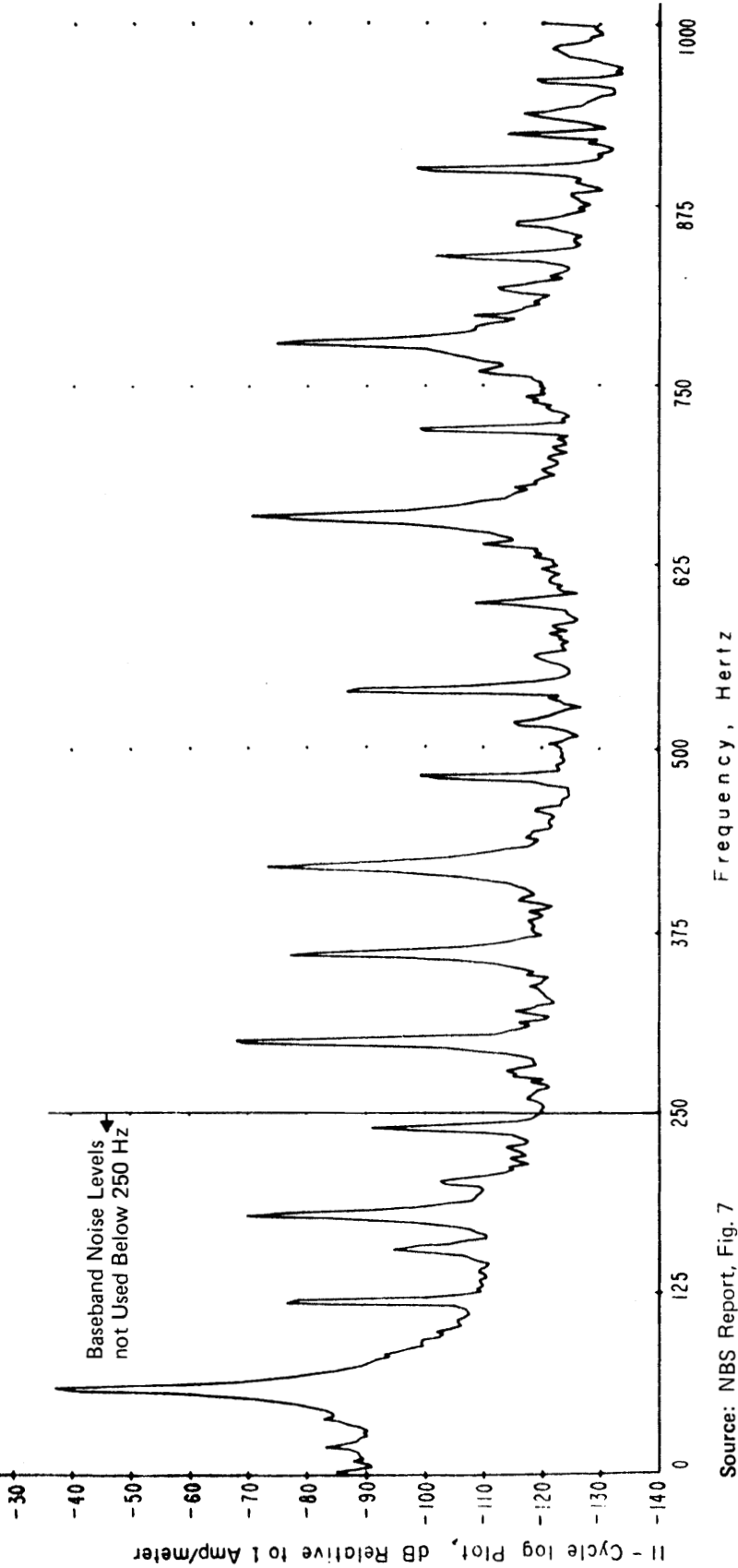
FIGURE 3-8 ALLEN MINE, UNDERGROUND, 750 Hz BW, 01-13
ANTENNA SENSITIVE AXIS POINTED VERTICAL



Source: Westinghouse Georesearch Laboratory (WGL)

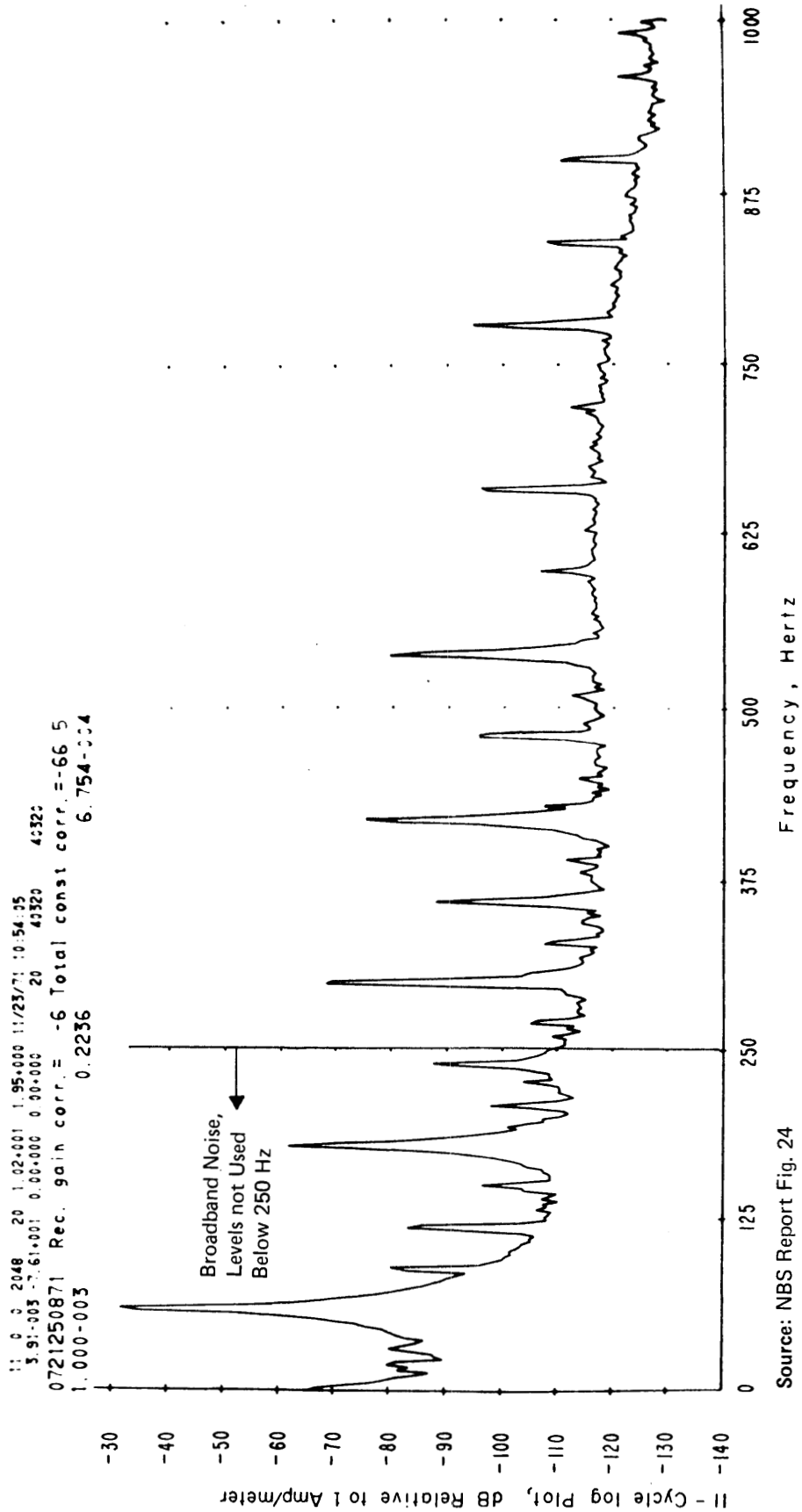
FIGURE 3-9 HORIZONTAL COMPONENT OF SUBSURFACE EM NOISE MAGNETIC FIELD, H_y , GUNN QUEALY MINE, ROCK SPRINGS WYOMING (Westinghouse Data)

11 5 0 2048 20 1.02+001 1.95+000 12/02/71 10 58.15 3
 3.91-003 -8.61+000 0.00+000 0.00+000 20 4.3325 4.3325
 0316210771 Rec. gain corr. = -12 Total const corr. = -76.3
 1.000-003 0.2236 1.876-004



Source: NBS Report, Fig. 7

FIGURE 3-10 ALLEN MINE, SURFACE, 750 Hz BANDWIDTH (BW), 03-16
ANTENNA SENSITIVE AXIS POINTED VERTICAL



Source: NBS Report Fig. 24

FIGURE 3-11 LINCOLN MINE, SURFACE, 750 Hz BW, 07-21
ANTENNA SENSITIVE AXIS POINTED VERTICAL

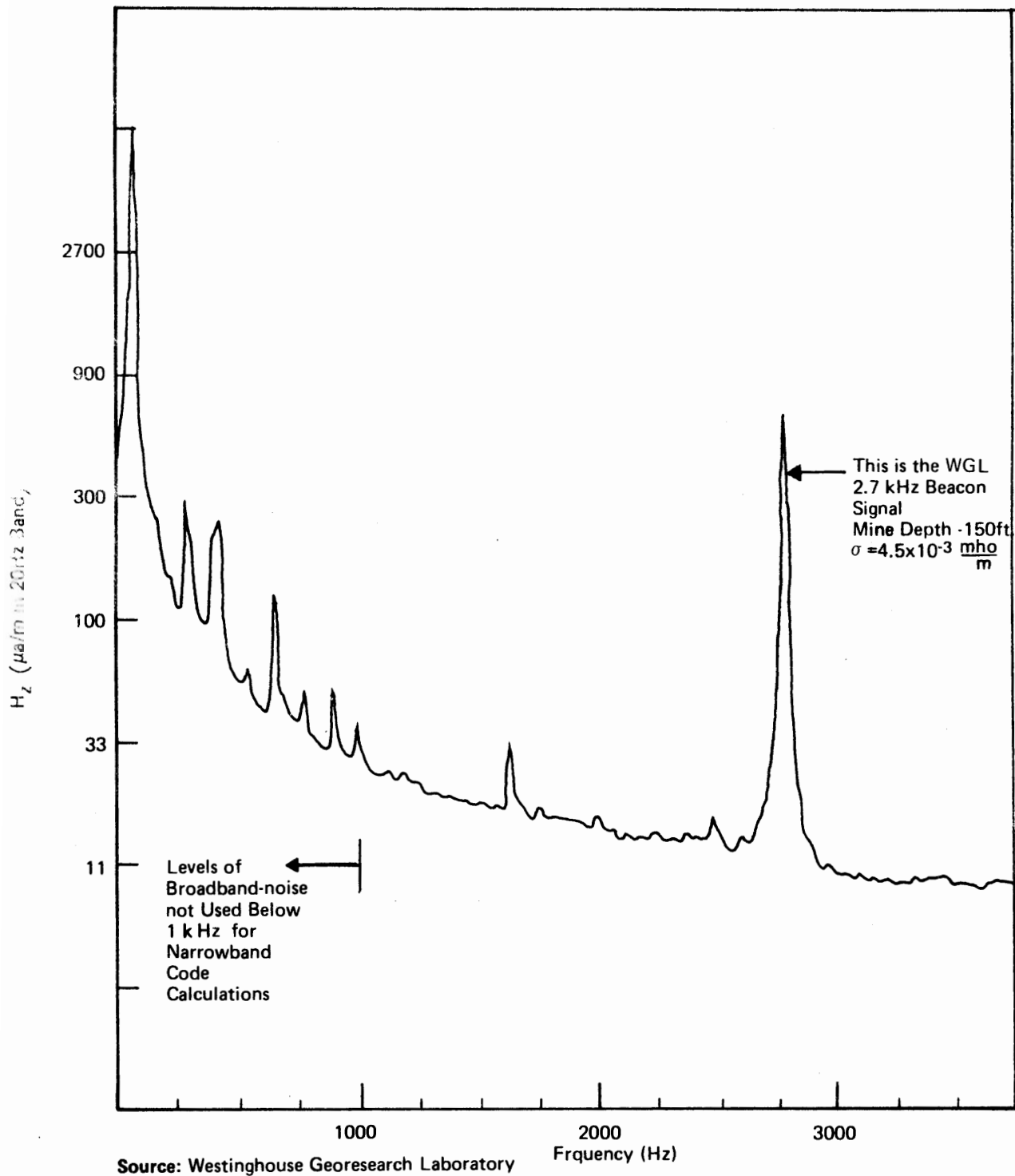
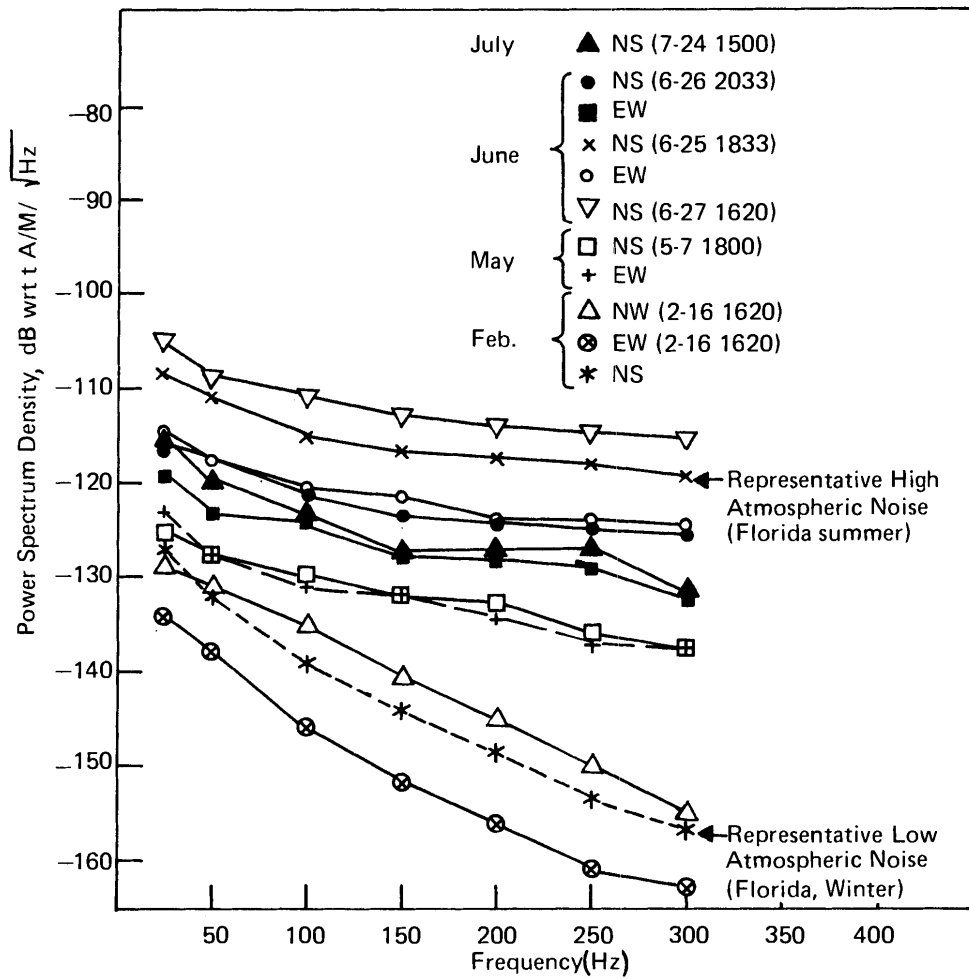


FIGURE 3-12 EM BACKGROUND NOISE ON SURFACE-VERTICAL COMPONENT, H_z , GUNN QUEALY MINE, ROCK SPRINGS, WYOMING



Source: Lincoln Laboratory - Evans, TN - 1969-18,26 March 1969 Fig. 4-3

FIGURE 3-13 WIDEBAND POWER DENSITY SPECTRUM FOR FLORIDA DATA (Feb., May, June, July 1968) MAGNETIC FIELD HORIZONTAL COMPONENTS

It is apparent from Figures 3-3 and 3-4 that in several instances the broadband noise density has not been plotted down to the minimum frequency at which noise measurements were made. For our plotting purposes, cut-off frequencies were chosen because of two factors which can significantly distort very-low-frequency broadband noise estimates made from the NBS and WGL plots. These can be illustrated by reference to Bensema's work. First, in the presence of a high-level harmonic (particularly 60Hz and 180Hz), the characteristics of the analysis filter used are such that the plotted level of the noise "floor" between harmonics may be raised significantly above its actual value. Secondly, as is apparent from the system test with the antenna disconnected (Figure 15, Bensema), tape recorder noise rises steeply below 100Hz, and may severely contaminate low-frequency broadband noise measurements under some conditions. Broadband noise levels between harmonic peaks at very low frequencies (e.g., below 250Hz or so), presented by NBS and WGL, may therefore represent upper limits, that are possibly 10db or more above the actual broadband noise floor. More-careful measurements, or reprocessing of existing noise recordings, are required before these low-frequency uncertainties can be removed.

B. SPOT SIGNAL-TO-NOISE RATIOS

The spot signal-to-noise ratios for the transmitter antennas and noise conditions just described are plotted in Figures 3-14 and 3-15 for the downlink and in Figures 3-16 and 3-17 for the uplink channels. In each case, two values of overburden conductivity have been used which represent moderate and high values (10^{-2} and 10^{-1} mhos/meter) for coal mine regions.

Figures 3-15 and 3-17 reveal that, for both the uplink and downlink channels, the optimum frequency for narrowband code communication systems for the deepest mines under conditions of high earth conductivity (10^{-1} mhos/meter) lies considerably below 1kHz. At a depth of 1,000 feet, a frequency on the order of 100Hz seems optimum. At a depth of only 300 feet there is little variation in the spot signal-to-noise ratio over frequencies in the range between 100 and 500Hz. The downlink channel calculation at moderate earth conductivity (10^{-2} mhos/meter), shown in Figure 3-14 indicates that a frequency near 1000Hz would be better than one in the 100-500Hz range. However, in all except the highest noise cases for deeper mines (i.e., Lincoln Mine noise at 600 and 1,000 feet), good spot signal-to-noise ratios of 10db or more are predicted down to a frequency of 200Hz. Note that this refers to a horizontal-wire antenna with a current of 1 ampere. A current of 4 amperes would provide a 10db spot signal-to-noise ratio at 200Hz even at 1,000 feet, under even Lincoln Mine high-noise conditions. The uplink channel calculation, shown in Figure 3-16, at moderate earth conductivity (10^{-2} mho/meter) demonstrates less sensitivity to frequency than the downlink case, and frequencies in the range of 100 to 1000Hz appear about equally satisfactory.

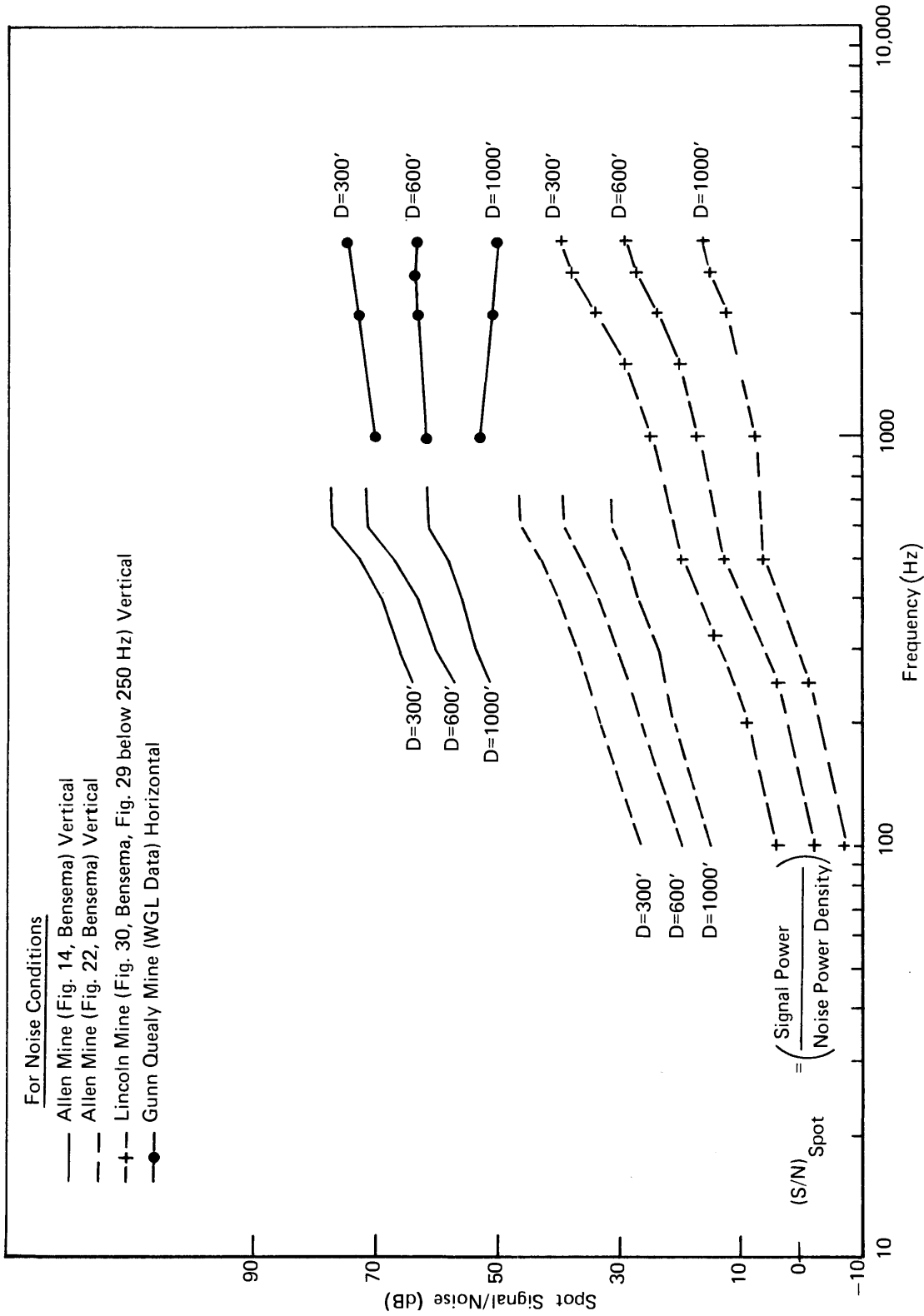


**FIGURE 3-14 DOWNLINK (IN MINE) SIGNAL TO NOISE RATIO FOR HORIZONTAL WIRE ANTENNA,
1 AMP. CURRENT (50 Watts for 50 ohm Resistance), OVERBURDEN CONDUCTIVITY
 $\sigma = 10^{-2}$ mho/meter**

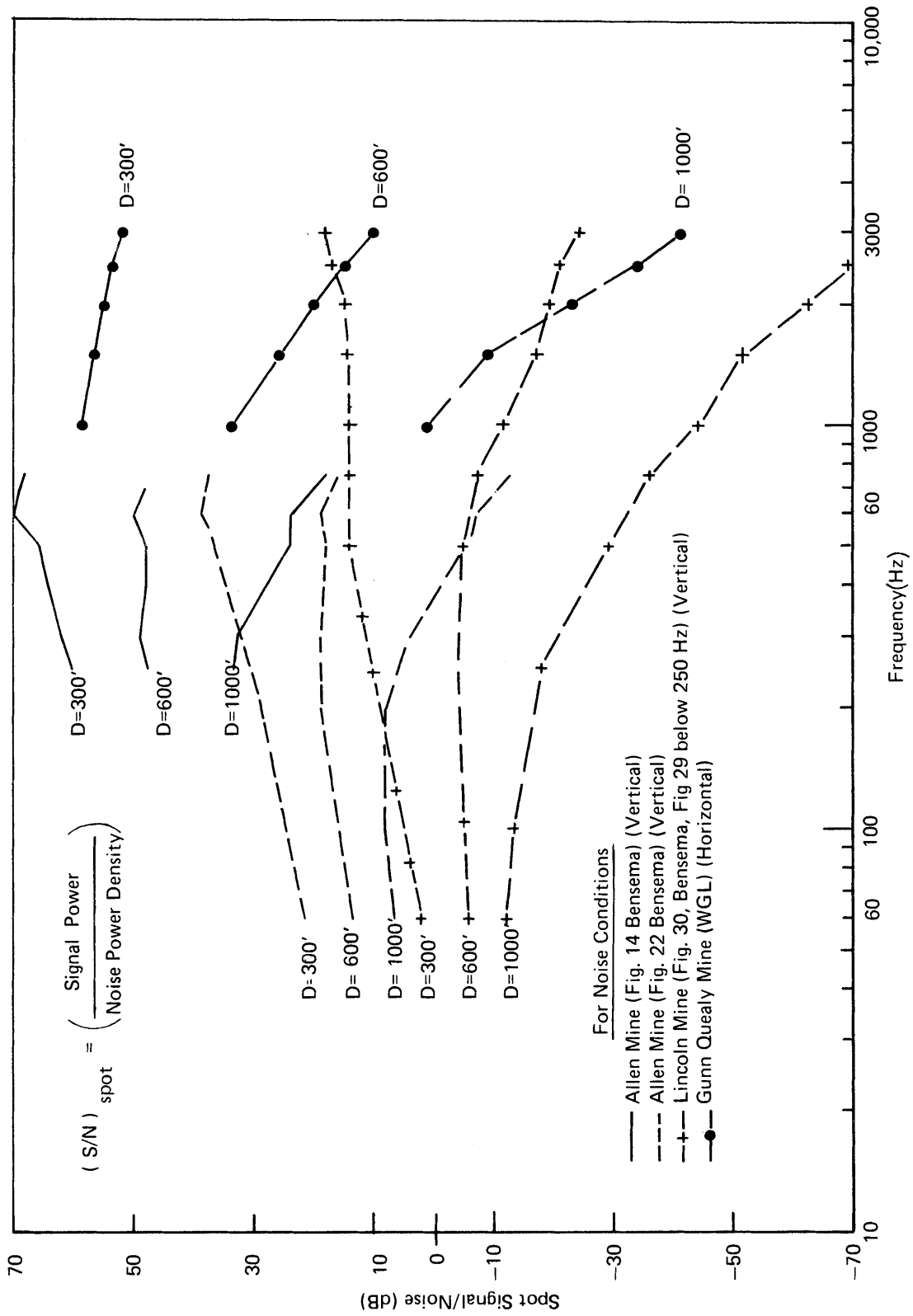


FIGURE 3-15 DOWNLINK (IN MINE) SIGNAL TO NOISE RATIO FOR HORIZONTAL WIRE ANTENNA,
 1 AMP CURRENT, $\sigma = 10^{-1}$ mho/meter

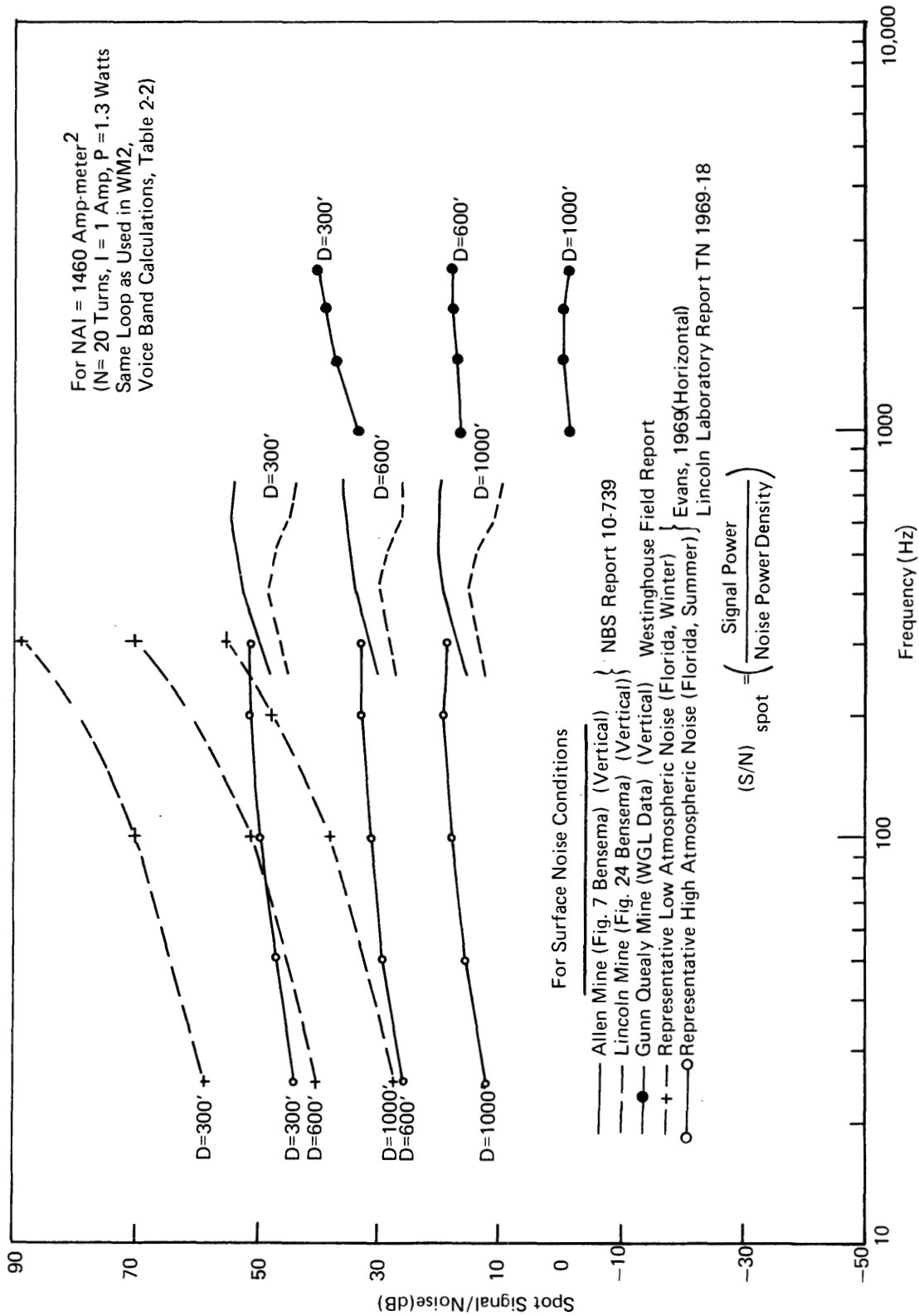


FIGURE 3-16 UPLINK SIGNAL-TO-NOISE RATIO FOR LOOP TRANSMIT ANTENNA, OVERBURDEN
 CONDUCTIVITY $\sigma = 10^{-2}$ mho/meter, LOOP MOMENT NAI = 1460 Amp-meter²

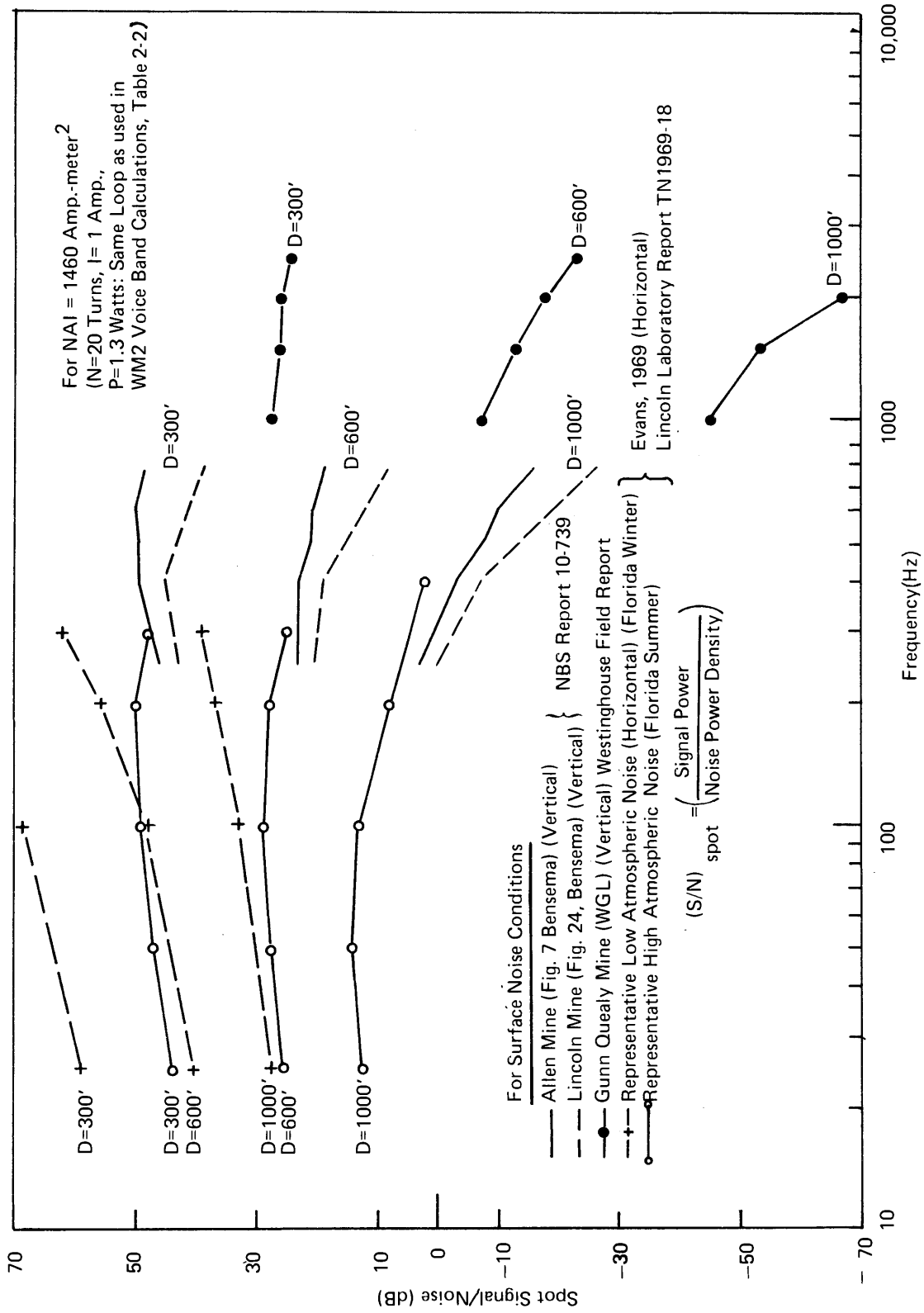


FIGURE 3-17 UPLINK SIGNAL-TO-NOISE RATIO FOR LOOP TRANSMIT ANTENNA, OVERBURDEN CONDUCTIVITY
 $\sigma = 10^{-1}$ mho/meter, LOOP MOMENT NAI = 1460 Amp-meter²

The spot signal-to-noise ratios plotted for Evans' noise measurements in Figures 3-16 and 3-17 are probably representative of the range of expected performance on the surface when broadband man-made noise is not dominant; the Florida Winter curve is characteristic of the cases when thunderstorms are distant, and the Florida Summer curve is characteristic of times of intense local thunderstorm activity. For communication via the vertical signal component, the S/N estimates are probably 12 to 20db too pessimistic, because the horizontal noise components (which are larger than the vertical) were used in the calculations. On the other hand, for EM location systems*that depend on detecting and locating a null in the horizontal component of signal magnetic field, the S/N curves are probably more than 30db too optimistic, because horizontal signal null depths can be more than 50db below the vertical component signal strength directly above a loop signal source.

C. CONCLUDING REMARKS

A generalized tentative conclusion is that frequencies on the order of 100 to 500Hz appear attractive for the design of narrowband code through-the-earth communications systems to cover a wide variety of mine depths, conductivities, and noise conditions. This holds for both uplink and downlink channels, and particularly under conditions of high-signal attenuation and high noise. The limited noise data available indicate that even for deep (1,000 ft) mines with high noise and conductivity, more-than-adequate signal-to-noise levels should be attainable for narrowband code systems with practical signal sources operating at 100 to 500Hz. However, for moderate conductivity mines, the data indicate that frequencies up to about 1-to-2kHz may provide improved performance.

If high conductivity, deep mine conditions assume a high priority, more accurate measurement of the broadband-noise power spectral density and/or processing of existing noise recordings at very low frequencies will be required to obtain more exact estimates of the noise densities; so that optimum frequency bands for narrowband code communications systems can be identified and selected with a higher degree of confidence. Since broadband man-made and atmospheric noise contributions are also nonstationary and non-Gaussian, it is important to obtain and utilize noise amplitude and time statistics, so that full advantage can be taken of existing methods for optimizing digital signaling in such noise environments.

This discussion has not touched on ways in which it may be possible to take advantage of certain broadband noise characteristics to improve the performance of narrowband code communications systems. For example, when broadband noise is highly impulsive in nature (which can be determined by observation and by measuring amplitude and time-interval exceedance probabilities), then it may be practical to use wideband-limiting

* Breadboard and prototype EM detection/location systems for trapped miners have been developed and tested for the Bureau of Mines by Westinghouse Georesearch Laboratory on Contract HO232049. In addition a miniaturized waveform generator is being developed for pre-production versions of the miner-carried EM location transmitter by Collins Radio Co. under Contract HO133045.

or other impulsive-noise-discrimination techniques to good advantage. Some of these techniques may not be usable in the presence of strong harmonic interference, but clearly they merit further investigation concerning their applicability and possible application.

IV. EFFECTS OF DIFFERENTIATION ON BASEBAND VOICE SIGNALS TRANSMITTED THROUGH THE EARTH FROM THE SURFACE TO MINES (DOWNLINK)

This Chapter of Part Two contains an extension of work on the downlink transmission of baseband voice signals from the surface to mines, as described in Chapter I. Calculations are presented of the effect on the signal-to-noise ratio across the 500Hz to 3kHz band of differentiating the voice signal at the transmitter, and differentiating both the signal and the noise on reception, including the influence of the receive loop. (Chapter I contained calculations of the ratio of the RMS signal to RMS noise magnetic field.) The effect of the overburden is essentially to integrate the transmitted signal, i.e., favor lower frequency components.

As discussed in Chapter I, spectrum shaping techniques should be examined, in order to determine whether significant increases in the intelligibility of voice communications can thereby be obtained, which will enable reasonably intelligible communication to be achieved at practical power levels even to deep mines (1000 feet) under high noise conditions.

A. RECEIVE LOOP OUTPUT

The induced voltage in the loop can be written

$$V = j\omega an\mu_0 H \text{ volts} \quad (1)*$$

where a is the area, and n the number of turns in the loop. Hence, the RMS signal voltage is

$$V_{\text{rms}}^S = 8\pi^2 \times 10^{-7} an \left[\int_{500}^{3000} f^2 H^2(f) df \right]^{1/2} \quad (2)$$

Assume $n = 1$, $a = 1 \text{ meter}^2$, and consider the following cases.

1. Signals

(a) Transmitted Signal as in Chapter I, i.e., with the same notation

$$I = \frac{S_o}{f}, \quad H(f) = \frac{S_o |A|}{2\pi Df} \quad (3a, b)$$

* References to Figures, Tables, and Equations apply to those in this Chapter unless otherwise noted.

so that

$$V_{\text{rms}}^s = \frac{8\pi^2 \times 10^{-7}}{2\pi D} S_o \left[\int_{500}^{3000} |A|^2 df \right]^{1/2}. \quad (4)$$

Hence, with an overburden conductivity of $\sigma = 10^{-2}$ mhos/meter, the received signal voltage is

<u>Depth D, feet</u>	<u>V_{rms}^s, volts $\times \frac{10^{-7}}{8\pi^2}$</u>	
300	0.080 S_o	<u>Table 4-1</u>
600	0.0287 S_o	
1000	0.0102 S_o	

(b) Signal Differentiated Before Transmission

$$I = S_1, \quad H(f) = \frac{S_1 |A|}{2\pi D} \quad (5a, b)$$

Hence,

$$V_{\text{rms}}^s = \frac{8\pi^2 \times 10^{-7}}{2\pi D} S_1 \left[\int_{500}^{3000} f^2 |A|^2 df \right]^{1/2} \quad (6)$$

For $\sigma = 10^{-2}$ mhos/meter, it follows that:

<u>Depth D, feet</u>	<u>V_{rms}^s, volts $\times \frac{10^{-7}}{8\pi^2}$</u>	
300	151.8 S_1	<u>Table 4-2</u>
600	46.23 S_1	
1000	13.47 S_1	

(c) Signal Differentiated Twice Before Transmission

$$I = S_2 f, \quad H(f) = \frac{S_2 f |A|}{2\pi D} \quad (7a, b)$$

Hence

$$V_{\text{rms}}^s = \frac{8\pi^2 \times 10^{-7}}{2\pi D} S_2 \left[\int_{500}^{3000} f^4 |A|^2 df \right]^{1/2} \quad (8)$$

For $\sigma = 10^{-2}$ mhos/meter, it follows that:

<u>Depth D, feet</u>	V_{rms}^s , volts $\times \frac{10^7}{8\pi^2}$
300	$3.527 \times 10^5 S_2$
600	$9.91 \times 10^4 S_2$
1000	$2.55 \times 10^4 S_2$

Table 4-3

2. Noise

The differentiation by the receive loop affects the noise output as follows; using a loop with a and n set equal to $1m^2$ and 1 respectively as above, and the noise data of Chapter I, we get:

(a) Harmonic Noise Components

$$V_{rms}^n = 8\pi^2 \times 10^{-7} \sqrt{\sum_i f_i^2 h_i^2} \quad (9)$$

Allen Mine, Colorado - W.D. Bensema (NBS measurements)*

$$V_{rms}^n = 8\pi^2 \times 10^{-7} \times 0.07 \text{ volts (low harmonic noise, Figure 16)}$$

$$V_{rms}^n = 8\pi^2 \times 10^{-7} \times 1.03 \text{ volts (high harmonic noise, Figure 23)}$$

(b) Noise Primarily Broadband Impulsive

$$\text{If } N = N_1 e^{-N_2 f} \text{ A/M} / \sqrt{\text{Hz}} \quad (10)$$

$$V_{rms}^n = 8\pi^2 \times 10^{-7} N_1 \left[\int_{500}^{3000} f^2 e^{-2N_2 f} df \right]^{1/2} \quad (11)$$

Lincoln Mine, Colorado - Figure 30 Bensema's Report

$$N_1 = 0.000316; N_2 = 0.00115$$

so that

$$V_{rms}^n = 8\pi^2 \times 10^{-7} \times 3.75 \text{ volts}$$

* Ref. I-1, NBS Report 10-739.

B. RECEIVE LOOP OUTPUT DIFFERENTIATED

Differentiating the received signal and noise once upon reception, in addition to the differentiating effect of the receive loop, provides greater emphasis to the higher frequencies of the noise and signal spectra.

1. Signal and Noise

The RMS signal-to-noise ratio may then be written

$$S/N = \frac{[\int_{500}^{3000} f^4 H(f)^2 df]^{1/2}}{N_{rms}} \quad (12)$$

where

$$N_{rms} = \sqrt{\sum_i f_i^4 h_i^2} \quad (\text{harmonic noise}) \quad (13)$$

$$= N_i [\int f^4 e^{-2N_2 f} df]^{1/2} \quad (\text{broadband noise of the type considered before}) \quad (14)$$

(a) Transmitted Signal as in Chapter I

We will assume that the original transmitted signal is the 1/f approximation to the voice spectrum, so that

$$H(f) = \frac{S_o |A|}{2\pi Df} \quad (15)$$

C. SIGNAL-TO-NOISE RATIO CALCULATIONS

Calculations of the signal-to-noise voltage ratio for examples of the situations discussed above are presented in Table 4-4 ($\sigma = 10^{-2}$ mhos/meter).

The values of the constants S_o , S_1 , and S_2 are chosen so that the RMS current, and therefore power, into the wire antenna is equal to its values in Chapter I under the same noise conditions. These were calculated to yield an RMS signal-to-noise magnetic field ratio of 4 (16 in terms of power or 12db). Figure 4-1 shows the effect of receive loop differentiation on the earth attenuation response and on an example of a broadband noise spectrum. Figure 4-2 demonstrates the shape of the original and differentiated voice spectra as transmitted and received at one selected mine depth, keeping the power fed into the antenna constant.

TABLE 4-4
VOICE BAND

SIGNAL-TO-NOISE RATIOS IN DB
FOR SEVERAL DIFFERENTIATION CONDITIONS (1)

Transmit Conditions	No Differentiation			Diff. Once	Diff. Twice	Mine Depth (Feet)
	Fields at (1) Receive Loop (dB)	Output of Receive Loop (dB)	Output of Receive Loop Differentiated Once (dB)			
<u>Noise Conditions</u>						
Allen Mine, Figure 16 Low Harmonic Noise	12 12 12	14.5 13.0 11.9	17.6 14.7 11.9	18.3 15.4 12.6	20.0 16.5 12.6	300 600 1000
Allen Mine, Figure 23 High Harmonic Noise	12 12 12	13.9 12.3 11.1	17.7 14.6 11.9	17.7 14.6 11.78	19.5 15.7 11.8	300 600 1000
Lincoln Mine, Figure 30 Broadband Impulsive Noise	12 12 12	13.5 12.1 11.0	15.7 12.9 10.0	17.3 14.5 11.6	19.1 15.6 11.6	300 600 1000

(1) Transmitter gain adjusted to keep transmit antenna input power equal to those (computed in Chapter I) that are required to achieve the 12db field signal-to-noise ratio (column 1) under each of the listed noise and depth conditions.

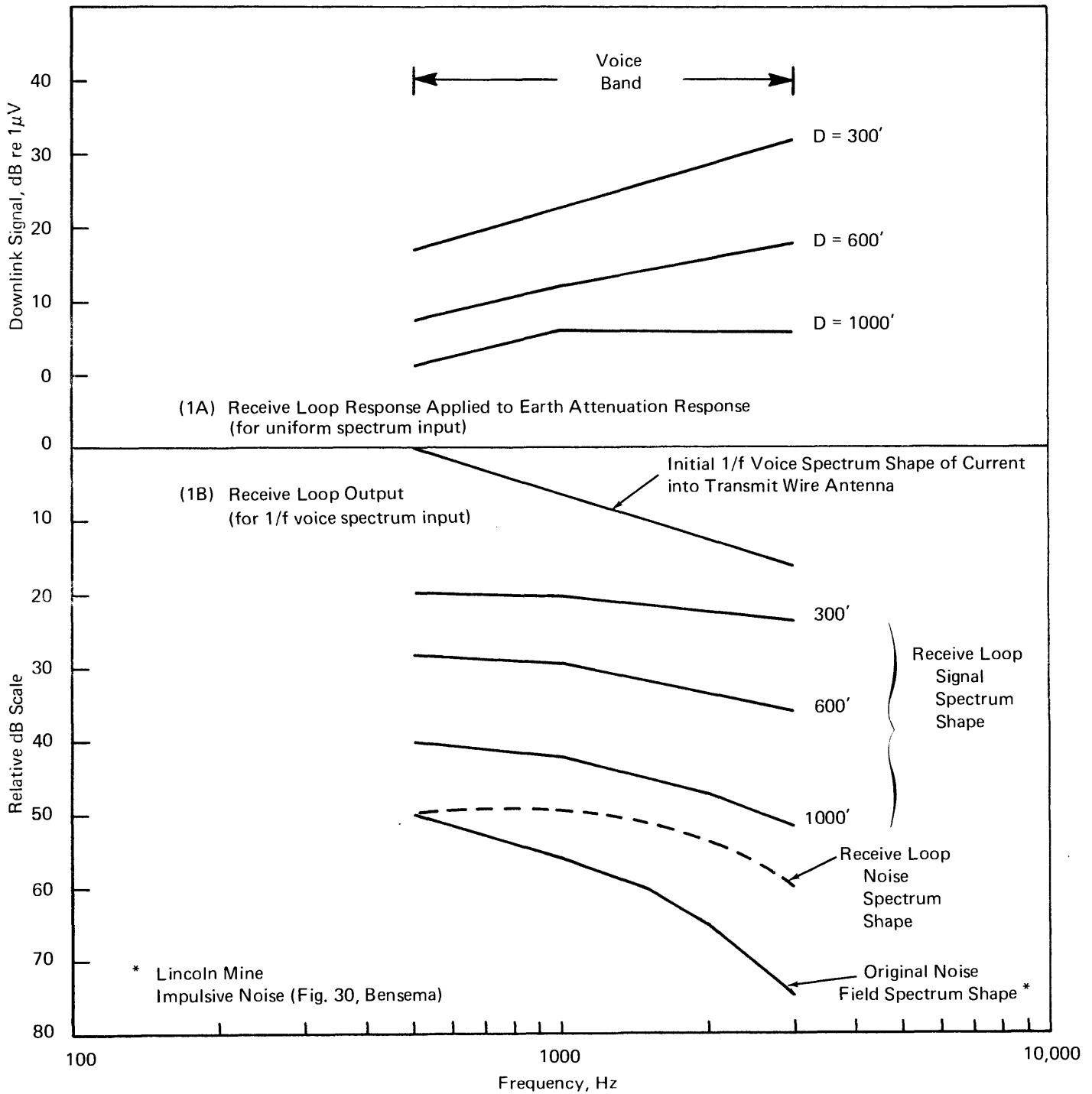


FIGURE 4-1 EFFECTS OF RECEIVE LOOP DIFFERENTIATION ON THE EARTH ATTENUATION RESPONSE AND ON A BROADBAND NOISE SPECTRUM, One-Turn Receive Loop, Area 1 Meter², Long-Wire Transmit Antenna, 1 amp. Current, $\sigma = 10^{-2}$ mhos/meter

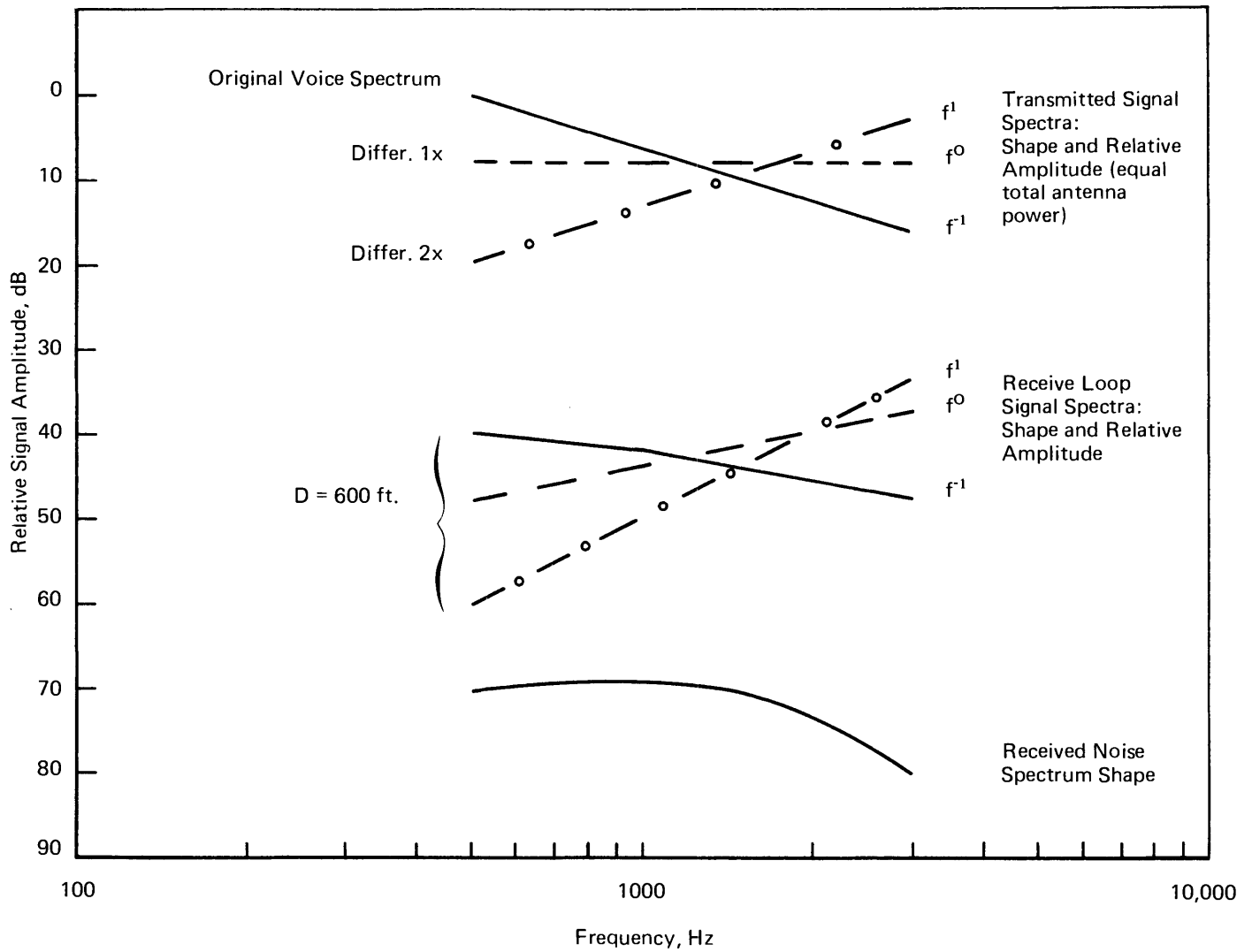


FIGURE 4-2 SHAPES OF ORIGINAL AND TRANSMITTED VOICE SPECTRA
 DOWNLINK: WIRE ANTENNA, $\sigma = 10^{-2}$ mho/meter

D. DISCUSSION

The results shown in Table 4-4 indicate that in deep mines or over long through-the-earth communications paths, there is nothing to be gained, and indeed something to be lost by differentiation either before transmission or upon reception or both. On the other hand, at lesser mine depths (300-600 feet), the signal-to-noise ratio is increased significantly by differentiation both before transmission and upon reception. Hence, under these circumstances, it may be possible to use differentiation to reduce power requirements for communications, and thus use less expensive communications gear than would otherwise be the case. It should be pointed out that the depth at which differentiation will lose its effectiveness will be a function of the conductivity of the overburden, which in these calculations has been fixed at 10^{-2} mhos/meter.

Thus far in the discussion, it has been assumed that the total signal-to-noise ratio over the voiceband is the measure of "goodness" or intelligibility of a received voice signal. In fact the intelligibility of a voice signal is a somewhat more subtle and complex phenomenon than can be explained by this straightforward criterion. In the work immediately following we describe and evaluate indices of the intelligibility of speech which enable more realistic estimates of the effectiveness of a voice communications system to be generated.

V. INTELLIGIBILITY OF THROUGH-THE-EARTH ELECTROMAGNETIC COMMUNICATIONS TO MINES (DOWNLINK)

Previous work in this report has presented calculations of the estimated power requirements for through-the-earth electromagnetic communications systems for various noise conditions and mine situations, using the simple criterion of a 12 dB speech signal-to-noise ratio across the voiceband of 500 to 3,000Hz as an indicator of "acceptable quality" of communication. However, the signal-to-noise ratio does not provide a meaningful index to the intelligibility of speech to be expected under widely differing noise conditions. For example, high noise intensities above a certain level produce a proportionately greater degree of masking; also masking at any one point on the frequency scale can be affected by bands of noise at higher or lower frequencies. Hence, in designing a voice communication system, it is essential to use a more broadly-based criterion for intelligibility, or the extent to which listeners correctly perceive the intended messages. Since the perception of speech is a psychological problem, precise quantitative procedures cannot provide for all possibilities in communications systems. Nevertheless, by appropriate test procedures, good results can be obtained for most communications systems on the effects of a number of system parameters.

A. BACKGROUND

A common procedure is to measure the percentage of words or individual speech sounds uttered by a talker which are perceived correctly by most listeners, using for example, a set of phonetically balanced word lists. The percentage of words heard correctly is termed percent word articulation.

From the results obtained in such experiments and information on the nature of speech and hearing, it has been possible to develop methods for computing from acoustical measurements a measure that is highly correlated with the intelligibility of speech as evaluated by speech perception tests. This measure, the Articulation Index (AI) is a weighted fraction which represents, for a given speech channel and noise condition, the effective proportion of the normal speech signal which is available to a listener for conveying speech intelligibility. The AI is computed from measurements or estimates of the speech spectrum and of the effective masking spectrum of noise that may be present at the ear of the listener.

Several methods are available for calculating AI, the most appropriate one being dependent upon the particular situation being evaluated. AI's give reasonable predictions of the effects of broadband continuous spectrum noise, and of bands of noise as narrow as 200 Hz, in the frequency range from about 200Hz to 6kHz. When the noise is not steady state, but its "duty cycle" or "burstiness" is known, corrective factors may be applied to the AI computed as if the noise were

steady state. AI's may be converted to estimated speech intelligibility scores (based principally upon male talkers) by use of Figure 5-1.* It should be noted that no single AI value can be specified as a criterion for an "acceptable" quality of communications. The efficiency of communications is a function of the messages to be transmitted, including the size of message set, and the proficiency of the talkers and listeners involved. Furthermore, "acceptable quality" must be established in terms of minimum level of intelligence and grade of service, which vary from application to application.

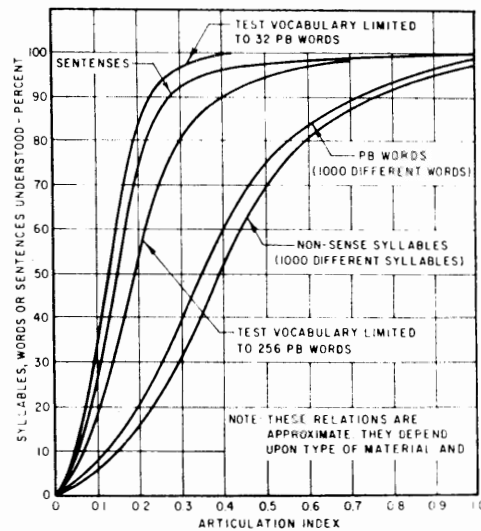


FIGURE 5-1 RELATION BETWEEN AI AND VARIOUS MEASURES OF SPEECH INTELLIGIBILITY (REF. 1)

Two criteria of acceptability are presented here:

- (a) Discrete word and sentence intelligibility expected, including preservation of sufficient tonal quality to permit recognition of the particular voice and transient emotions of the speaker (corresponding essentially to public telephone service requirements).
- (b) Discrete word intelligibility is desirable, but sentence intelligibility may be acceptable. Recognition of a particular voice or tonal quality is not essential.

Criterion (b) is probably close to that appropriate for mine communications systems.

(1) K.D. Kryter, J. Acoust. Soc. Am. 34 (1962) 1689-97.

* References to Figures, Tables, and Equations apply to those in this Chapter unless otherwise noted.

Naturally, it is also possible to measure directly the intelligibility performance of a given communications system, by articulation tests similar to the ones described above, carried out in conditions simulating normal use of the communications equipment. These tests, because of uncontrollable variables in the environment, talker, and listeners require very careful design to permit a statistical test for significance.

B. ARTICULATION INDEX: METHOD OF COMPUTATION

A basic method for computing AI's which seems to be applicable under many of the circumstances relevant to coal mine communications is the 20-band method (2). This is based on measurements or estimates of the spectrum level of the speech and noise present in each of twenty contiguous bands of frequencies that contribute equally to speech intelligibility at equal signal-to-noise ratios.

These bands are given in Table 5-1. Note that the contents of this table and the following discussion refer to male voices.

<u>Band No.</u>	<u>Limits</u>	<u>Mid-Frequency</u>	<u>Band No.</u>	<u>Limits</u>	<u>Mid-Frequency</u>
1	200 to 330 cps	270 cps	11	1660 to 1830 cps	1740 cps
2	330 to 430	380	12	1830 to 2020	1920
3	430 to 560	490	13	2020 to 2240	2130
4	560 to 700	630	14	2240 to 2500	2370
5	700 to 840	770	15	2500 to 2820	2660
6	840 to 1000	920	16	2820 to 3200	3000
7	1000 to 1150	1070	17	3200 to 3650	3400
8	1150 to 1310	1230	18	3650 to 4250	3950
9	1310 to 1480	1400	19	4250 to 5050	4650
10	1480 to 1660	1570	20	5050 to 6100	5600

Table 5-1: Twenty Frequency Bands of Equal Contribution to Speech Intelligibility [from Beranek (3)]

The average speech spectrum (1/f approximation, Chapter I) which has been used in computations until now is based on stable, long-term speech spectra obtained by integration over periods of one minute or more. In fact, the ear appears to integrate over shorter periods of about 1/8 sec. (the average duration of a phoneme). When RMS levels are taken over 1/8 sec. intervals, it is found that 1% of the short-term RMS values exceed the long-term RMS value by 12 dB or more. Hence, this value average RMS plus 12dB, is used to represent the peak levels of speech which are used in computations of AI's.

(2) N.R. French and J.C. Steinberg, J. Acoust. Soc. Am. 19 (1949), 90-119.

(3) L.L. Beranek, Proc. IRE 35 (1947), 880-890.

The fundamentals of the twenty-band method for AI computation are as follows, in greatly simplified form (Ref. 1):

- (1) The RMS speech peak spectrum level signal at the listener's ear is plotted.
- (2) The spectrum level of the steady state noise reaching the listener's ear is plotted, and the masking spectrum of the noise drawn as follows:
 - (a) Find the extreme right-hand point at which a horizontal line 3dB below the maximum of the noise spectrum intersects the noise spectrum.
 - (b) Drop 57dB vertically from this starting point, and then draw a line to the left, sloping upwards at 10dB per octave. This line is the low frequency part of the masking spectrum.
 - (c) Also draw a line to the right from this point, first horizontally and then downward. The length of the horizontal portion of this line and the slope of its downward portion depend upon the frequency of the starting point and the maximum spectrum level of the noise as shown in Table 5-2. This line represents the high frequency part of the masking spectrum.
- (3) Determine at the mid-frequency of each of the twenty frequency bands shown in Table 5-1 the difference Δ in dB between the spectrum level of the speech peaks and that of the noise spectrum or the masking spectrum, whichever is higher.

If $\Delta \leq 0$, set $\Delta = 0$.

If $\Delta \geq 30$, set $\Delta = 30$.

- (4) The articulation index is given by

$$AI = \frac{1}{600} \sum_{i=1}^{20} \Delta_i \quad (1)$$

C. ARTICULATION INDEX: SPECIFIC CALCULATIONS

The above method has been applied to a few examples of cases previously discussed for through-the-earth downlink electromagnetic communications to mines, and the results are shown in Figures 5-2 and 5-3. In Figure 5-2, the magnetic field signal was taken to be the speech signal, whereas in Figure 5-3 the receive loop voltage played this role. No low frequency masking spectra are shown, because they play no role for the Lincoln Mine* noise spectrum which was chosen as an example. The high frequency masking spectra were drawn under the arbitrary assumption that the actual maximum level of the noise sound pressure would lie between 76-85 dB re 0.0002 μ bar, a comfortable listening level.

* Ref. I-1, NBS Report 10-739.

It should be emphasized that the optimum overall level at which the signal (and noise) should be delivered to the listener has not been considered here. Thus, for example, no notice has been taken of corrections which may have to be applied to take account of the faster rate of increase in the masking effectiveness of sound when the band sensation level of the sound exceeds 80dB re 0.0002 μ bar. Also no account has been taken of ambient audio noise in the mine environment, (as against the electromagnetic noise considered here which is converted into audio noise by the communications receiver) which may also affect communications intelligibility.

Maximum spectrum level or masking level, which- ever is higher, of noise above 0.0002 μ bar in dB	Frequency of starting point located in Step 3									
	50-800Hz		800-1600Hz		1600-2400Hz		2400-3200Hz		3200-5200Hz	
	A ^a	B ^b	A ^a	B ^b	A ^a	B ^b	A ^a	B ^b	A ^a	B ^b
96dB - ..	250	10	500	8	1000	5	1500	3	3000	0
86 - 95	200	15	500	13	1000	10	1500	5	3000	0
76 - 85	200	20	400	18	800	15	1500	10	3000	0
66 - 75	150	25	250	23	500	20	1000	15	2000	5
56 - 65	75	35	150	30	300	25	500	25	800	20
46 - 55	50	45	100	40	200	35	200	40	200	40

^a Draw from starting point horizontal line to right for this number of Hz.

^b Draw from right-hand end of horizontal line a downward line that has this slope in dB/octave

Table 5-2: High-Frequency Part of Masking Spectrum--
Upward Spread of Masking (Ref. 1)

Calculations of the articulation index were carried out for a voice bandwidth of 500-3000Hz. This corresponds to bands 4 through 15, plus about half of band 3 and band 16 shown in Table 5-1. The signal-noise spectrum difference Δ was set equal to zero for all bands other than these, and given half its actual value at 500Hz and 3000Hz for the two end bands. The articulation index has a theoretical maximum value of 0.65 under these conditions.

The articulation index was computed for two cases with equal total power into the transmit wire antenna:

Case A: 1/f voice spectrum transmitted : AI = 0.47

Case B: Differentiated (flat) voice spectrum : AI = 0.49

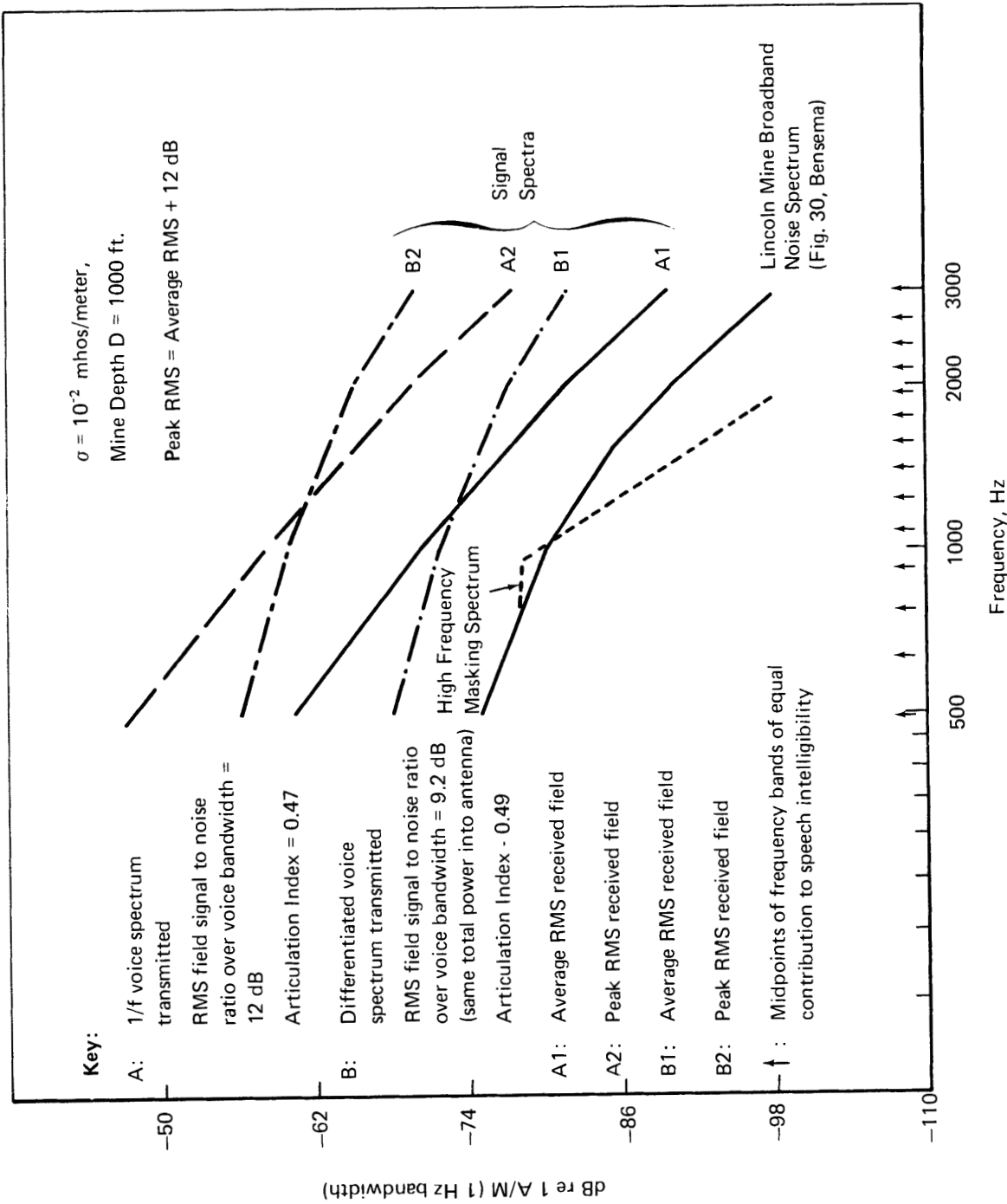


FIGURE 5-2 RECEIVED MAGNETIC FIELD SPECTRA

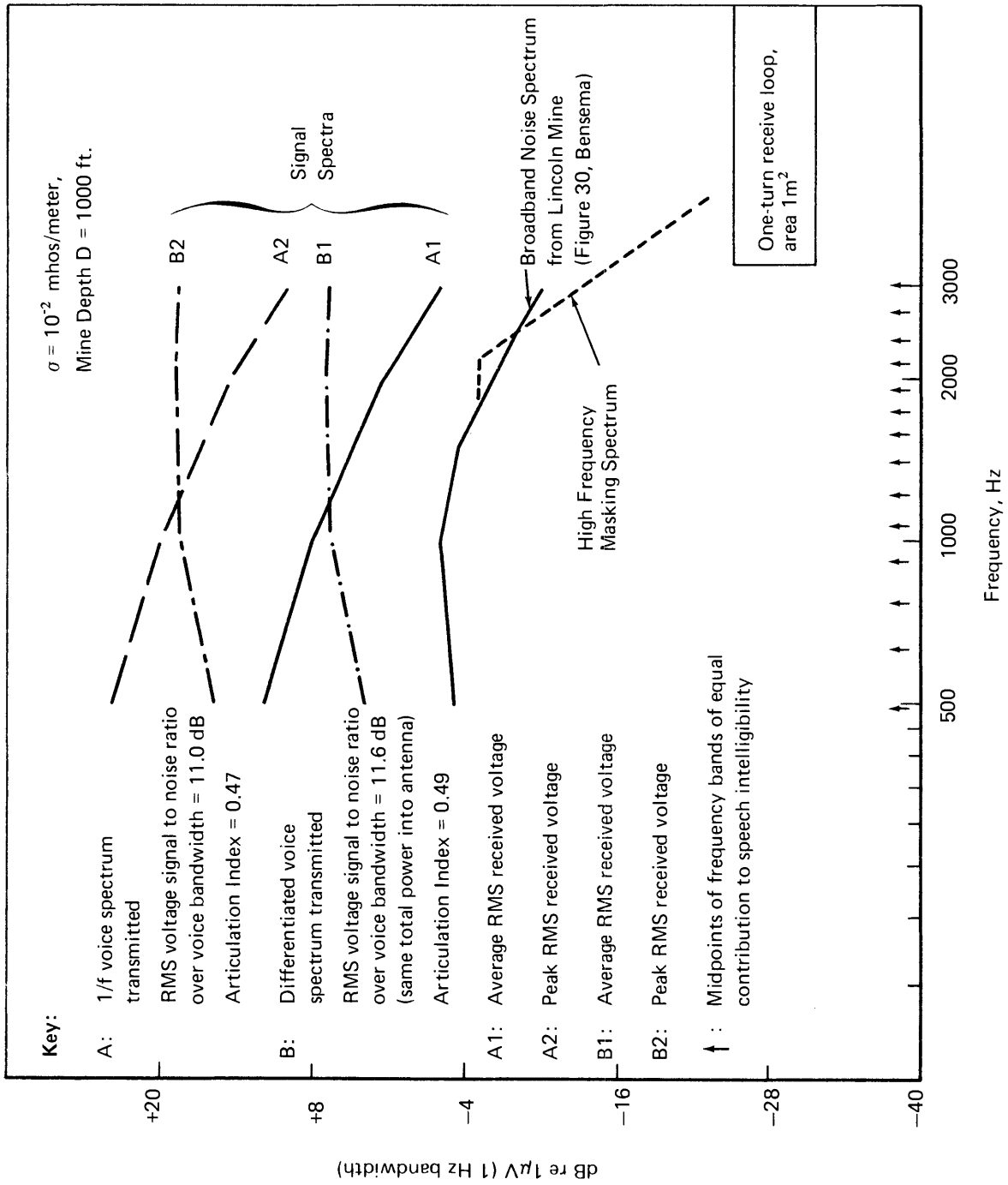


FIGURE 5-3 RECEIVE LOOP VOLTAGE SPECTRA

The articulation index is essentially unchanged for both cases whether the magnetic field or the receive loop voltage is taken as the speech signal. In the method of calculation described above, since the receive loop performs the same operation on both the signal and the noise spectra, the articulation index can only be changed by differences in the effects of the masking spectra between Figures 5-2 and 5-3. It can be seen that the masking spectrum has only a small influence in both situations; hence, the articulation index is not affected by the receive loop differentiation. This result would not necessarily hold for all noise spectra of interest.

In both instances Case B (the differentiated voice spectrum) exhibits a slightly greater AI than Case A although its signal-to-noise ratio over the voice bandwidth is 9.2dB in Figure 5-2 (as against 12dB for Case A), and 11.6dB in Figure 5-3 (Case A is now down to 11.0dB). Hence, it is clear that the AI is a noticeably different criterion for speech intelligibility than the overall spectrum signal-to-noise ratio. The relation between AI and various measures of speech intelligibility was shown in Figure 5-1.

While no single value of the AI can be specified as a criterion for acceptable communications, as a rough guide (Ref. 3) a communications system with an AI of less than 0.3 should be considered unsatisfactory for everyday speech communications, an AI of between 0.3 and 0.5 should be regarded as barely acceptable, and an AI greater than 0.5 should be rated as satisfactory. The criteria of acceptability for mine communications may, of course, be somewhat less stringent than for "everyday" speech.

D. SPEECH PEAK CLIPPING

Sharp, symmetrical speech peak clipping (amplitude limiting), while it affects the quality or naturalness of speech markedly, does not greatly reduce intelligibility. In fact, the articulation score of monosyllabic words heard in quiet at a comfortable listening level is reduced to about 70% even with infinite peak clipping, where the speech has been reduced to a succession of rectangular waves.

The value of peak clipping on transmission can be appreciated from two viewpoints:

- (a) In order to reproduce the speech spectrum faithfully with, say X watts RMS output power, an amplifier has to be capable of about 10X or more watts in order to cope with the peaks of the speech. To avoid the added expense involved, it is possible to clip the speech spectrum and remove these peaks, with essentially no effect on the average RMS output power, and little effect on the intelligibility of the received speech.
- (b) Alternatively, if the maximum capability of the amplifier is to be used effectively, the speech can be clipped and then post-amplified, so that the average RMS power is more nearly equal to the peak power. There can then be a significant increase in the intelligibility of the received speech, at the cost, of course, of a greater overall power requirement.

In other words, if the communication system has insufficient amplitude handling capacity to pass the peaks of the speech wave and still provide an adequate intensity level, the best intelligibility is obtained by clipping off the peaks and using the available power for the remainder of the wave.

Intelligibility is very resistant to peak clipping; at a comfortable listening level, 95% of monosyllabic words are heard correctly even after 24dB peak clipping, and 70% of the words can be understood even after infinite peak clipping, as mentioned above. Greater care has to be taken in evaluating the effects of peak clipping in the presence of significant amounts of noise. If the noise enters the system at the talker's end of the line, intermodulation resulting from the non-linear clipping circuit may have severe effects on intelligibility; on the other hand, if this noise consists largely of sharp pulses, the interaction will be more favorable since the peak clipping can then get rid of more noise than speech. The situation with respect to severe background noise at the listener's end of the line can be ameliorated by peak clipping followed by amplification so that low level portions of the speech signal, previously masked by noise, may now be heard. Advantages can also accrue from peak clipping upon reception in situations where noise picked up at the listener's end of the transmission link is highly impulsive in nature.

The increase in intelligibility obtainable by use of peak clipping (situation (b)) has been calculated for the mine communications cases considered above. Figure 5-4 shows the increase in the long-term or average RMS speech level as a result of peak clipping and post-clipping amplification which equates the clipped and unclipped speech waves in peak-to-peak amplitude. Essentially, an increase in average transmitting power with no increase in overload capabilities buys an increase in intelligibility.

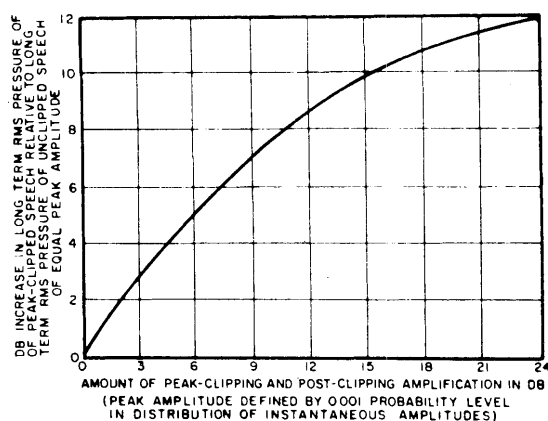


FIGURE 5-4 INCREASE IN RMS SPEECH POWER AS A FUNCTION OF CLIPPING WHEN CLIPPED LEVEL IS RAISED TO CLIPPING REFERENCE LEVEL (REF. 1)

The effect of this type of clipping may be applied to the computations of AI for coal mine communications discussed above. All that is required, in Step 1 of the computation process, is to add to the speech peaks the increase in the long-term RMS speech level as derived from Figure 5-4 for the selected amount of peak clipping and equal post-clipping amplification, and then proceed as before.

The results are shown in Table 5-3 for the signal and noise conditions of Figures 5-2 and 5-3.

Table 5-3: The Effects on Speech Intelligibility of Peak Clipping with Equal Post-Clipping Amplification

Increase in Average Power Required	<u>No Peak Clipping</u>		<u>12 dB Peak Clipping</u>		<u>24 dB Peak Clipping</u>	
	0 dB		8.5 dB		12.0 dB	
Articulation Index	<u>Case A⁽⁴⁾</u>		<u>Case A</u>		<u>Case A</u>	
	<u>Case B</u>		<u>Case B</u>		<u>Case B</u>	
	0.47;0.47	0.49;0.49	0.64;0.64	0.64;0.64	0.65;0.65	0.65;0.65

It is worth noting that the articulation index has reached its theoretical maximum for the 500-3kHz bandwidth employed when 24 dB peak clipping is used. However, the minute gain in speech intelligibility obtained in going from 12 dB to 24 dB peak clipping is clearly not worth the extra 3.5 dB in average power required.

E. DISCUSSION

The results obtained from calculations of the articulation index indicate that spectrum shaping techniques are not likely to improve communications intelligibility significantly for deep mines, where power requirements pose the most severe problems. They will probably be more effective in shallower mines, as calculations of signal-to-noise ratios have already indicated (Chapter IV of this Part).

The results derived here have, of course, been based on limited noise data available from NBS' measurements in mines. Among other factors, no account has been taken of the "burstiness" of electromagnetic noise in mines, nor of the effect on intelligibility of pure or complex "tones" of noise, such as those created by harmonics of 60Hz or 360Hz commonly found in mines. The latter can probably be reduced to a satisfactory level by use of a harmonic rejection filter, should they have a very deleterious effect on communications intelligibility. A potentially attractive design for a harmonic rejection filter is described in the following Chapter VI. The effect of the "burstiness" of noise on intelligibility can be estimated from Figure 5-5 and 5-6, once the necessary data have been gathered.

(4) Each pair of results under Case A (undifferentiated voice spectrum) or Case B (differentiated voice spectrum) represents the two situations where the magnetic field (left) and the receive loop voltage (right) are taken as the speech signal. No difference is observable within the accuracy of these computations.

Figure 5-5 shows the effect on speech intelligibility of the duty cycle or fraction of time that a masking noise is on, and Figure 5-6 presents the further correction that should be applied to the AI when noise having a definite on-off duty cycle is present.

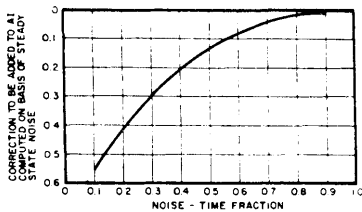


FIGURE 5-5 CORRECTION TO AI

The ordinate shows a correction to be applied to the articulation index computed on the assumption that a masking noise is steady-state for various noise-time fractions. The corrected AI cannot exceed 1.0. (Ref. 1)

The technique of peak clipping is likely to be useful to mine communications in several ways. At transmission, it can reduce the necessary peak power handling capacity and hence cost of, for example, an amplifier. Alternatively, for any fixed power transmission capability, peak clipping can significantly increase the intelligibility of the communications channel. Finally, peak clipping or limiting upon reception will be helpful where the local mine electromagnetic noise is very impulsive.

It should be mentioned that in designing a communications system for acceptable intelligibility in a given environment, careful attention must be paid to the effect of direct audio noise reaching the listener, and to consideration of the optimum overall level of sound which should be delivered to him.

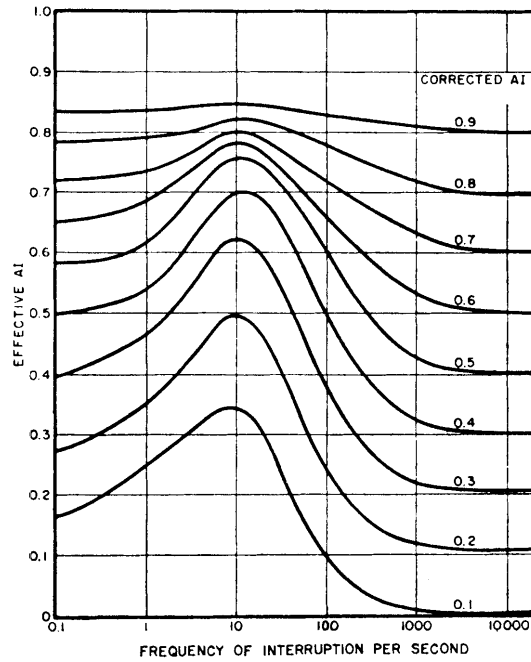


FIGURE 5-6 EFFECTIVE AI

Showing the effective AI as a function of the frequency with which a masking noise is interrupted. The parameter of the curves is the corrected AI calculated on the assumption that the masking noise is steady-state and then adjusted according to Fig. 5-5 for the fraction of the time the noise is on. (Ref. 1)

VI. A MEANS FOR OVERCOMING POWER LINE INTERFERENCE

Through-the-earth electromagnetic communication from the surface to miners below the surface in working areas of a mine is plagued by the presence of very substantial amounts of electromagnetic noise in the receiving area. The enormity of this noise is illustrated by the work of Bensema* at the National Bureau of Standards. Figure 6-1** is taken from Bensema's report and illustrates the spectral character of typical in-mine noise. It is evident from this plot that the largest contributor to noise for the example given is 60 Hz, and its harmonics, at least within the baseband voice region where the present through-the-earth electromagnetic communication systems operate. For this reason, it seems appropriate to consider a means of rejecting 60 Hz and its harmonics if it can be done effectively and economically. Rejection of power line harmonics presents the possibility, discussed in previous Chapters of this Part, of permitting a marked increase in the intelligibility of through-the-earth voice communications, or of allowing a substantial reduction in the transmitter power requirements.

A. METHODS TO OVERCOME HARMONICS

Classically the means for rejecting harmonics of a single frequency has been to use a multiple notch filter. These multiple notch filters belong to the class known as comb filters and have been realized in the past largely by multiple tuned stages or by the use of delay lines, which are able to achieve some degree of rejection for situations similar to those encountered in mines.

There is an alternative kind of filter the theory of which is relatively old, but whose implementation has only recently become practical. The form of this filter is illustrated in Figure 6-2, and comprises a commutator switch, a series of capacitors, and one resistor. To make this into a harmonic rejection filter, the commutator is caused to rotate once per fundamental cycle of the harmonic set which is to be rejected. The generic frequency response for such a filter is shown in Figure 6-3. With a sufficiently large number of switches and capacitors to sample and store the input waveform, this multiple notch filter can be made to be a near ideal rejector of harmonics. One of the characteristics of importance in this filter is that each of the notches has the same bandwidth, so that if it is 1 Hz wide at the fundamental frequency, it is still 1 Hz wide at each harmonic.

The functioning of this filter is made apparent in Figure 6-4 for a signal which has a fundamental plus many harmonics. Each capacitor in the filter stores the average value of the waveform that occurs in the interval for which that capacitor switch is closed. Thus a replica of the repeating part of the waveform is stored on the capacitors, and the incoming wave is compared to this

* Ref. I-1, Bensema, W.D., "Coal Mine ELF Noise Measurements", NBS Report 10-739, 28 April 1972.

** References to Figures, Tables, and Equations apply to those in this Chapter unless otherwise noted.

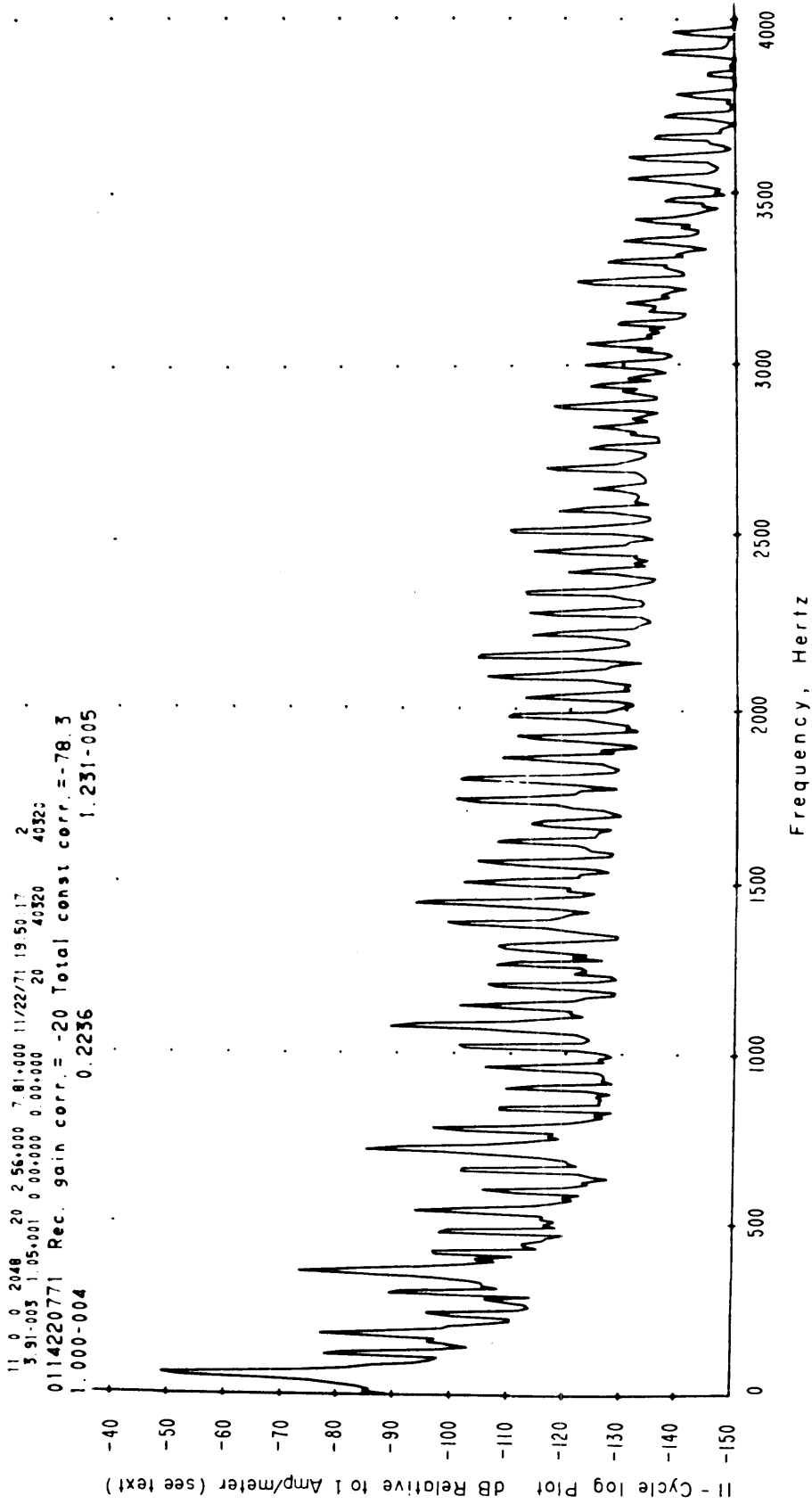


FIGURE 6-1 ALLEN MINE, UNDERGROUND, 3000 Hz BW, 01-14.
 ANTENNA SENSITIVE AXIS POINTED VERTICALLY.

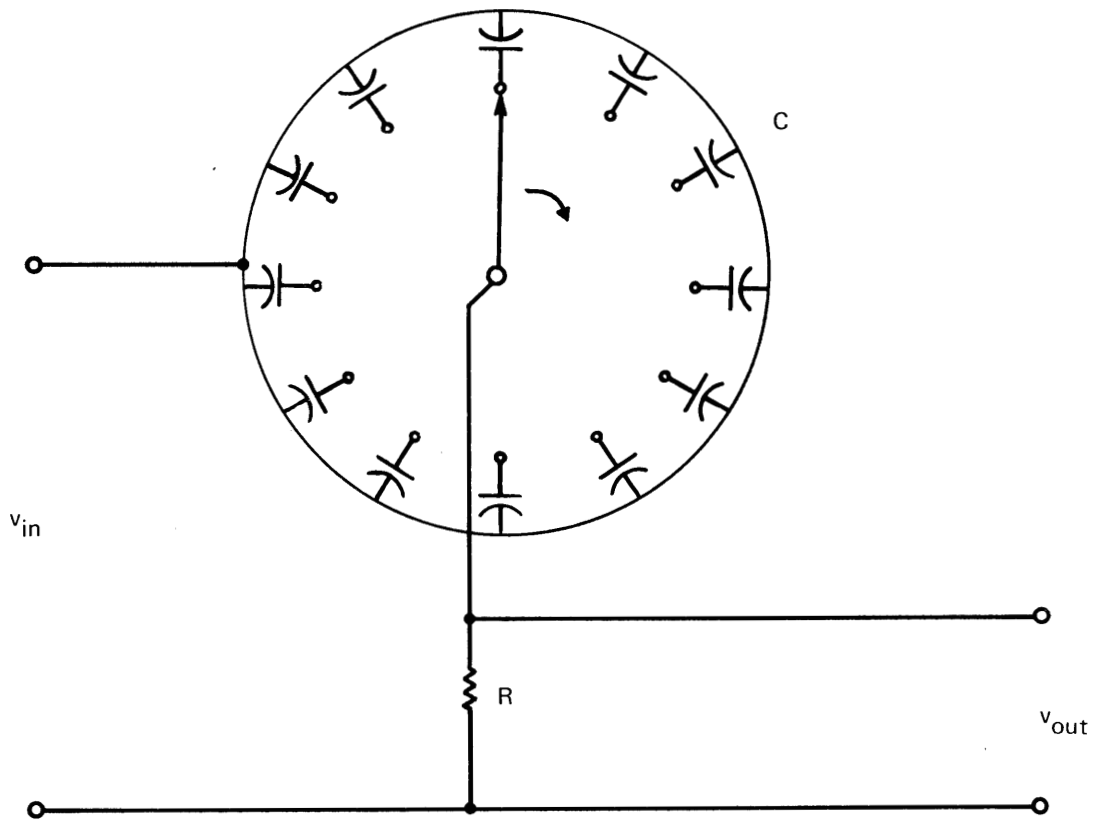


FIGURE 6-2 FUNCTIONAL REPRESENTATION OF HYBRID FILTER

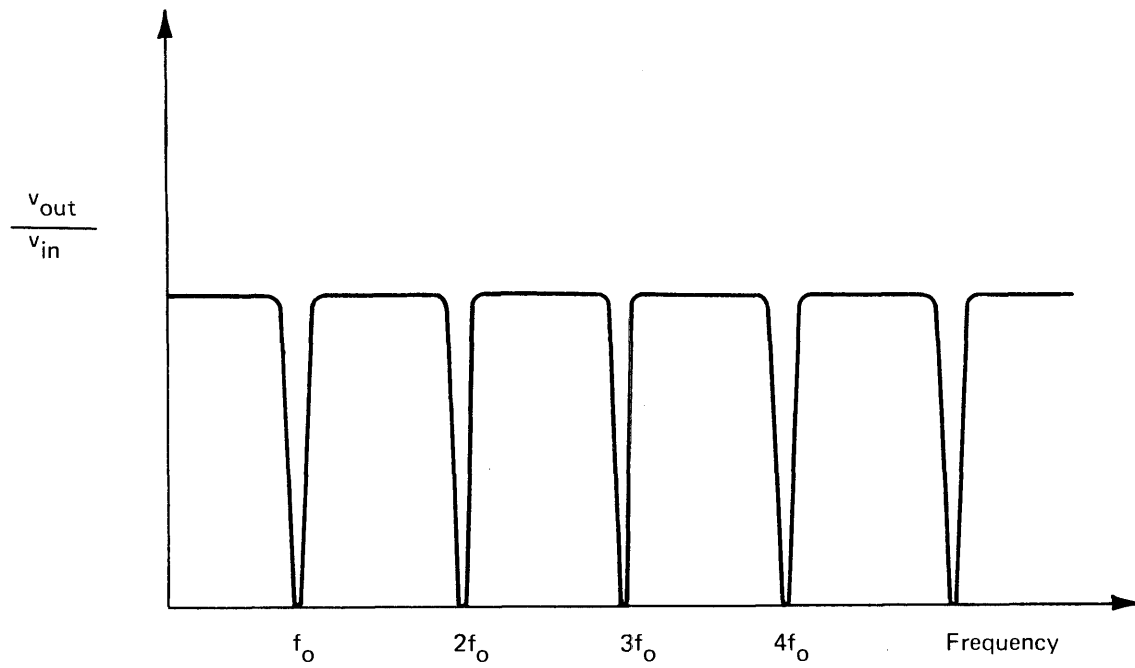


FIGURE 6-3 FILTER FREQUENCY RESPONSE

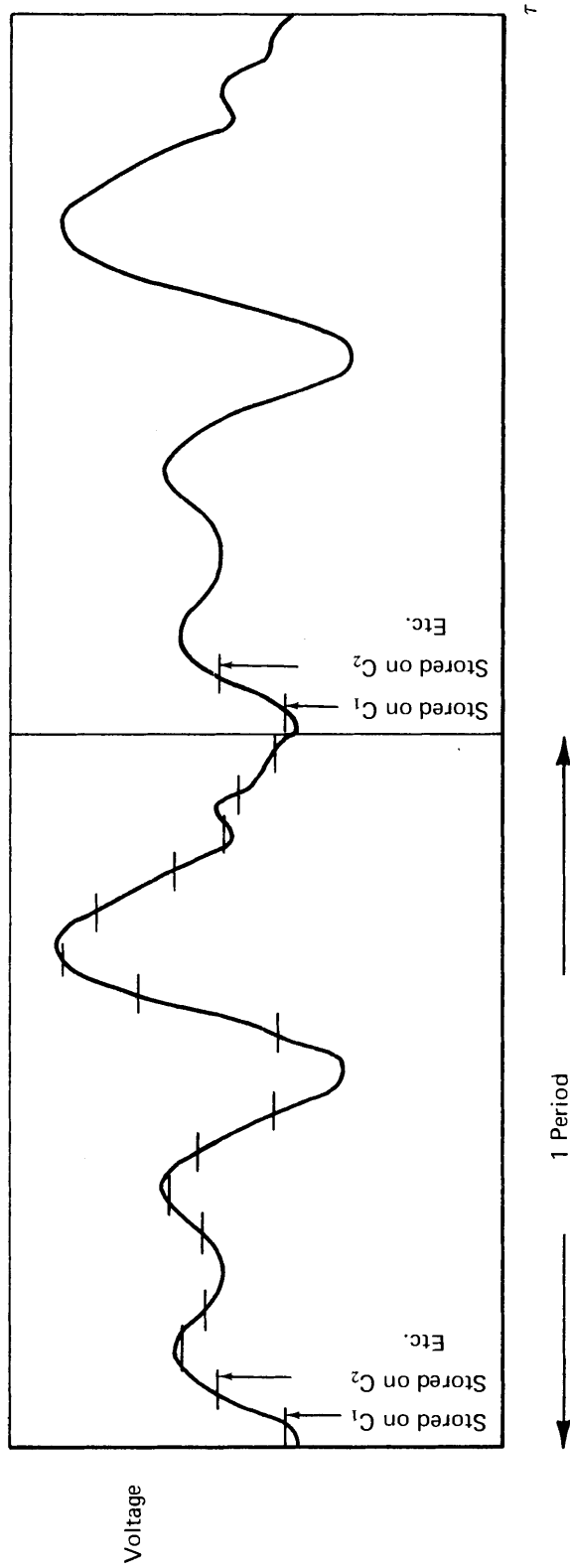


FIGURE 6-4 SIGNAL WAVEFORM AND STORED SAMPLES

stored waveform. Since the stored waveform is a step-wise approximation to the recurring part of the waveform, the only current that flows in the output circuit is that caused by features of the waveform which depart from its repetitive character. It can be foreseen that the stored step-wise approximation to the waveform will deteriorate for those fairly high-order harmonics where the number of samples stored by the corresponding capacitor segments per period of the respective harmonics is low in number, say 4 or 8. Therefore, this harmonic notch filter is not as good a rejector of signals at a higher order harmonic as it is at a lower order harmonic.

We calculated the rejection capability for a filter with 8 and 10 stored samples, or segments, per cycle of the harmonic to be rejected. Values of 31db for the 10-segment representation, and 26db for the 8-segment representation were obtained. These results were arrived at by making a harmonic analysis of the step-wise approximation to a sine wave, and determining the error thereby incurred in representing the true input wave. This error waveform is passed by the filter. A 40-segment breadboard unit was built to demonstrate feasibility.

One of the advantages that this filter offers which makes it promising for the Bureau of Mines communication problem, is that the bandwidth of the notch is completely controllable by adjusting only one circuit element, that is, the series resistor. The controllable rejection bandwidth is specified as $\frac{1}{\pi NRC}$; where N is the number of capacitor segments in the filter and R and C are the resistance and capacitance values; and it can be tailored to the natural bandwidth of the interference signals. The electronic implementation of the commutator switch can also easily be made such that the filter becomes a tracking filter, that tracks the interference fundamental frequency and thereby always rejecting the interference present, in spite of frequency variations of the fundamental about its nominal value of 60Hz. Such a tracking feature will most likely be required for coal mine applications.

B. CIRCUIT IMPLEMENTATION

Figure 6-5 illustrates a circuit diagram of the breadboard version of the filter that was constructed in order to evaluate the filter's performance. The breadboard was a 40-segment design using 40 capacitors in conjunction with 40 CMOS* analog switches. During operation only one switch at a time is turned on, the selection being based on where a "one" pulse is in a 40-bit twisted ring shift register. This keying is controlled by the five 74164 8-bit shift registers shown in the lower portion of the diagram. A single "one" advances stage by stage through this 40-bit shift register in accordance with clock pulses applied externally to the circuit. These clock pulses occur at 40 times the fundamental frequency of rejection for the filter. In principle, the outputs from the shift registers may be used directly to control the analog switches connected to the capacitors. However, for practical reasons we chose to use 40 buffer amplifiers

* CMOS: Complementary Metal Oxide Semiconductor.

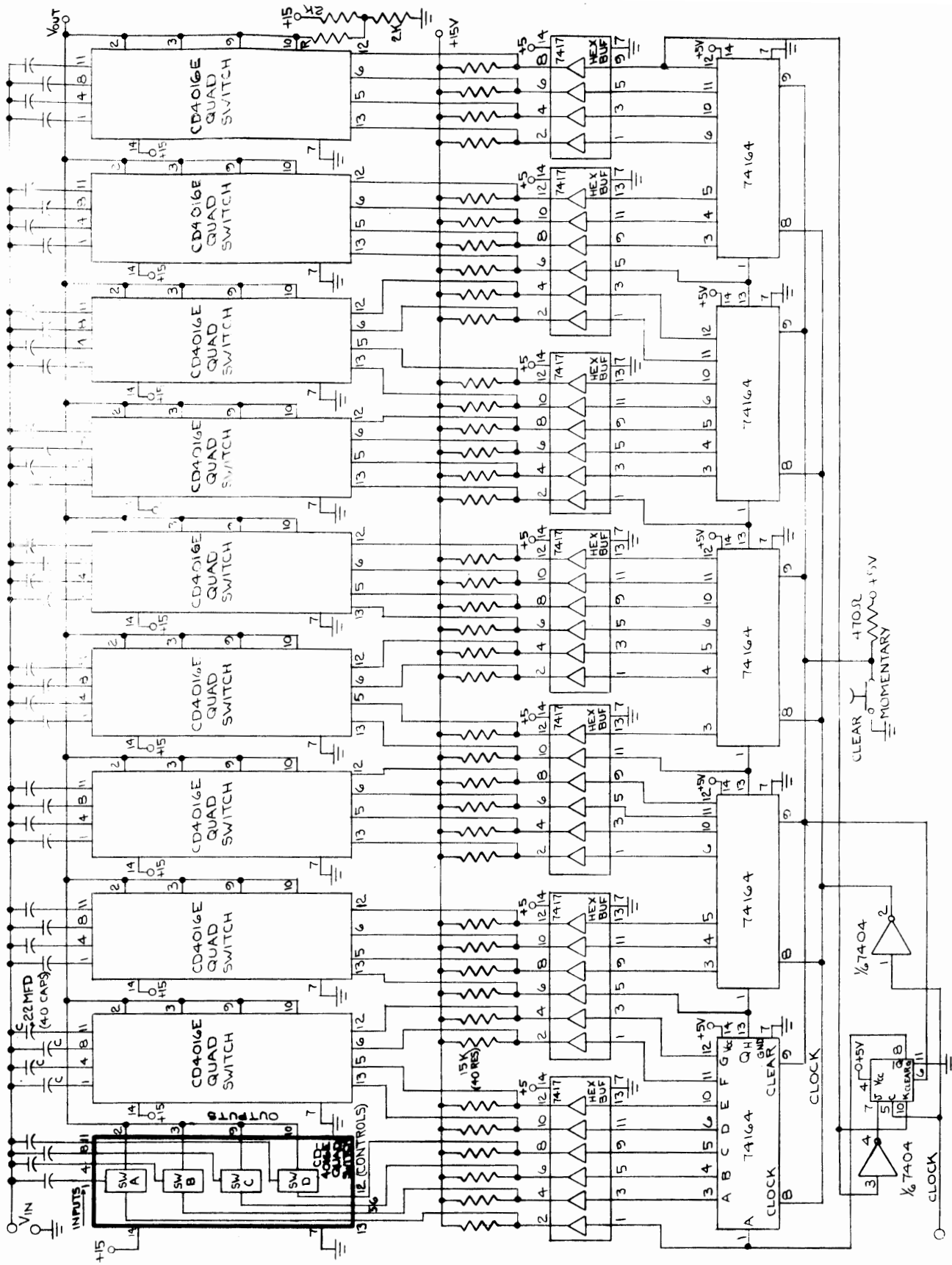


FIGURE 6-5 FORTY SECTION HYBRID FILTER

to provide the 15 volt switching signal to the CMOS switches. The buffer amplifiers are indicated as the hex buffers #7417. The outputs from these hex buffers feed 10 quad switches, i.e., each of the CD4016E CMOS switches has four elements in the package. One side of each switch is fed to a common bus shown terminating in a resistor biased to the 15 volt supply. The other side of each switch goes to its individual capacitor, then back to a common input line. The commutating function of the switch shown in the earlier diagram (Figure 6-2) is thus accomplished by this circuit. The breadboard used 30 14-pin dual in-line integrated circuit packages to accomplish the required functions. Thirteen of these packages were associated with the buffer circuits used to connect the shift registers to the switching elements.

One of the major contributors to the volume occupied by the circuit was the bank of 40 equal capacitors for waveform storage. The capacitance value of 0.22 μf was chosen large enough to provide quite a degree of flexibility in selecting the circuit time constant. The choice of a specific capacitor was made largely on the basis of cost--not size, so they were fairly large.

The reason that the output signal is biased to a +7.5 volt return is because the CMOS switches must have their analog input signal confined to the space between 0 volts and the control voltage of +15 volts used to turn the switch on. Hence, the return was made midway between these two voltages at +7.5 volts. This operation biases the capacitors during operation but does not affect the performance of the circuit. The effective resistance associated with the capacitor is that of this return circuit, and for most tests it was set at 10,000 ohms.

C. TESTS AND RESULTS

Figure 6-6 illustrates in block diagram form the equipment assembled for testing the filter. The most interesting test was that done to determine the depth of the notches as a function of harmonic number. For this test, a 2000 Hz square wave was used to program the commutator. This means that the commutator rotated at a 50 Hz rate. Fifty Hz was chosen to assure that 60 Hz pickup did not present problems. The output of the filter was passed through a Krohn-Hite filter prior to measurement so that the out-of-band contamination produced by switching transients would not interfere with the in-band measurements.

The plot of Figure 6-7 illustrates the depths of notches as a function of harmonic number. Also shown on this plot are two computed points derived as discussed earlier, and the depth of notches that would be experienced for filters containing larger numbers of segments. It is seen from these plots that rejection of harmonics can be in excess of 40 db, and that this rejection is controlled by the number of segments used in the filter, thereby providing the ability to tailor the design to desired rejection levels.

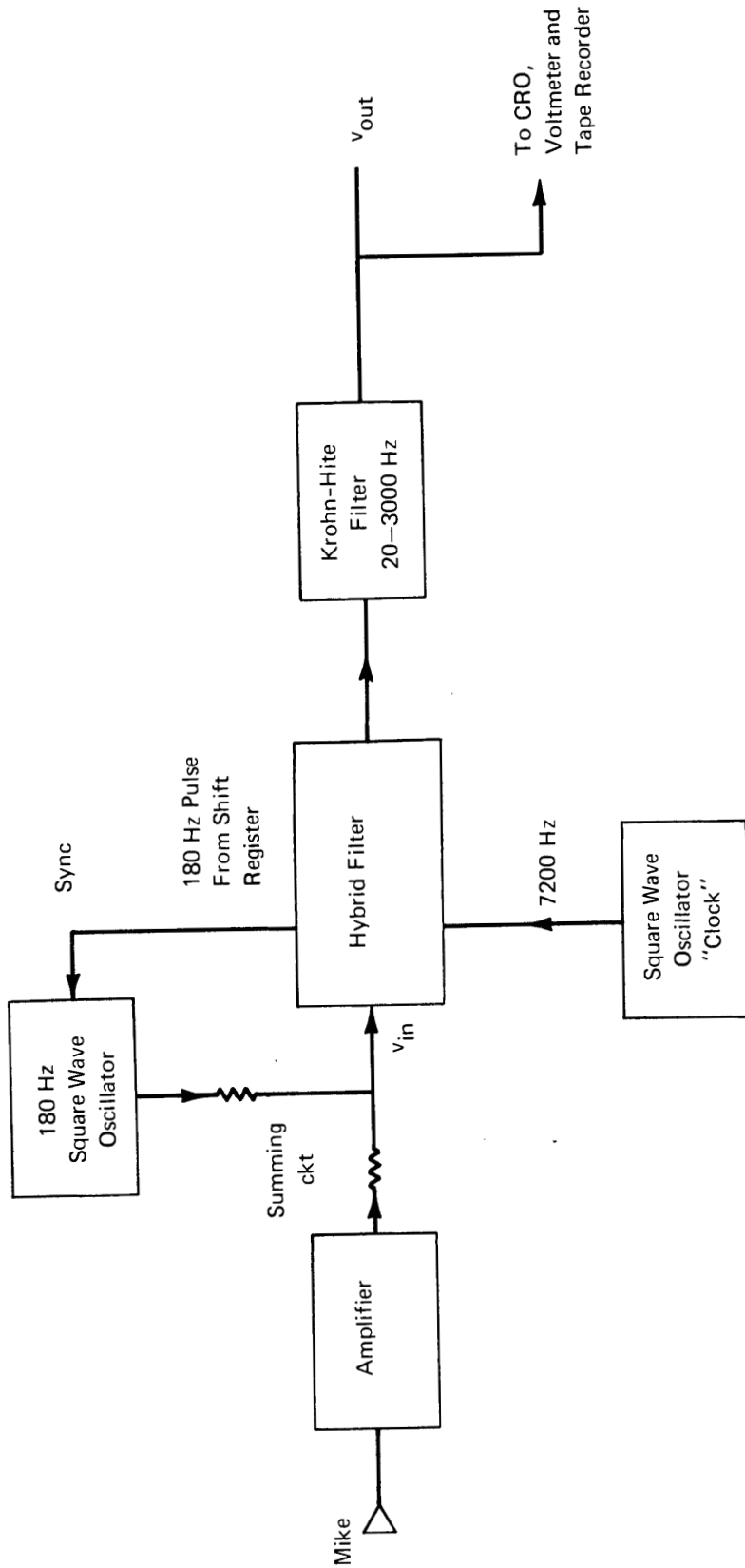


FIGURE 6-6 BLOCK DIAGRAM OF TEST CONFIGURATION

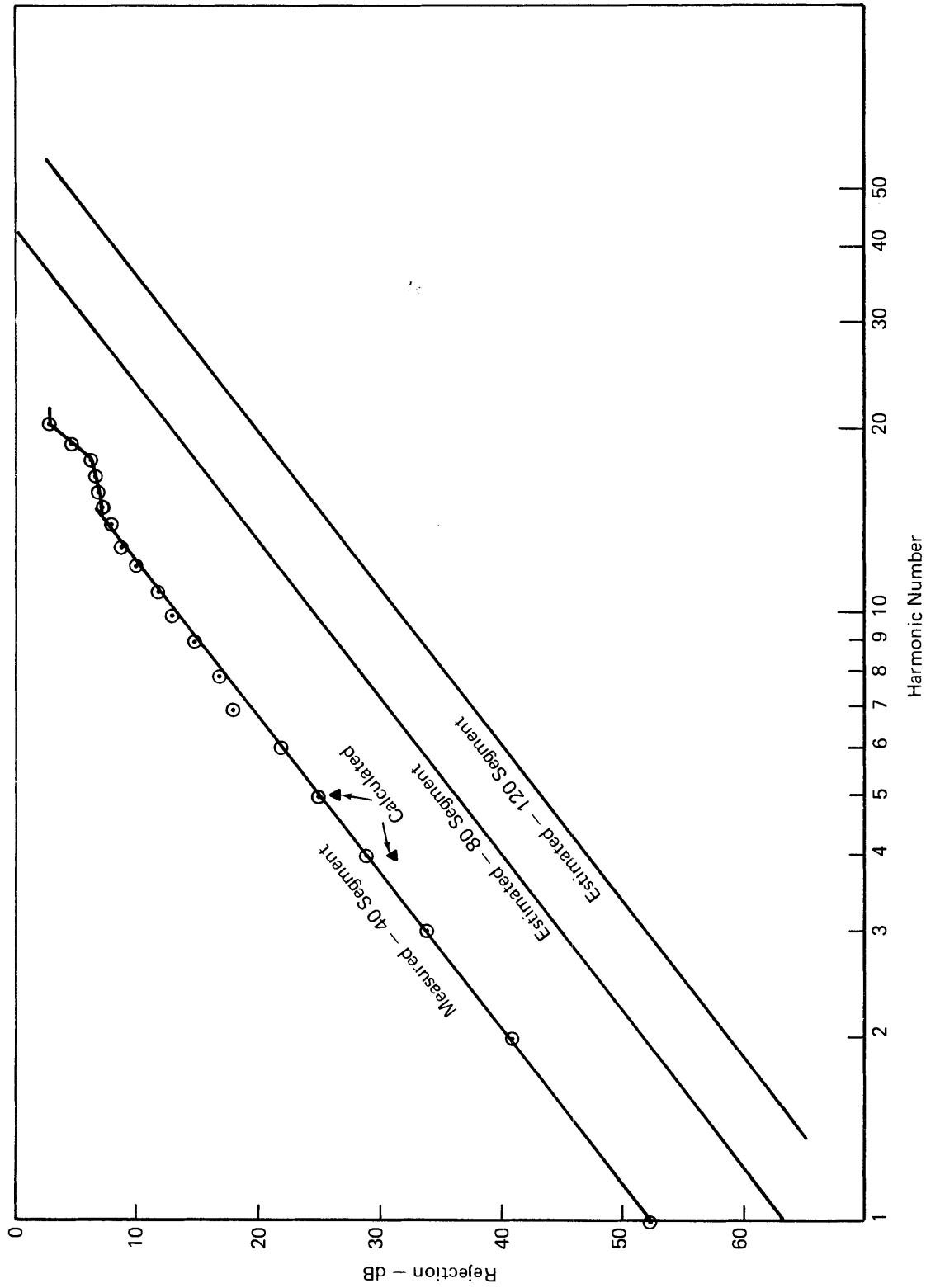


FIGURE 6-7 HARMONIC REJECTION
40 SEGMENT HYBRID FILTER

Figure 6-8 illustrates an expanded version of the transmission frequency response around the fourth harmonic notch. The results of these tests clearly indicate that this harmonic rejection filter can be used for the purpose of rejecting harmonics in a mine communication system.

One of the unresolved questions at the time we started construction of this circuit was what would happen to voice signals when passed through such filters with the notch bandwidths we used. We found, upon test of running voice signals through the filter in the absence of interfering signals and recording the results, that voice quality was preserved remarkably well. One feature noted by paying careful attention to the quality of the voice was a very faint echo in the voice signals coming out of the filter. This is as expected.

In order to provide qualitative evaluation of the rejection capabilities of the filter, square waves of interference were applied to the input of the filter and combined with voice signals arriving from a microphone. A VCO (voltage controlled oscillator) was used to cause the filter to synchronize with the interfering signal. Recordings were made of the unfiltered and filtered versions of the waves, which demonstrate the dramatic improvements in voice reception provided by the harmonic rejection filter.

D. EXTENSIONS OF WORK

There are several extensions of the basic work which could be done to aid in improving mine communications. First of all, a VCO and phase-lock loop could be fabricated and added to the circuit to demonstrate the feasibility of producing a tracking version of the filter. Secondly, a filter with more segments to provide higher rejection of the higher order harmonics could be assembled and tested. Thirdly, there is the distinct possibility that in terms of size and power consumption, an all-digital version may have significant promise. Such a version would be easier to implement in a Large Scale Integrated, LSI, version than would be the hybrid analog/digital system represented by the present breadboard. A possible block diagram for an all-digital version is illustrated in Figure 6-9. The advantage of the all-digital version arises from the fact that one of the most significant volume elements of the present circuit, LSI version included, is the bank of storage capacitors. Since storage capacitors would have to be external elements in an LSI version of the hybrid circuit, they would even limit the attractiveness of this concept somewhat.

E. CONCLUSIONS

The hybrid commutator-type filter has been demonstrated to be an effective rejector of harmonic signals. This effective rejection is accomplished without altering significantly the quality of the voice which is desired to be passed through the filter. In those cases where the noise environment is

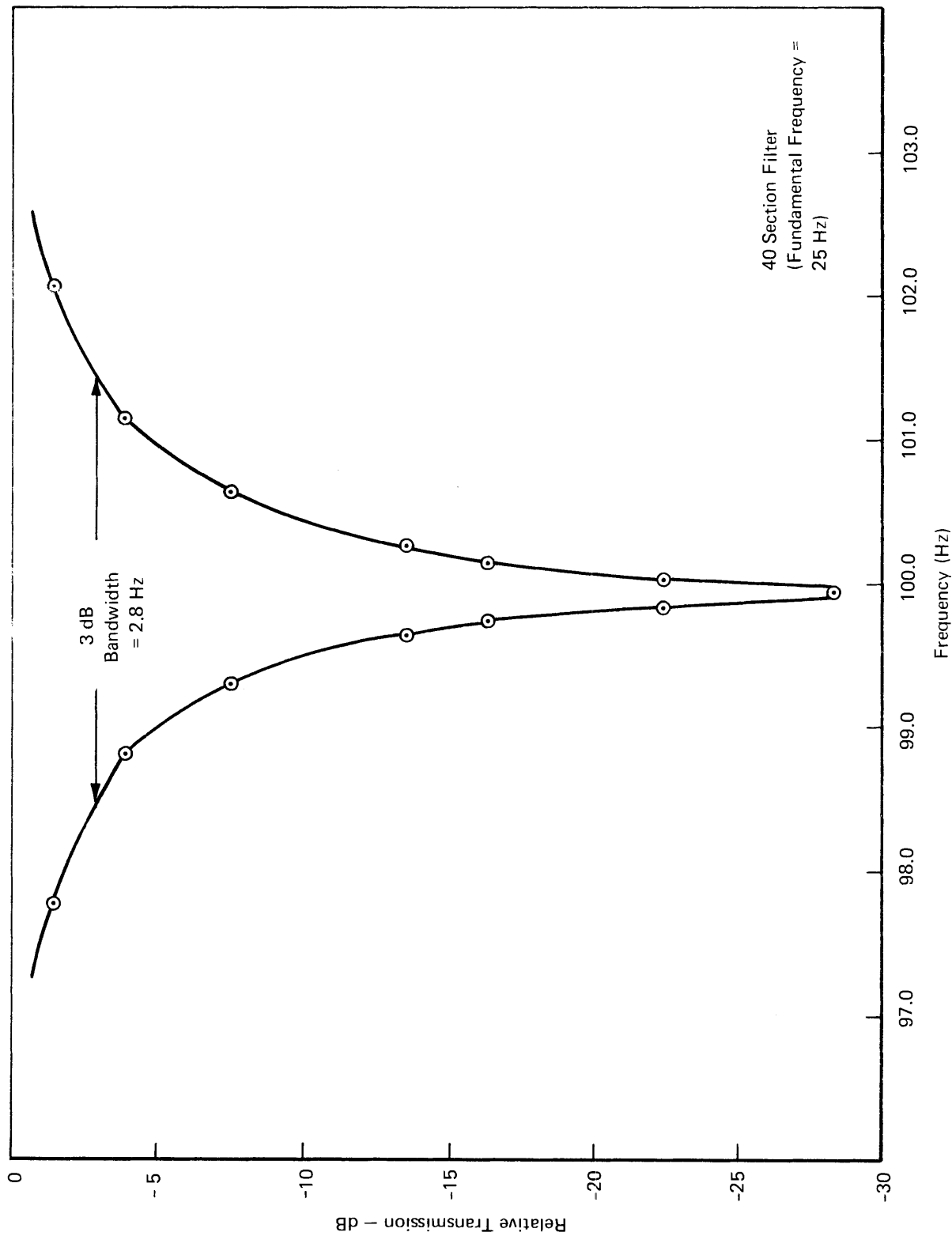


FIGURE 6-8 REJECTION OF FOURTH HARMONIC

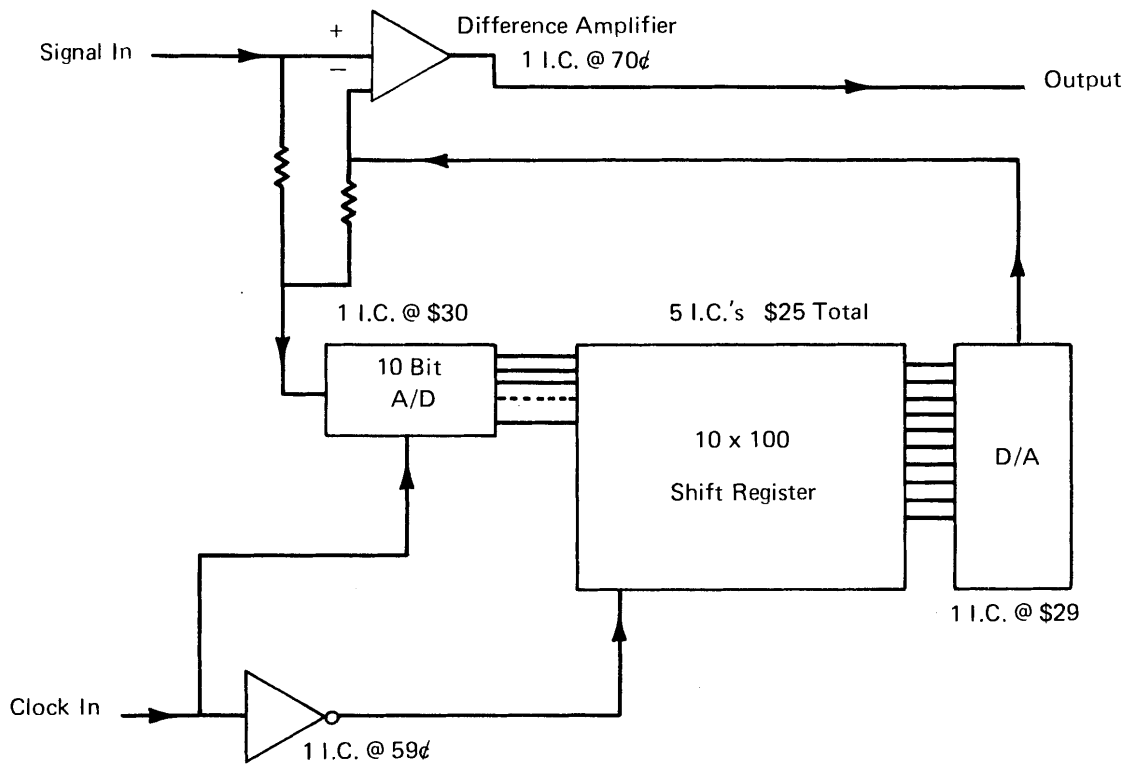


FIGURE 6-9 100 SEGMENT DIGITAL HARMONIC FILTER

dominated by harmonic components, the use of this filter can significantly decrease the amount of transmitter power required to achieve reliable voice communications through-the-earth. For example, in the case of a harmonic filter that reduced all harmonic components by an equal amount of say Rdb, the transmitter power requirement would also be reduced by the same Rdb. In the case of the harmonic filter described in this report, the improvement could be well in excess of the minimum rejection provided by the highest harmonic to be rejected in the voice band of interest.

PART THREE

LEAKY COAXIAL CABLE FOR GUIDED WIRELESS
MINE COMMUNICATION SYSTEMS

PART THREE

LEAKY COAXIAL CABLE FOR GUIDED WIRELESS
MINE COMMUNICATION SYSTEMS

TABLE OF CONTENTS

	<u>Page</u>
List of Tables	3.iii
List of Figures	3.iv
INTRODUCTION	3.1
I. APPLICATION OF LEAKY COAXIAL CABLE COMMUNICATION SYSTEMS	3.2
II. THEORETICAL CALCULATIONS OF PERFORMANCE OF LEAKY COAXIAL CABLE COMMUNICATION SYSTEMS	3.3
A. SOLID SHIELD MODEL	3.5
B. LEAKY BRAID SHIELD MODEL	3.9
C. BEHAVIOR VERSUS OPERATING FREQUENCY	3.11
D. ATTAINABLE LONGITUDINAL COMMUNICATION RANGE	3.16
E. DISCUSSION OF RESULTS	3.17
III. EUROPEAN WORK WITH LEAKY COAXIAL CABLE COMMUNICATION SYSTEMS	3.21
A. STATE-OF-THE-ART	3.21
B. DISCUSSION	3.23
IV. REFERENCES	3.24

PART THREE

LEAKY COAXIAL CABLE FOR GUIDED WIRELESS
MINE COMMUNICATION SYSTEMS

LIST OF TABLES

<u>Table No.</u>	<u>Title</u>	<u>Page</u>
1	Coaxial Cable Parameters, RG 58/U Cable	3.13
2	Braid Dimensions, RG 58/U Cable	3.13
3	Longitudinal Attenuation (α), RG 58/U Cable	3.13
4	Maximum Two-Way Longitudinal Communication Range Via Leaky Coaxial Cable (50 Ω , RG 58/U)	3.18

PART THREE

LEAKY COAXIAL CABLE FOR GUIDED WIRELESS
MINE COMMUNICATION SYSTEMS

LIST OF FIGURES

<u>Figure No.</u>	<u>Title</u>	<u>Page</u>
1	Characteristic Quantities and Dimensions Associated with a Four Region Coaxial Line Geometry	3.4
2	Braid Shield Mesh Structure	3.10
3	Magnetic Field $ H_{\phi} $ at r Meters from Cable Axis vs Frequency	3.12
4	Receive Loop Voltage at r Meters from Cable Axis vs Frequency (For Loop Located 300 Meters From Transmitter End of Cable)	3.15

PART THREE

LEAKY COAXIAL CABLE FOR GUIDED WIRELESS MINE COMMUNICATION SYSTEMS

INTRODUCTION

Coaxial cable structures form the subject of substantial theoretical and experimental investigations either directly related, or which can be extrapolated, to the communications needs and environments of U.S. coal mines. Communication systems based on "guided" waves, of which "leaky" coaxial cables are one implementation, are attractive candidates for providing a range of communication functions primarily along haulage ways, and possible also within sections up to the working face. (However, there are still strong reservations as to whether a practical coaxial cable system could provide sufficient communications coverage within a section.) In this Part, we present the results of some theoretical calculations of the performance of leaky coaxial cable communication systems. We also analyze the applicability of the theoretical and experimental results obtained by other researchers to the needs of U.S. coal mines. In particular, this investigation has been focused on the utility of relatively low cost, conventional, flexible, coaxial cable at frequencies covering the LF through HF bands and extending into the lower part of the VHF band, as opposed to relatively high cost, special semi-rigid, coaxial cable* at frequencies in the VHF and UHF bands.

There are three major design alternatives for coaxial cable communication systems considered in this chapter:

- Base station feeding a coaxial cable with high surface transfer impedance (holes in outer conductor, e.g., braid construction).
- Base station feeding a coaxial cable with repeaters (U.K. experiments).
- No base station, direct communication via a coaxial cable with periodic radiative structures.

* The utility of special Radiax^{T.M.} cable in the UHF band is treated in a paper coauthored by R. Lagace of ADL and H. Parkinson of PMSRC, and published in U.S. Bureau of Mines Information Circular No. 8635, and in Part Eight of this Volume.

Our discussion of the latter two alternatives consists primarily of descriptions of the progress and results achieved in Europe. In the first case, which is the simplest in the sense of requiring no special devices added to the coaxial cable, we have analyzed the performance that can be hoped for based on simplified theoretical models.

I. APPLICATION OF LEAKY COAXIAL CABLE COMMUNICATION SYSTEMS

The communication function for which coaxial cable structures are being considered is first and foremost:

- Two-way communication along main haulage ways up to 4-5 miles long, to vehicles and to key individuals on-the-move.

A less likely application involves:

- Two-way communication in sections up to working faces; all entries near the working face should be covered, but possibly only a limited portion of those at or near main haulage ways. Communication with roving personnel at up to 3,000 feet away from main haulage ways needs to be established. More than one kind of working face must be dealt with, i.e., room and pillar (predominant in the U.S.) and longwall.

A major disadvantage of conventional flexible coaxial cable structures in the latter application arises from their seeming inability to provide communications coverage at more than 10 to 20 meters lateral distance from the cable in the above mentioned frequency bands which are suitable for use with these cables. Thus in order to provide wide area communications coverage within the network of tunnels in a coal mine section, it would be necessary to string cables along most of them. There are however severe practical and economic obstacles to stringing all this cable in the continually changing geography of a section. Hence the majority of the remarks and analyses described in this chapter are directed towards the primary application of essentially longitudinal communication along haulage ways.

II. THEORETICAL CALCULATIONS OF PERFORMANCE OF LEAKY COAXIAL CABLE COMMUNICATION SYSTEMS

This section describes the methods and results of calculations of the leakage of electromagnetic energy from coaxial cable structures. These calculations were performed to give preliminary estimates of the optimum design of inductively coupled communication systems based on partially shielded transmission lines, and to suggest the experimental data needed to confirm or modify existing theories of their operation.

The situations considered include the behavior of fields in an air outer medium using a solid wall shield model approximation, and an ideally conducting braid shield model.

Electromagnetic fields in and around coaxial lines can be calculated using the simplest available geometrical model (Figure 1). The following assumptions are made:

- 1) As the outer shield of the coaxial line is made slightly "transparent" to the electromagnetic fields, the inside fields (in Regions 1 and 2) are not affected drastically; hence the error introduced by using the "opaque" shield field distribution inside will be negligible.
- 2) The axial attenuation of the field, although always non-zero, is small enough that its effect on the radial components k_r of the propagation vector is negligible.
- 3) All four regions are non-magnetic, i.e., $\mu_1 = \mu_2 = \mu_3 = \mu_0$. This is not a significant restriction on the materials of the coaxial cable in the frequency range of interest (roughly 10^5 - 10^8 Hz).

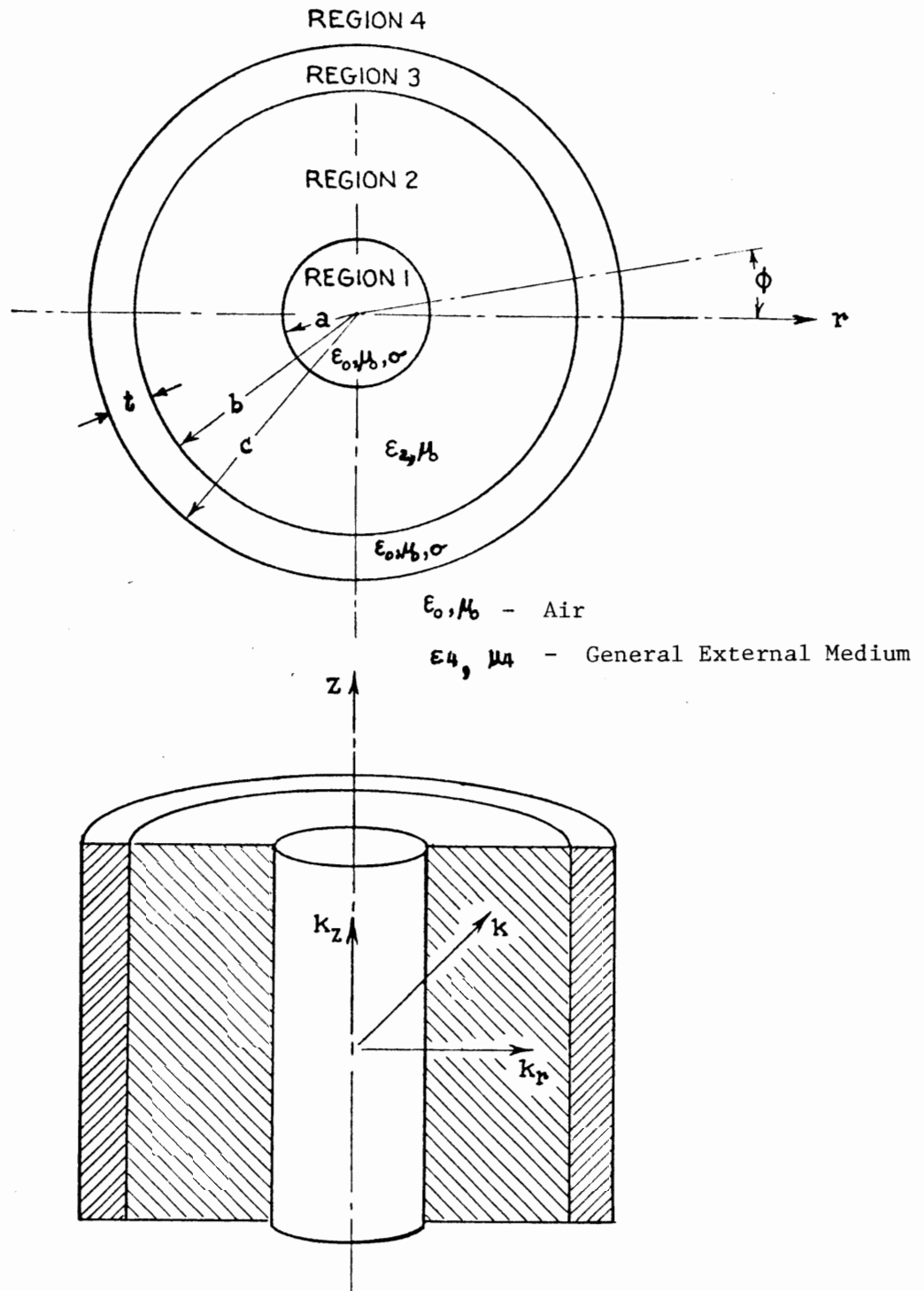


FIGURE 1 CHARACTERISTIC QUANTITIES AND DIMENSIONS ASSOCIATED WITH A FOUR REGION COAXIAL LINE GEOMETRY

The mathematical formalism of the wave theoretical analysis starts from the wave equation for the vector potential for a four-region system (3 concentric cylindrical boundary surfaces with radii a , b , c). The transmission line is straight, infinitely long, and uniform, and its cross-sectional dimensions are negligibly small with respect to the wavelength of the signals. There are six boundary conditions, since the tangential components of the electrical and magnetic field intensities are continuous across each of the three boundaries. We assume a coaxial line operating in a TEM mode.

The outer shield of the coaxial cable does not provide complete shielding at low frequencies, but in fact allows a more-than-adequate field to propagate as a loosely-bound surface wave along the outside of the cable. The wave phase velocity of the cable, and therefore the degree to which the external field is confined to the vicinity of the cable, can be adjusted by changing the cable internal dielectric constant. The higher the dielectric constant, the more confined the external field. Coaxial cable also assures that field behavior will be relatively insensitive to the surrounding physical environment, since most of the power is transported inside the cable. The insensitivity to the external environment not only simplifies analysis, but is an advantageous, if not indispensable, characteristic of the cable, particularly in those applications where the communications corridor may be strewn with large metal objects and contain several bends or corners.

A. Solid Shield Model

The external fields can be analyzed using a solid cylindrical shield model, since braided shields appear solid below about 5 MHz.⁽¹⁾

(1) K. Ikrath, "Leakage of Electromagnetic Energy from Coaxial Cable Structures", U.S. Army Signal Research and Development Laboratory, Fort Monmouth, N. J., USASRD Tech. Dept. 1964 (1958).

The nature of the electromagnetic wave fields external to a long length of dielectric-filled coaxial cable placed in an air medium is described below. The field equations represent an external surface wave propagating in the positive axial (z) direction. The external wave has two electric field components E_r , E_z , and one circumferential magnetic field component H_ϕ , all circularly symmetric about the z-axis.

$$E_z = IS \frac{K_0(\eta r)}{K_0(\eta c)} e^{-jk_z z} \quad (1)$$

$$E_r = jIS \left(\frac{k_z}{\eta}\right) \frac{K_1(\eta r)}{K_0(\eta c)} e^{-jk_z z} \quad (2)$$

$$H_\phi = jIS \left(\frac{\epsilon_0}{\mu_0}\right)^{1/2} \left(\frac{k}{\eta}\right) \frac{K_1(\eta r)}{K_0(\eta c)} e^{-jk_z z} \quad (3)$$

where the coordinate system is defined by Figure 1; and

E_r (volts/meter) is the component of electric field in the radial direction - r.

E_z (volts/meter) is the component of electric field in the axial direction - z.

H_ϕ (amperes/meter) is the component of magnetic field in the circumferential direction - ϕ .

E_z (volts/meter) is the component of electric field in the axial direction - z.

H_ϕ (amperes/meter) is the component of magnetic field in the circumferential direction - ϕ .

$$S = \frac{E_z^{\text{out}}(\text{at shield})}{I} ; S \text{ is the complex surface transfer impedance. It represents the magnitude and phase of the axial component of electric field } (E_z) \text{ at the outer surface of the coaxial cable shield per unit current in the center conductor.} \quad (4)$$

$$S = \frac{\sqrt{2}e^{-t/\delta}}{\pi\sqrt{bc}\sigma\delta} \text{ ohms/meter, (for } t/\delta \gtrsim 1) \quad (5)$$

b, c are the shield radii shown in Figure 1 in meters
 t = c-b is the thickness of the cable outer shield (6)

$$\delta = \frac{\sqrt{2}}{\omega\mu\sigma} = \text{skin depth in the conducting shield} \quad (7)$$

ω is the radian frequency ($=2\pi f$)

ϵ_0, μ_0 are the permittivity and permeability of free space in farads/meter and henries/meter respectively.

σ is the conductivity of the shield and center conductor in mho/meter

$$k = \omega(\mu_0\epsilon_0)^{1/2} \text{ is the resultant propagation vector in the external medium} \quad (8)$$

$$k_z = \beta_z - j\alpha_z \approx \omega(\mu_0\epsilon)^{1/2} = \left(\frac{\epsilon}{\epsilon_0}\right)^{1/2} k \text{ is the axial component of the propagation vector for the cable structure (z-attenuation constant } \alpha_z \text{ small)} \quad (9)$$

ϵ is the permittivity of the cable dielectric

$$k_r = -j \left(\frac{\epsilon}{\epsilon_0} - 1\right)^{1/2} k \text{ is the radial component of the propagation vector in the external medium} \quad (10)$$

$$\eta = \left(\frac{\epsilon}{\epsilon_0} - 1\right)^{1/2} k = jk_r \quad (11)$$

z is the axial coordinate distance in meters

$K_0(nr)$ is the zero-order modified Bessel function of the third kind

$K_1(nr)$ is the first-order modified Bessel function of the third kind.

The external E_r and H_ϕ components are in phase with each other, thereby propagating power down the outside of the line. E_r and H_ϕ are simply related by the ratio

$$E_r/H_\phi = \left(\frac{\mu_0 \epsilon}{\epsilon_0}\right)^{1/2},$$

which equals 570 ohms for polyethylene-filled cables such as RG-58 and RG-8. In applications where the radial distance r and frequency are such that $\eta r < 0.15$, $K_0(nr)$ and $K_1(nr)$ can be approximated by the simpler small argument forms

$$K_0(\eta r) = \ln(\eta r) \quad (12a)$$

$$K_1(\eta r) = 1/\eta r, \quad (12b)$$

to give:

$$E_z = \frac{IS}{\ln(\eta c)} \ln(\eta r) e^{-jk_z z} \quad (13)$$

$$E_r = -j \frac{IS}{\ln(\eta c)} \left(\frac{k_z}{\eta}\right) \frac{1}{\eta r} e^{-jk_z z} \quad (14)$$

$$H_\phi = -j \left(\frac{\epsilon_0}{\mu_0}\right)^{1/2} \frac{IS}{\ln(\eta c)} \left(\frac{k}{\eta}\right) \frac{1}{\eta r} e^{-jk_z z}. \quad (15)$$

A coal mine haulage way communications system operating below about 100 kHz is one such application.

Equations 13 through 15 reveal that in the vicinity of the cable the radial electric field E_r and circumferential magnetic field H_ϕ fall off inversely with distance r from the cable, while the axial electric E_z field falls off as the logarithm of r . When $\eta r > 0.15$, i.e. at higher frequencies or greater distances from the cable, the exact expressions for $K_0(\eta r)$ and $K_1(\eta r)$ must be used.

When air is the outside medium, the fields in Region 4 represent a surface wave along the outside of the coaxial shield. There is power transfer in the axial direction, and only reactive power in the radial direction (E_r and H_ϕ in phase, E_z in phase quadrature with both E_r and H_ϕ).

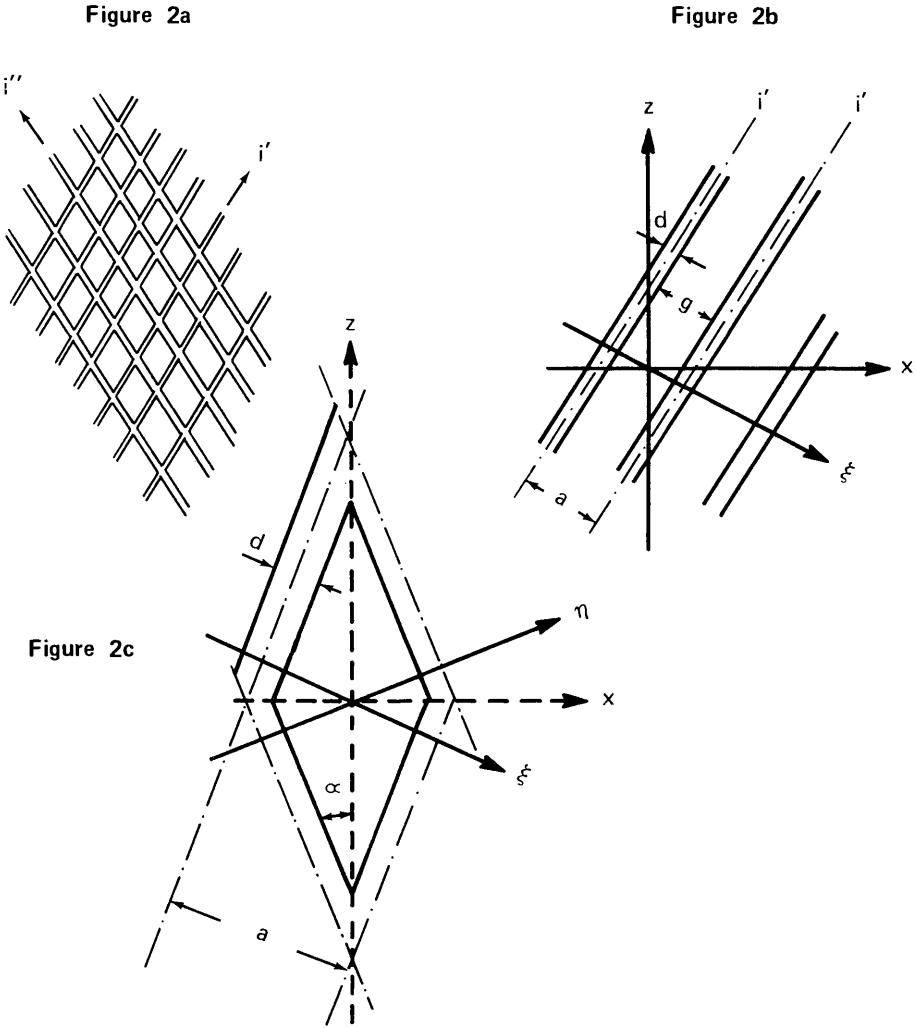
B. Leaky Braid Shield Model*

This model explores leakage of electromagnetic energy through the apertures in braided shields. The external magnetic field is obtained by superposition of the field configurations from each braid wire current as a function of the distance from the wire. Leakage through the conducting braid wire itself is neglected (ideally conducting assumption). The braid is regarded as a mesh of diamond shaped apertures (Figure 2) and the following assumptions are made in order to be able to apply the analytical results of a plane meshwire model to the curved shields of coaxial cables.

1. Stationary DC like behavior of the flux patterns in the immediate vicinity of the braid apertures is assumed at wavelengths which are large compared to the dimensions of the braid apertures.
2. Magnetic field distortions due to geometry and contact conditions at the braid wire crossing are neglected.
3. The number of mesh apertures is large in a surface portion of the braid which can be considered to be almost flat.

* K. Ikrath, ref. (1).

Under symmetry conditions currents i' and i'' are equal.



* K. Ikrath, ref. 1

FIGURE 2 BRAID SHIELD MESH STRUCTURE*

4. Geometric symmetry and equal size of the diamond shaped braid apertures is assumed (a perturbation of the symmetrical model would exceed the scope of this presentation).
5. The braid is made of infinitely conducting material (leakage through the apertures only).

The expression for the surface transfer impedance per unit length is then*

$$S = 0.3 \frac{\mu_0 f}{n} \left(\frac{g}{a}\right)^4 (1 + \tan^4 \alpha - \sin^4 \alpha), \quad (16)$$

for small leakage factor

$$\frac{g}{4a \sin^2 \alpha} < 1, \quad (17)$$

where n is the number of braid wire strands which form the diamond shaped mesh apertures. The leakage fields for the braid shield model can then be calculated from eqs. (13)-(15) or (1)-(3) by substituting the expression (16) for S .

C. Behavior Versus Operating Frequency

In Figure 3 the lateral leakage fields in air (again ignoring z dependence) are shown as a function of frequency at two distances from RG 58/U cable. These plots were obtained using both the solid wall and ideally conducting braid shield approximations. The cable parameters and braid dimensions are given in Tables 1, 2 and 3. In these calculations the exact expressions for the Bessel functions $K(\eta r)$ were used when $\eta r > 0.15$.

* K. Ikrath, ref. (1).

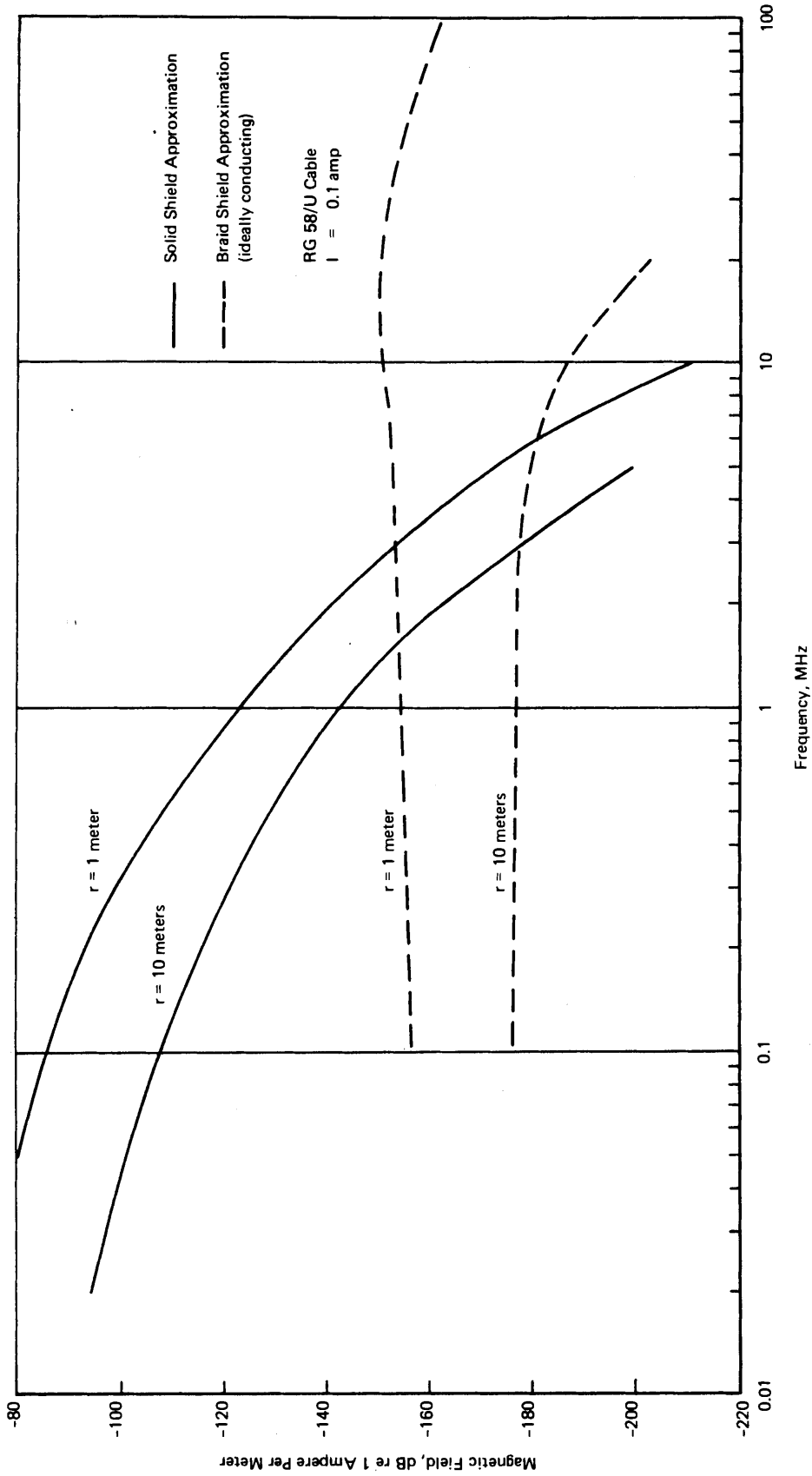


FIGURE 3 MAGNETIC FIELD $|H_\phi|$ AT r METERS FROM CABLE AXIS VS FREQUENCY

TABLE 1
COAXIAL CABLE PARAMETERS, RG 58/U CABLE
(For Figure 1 Geometry)

a (meters)	4.13×10^{-4}
b (meters)	1.524×10^{-3}
c (meters)	1.816×10^{-3}
t (meters)	2.92×10^{-4}
σ (mho/m)	5.7×10^7
ϵ_2 (relative)	$2.26 \epsilon_0$

TABLE 2
BRAID DIMENSIONS, RG 58/U CABLE
(as measured on a small sample)

a =	1.02×10^{-3}	m.
g =	0.18×10^{-3}	m.
d =	0.84×10^{-3}	m.
$2\alpha =$	45°	
n =	18	

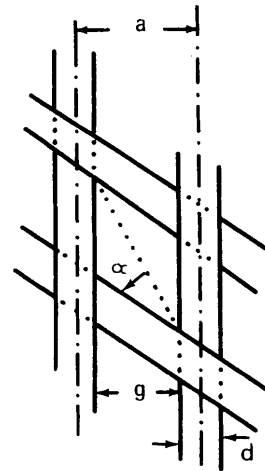


TABLE 3
LONGITUDINAL ATTENUATION (a), RG 58/U CABLE

Frequency (MHz)	.1	.5	1	2	5	10	15	20	50
a (dB per 100 ft.)	.1	.25	.35	.54	.95	1.45	1.8	2.1	3.6

Examination of Figure 3 reveals that leakage through the conducting shield material dominates over that through the braid apertures at frequencies below about 5 MHz. It is also clear that lower frequencies are favored overall with no optimum frequency occurring above 100 kHz in terms of achievable leakage fields. However, a secondary "plateau" region is produced between 5 and 50 MHz by the broad maximum in external field strength predicted when using only the braid shield model. The frequency band in which this field maximum occurs using the braid shield model varies with distance from the cable. At 1 meter from the cable the field maximum occurs between 10 and 20 MHz, while at a distance of 10 meters, the maximum occurs around 1 MHz.

It should be noted that the plots of Figure 3 have taken no account of longitudinal attenuation (Table 3) of the fields as they travel along the cable. This attenuation increases with frequency. In Figure 4 are shown plots of the open circuit voltage induced by the magnetic fields of Figure 3 into a transceiver loop antenna having a nominal effective area, A_{eff} , of 1m^2 . Unlike Figure 3, a frequency dependent attenuation factor which corresponds to transmission along 300 meters of RG-58/U cable has been applied to the signal. Again, no maximum is found in the signal above 100 kHz using the solid shield approximation; and broad voltage maxima for the braid shield model remain at roughly the same frequencies as the field maxima, falling between 10-20 MHz at the distance of 1 meter and between 1 and 5 MHz at a distance of 10 meters. The overall result is as before with the low frequencies favored and a secondary plateau region between 5 and 50 MHz. This result is similar to the original field results because of the approximate cancellation of two opposing effects, (a) the differentiating effect of the receive loop, which favors higher frequencies and (b) the attenuation within the cable, which is greater at higher frequencies. It will also be observed that the open circuit voltage of the receive loop is only a very weak function of frequency below 100 kHz down to about 20 kHz.

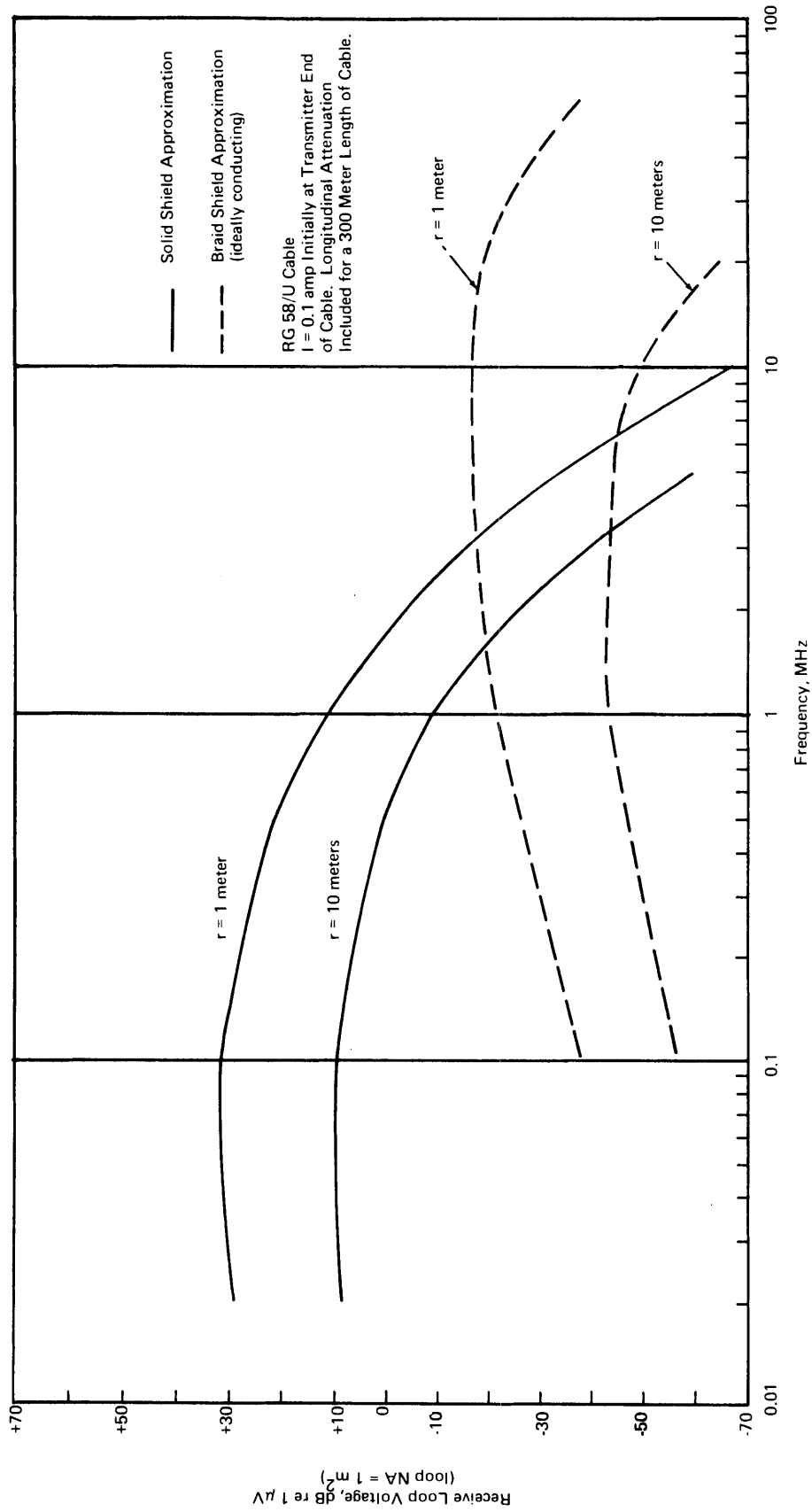


FIGURE 4 RECEIVE LOOP VOLTAGE AT r METERS FROM CABLE AXIS VS FREQUENCY
 (For Loop Located 300 Meters From Transmitter End of Cable)

It is worth noting from Figure 4 that the receive signal voltage at a distance of 1 meter from the cable is about 39dB higher at 100 kHz (solid shield approximation) than the maximum value for the braid shield approximation around 15 MHz. At $r = 10$ meters, this difference increases to about 54dB, when comparing the voltage maximum for the braid shield approximation at about 3 MHz with the higher voltage at the same frequency of 100 kHz for the solid shield case.

D. Attainable Longitudinal Communication Range

This section contains the results of calculations of the two-way longitudinal communication range attainable between a roving miner with a portable transceiver and a fixed base station connected to a leaky coaxial cable hung against the rib of a haulage way. In these calculations it has been assumed that the haulage way environment does not appreciably affect the fields leaked out of the cable into the haulage way cross-section because most of the power is transported inside the cable. Thus, the calculated ranges are those for a cable in free space. Furthermore, the longitudinal range of the communication system has been defined as that point where the leakage field induces a voltage across the matched input of the receiver, at a lateral distance r meters from the cable, which is just equal to the sensitivity of that receiver.* In the following all quantities should be understood as having their RMS values where appropriate.

Assuming a loop antenna,

$$V_r = 1/2 V_{oc} = \pi f \mu_c NAB \quad (18)$$

* This assumes that system performance will be limited by intrinsic receiver noise as opposed to external electromagnetic noise in the mine. As such, the ranges calculated in this section can be considered as upper bounds on performance that will only be further degraded by external noise levels. The electromagnetic noise data recently taken up to 32 MHz by the National Bureau of Standards in several coal mines should allow more realistic estimates of communication range to be made when the reduced data become available in the near future.

where V_r is the voltage across the receiver's matched input,
 V_o is the open circuit voltage across the loop,
 B is the magnetic flux density ($\mu_o H$) in webers/meter²
 μ_c is the effective permeability factor, and NA , the
product of the number of turns times the area of the loop.

In more convenient units for this calculation, the maximum acceptable field intensity H_ϕ is given by

$$H_\phi \text{ (dB re 1 ampere per meter)} = V_r^s \text{ (dB re 1 } \mu\text{V)} \\ - \mu_c NA \text{ (dB re 1 m}^2) - f \text{ (dB re 1 MHz)} - 132, \quad (19)$$

where V_r^s is the sensitivity of the receiver.

The maximum longitudinal two-way communication range has been calculated for RG 58/U coaxial cable using equation (19), in conjunction with previous computations of H_ϕ and the longitudinal attenuation associated with this cable given in Table 3. The variation in longitudinal communication range with operating frequency, lateral range, and loop effective area, based on the two simplified models of field behavior discussed earlier, is presented for RG 58/U cable in Table 4. These tabulated values, as noted in the table, are for a portable FM system having a nominal transmitter power of 1 watt and receiver sensitivity of 1 microvolt, under the most favorable signal conditions when the mobile unit antenna is oriented for maximum coupling to the coaxial cable leakage fields and no destructive interference (fading) is present. The range implications of nominal polarization and/or fading losses are also noted.

E. Discussion of Results

The results tabulated in Table 4 indicate that one can hope to achieve base station-to-portable unit communications along cable lengths of up to about one mile only at operating frequencies around 100 kHz and below, with reasonable portable transmitter and receiver parameters and without

TABLE 4

MAXIMUM TWO-WAY LONGITUDINAL COMMUNICATION RANGE VIA
LEAKY COAXIAL CABLE (50Ω, RG 58/U)

FM System

Transmitter Power = 1 watt[‡]

Injected Current = 141 milliamperes rms

Receiver-Noise-Limited Case for a Receiver Sensitivity of $V_r^S = 1\mu V$
for 20 dB of Quieting

Loop Effective Area = $\mu_c NA$ [‡]

Lateral Range (meters)	Frequency (MHz)	Maximum Longitudinal Communication Range [§] (feet)		
		$\mu_c NA = 0.1m^2$	$\mu_c NA = 1m^2$	$\mu_c NA = 10m^2$
1	0.1	8,000	28,000	48,000
	0.5	400	8,400	16,400
	1	0	3,700	9,300
	2	0	0	3,900
	5	(0)*	(300)*	(2,500)*
	10	(0)	(800)	(2,200)
	20	(0)	(800)	(1,800)
2	0.1	2,000	22,000	42,000
	0.5	0	6,000	14,000
	1	0	1,900	7,700
	2	0	0	2,600
	5	(0)*	(0)*	(1,800)*
	10	(0)	(300)	(1,700)
	20	(0)	(400)	(1,400)
3	0.1	0	18,500	38,500
	0.5	0	4,600	12,600
	1	0	1,000	6,700
	2	0	0	2,000
	5	(0)*	(0)*	(1,400)*
	10	(0)	(300)	(1,700)
	20	(0)	(100)	(1,100)

*Ranges in parentheses are obtained by use of field strengths calculated from the leaky braid model. In all cases where ranges are given for the braid model, the solid shield model gives zero range.

‡ Representative values of effective loop area and transmitter power for portable personal transceiver units are $0.5m^2$ – for a ferrite-loaded loop, and 1 watt, respectively; and for mobile vehicular units, $5m^2$ for an air-core loop, and 10 watts. The ferrite-loaded loop effective area reduces to unacceptable levels for a practical design as the frequency increases (falling to about $0.005m^2$ around 20 MHz), thereby indicating that a whip antenna about 2 feet long will be needed to obtain the required signal levels at the higher frequencies.

§ The maximum ranges tabulated above are for the most favorable signal and noise conditions. If a nominal safety margin of 14 dB is also included to account for likely polarization and fading losses (the former at lower frequencies and the latter at higher frequencies), ranges that are more realistic for routine use of portable units in haulage ways are probably those in the $\mu_c NA = 0.1m^2$ column above. The corresponding ranges for vehicular units should lie approximately half way between those in the $1m^2$ and $10m^2$ columns. These ranges apply when receiver noise, not external electromagnetic mine noise, is the dominating noise source. Longitudinal ranges for different values of power, loop area, safety margin, receiver sensitivity or corresponding levels of external noise, can also be obtained by relating the total dB change to the equivalent change in cable length using the Table 3 longitudinal attenuation values for each frequency.

Finally, though the lower frequencies offer the greatest signal levels for a given transmitter current, these levels unfortunately can require rf transmitter voltages on the order of 100 volts for a portable unit with a 100 milliamper loop current. Therefore, the implications of these voltage and current levels on the intrinsic safety of such portable units should be investigated if they are to be used in the face areas of working sections.

repeaters placed in the cable. Larger, higher-powered vehicle-mounted mobile units will achieve greater longitudinal ranges as indicated. Table 4 also reveals that lateral distance from the cable in the haulage way is not a significant factor with respect to determining the optimum frequency band. Furthermore, the evidence of Figure 4 shows that below about 100 kHz, there is not much to choose between frequencies in terms of signal strength. At longitudinal communication distances of more than one to two miles, frequencies of a few tens of kHz will be slightly favored over 100 kHz, from the point of view of signal strength, because of the lower attenuation along the cable at lower frequencies. However, these differences in signal strength with frequency are no larger and perhaps even smaller (2-3 dB) than the uncertainties presented by the external noise environment in the haulage way. This external noise may in fact turn out to be the limiting factor on communication range, and hence be the final influence on the choice of operating frequency.

The choice of an optimum operating frequency is a function of four factors* which vary differently with frequency, namely longitudinal attenuation of the signal within the line, leakage of the field to the outside, propagation of the "leaked" field outside the cable, and external noise levels. External noise levels were not included in the above calculations because significant data were not yet conveniently available to adequately characterize the haulage way noise environment. Preliminary data from noise measurements taken in mines by National Bureau of Standards personnel indicate that under some circumstances, external noise will be the limiting factor on performance. Therefore, it will be important to monitor and apply the results of NBS's noise measurement program in order to determine when and how seriously external noise may impede the performance of coaxial cable communication systems. It will then be possible to determine if a distinctly optimum operating frequency is identifiable from a practical standpoint within the presently favored 10 kHz to 100 kHz band or at higher frequencies for two-way base station-to-portable

* As mentioned in Table 4, intrinsic safety and practical design considerations may also play important roles, particularly for the portable units.

communications in haulage ways. On the other hand, a few brief calculations have shown that at no frequency is it possible to obtain portable-to-portable communication via conventional coaxial cable without repeaters or radiating devices inserted in the cable.

In the above work, the effect upon the leaked fields of the characteristics of the tunnels and rock found in mines has been neglected. This approximation is probably reasonably valid in the haulage way close to the cable itself (at a lateral separation of one to perhaps two meters, for example), but should be investigated further. On the other hand, the approximation should be grossly inadequate for predicting lateral range down entries crossing the haulage way containing the cable. As shown in Part Four of this report, radio waves propagating down entries without conductors will be severely attenuated by losses in the surrounding rock at frequencies suitable for the conventional leaky coaxial cables discussed in this Part (Three) of the report.

The theories of leakage fields used to derive the attainable communication ranges in Table 4 contain other assumptions and approximations which must of course be tested experimentally before the conclusions drawn using them can be regarded as firm. For example, the relative amplitudes of the leakage fields calculated in the regions of validity of the two different models (solid wall and infinitely-conducting braid shield approximations) have to be verified before definitive statements concerning the optimum operating frequency for a leaky conventional coaxial cable transmission system can be made.

The application of the braid shield model to the calculation of leakage fields from RG 58/U cable must also be viewed as subject to some uncertainty. It appears to us that the model as it stands may only give accurate results when applied to cables with braid shields in which the apertures and shield radius are substantially larger than is the case

with standard RG 58/U cable. However, while the absolute values of the leakage field for the braided shield model are subject to doubt, the predicted behavior of this field with frequency, i.e., a broad maximum between 10 and 20 MHz, is on more certain ground.

Relatively straightforward experiments are required to measure the magnetic field signal strengths as functions of frequency and distance from long lengths of conventional coaxial cables in air and in mine haulage ways. Then curves such as those shown in Figures 3 and 4 can be verified in terms of both shape and amplitude, or corrections made to them and the theory if appropriate. It would also be instructive and worthwhile to reconcile and compare the method of calculation described in this report with those followed by workers in other countries, notably France (1), the U.K. (2), and Canada (3), in their investigations of radio communication in mines by means of coaxial cable.

III. EUROPEAN WORK WITH LEAKY COAXIAL CABLE COMMUNICATION SYSTEMS

A. State-of-the-Art

Three major classes of coaxial cable communication systems designed for use in mines have been reported as being in various stages of development in Europe.

- (1) INIEX/Delogne system (Belgium) employing regularly spaced radiating devices along conventional RG-8/U coaxial cable (4).

Much experimental and theoretical investigation of this system has been performed including trials at the Bruceton, Pa. Safety Research mine of the USBM. The optimum operational frequency is believed to fall in the range of 2-20 MHz. Prototype installations are on order in Belgium, at a price of about \$2500/km. Firm production sales prices are not yet available. The INIEX/Delogne scheme appears potentially suitable for

application in U.S. mines, although several uncertainties regarding performance/cost trade-offs in typical U.S. mine environments still have to be resolved. These uncertainties are connected in particular with the restraint in U.S. mines of having to install the cable close to the rib with consequent increases in attenuation, in contrast to the more central location in an arched tunnel allowed in Europe, and with the influences on performance of dirt and water on the cable and radiative devices.

- (2) Coaxial cable with high surface transfer impedance -- specially designed "leaky" braid outer conductor (France).

Theoretical investigations carried out at the University of Lille in France indicate that effective communication along several miles of mine haulage way may be achieved by use of a coaxial cable whose braid outer conductor is designed and fabricated for "optimum" leakage of radiation. Experimental investigations of this scheme in a French mine are planned to be carried out near the end of 1973. The optimum operational frequency is believed to be between 5-10 MHz.

Similar uncertainties exist with regard to the effects of dirt, water, and proximity to the walls of the tunnel on the performance of the proposed French scheme in U.S. mine environments, as were mentioned in the context of the Belgian cable system.

- (3) Conventional coaxial cable with repeaters (U.K.)

It has been reported that a conventional coaxial cable communication system incorporating repeaters is being tested experimentally in the U.K. Little information on the cost and performance of this system is yet available in the U.S. Additional uncertainties in the performance and cost evaluations of this system are introduced by questions associated with the reliability and maintainability of the repeaters that can realistically be expected in a mine environment.

B. Discussion

Progress achieved in Europe in the development of the coaxial cable communication systems mentioned above should be carefully and continually monitored and evaluated. In particular, cost estimates and further operating performance data should be obtained.

Nevertheless, European results, while valuable and to date encouraging, cannot be directly applied to the different environment of U.S. mines. In particular it appears impossible to install communication cables in U.S. mines in the locations recommended by European researchers. Specifically, cables will have to be installed close to the ribs or walls in U.S. mines. Accordingly different attenuation rates, and correspondingly different optimum operating frequencies or tradeoffs between the rate of "leakage" of power and total communication system length may prevail than in the European situation. Experimental investigations in U.S. mines with the proposed European coaxial cable systems are required before their applicability in this country can be definitively confirmed or denied, and if confirmed, operational specifications written (for frequency, design of radiative structure or "leaky" outer conductor, and so forth).

IV. REFERENCES

1. J. Fontaine, et al., Universite des Sciences de Lille, "Feasibility of Radiocommunication in Mine Galleries," paper presented at the Through-the-Earth Electromagnetics Workshop, Colorado School of Mines, Golden, Colorado, August, 1973.
2. D.J.R. Martin, "Full Coverage of the Mine by Line-Propagated VHF Radio," Mining Technology, November, 1970.
3. V. Rawat, et al., Queen's University, Ontario, "Transmission Lines for Continuous-Access Guided Communications in Mines and Tunnels," Proceedings of the 1972 IEEE-G-MTT International Microwave Symposium, May 22-24, 1972.
4. P. Delogne and R. Liegeois, "Le Rayonnement d'une Interruption du Conducteur Exterieur d'un Cable Coaxial," Annales des Telecommunications, 26 (1971), p. 85.

PART FOUR
THEORY OF WIRELESS PROPAGATION
OF UHF RADIO WAVES
IN COAL MINE TUNNELS

PART FOUR
THEORY OF WIRELESS PROPAGATION
OF UHF RADIO WAVES
IN COAL MINE TUNNELS

TABLE OF CONTENTS

	<u>Page</u>
List of Tables	4.iv
List of Figures	4.v
INTRODUCTION	4.1
I. RAY THEORY	4.3
II. WAVE METHOD	4.4
III. COMPARISON WITH EXPERIMENT	4.6
IV. DIFFUSE RADIATION CALCULATIONS	4.10
A. ROUGHNESS EFFECTS	4.11
B. TILT EFFECTS	4.12
C. COUPLING OF INDIVIDUAL MODES	4.14
V. PROPAGATION AROUND A CORNER	4.16
VI. EFFECT OF ANTENNA ORIENTATION	4.23
VII. INSERTION LOSS	4.24
VIII. OVERALL LOSS IN A STRAIGHT TUNNEL	4.26
IX. OVERALL LOSS ALONG A PATH WITH ONE CORNER	4.29
X. CONCLUSIONS	4.33
XI. REFERENCES	4.34
APPENDIX A - RAY METHOD	4.35
APPENDIX B - WAVE METHOD	4.37
APPENDIX C - COUPLING OF E_h and E_v MODES	4.43

PART FOUR

THEORY OF WIRELESS PROPAGATION
OF UHF RADIO WAVES
IN COAL MINE TUNNELS

TABLE OF CONTENTS
(Continued)

	<u>Page</u>
APPENDIX D - PROPAGATION AROUND A CORNER	4.49
APPENDIX E - ANTENNA INSERTION LOSS BY CURRENT- DISTRIBUTION METHOD	4.53
APPENDIX F - EXPECTED COMMUNICATION RANGE BETWEEN TWO ROVING MINERS	4.55

PART FOUR
THEORY OF WIRELESS PROPAGATION
OF UHF RADIO WAVES
IN COAL MINE TUNNELS

LIST OF TABLES

<u>Table No.</u>	<u>Title</u>	<u>Page</u>
I	Diffuse Radiation Component in Main Tunnel and at Beginning of Cross Tunnel	4.18
II	Excitation of E_h Mode in Cross Tunnel by Diffuse Component in Main Tunnel	4.20
III	Effect of Antenna Orientation	4.24
IV	Insertion Loss (L_i) (For a Half-Wave Antenna)	4.26
V	Calculation of Overall Loss for E_h Mode with Two Half Wave Dipole Antennas	4.27
VI	Overall Loss Along a Path Including One Corner E_h Mode with Half Wave Dipole Antennas	4.32
A1	Ray Method Calculations (For E_h Mode)	4.36
B1	Loss Rates for Various Modes	4.42
C1	Coupling Between E_h and E_v Modes	4.48

PART FOUR
THEORY OF WIRELESS PROPAGATION
OF UHF RADIO WAVES
IN COAL MINE TUNNELS

LIST OF FIGURES

<u>Figure No.</u>	<u>Title</u>	<u>Page</u>
1	Refraction Loss for E_h and E_v Modes in High Coal	4.7
2	Refraction Loss for E_h Mode in Low Coal	4.8
3	Resultant Propagation Loss for E_h Mode in High Coal (Refraction, Wall Roughness and Tilt)	4.15
4	Corner Loss in High Coal - 415 MHz	4.21
5	Corner Loss in High Coal - 1000 MHz	4.22
6	Total Loss for Various Distances Along a Straight Tunnel	4.28
7	Overall Loss in a Straight Tunnel in High Coal (for Isotropic Antennas) - 415 MHz	4.30
8	Overall Loss in a Straight Tunnel in High Coal (for Isotropic Antennas) - 1000 MHz	4.31
C1	Incident and Reflected Fields Relative to a Rotated Portion of the Roof of the Tunnel	4.44
D1	Geometry for Coupling to Cross Tunnels	4.50
F1	Predicted UHF Wireless Radio Coverage	4.56

PART FOUR

THEORY OF WIRELESS PROPAGATION
OF UHF RADIO WAVES
IN COAL MINE TUNNELS

INTRODUCTION

This Part is concerned with the theoretical study of UHF radio communication in coal mines, with particular reference to the rate of loss of signal strength along a tunnel, and from one tunnel to another around a corner. Of prime interest are the nature of the propagation mechanism and the prediction of the radio frequency which propagates with the smallest loss. Our theoretical results are compared with measurements made by Collins Radio Co.

This work was conducted as part of the Pittsburgh Mining and Safety Research Center's investigation of new ways to reach and extend two-way communications to the key individuals that are highly mobile within the sections and haulage ways of coal mines.

At frequencies in the range of 200-4,000 MHz the rock and coal bounding a coal mine tunnel act as relatively low loss dielectrics with dielectric constants in the range 5-10. Under these conditions a reasonable hypothesis is that transmission takes the form of waveguide propagation in a tunnel, since the wavelengths of the UHF waves are smaller than the tunnel dimensions. An electromagnetic wave traveling along a rectangular tunnel in a lossless dielectric medium can propagate in any one of a number of allowed waveguide modes. All of these modes are "lossy modes" owing to the fact that any part of the wave that impinges on a wall of the tunnel is partially refracted into the surrounding dielectric and partially reflected back into the waveguide. The refracted part propagates away from the waveguide and represents a power loss. This type of waveguide mode differs from the light-pipe modes in glass fibers in which total internal reflection occurs at the wall of the fiber, with zero power loss if the fiber and the matrix in which it is embedded are both lossless. It is to be noted that the attenuation rates of the waveguide modes studied in this paper depend almost entirely on refraction loss, both for the dominant mode and higher modes excited by scattering, rather than on ohmic loss. The effect of ohmic loss due to the small conductivity of the surrounding material is found to be negligible at the frequencies of interest here, and will not be further discussed.

The study reported here is concerned with tunnels of rectangular cross-section and the theory includes the case where the dielectric constant of the material on the side walls of the tunnel is different from that on top and bottom walls. The work extends the earlier theoretical work by Marcatili and Schmeltzer⁽¹⁾ and by Glaser⁽²⁾ which applies to waveguides of circular and parallel-plate geometry in a medium of uniform dielectric constant.

I. RAY THEORY

The allowed modes in a rectangular tunnel in a dielectric can be determined approximately either by a ray theory or a wave theory approach. In the ray method we consider a ray of the radiation which bounces from wall to wall of the tunnel making a grazing angle ϕ_1 with the side walls and ϕ_2 with the floor and roof. The propagation modes with the lowest attenuation rates are the two (1, 1) modes which have the electric field, E, polarized predominantly in the horizontal and vertical directions, respectively. These two modes, which we will refer to as the E_h and E_v modes, are both defined in the ray picture by the phase relations

$$\sin\phi_1 = \frac{\lambda}{2d_1} \quad (1)*$$

$$\sin\phi_2 = \frac{\lambda}{2d_2} \quad (2)$$

where λ is the free space wavelength of the radiation and d_1 , d_2 are the horizontal and vertical dimensions of the tunnel. Equations (1) and (2) are the conditions that the phase shift undergone by the ray is exactly 360° after successive reflections from the two side walls or from the floor and roof.

For frequencies around 1,000 MHz, λ is small compared with d_1 and d_2 . Therefore we can use the approximate relations

$$\phi_1 = \frac{\lambda}{2d_1} \quad (3)$$

$$\phi_2 = \frac{\lambda}{2d_2} \quad (4)$$

The numbers of reflections N_1 and N_2 experienced by a ray at the vertical and horizontal walls of the tunnel, while traveling a distance z along the tunnel, are given by

$$N_1 = \frac{z\phi_1}{d_1} \quad (5)$$

$$N_2 = \frac{z\phi_2}{d_2} \quad (6)$$

The attenuation factor for the ray intensity for this distance is

$$\frac{I}{I_0} = R_1^{N_1} R_2^{N_2} \quad (7)$$

where R_1 and R_2 are the power reflectances of the vertical and horizontal surfaces at the grazing angles ϕ_1 and ϕ_2 , respectively.

* References to Figures, Tables and Equations apply to those in this Part unless otherwise noted.

On combining equations (3)-(7) we find for the loss L in decibels

$$L = 5\lambda z \left(\frac{1}{d_1^2} \log_{10} \frac{1}{R_1} + \frac{1}{d_2^2} \log_{10} \frac{1}{R_2} \right) \quad (8)$$

In using this formula to calculate the loss rate one must calculate R_1 and R_2 by means of the standard Fresnel reflection formulas for the angles ϕ_1 and ϕ_2 , and the corresponding dielectric constants K_1 and K_2 . The result is different for the E_h and E_v modes because the Fresnel formulas are different for the two polarizations. Appendix A gives the Fresnel formulas and ray-method calculations for the E_h mode.

II. WAVE METHOD

In the wave method we obtain an approximate solution of Maxwell's equations for lossy modes in a rectangular waveguide with dielectric walls. We use Cartesian coordinates with origin at the center of the tunnel cross-section, the z-axis along the tunnel axis, the x-axis horizontal, and the y-axis vertical. In the case of the E_h mode the main field components of the mode are given approximately by

$$E_x = E_o \cos k_1 x \cos k_2 y e^{-ik_3 z} \quad (9)$$

$$H_y = \frac{k_3}{\omega \mu_o} E_o \cos k_1 x \cos k_2 y e^{-ik_3 z} \quad (10)$$

where the symbols have their customary meaning and

$$k_1^2 + k_2^2 + k_3^2 = k_o^2 = 4\pi^2/\lambda^2. \quad (11)$$

In addition to these transverse field components there are small longitudinal components E_z and H_z and a small transverse component H_x .

The simple solution given by (9) and (10), along with the small longitudinal and transverse components, does not allow the boundary conditions of continuity of the tangential components of E and H to be accurately satisfied over the whole surface of the waveguide. An approximation to the boundary conditions gives values for k_1 and k_2 as follows:

$$k_1 \cong \frac{\pi}{d_1} \left(1 - \frac{2iK_1}{k_o d_1 \sqrt{K_1 - 1}} \right) \quad (12)$$

$$k_2 \cong \frac{\pi}{d_2} \left(1 - \frac{2i}{k_o d_2 \sqrt{K_2 - 1}} \right) \quad (13)$$

where K_1 and K_2 are the dielectric constants of the sidewalls and of the floor and roof, respectively.

From (11)-(13) we obtain the imaginary part of the wave number z-component k_3 and from it the power loss over a distance z. The result in decibels is

$$L_{Eh} = 4.343\lambda^2 z \left(\frac{K_1}{d_1^3 \sqrt{K_1 - 1}} + \frac{1}{d_2^3 \sqrt{K_2 - 1}} \right) . \quad (14)$$

In like manner the loss for the E_v mode is found to be

$$L_{Ev} = 4.343\lambda^2 z \left(\frac{1}{d_1^3 \sqrt{K_1 - 1}} + \frac{K_2}{d_2^3 \sqrt{K_2 - 1}} \right) . \quad (15)$$

These results show that the loss rate increases with the square of the wavelength and decreases with the cube of the linear dimensions of the tunnel. Losses calculated by (14) and (15) agree closely with those calculated by the ray loss formula (8). Since (14) and (15) do not require evaluation of the Fresnel reflectances R_1 and R_2 , they are considerably simpler to use. Details of the wave theory, including loss calculations for higher modes, are given in Appendix B.

III. COMPARISON WITH EXPERIMENT

Figure 1 shows loss rates in dB/100 ft. as functions of frequency calculated by equations (14) and (15) for the E_h and E_v modes in a tunnel of width 14 ft. and height, 7 ft., representative of a haulage way in a seam of high coal, for $K_1 = K_2 = 10$, corresponding to coal on all the walls of the tunnel. It is seen that the loss rate is much greater for the E_v mode. Figure 2 shows the calculated E_h loss rate for a tunnel of half the height. The higher loss rate is due to the effect of the d_2^3 term in equation (14).

Two experimental values obtained by Collins Radio Co.⁽³⁾ for horizontal-horizontal antenna orientations are also shown in Figure 1. These values agree well with theory for the E_h mode for 415 MHz, but not so well at 1,000 MHz. The departure suggests that some additional loss mechanism sets in at higher frequencies.

It is also to be noted that the experimental values of the loss rates for all three orientation arrangements of the transmitting and receiving dipole antennas, namely, horizontal-horizontal, vertical-horizontal, and vertical-vertical, are surprisingly close to each other. The independence of loss rate with respect to polarization is not predicted by the theory discussed so far, as seen in Figure 1 for the E_h and E_v modes. Indeed the theory predicts no transmission at all for the VH antenna arrangement.

FIGURE 1
 REFRACTION LOSS FOR E_h AND E_v MODES
 IN HIGH COAL

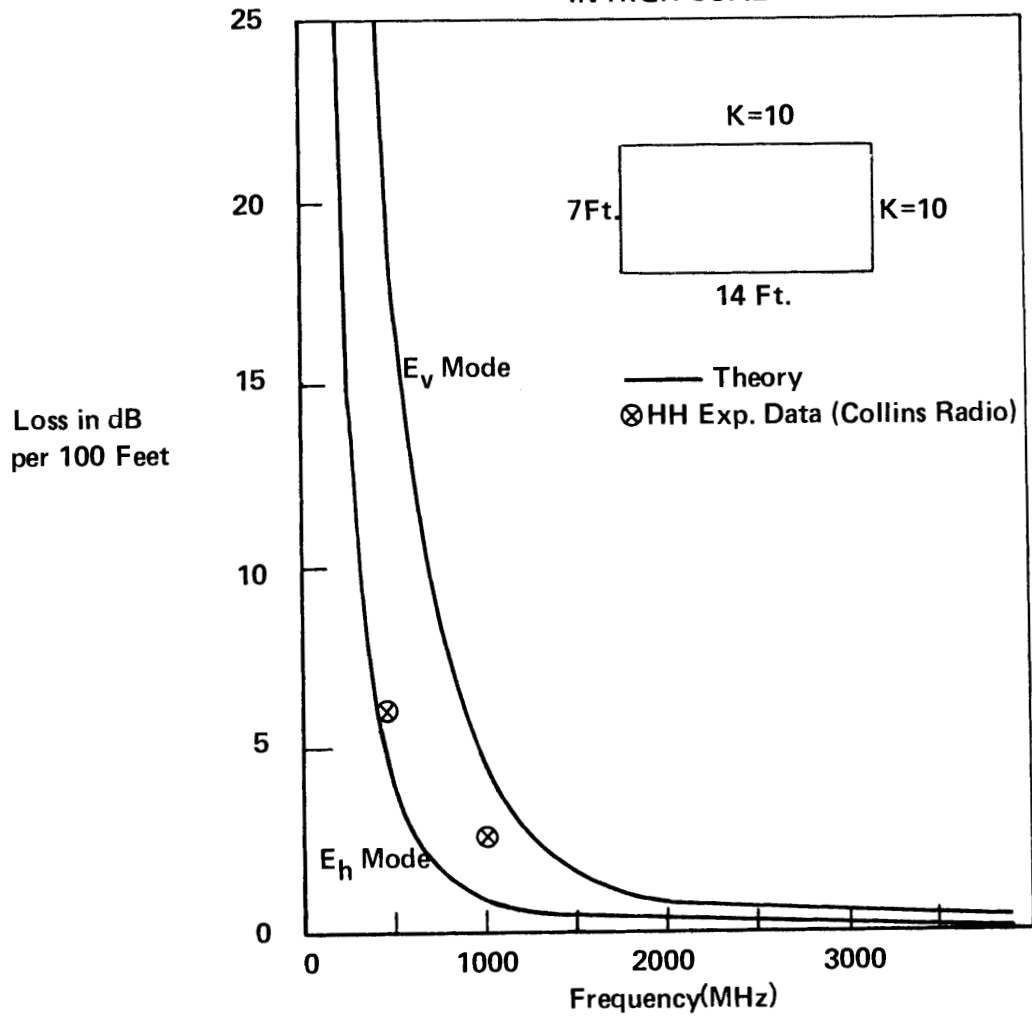
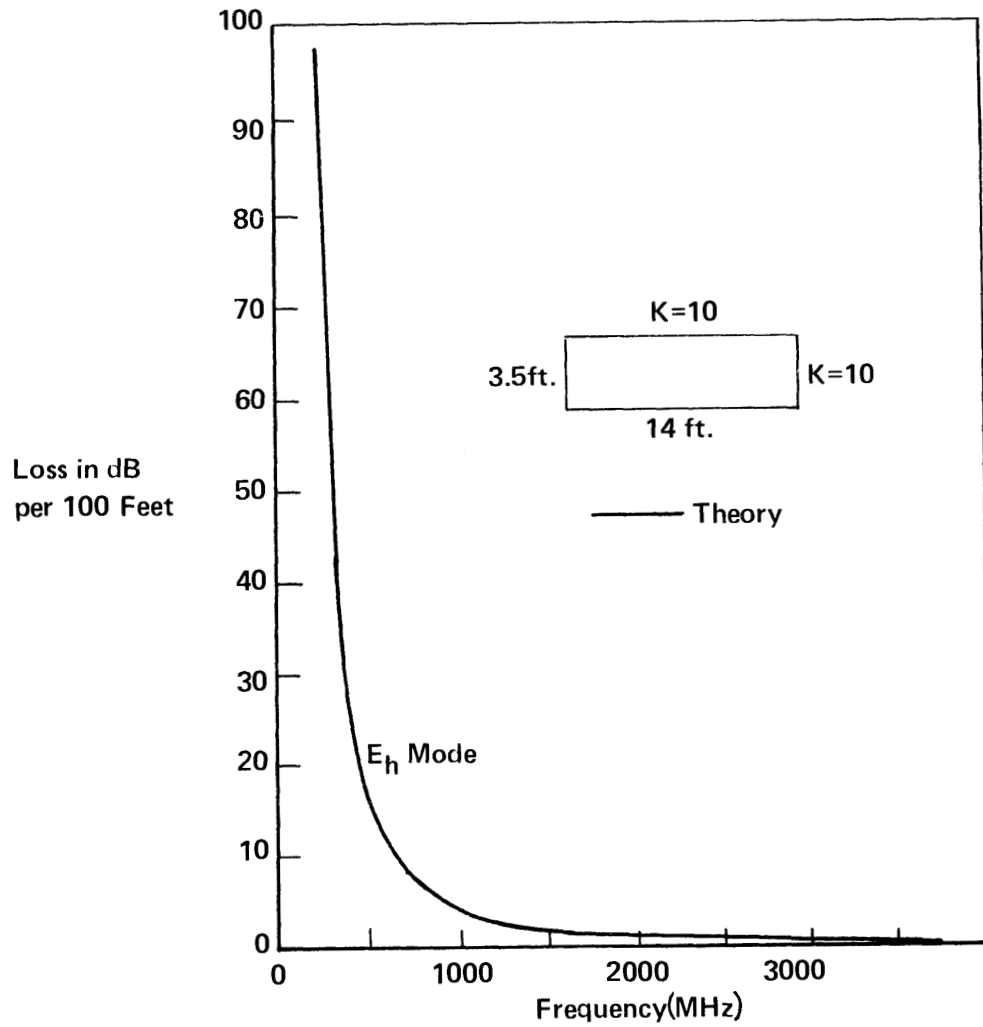


FIGURE 2
REFRACTION LOSS FOR E_h MODE IN LOW COAL



To explain both the higher observed loss rate at the higher frequencies, relative to the calculated E_h mode values, and the independence of the loss rate on antenna orientation, we postulate that roughness and variable tilt of the four tunnel walls combine to cause scattering of the dominant E_h mode. The scattered radiation goes into many higher modes and can be regarded as a diffuse component that accompanies the E_h mode. The diffuse component is in dynamical equilibrium with the E_h mode in the sense that its rate of generation by the E_h mode is balanced by its rate of loss by refraction into the surrounding dielectric. Since the diffuse component consists of higher waveguide modes for which the refractive loss rate is much higher than for the fundamental E_h mode, the dynamical balance point is such that the level of the diffuse component is many dB below that of the E_h mode at any point in the tunnel.

The scattering loss from the E_h mode into the diffuse component begins to increase rapidly when the wavelength is so short that the mode grazing angles ϕ_1 and ϕ_2 , defined earlier, become comparable with the root mean square tilt of the walls of the tunnel. This accounts for the higher experimental loss at 1,000 MHz than that predicted for the E_h mode by the theory for a perfect dielectric waveguide shown in Figure 1.

The diffuse radiation component also accounts for the observed independence of loss rate on antenna orientation. The argument here is that, irrespective of whether the transmitting antenna is oriented horizontally or vertically, at a sufficient distance down the tunnel the radiation ultimately settles down into the dominant E_h component and a weaker diffuse component. If the transmitting antenna is oriented vertically it initially excites the E_v mode which dies out relatively rapidly by refractive loss and scattering into the unpolarized diffuse component. The diffuse component in turn couples to the E_h mode which, owing to its much lower loss rate finally becomes dominant. When dynamical

equilibrium is reached the diffuse component remains at a fixed number of dB below the E_h mode. Therefore a vertically oriented receiving antenna carried down the tunnel measures the loss rate of the E_h mode. A horizontal receiving antenna measures the E_h mode directly and the loss rate is the same as before although the insertion loss of the antenna is considerably less.

Experiments by Collins Radio Co. on the signal strength transmitted around a corner into a cross tunnel give further convincing proof of the diffuse component hypothesis. They found that a large loss occurred when the receiving antenna was moved around the corner, but that the received signal strength was then independent of antenna orientation. This is exactly what one would expect from the diffuse radiation hypothesis since the well collimated E_h mode in the main tunnel couples very weakly into the cross tunnel, whereas the uncollimated diffuse component couples fairly efficiently. Since the diffuse radiation is likely to be largely unpolarized the observed independence of signal strength on antenna orientation is understandable.

Another observation by Collins Radio is that the initial attenuation rate on entering the cross tunnel is much higher than the rate in the main tunnel. This is also in accord with the diffuse radiation component which has a much larger loss rate than the E_h mode owing to its steeper angles of incidence on the tunnel walls.

IV. DIFFUSE RADIATION CALCULATIONS

We discuss two different mechanisms by which diffuse radiation is generated by scattering out of the dominant E_h mode. The first of these is roughness of the walls of the tunnel which is here regarded as variations in local surface level relative to the mean surface level. The second is long range tilt of the tunnel walls relative to the mean planes which define the dimensions d_1 and d_2 of the tunnel.

A. Roughness Effects

When a parallel beam of radiation of intensity I_0 strikes a rough surface at normal incidence the reflected radiation consists of a parallel beam of reduced intensity I together with a diffuse component. If the surface is a perfect reflector

$$I = I_0 e^{-2\left(\frac{2\pi h}{\lambda}\right)^2} \quad (16)$$

where λ is the wavelength and h is the root mean square roughness. For incidence at a grazing angle ϕ one may assume that the effective roughness is now $h \sin\phi$, so the loss factor becomes⁽⁴⁾

$$f = e^{-2\left(\frac{2\pi h \sin\phi}{\lambda}\right)^2} \quad (17)$$

In the case of the dominant mode in a dielectric waveguide we can from equations (1) and (2) write for the roughness loss factors per reflection for the vertical and horizontal walls:

$$f_1 = e^{-2\left(\frac{\pi h}{d_1}\right)^2} \quad (18)$$

$$f_2 = e^{-2\left(\frac{\pi h}{d_2}\right)^2} \quad (19)$$

The loss factor for a distance z is therefore, from equations (3)-(6)

$$f = e^{-2N_1\left(\frac{\pi h}{d_1}\right)^2 - 2N_2\left(\frac{\pi h}{d_2}\right)^2} \approx e^{-\pi^2 h^2 \lambda \left(\frac{1}{d_1^4} + \frac{1}{d_2^4}\right) z} \quad (20)$$

The loss in dB is then

$$L_{\text{roughness}} = 4.343\pi^2 h^2 \lambda \left(\frac{1}{d_1} + \frac{1}{d_2} \right) z \quad (21)$$

B. Tilt Effects

The effect of wall tilt can be estimated as follows. Suppose that a ray of the E_h mode encounters a portion of a side wall that is tilted through a small angle θ about a vertical axis. Then the reflected beam is rotated through an angle 2θ . This means that the electric field is changed from

$$E_x = F(x,y) e^{-ik_3 z} \quad (22)$$

to

$$E_x' = F(x,y) e^{-ik_3 (z \cos 2\theta + x \sin 2\theta)} \quad (23)$$

The power coupling factor g_1 of the disturbed field (23) back into the mode (22) is given by

$$g_1 = \frac{|\iint E_x \bar{E}_x' dx dy|^2}{\iint |E_x|^2 dx dy \iint |E_x'|^2 dx dy} \quad (24)$$

where the integrations are over the cross-section of the tunnel. The bar over E_x indicates complex conjugate. Since θ is small we can replace $\cos 2\theta$ by 1 and $\sin 2\theta$ by 2θ . Then (24) becomes

$$g_1 = \frac{|\iint |F|^2 e^{2ik_3 x \theta} dx dy|^2}{(\iint |F|^2 dx dy)^2} \quad (25)$$

Instead of using the actual function $\cos k_1 x \cos k_2 y$ for F , we find it more convenient to use an equivalent Gaussian function

$$F = F_0 e^{-\left(\frac{x^2}{a^2} + \frac{y^2}{b^2}\right)} \quad (26)$$

and integrate over infinite limits. The result is

$$g_1 = e^{-\frac{1}{2} k_3^2 a^2 \theta^2} \quad (27)$$

Next we assume that F^2 falls to $1/e$ at the point $x = d_1/2$, $y = 0$, which is at the surface of the waveguide. Then $a^2 = 1/2 d_1^2$ and

$$g_1 = e^{-\frac{1}{4} k_3^2 d_1^2 \theta^2} \quad (28)$$

Likewise, tilting of the floor or roof gives a coupling factor

$$g_2 = e^{-\frac{1}{4} k_3^2 d_2^2 \theta^2} \quad (29)$$

The loss factor for a distance z is

$$g = g_1^{N_1} g_2^{N_2} = e^{-\frac{\pi^2 \theta^2 z}{\lambda}} \quad (30)$$

where we have replaced k_3 by k_0 .

The loss in dB is therefore

$$L_{\text{Tilt}} = \frac{4.343 \pi^2 \theta^2 z}{\lambda} \quad (31)$$

On comparing equation (21) with equation (31) we see that whereas the roughness loss depends strongly on the waveguide dimensions the tilt loss is independent of them. Another important difference is that the roughness increases with wavelength while the tilt loss decreases.

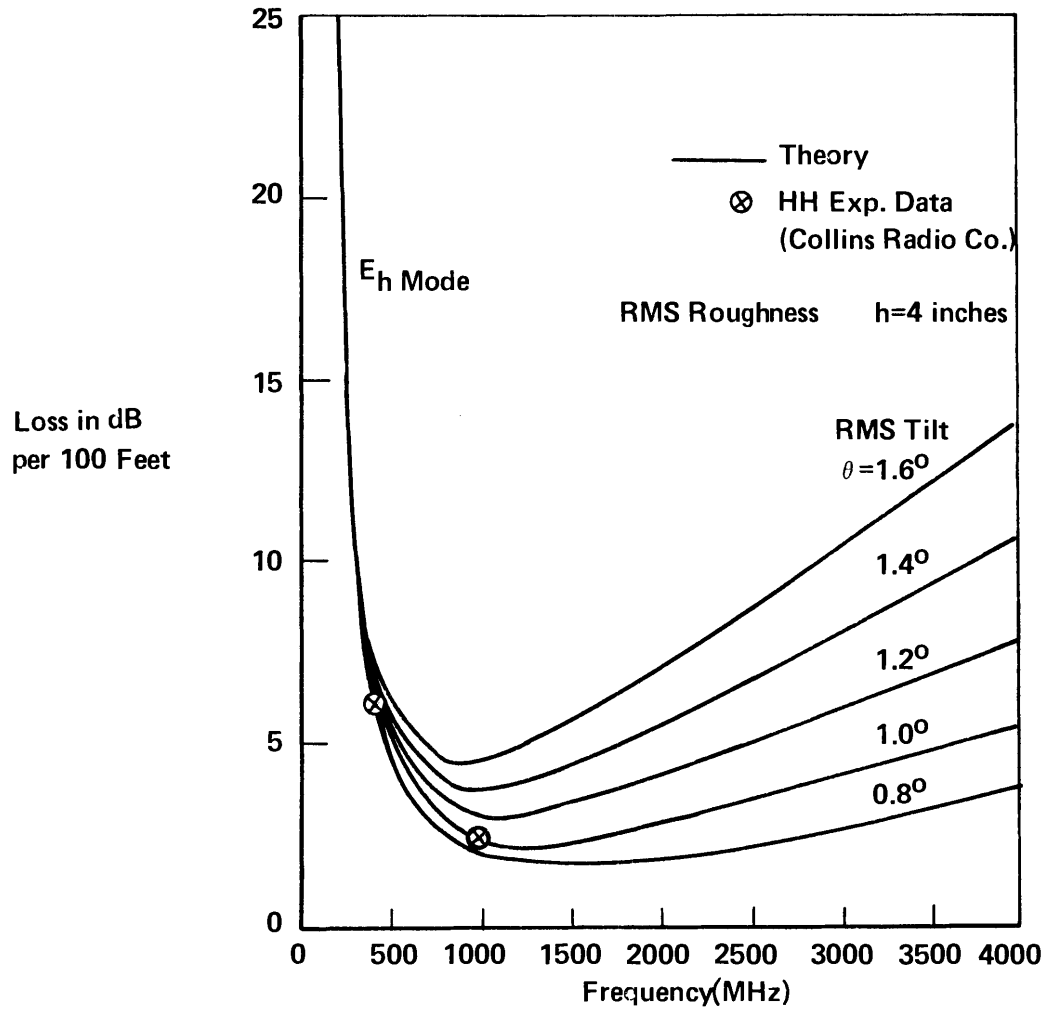
Figure 3 shows the effect on the E_h mode propagation of adding the loss rates due to roughness and tilt to the refraction loss given in Figure 1. The curves are calculated for a root mean square roughness of 4 inches and for various assumed values of the root mean square tilt angle θ . It is seen that a value $\theta = 1^\circ$ gives good agreement with the experimental values measured by Collins Radio Co. The effect of tilt is much greater than that of roughness.

The results indicate that for a 14 ft. x 7 ft. tunnel in a medium of dielectric constant 10 the optimum frequency is about 1,000 MHz.

C. Coupling of Individual Modes

The diffuse radiation method is a convenient first approximation to the solution of the difficult problem of the mutual interactions of all the allowed waveguide modes caused by irregularities of the waveguide walls. As a first step in this interaction problem we have considered the coupling between the (1,1) E_h and E_v modes due to longitudinal ridges on the roof of the tunnel. The results of the calculation are given in Appendix C.

FIGURE 3
 RESULTANT PROPAGATION LOSS FOR E_h MODE IN HIGH COAL
 (Refraction, Wall Roughness and Tilt)



V. PROPAGATION AROUND A CORNER

As mentioned earlier, signal propagation from a main tunnel around a corner into a cross tunnel arises from the diffuse component that accompanies the E_h mode wave in the main tunnel. The intensity I_d of this diffuse component in the main tunnel relative to the intensity I_h of the E_h mode is given by the relation

$$\frac{I_{d,\text{main}}}{I_{h,\text{main}}} = \frac{L_{hd}}{L_d} \quad (32)$$

where L_{hd} is the loss rate from the E_h mode into the diffuse component and L_d is the loss rate of the diffuse component by refraction.

To calculate L_d approximately, we take the loss rate to be that of an "average" ray of the diffuse component having direction cosines $(1/\sqrt{3}, 1/\sqrt{3}, 1/\sqrt{3})$. Then

$$L_d = 10 \left(\frac{z}{d_1} + \frac{z}{d_2} \right) \log_{10} \frac{1}{R} \quad (33)$$

where R is the Fresnel reflectance of the average ray at the walls of the tunnel. R is 0.28 for the case $K_1 = K_2 = 10$. Then for $d_1 = 14$ ft., $d_2 = 7$ ft., $z = 100$ ft., we find that $L_d = 119$ dB/100 ft. This value has to be corrected for the loss of diffuse radiation into cross tunnels which we assume have the same dimensions as the main tunnel and occur every 75 ft. From relative area considerations we find that this loss is 2 dB/100 ft. The corrected value is therefore

$$L_d = 121 \text{ dB/100 ft} \quad (34)$$

which is independent of frequency.

The loss rate L_{hd} is shown in Table I as a function of frequency for the 14 ft. x 7 ft. tunnel. The values are the sum of the roughness and tilt losses calculated by equations (21) and (31) for a roughness of 4 inch rms and tilt of 1° rms. The ratio $I_{d,\text{main}} / I_{h,\text{main}}$, calculated by equation (32) and expressed in dB, is also shown. It is seen that the diffuse component is larger at the higher frequencies. The reason is that scattering out of the E_h mode due to tilt increases with frequency.

From solid angle considerations (see Appendix D) one finds that the fraction of diffuse radiation in the main tunnel that enters the 14 ft. x 7 ft. aperture of the cross tunnel is 0.15 or -8.2 dB. The diffuse level just inside the aperture of the cross tunnel, relative to the E_h wave in the main tunnel is shown in the last column of Table I, which is obtained by subtracting 8.2 dB from the numbers in column 4. A dipole antenna placed at this point and oriented either horizontally or vertically responds to half of the diffuse component or 3 dB less than the figures in column 5. At 1,000 MHz, for example, the signal received by an antenna at this point is -30.2 dB relative to that received in the main tunnel with the antenna oriented horizontally. At 415 MHz the corresponding number is -31.8 dB. These values agree moderately well with the measurements of Collins Radio Co.

The diffuse radiation that enters the cross tunnel decays at a rate of 121 dB/100 ft., according to the rather crude "average" ray approximation. This means that at 100 ft. down the cross tunnel the signal level at 1,000 MHz should be -151 dB. However, the level measured by Collins Radio is about -68dB. We attribute this large difference to the fact that the diffuse component in the main tunnel excites the E_h mode in the cross tunnel, and that this mode travels down the cross tunnel with much less attenuation than the diffuse component.

To calculate the coupling of the diffuse component in the main tunnel into the E_h mode in the cross tunnel, we determine the fraction

TABLE I
 DIFFUSE RADIATION COMPONENT IN MAIN TUNNEL
 AND AT BEGINNING OF CROSS TUNNEL

f (MHz)	λ (Ft.)	L_{hd} (dB/100 ft.)	$\frac{I_{d, main}}{I_{h, main}}$ (dB)	$\frac{I_{d, cross}}{I_{h, main}}$ (dB)
4,000	.245	5.4	-13.5	- 21.7
3,000	.327	4.1	-14.7	- 22.9
2,000	.49	2.8	-16.4	- 24.6
1,000	.98	1.5	-19.0	- 27.2
415	2.37	1.1	-20.6	- 28.8
200	4.92	1.3	-19.7	- 27.9

$(I_{h, \text{cross}})/(I_{d, \text{main}})$ of diffuse radiation leaving the exit aperture of the main tunnel which lies within the solid angle of acceptance of the E_h mode in the cross tunnel. The result (see Appendix D) is

$$\frac{I_{h, \text{cross}}}{I_{d, \text{main}}} = \frac{\lambda^3}{16\pi d_1^2 d_2} \quad (35)$$

This ratio is given in dB in Table II.

The E_h level in the cross tunnel relative to the E_h level in the main tunnel is found by adding column 2 in Table II and column 4 in Table I. The result is shown as $(I_{h, \text{cross}}/I_{h, \text{main}})_0$ in Table II. At 100 ft. down the cross tunnel we find the corresponding ratio by adding the loss rate given in Figure 3 for a tilt of 1° . The result is shown in the last column of Table II. The value of -70.1 dB at 1,000 MHz agrees very well with the measured value of -68 dB.

Our model of the propagation around a corner into a cross tunnel therefore consists of a relatively strong diffuse component at the beginning of the cross tunnel at a level of around -20 to -30 dB together with a much weaker E_h mode at a level of -50 to -80 dB, depending on frequency. These two components propagate down the cross tunnel with a very high loss rate of around 120 db/100 ft. for the diffuse component, and a very low loss rate for the E_h component. Therefore the E_h component overtakes the diffuse component at about 100 ft. down the tunnel, while the radiation changes its character from almost completely unpolarized to very highly polarized. This description of the propagation is in good general agreement with measurement, as shown in Figures 4 and 5.

TABLE II

EXCITATION OF E_h MODE IN CROSS TUNNEL
BY DIFFUSE COMPONENT IN MAIN TUNNEL

f (MHz)	$\frac{I_{h, \text{cross}}}{I_{d, \text{main}}}$ (dB)	$\left(\frac{I_{h, \text{cross}}}{I_{h, \text{main}}}\right)_0$ (dB)	$\left(\frac{I_{h, \text{cross}}}{I_{h, \text{main}}}\right)_{100'}$ (dB)
4,000	-66.7	-80.2	85.6
3,000	-62.9	-77.6	81.8
2,000	-57.7	-74.1	77.1
1,000	-48.6	-67.6	70.1
415	-37.1	-57.7	64.1
200	-27.6	-47.3	71.6

FIGURE 4
CORNER LOSS IN HIGH COAL

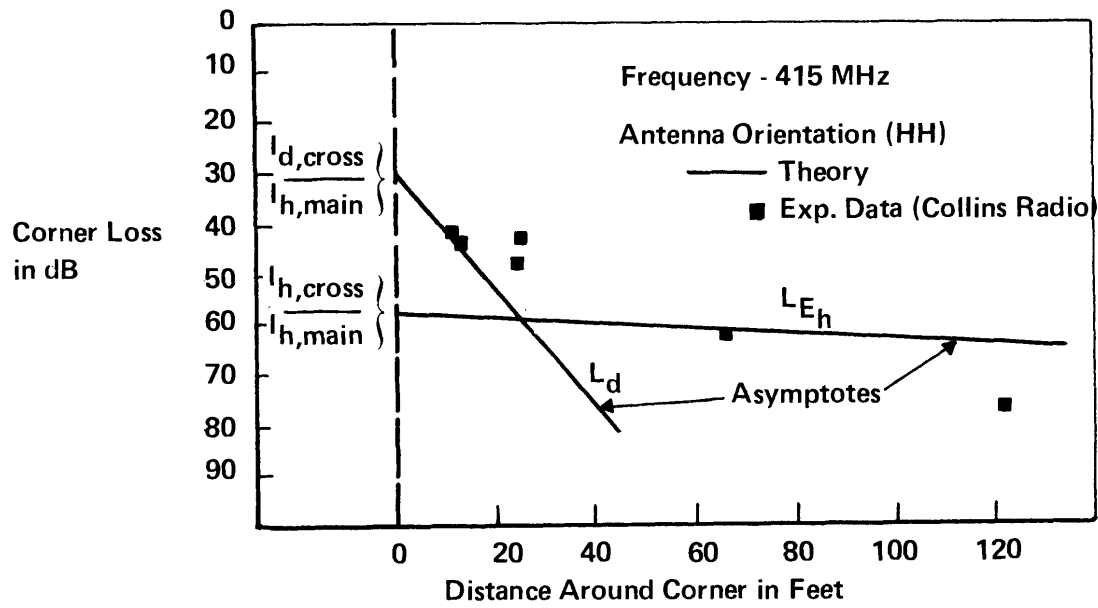
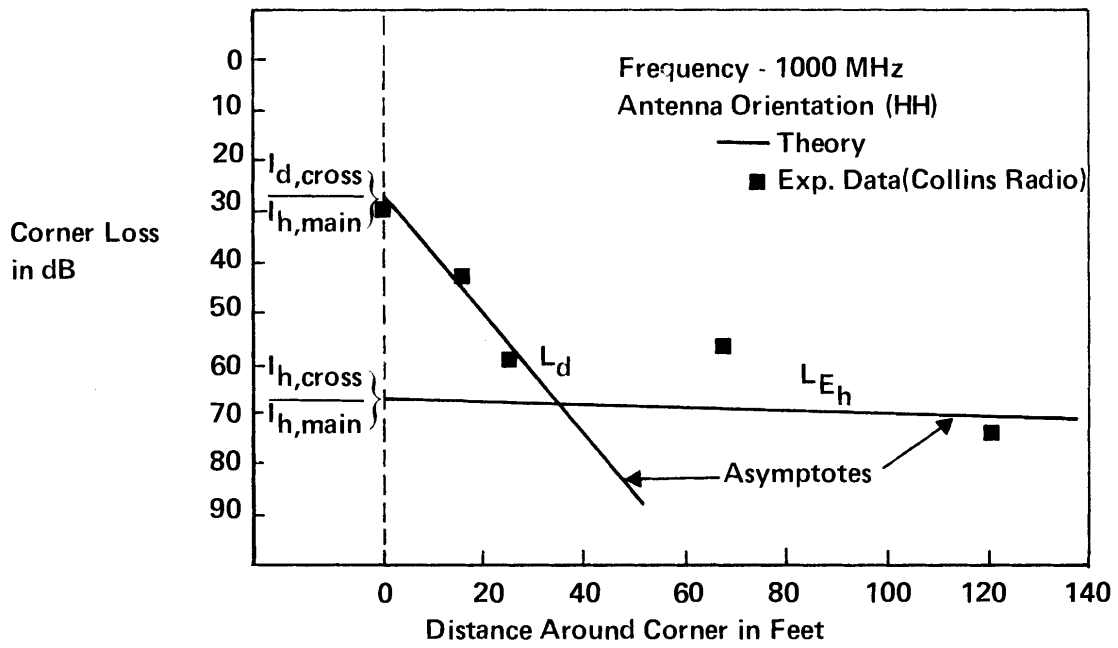


FIGURE 5
CORNER LOSS IN HIGH COAL



VI. EFFECT OF ANTENNA ORIENTATION

We now return to the effect on signal loss of the orientations of the transmitting and receiving antennas. In the case of identical antennas the principle of reciprocity states that the VH and HV losses are equal, where the first and second letters signify the orientation of the transmitting and receiving antennas, respectively. We will assume that the actual antennas are so small compared with the dimensions of the tunnel that interactions with the tunnel are negligible and therefore reciprocity is still valid.

We also invoke the principle that at great distances down the tunnel the radiation consists of the E_h mode together with a related diffuse component, for either orientation of the transmitting antenna.

From these two principles it follows that the HV or VH loss in dB is half way between HH and VV losses, or that

$$VV - HH = 2(HV-HH) \quad (36)$$

Now we obtain the relative loss HV-HH by subtracting 3 dB from column 4 of Table I. The results are shown in Table III along with VV-HH calculated from (36). The last column in the Table gives average experimental values of VV-HH determined by Collins Radio Co. Since no data were obtained by Collins for a horizontal transmitting antenna at 200 MHz, we have doubled their reported value of -25 dB for VV-VH at this frequency.

Comparison of theory and experiment in Table III indicates that the average value of VV-HH is predicted quite well by the theory but the variation with frequency is not well predicted. The discrepancy may result from failure of the reciprocity principle owing to the fact that a $\lambda/4$ groundplane transmitting antenna was used whereas the receiving

TABLE III
EFFECT OF ANTENNA ORIENTATION

f (MHz)	HH (dB)	HV (dB)	VH (dB)	VV (dB)
1000	0	-22.0	-22.0	-44.0
415	0	-23.6	-23.6	-47.2
200	0	-22.7	-22.7	-45.4

antenna was a standard dipole antenna of the type normally used for field strength measurements. However, the data for 415 MHz agree well with the theory since VH appears to be about halfway between HH and VV over a considerable distance down the tunnel.

VII. INSERTION LOSS

Dipole or whip antennas are the most convenient for portable radio communications between individuals. However, a considerable loss of signal power occurs at both the transmitter and receiver when simple dipole antennas are used, because of the inefficient coupling of these antennas to the waveguide mode. The insertion loss of each antenna can be calculated by two methods.

In the first method we make use of the effective transmitting or receiving area A_{ant} of a half-wave dipole antenna which is given by

$$A_{ant} = \frac{1.64\lambda^2}{4\pi} \quad (37)$$

The coupling factor C to the E_h waveguide mode is then, from (9),

$$C = \frac{|\int_{A_{ant}} E_o \cos k_1 x \cos k_2 y dA|^2}{\int_{A_{guide}} |E_o \cos k_1 x \cos k_2 y|^2 \int_{A_{ant}} dA} \quad (38)$$

where A_{guide} is the area of cross-section of the waveguide. At frequencies on the order of 1,000 MHz where the wavelengths become small compared to tunnel cross-section dimensions, the cosine factors of the (1,1) E_h mode are approximately zero at the walls of the tunnel and $A_{\text{ant}} \ll A_{\text{guide}}$. Under these conditions (38) gives approximately

$$C \cong \frac{4A_{\text{ant}}}{A_{\text{guide}}} \cos^2\left(\frac{\pi x_0}{d_1}\right) \cos^2\left(\frac{\pi y_0}{d_2}\right) \quad (39)$$

for a dipole centered at x_0, y_0 in the tunnel. When the dipole is placed at the center of the tunnel (39) reduces to

$$C \cong \frac{4A_{\text{ant}}}{A_{\text{guide}}} = \frac{1.64}{\pi} \frac{\lambda^2}{d_1 d_2} \quad (40)$$

In the second method we make use of a standard microwave circuit technique for computing the amount of power coupled into a waveguide mode by a probe. A half-wave dipole antenna centered at x_0, y_0 in the tunnel and oriented in the x-direction is approximated by a surface current distribution, and the power coupled into the (1,1) E_h mode by the current distribution is compared with the power radiated by the dipole in free space. The coupling coefficient so obtained is shown in Appendix E to be

$$C = 0.52 \frac{\lambda^2}{d_1 d_2} \cos^2\left(\frac{\pi x_0}{d_1}\right) \cos^2\left(\frac{\pi y_0}{d_2}\right) \quad (41)$$

which is numerically equal to (39), and therefore to (40), when the dipole is located at the center of the tunnel ($x_0 = y_0 = 0$).

The insertion loss L_i is then

$$L_i = -10 \log_{10} \left(0.52 \frac{\lambda^2}{d_1 d_2}\right) \quad (42)$$

for a dipole centrally located in the tunnel. Table IV gives values of L_i for various frequencies, for a 14 ft. x 7 ft. tunnel.

TABLE IV
 INSERTION LOSS (L_i)
 (For a Half-Wave Antenna)

F (MHz)	λ (Feet)	L_i (dB)
4000	0.245	35.0
3000	0.327	32.4
2000	0.49	28.9
1000	0.98	22.9
415	2.37	15.2
200	4.92	8.9

It is seen that the insertion loss decreases rapidly with increasing wavelength, as one would expect, since the antenna size occupies a larger fraction of the width of the waveguide. The overall insertion loss, for both antennas, is twice the value given in the Table. A considerable reduction in the loss would result if high gain antenna systems were used.

VIII. OVERALL LOSS IN A STRAIGHT TUNNEL

The overall loss in signal strength in a straight tunnel is the sum of the propagation loss and the insertion losses of the transmitting and receiving antennas. Table V lists the component loss rates for the E_h mode due to direct refraction, roughness, and tilt; the total propagation loss rate; the insertion loss for two half-wave antennas; and the overall loss for three different distances. The results are also shown in Figure 6, where it is seen that the optimum frequency for minimum overall loss is the range 500-1000 MHz, depending on the desired communication distance.*

It is also of interest to combine the results in Table V with those in Table IV to obtain the overall loss versus distance for the HH, HV (or VH), and VV antenna orientation. In order to compare the theoretical

* For roving miner mobile applications using portable transceivers, some frequency independent factors accounting for polarization, efficiency and fade margin losses, should also be applied to these results, as described in Appendix F, to obtain practical estimates of communication range.

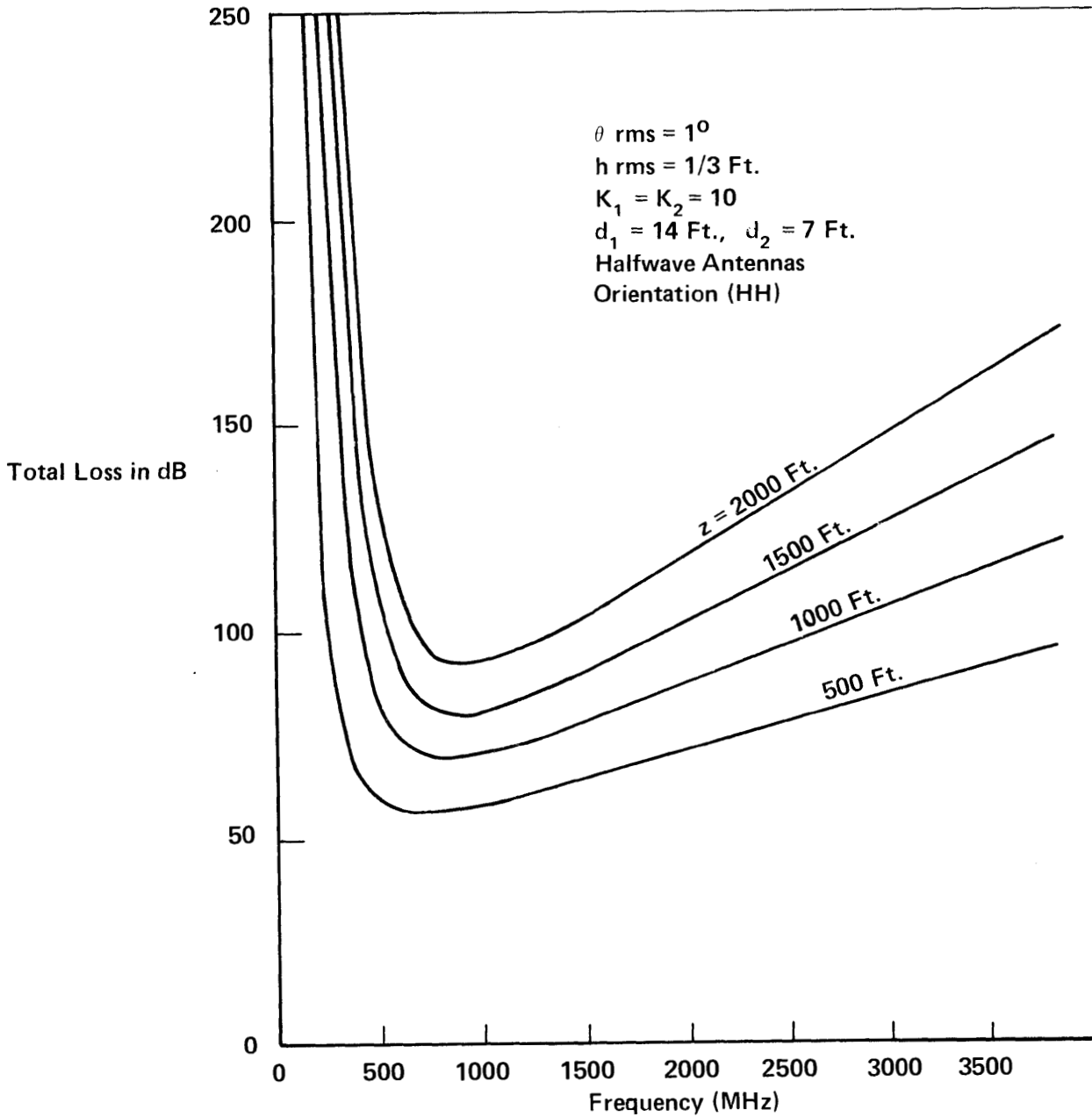
TABLE V
 CALCULATION OF OVERALL LOSS FOR E_h MODE WITH TWO HALFWAVE DIPOLE ANTENNAS

(h = 1/3 Ft. $\theta = 1^\circ$, $K_1 = K_2 = 10$, $d_1 = 14$ Ft., $d_2 = 7$ Ft.)

f (MHz)	L _{refraction} (dB/100')	L _{roughness} (dB/100')	L _{tilt} (dB/100')	L _{propagation} (dB/100')	L _{insertion} (dB)	L _{overall} (dB)				
						100'	500'	1000'	1500'	2000'
4000	.06	.05	5.33	5.44	69.90	75	97	124	152	179
3000	.10	.07	3.99	4.16	64.88	69	86	107	127	148
2000	.23	.10	2.66	2.99	57.86	61	73	88	103	118
1000	.91	.21	1.33	2.45	45.82	48	58	70	81	93
415	5.34	.50	0.55	6.39	30.48	37	62	94	126	158
200	23.00	1.04	0.27	24.31	17.80	42	139	261	383	504
100	92.00	2.08	0.14	94.20	5.80	100	477	948	1419	1890

FIGURE 6

TOTAL LOSS FOR VARIOUS DISTANCES ALONG A STRAIGHT TUNNEL



values with the experimental data of Collins Radio Co., which are expressed with reference to isotropic antennas, we add 4.3 dB to the overall loss calculated for half-wave dipoles. The theoretical results for the three different antenna orientations for frequencies of 415 MHz and 1,000 MHz are compared with the experimental data in Figures 7 and 8. It is seen that the theory agrees quite well with the general trend of the data. The agreement could probably be improved by better choices of the roughness and tilt parameters h and θ and by a more sophisticated treatment of the attenuation of the diffuse component than the simple "average ray" approach.

IX. OVERALL LOSS ALONG A PATH WITH ONE CORNER

Table VI gives the overall E_h mode loss for a path from one tunnel to another, including the corner loss involved in re-establishing the E_h mode in the second tunnel. The loss is the sum of the corner loss, given in column 3 of Table II and repeated in Table VI, and the straight tunnel loss given in Table V for various total distances. The results in Table VI are for the case of half-wave dipole transmitting and receiving antennas* and are valid when neither antenna is within about 100 ft. of the corner. The overall loss is smaller than the values in Table VI if the receiving antenna is within this distance, owing to the presence of the rapidly attenuating diffuse component that passes around the corner. From the principle of reciprocity, the same is true if the transmitting antenna is within 100 ft. of the corner.

The results indicate that the optimum frequency lies in the range 400-1,000 MHz. However, if one installs horizontal half-wave resonant scattering dipoles with 45° azimuth in the important tunnel intersections, in order to guide the E_h mode around the corner, the optimum may shift to somewhat lower frequencies since a greater fraction of the incident E_h wave will be deflected by the longer low-frequency dipoles.

* As in the straight tunnel case, refer to Appendix F for the additional loss factors needed to estimate communication range for roving miner applications using portable transceivers.

FIGURE 7
 OVERALL LOSS IN A STRAIGHT TUNNEL IN HIGH COAL
 (For Isotropic Antennas)

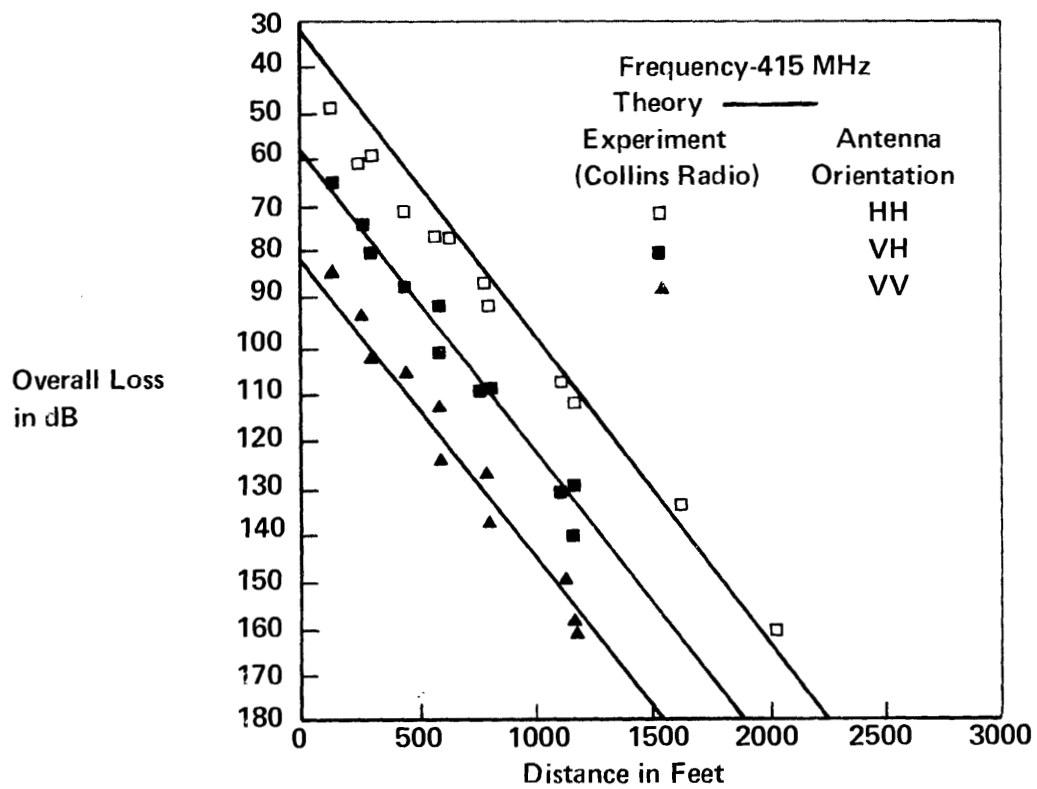


FIGURE 8
 OVERALL LOSS IN A STRAIGHT TUNNEL IN HIGH COAL
 (For Isotropic Antennas)

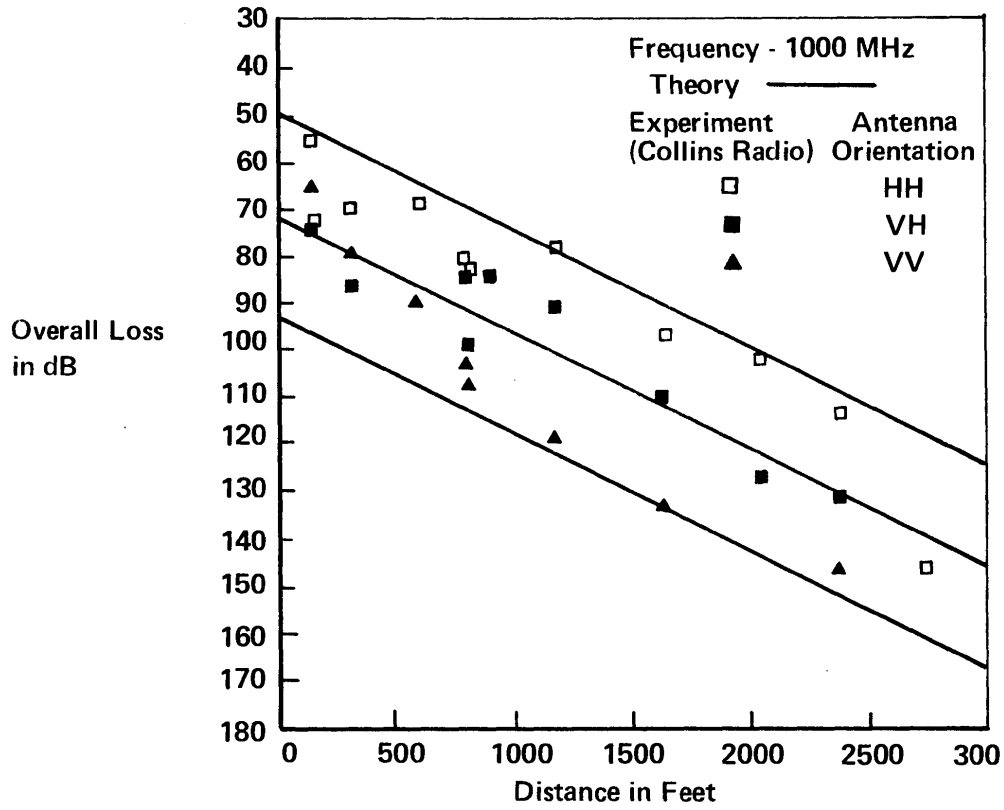


TABLE VI
OVERALL LOSS ALONG A PATH INCLUDING ONE CORNER
 E_h MODE WITH HALFWAVE DIPOLE ANTENNAS

f (MHz)	E_h Loss per Corner (dB)	Overall Loss (dB)			
		500'	1000'	1500'	2000'
4000	80.2	177	205	232	259
3000	77.6	163	184	205	226
2000	74.1	147	162	177	192
1000	67.6	126	138	148	161
415	57.7	120	152	184	216
200	47.3	187	308	430	551

X. CONCLUSIONS

The kind of propagation model developed in this paper, involving the (1,1) E_h waveguide mode accompanied by a diffuse component in dynamical equilibrium with it, seems to be necessary to account for the many effects observed in the measurement of Collins Radio Company: the exponential decay of the wave; the marked polarization effects in a straight tunnel; the independence of decay rate on antenna orientation; the absence of polarization at the beginning of a cross tunnel; the two-slope decay characteristic in a cross tunnel; and overall frequency dependence. All of these effects are moderately well accounted for by the theoretical model. However, considerable refinement of the theory could be made by removing some of the present oversimplifications, such as: the assumption of perfectly diffuse scattering both in the main tunnel and immediately around a corner in a cross tunnel; the use of the "average ray" approximation; and the description of the propagation around a corner in terms of two asymptotes only.

The last item particularly deserves more attention since we have not included the conversion of the diffuse component in the transition region near the beginning of the cross tunnel into the E_h mode. For this reason we think that the good fit of the theory to the experimental data in Figures 4 and 5 may be somewhat fortuitous. More data at greater distances down a cross tunnel would be very desirable to settle this question. Data covering a wider frequency range in both main and cross tunnels would also allow a more stringent test of the theory.

XI. REFERENCES

- (1) E.A.J. Marcatili and R.A. Schmelzter, "Hollow Metallic and Dielectric Waveguides for Long Distance Optical Transmission and Lasers," The Bell System Technical Journal, Vol 43, 1783, 1964.
- (2) J.I. Glaser, "Attenuation and Guidance of Modes in Hollow Dielectric Waveguides," IEEE Transactions on Microwave Theory and Techniques, March 1969, p. 173; and M.I.T. Ph.D. Thesis, "Low-Loss Waves in Hollow Dielectric Tubes," February 1967.
- (3) Collins Radio Company, Cedar Rapids, Iowa, "Coal Mine Communications Field Test Report," December 29, 1972 prepared for U.S. Department of the Interior, Bureau of Mines, Pittsburgh, Pa.; and a paper entitled "Radio Propagation Measurements in Coal Mines at UHF and VLF," published in Proceedings*of Through-the-Earth Electromagnetics Workshop at Colorado School of Mines, Golden, Colorado, August 1973.
- (4) P. Beckmann and A. Spizzichino, "The Scattering of Electromagnetic Waves from Rough Surfaces," Macmillan, New York, 1963, p. 81, Eq.(6).
- (5) E.M. Sparrow and R.D. Cess, "Radiation Heat Transfer," Wadsworth Publishing Co., 1966, Appendix A.

* Proceedings to be published as part of Colorado School of Mines Final Report on Bureau of Mines Grant G133023.

APPENDIX A

RAY METHOD

1. Fresnel Formulas

For the Eh mode the reflectances R_1 and R_2 of the vertical and horizontal walls, respectively, are

$$R_1^{Eh} = \left| \frac{K_1 \sin \phi_1 - \sqrt{\sin^2 \phi_1 + K_1 - 1}}{K_1 \sin \phi_1 + \sqrt{\sin^2 \phi_1 + K_1 - 1}} \right|^2 \quad (A1)$$

$$R_2^{Eh} = \left| \frac{\sin \phi_2 - \sqrt{\sin^2 \phi_2 + K_2 - 1}}{\sin \phi_2 + \sqrt{\sin^2 \phi_2 + K_2 - 1}} \right|^2 \quad (A2)$$

For the Ev mode the corresponding formulas are

$$R_1^{Ev} = \left| \frac{\sin \phi_1 - \sqrt{\sin^2 \phi_1 + K_1 - 1}}{\sin \phi_1 + \sqrt{\sin^2 \phi_1 + K_1 - 1}} \right|^2 \quad (A3)$$

$$R_2^{Ev} = \left| \frac{K_2 \sin \phi_2 - \sqrt{\sin^2 \phi_2 + K_2 - 1}}{K_2 \sin \phi_2 + \sqrt{\sin^2 \phi_2 + K_2 - 1}} \right|^2 \quad (A4)$$

2. Loss Rates

Table 1A gives calculated values of grazing angle, number of reflections, reflectance, and loss for the Eh mode in a 14 x 7 high-coal tunnel with $K_1=K_2=10$. L_1 and L_2 are the loss rates at the side walls and at the roof and floor, respectively.

TABLE A1

Ray Method Calculations (For Eh Mode)

f (MHz)	λ (ft)	ϕ_1 (deg)	ϕ_2 (deg)	N_1 $\left(\frac{\text{Bounces}}{100 \text{ ft}}\right)$	N_2 $\left(\frac{\text{Bounces}}{100 \text{ ft}}\right)$	R_1	R_2	L_1 $\left(\frac{\text{dB}}{100 \text{ ft}}\right)$	L_2 $\left(\frac{\text{dB}}{100 \text{ ft}}\right)$	L $\left(\frac{\text{dB}}{100 \text{ ft}}\right)$
1000	0.984	2.0	4.0	0.25	1.00	0.62	0.90	0.51	0.41	0.92
415	2.370	4.9	9.7	0.60	2.42	0.37	0.79	3.05	2.38	5.43
200	4.918	10.1	20.1	1.25	5.02	0.068	0.62	11.40	10.17	21.57

APPENDIX B
WAVE METHOD

1. (1,1) E_h and E_v Modes

The fundamental (1,1) E_h mode is approximately a TEM wave given by (9) and (10). The complete field of this form in the tunnel ($-d_1/2 \leq x \leq d_1/2$, $-d_2/2 \leq y \leq d_2/2$), satisfying Maxwell's equations, is

$$E_x = E_0 \cos k_1 x \cos k_2 y e^{-ik_3 z} \quad (B1)$$

$$E_y = 0 \quad (B2)$$

$$E_z = \frac{ik_1}{k_3} E_0 \sin k_1 x \cos k_2 y e^{-ik_3 z} \quad (B3)$$

$$H_x = \frac{k_1 k_2}{\omega \mu_0 k_3} E_0 \sin k_1 x \sin k_2 y e^{-ik_3 z} \quad (B4)$$

$$H_y = \frac{(k_1^2 + k_3^2)}{\omega \mu_0 k_3} E_0 \cos k_1 x \cos k_2 y e^{-ik_3 z} \quad (B5)$$

$$H_z = \frac{ik_2}{\omega \mu_0} E_0 \cos k_1 x \sin k_2 y e^{-ik_3 z}, \text{ where} \quad (B6)$$

$$k_1^2 + k_2^2 + k_3^2 = k_0^2 = 4\pi^2/\lambda^2. \quad (B7)$$

Since the wavelengths of interest are small compared with the tunnel dimensions, the wave vector components k_1 and k_2 are small compared with k_3 , which is close to $k_0 = 2\pi/\lambda$. Therefore H_y reduces to the expression given in (10) and E_z , H_x , and H_z are very small.

In the roof ($y \geq d_2/2$) of dielectric constant K_2 , the field must represent an outgoing wave in the y -direction and therefore has the form

$$E_x = B \cos k_1 x e^{-ik_2' y} e^{-ik_3 z} \quad (B8)$$

$$E_y = 0 \quad (B9)$$

$$E_z = \frac{ik_1}{k_3} B \sin k_1 x e^{-ik_2' y} e^{-ik_3 z} \quad (B10)$$

$$H_x = \frac{k_1 k_2'}{\omega \mu_0 k_3} B \sin k_1 x e^{-ik_2' y} e^{-ik_3 z} \quad (B11)$$

$$H_y = \frac{(k_3^2 + k_1^2)}{\omega \mu_0 k_3} B \cos k_1 x e^{-ik_2' y} e^{-ik_3 z} \quad (B12)$$

$$H_z = \frac{k_2'}{\omega \mu_0} B \cos k_1 x e^{-ik_2' y} e^{-ik_3 z} \quad (B13)$$

which satisfies Maxwell's equations. The wave number component k_2' in the dielectric is given by the relation

$$k_1^2 + k_2'^2 + k_3^2 = K_2 k_0^2. \quad (B14)$$

The boundary conditions at $y = d_2/2$ are that the tangential components of E and H are continuous. These conditions require that

$$E_o = \cos \left(\frac{k_2 d_2}{2} \right) = B e^{-\frac{ik_2' d_2}{2}} \quad (B15)$$

and

$$k_2 E_o \sin \left(\frac{k_2 d_2}{2} \right) = ik_2' B e^{-\frac{ik_2' d_2}{2}}, \quad (B16)$$

from which we obtain the condition

$$k_2 \tan \frac{k_2 d_2}{2} = ik_2' \quad (B17)$$

Since k_1 and k_2 are small compared with k_0 we find from (B7) and (B14) that k_2' is given approximately by

$$k_2' = k_0 \sqrt{K_2 - 1}. \quad (\text{B18})$$

Therefore, from (B17) and (B18) we obtain the following mode condition for k_2 , for modes that are even functions of y :

$$k_z \tan \frac{k_2 d_2}{2} = i k_0 \sqrt{K_2 - 1}. \quad (\text{B19})$$

Since $k_2 d_2 / 2 \ll 1$ we find for the lowest E_h mode

$$k_2 \approx \frac{\pi}{d_2} - \frac{i\lambda}{d_2^2 \sqrt{K_2 - 1}} \quad (\text{B20})$$

This result shows that, except for a small imaginary part, k_2 has the same value as for a metal waveguide. The imaginary part arises from the power loss due to the outgoing refracted wave.

In the side wall ($x \geq d_1/2$), of dielectric constant K_1 , the field has the form

$$E_x = A e^{-ik_1'x} \cos k_2 y e^{-ik_3 z} \quad (\text{B21})$$

$$E_y = 0 \quad (\text{B22})$$

$$E_z = \frac{k_1'}{k_3} A e^{-ik_1'x} \cos k_2 y e^{-ik_3 z} \quad (\text{B23})$$

$$H_x = \frac{ik_1'k_2}{\omega\mu_0 k_3} A e^{-ik_1'x} \cos k_2 y e^{-ik_3 z} \quad (\text{B24})$$

$$H_y = \frac{(k_1'^2 + k_3^2)}{\omega\mu_0 k_3} A e^{-ik_1'x} \cos k_2 y e^{-ik_3 z} \quad (\text{B25})$$

$$H_z = \frac{ik_2}{\omega\mu_0} A e^{-ik_1'x} \sin k_2 y e^{-ik_3 z} \quad (\text{B26})$$

where

$$k_1'^2 + k_2^2 + k_3^2 = K_1 k_0^2. \quad (\text{B27})$$

Continuity of the tangential E field gives the condition

$$k_1 E_0 \sin\left(\frac{k_1 d_1}{2}\right) = ik_1' A e^{-\frac{ik_1' d_1}{2}} \quad (\text{B28})$$

Continuity of H_y and H_z requires that

$$(k_3^2 + k_1^2) E_0 \cos\left(\frac{k_1 d_1}{2}\right) = (k_3^2 + k_1'^2) A e^{-\frac{ik_1' d_1}{2}} \quad (\text{B29})$$

and

$$k_2 E_0 \cos\left(\frac{k_1 d_1}{2}\right) = k_2 A e^{-\frac{ik_1' d_1}{2}} \quad (\text{B30})$$

Since (B29) and (B30) are inconsistent we can only satisfy the H boundary condition approximately. We note that since $K_1 \gg 1$, $|k_1'|$ is of the same order as k_0 , whereas $|k_2|$ is much smaller. Therefore we may ignore (B30) and also, from (B7) and (B27), write

$$k_1^2 + k_3^2 \approx k_0^2 \quad (\text{B31})$$

$$k_1'^2 + k_3^2 \approx K_1 k_0^2. \quad (\text{B32})$$

Then from (B28) and (B29) we obtain, approximately,

$$K_1 \tan\left(\frac{k_1 d_1}{2}\right) = \frac{ik_1'}{K_1}. \quad (\text{B33})$$

Again taking advantage of the smallness of k_1 and k_2 relative to k_0 , we find for the lowest E_h mode that

$$k_1 \approx \frac{\pi}{d_1} - \frac{iK_1 \lambda}{d_1^2 \sqrt{K_1 - 1}}, \quad (\text{B34})$$

which shows that the mode shape in the x-direction is also the same as for a metal waveguide, except for a small imaginary part.

On substituting for k_1 and k_2 from (B33) and (B34) into (B7) we find, on neglecting second order terms, that the propagation constant in the z-direction is

$$k_3 = k_o - \frac{i\lambda^2}{2} \left(\frac{K_1}{d_1^3 \sqrt{K_1-1}} + \frac{1}{d_2^3 \sqrt{K_2-1}} \right) \quad (B35)$$

The power loss in dB for the (1,1) E_h mode for a distance z is therefore

$$\begin{aligned} L_{Eh} &= -8.686 \operatorname{Im}(k_3) \\ &= 4.343 \lambda^2 z \left(\frac{K_1}{d_1^3 \sqrt{K_1-1}} + \frac{1}{d_2^3 \sqrt{K_2-1}} \right) \cdot \end{aligned} \quad (B36)$$

We obtain the loss for the (1,1) E_v mode by interchanging the subscripts 1 and 2 in (B36):

$$L_{Ev} = 4.343 \lambda^2 z \left(\frac{1}{d_1^3 \sqrt{K_1-1}} + \frac{K_2}{d_2^3 \sqrt{K_2-1}} \right) \cdot \quad (B37)$$

As a check on these formulas we find that exactly the same results are obtained if one adds the losses for two infinite slot waveguides of slot widths d_1 , d_2 and dielectric constants K_1 , K_2 , respectively. The numerical results given by (B36) and (B37) also agree well with those given by the ray method.

2. Higher Modes

One can readily generalize (B36) and (B37) to the case of a higher mode (n_1, n_2) with approximately n_1 half-wave loops in the x-direction and n_2 in the y-direction. The results are

$$L_{Eh} (n_1, n_2) = 4.343 \lambda^2 z \left(\frac{n_1^2 K_1}{d_1^3 \sqrt{K_1 - 1}} + \frac{n_2^2}{d_2^3 \sqrt{K_2 - 1}} \right) \quad (B38)$$

$$L_{Ev} (n_1, n_2) = 4.343 \lambda^2 z \left(\frac{n_1^2}{d_1^3 \sqrt{K_1 - 1}} + \frac{n_2^2 K_2}{d_2^3 \sqrt{K_2 - 1}} \right) \quad (B39)$$

Table B1 shows the loss rates for a number of modes for $f = 1000$ MHz, $\lambda = 0.98$ ft, $d_1 = 14$ ft, $d_2 = 7$ ft, $K_1 = 10$, $K_2 = 10$, $z = 100$ ft. It is to be noted that formulas (B38) and (B39) become increasingly inexact as n_1 and n_2 increase, since our approximations based on $k_1, k_2 \ll k_0$ become progressively less valid.

TABLE B1
LOSS RATES FOR VARIOUS MODES

n_1	n_2	L_{Eh} (dB/100 ft)	L_{Ev} (dB/100 ft)
1	1	0.9	4.1
1	2	2.1	16.3
2	1	2.4	4.3
2	2	3.6	16.4
1	3	4.2	36.5
3	1	5.0	5.0
2	3	5.7	36.7
3	2	6.2	16.7
3	3	8.2	36.9

APPENDIX C

COUPLING OF E_h AND E_v MODES

We first consider the Eh wave incident at a small grazing angle ϕ_2 on a perfectly flat and horizontal part of the roof of the tunnel. The reflected wave is then also polarized with the E field horizontal. If the plane on the roof is locally rotated through some angle about the x-direction, i.e., about a transverse horizontal axis, then the E-field in the reflected wave remains horizontal, from symmetry. Rotation about the vertical y-direction also produces no effect since the plane of the roof remains unchanged. Rotation about the z-direction produced by longitudinal ridges can however tilt the E-field of the reflected wave. Figure C1 shows a crosssectional view of the tunnel with the roof rotated through an angle θ around the z-axis. The E-field of the incident wave is represented by E_i and that of the reflected wave by E_r , which is tilted by an angle δ_2 relative to E_i . We wish to calculate δ_2 in terms of θ and the grazing angle of incidence ϕ_2 .

Relative to axes x' , y' attached to the rotated portion of the roof the incident E-field has components

$$E_{i,x'} = E_i \cos\theta \quad (C1)$$

$$E_{i,y'} = -E_i \sin\theta. \quad (C2)$$

The reflected field has components

$$E_{r,x'} = E_r \cos(\theta - \delta_2) \quad (C3)$$

$$E_{r,y'} = -E_r \sin(\theta - \delta_2). \quad (C4)$$

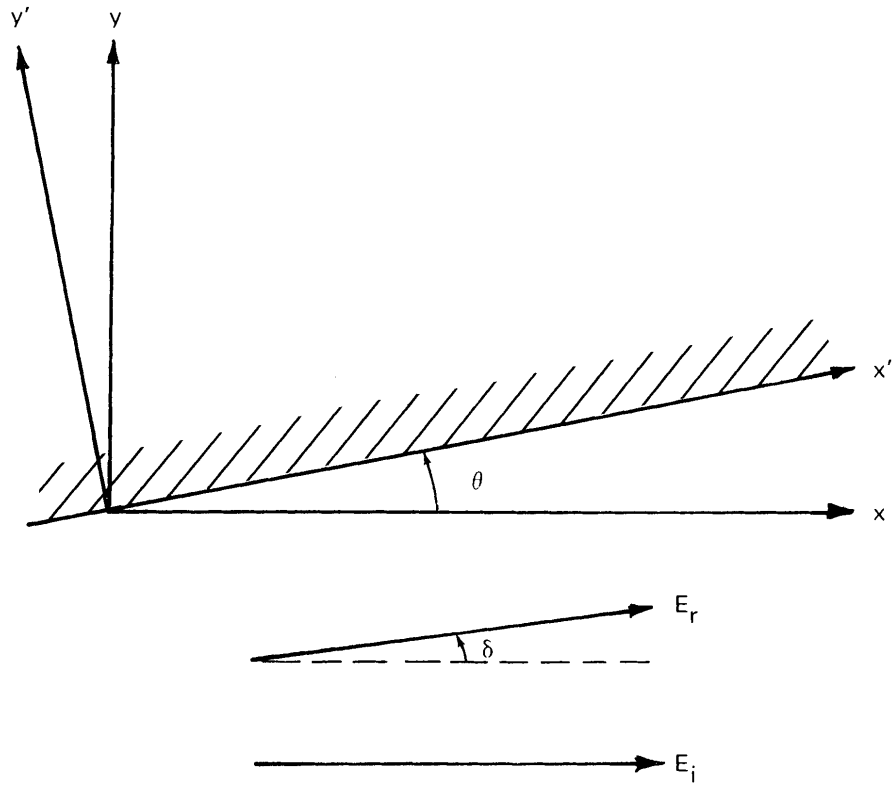


FIGURE C1 INCIDENT AND REFLECTED FIELDS RELATIVE TO A ROTATED PORTION OF THE ROOF OF THE TUNNEL

With respect to the roof the x' components can be regarded as the TE wave with amplitude reflection r_{TE_2} . Therefore

$$\frac{E_{r,x'}}{E_{i,x'}} = r_{TE_2}. \quad (C5)$$

Likewise the y' components act as a TM wave, so that

$$\frac{E_{r,y'}}{E_{i,y'}} = r_{TM_2}. \quad (C6)$$

From (C1)-(C6) we obtain

$$\frac{\tan(\theta - \delta_2)}{\tan\theta} = \frac{r_{TM_2}}{r_{TE_2}}. \quad (C7)$$

This result shows that rotation of the E-field occurs only because r_{TM} is different from r_{TE} .

The amplitude reflectances r_{TE_2} and r_{TM_2} are given in terms of the grazing angle ϕ_2 and the dielectric constant K_2 of the roof by the Fresnel formulas

$$r_{TE_2} = \frac{\sin\phi_2 - \sqrt{\sin^2\phi_2 + K_2 - 1}}{\sin\phi_2 + \sqrt{\sin^2\phi_2 + K_2 - 1}}$$

$$r_{TM_2} = \frac{K_2 \sin\phi_2 - \sqrt{\sin^2\phi_2 + K_2 - 1}}{K_2 \sin\phi_2 + \sqrt{\sin^2\phi_2 + K_2 - 1}} \quad (C9)$$

Equations (C7)-(C9) allow one to calculate the tilt angle δ_2 of the electric field of the reflected wave for given values of θ , ϕ_2 and K_2 . The corresponding equations for the effect of the side walls of the tunnel are

$$\frac{\tan(\theta - \delta_1)}{\tan\theta} = \frac{r_{TE_1}}{r_{TM_1}} \quad (C10)$$

$$r_{TE_1} = \frac{\sin\phi_1 + \sqrt{\sin^2\phi_1 + K_1 - 1}}{\sin\phi_1 + \sqrt{\sin^2\phi_1 + K_1 - 1}} \quad (C11)$$

$$r_{TM_1} = \frac{K_1 \sin\phi_1 - \sqrt{\sin^2\phi_1 + K_1 - 1}}{K_1 \sin\phi_1 - \sqrt{\sin^2\phi_1 + K_1 - 1}} \quad (C12)$$

We have assumed for simplicity that the rms rotation angle θ is the same for all four walls of the tunnel. The angles ϕ_1 and ϕ_2 are given by equations (1) and (2).

We now obtain an expression for the power coupling coefficient between the Eh and Ev modes. From a ray point of view the fraction of the power coupled per reflection is $\sin^2\delta_1$ for the side walls and $\sin^2\delta_2$ for the top and bottom walls. The coupling coefficient per foot along the tunnel is therefore

$$\begin{aligned} \alpha_{hv} &= \frac{N_1}{z} \sin^2\delta_1 + \frac{N_2}{z} \sin^2\delta_2 \\ &= \frac{\phi_1}{d_1} \sin^2\delta_1 + \frac{\phi_2}{d_2} \sin^2\delta_2, \end{aligned} \quad (C13)$$

where N_1 and N_2 , the number of reflections for a distance z , are given by (5) and (6).

It is to be noted that we have added the contributions of the various reflections to α_{hv} incoherently. The reason is that the Eh and Ev modes are orthogonal, which means that the various contributions from one mode to the other have random phases.

The rate of change of the intensity I_v in the Ev mode is given by the equation

$$\frac{dI_v}{dz} = -\alpha_v I_v + \alpha_{hv} I_h \quad (C14)$$

where I_h is the intensity of the Eh mode and α_v is the attenuation coefficient of the Ev mode due to refraction loss. Now, as will be shown later, the coupling coefficient α_{hv} is small compared with the loss rates α_h and α_v of the two modes. Therefore under steady state conditions both modes decay at a rate close to α_h . This means that

$$\frac{dI_v}{dz} \approx -\alpha_h I_v. \quad (C15)$$

Thus from (C14) we find that

$$\frac{I_v}{I_h} = \frac{\alpha_{hv}}{\alpha_v - \alpha_h} \quad (C16)$$

Table C1 shows values of δ_1 , δ_2 , α_{hv} , and I_v/I_h calculated by the foregoing equations for three values of the rms rotation angle θ of the tunnel walls. The measurements of Collins Radio with the receiving antenna first vertical, then horizontal indicate that I_v/I_h is in the range -20 to -25 dB for the 1000 and 415 MHz data. Therefore if one assumes that the measured Ev arises entirely from coupling between the two (1,1) modes, a value of θ between 10° and 20° is needed to make the theory agree with the experimental data.

TABLE C1

Coupling Between Eh and Ev modes

f (MHz)	θ (deg)	δ_1 (deg)	δ_2 (deg)	α_{hv} (dB/ft.)	α_h (dB/ft.)	α_v (dB/ft.)	$\frac{I_v}{I_h}$ (dB)
1,000	30	5.5	-6.5	.00066	.010	.0311	-15.0
1,000	20	4.2	-4.7	.00035	.010	.0311	-17.8
1,000	10	2.3	-2.4	.000096	.010	.0311	-23.4
415	30	14.3	-14.4	.0081	.060	.1802	-11.7
415	20	11.6	-10.0	.0042	.060	.1802	-14.6
415	10	6.6	- 5.1	.0012	.060	.1802	-20.0

APPENDIX D

PROPAGATION AROUND A CORNER

1. Transmission of Diffuse Component Around a Corner.

To calculate the fraction of the diffuse component in the main tunnel that goes around a corner into a cross tunnel, we use results given in graphical form by Sparrow and Cess⁽⁵⁾ for the angle factors for diffuse radiation transfer between rectangular areas, on the assumption that the radiation in the main tunnel is perfectly diffuse. In the high coal case of intersecting tunnels each of dimensions 14 ft by 7 ft, the angle factor between the main-tunnel aperture 1 and the cross-tunnel aperture 2 is

$$F_{1 \rightarrow 2} \text{ (High Coal)} = 0.15 = -8.2 \text{ dB} \quad (D1)$$

In the case of low-coal tunnels of dimensions 14 ft x 3.5 ft, the result is

$$F_{1 \rightarrow 2} \text{ (Low Coal)} = 0.10 = -10 \text{ dB} \quad (D2)$$

2. Excitation of Eh Mode in Cross Tunnel by Diffuse Component in Main Tunnel.

Figure D1 depicts the geometry used for computing the degree to which the Eh mode in the main tunnel couples to the Eh mode in a cross tunnel. Diffuse radiation passing through a cross section A of the main tunnel has the angular distribution

$$dP = \frac{P_0 \cos \theta}{\pi A} d\Omega dA \quad (D3)$$

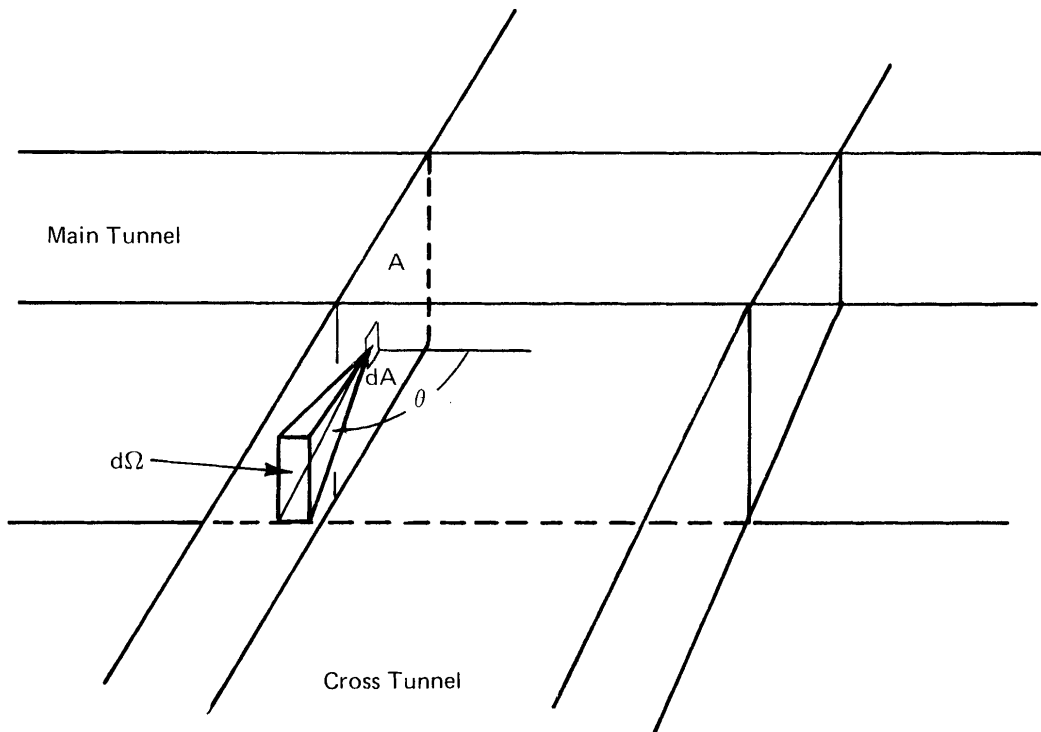


FIGURE D1 GEOMETRY FOR COUPLING TO CROSS TUNNELS

where

dP = power in element of solid angle $d\Omega$
from element of area dA

θ = angle with normal to dA

P_o = total diffuse power

A = total area of cross section

The power entering the Eh mode in the cross tunnel is therefore

$$P = 1/2 \frac{P_o}{\pi A} \int_{\Omega} \int_A \cos\theta d\Omega dA \quad (D4)$$

where the integration is taken over the whole area A of the cross section and over the solid angle Ω of the mode. The factor $1/2$ allows for the horizontal polarization of the mode.

$$\phi_1 = \lambda/2d_1 \quad (D5)$$

$$\phi_2 = \lambda/2d_2 \quad (D6)$$

d_1 and d_2 being the horizontal and vertical dimensions of the tunnel.

Therefore

$$\Omega = 2\phi_1\phi_2 = \frac{\lambda^2}{2d_1d_2} \quad (D7)$$

Since ϕ_1 and ϕ_2 are small the contributions of various elements dA are approximately equal since shadowing effects can be neglected. Therefore (D4) becomes

$$\begin{aligned}
 P &= (2\phi_2) \frac{P_o}{2\pi} \int_{\frac{\pi}{2}-\phi_1}^{\pi} \cos\theta \sin\theta d\theta \\
 &= \frac{2\phi_2 P_o}{2\pi} \cdot \frac{1}{2} [1 - \sin^2(\frac{\pi}{2} - \phi_1)] \\
 &= \frac{\phi_2 P_o}{2\pi} (1 - \cos^2\phi_1) \\
 &\approx \frac{\phi_2 \phi_1^2 P_o}{4\pi} \\
 P &= \frac{\lambda P_o}{16\pi d_1^2 d_2} \quad . \quad (D8)
 \end{aligned}$$

The power ratio of the Eh mode in the cross tunnel and main tunnel is

$$\frac{P_{\text{Eh-cross}}}{P_{\text{Eh-main}}} = \frac{P}{P_{\text{Eh-main}}} = \frac{P_o}{P_{\text{Eh-main}}} \cdot \frac{\lambda^3}{16\pi d_1^2 d_2} \quad (D9)$$

where P_o is the diffuse power level in the main tunnel. This result neglects any contribution from scattering by the floor and roof of the intersection area between the two tunnels.

APPENDIX E

ANTENNA INSERTION LOSS BY CURRENT-DISTRIBUTION METHOD

A half-wave dipole antenna centered at x_0, y_0 in the tunnel and oriented in the x-direction is approximated by a surface current distribution

$$\bar{K}(x,y) = \bar{i}_x I_0 \cos\left(\frac{2\pi x}{\lambda}\right) u_0(y-y_0) \{u_{-1}[x+(x_0 - \frac{\lambda}{2})] - u_{-1}[x-(x_0 + \frac{\lambda}{2})]\} \quad (E1)$$

where u_0 and u_{-1} are the unit impulse and step functions.

For the case of an infinite tunnel extending to either side of the dipole, the tangential field components take on the usual form

$$\bar{H}_{\pm} = \sum_{j,k} \bar{h}_{jk} \frac{1}{Z_{ojk}} V_{\pm jk} e^{\pm \gamma_{jk} z} \quad (E2)$$

$$\bar{E}_{\pm} = \sum_{j,k} \bar{e}_{jk} V_{\pm jk} e^{\pm \gamma_{jk} z} \quad (E3)$$

$$\bar{h}_{jk} = \bar{h}_{ojk} \cos k_1 x \cos k_2 y \quad (E4)$$

$$\bar{e}_{jk} = \bar{e}_{ojk} \cos k_1 x \cos k_2 y \quad (E5)$$

where Z_{ojk} , $V_{\pm jk}$, \bar{h}_{ojk} and \bar{e}_{ojk} are the characteristic impedance, + and -wave voltage coefficients, and normalization constants, respectively, for each waveguide mode. By matching the tangential boundary conditions over the cross-section containing the dipole and selecting the dominant (1,1) E_h mode contribution by using the mode orthogonality properties, we obtain

$$V_{+,1,1} = V_{-,1,1} \quad (E6)$$

$$V_{+,1,1} = - \frac{Z_{o,1,1}}{2} \iint_{x,y} (\bar{i}_z x \bar{K}(x,y)) \cdot \bar{h}_{1,1}(x,y) dx dy \quad (E7)$$

Carrying out the integration we get

$$V_{+,1,1} = \frac{I_o \lambda}{2\pi} Z_{o,1,1} h_{o,1,1} \cos k_1 x_o \cos k_2 y_o \quad (E8)$$

The total power coupled into the dominant (1,1) E_h waveguide mode propagating in both tunnel directions, to the left and to the right of the dipole, is

$$P_{\text{mode}} = \frac{|V_{+,1,1}|^2}{Z_{o,1,1}} \quad (E9)$$

The power radiated by the dipole is

$$P_{\text{dipole}} = \frac{1}{2} I_o^2 R_r \quad (E10)$$

where R_r is the dipole radiation resistance. The desired coupling factor C is the fraction of the dipole radiated power that is coupled to the (1,1) E_h mode propagating in one of the tunnel directions for a half-wave dipole; C is given by

$$C = \frac{1/2 P_{\text{mode}}}{P_{\text{dipole}}} = \frac{\lambda^2}{4\pi^2} \frac{Z_{o,1,1}}{R_r} h_{o,1,1}^2 \cos^2 k_1 x_o \cos^2 k_2 y_o. \quad (E11)$$

As in the first method, when the wavelength is small compared with the tunnel cross-sectional dimensions, the cosine factors are approximately zero at the tunnel walls, so that $k_1 \cong \pi/d_1$, $k_2 \cong \pi/d_2$ and $h_{o,1,1} \cong \frac{2}{\sqrt{d_1 d_2}}$. In addition $Z_{o,1,1}$ and R_r become, to good approximation, 377 ohms and 73 ohms, respectively, their corresponding free space values. Under these conditions (E11) becomes

$$C = 0.52 \frac{\lambda^2}{d_1 d_2} \cos^2 \frac{\pi x_o}{d_1} \cos^2 \frac{\pi y_o}{d_2} \quad (E12)$$

APPENDIX F

EXPECTED COMMUNICATION RANGE BETWEEN TWO ROVING MINERS

Communication can be maintained between two separated individuals until the separation distance increases to a point where the signal strength is not sufficient to overcome the background electrical noise. To obtain estimates of this communication range for a mobile application involving roving miners equipped with portable handy talkie transceivers, three frequency independent loss factors should be added to the values of overall loss presented in Tables V and VI. These factors are: -polarization loss-to account for likely misalignment of transmit and receive antennas, -antenna efficiency loss-to account for the non-ideal antenna installation on handy talkies, and -fade margin-to account for signal cancellation effects due to destructive interference. Nominal values which appear reasonable for these factors are 12dB, 4dB, and 12dB, respectively, resulting in a total of 28dB to be added to the above mentioned values of overall loss. By exercising care in the orientation and position of the handy talkies in the mine tunnel cross-section while communicating, these polarization and signal fading losses can of course be reduced, thereby producing a corresponding increase in range.

Representative values of receiver sensitivity and transmitter power for FM portable handy talkies in the UHF 450-MHz band are 0.5 microvolt for 20dB of quieting (-113 dBm into a 50-ohm input resistance) and 2 watts (33 dBm), respectively, resulting in a total allowable loss of 146dB. In this frequency band measurements in mines have shown that the intrinsic electrical noise of the UHF receiver will predominate over externally generated electrical noise. Using the above parameter values in conjunction with the 415-MHz overall loss values presented in Tables V and VI for straight line transmission paths and paths including one corner, predictions of communication range along haulageways and in working sections of mines can be obtained, as shown in Figure F1. Figure F1 illustrates the coverage expected in a high-coal mine between a centrally located miner with a handy talkie unit and a second miner roving throughout a typical 600 x 600 foot mine section with another unit at an operating frequency of 415 MHz.

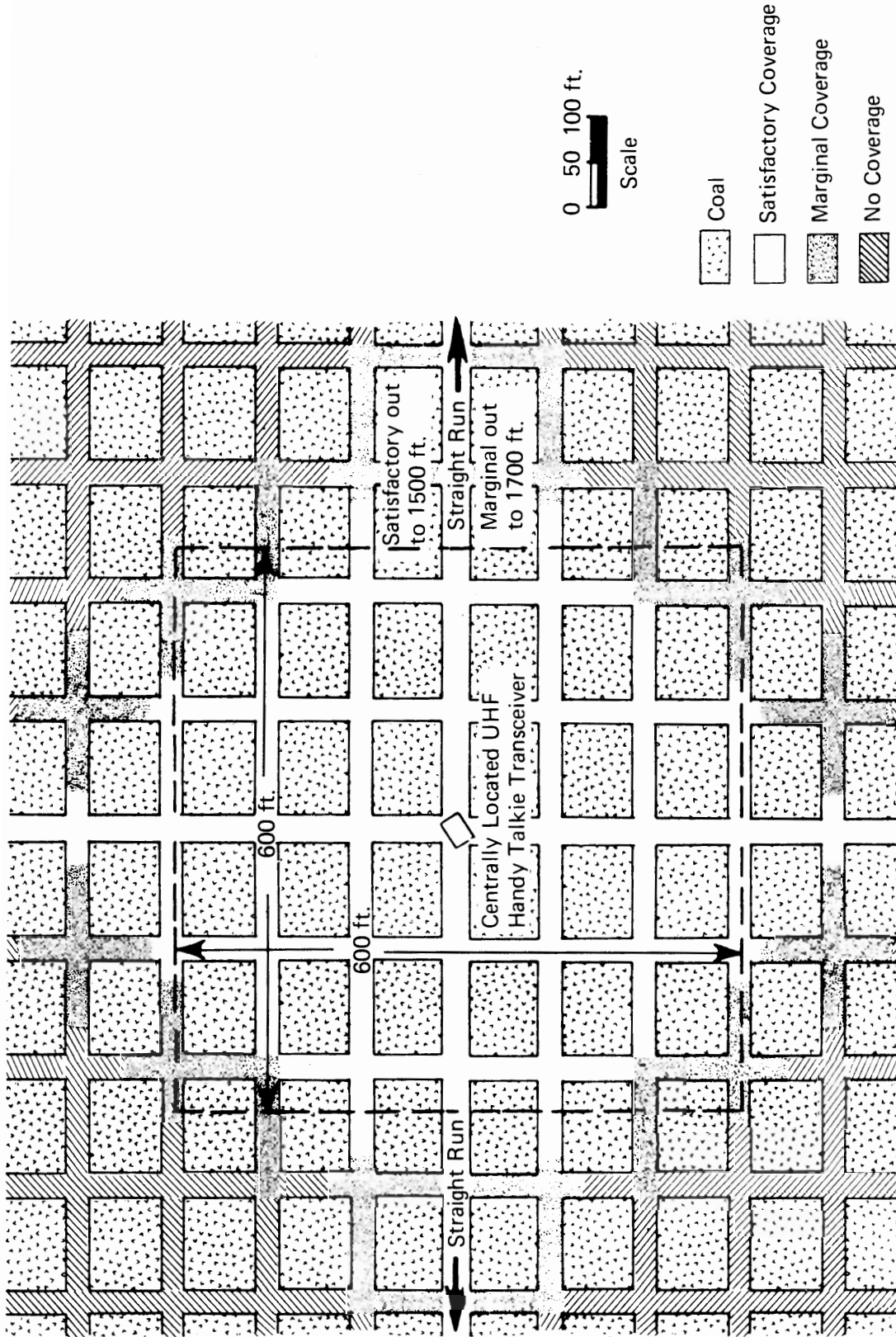


FIGURE F1 PREDICTED UHF WIRELESS RADIO COVERAGE
 For 2-Watt Handy Talkies in a High (7-foot) Coal Mine Section
 Frequency — 415 MHz

When the signal must go around only one corner, satisfactory communication can be expected over a linear distance of approximately 500 feet down an entry and cross-cut. When no corners are encountered, as in a haulageway transmission path, satisfactory straight line communication can be expected over distances in excess of 1500 feet. These range limits are somewhat conservative estimates, and as mentioned above, can usually be somewhat extended if the handy talkies are rotated into the horizontal plane, pointed across the tunnel, and translated a little to a more favorable signal strength position, thereby taking full advantage of the dominant horizontal field component and minimizing destructive interference effects.

Wireless coverage was estimated using the 415 MHz frequency results because the 450 MHz UHF frequency band is the present upper limit for commercially available portable radio transceivers, and because operating frequencies near 400 MHz are most favorable for high-coal section applications where transmission paths typically include one corner. Additional information regarding the practical application of UHF wireless radio systems to mine haulageways and sections is given in a paper coauthored by R. Lagace of ADL and H. Parkinson of PMSRC entitled "Two-Way Communications with Roving Miners," and published in U.S. Bureau of Mines Information Circular No. 8635.

PART FIVE
HOIST SHAFT MINE COMMUNICATIONS

PART FIVE
HOIST SHAFT MINE COMMUNICATIONS
TABLE OF CONTENTS

	<u>Page</u>
List of Tables	5.iii
List of Figures	5.iv
INTRODUCTION	5.1
I. THE MODE CONDITION	5.2
II. PROPAGATION LOSS	5.4
III. SURFACE IMPEDANCE METHOD	5.6
IV. CHARACTERISTIC IMPEDANCE	5.11
V. CURRENT DISTRIBUTION IN THE SOURROUNDING MEDIUM	5.12
VI. COUPLING TO THE TRANSMISSION LINE	5.14
A. SPATIAL COUPLING FACTORS FOR THE RETURN PATHS	5.14
B. CAGE CAPACITIVE TERMINATION	5.20
C. INDUCTIVE COUPLING AND IMPEDANCE MATCHING TO THE HOIST ROPE	5.21
VII. CONCLUDING REMARKS	5.23

PART FIVE

HOIST SHAFT MINE COMMUNICATIONS

LIST OF TABLES

<u>Table No.</u>	<u>Title</u>	<u>Page</u>
1	Surface Impedance	5.8
2	Resistance of Center Conductor for $a = .0222\text{m}$, $\sigma = 10^6$ mho/m	5.9
3	Propagation Loss, L(dB) (for $b = 1.2\text{m}$, $a = 0.0222\text{m}$, $z = 3050\text{m}$)	5.10
4	Characteristic Impedance (for $\sigma = 10^{-2}$ mho/m, $b = 1.2$ m, $a = 0.0222$ m)	5.11
5	Capacitive Reactance of Cage Termination (for $C = 224$ pf)	5.20
6	Inductive Reactance, Resonant Impedance, and Q for a Small Single-Turn Toroidal Coupler/ Isolator	5.22

PART FIVE

HOIST SHAFT MINE COMMUNICATIONS

LIST OF FIGURES

<u>Figure No.</u>	<u>Title</u>	<u>Page</u>
1	Dimensionless Current Factors for Annulus at Radius X	5.15
2	Dimensionless Cumulative Current $I(x)$ Versus x	5.16

PART FIVE

HOIST SHAFT MINE COMMUNICATIONS

INTRODUCTION

During the summer of 1973 we were asked to perform a theoretical investigation of the propagation of low frequency (LF) radio waves down deep (10,000 feet) hoist shafts* for the case where the hoist cable ("rope") is the only metal conductor present. Propagation is by means of the TEM coaxial mode of transmission in which the hoist cable serves as the inner conductor and the surrounding rock acts as the outer conductor.

Since the rock is a relatively poor electrical conductor the current in the outer conductor of the coaxial line is not confined to a very thin surface layer as in a metal coaxial cable, but spreads radially to a distance that is generally many times the shaft diameter. This feature of the wave propagation requires a more sophisticated theoretical treatment than the approximate skin-depth theory that is adequate for metal coaxial lines.

In this Part we treat the hoist shaft wave propagation loss, characteristic impedance, and the field current distributions in the surrounding rock medium. We also show that the large penetration of the wave into the rock outer conductor does not present a difficult problem with regard to coupling the transmitter or receiver to the transmission line with a minimum of insertion loss, but that the large impedance mismatch caused by the capacitance termination between the cage and shaft wall may well be the most significant contribution to overall system loss. Inductive coupling and impedance matching to the hoist rope/shaft transmission line are also treated briefly. Preliminary results indicate that a broad minimum in overall system loss should occur between 100 kHz and 1 MHz, possibly centered around 300 kHz. Further work is needed to better quantify this signal loss behavior, compare it with hoist shaft electromagnetic noise spectral data recently acquired by NBS, and identify the most favorable operating frequencies.

*This work complemented the hardware development of a new hoist radio system for deep shafts by Collins Radio Co. under Contract H0232056 for the Bureau of Mines.

I. THE MODE CONDITION

We approximate the actual rectangular shaft by a cylinder of circular cross-section of radius \underline{b} containing a steel cable of radius \underline{a} along its axis. The dominant mode of propagation in such a transmission line has a radially-symmetric transverse magnetic field H_θ which, for $\underline{a} \leq r \leq \underline{b}$ has the form

$$H_\theta = [AJ_1(k_r r) + B Y_1(k_r r)] e^{-ik_z z} \quad (1)*$$

where A and B are arbitrary constants and J_1 and Y_1 are first order Bessel functions of the first and second kind, respectively. The radial and longitudinal wave vector components k_r and k_z satisfy the condition

$$k_r^2 + k_z^2 = k_o^2 = \frac{4\pi^2}{\lambda^2} \quad (2)$$

where λ is the free space wavelength.

The electric field components are given by the curl components

$$E_r = - \frac{1}{i\omega\epsilon_o} \frac{\partial H_\theta}{\partial z} \quad (3)$$

$$E_z = \frac{1}{i\omega\epsilon_o} \frac{1}{r} \frac{\partial}{\partial r} (rH_\theta) \quad (4)$$

which, from (1) and the properties of the Bessel functions, give

$$E_r = \frac{ik_z}{i\omega\epsilon_o} [AJ_1(k_r r) + BY_1(k_r r)] e^{-ik_z z} \quad (5)$$

$$E_z = \frac{k_r}{i\omega\epsilon_o} [AJ_o(k_r r) + BY_o(k_r r)] e^{-ik_z z} \quad (6)$$

The fields given by (1), (5), and (6) represent an exact solution of Maxwell's equations.

* References to Figures, Tables, and Equations apply to those in this Part unless otherwise noted.

In the conducting rock surrounding the shaft ($r > b$) the radial part of the solution must correspond to an outgoing traveling wave. The solution therefore has the form

$$H_{\theta} = C H_1^{(2)}(k_r' r) e^{-ik_z z} \quad (7)$$

$$E_r = \frac{ik_z}{i\omega\epsilon} C H_0^{(2)}(k_r' r) e^{-ik_z z} \quad (8)$$

$$E_z = \frac{k_r'}{i\omega\epsilon} C H_0^{(2)}(k_r' r) e^{-ik_z z} \quad (9)$$

where $H_1^{(2)}$ and $H_0^{(2)}$ are the Hankel functions given by

$$H_1^{(2)} = J_1 - iY_1 \quad (10)$$

$$H_0^{(2)} = J_0 - iY_0 \quad (11)$$

C is an arbitrary constant, ϵ is the complex permittivity of the rock, and k_r' is given by the relation

$$k_r'^2 + k_z^2 = K k_0^2 \quad (12)$$

where $K = \epsilon/\epsilon_0$ is the complex dielectric constant of the rock.

At the wall of the shaft the boundary conditions that H_{θ} and E_z are continuous give the relations

$$A J_1(k_r b) + B Y_1(k_r b) = C H_1^{(2)}(k_r' b) \quad (13)$$

$$k_r [A J_0(k_r b) + B Y_0(k_r b)] = \frac{k_r'}{K} C H_0^{(2)}(k_r' b) \quad (14)$$

At the inner conductor ($r = a$) the conductivity of the steel is so high that the boundary condition is simply $E_z = 0$. Therefore from (6),

$$A J_0(k_r a) + B Y_0(k_r a) = 0. \quad (15)$$

Equations (13), (14), and (15) are homogeneous in A, B and C. The requirement for consistency of these equations gives the mode condition

$$\frac{1}{k_r} \left[\begin{array}{c} \frac{J_1(k_r b)}{J_0(k_r a)} - \frac{Y_1(k_r b)}{Y_0(k_r a)} \\ \frac{J_0(k_r b)}{J_0(k_r a)} - \frac{Y_0(k_r b)}{Y_0(k_r a)} \end{array} \right] = \frac{K}{k_r'} \frac{H_1^{(2)}(k_r' b)}{H_0^{(2)}(k_r' b)} \quad (16)$$

Equations (16), (2) and (12) determine exactly the allowed values of k_r , k_z and k_r' for all modes of propagation having a transverse axially-symmetric magnetic field. We are only interested in the lowest such mode, which approximates a TEM mode.

II. PROPAGATION LOSS

For frequencies in the range 20-200 kHz, $k_r a$, $k_r b$ and $k_r' b$ are all small quantities. Therefore the Bessel functions in (16) can be approximated by the first terms in their series expansions, namely

$$J_0(x) = 1 \quad (17)$$

$$J_1(x) = \frac{x}{2} \quad (18)$$

$$Y_0(x) = \frac{2}{\pi} (\log x + 0.577 - \log 2) \quad (19)$$

$$Y_1(x) = -\frac{2}{\pi x} \quad (20)$$

$$H_0^{(2)}(x) = 1 - \frac{2i}{\pi} (\log x + 0.577 - \log 2) \quad (21)$$

$$H_1^{(2)}(x) = \frac{2i}{\pi x} \quad (22)$$

Equation (16) then reduces to

$$k_r^2 = \frac{\pi i k_r'^2}{2K \log \frac{b}{a}} \left[1 - \frac{2i}{\pi} (\log k_r' b + 0.577 - \log 2) \right] \quad (23)$$

The dielectric constant of a conducting medium is given approximately by the relation

$$K = - \frac{i\sigma}{\omega \epsilon_0} \quad (24)$$

For the case $\sigma = 0.01$ mho/m and $f = 50$ kHz, $K = -3597 i$. Therefore from (12), to a very good approximation,

$$k_r'^2 = K k_o^2 \quad (25)$$

since k_r^2 is of the same order as k_o^2 and can therefore be neglected compared with $K k_o^2$. On substituting this value of $k_r'^2$ into (23), and then solving (2) for k_z^2 , we find that

$$k_z^2 = k_o^2 \left[1 - \frac{\pi i}{2 \log \frac{b}{a}} - \frac{1}{\log \frac{b}{a}} (\log k_o b \sqrt{K} + 0.577 - \log 2) \right] \quad (26)$$

We take the following values of the constants:

$$\begin{aligned} f &= 50 \text{ kHz} \\ \lambda &= 6,000 \text{ m} \\ k_o &= 1.047 \times 10^{-3} \text{ m}^{-1} \\ b &= 4 \text{ ft.} = 1.2 \text{ m} \\ a &= 0.875 \text{ in.} = 0.0222 \text{ m} \\ \sigma &= 0.01 \text{ mho/m} \\ \epsilon_o &= 8.85 \times 10^{-12} \text{ farad/m} \\ K &= -3597 i \end{aligned}$$

Then we find

$$k_z = 1.358 \times 10^{-3} - 7.948 \times 10^{-5}i \text{ (m}^{-1}\text{)}$$

For a 10,000 foot shaft (3050m), the propagation loss is therefore

$$L = (8.686) (7.948 \times 10^{-5} \text{ m}^{-1}) (3050\text{m}) = 2.11 \text{ dB}$$

III. SURFACE IMPEDANCE METHOD

An alternative way to calculate the propagation loss is by means of the surface impedance Z_s of the wall of the shaft which is defined as

$$Z_s = - \frac{E_z(b)}{2\pi b H_\theta(b)} \quad (27)$$

From (7) and (9) this becomes

$$Z_s = \frac{ik_r' H_0^{(2)}(k_r'b)}{2\pi b \omega \epsilon H_1^{(2)}(k_r'b)} \quad (28)$$

With the same approximations as before this becomes

$$Z_s = \frac{k_o^2}{4\omega\epsilon_o} \left[1 - \frac{2i}{\pi} (\log k_o b \sqrt{K} + 0.577 - \log 2) \right] \quad (29)$$

We now insert Z_s as a series impedance into the usual transmission line formula for the propagation constant:

$$\gamma = \sqrt{(R + i\omega L) (G + i\omega C)} \quad (30)$$

to obtain the formula

$$\gamma = \sqrt{(Z_s + i\omega L) i\omega C} \quad (31)$$

where we assume that the resistance R per unit length of the inner conductor is negligible compared with Z_s and that there is no shunt conductance.

Since

$$\gamma^2 = -k_z^2, \quad (32)$$

$$L = \frac{\mu_o}{2\pi} \log \frac{b}{a}, \quad (33)$$

$$C = \frac{2\pi\epsilon_o}{\log \frac{b}{a}} \quad (34)$$

$$\text{where } \mu_o = 4\pi \times 10^{-7} \text{ henry/m.} \quad k_o^2 = \omega^2 \epsilon_o \mu_o, \quad (35)$$

Equation (31) becomes

$$k_z^2 = k_o^2 - \frac{2\pi i\omega\epsilon_o Z_s}{\log \frac{b}{a}} \quad (36)$$

This formula becomes identical with Equation (26) when the expression (29) is substituted for Z_s .

Table 1 gives values of Z_s calculated by means of Equation (29) for frequencies in the range 30-3,000 kHz and conductivities in the range 10^{-4} to 10^{-1} mho/m. It is of interest that the real part of the surface impedance $R_s = \omega\mu_o/8$, is independent of the conductivity and the radius of the shaft. The value of Z_s for 3,000 kHz and 0.01 mho/m is somewhat uncertain, since the approximations used are near the limit of their validity for these values.

Table 1

Surface Impedance

Z_s (ohm/m) for $b = 1.2$ m = 4 ft.

f (kHz)	σ (mho/m)			
	10^{-4}	10^{-3}	10^{-2}	10^{-1}
30	.0296 + .1982i	.0296 + .1548i	.0296 + .1114i	.0296 + .0680i
50	.0493 + .3141i	.0493 + .2418i	.0493 + .1695i	.0493 + .0973i
100	.0986 + .5847i	.0986 + .4402i	.0986 + .2956i	.0986 + .1511i
150	.1479 + .8389i	.1479 + .6221i	.1479 + .4053i	.1479 + .1885i
200	.1972 + 1.0824i	.1972 + .7933i	.1972 + .5043i	.1972 + .2152i
250	.2465 + 1.3180i	.2465 + .9567i	.2465 + .5953i	.2465 + .2340i
300	.2958 + 1.547i	.2958 + 1.114i	.2958 + .6801i	.2958 + .2464i
3000	2.958 + 11.14i	2.958 + 6.801	2.958 + 2.465i	-----

The resistance of the stainless steel center conductor of radius 0.0222m and conductivity 10^6 mho/m is given in Table 2. The results include the effect of the skin depth of penetration into the cable. It is seen that the cable resistance is small compared with the real part of the surface impedance given in Table 1 at all frequencies, and therefore has little effect on propagation loss.

Table 2

Resistance of Center Conductor for
 $a = .0222\text{m}, \sigma = 10^6 \text{ mho/m}$

<u>f</u> (kHz)	<u>R</u> (ohm/m)
30	.0025
50	.0032
100	.0045
150	.0055
200	.0064
250	.0071
300	.0078
3000	.0246

Table 3 gives the propagation loss in dB for the same range of frequency and conductivity, calculated by means of Equation (36) for a 10,000 foot shaft. It is seen that the loss is very low at 30 kHz and quite moderate at 300 kHz. However the loss is excessive at 3,000 kHz. It is to be noted that the loss is almost independent of conductivity.

Table 3

Propagation Loss, L(dB)
 (for b = 1.2m, a = 0.0222m, z = 3050m)

σ (mho/m) f (kHz)	10^{-4}	10^{-3}	10^{-2}	10^{-1}
30	1.1	1.1	1.2	1.4
50	1.8	1.9	2.1	2.3
100	3.7	4.0	4.3	4.8
150	5.6	6.1	6.6	7.3
200	7.6	8.1	8.9	9.9
250	9.5	10.3	11.2	12.5
300	11.5	12.4	13.6	15.0
3000	124.1	135.7	151.4	--

IV. CHARACTERISTIC IMPEDANCE

The characteristic impedance of a transmission line is given by the expression

$$Z_o = \sqrt{\frac{R + i\omega L}{G + i\omega C}} \quad (37)$$

In the case of the shaft transmission line $G = 0$ and $R = Z_s$, which is the surface impedance given by Equation (29) or Table 1. Then (37) becomes,

$$Z_o = \sqrt{\frac{Z_s + i\omega L}{i\omega C}} \quad (38)$$

where L and C are given by (33) and (34).

For $f = 100$ kHz and $\sigma = 10^{-3}$ mho/m, we find that $Z_s = 0.0986 + 0.4402i$ ohm/m, $i\omega L = (0.501) i$ ohm/m, $i\omega C = (8.76 \times 10^{-6}) i(\text{ohm/m})^{-1}$, and $Z_o = 327 - 17 i$ ohms. For $\sigma = 10^{-2}$ mho/m, we get:

Table 4

Characteristic Impedance
(for $\sigma=10^{-2}$ mho/m, $b=1.2$ m, $a=0.0222$ m)

<u>f</u> <u>(kHz)</u>	<u>Z_o</u> <u>(ohms)</u>
50	310-18i
300	283-20i

For comparison, $Z_o = 239$ ohms for an all-metal transmission line with the same dimensions.

V. CURRENT DISTRIBUTION IN THE SURROUNDING MEDIUM

From Equation (7) the magnetic field in the rock is given by

$$\frac{H_{\theta}(r)}{H_{\theta}(b)} = \frac{H_1^{(2)}(k_r' r)}{H_1^{(2)}(k_r' b)} \quad (39)$$

The current density is therefore given by

$$\frac{J_z(r)}{J_z(b)} = \frac{\frac{1}{r} \frac{\partial}{\partial r}(rH_{\theta})}{J_z(b)} = \frac{H_0^{(2)}(k_r' r)}{H_0^{(2)}(k_r' b)} \quad (40)$$

Although $k_r' r$ is small compared with 1 at the wall of the shaft, this is not true for larger values of r where the current density is still appreciable. Therefore we cannot now use only the first term of the expansion of the Hankel function. However, since, from (24) and (25), k_r' has equal real and imaginary parts, we can write

$$k_r' r = x e^{-\pi i/4} \quad (41)$$

and use the tabulated functions* $\ker(x)$ and $\kei(x)$ to obtain the real and imaginary parts of the Hankel function. The relationships are

$$\ker(x) = \operatorname{Re} \left[-\frac{\pi i}{2} H_0^{(2)}(x e^{-\pi i/4}) \right] \quad (42)$$

$$\kei(x) = \operatorname{Im} \left[-\frac{\pi i}{2} H_0^{(2)}(x e^{-\pi i/4}) \right] \quad (43)$$

where

$$x = |k_r'| r \quad (44)$$

* Handbook of Mathematical Functions, Ed. M. Abramowitz and I.A. Stegun, National Bureau of Standards, U.S. Department of Commerce, June 1964, p. 431.

from (41) above, so that

$$J_z(x) = J_{\text{real}}(x) + iJ_{\text{imag}}(x) \quad (45)$$

where $J_{\text{real}}(x) \propto \ker(x)$ and $J_{\text{imag}}(x) \propto \text{kei}(x)$

Of particular interest to the coupling of signals to the shaft is the cumulative distribution of vertical current in the rock as a function of radial distance, r .

$$I_z(r) = \int_b^r 2\pi r J_z(r) dr \quad (46)$$

Therefore we have computed the dimensionless quantity

$$I(x) = \sqrt{I_{\text{real}}^2 + I_{\text{imag}}^2} \quad (47)$$

which is proportional to $I_z(r)$, where

$$I_{\text{real}} = \int_{x_0}^x \frac{x J_{\text{real}}(x) dx}{x_0 J_{\text{real}}(x_0)} \quad (48)$$

$$I_{\text{imag}} = \int_{x_0}^x \frac{x J_{\text{imag}}(x) dx}{x_0 J_{\text{real}}(x_0)} \quad (49)$$

and $x_0 = |k_r'|b$ (50)

The quantities $\frac{x J_{\text{real}}(x)}{x_0 J_{\text{real}}(x_0)}$ and $\frac{x J_{\text{imag}}(x)}{x_0 J_{\text{real}}(x_0)}$, which are proportional to the real and imaginary parts of the current flowing in an annulus of infinitesimal width dx at radius x , are plotted in Figure 1, while the quantity $I(x)$ is plotted in Figure 2.

In each plot, the dimensionless radius of the shaft wall, x_0 , has been set equal to 0.1. In view of equation (50), for a shaft radius $b = 4 \text{ feet} = 1.2 \text{ meters}$, $x = 0.1$ corresponds to a $k_r = 0.083 \text{ m}^{-1}$. Since $|k_r'| = k_0 \sqrt{|K|}$ and $k = -\frac{i\sigma}{\omega\epsilon_0}$ this means that for a rock conductivity $\sigma = 0.01 \text{ mho/m}$, the corresponding frequency is equal to 87 kHz and $K = -2067i$. Other combinations of f , σ , and b will produce different values of x_0 .

VI. COUPLING TO THE TRANSMISSION LINE

The overall communication efficiency between transmitter/receiver units located on the surface and in the cage will be influenced not only by the line attenuation loss. It will also depend on the losses caused by the methods used to establish the return current path in the rock, and more importantly on the losses due to impedance mismatches and standing waves. These latter losses will be caused by the high impedance capacitive termination at the cage end of the line, the low resistance sheave wheel grounding termination on the surface, and the couplers used to inductively couple signals onto the transmission line via the hoist rope.

A. Spatial Coupling Factors for the Return Paths.

Examination of Figure 2 reveals that the return current is widely distributed in the rock for typical values of $b = 1.2\text{m}$, $\sigma = 0.01 \text{ mho/m}$, and $f = 87 \text{ kHz}$. At first this would seem to imply that low loss coupling from the transmitter into the fundamental transmission-line mode requires a system of return-current electrodes implanted in the ground over a circular area of diameter equal to about 10-20 hoist-shaft diameters. We will now show, however, that the loss is actually quite small even when the area covered by the electrodes is only comparable with the cross-sectional area of the shaft itself.

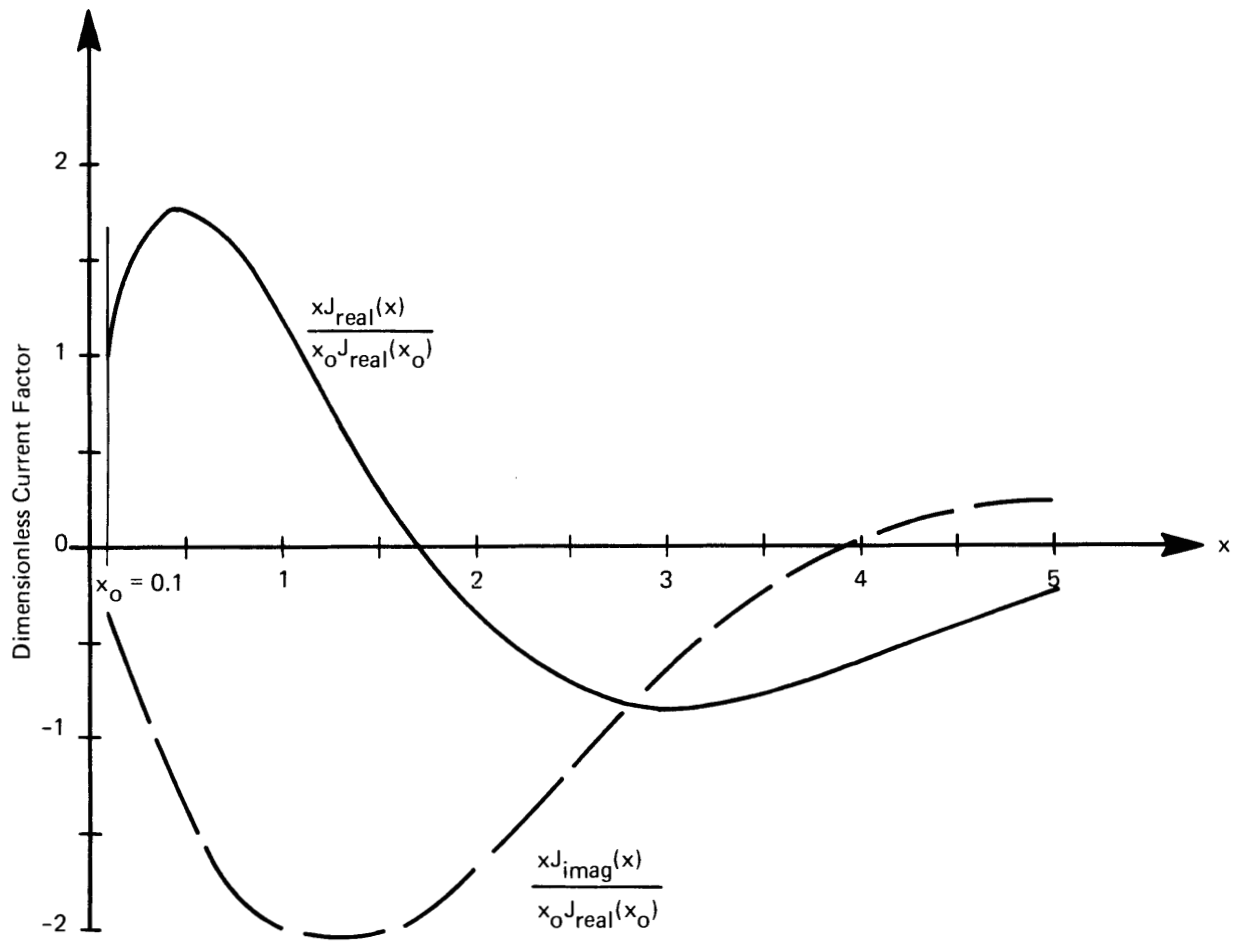


FIGURE 1 DIMENSIONLESS CURRENT FACTORS FOR ANNULUS AT RADIUS X

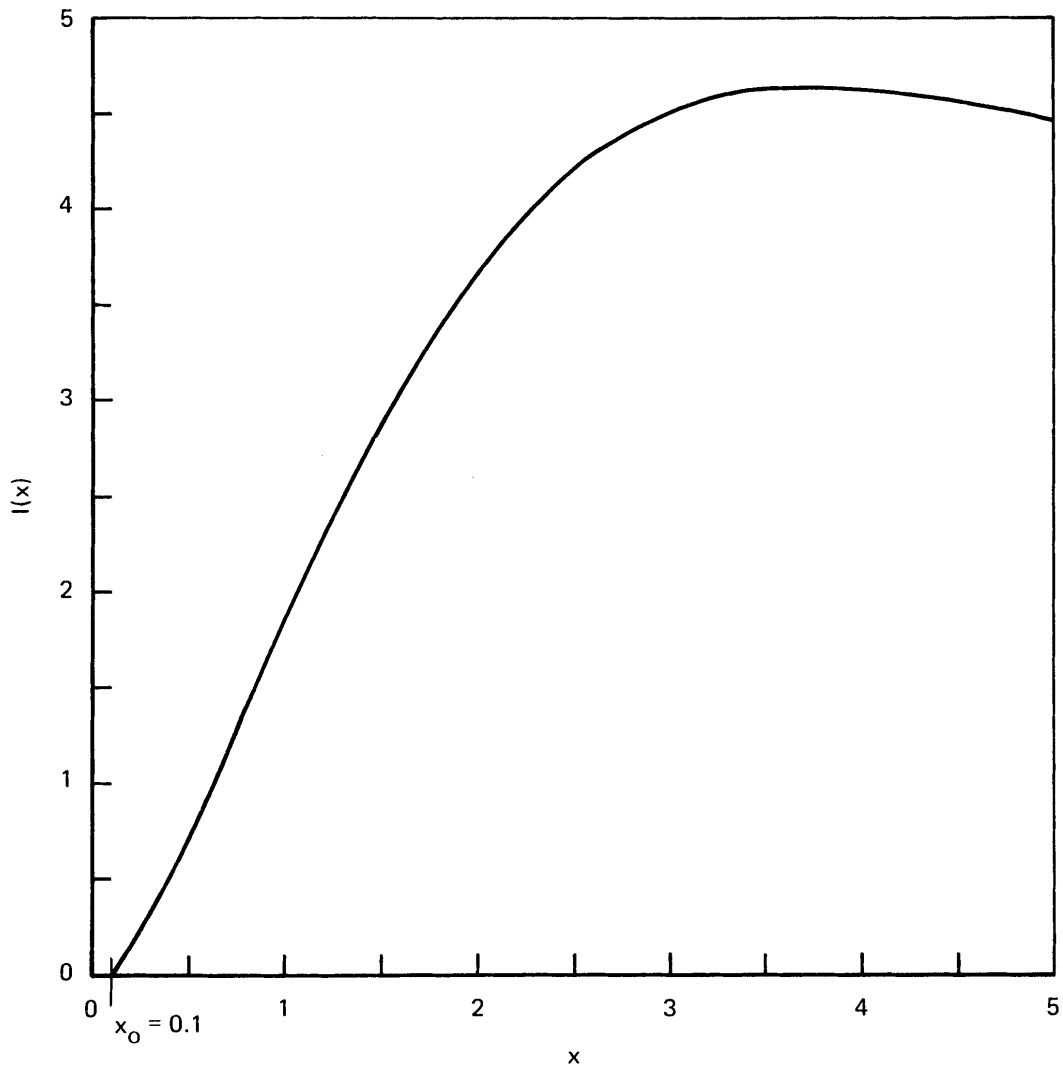


FIGURE 2 DIMENSIONLESS CUMULATIVE CURRENT $I(x)$ VERSUS x

The argument is that we can divide this coupling problem into two parts, the first being concerned with current flow from an electrode out to about one skin-depth, and the second having to do with the transition from this region, of essentially spherical spreading (or converging) of the current, to the region of transmission-line propagation beyond one skin-depth, in which the current flow is mainly in the z-direction.

In the first region the current flow pattern is approximately like that of direct current from a hemispherical electrode embedded in a semi-infinite resistive medium, with its flat face flush with the surface of the medium. The current flow in this case is radial, and the total resistance to flow is contributed almost entirely by the volume within a few hemisphere radii. The spreading resistance is

$$R_s = \frac{1}{2\pi a_o \sigma}, \quad (51)$$

where a_o is the radius of the hemisphere and σ is the conductivity of the rock.

The spreading resistance is not very sensitive to the exact electrode shape. A shape of interest in the hoist problem, at both the transmitter and receiver, is that of a hollow cylindrical electrode of length ℓ in contact with the wall of the shaft. In practice, such an electrode at the surface end of the shaft will most likely be approximated by three or more roof bolts connected in parallel and driven into the wall of the shaft, equally spaced around its perimeter. At the cage end, the "electrode" will be a cylindrical capacitance "connection" formed by the air space between the outer walls of the cage and the walls of the shaft. At the transmitter, the cylinder will act approximately like the above mentioned hemisphere having the same area of curved surface as the cylinder. The equivalent hemispherical radius is then

$$a_o = \sqrt{b\ell}, \quad (52)$$

where b is the shaft radius. For $\sigma = 0.01$ mho/m, $b = 1.2$ m, $\ell = 3$ m, we find from (51) and (52) that R_s is only 8.4 ohms. This resistance is in series with the characteristic impedance of the transmission line, which has a real part of about 300 ohms. Therefore, for $\sigma = .01$ ohm/m, the spreading resistance has negligible effect. For $\sigma = .001$ ohm/m, R_s is 84 ohms, and should be allowed for in the design of the driving circuit.

At the receiver the equivalent sphere radius is $a_0 = \sqrt{b\ell/2}$ but the spreading resistance is now $1/(4\pi a_0 \sigma)$. Thus, the spreading resistance is lowered by a factor of 2. This resistance is in series with the capacitive reactance between the cage and the shaft wall as well as with the characteristic impedance of the transmission line.

We now turn to the transition from spherical spreading to the transmission line mode of current flow. For simplicity we assume that the transition occurs sharply at the plane $z = \delta$, where δ is the skin-depth given by the formula

$$\delta = \sqrt{\frac{1}{\pi f \mu_0 \sigma}} . \quad (53)$$

For the values $f = 87$ kHz and $\sigma = 0.01$ mho/m corresponding to $b = 1.2$ m and $x_0 = 0.1$, as in Figures 1 and 2, we find that $\delta = 17$ m.

In the spherical-spreading region the current density depends on the spherical radius r_s according to the relation

$$j = \frac{A}{r_s^2} , \quad (54)$$

where A is an arbitrary constant. On the plane $z = \delta$ the z component of j is given by

$$j_z(r) = \frac{A\delta}{(\delta^2 + r^2)^{3/2}} , \quad (55)$$

where r is the cylindrical radial coordinate.

We regard $j_z(r)$ as driving the various modes of the transmission line. The power coupling constant C for the fundamental TEM mode is given by the formula

$$C = \frac{\left| \int_b^\infty J_z^* j_z r dr \right|^2}{\int_b^\infty |J_z|^2 r dr \int_b^\infty |j_z|^2 r dr}, \quad (56)$$

where J_z is the z - component of current density in the transmission line mode. The numerator is the overlap integral between J_z and j_z . The integrals in the denominator are normalizing factors. It is seen that when j_z has the same r -dependence as J_z , $C=1$. On the other hand, when j_z is orthogonal to J_z , $C=0$.

On changing to the dimensionless variable x given by (44) and substituting from (40) for $J_z(r)$ and from (55) for j_z we find approximately on expressing the result in terms of the \ker and \kei functions (Equations 42 and 43);

$$C = \frac{4 \left(\frac{x_o \delta}{b} \right)^4 \left\{ \left(\int_{x_o}^\infty \frac{\ker(x) x dx}{\left[\left(\frac{x_o \delta}{b} \right)^2 + x^2 \right]^{3/2}} \right)^2 + \left(\int_{x_o}^\infty \frac{\kei(x) x dx}{\left[\left(\frac{x_o \delta}{b} \right)^2 + x^2 \right]^{3/2}} \right)^2 \right\}}{\int_{x_o}^\infty \left[(\ker(x))^2 + (\kei(x))^2 \right] x dx}. \quad (57)$$

On taking $x_o = 0.1$, $\delta = 17$ m, and $b = 1.2$ m, we find by numerical integration of the integrals in (57) that $C = 0.7 = -1.5$ dB.

Therefore, the initial spherical spreading of the current, over a distance of the order of a skin depth (from relatively small electrodes such as the above mentioned cylindrical electrode approximations for the surface ground connection and the cage capacitive coupling geometries) yields a current distribution that matches the fundamental mode shape quite well, thereby contributing only a very small loss factor. Taken together with the relatively small spreading resistance effects, the losses due to spatial coupling factors for the return current path will not be major contributors to overall system loss at the frequencies of interest.

B. Cage Capacitive Termination

First order calculations for the cage-to-shaft-wall capacitance yield values between 110 and 460 pf. The smaller of these values is the free space capacitance of a one-meter radius conducting sphere, while the larger is the capacitance between a 5.5 x 5.5 x 13 foot conducting box placed in an 8.8 x 8.8 foot conducting enclosure, neglecting fringing effects. Choosing a nominal capacitance value equal to the geometric mean, 224 pf, we obtain the following capacitive reactance values over the frequency range of interest (see Table 5).

Table 5

Capacitive Reactance of Cage Termination
(for C = 224 pf)

<u>f</u> <u>(kHz)</u>	<u>X_C</u> <u>(Ohms)</u>
10	71,000
30	24,000
50	14,000
100	7,100
300	2,400
500	1,400

At frequencies below about 100 kHz, this reactance in series with the nominal 300 ohm characteristic impedance of the lines will produce a large mismatch and standing wave voltage and current variations down the shaft. It will also produce substantial reductions in the signal voltages appearing across the transmitter/receiver units, which are in series with, and of considerably lower impedance than, the capacitive reactance of the cage at these frequencies. Two potential solutions to these problems are to raise the impedance levels of the transmitter/receiver units and to raise the operating frequency. The latter solution also helps to achieve the former, as will be discussed briefly in the next section.

C. Inductive Coupling and Impedance Matching to the Hoist Rope.

Since it is not feasible to place a break in the hoist rope to insert the surface and cage transmitter/receiver units, the signals must be inductively coupled onto and off the hoist rope/shaft transmission line. One way to accomplish this is through the use of ferrite or powdered iron toroidal core coupler/isolators similar to the one described in Chapter II of Part Six of this Volume, and shown in Figures 1 and 6 of that Chapter. In Part Six, the toroidal coupler/isolator with its associated capacitor is placed around the trolley pole drop wire, as shown in Figure 1A of Chapter II, to add impedance in series with the trolley motors at the trolley wire carrier phone frequency of 88 or 100 kHz. This is to prevent the trolley motors from acting as a signal "shorts" across the trolley wire transmission line. It also provides an alternative method for coupling the carrier phone to the trolley wire transmission line. The capacitor and optional resistor shown in these figures are used to tune the toroidal core isolator and adjust its Q, to obtain the desired impedance level and isolator selectivity at the frequency of interest.

This type of toroidal coupler/isolator should be applicable to hoist rope communication systems, first as a signal coupler and second as an impedance matching isolator. For example, at the surface end of the hoist rope it could be used not only to couple the transmitter/receiver units to the hoist rope-shaft transmission line, but to also add the appropriate amount of matching impedance in series with the low impedance sheave wheel/ground connectors, thereby preventing standing wave interference effects during cage to surface transmissions. At the cage end of the hoist rope, the role of the toroidal device will most likely be limited only to transmitter/receiver hoist rope coupling, because of the already large reactance termination presented by the cage-to-shaft wall capacitance, as given in Table 5.

The impedance levels obtainable from reasonably small coupler/isolator structures can be easily estimated by utilizing the design data established for the trolley motor isolator described in Chapter II of Part Six. For the same six pairs of I and U ferrite cores used in the isolator pictured in Figures 6 and 7 of that Chapter, Figure 7 reveals that for a nominal minimum air gap* of 0.005", the single-turn inductance will be 19 microhenries. The corresponding reactance and resonant impedance levels are given below in Table 6 of this section for the indicated selectivities. The 3 kHz bandwidth selectivity chosen for frequencies below 80 kHz is applicable to single sideband modulation, while the 12 kHz bandwidth chosen for frequencies above 80 kHz is applicable to narrowband frequency modulation.

Table 6

Inductive Reactance, Resonant Impedance, and Q
for a Small Single-Turn Toroidal Coupler/Isolator

(kHz)	(ohms)	<u>For 3 kHz Bandwidth</u>		<u>For 12 kHz Bandwidth</u>	
		<u>Z_{res} (ohms)</u>	<u>Q</u>	<u>Z_{res} (ohms)</u>	<u>Q</u>
10	1.2	4	3.3	-	-
20	2.4	16	6.7	-	-
40	4.8	64	13.3	16	3.3
80	9.6	256	26.7	64	6.7
160	19.2	-	-	256	13.3
320	38.4	-	-	1024	26.7

* A much larger air gap was required for the trolley wire carrier phone application, to prevent core saturation by the large DC currents flowing in the trolley wire to power the trolley motors.

Table 6 indicates that values of impedance comparable to the hoist rope transmission line characteristic impedance of about 300 ohms are easily achieved above 100 kHz, even for this small-sized isolator.* Consequently, larger toroidal coupler/isolators of this type should be investigated further for their potential application as couplers and impedance matching devices in hoist shaft communication systems.

VII. CONCLUDING REMARKS

As stated in Chapter VI of this Part, raising the operating frequency to above 100 kHz offers several advantages for reducing the overall system loss. For example, examination of Tables 3, 5, and 6 for propagation loss, cage reactance, and coupler impedance, respectively, reveals that operation at a frequency in the vicinity of 300 kHz should lead to substantially reduced overall loss over that obtainable at frequencies below 100 kHz or at frequencies above 1000 kHz. As the frequency is increased to around 300 kHz, the gain in signal voltage across the transmitter/receiver coupling units due to reduced cage reactance and increased coupler impedance, more than offsets the effects of increased propagation loss. However, these minima should be less severe (i.e., have a smaller VSWR) at the higher frequency of 300 kHz because of the greater difference in relative strengths of the incident and reflected waves (as a result of the higher attenuation rate along the transmission line and the smaller mismatches achievable for the cage and coupler impedances relative to the transmission line characteristic impedance).

* The outside dimensions of this particular isolator are 4-1/2" x 4-1/4" x 6", the inside dimension 1-1/4" x 2" x 6", making it too small, especially in cross-section, for use with the 1-3/4" diameter hoist rope application of interest. The hoist rope application requires a much larger central opening in the core; not only to accommodate the large diameter hoist rope, but also the lateral motion of the rope particularly at the top of the shaft. This need may require the use of non-standard custom-made cores.

In sum, our preliminary findings indicate that an operating frequency in the vicinity of 300 kHz may offer decided performance advantages over that obtainable at substantially higher and lower frequencies. These findings need to be verified and better quantified by conducting a more comprehensive overall systems analysis and optimization, including the effects of electromagnetic noise.

PART SIX
TROLLEY WIRE MINE COMMUNICATIONS

PART SIX
TROLLEY WIRE MINE COMMUNICATIONS

TABLE OF CONTENTS

	<u>Page</u>
List of Figures	6.iii
INTRODUCTION	6.1
I. CALCULATIONS RELATED TO TROLLEY WIRE COMMUNICATIONS	6.1
A. ESTIMATION OF INDUCTANCE AND CAPACITANCE PER UNIT LENGTH OF TROLLEY LINES	6.1
B. EQUIVALENT CIRCUIT APPROXIMATION FOR THE TROLLEY POLE DROP WIRE TO MINE MOTORS	6.2
C. IMPEDANCE SEEN BY TROLLEY PHONES DUE TO CONNECTION METHOD	6.5
D. INDUCTANCE OF AIR-CORE COILS	6.8
E. THE EFFECT OF AN ATTACHED PARALLEL DC FEEDER CABLE ON TROLLEY LINE CHARACTERISTIC IMPEDANCE	6.8
F. SOME TROLLEY LINE IMPEDANCE BEHAVIOR PREDICTED BY TRANSMISSION LINE THEORY	6.11
G. CHARACTERISTIC IMPEDANCE ESTIMATES FOR MINE TROLLEY LINES	6.17
II. RF ISOLATORS FOR MINE MOTORS	6.22
A. BACKGROUND	6.22
B. APPROACH	6.22
C. DESIGN CALCULATIONS	6.25
D. LABORATORY TEST DATA	6.27
E. CONCLUDING REMARKS	6.30
ADDENDUM - FERRITE CHARACTERISTICS	
III. A DIVERSITY METHOD FOR COMBATTING STANDING WAVE NULLS	6.36

PART SIX
TROLLEY WIRE MINE COMMUNICATIONS
LIST OF FIGURES

<u>Figure No.</u>	<u>Title</u>	<u>Page</u>
	<u>Chapter I</u>	
1	Eccentric Line Model of Trolley Line	6.1
2	Trolley Line Model	6.3
3	Drop Wire and Equivalent Shunt Inductance	6.3
4	Geometry for Drop Wire	6.4
5	Trolley Line and Associated Impedances	6.4
6	Trolley Phone Connection to Trolley Wire	6.5
7	Model Geometries	6.5
8	Model Inductance Network	6.6
9	Equivalent Circuits	6.7
10	DC Feeder Cable and Trolley Wire Geometries	6.9
11	Trolley Line Routing Near Shop Area	6.10
12	Transmission Line and Load Impedance	6.11
13	Locus of Normalized Impedance Z/Z_0 Along Line-Case 1	6.13
14	Locus of Normalized Impedance Z/Z_0 Along Line-Case 2	6.16
15	Cross-Sectional Views of Trolley Line Geometries	6.17
16	Case 1 - Eccentric Line	6.19
17	Case 2 - Single Wire, Near Ground	6.19
18	Case 3 - Balanced 2-Wire-Unequal Diameters	6.19
19	Case 4 - Open 2-Wire Line in Air	6.19
20	Plots of Characteristic Impedance Z_0 Versus D	6.21

PART SIX

TROLLEY WIRE MINE COMMUNICATIONS

LIST OF FIGURES

(Continued)

<u>Figure No.</u>	<u>Title</u>	<u>Page</u>
<u>Chapter II</u>		
1A	Representation of Single-Turn Coupled Impedance Element Installed on a Trolley Pole	6.24
1B	Equivalent Circuit of Impedance Element	6.24
2	Toroid With Air Gap	6.26
3	Ferroxcube 3C5 Material Inductance Per Square Inch of Cross Section Versus Maximum DC Current - Single Turn Winding	6.28
4	Inductance Versus Current	6.29
5	Cores Used in Experiment	6.31
6	Configuration of Cores for Isolator	6.32
7	Single-Turn Inductance	6.33
<u>Chapter III</u>		
1	Sample Voltage and Current Standing Wave Patterns	6.37
2	Carrier Phone with Modifications for Switching Diversity-Simplified Block Diagram	6.38

PART SIX

TROLLEY WIRE MINE COMMUNICATIONS

INTRODUCTION

This part of the final report treats some problems related to coal mine carrier frequency communication systems using the trolley wire/track transmission line. This work was undertaken for a brief period of time during the summer of 1972 to help understand, quantify, and improve some of the trolley wire carrier system behavior observed and/or predicted. Calculations and estimates of transmission line characteristic impedance, inductance and capacitance per unit length, mine motor loading effects, parallel line effects, and connection impedances are presented in Chapter I. Chapter II treats the design of r-f isolators for reducing the undesired and troublesome r-f loading that mine motors present to the trolley transmission line. Chapter III treats a diversity method for combatting standing wave nulls.

I. CALCULATIONS RELATED TO TROLLEY WIRE COMMUNICATIONS

A. ESTIMATION OF INDUCTANCE AND CAPACITANCE PER UNIT LENGTH OF TROLLEY LINES

To estimate the L and C per unit length of trolley lines, we use the eccentric line model of Section G of this Chapter, "Characteristic Impedance Estimates for Mine Trolley Lines." The capacitance per unit length for an eccentric line is given by (1)

$$C = \frac{2\pi\epsilon}{\left[\cosh^{-1} \frac{m_2}{R_2} - \cosh^{-1} \frac{m'_1}{R'_1} \right]} \quad (1)*$$

where $m'_1 = \frac{c}{2} [(\eta_1^2 - \eta_2^2) + 1]$

$m_2 = \frac{c}{2} [(\eta_1^2 - \eta_2^2) - 1]$ (3)

$\eta_1 = \frac{R'_1}{c}, \eta_2 = \frac{R_2}{c}$ (4a,b)

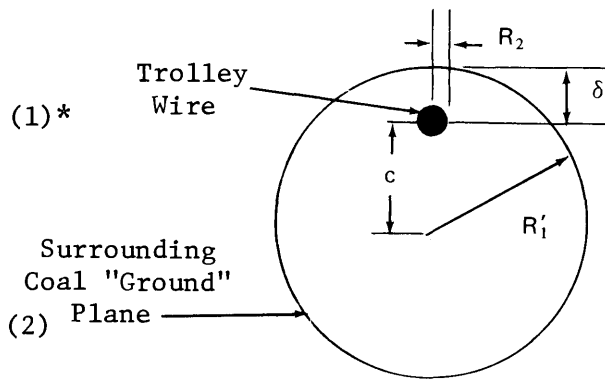


FIGURE 1 ECCENTRIC LINE MODEL OF TROLLEY LINE

(1) E. Weber, Electromagnetic Fields, Theory and Applications, Vol. 1, 1957, pp. 119-121.

* References to Figures, Tables, and Equations apply to those in this Chapter unless otherwise noted.

The inductance per unit length can be obtained indirectly by substituting values for Z_o and C into the characteristic impedance expression.

$$Z_o = \sqrt{\frac{L}{C}} \quad (5)$$

The values for Z_o can be obtained from Figure 20, which were computed using the following equations⁽²⁾

$$Z_o = \frac{60}{\epsilon^{1/2}} \cosh^{-1} U \quad (6)$$

$$U = 1/2 [D/d + d/D - 4c^2/dD] \quad (7)$$

$$c = \frac{D}{2} - \delta, \quad \epsilon = 1 \quad (8)$$

Substituting the appropriate values for high and low coal conditions, we get:

	<u>High Coal</u>	<u>Low Coal</u>
R_2	0.25"	0.25"
R'_1	36"	24"
δ	6"	3"
c	30"	21"
Z_o	230 Ω	190 Ω
C	15pf/m	18pf/m
L	0.8 μ h/m	0.65 μ h/m

B. EQUIVALENT CIRCUIT APPROXIMATION FOR THE TROLLEY POLE DROP WIRE TO MINE MOTORS

Using the eccentric transmission line model of Figure 1 which provides a good approximation to the trolley transmission line characteristic impedance, consider the effect of a vertical trolley pole wire to a motor, which is in turn connected to ground via the rails. Figure 2 depicts the trolley line

(2) ITT Reference Data for Radio Engineers, 5th Edition, Chapter 22, Transmission Lines, pp. 22-24.

and drop wire geometries, where the characteristic impedance is taken equal to 200 ohms and Z_m is the impedance of the motor at the trolley phone frequency.

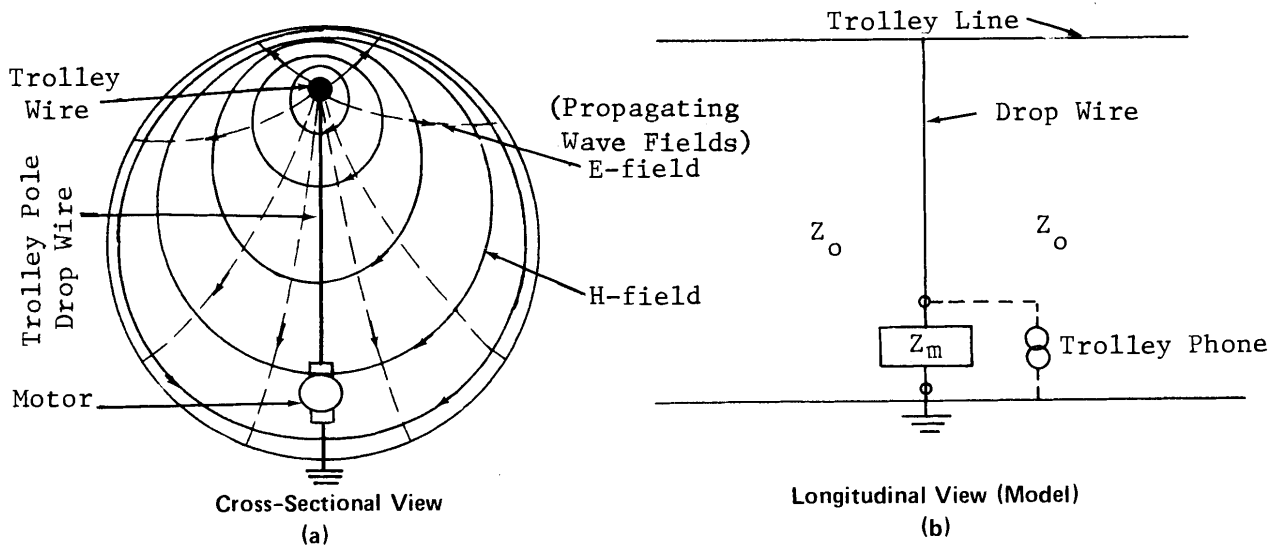


FIGURE 2 TROLLEY LINE MODEL

The trolley drop wire and low impedance motor do not represent a true or ideal short circuit in this situation, because the fields of a traveling wave are not prevented from coupling to the other side of the drop wire, as would be the case if the wire were replaced by a perfectly conducting plate across the whole haulageway cross-section. Therefore, the drop wire will allow energy to be inductively coupled between the sections of trolley line on each side of the drop wire, although this coupling will generally be weak.

Since the dimensions of the drop wire are small compared to a wavelength at 88kHz, it can be represented by a lumped inductance shunt element, L_s , as shown in Figure 3.

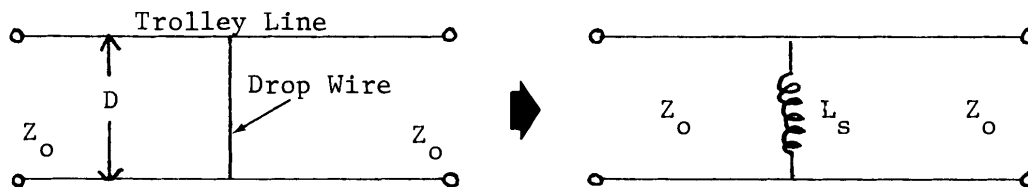


FIGURE 3 DROP WIRE AND EQUIVALENT SHUNT INDUCTANCE

The shunt inductance contribution L_s of the drop wire was estimated by computing the flux produced by the drop wire over the cross-sectional area $D_1 \times D_2$ shown in Figure 4.

$$\bar{H} = \bar{i}_\phi \frac{I}{2\pi r} \quad (9)$$

$$\Phi = \int_0^{D_2} \int_0^{D_1} B \, da = L_s I \quad (10)$$

$$L_s \cong \frac{\mu_0}{2\pi} D_1 \ln \left(\frac{D_2}{a} \right) \quad (11)$$

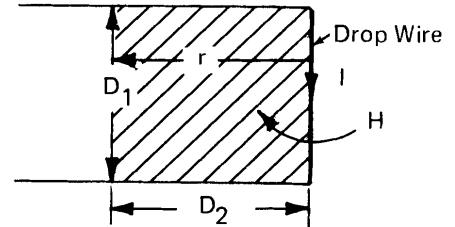


FIGURE 4 GEOMETRY FOR DROP WIRE

where a is the wire radius.

Letting $a = 0.25$ inches, and $D_2 = D_1 = 5.5$ feet for high coal and 4 feet for low coal, we get

	L_s	X_{L_s}
for high coal	$1.9\mu\text{h}$	1.1Ω
for low coal	$1.3\mu\text{h}$	0.75Ω

where X_{L_s} is the associated inductive reactance at 88 kHz (shown in Figure 5).

By comparison with these values of shunt reactance, the characteristic impedance of the trolley line $Z_0 \cong 200$ ohms, the trolley phone impedance Z_T is a nominal 25 ohms, and the magnitude of the impedance Z_m of the motor in series with the drop wire is alleged to be on the order of 0.5 ohm when hauling at nominal speed. More measurements of the impedance behavior of typical locomotive motors at the trolley phone frequencies of 88 and 100 kHz are needed to confirm this reputed low impedance behavior and to determine whether it is representative for different motor installations on locomotives.

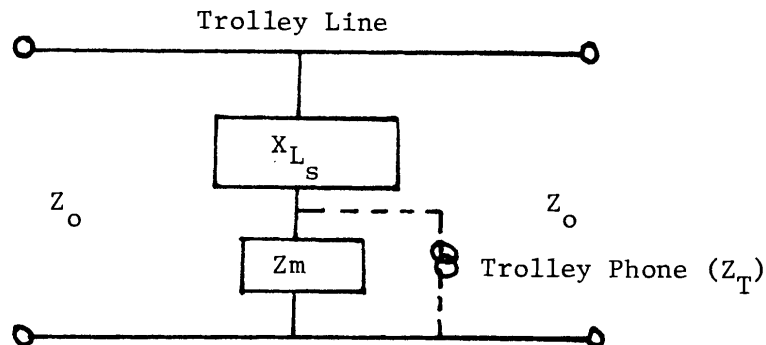


FIGURE 5 TROLLEY LINE AND ASSOCIATED IMPEDANCES

C. IMPEDANCE SEEN BY TROLLEY PHONES DUE TO CONNECTION METHOD

The trolley phones are presently coupled to the trolley line by connecting them in parallel with the low impedance trolley motors. The connections are made relatively close to the motor terminals so that little or no advantage is taken of any increase in impedance offered by the trolley pole drop wire inductance. Figure 6 illustrates typical geometry (6a) and an approximate equivalent circuit (6b).

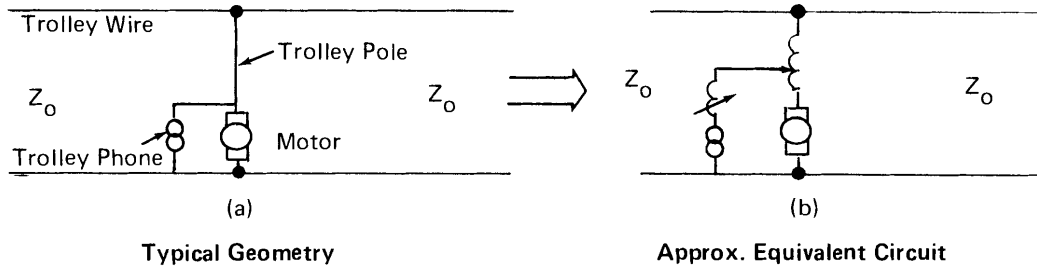


FIGURE 6 TROLLEY PHONE CONNECTION TO TROLLEY WIRE

Since the trolley motor impedance at 88kHz is reported to be on the order of 0.5 ohms, the motors will shunt most of the trolley signal away from the trolley line. By making the connection further up the drop wire, the shunt impedance presented by the motor can be increased by the drop wire inductive reactance. The objective of this section is to provide an estimate of the magnitude of this potential increase in impedance.

To estimate the shunt and series impedance for two different connections, the geometries of Figure 7 for the case of high coal were used.

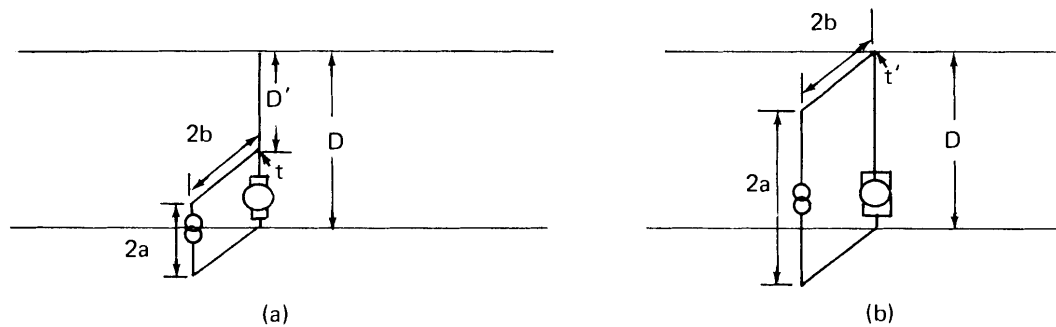


FIGURE 7 MODEL GEOMETRIES

Figure 7a approximates the present connection, t, while Figure 7b approximates a connection, t', to the top of the trolley pole. As seen from the trolley phone generator, simplified inductance networks can be drawn as in Figure 8.

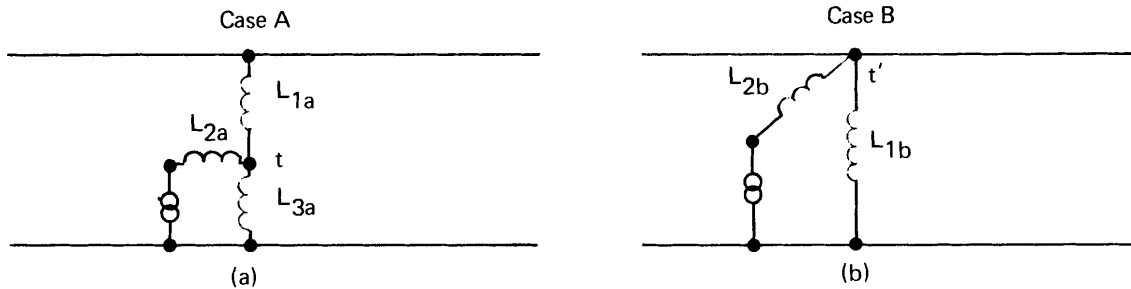


FIGURE 8 MODEL INDUCTANCE NETWORK

CASE A

In Case A the drop wire inductance formula (11) of Section C can be used for computing L_{1a} ,

$$L_{1a} = \frac{\mu D'}{2\pi} \ln \left(\frac{D}{r_o} \right) \quad (12)$$

where $D' = D - 2a$, and r_o is the wire radius, in Figure 7a. The other inductance components of Cases A and B can be estimated using the following formula for a rectangular loop from Weber(3).

$$L = \frac{2\mu}{\pi} \left\{ 2 \sqrt{a^2 + b^2} + a \ln \left(\frac{8a}{d} \right) + b \ln \left(\frac{8b}{d} \right) - 2(a+b) - a \ln \left[1 + \sqrt{1 + \left(\frac{b}{a} \right)^2} \right] - b \ln \left[1 + \sqrt{1 + \left(\frac{a}{b} \right)^2} \right] \right\} \quad (13)$$

where $2a$, $2b$ are the lengths of the rectangle sides and d is the wire diameter.

For Case A: $D = 5.5$ ft., $2a = 2b = 1$ ft., $d = 0.5$ in.

Therefore using (12) we get,

$$L_{1a} \approx 1.5 \mu\text{h}, \quad (14)$$

and using (13), we get,

$$L \approx 0.8 \mu\text{h}, \quad (15)$$

for the square loop of Figure 7a. Now by separating out equal inductance contributions of $0.2 \mu\text{h}$ for each leg of the square loop to form L_{2a} and L_{3a} ,

$$\text{we get} \quad L_{2a} \approx 0.6 \mu\text{h} \quad , \quad L_{3a} \approx 0.2 \mu\text{h}. \quad (16a,b)$$

(3) E. Weber, "Electromagnetic Fields, Theory and Applications", Vol. 1, 1957, p. 131-133.

CASE B

For Case B: $2a = 5.5$ ft., $2b = 1$ ft., $d = 0.5$ in. Using Equation (13) for a rectangular loop we get:

$$L = 3.8 \mu\text{h}. \tag{17}$$

By approximating the inductance contribution of each short rectangular leg by the $0.2\mu\text{h}$ value for the square loop case, and therefore assigning $1.7\mu\text{h}$ to each long 5.5 ft. leg, we get:

$$L_{1b} = 1.7\mu\text{h}, L_{2b} = 2.1\mu\text{h}. \tag{18, 19}$$

Therefore, the simplified equivalent circuits become as shown in Figure 9 with the indicated impedance values at 88 kHz. These circuits are not meant to be exact representations, but simple approximations to provide workable means for estimating likely effects on performance. A more exact treatment would include the influence of mutual coupling on the specification of equivalent circuit components.

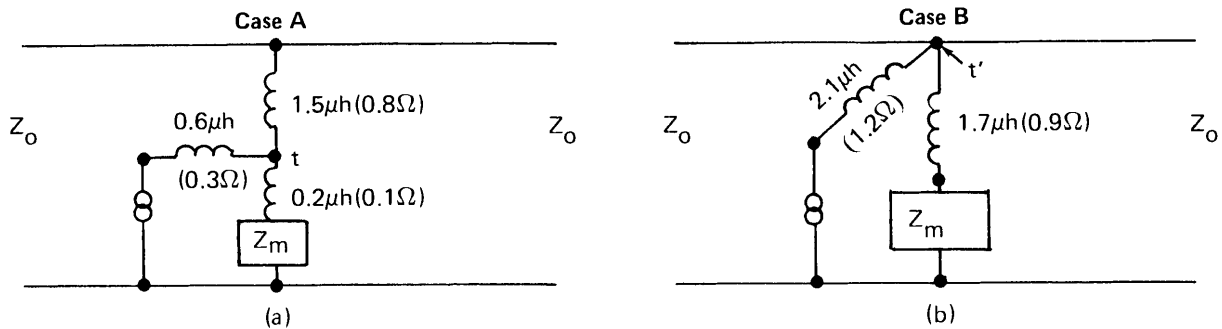


FIGURE 9 EQUIVALENT CIRCUITS

Raising the connection point, t , to the top of the trolley pole, t' , changes the impedance level from $[Z_m + 0.1$ ohms (t -to-ground) to $[Z_m + 0.9]$ ohms (t' -to-ground), an increase of only 0.8 ohms. In view of the high 200 ohm characteristic impedance of the trolley line, and the changing line impedance levels produced across the t' -to-ground connection as a result of other normal line loads, the small increase of about 0.8 ohms obtained by making connections at the top of the trolley pole appears to be grossly insufficient to provide significant improvements in trolley phone performance.

D. INDUCTANCE OF AIR-CORE COILS

Untuned air-core inductors have been and are still used in some mines to isolate the low impedance of rectifier power substations at the trolley phone frequency of 88 khz. This has been accomplished by forming a coil inductor consisting of about ten turns, three feet in diameter and three feet in length, which is placed in series with the substations. A good formula for estimating the approximate inductance of such air-core coils is given by

$$L = \frac{N^2 r^2}{9r + 10\ell} \text{ in } \mu\text{h} \quad (4) \quad (20)$$

where r is the coil radius in inches, ℓ is the coil length in inches, and N is the number of turns. For the above described coil, equation (20) predicts an inductance value of $L = 62 \mu\text{h}$, which results in an inductive reactance of 34 ohms at 88kHz. This value of reactance apparently is sufficient to improve trolley phone performance in many cases.

By resonating such an air-core coil with a parallel capacitance, much less inductance would be required to produce the desired impedance level. For example, using a circuit with a Q of 10, a desirable Q value for trolley phone applications, only $6.2\mu\text{h}$ are needed to get 34 ohms of reactance. Therefore a coil of the same number of turns and length would need only a diameter of 8.5 inches instead of 36 inches to produce the $6.2\mu\text{h}$ of inductance. If we further assume that the turns per unit length can be increased by at least a factor of two for the size wire required to carry the high current loads of coal mine trolley lines, then the length of the above 8.5 inch diameter coil can be reduced from 36 to 14 inches. Consequently, tuned air-core coils occupying about 1/2 cubic foot of volume may be practical alternatives, in some locations, to the ferrite or iron rf isolators described in Chapter III. The increased sensitivity of air-core coil behavior to nearby metal structures, however, may still make air-core coils less attractive for use in confined spaces as found inside locomotives.

E. THE EFFECT OF AN ATTACHED PARALLEL DC FEEDER CABLE ON TROLLEY LINE CHARACTERISTIC IMPEDANCE

At the Bethlehem Steel Marianna Mine in Uniontown, Pa., we noticed that the one million circular mil DC trolley feeder cable was made to run above, parallel to, and frequently connected to the trolley wire as shown in Figure 10.

(4)

ITT Reference Data for Engineers, 5th Edition, Chapter 6, Fundamentals of Networks, pp. 6-3.

This kind of arrangement is sometimes used in mines to help maintain the

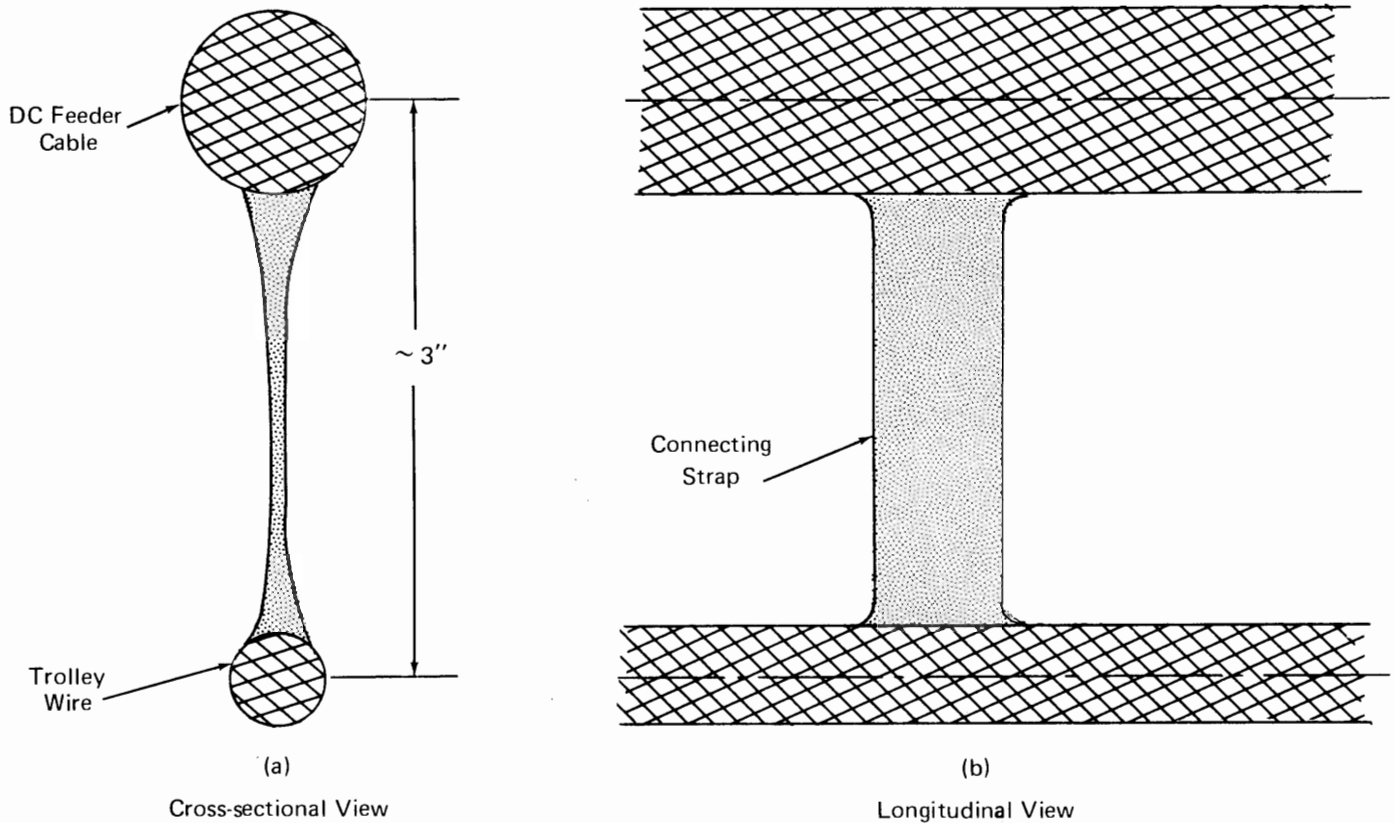


FIGURE 10 DC FEEDER CABLE AND TROLLEY WIRE GEOMETRIES

DC line voltage by decreasing the effective resistance of the trolley line, the diameter of which is only about 1/2 inch. Since this geometry increases the effective diameter of the trolley wire as far as the rf characteristic impedance of the line is concerned, an estimate was made of how much the characteristic impedance would be changed. An upper bound on this effect can be obtained by assuming that the Figure 10 geometry can be approximated by a cylindrical wire of 3" diameter centered at the nominal 6" level down from the roof in a high-coal haulageway. Using equations 41a,b

$$Z_o = \frac{60}{\epsilon^{1/2}} \cosh^{-1} U \quad (21)$$

$$U = \frac{1}{2} [D/d + d/D - 4c^2/dD] \quad (22)$$

$$c = D/2 - \delta \quad (23)$$

with $\epsilon = 1$, $d = 3''$, $D = 6'$, $\delta = 6''$,

$$\text{we get } \underline{Z_o = 118 \text{ ohms}}, \quad (24)$$

which is about one-half the expected Z_o value for the trolley wire without the DC feeder cable.

The trolley wire at the Marianna mine was displaced, as is customary, about one foot to the outside of the rails as opposed to being centered above and between the rails as we first assumed. The utility of the eccentric line model of Figure (1) for such practical trolley line geometries should not be impaired, but in fact may even make the model more representative.

The lower Z_o value computed for the case of the DC feeder cable attachment also supports a measurement of net trolley line impedance as seen from our position near the shop area termination of the line. Figure 11 illustrates the track and trolley line routing in that immediate area. Trolley line continuity was maintained at the indicated branchings. Since all the distances to the branchings were small compared to wavelength at 88kHz, the network can be considered as five lines in parallel. If we further assume that each individual branch line looks matched in a characteristic impedance value of 118 ohms, then the net impedance seen at the starred shop location should be close to 24 ohms. A value of 22 ohms was measured with the PMSRC impedance measuring box. Future measurements should reveal whether this was just a coincidence.

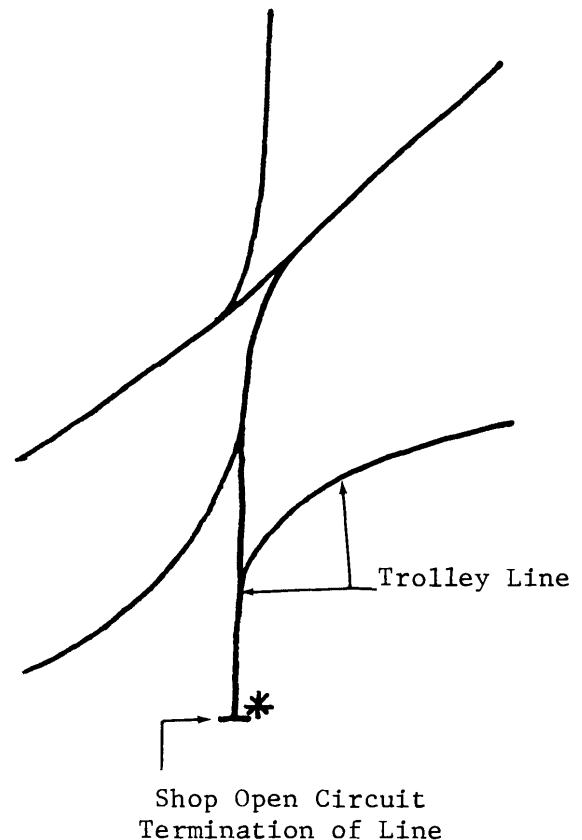


FIGURE 11 TROLLEY LINE ROUTING NEAR SHOP AREA

F. SOME TROLLEY LINE IMPEDANCE BEHAVIOR PREDICTED BY TRANSMISSION LINE THEORY

For a general lossy transmission line, the voltage and current along the line are given by

$$V(z) = V_+ e^{-\gamma z} + V_- e^{+\gamma z} \quad (25)$$

$$I(z) = \frac{1}{Z_o} [V_+ e^{-\gamma z} - V_- e^{+\gamma z}] \quad (26)$$

where $\gamma = \alpha + j\beta$ is the propagation constant and $Z_o = R + jX_o$ is the characteristic impedance.

Put in the classical convenient form, we have

$$V(z) = V_+ e^{-\alpha z} e^{-j\beta z} [1 + \Gamma(z)] \quad (27)$$

$$I(z) = \frac{V_+}{Z_o} e^{-\alpha z} e^{-j\beta z} [1 + \Gamma(z)] \quad (28)$$

where $\Gamma(z) = \frac{V_-}{V_+} e^{2\alpha z} e^{j2\beta z} = \Gamma_L e^{2\alpha z} e^{j2\beta z}$, is the reflection (29)

coefficient at an arbitrary point z on the line, and

$$\Gamma(o) = \Gamma_L = \frac{V_-}{V_+} \text{ is the reflection coefficient of the load term- (30)}$$

minating the line at $z = o$. $\Gamma(o) = \Gamma_L$ can be computed using

$$\Gamma_L = \frac{Z_L - Z_o}{Z_L + Z_o}, \text{ where } Z_L \text{ is the impedance of the load. (31)}$$

The geometry in question is shown in Figure 12.

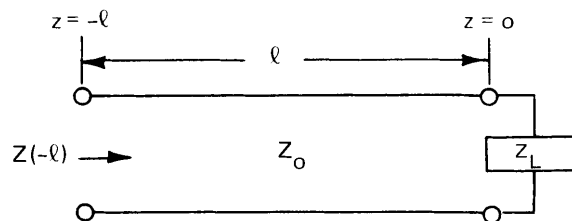


FIGURE 12 TRANSMISSION LINE AND LOAD IMPEDANCE

At a distance " ℓ " away from the load (e.g. $z = -\ell$), we get

$$V(z = -\ell) = V_+ e^{\alpha\ell} e^{j\beta\ell} [1 + \Gamma(-\ell)] \quad (32)$$

$$I(z = -\ell) = \frac{V_+}{Z_0} e^{\alpha\ell} e^{j\beta\ell} [1 - \Gamma(-\ell)], \quad (33)$$

so that the line impedance presented to a generator at $z = -\ell$ is given by

$$Z(-\ell) = \frac{V(-\ell)}{I(-\ell)} = Z_0 \left[\frac{1 + \Gamma(-\ell)}{1 - \Gamma(-\ell)} \right]. \quad (34)$$

$Z(-\ell)$ can be conveniently plotted in normalized form $Z(-\ell)/Z_0$ on a Smith Chart to examine its behavior as a function of line length, frequency, and the introduction of series and parallel loads.

The propagation constant and characteristic impedance are given by the following expressions.

Propagation Constant

Characteristic Impedance

$$\gamma = \sqrt{(R+j\omega L)(G+j\omega C)} \quad (35) \quad Z_0 = \sqrt{\frac{R+j\omega L}{G+j\omega C}} \quad (36)$$

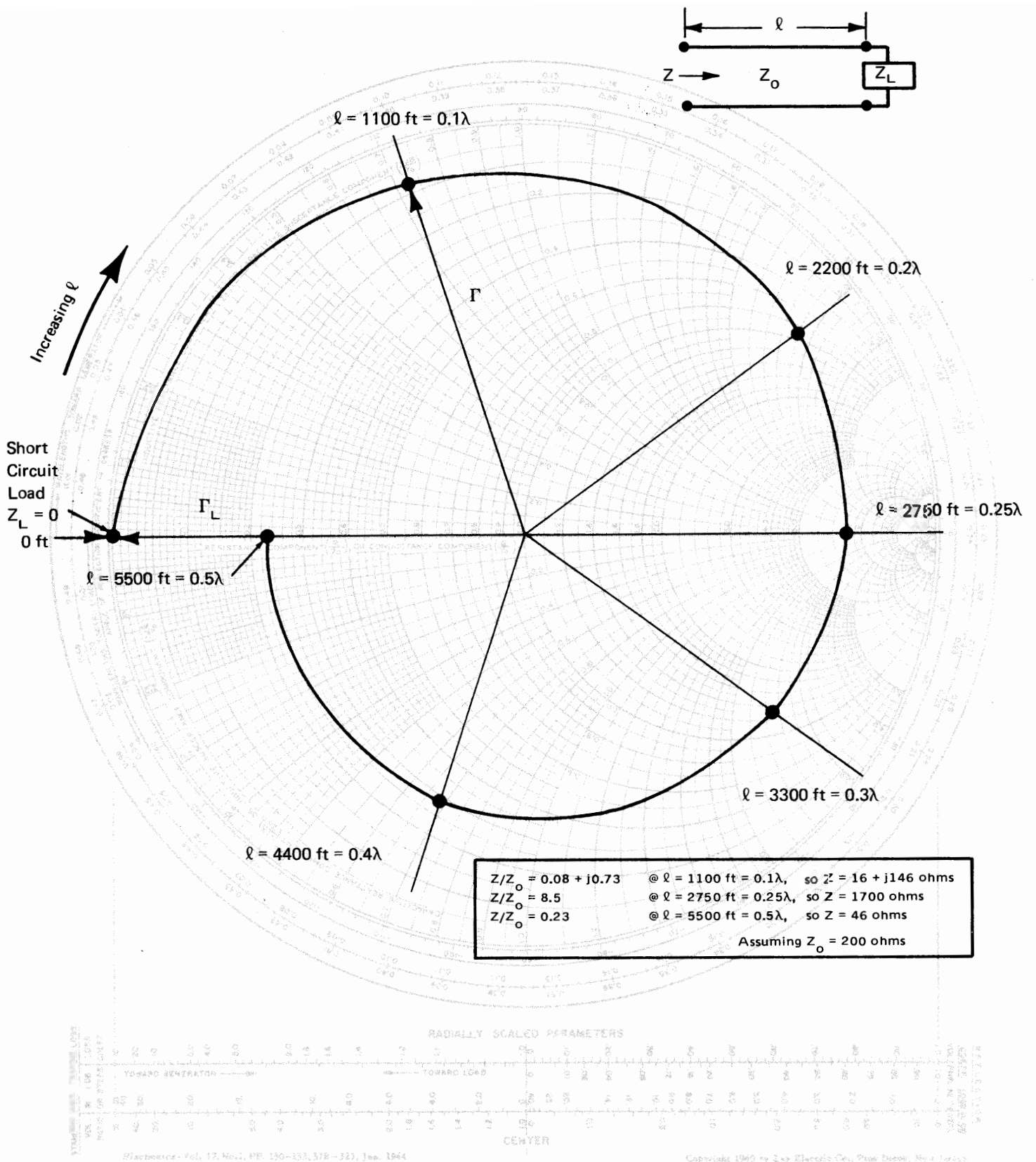
$$\gamma = \alpha + j\beta \quad (37) \quad Z_0 = R_0 + jX_0 \quad (38)$$

where R, G, L, C are the normal per unit length electrical parameters of the transmission line.

At first glance it appears that mine trolley lines can be considered "low loss" lines, having characteristic impedances that are essentially real, and lossless propagation constants $\gamma = j\beta = j 2\pi/\lambda$ modified by a small attenuation factor α , $\gamma = \alpha + j\beta$. Some investigators have observed attenuation rates on the order of 2 db per mile.* This is about 4 db per wavelength at 88 kHz, the wavelength being approximately 11,000 feet.

Using these values of wavelength and attenuation, the line impedance behavior produced by a short circuit placed across the line, as a function of distance away from the short circuit has been plotted on a Smith Chart in Figure 13. A short circuit was chosen as a first approximation to a DC rectifier power substation, and possibly a locomotive motor.

* More data are needed to determine whether this value is a representative one for different mines and installations.



$Z/Z_0 = 0.08 + j0.73$	@ $l = 1100 \text{ ft} = 0.1\lambda$, so $Z = 16 + j146 \text{ ohms}$
$Z/Z_0 = 8.5$	@ $l = 2750 \text{ ft} = 0.25\lambda$, so $Z = 1700 \text{ ohms}$
$Z/Z_0 = 0.23$	@ $l = 5500 \text{ ft} = 0.5\lambda$, so $Z = 46 \text{ ohms}$
Assuming $Z_0 = 200 \text{ ohms}$	

FIGURE 13 LOCUS OF NORMALIZED IMPEDANCE Z/Z_0 ALONG LINE – CASE 1
For: Short Circuit Termination (Load)
Frequency – 88 kHz
Attenuation Factor: $\alpha = 4 \text{ dB per } \lambda$
(2 dB/mile)

The Smith Chart is used here as an impedance chart so that a short circuit of zero impedance occurs at the left hand side of the real (horizontal) axis. The reactance axis runs along the circumference, inductive reactance occurring in the top hemisphere and capacitive reactance in the lower. The real and imaginary impedance values are normalized to that of the characteristic impedance, Z_0 . Distances expressed in fractions of a wavelength from the load moving towards the generator are also found along the circumference. Rotation once around the chart represents one-half wavelength of travel. The vector drawn from the center of the chart to any normalized impedance point is the reflection coefficient Γ . The center of the chart $Z/Z_0 = 1 + j0$ describes the impedance $Z = Z_0$, namely that of a line matched to its characteristic impedance Z_0 . Since power substations are spaced roughly a mile apart in typical coal mines, the impedance behavior has been plotted up to one mile away, which is roughly $1/2$ wavelength at 88kHz. A short circuit $Z_L = 0$ represents a reflection coefficient $\Gamma_L = -1$. If the attenuation factor were zero, the Γ vector would be rotated at constant amplitude around the chart as the distance from the short increased, thereby giving rise to only reactive components of line impedance. Since the attenuation factor is not zero, but on the order of 4db per wavelength, the Γ vector will be reduced in size by twice this factor as prescribed by equation (29), thereby producing both resistive and reactive components of line impedance as the vector is rotated around the chart.

Examination of the Smith Chart plot of Figure 13 reveals several items of interest. It apparently is common practice in some mines to place the dispatcher's trolley phone station about 1000 feet from the DC substations in order to get satisfactory performance. From Figure 13 we see a healthy impedance level of $Z = 16 + j 146$ ohms is obtainable 1100 feet away from a substation short circuit placed across a $Z_0 = 200$ ohm trolley line. Even if the Z_0 is on the order of 100 ohms as may be the case in the Marianna mine, $Z = 8 + j 72$ ohms would be available. These reactive impedance values should be more than enough to allow satisfactory trolley phone signals to be put onto the trolley line from a 25 ohm transmitter, if the transmitter is not adversely affected by reactive loads, thereby supporting the above practice. Figure 13 also indicates that a mobile unit should encounter its worst performance, due to the presence of a low impedance substation or mine motor, when the mobile is in the immediate vicinity of the substation or motor, say within about 100 feet. Once beyond the very low impedance region near the substation or motor, the magnitude of the impedance will not decrease below the 46 ohm level found at the one-half wavelength distance, for the line described. The finite attenuation factor makes the impedance locus gradually spiral in towards the center of the Smith Chart. This prevents the impedance from going to zero again at the half wave length distances, and eventually makes Z approach the Z_0 value if no other impedances are placed across the line. The finite attenuation factor also prevents infinite values of impedance from occurring at the quarter wavelength distances, a maximum of 1700 ohms being the upper limit at $\lambda/4$ for the case described.

One last case of interest is that of a 25 ohm resistive trolley phone load. The impedance variation as a function of line length for the 25 ohm resistive load has been plotted in Figure 14. Note that reactive impedances are still produced, but that the maximum impedance level achieved (at $\lambda/4$) is half of that for the short circuit case, while the $\lambda/2$ impedance value has been increased by half again over that for the short circuit case, for the line in question. The effects of placing additional 25 ohm and/or short circuit "mobile" loads across the line at arbitrary locations can also be treated. This can most conveniently be done by using the Smith Chart as an admittance chart, which allows the addition of parallel admittances in a simple manner graphically. However, one can get a good feel for the impedance behavior expected at an arbitrary attachment point between two loads on a continuous line by placing to the left of the $z = -\ell$ point of Figure 12, a second line section of length ℓ' and load Z_L' appropriate to what is present to the left of the attachment point; computing the impedance seen looking to the left Z_ℓ per Figures 13 and 14; and summing them together as a parallel impedance connection.

G. CHARACTERISTIC IMPEDANCE ESTIMATES FOR MINE TROLLEY LINES

The characteristic impedance of a uniform transmission line is given by

$$Z_o = \sqrt{\frac{R+j\omega L}{G+j\omega C}} \text{ ohms} \quad (39)$$

where ω is the radian frequency, R and L are the series resistance and inductance per unit length, and G and C are the shunt conductance and capacitance per unit length. For lossless lines, which most practical lines approach, R and G = 0. Then Z_o reduces to

$$Z_o = \sqrt{\frac{L}{C}} \text{ ,} \quad (40)$$

and the characteristic impedance is a function only of the cross-sectional geometry and the dielectric and magnetic properties of the cross-sectional media.

To get a first-order analytical estimate of Z_o for trolley lines in coal mines, losses were neglected and the mine haulageway geometry approximated by some classical geometries for which equations are readily available for Z_o . The trolley haulageway cross-sections in Figure 15 are considered representative.

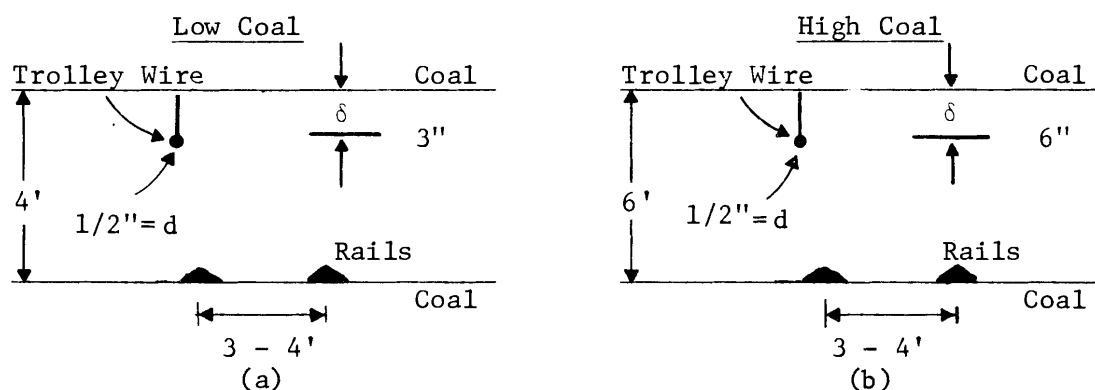


FIGURE 15 CROSS-SECTIONAL VIEWS OF TROLLEY LINE GEOMETRIES

The trolley transmission line consists of an overhead trolley wire isolated from the haulageway ceiling, together with two trolley rails serving as return path conductors. The rails are in turn grounded to the coal which has a moderate conductivity ranging from about 10^{-1} to 10^{-3} mho/meter. So the surrounding coal may produce behavior similar to that of a ground plane in place of the rails, or that of a surrounding conducting shield.

1. Impedances for Approximate Geometries

Two geometries, with readily available equations for Z_o , that may approximate these trolley wire situations, are shown in Figures 16 and 17. Figure 16 is Case 1, an eccentric shielded line, and Figure 17 is Case 2, a single wire above a ground plane. Two other cases that do not include the effects of the surrounding coal are also included for ready comparison. They are Case 3, the open two-wire line with unequal diameters in Figure 18 and Case 4, open two-wire line with equal diameters in Figure 19.

Case 1: Eccentric Line

$$Z_o = \frac{60}{\epsilon^{1/2}} \cosh^{-1} U \quad (41a,b)$$

$$U = \frac{1}{2} [D/d + d/D - 4C^2/dD]$$

$$\epsilon = 1, d = 0.46", C = \frac{D}{2} - \delta$$

D(variable) 3 to 10 ft., $\delta = 3"$ low coal, $6"$ high coal

Case 2: Single Wire Above a Ground Plane

$$Z_o = \frac{138}{\epsilon^{1/2}} \log_{10} (4D/d) \text{ for } d \ll h \quad (42)$$

$\epsilon = 1, d = 0.46"$ nominal diameter of 0000 trolley wire
D(variable) 3 to 10 ft. - (low to high coal)

Case 3: Open Two-Wire Line with Unequal Diameters

$$Z_o = \frac{60}{\epsilon^{1/2}} \cosh^{-1} N \quad (43a,b)$$

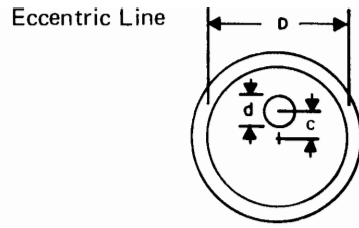
$$N = \frac{1}{2} \left[\frac{4 D^2}{d_1 d_2} - \frac{d_1}{d_2} - \frac{d_2}{d_1} \right]$$

$\epsilon = 1, d_2 = 0.46", D(\text{variable}) - 3 \text{ to } 10 \text{ ft.}$

Do for two values of d_1

$d_1' = 4.6"$ approximate diameter of a single rail

$d_1'' = 46"$ approximate maximum separation between rails--
assuming a cylinder of that diameter

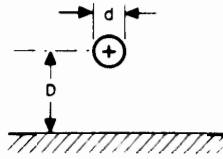


$$Z_0 = (60/\epsilon^{1/2}) \cosh^{-1} U$$

$$U = \frac{1}{2} \left[(D/d) + (d/D) - (4c^2/dD) \right]$$

FIGURE 16 CASE 1

Single wire, near ground

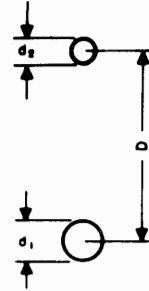


For $d \ll D$

$$Z_0 = (138/\epsilon^{1/2}) \log_{10}(4D/d)$$

FIGURE 17 CASE 2

Balanced 2-wire—unequal diameters



Source: *ITT Reference Data for Radio Engineers*,
5th Edition Chapter 22

$$Z_0 = (60/\epsilon^{1/2}) \cosh^{-1} N$$

$$N = \frac{1}{2} \left[(4D^2/d_1 d_2) - (d_1/d_2) - (d_2/d_1) \right]$$

FIGURE 18 CASE 3

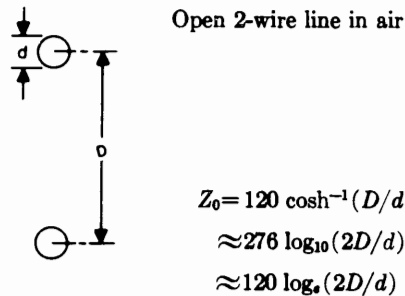


FIGURE 19 CASE 4

Case 4: Open Two-Wire Line

$$Z_o = 120 \cosh^{-1} (D/d) \quad (44)$$

$d = 0.46"$, $D(\text{variable}) - 3$ to 10 feet.

The computed values of characteristic impedance for each case are presented in Figure 20 for convenient comparison of limits, trends, and effects of nearby conducting walls or floors.

2. Discussion of Results

Examination of Figure 20 and the equations reveals that once the spacing D becomes large compared to the trolley wire diameter d , the characteristic impedance is not very sensitive to further increases in D . Furthermore, the oversimplified geometries of Cases 3 and 4 give values of Z_o that far exceed any line impedance values apparently encountered to date in mines. Case 2, although giving lower values, still appears somewhat high. Only Cases 1a and 1b approach the high side of the impedance values that have been observed experimentally by past investigators on trolley lines under typical conditions. Z_o for the Case 1 structure is relatively insensitive to both the roof-to-floor distance D and the distance d of the trolley wire from the roof, for values typical of those found in mines. Similarly, other investigators have experimentally observed only small changes in trolley line Z_o behavior under both high and low coal conditions.

The above calculations indicate that the Z_o 's of lossless lines with geometries and dimensions similar to coal mine trolley lines will not fall much below about 200 ohms. The presence of substantial distributed shunt loss, G , with its corresponding high attenuation, could reduce Z_o dramatically from its lossless line value. However, other investigators have observed only little attenuation (approximately 2db per mile) on long runs of trolley line. Consequently, the variable impedance values (generally below 200 ohms) often observed on trolley lines, are most likely caused by the moving low impedance motor loads placed across the trolley lines via locomotive trolley poles. Therefore, in our quest for a solution to motor loading, the Case 1 eccentric line structure with a nominal Z_o value of $Z_o = 200$ ohms, presently looks like a reasonable approximation to use for haulageway trolley lines.

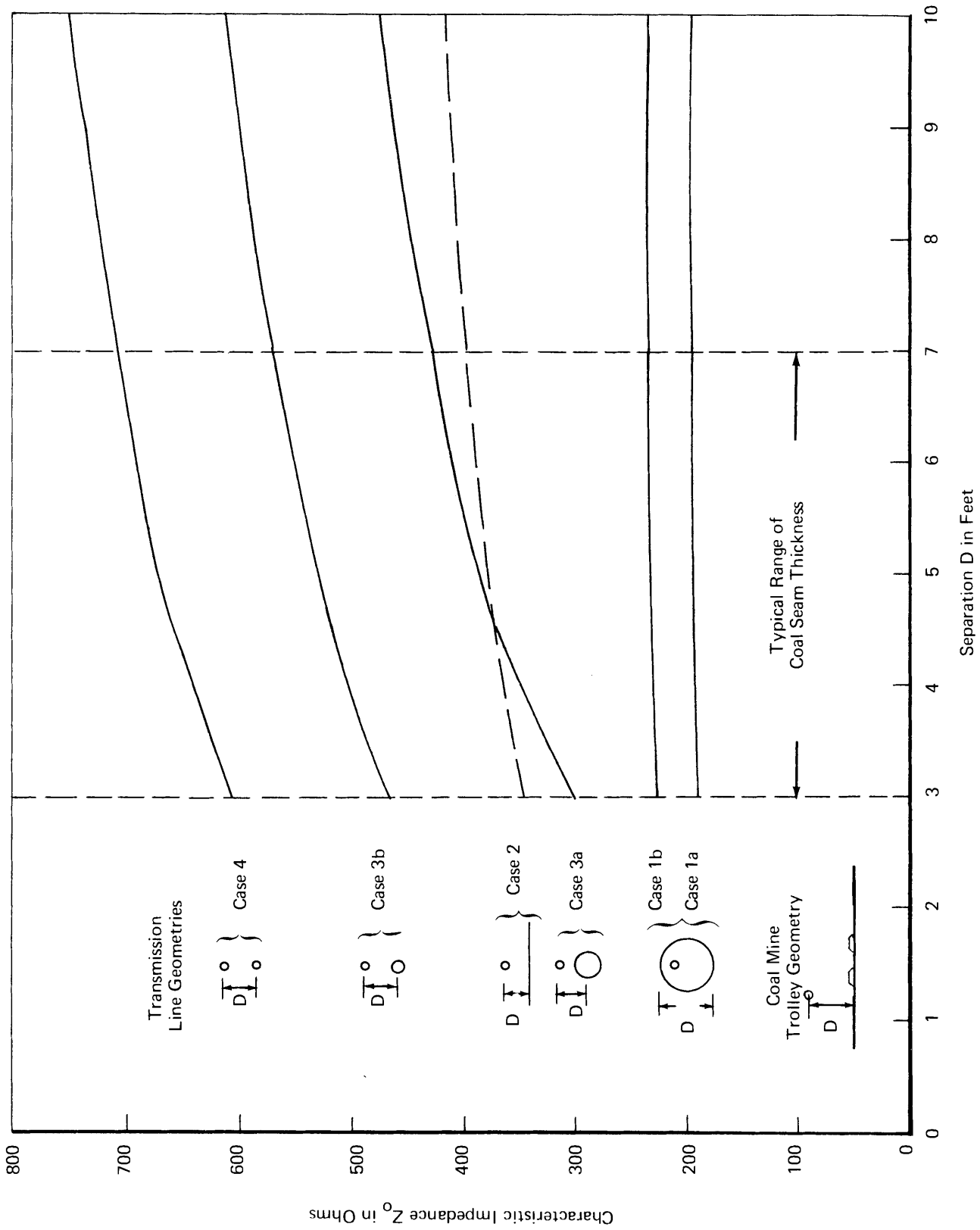


FIGURE 20 PLOTS OF CHARACTERISTIC IMPEDANCE Z_0 VERSUS D

II. RF ISOLATORS FOR MINE MOTORS

A. BACKGROUND

The mine trolley phone systems presently in use can frequently suffer from low signal strength problems attributed to trolley motors acting as extremely low impedances across the trolley line signal pair used for the transmission of carrier communication signals. To obviate the problem caused by these low impedance "shorts", it is desirable to add impedance in series with the trolley motors, thus preventing each trolley motor from acting as a signal "short".

The most severe problem met in implementing such a scheme is due to the fact that, while providing the added impedance at the carrier frequency (typically 88 kHz or 100 kHz), it must: act as an extremely low resistance at dc, be able to pass up 2000 amperes without sustaining damage, and be able to maintain its 88 kHz impedance level while passing in excess of 400 dc amperes.*

B. APPROACH

Techniques that have been used in power and electronic systems suggest a means of adding the desired impedance to a trolley without imposing difficulties in installation or any added dc resistance. One of these techniques is the use of a single-turn transformer winding, such as the current transformers with single-turn primaries commonly used in power monitoring systems. A second technique is one commonly used in digital electronic printed circuit boards. Most of the circuits found on these boards are extremely sensitive to electrical spikes that occur on power supply lines. Frequently, use is made of a ferrite toroid together with a capacitor. The power supply lead is fed through the toroid, thus adding inductance to the power supply line. This inductance, combined with the capacitor, serves to block the voltage spikes from penetrating to the sensitive circuit elements.

*We have since learned that a 400 ampere operating current is more typical of small 10-12 ton locomotives on 600V DC trolley lines, and not of the more important 50-ton locomotives on 300V dc lines which will draw 3000-4000 amperes under full load conditions. Under these 3000-4000 amperes current conditions, the isolators designed for 400 ampere dc currents will saturate and be totally ineffective. If provisions are made to prevent saturation until beyond 4000 amperes by increasing the core air gap, the isolators in their present configuration will have to be increased beyond their present overall length of 6 inches by about a factor of 10 to maintain the required inductance to produce the desired 20 ohm isolator impedance at 88kHz. The cost, length, and weight of such a 4000 ampere unit is no longer as attractive as the 400 ampere unit, and as such is probably an impractical isolator solution for 50-ton locomotives. Special ferrite castings to improve the core geometry, and therefore, reduce the overall volume of the core may be possible, but significant reductions in volume don't look too promising upon first examination.

A representation of how such a technique can be applied to the trolley problem is illustrated in Figure 1A.* Figure 1B* shows an equivalent circuit for the configuration of Figure 1A. In this equivalent circuit, the terminal-to-terminal impedance is that which is added in series with the trolley. It should be noted that the magnetic element does not affect the trolley cable in terms of dc resistance, since the capacitor and resistor are inductively coupled to the core as opposed to being connected to the trolley wire. The equivalent circuit shows that there can be considerable impedance at the carrier frequency if the circuit is tuned to the carrier. The capacitor is used to accomplish this tuning, while the resistor is used to set the Q or quality factor of the circuit, and thus the circuit impedance ($Z = Q\omega_0 L$) at the carrier frequency.

There are two problems associated with implementing this scheme. First, and most important, the magnetic core is subject to saturation by the very substantial dc currents drawn by the trolley motors. Secondly, the transformer must have sufficient Q at the carrier frequency in order that tuning will produce the desired impedance value.

We have investigated several materials which seemed to be potentially applicable for this use, and the following conclusions apply:

1. Powdered iron cores. In principle these cores will perform the function; however, the cost is high.
2. Laminated transformer iron. The effective μ and quality factor at 88kHz are marginal, while the cost and weight are also high.
3. Ferrite materials. The cost is moderate, the μ and quality factors are adequate, but the saturation levels marginal for trolley applications.

The following target specifications were set by us for an rf isolator of this type:

- . DC current rating: 0 to 2000 amperes (without damage to circuit).
- . DC operating current: 0 to 400 amperes (impedance will be within $\pm 30\%$ of target).
- . Impedance: Larger than 20 ohms at 88kHz or at 100kHz.
- . Bandwidth: 8.8kHz or 10kHz.

* References to Figures, Tables, and Equations apply to those in this Chapter unless otherwise noted.

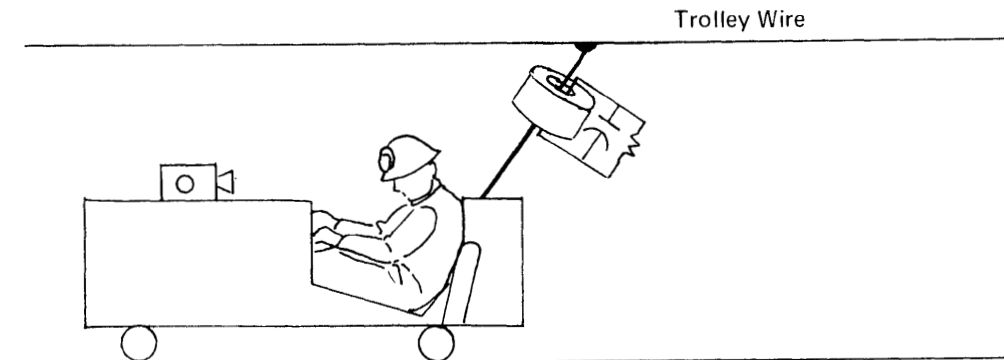


FIGURE 1A REPRESENTATION OF SINGLE-TURN COUPLED IMPEDANCE ELEMENT INSTALLED ON A TROLLEY POLE

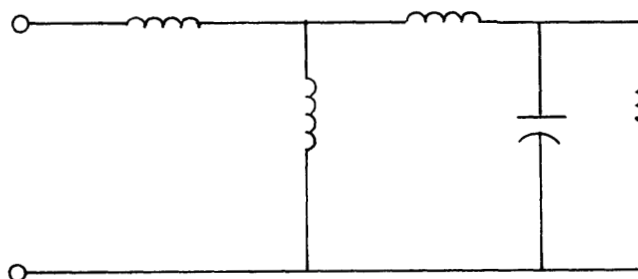


FIGURE 1B EQUIVALENT CIRCUIT OF IMPEDANCE ELEMENT

C. DESIGN CALCULATIONS

The first-order design is extremely simple and for most configurations yields results within several percent of actual design values. Consider the core configuration as shown in Figure 2. The reluctance of the magnetic path is:

$$R = \frac{1}{A} \left(\frac{\ell_M}{\mu_M} + \frac{\ell_A}{\lambda_A} \right) \quad (1)*$$

where ℓ_M = length of path in magnetic material
 ℓ_A = length of path in air
 μ_M = permeability of magnetic material
 μ_A = permeability of air.

If the μ of the magnetic material is 1000 times that of air, then for an air gap that is more than 1/100 of the magnetic path length, the reluctance and hence the inductance of a winding on the core is dominated by the air gap. Thus, for our purposes where the air gap and magnetic material paths are known to have about the right relationships, the first-order design proceeds on the basis that the air gap dominates completely. This fact is true up to the point where the dc current, and hence the magnetic flux density, becomes so large that the magnetic material saturates and reduces the effective permeability to a value significantly less than 1000.

The design procedure is to select the value of flux density (B_o gauss) in the magnetic material at which the incremental permeability is^o reduced by saturation to the minimum acceptable value. The air gap in the magnetic path is selected so that the maximum motor current for which the isolator must work, I_o , produces just this flux density in the gap and in the magnetic material. Because we are dealing with a single turn, the number of ampere turns becomes I_o , the flux density is B_o , and the magnetic field intensity H in the air gap numerically equals B_o expressed in oersteds (cgs units). The ampere turns per inch then become

$$\frac{I_o}{\ell_A} = H = B_o. \quad (2)$$

Thus the air gap is given by

$$\ell_A = \frac{I_o}{B_o} \text{ cm} = \frac{I_o}{B_o (2.54)} \text{ inch.} \quad (3)$$

* References to Figures, Tables, and Equations apply to those in this Chapter unless otherwise noted.

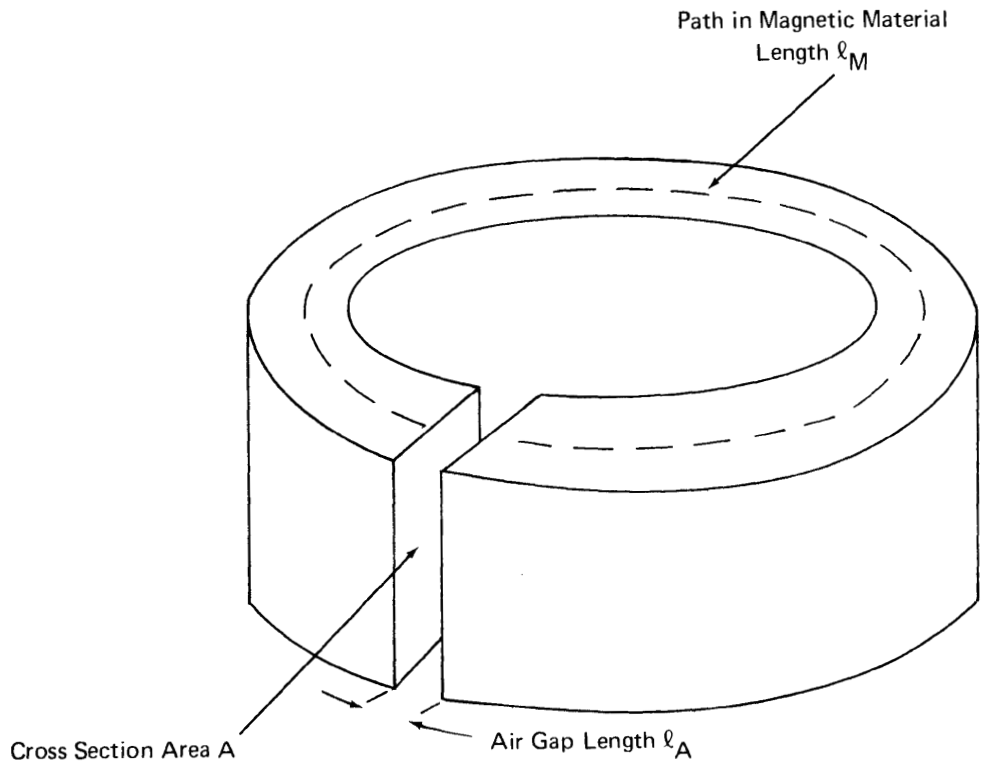


FIGURE 2 TOROID WITH AIR GAP

The inductance is $L = \frac{\lambda}{I_0} = \frac{B_0 A}{I_0}$ (4)

where λ equals flux linkages in Weber turns, I_0 in amperes, and A is cross-sectional area.

Thus we can plot the inductance per unit area as a function of I_0 for various candidate materials. The Ferroxcube, 3C5 material, can be operated at 2500 gauss and still maintain sufficient incremental permeability for the air gap to dominate. A plot of inductance per square inch of cross-section for this material is shown in Figure 3. Using this plot one can determine the core cross-section area required to meet a specific design. As an example, assume that the isolator must function for currents up to 400 amperes. From the plot of Figure 3, it is seen that an inductance of .4 microhenries per square inch is usable.*

The desired resonant impedance is 20 ohms. For a Q of 10, this impedance is ten times the inductive reactance provided by the core itself at 88kHz. Thus the inductive reactance required of the core is 2 ohms, corresponding to an inductance of 3.68 microhenries. The cross-sectional area required is thus 9.2 square inches. Were arbitrary shapes of ferrite material available, one could select the shape that would provide this cross-sectional area to best match the space available in a locomotive for installation. For example, a toroid of outside diameter 5", inside diameter 1", and a length of 4.5" would provide the required core cross-sectional area. Similar calculations can be performed for both larger and smaller current ratings.

D. LABORATORY TEST DATA

Unfortunately, for present experimental investigations, use must be made of available cores which are quite limited in the sizes and shape factors that are attractive for our purpose. We have done experiments on available standard cores. The results of these experiments are shown in Figure 4, which illustrates the effects of the saturation of a ferrite core pair.

These data were sufficiently encouraging that a set of tuned isolators were assembled for test in a laboratory in preparation for field evaluation in an actual trolley phone system. The goal was to achieve a 20 ohms impedance at 88kHz with a bandwidth of 8.8kHz and a dc operating current rating of 400 amperes. We believe that a rating of 400 amperes will suffice for many conditions**, although it does preclude operation during starting and under extremely

*Similar calculations were made for powdered iron and laminated iron cores. The powdered iron cores were rejected on the basis of excessive cost. Laminated cores with 4 mil and 2 mil thick laminations were purchased and tested as were the ferrite cores. The laminated cores were then rejected because their inadequate Q factor required an excessive number of the expensive cores to achieve the desired impedance.

** See note on first page of this Chapter.

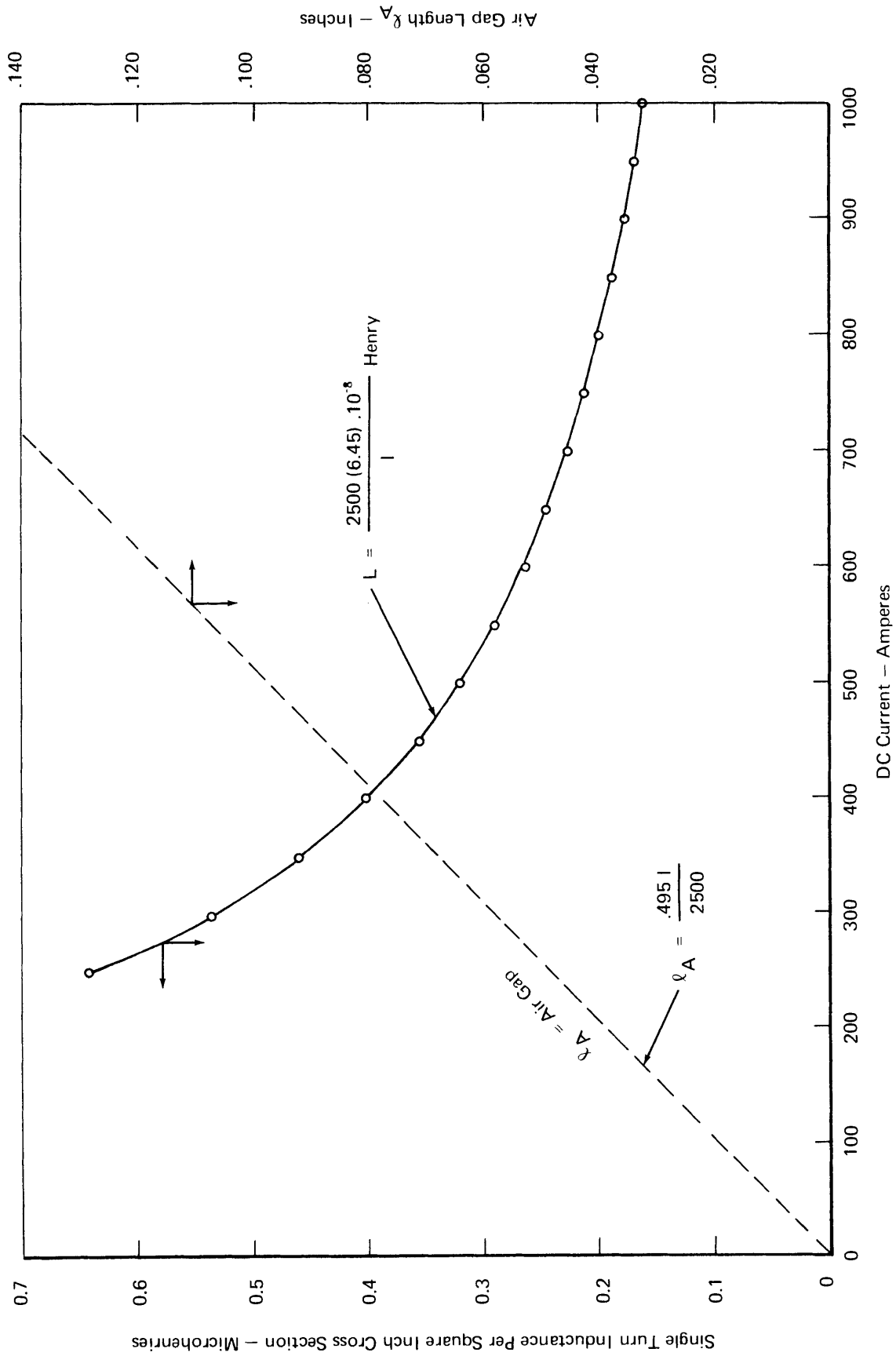


FIGURE 3 FERROXCUBE 3C5 MATERIAL INDUCTANCE PER SQUARE INCH OF CROSS SECTION VERSUS MAXIMUM DC CURRENT - SINGLE TURN WINDING

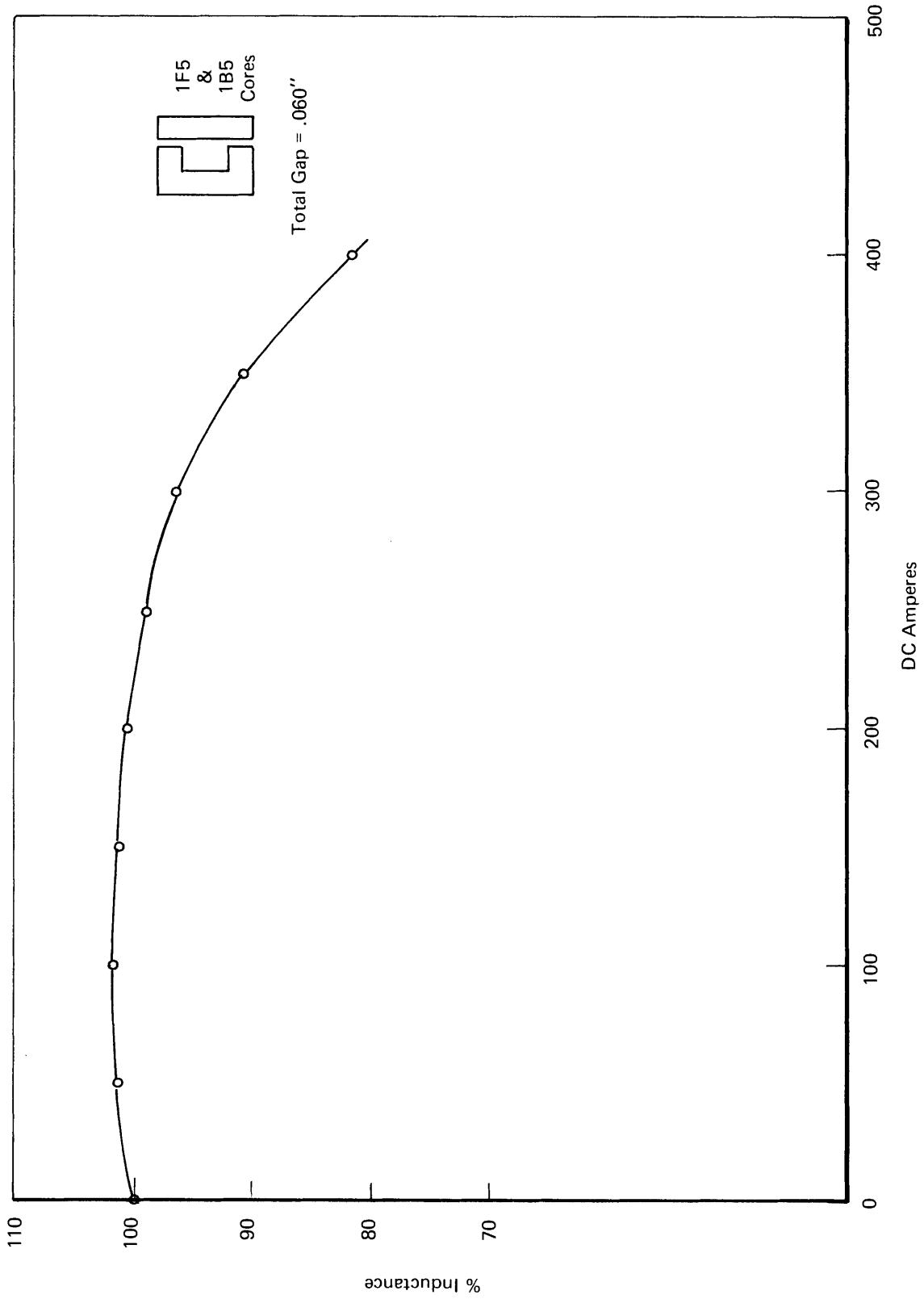


FIGURE 4 INDUCTANCE VERSUS CURRENT

heavy load conditions. The system will not be damaged by much larger currents but will merely be detuned from 88kHz. The isolator unit was comprised of six U sections and six I sections of a standard commercial ferrite core as shown in Figure 5. The configuration of the isolator is illustrated in Figure 6. For this configuration the reluctance:

$$R = \frac{1}{A} \left(\frac{\ell_M}{\mu_M} + \frac{\ell_A}{\mu_A} \right) \quad \text{and} \quad (5)$$

$$L = \frac{A}{\left(\frac{\mu_A}{\mu_M} + \ell_A \right)} \quad (6)$$

$$\text{and thus the inductance } L = \frac{(6.45) \times 10^{-8}}{2.54 \left(\frac{10.5}{1500} + \ell_A \right)} \quad \text{henry.} \quad (7)$$

The magnetic material path length ℓ_M is 10.5 inches, μ_M is assumed to be 1500, and A is 1 square inch.

A plot of the calculated and measured inductance for a single pair of these cores is shown in Figure 7. The Q when tuned to 88kHz was between 20-30. The measured value of inductance is higher than the calculated for most points. This can be attributed to the fact that the relatively large air gaps cause part of the flux to follow paths outside the air gap. These uncertainties mean that while the formulas discussed above are useful in determining the nominal values of circuit parameters, their exact values will have to be determined empirically. An optional resistor may be added in parallel with the tuning capacitor to adjust the Q downward if desired.

E. CONCLUDING REMARKS

An isolator made of Ferroxcube 3C5 ferrite that provides 20 ohms impedance at 88kHz in the face of 400 amperes dc current, with a bandwidth of 8.8kHz, weighs 8.7 lbs., and has outside dimensions of 4-1/2" x 4-1/4" x 6" when made of available core parts. This isolator has an opening of 1.25" x 2" as a passage for the power cable. Cost of the core parts in small quantities is \$48.

We recommend that experiments be done on a trolley phone system to test isolator performance under typical conditions. A minimum experiment would involve measuring the trolley line rf voltage as a locomotive passes a measuring station for different levels of locomotive power, both with and without the rf isolator described above.*

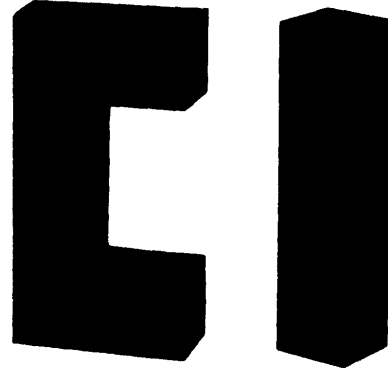
*A very short experiment similar to this was performed at the Bethlehem Steel Marianna Mine in Ellsworth, Pennsylvania on a 50 ton tandem locomotive. Rf line voltage was measured under stationary simulated load conditions of applying full power to 1, 2 or 4 motors with full braking also applied. Full rf voltage appeared as expected under no-load conditions, but dropped essentially to levels achieved in the absence of the isolator under all three load conditions, because the 400 ampere saturation rating was exceeded for all 3 loads. Further detailed inquiry of mine operators and equipment manufacturers revealed the 3000-4000 ampere loads typical of 50-ton locomotives operating at 275 volts, and led to the conclusions of the asterisked note on the first page of this Chapter.

U CORE, Part Number 1F5
I CORE, Part Number 1B5

This core is

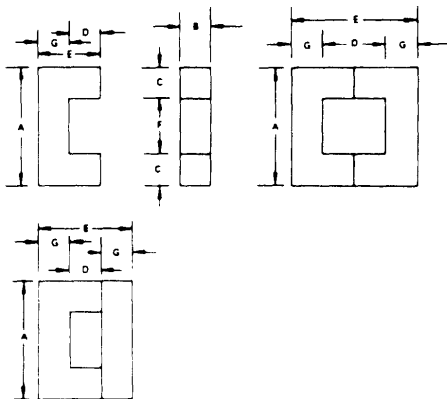
- manufactured in 3C5 ferrite material only.
(See Section 1 for material characteristics)
- available in U-U and U-I configurations.
(for a complete U-I core set, specify both part numbers)
- not available with bobbins or mounting hardware.

When ordering cores, specify core part number and ferrite material.
e.g.: 1F5-3C5 or 1B5-3C5



HALF ACTUAL SIZE

CHARACTERISTICS
& DIMENSIONS



NOMINAL DIMENSIONS IN INCHES

DIMENSION	SINGLE U CORE	U-U	U-I
A	4.00	4.00	4.00
B	1.00	1.00	1.00
C	1.00	1.00	1.00
D	1.25	2.50	1.25
E	2.25	4.50	3.250
F	2.00	2.00	2.00
G	1.00	1.00	1.00

ELECTRICAL CHARACTERISTICS

CONFIGURATION	U-U	U-I	U-U	U-I
AL mH per 1000 turns	≥5500	≥6900	≥7850	≥9850
μ_e ref. (min.)	2100 at 25°C 1000 Gauss		3000 at 100°C 2000 Gauss	

MECHANICAL CHARACTERISTICS

CORE SET		U-U	U-I
MAGNETIC PATH LENGTH	l_e	12.4 in. 31.5 CM	9.64 in. 24.5 CM
CORE CONSTANT	$\sum \frac{l_e}{A_e}$	12.4 in. ⁻¹ 4.884 CM ⁻¹	9.64 in. ⁻¹ 3.798 CM ⁻¹
EFFECTIVE CORE AREA	A_e	1.00 in. ² 6.45 CM ²	1.00 in. ² 6.45 CM ²
EFFECTIVE CORE VOLUME	V_e	12.1 in. ³ 198. CM ³	9.64 in. ³ 158. CM ³
WINDING AREA	A_c	5.00 in. ² 32.25 CM ²	2.50 in. ² 16.125 CM ²
WEIGHT		32.5 oz. 930 grams	23.1 oz. 660 grams

FIGURE 5 CORES USED IN EXPERIMENT

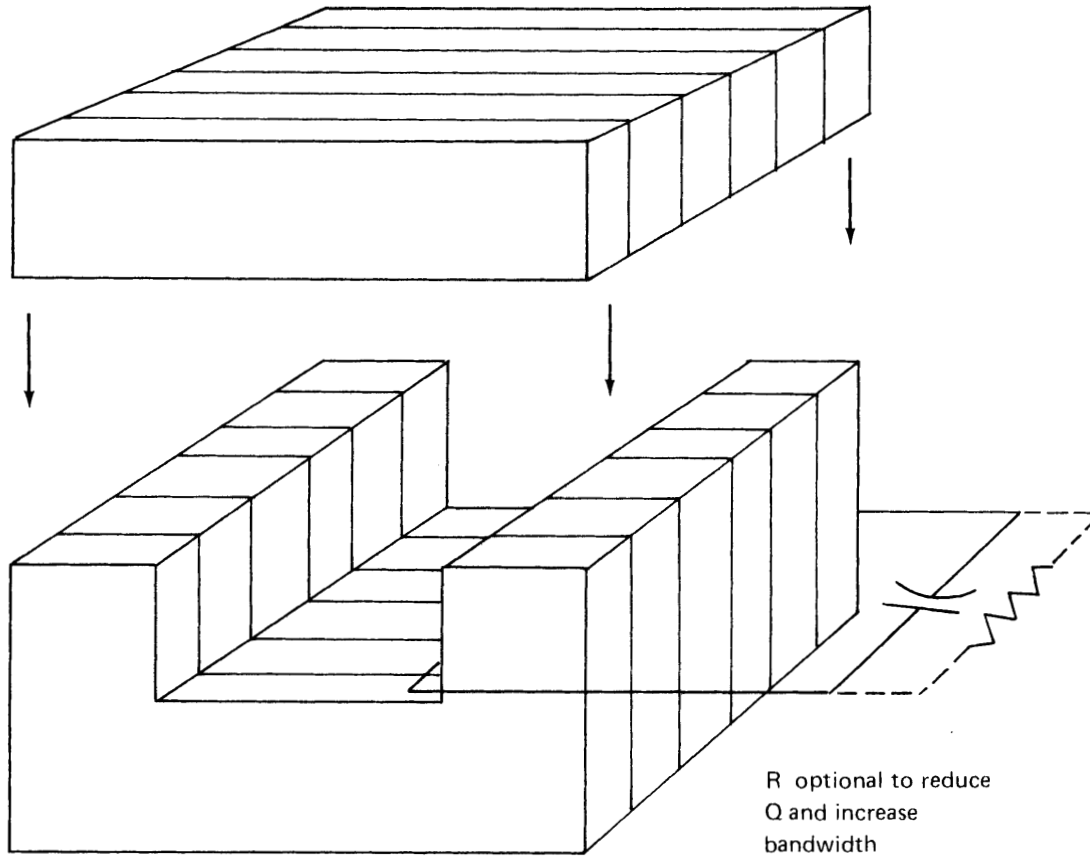


FIGURE 6 CONFIGURATION OF CORES FOR ISOLATOR

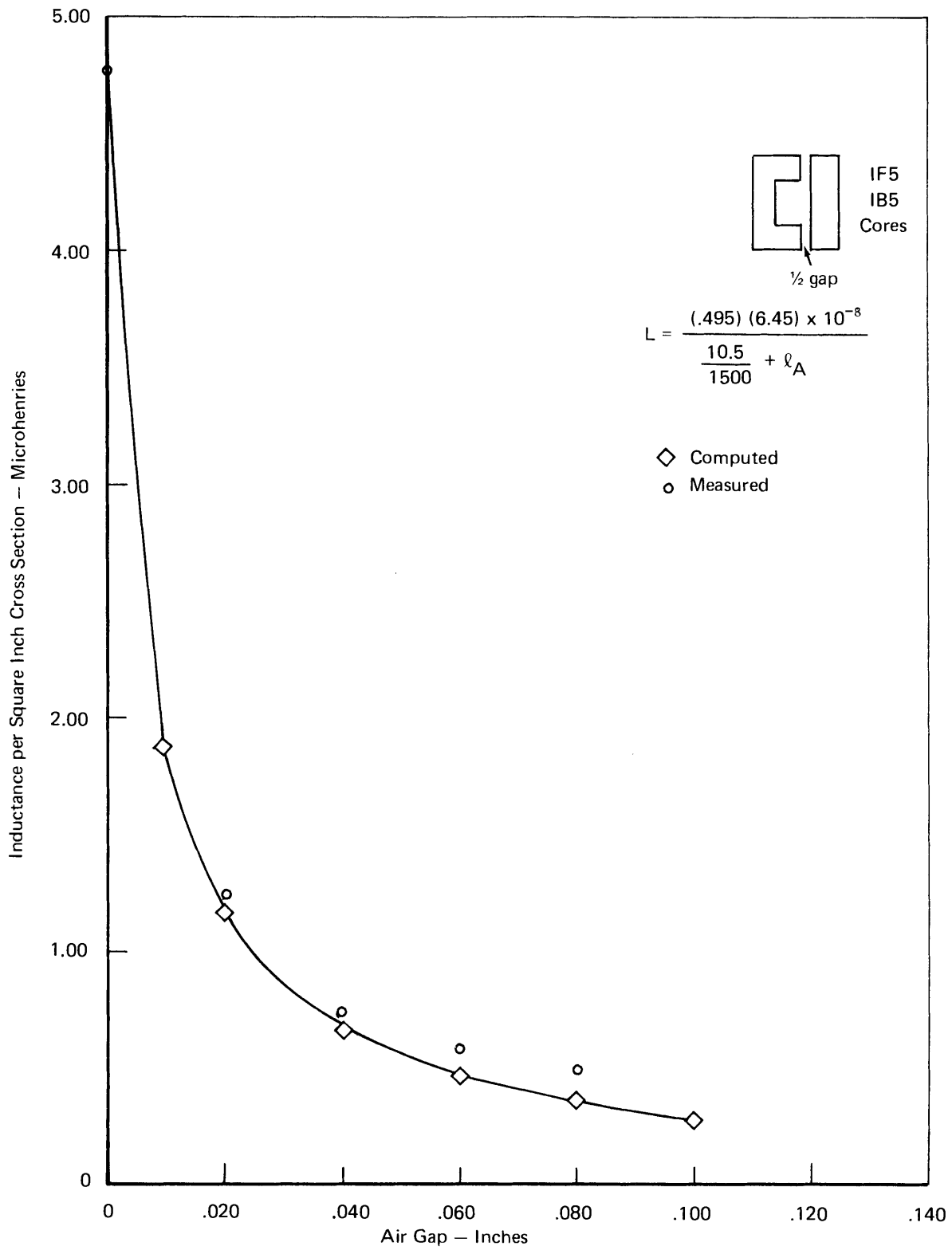


FIGURE 7 SINGLE-TURN INDUCTANCE

1 **3C5 FERRITE**

3C5 FERRITE

3C5 MATERIAL

A MnZn ferrite for high flux density applications. The losses and permeability are controlled under high flux density, high temperature conditions. This will ensure proper performance in the actual applications.

This 3C5 material is available in the largest standard core configurations produced by Ferroxcube.

Available in:
 TOROIDS
 E, U & I CORES

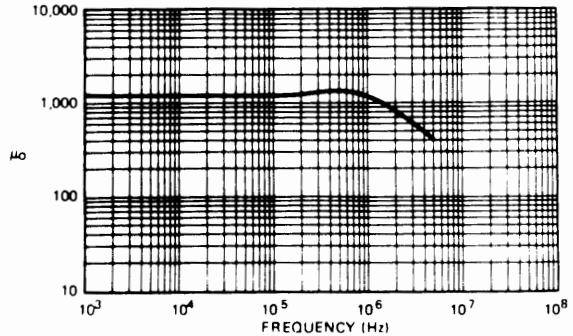
3C5 CHARACTERISTICS

Parameters shown are typical values, based upon measurements of a 1" toroid.

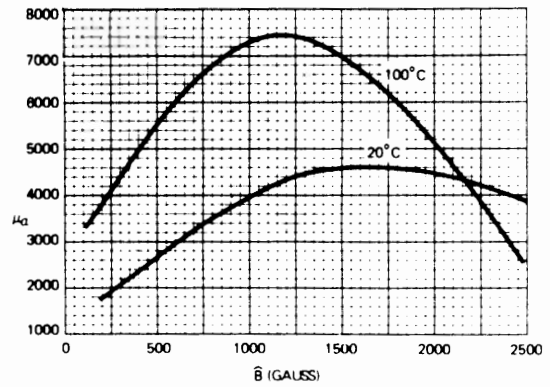
Permeability at 25°C, B = 1000 gauss	μ_i	≥ 3000
at 100°C, B = 2000 gauss		≥ 4000
Losses 100°C, 2000 gauss		160 mW/CM ³ *
Saturation Flux Density at 25°C, H = 2 oersteds	B_s	3800 gauss*
Coercive Force	H_c	0.2 oersted*
Curie Temperature	T_c	$\geq 200^\circ\text{C}$

*Typical value

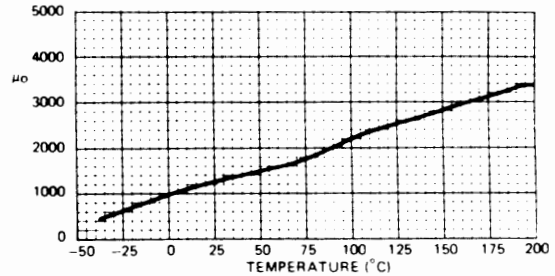
INITIAL PERMEABILITY (μ_0) vs. FREQUENCY



PERMEABILITY (μ_0) vs. FLUX DENSITY (\hat{B})

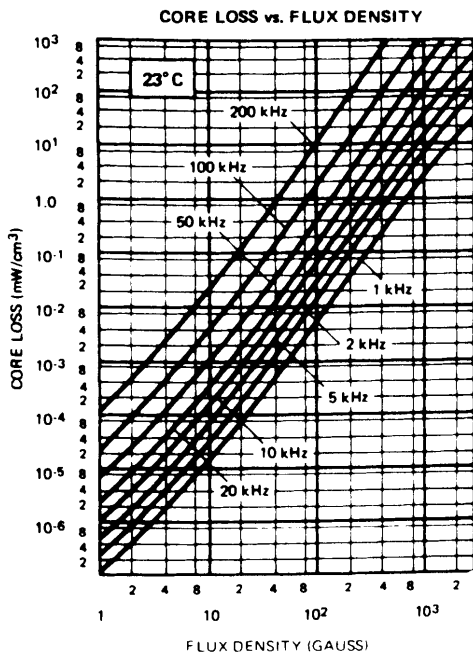
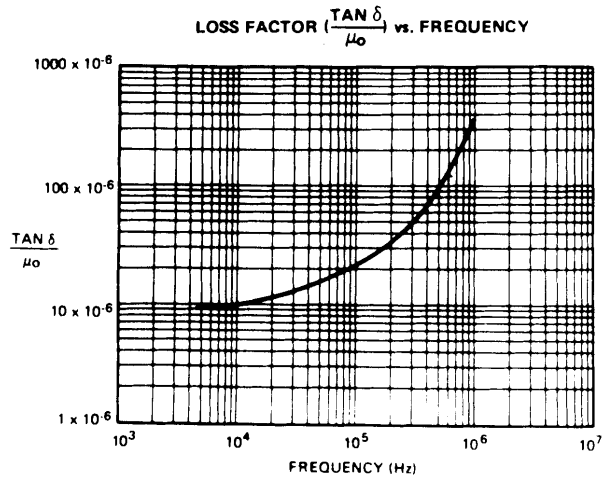
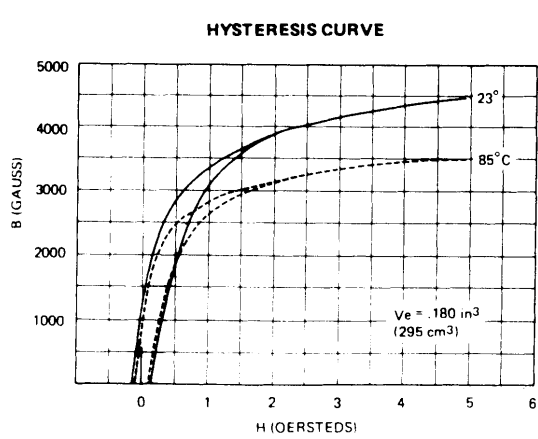


INITIAL PERMEABILITY (μ_0) vs. TEMPERATURE



Source: Ferroxcube Corp., *Linear Ferrite Materials & Components Catalogue*

**3C5 FERRITE
CHARACTERISTIC CURVES**



III. A DIVERSITY METHOD FOR COMBATting STANDING WAVE NULLS

As discussed in Section F of Chapter I of this Part, unmatched loads placed across the trolley wire/rail transmission line produce reflections that result in standing wave variations in voltage, current, and impedance along the line. In mines, these loads include DC power substations, pumps, motors of haulage vehicles, etc., distributed along the length of the trolley rail network. An example of the voltage and current standing wave patterns produced by a single mismatched load across a lossless line is shown in Figure 1.* The magnitude of the current is greatest when the magnitude of the voltage is smallest, and vice versa; the repetition period of the patterns is a half wave length (approximately one mile at 100 kHz) and the ratio of maximum to minimum magnitudes, VSWR,** (the voltage, or current, standing wave ratio) indicates the degree of mismatch between the load, Z_L , and the line characteristic impedance, Z_0 .

Trolley wire carrier phones on mine vehicles are capacitively coupled to the transmission line via the trolley pole drop wire. Consequently, when a vehicle moves into a region containing one of the voltage minima depicted in Figure 1, signal reception may be significantly degraded, and even lost, if the null is deep enough. In those mines where this is a significant and bothersome problem, it may be possible to overcome it in an economical manner; namely, by using modified carrier phones that employ a relatively simple form of switching diversity*** which takes advantage of the fact that the line carrier current and, therefore, the magnetic field are maximum when the voltage is minimum. The method consists of adding a second signal sensor, namely a loop oriented for maximum coupling to the trolley wire magnetic field, and a controlled switch that applies the loop voltage to the carrier phone receiver input whenever the voltage from the drop wire capacitive pick-off falls below a preset reference threshold. The switching process is reversed when the loop voltage falls below the threshold.

Figure 2 depicts in block diagram form the basic elements that need to be added (dashed lines) to the present carrier phones to provide this switching diversity. As shown, the carrier signal, V_1 , from one of the sensors is applied to the carrier phone receiver through the diversity switch. In addition to the receiver's normal operations, the amplitude of this signal is measured by means of an envelope detector and then compared with an appropriate preset reference threshold. Whenever the signal, V_1 , falls below this threshold, the logic sends a switching control signal to the diversity switch,

* References to Figures, Tables, and Equations apply to those in this Chapter unless otherwise noted.

** On a lossy line, the VSWR will eventually decrease to a value of unity as one moves further away from the load, because the reflected wave gradually becomes negligible compared with the incident wave as a result of the line's attenuation.

*** Several types of space, frequency, and polarization diversity reception techniques are commonly used in mobile and point-to-point communications. The switching diversity technique discussed here appears to be the most suited to the mine carrier phone application from the standpoints of simplicity, economy, and performance.

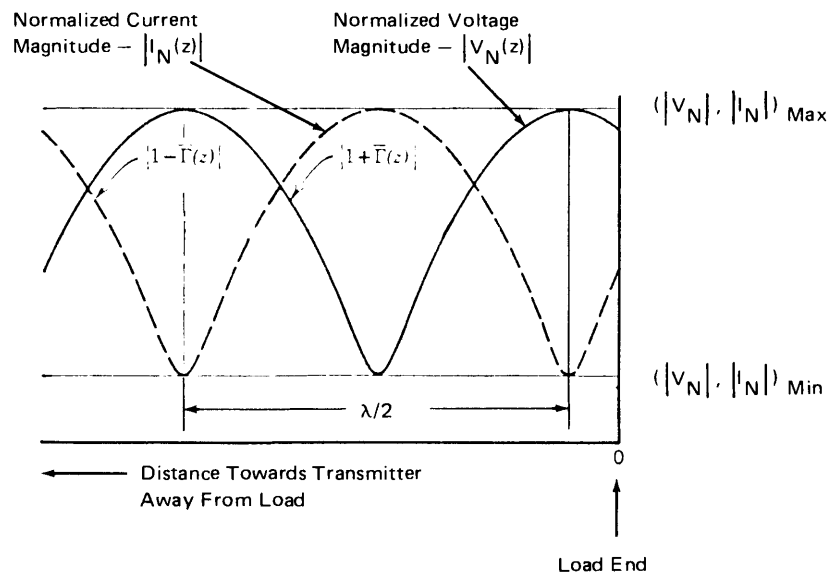


FIGURE 1 SAMPLE VOLTAGE AND CURRENT STANDING WAVE PATTERNS

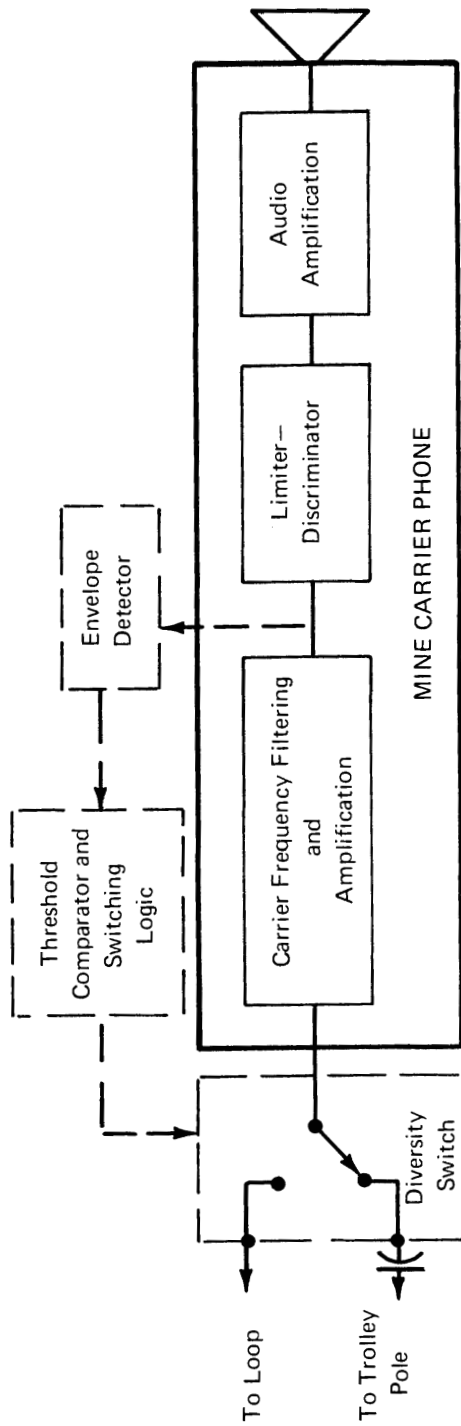


FIGURE 2 CARRIER PHONE WITH MODIFICATIONS FOR SWITCHING DIVERSITY -- SIMPLIFIED BLOCK DIAGRAM

which in turn, connects the output, V_2 , of the other sensor to the receiver input. Special filtering or integration may also be required in the comparator to avoid false switching caused by impulsive noise transients on the trolley line. This switching process is repeated whenever the applied carrier voltage falls below the threshold.

Preliminary calculations indicate that loop sensors with equivalent cross-sections, NA , of 1-to-10 square meters, should provide loop pick-up voltages well above 10 mv for typical trolley wire carrier currents of about 0.5- to-1 ampere. Although loop orientation for maximum response will be somewhat influenced by the haulage vehicle material and structure, best results should be obtained when the trolley wire lies in, or near to, the plane of the loop. Loops loaded with magnetic material, such as ferrite, should probably be avoided because of the presence of high DC background magnetic fields which may saturate such materials. In fact, a rectangular multi-turn air core loop of heavy construction, attached to the vehicle with the short dimension vertical and the long dimension running the length available on top of the vehicle, may offer the right combination of performance, convenience, and ruggedness.

Further investigation, including experiments, is required to define the most suitable loop sensor size and configuration, and to assess the effectiveness and practicality of the above described switching diversity method for application to mine haulage vehicles for improving transmission as well as reception performance. Finally, the mine carrier phone application may well lend itself to the simplest embodiment of this diversity method, namely, a completely manual switching operation. This possibility arises because of the gradual manner in which the communication performance will be degraded as the haulage vehicle approaches null regions, as opposed to the fast fading phenomena experienced with surface mobile communications at much higher frequencies. In this manual mode, the only modifications required will be associated with the additional loop attached to the vehicle and an appropriate mechanical switch that the vehicle operator can throw when the reception is poor or nonexistent on one of the sensors. In fact, this rudimentary configuration should provide a simple and quick way to check the practical feasibility of this type of diversity in operational mine environments and with currently installed carrier phones on mine haulage vehicles.

PART SEVEN

MINE PAGER PHONE TO PUBLIC
TELEPHONE INTERCONNECT SYSTEM

PART SEVEN

MINE PAGER PHONE TO PUBLIC
TELEPHONE INTERCONNECT SYSTEM

TABLE OF CONTENTS

	<u>Page</u>
List of Figures	7.iii
INTRODUCTION	7.1
I. OPERATIONAL DESCRIPTION	7.3
A. OVERVIEW	7.3
B. INCOMING CALL SEQUENCE	7.7
C. OUTGOING CALL SEQUENCE	7.8
II. SUMMARY OF OPERATIONAL FEATURES	7.9
A. PRESENT DESIGN	7.9
B. ADDITIONAL FEATURES FOR FUTURE DESIGNS	7.10
III. INSTALLATION PROCEDURE	7.10

PART SEVEN

MINE PAGER PHONE TO PUBLIC
TELEPHONE INTERCONNECT SYSTEM

LIST OF FIGURES

<u>Figure No.</u>	<u>Title</u>	<u>Page</u>
1	Selective Interconnect Between Mine Pager Phone and Public Telephone Systems	7.2
2	Mine Pager to Public Telephone Interconnect System	7.4
3	Interconnect System - Internal Top View	7.5
4	Operational Flow Diagram - Mine Pager to Public Telephone Interconnect System	7.6

PART SEVEN

MINE PAGER PHONE TO PUBLIC TELEPHONE INTERCONNECT SYSTEM

INTRODUCTION

This Part describes a mine pager phone to public telephone interconnect system that permits mine paging telephones to be selectively interconnected with the public telephone system, as illustrated by Figure 1. This interconnect concept was first conceived and demonstrated in breadboard form by H. E. Parkinson of Industrial Hazards and Communications, PMSRC, as one means for providing improved emergency and off-hours communications. The third-generation prototype unit described in this Part was designed and fabricated by Arthur D. Little, Inc. This unit is a small desk-top or wall-mounted unit that connects directly to both the public telephone line and the mine pager phone line, and requires no modifications to either the public dial telephone or mine pager phones. As part of this task, ADL also built, under a very compressed time schedule, a second-generation prototype unit suitable for reliable demonstration of the interconnect concept during the Bureau's technology transfer seminar on mine communications in March 1973.*

A major objective of the design of the third-generation unit described in this Part was that it be compatible with present mine pager phone systems utilizing DC voltage on the mine phone line to activate the phone loudspeakers. Therefore, this unit was designed to operate in a push-to-talk, push-to-listen mode that accommodates the inherent design differences and operation modes of the mine phones of different manufacturers. Though this push-to-talk, push-to-listen mode of operation may seem slightly unusual at first sight, we have found it is easily learned by new users. However, mine phone manufacturers wishing to expand their product lines with such an interconnect system will probably find it to their advantage to customize the design of this system to their particular mine phones, thereby utilizing the unique attributes offered by their individual product lines. This customization should not be difficult, and Section III below suggests some of the features that can be easily added to future designs. Detailed parts lists and circuit schematics for the present third-generation prototype system can be obtained from the system manual submitted to PMSRC and placed on public file.

* Manufacture of a new version of this interconnect unit has since been undertaken by a major manufacturer of mine communication equipment.

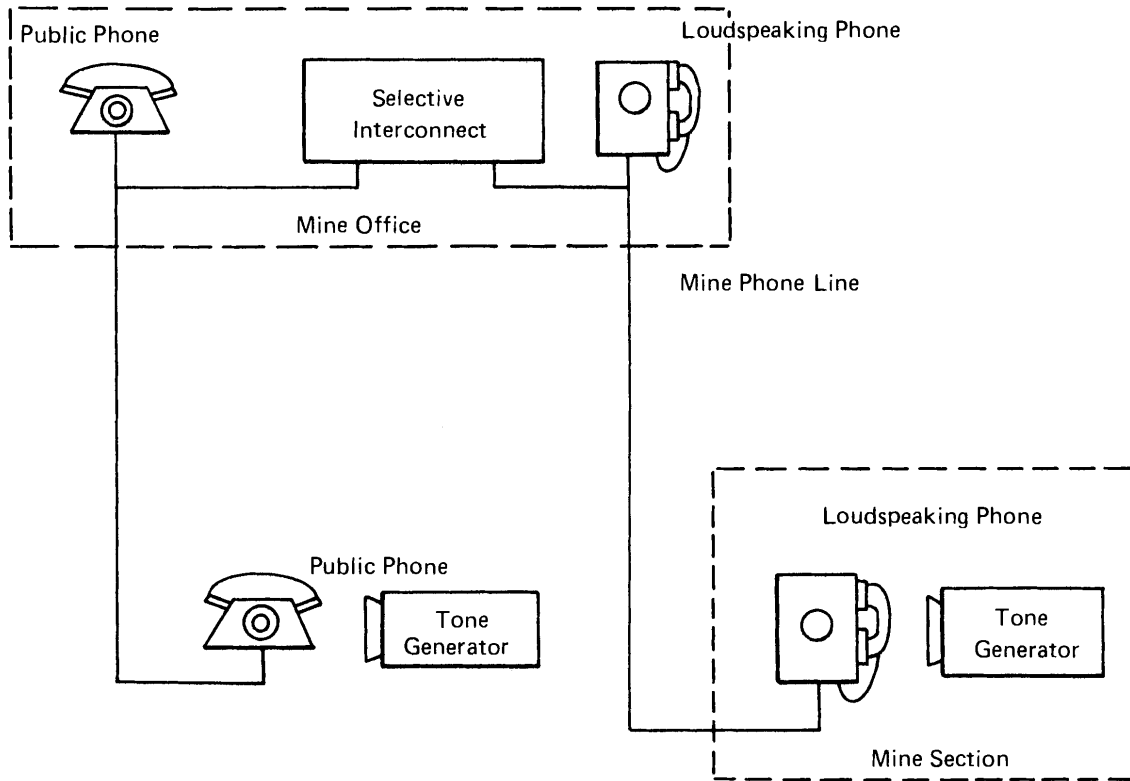


FIGURE 1 SELECTIVE INTERCONNECT BETWEEN MINE PAGER PHONE AND PUBLIC TELEPHONE SYSTEMS

I. OPERATIONAL DESCRIPTION

A. OVERVIEW

The Mine Pager Phone to Public Telephone Interconnect System is a Push-to-talk, Push-to-listen system designed to allow any mine pager system using DC voltage on the line to page, to be connected to the public telephone system. The system allows authorized personnel to communicate from the public telephone system into the mine pager system and vice versa.

An outside caller dials a telephone number assigned to the mine. Then, he gains access into the mine pager system by transmitting a proper tone from a hand-held tone generator into his phone for five seconds. Once access is gained into the mine pager system the tone is transmitted over the loudspeaker system for a few seconds, signalling that an outside call is coming in. The caller then pages over the loudspeakers until the page is answered.

The various mine pager systems have functionally similar switches located in different places and operate in slightly different fashion. All of these systems will be operated normally when used in conjunction with the Interconnect system with the exception of additional switching of the Page switch. This operational description will only describe operations that are in addition to those normally required to operate the mine pager phone.

The person in the mine answers the page by momentarily depressing the Page switch, which allows him to speak and also removes the paging signal from the line, disconnecting the loudspeakers. (The MSA system designates this switch as the Push-to-Page switch and it is located on the handset; it is called the Page Button on the Gai-Tronics system and is located on the front panel; the switch is also located on the front panel of the Femco system and is designated the Page switch.) To carry on a two-way conversation the user of the mine phone must momentarily depress the Page switch each time he wishes to change from the talk mode to the listen mode or vice versa.

The Interconnect system also works in the reverse direction, from the mine onto the outside telephone system. The in-mine user removes the handset from the mine phone and with the proper hand-held tone generator applies a tone into the mouthpiece of his handset for five seconds. The tone activates the Interconnect system which automatically dials a preprogrammed telephone number. The telephone number is programmed by setting the number on the thumb-wheel switches on the front panel of the Interconnect system housing. External and internal photographs of the interconnect system are shown in Figures 2 and 3. Detail operational descriptions of the incoming and outgoing call sequences are given below. Operation of the system during each of these sequences can be followed on the overall flow diagram in Figure 4.

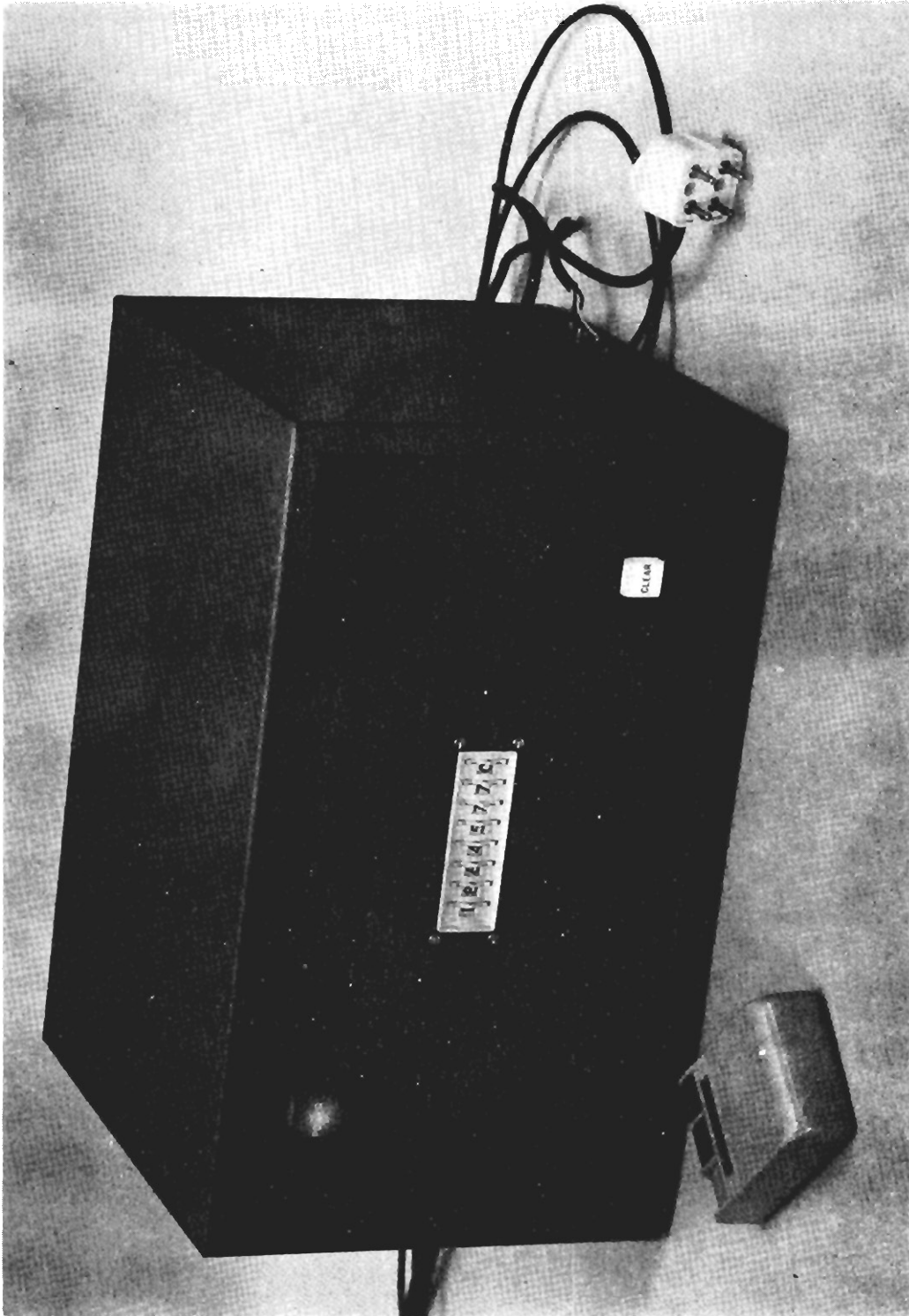


FIGURE 2 MINE PAGER TO PUBLIC TELEPHONE
INTERCONNECT SYSTEM

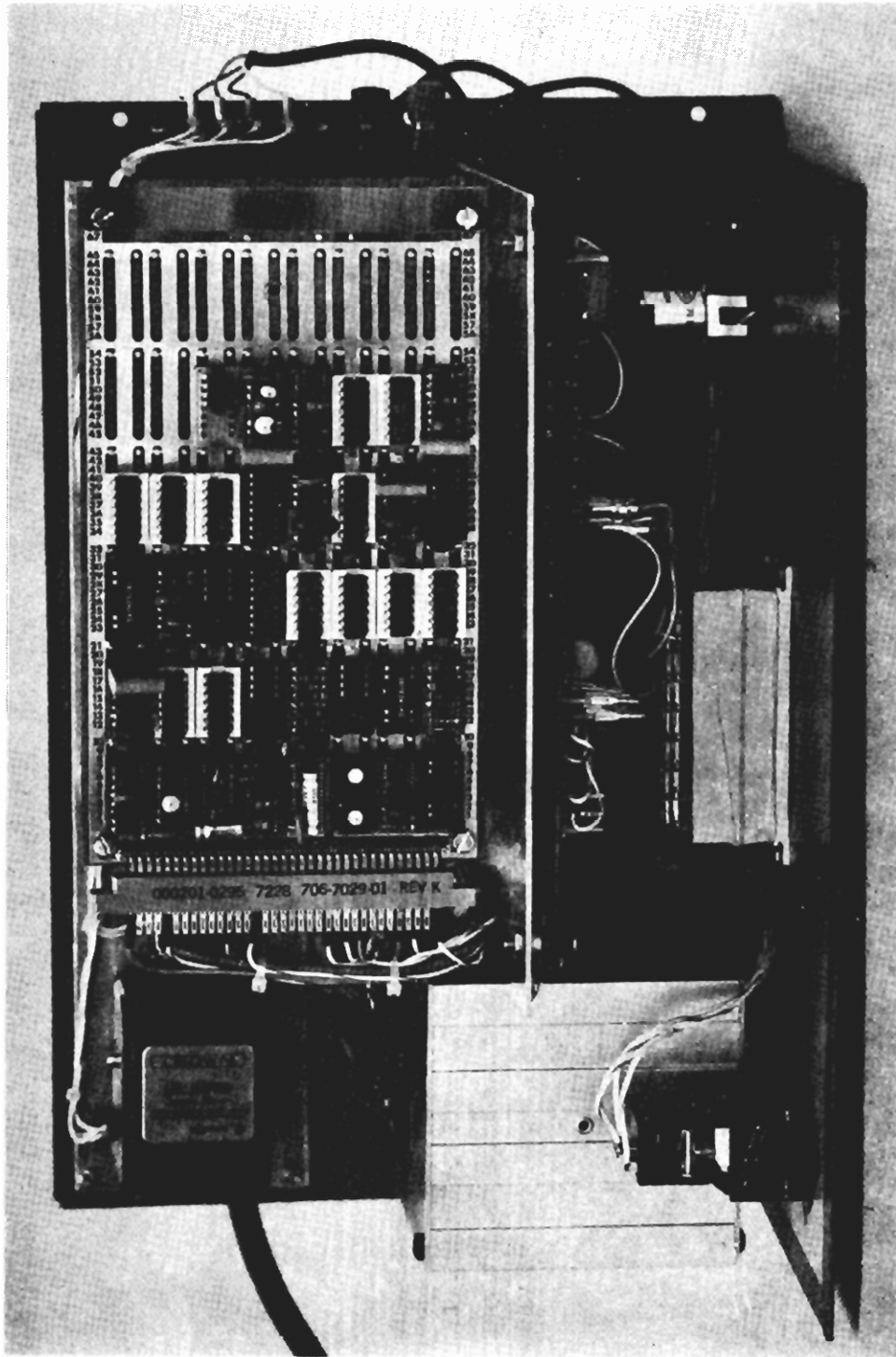
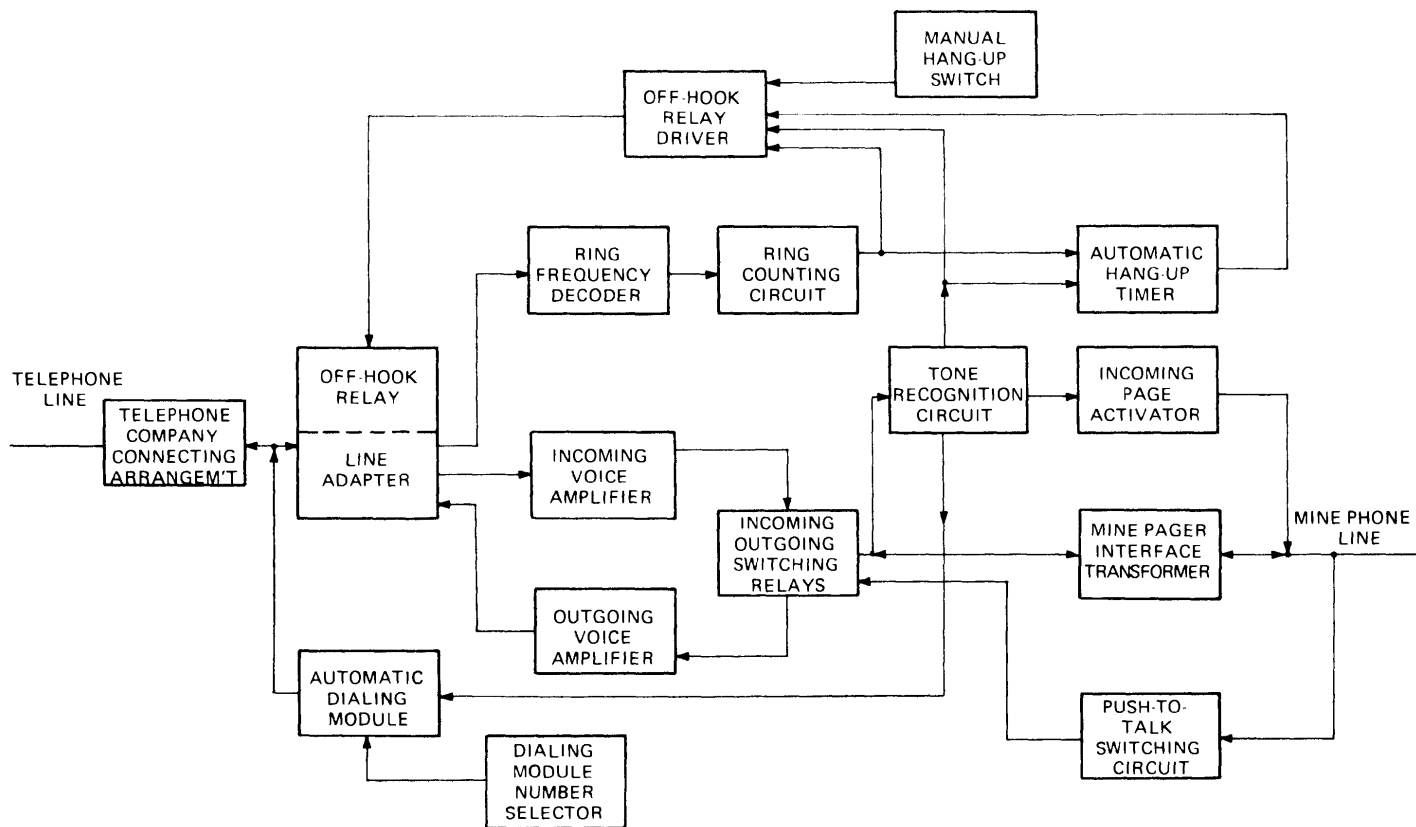


FIGURE 3 INTERCONNECT SYSTEM
INTERNAL TOP VIEW



**FIGURE 4 OPERATIONAL FLOW DIAGRAM
MINE PAGER TO PUBLIC TELEPHONE
INTERCONNECT SYSTEM**

B. INCOMING CALL SEQUENCE

To actuate the Interconnect system from an outside telephone, the caller must first know the telephone number of the system and must also have the proper frequency tone generator. Possessing these, the caller dials the number, which generates the ring signal. The ring goes over the telephone lines, through the telephone company's connecting arrangement and the transformer of the Crown Adapter and into the ring frequency decoder. The ring frequency decoder is designed to discriminate against all signals except the 20 Hz ring signal generated by the telephone system. The output of the ring frequency decoder goes to the ring counting circuit. When the circuit recognizes two rings, it drives the off-hook relay, "answering" the phone, and activates the automatic hang-up timer.

Once the phone has been automatically "answered", the caller must gain access to the mine pager system. In order to allow only authorized calls into the mine pager system, the Interconnect system uses a tone recognition circuit that is only activated by a proper frequency tone. Thus an authorized caller has only to generate that tone into the mouthpiece of his phone for five seconds. This tone is recognized, activating the paging portion of the mine pager system through the Incoming Page Activator. The caller may then talk over the loudspeakers of the mine phones paging the person to whom he wishes to speak.

If, once the call is "answered", the proper frequency tone is not transmitted into the system within 20 seconds, the system will be "hung-up" by the automatic hang-up timer. This allows off-hook time due to improper calls to be kept to a minimum.

When the page is answered, the answerer must momentarily depress the Page switch of the mine phone. This activates the Push-to-talk switching circuit which serves a twofold purpose. One, it disconnects the loudspeakers in the mine system and two, it opens the incoming relay and closes the outgoing relay of the Interconnect system. The answerer can then talk into his handset through the outgoing voice amplifier to the telephone system. When he has finished talking, he must again momentarily depress the Page switch in order to listen. The Page switch must be depressed each time the transmission mode changes. In other words, pushed to talk and pushed again to listen. The button need not be held in, as a matter of fact, it is best not held in since this would cause the conversation to be broadcast over all the loudspeakers in the mine pager system.

There are two normal methods of disconnecting the mine pager system from the telephone system. One is manually, after the

end of the conversation, and the other is automatically, after a specified time. In order to manually hang-up the system, a tone has to be transmitted into the handset mouthpiece by either the caller or the answerer. This tone again goes through the tone recognition circuit which decodes it and removes the drive from the off-hook relay, "hanging the phone up". The automatic hang-up occurs when the hang-up timer turns off after six minutes, removing the drive from the off-hook relay. The automatic hang-up feature insures that the Interconnect system will not be disabled for more than the preset time because of an incorrect hang-up. The system may also be manually hung-up in an emergency by using the manual hang-up switch, labeled "Clear", on the front panel of the Interconnect system's housing. This lighted pushbutton, when lit, indicates that the system is in the off-hook mode. If need be, the system can be hung-up by pushing this push-button, which hangs up the system, extinguishing the lamp.

C. OUTGOING CALL SEQUENCE

An outgoing call can be originated from any mine pager phone connected to the Interconnect system. Again, only authorized personnel can call out since a proper frequency tone generator is needed. When someone wishes to call out, he goes to the nearest mine phone and removes the handset from its cradle. He then transmits the tone into the handset mouthpiece for five seconds. It should be noted that this is the same as talking; and if the system in use requires depression of a Talk switch, this must be done.

The generated tone goes to the tone recognition circuit where it is decoded, thereby activating the automatic hang-up timer and driving the off-hook relay in the Crown Adapter, "picking up the phone". Simultaneously, the relay of the incoming amplifier is activated, as is the automatic dialer.

The automatic dialer is a module in the Interconnect system with a programmed number than can be manually selected in the mine office. When it is activated by the tone decoder circuit, it automatically dials that number. Thus the caller has no ability to determine the number dialed, just the ability to have it dialed.

Once the number is dialed, the caller can listen to the ring and hear when the outside phone is answered. The caller must then momentarily depress the Page switch, which opens the incoming relay and closes the outgoing relay in order for the inside caller to be heard by the outside party. The Page switch must be momentarily depressed each time the transmission mode changes.

The hang-up modes are exactly the same as in the incoming call sequence: manually, a tone must be generated; or automatically, when the automatic hang-up timer times out. Also the emergency manual hang-up switch can be used to clear the system.

II. SUMMARY OF OPERATIONAL FEATURES

A. PRESENT DESIGN

- (1) Direct connection to outside telephone lines. No acoustic coupler required.
- (2) Direct connection to mine pager phone line. No acoustic coupler or pager phone modifications required.
- (3) System compatible with any mine paging system utilizing DC voltage on the line to enable paging.
- (4) Only authorized personnel can use system. Proper frequency tone is needed.
- (5) Pocket-sized tone generator is all that is required for authorized person to initiate call.
- (6) Standard 8-pin dual-in-line integrated circuit used for tone recognition.
- (7) Designated tone frequency completely variable, being determined by a resistor and/or capacitor, thus system is compatible with all tone generators.
- (8) Tone transmitted over loudspeakers to signal incoming outside call.
- (9) Outside caller can page over mine pager system loudspeakers.
- (10) Convenient dial-out number selection via thumb-wheel switches located on interconnect unit housing.
- (11) System automatically dials preprogrammed outside telephone number.
- (12) Automatic hang-up timer. System only off-line for 20 seconds due to wrong number and six minutes due to incorrect hang-up.
- (13) Manual hang-up switch allows automatic hang-up timer to be overridden. System can be cleared instantaneously from interconnect unit.
- (14) Small-sized unit can be easily mounted on a table or wall bracket.

B. ADDITIONAL FEATURES FOR FUTURE DESIGNS

- (1) Dual frequency detection allowing either of two numbers to be dialed automatically, or one of several by tone combination.
- (2) Status indicator lamps.
- (3) Complete duplex system eliminating Push-to-talk operation.
- (4) Operation with 24 volt systems.
- (5) Audio warning signal one minute prior to automatic hang-up.
- (6) Retriggering of automatic hang-up timer through use of second tone, thereby extending conversation time beyond six minutes.
- (7) Interconnection of two separate mine paging systems in different mines by using two Interconnect units.

III. INSTALLATION PROCEDURE

In order to connect a mine pager phone system to the Mine Pager Phone to Public Telephone Interconnect System, it must meet two criteria: first, the Pager system must use 12 volts DC to activate its paging circuit and second, it must be installed with all cable connections observing polarity. If these requirements are met, the Interconnect system will enable the mine pager phone system to interconnect with the public telephone system.

The actual installation of the Interconnect system is simple and can be performed by any mechanic. The first connection made is the connection to the Mine Pager Phone cable. This requires connection of the two wires of the pager cable to the Pager Connection binding posts on the Interconnect system housing. As stated above, polarity must be observed, with the + side of the batteries going to the + (red) post and the - side to the - (black) post.

The next connection required is the connection to the telephone company supplied connecting arrangement. This just entails matching four wires to their appropriate colors on both the connecting arrangement and the Interconnect system housing. Thus, red goes to red, green to green, yellow to yellow and black to black. This connects the mine pager phone system to the telephone line through the Interconnect system.

The final connection is simply plugging in the line cord of the Interconnect system to an AC outlet. The entire system can then be energized by pushing the POWER switch on the front panel of the Interconnect Unit housing. This lightened push-button switch will light, verifying that the system is energized and operable.

It should be noted that the telephone company supplied connecting arrangement may vary among the local telephone companies. The connecting arrangement will entail fixed charges which have been spelled out in the local telephone tariffs. In order to comply with the telephone tariffs the local telephone company should be informed by the mine that a customer furnished telephone device is being interconnected with the public switched network. Contact should be made with the local telephone company accounts manager responsible for telephone service to that mine. The accounts manager will then identify the proper technical telephone company employee who can identify which telephone company voice interconnecting arrangement is suitable from a standard list available from the telephone company. At that time the telephone company should be in a position to supply the following information:

- lead time required for installation of the arrangement,
- one time installation charge,
- monthly charges thereafter.

We expect that the above charges will fall in the range of \$50-\$75 for installation and \$5-\$10 per month.

PART EIGHT

TECHNOLOGY TRANSFER SEMINARS ON MINE COMMUNICATIONS
AND THROUGH-THE-EARTH ELECTROMAGNETICS WORKSHOP

PART EIGHT

TECHNOLOGY TRANSFER SEMINARS ON MINE COMMUNICATIONS
AND THROUGH-THE-EARTH ELECTROMAGNETICS WORKSHOP

TABLE OF CONTENTS

	<u>Page</u>
List of Tables	8.iii
List of Figures	8.iv
I. TECHNOLOGY TRANSFER SEMINARS ON MINE COMMUNICATIONS	8.1
A. INTRODUCTION	8.1
B. ROVING MINER, PAGING	8.3
C. TWO-WAY COMMUNICATIONS WITH ROVING MINERS	8.33
II. THROUGH-THE-EARTH ELECTROMAGNETICS WORKSHOP	8.77
A. INTRODUCTION	8.77
B. THEORY OF THE PROPAGATION OF UHF RADIO WAVES IN COAL MINE TUNNELS	8.78
C. SUMMARY REPORT OF UPLINK AND DOWNLINK COMMUNICATIONS WORKING GROUP	8.89
D. SUMMARY REPORT OF OPERATIONAL COMMUNICATIONS WORKING GROUP	8.113

PART EIGHT

TECHNOLOGY TRANSFER SEMINARS ON MINE COMMUNICATIONS
AND THROUGH-THE-EARTH ELECTROMAGNETICS WORKSHOP

LIST OF TABLES

<u>Table No.</u>	<u>Title</u>	<u>Page</u>
	<u>Chapter I, Section B</u>	
1	Roving Miner Paging	8.32
	<u>Chapter I, Section C</u>	
1	UHF Radio in Mines for Roving Miner-to-Miner Communications	8.75
	<u>Chapter II, Section B</u>	
I	Diffuse Radiation Component in Main Tunnel and at Beginning of Cross Tunnel	8.88
II	Excitation of E_h Mode in Cross Tunnel by Diffuse Component in Main Tunnel	8.88
III	Effect of Antenna Orientation	8.88
IV	Insertion Loss (L_i)	8.88
V	Calculation of Overall Loss for E_h Mode with Two Halfwave Dipole Antennas	8.88
VI	Overall Loss Along a Path Including One Corner E_h Mode with Halfwave Dipole Antennas	8.88

PART EIGHT

TECHNOLOGY TRANSFER SEMINARS ON MINE COMMUNICATIONS
AND THROUGH-THE-EARTH ELECTROMAGNETICS WORKSHOP

LIST OF FIGURES

<u>Figure No.</u>	<u>Title</u>	<u>Page</u>
	<u>Chapter I, Section B</u>	
1	Illustration of Current Flow Produced by Driving Roof Bolts	8.7
2	Block Diagram of Roof Bolt Experiment	8.9
3	Roof Bolt Attachment	8.10
4	88-kHz Repeater	8.11
5	Roof Bolt Coverage	8.12
6	Whole Mine Paging System	8.14
7	Reach Encoder Installation	8.16
8	88-kHz Transmitter in Mine Office	8.17
9	Pilot Wire Termination	8.18
10	Miner Wearing Pocket Pager	8.19
11	Paging on Trailing Cable	8.21
12	Call Alert Antenna Illustrating Magnetic Field	8.24
13	Call Alert Coverage	8.25
14	Call Alert Transmitter	8.27
15	Call Alert Receiver Worn by Miner	8.28
16	Call Alert Paging System	8.29
17	Keying Transmitter and Keying Receiver (Control Unit)	8.31

PART EIGHT

TECHNOLOGY TRANSFER SEMINARS ON MINE COMMUNICATIONS
AND THROUGH-THE-EARTH ELECTROMAGNETICS WORKSHOP

LIST OF FIGURES
(Continued)

<u>Figure No.</u>	<u>Title</u>	<u>Page</u>
	<u>Chapter I, Section C</u>	
1	Two-Way Wireless Section Radio System	8.38
2	UHF Wireless Radio in Coal Mines, Principle of Operation	8.40
3	UHF Wireless Radio Signal Attenuation Loss in Coal Mine Entries	8.41
4	Predicted UHF Wireless Radio Coverage	8.44
5	UHF Two-Way Wireless Section Radio Coverage in the Safety Research Mine	8.46
6	Two-Way Wireless Section Radio System Block Diagram	8.48
7	Miner Using Intrinsically Safe Handy Talkie Unit	8.51
8	Handy Talkie Operation Using Hardhat with Ear Speakers and Bone Conductance Microphone	8.52
9	Roof-Mounted Radio-to-Carrier Surface Inter- connect Unit and Handy Talkie Unit	8.53
10	Guided Wireless Radio System	8.55
11	Guided Wireless Radio with Coaxial Cable, Principle of Operation	8.57
12	Radiax Coaxial Cable, Cut-Away View	8.59
13	Two-Way Communication Range for Radiax Guided Wireless Radio System	8.61
14	Guided Wireless Radio System, Propagation Down Cross-Cuts Off Haulage Ways	8.63
15	A UHF Guided Wireless Radio System Using Radiax Cable	8.66

PART EIGHT

TECHNOLOGY TRANSFER SEMINAR ON MINE COMMUNICATIONS
AND THROUGH-THE-EARTH ELECTROMAGNETICS WORKSHOP

LIST OF FIGURES
(Continued)

<u>Figure No.</u>	<u>Title</u>	<u>Page</u>
<u>Chapter I, Section C (Continued)</u>		
16	UHF 420 MHz Guided Wireless Radio System Installed in the Safety Research Mine	8.69
17	System Control Console	8.70
18	Two-Frequency 12-Watt Repeater Station	8.71
19	Single Frequency 40-Watt Base Station and Special Power Supply Unit	8.72
20	Surface Transmitter/Receiver/Antenna Station for Overland Radio Loopback	8.74
<u>Chapter II, Section B</u>		
1	Refraction Loss for E_h and E_v Modes in High Coal	8.86
2	Refraction Loss for E_h Mode in Low Coal	8.86
3	Resultant Propagation Loss for E_h Mode in High Coal	8.86
4	Corner Loss in High Coal (Frequency-415 MHz)	8.86
5	Corner Loss in High Coal (Frequency-1000 MHz)	8.87
6	Total Loss for Various Distances Along a Straight Tunnel	8.87
7	Overall Loss in a Straight Tunnel in High Coal (Frequency-415 MHz)	8.87
8	Overall Loss in a Straight Tunnel in High Coal (Frequency-1000 MHz)	8.87
<u>Chapter II, Section D</u>		
1	Predicted Coverage of Mine Section by UHF Radio for Two Assumed Situations	8.125

PART EIGHT

TECHNOLOGY TRANSFER SEMINARS ON MINE COMMUNICATIONS AND THROUGH-THE-EARTH ELECTROMAGNETICS WORKSHOP

I. TECHNOLOGY TRANSFER SEMINARS ON MINE COMMUNICATIONS

A. INTRODUCTION

During the first quarter of 1973 ADL worked closely with PMSRC staff, under an extremely compressed time schedule, on all aspects of the detailed planning, organization and overall coordination and preparation of the lectures and in-mine demonstrations for the Bureau's Technology Transfer Seminar on Mine Communications given in March of 1973 to representatives of the mining industry.

Our efforts centered on the detailed organization and preparation of each of the five technical seminar lectures and associated supporting material, and the coordination of tasks assigned to ADL and other seminar participants. Revised and expanded drafts of the seminar papers were prepared from rough draft versions obtained from PMSRC, Collins Radio and ADL staff. Measurements were made to gather key data on the operation and performance of each of the following systems installed in the Bruceton Safety Research Mine; call alert paging, roof bolt paging, section wireless radio, and guided wireless radio systems. These data were analyzed, manufacturer's equipment specifications utilized, and calculations made to provide performance curves and data for each of the above systems.

A substantial amount of artwork was conceived and prepared for 35 mm slides, system identification posters in the mine, and seminar handouts. This artwork included some forty 8-1/2" x 11" line sketches, graphs, block diagrams, circuit diagrams, coverage maps, and other line drawings; five 30" x 40" block diagram system identification posters suitable for in-mine use; a 20" x 30" detail perspective illustration of a representative coal mine layout; forty viewgraphs; and seventy 35 mm slides of the artwork and word charts.

Conferences, discussions and review sessions were held with conference participants to help coordinate the various efforts, obtain technical information, and make final plans regarding the lecture presentations, associated visual aids, and the communication system installations to be demonstrated in the Bruceton mine. These meetings included final systems checkouts and dry run presentations and reviews of the lectures and mine demonstrations. This phase of the seminar effort concluded with R. Lagace and R. Spencer of ADL participating in two days of seminar presentations in the lecture hall and in the Bruceton mine.

This participation included the presentation of two papers coauthored with H. Parkinson of PMSRC, and entitled "Roving Miner, Paging" and "Two-Way Communications with Roving Miners."

The second phase of this seminar effort consisted primarily of preparing final edited versions of each of the five seminar papers, and typing them in a special draft format for subsequent processing and publication as an Information Circular*(IC) on Mine Communications by the Bureau's publication office. The specially formatted drafts of the two papers coauthored by ADL staff have been included in the following sections for convenient reference.

The final phase of the ADL seminar effort consisted in providing minor assistance to the Bureau in additional presentations of this seminar to the mining industry.

* Information Circular No. 8635.

B. ROVING MINER, PAGING

by

Richard H. Spencer¹ and Howard E. Parkinson²

ABSTRACT

Mine paging telephones increase the effectiveness of the mine personnel. The page message reaches the personnel within hearing distance of the phone. Personnel paging extends the page to the individual roving miner wherever he may be.

One system installed at the Bureau of Mines Safety Research mine is a "dial-in" system. An in-mine page can originate from any mine public phone. The system, exclusive of the Bell System equipment, includes an encoder, 88-kHz transmitter, pilot wire signal coupler, 88-kHz repeater, a roof bolt signal coupler, and pocket receivers.

There are two configurations of the system. One configuration is a whole mine configuration and the other is a working section configuration. There are two forms of the working section configuration. One form puts the selective page onto the mine phone line and converts the message to 88-kHz at the section, thereby extending the page area to the face.

The second form is a call alert system. This system keys a call alert transmitter on the section. The system has a capacity to handle 24 sections. It is a cost-effective system with an added feature of providing an emergency beacon locator at the time of a mine emergency.

¹Arthur D. Little, Inc., Cambridge, Mass.

²Supervisory Electrical Research Engineer, Industrial Hazards and Communications, Pittsburgh Mining and Safety Research Center, Bureau of Mines, U.S. Department of the Interior, Pittsburgh, Pa.

INTRODUCTION

Current Paging Systems

Mine telephones are the backbone of most present mine communications systems. There are two main telephone instruments: the magneto telephone and the mine pager telephone. A large mine may have 40 or more of these phones. Selective calling is attempted on both types of phones. The magneto phone is used to make a selective call by a coded ring that is audible near each phone location. The mine pager phone is used to make a selective call by paging a particular individual by name over loudspeakers at the phone locations. The selective call feature of the mine pager phone is an improvement over that of the magneto phone, and as a result the mine pager phone has gained wide acceptance. These phones can be made permissible and because of their battery operation are ready for using during an emergency.

Additional Paging Needs

The effectiveness of communication with roving miners underground would be significantly improved by meeting the following additional paging needs:

- (1) Selective page to the desired individual

- (2) Extension of paging coverage to individuals in all working places

Currently, there is confusion on the mine phone paging system. Individuals hear pages that are not meant for them, since it is a party line system. Individuals are frequently not within the acoustic range of a page phone loudspeaker, or may be in an area of high acoustic noise near machinery. Thus, many pages are not heard, and even if a page is heard, it is fre-

quently hard to tell who is being paged, As a result, it is customary for many individuals to ignore pages unless a particular call is expected. This makes it difficult to get a reply to an incoming call, resulting in people often having to be dispatched into the mine to locate specific individuals. The root cause of this situation is that the mine pager phone message goes to the pager phones rather than to the specific individual being paged.

PERSONAL PAGING VIA ROOF BOLTS

Personal paging extends the page message to the individual . A small pocket pager is carried by the individual. This pager receives a message only when the particular individual is being paged. The selective call feature of the page removes the confusion that is common in the mine page telephone system. Many personal paging systems are in use in a variety of communication applications. These systems are very effective in hospitals, industrial plants, and other large buildings. In their original form they are not satisfactory for mine use; however, relatively straightforward adaptations based on extensions of existing mine communication systems have proved to be fruitful. These adaptations are based on existing trolley wire and mine telephone systems, as described below.

Demonstration of paging capabilities was made by using carrier frequency equipment operating at the 88-kHz trolley wire phone frequency. Signals from the 88-kHz transmitter were connected to the leads of the main power system of the mine. The paging function was incorporated by using a commercial encoder manufactured by Reach to provide an input to the 88-kHz

transmitter. This encoder provided 200 selective call numbers. Pocket pagers were given to several individuals to carry with them as they were roving underground. It was possible to reach them in most of the working places.

There were places, however, where the page signal was too weak thereby requiring the addition of equipment, namely an 88-kHz repeater. This repeater is fed by the 88-kHz signals on the power mains, and the output of the repeater is connected to roof bolts. This addition provided page capability up to the very face of the working sections.

The pocket pagers are selective and are operated only when the page messages are being transmitted. The normal trolley wire communications are not heard by an individual not being paged unless a button on the pager unit is depressed. We have continued to operate the equipment at 88-kHz; however, we recognize that it could be used at some other frequency that would preclude interference with normal 88-kHz transmissions.

Principles of Operation

Figure 1 illustrates the current flow that results when two roof bolts are driven by a source of power. It is noted on this figure that

FIGURE 1. - Illustration of Current Flow Produced by Driving Roof Bolts.

the current flow extends far into the material surrounding the roof bolts. Indeed, at very great distances there is still current flow; the problem is that the currents are quite small compared to the background noise currents. One can easily see that if a pair of probes is attached to the material surrounding the roof bolts, even at great distances, voltages

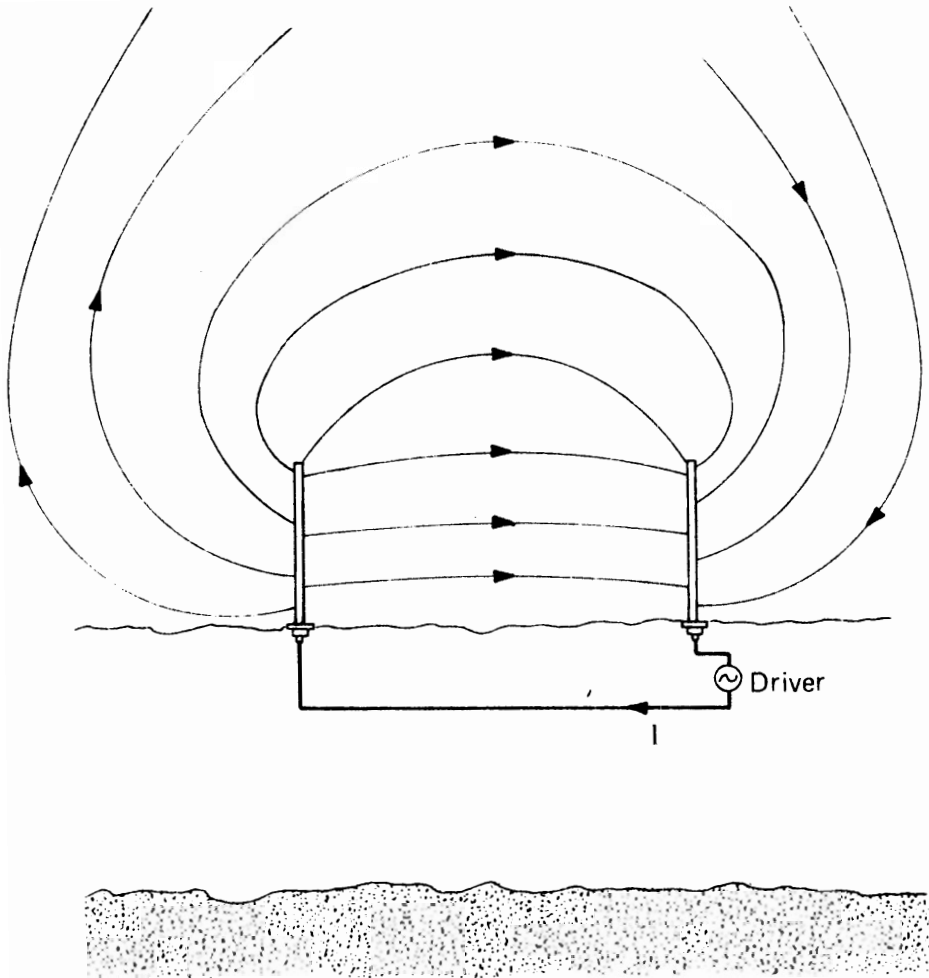


FIGURE 1 ILLUSTRATION OF CURRENT FLOW PRODUCED BY DRIVING ROOF BOLTS

produced by the current flow will be obtained from these probes. It is also evident that if the current flow is alternating, there will be associated magnetic fields which occur in the material and in the surrounding regions. These fields extend into the open areas of the mine and hence may be picked up by loop antennas throughout the mine region. It is important to know how far from the roof bolts one may obtain usable signals in this fashion.

Expected Coverage

An experiment was conducted in the Bruceton Experimental mine as illustrated in Figure 2. An 88-kHz repeater of nominal 20-watt capability was attached to two roof bolts separated by a distance of approximately 120 feet. The repeater was driven from a sine-wave source, and a calibrated loop together with a calibrated receiver was used to measure the vertical magnetic field strength throughout all regions of the Bruceton mine. The manner in which roof bolt attachments were made is illustrated in Figure 3. A simple, direct electrical connection to roof bolts is illustrated here. The repeater is shown in Figure 4. Figure 5 shows the coverage to be expected with a Reach pocket pager receiver using the roof bolt system in the Bruceton mine. Three contours are shown on this

- FIGURE 2. - Block Diagram of Roof Bolt Experiment.
- FIGURE 3. - Roof Bolt Attachment.
- FIGURE 4. - 88-kHz Repeater.
- FIGURE 5. - Roof Bolt Coverage.

plot. The first contour is for a received signal-to-noise ratio of 15 db. This contour was determined by comparing the measured values of vertical

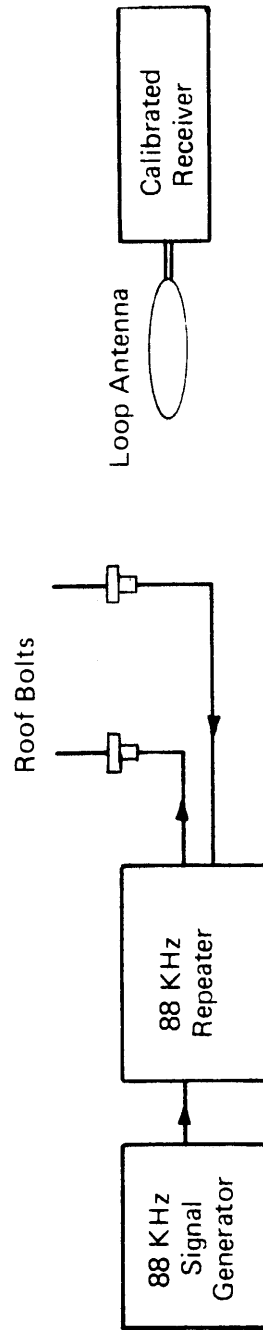


FIGURE 2 BLOCK DIAGRAM OF ROOF BOLT EXPERIMENT



FIGURE 3 ROOF BOLT ATTACHMENT

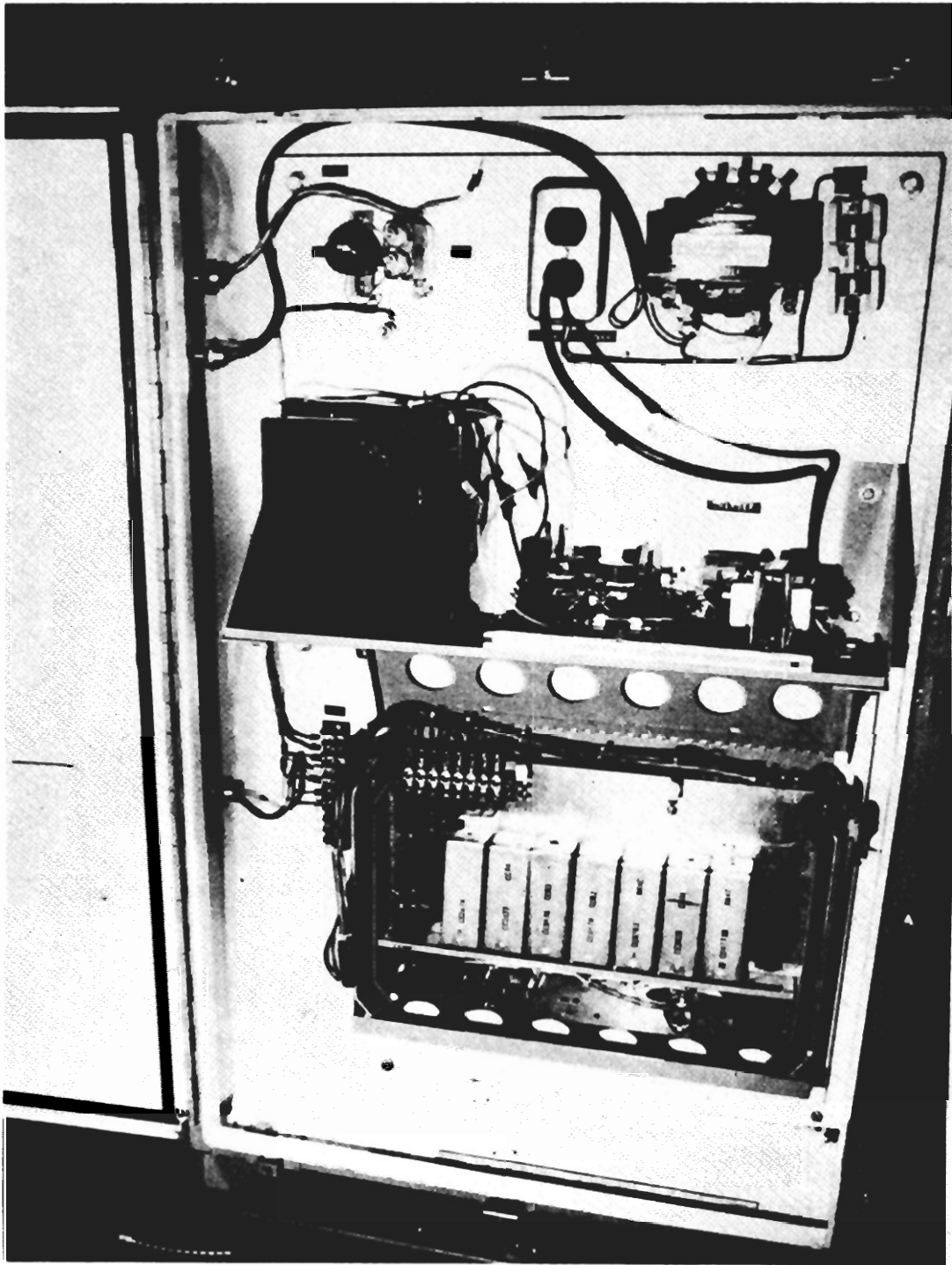
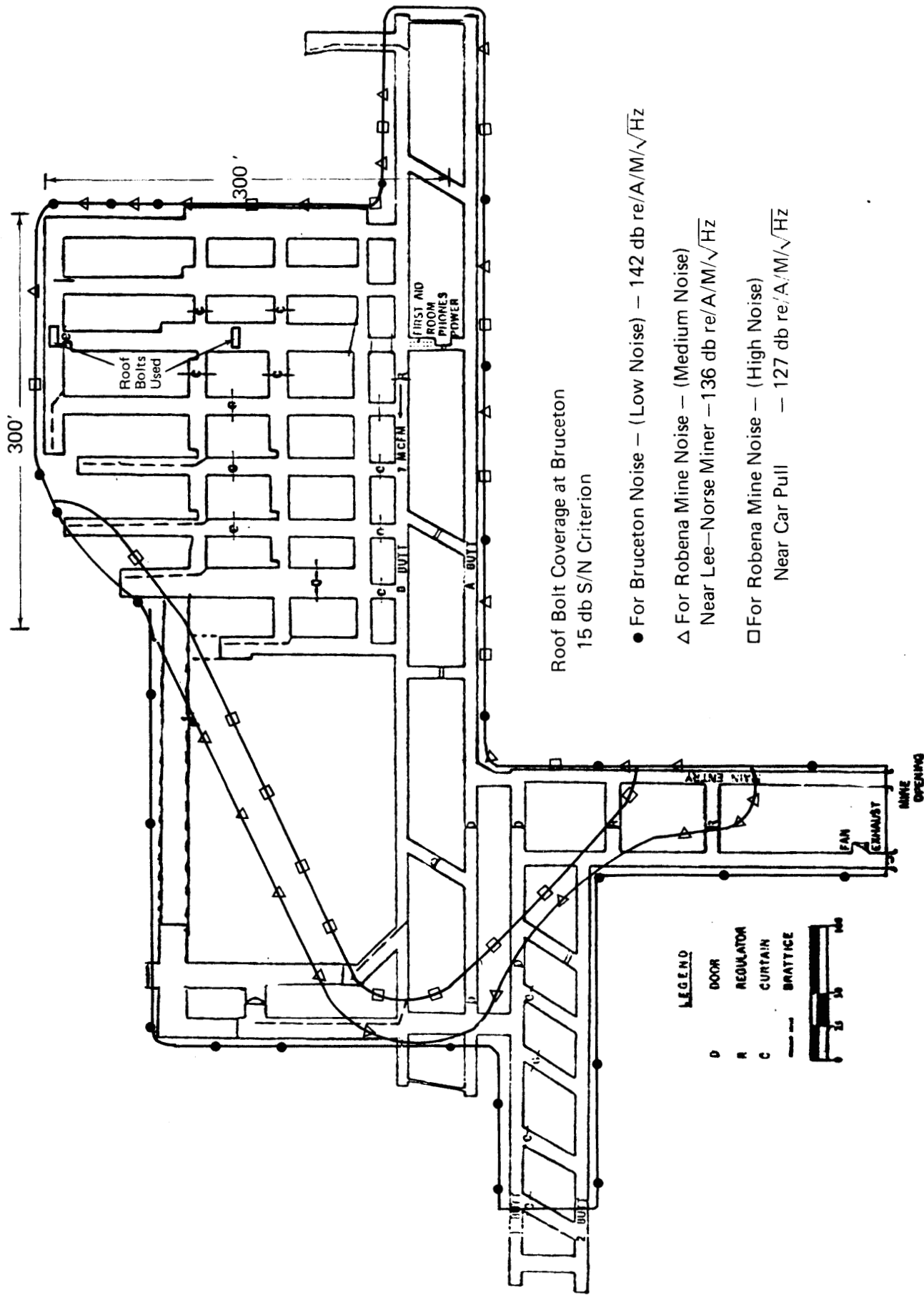


FIGURE 4 88 kHz REPEATER
8.11



- For Bruceston Noise – (Low Noise) – 142 db re/A/M/√Hz
- △ For Robena Mine Noise – (Medium Noise)
Near Lee–Norse Miner – 136 db re/A/M/√Hz
- For Robena Mine Noise – (High Noise)
Near Car Pull – 127 db re/A/M/√Hz

FIGURE 5 ROOF BOLT COVERAGE

magnetic field strength and the measured values of vertical magnetic field noise present during the experiment. A 2,000 Hz bandwidth was assumed for these determinations. It is seen that this boundary encloses essentially all of the Bruceton mine with the exception of a region at the far left extremity. Using the measured field strength data and noise obtained by the National Bureau of Standards (NBS) in their mine electromagnetic noise measurement program, two other contours are overlaid on this plot. The first one is the expected limit of coverage were the noise like that in the face area of a working mine near a Lee Norse miner. It is noted that this coverage is less than that for the Bruceton noise. The third contour represents the expected coverage were the noise like that found in the same working mine near a car pull while the car pull was operating. This machine produced the highest electromagnetic noise levels found by NBS in their mine measurements, and as such probably represent an upper limit of expected noise in mines at the frequencies of interest for mine communications. From these plots, it can be seen that coverage of a typical working section can be expected from roof bolt attachments made near the center of that section.

System Description

The overall block diagram of the system as installed in Bruceton is shown in Figure 6. The paging system demonstrated in Bruceton can originate

FIGURE 6. - Whole Mine Paging System.

pages from any dial phone within the PBX at Bruceton. The caller dials 1, followed by a three-digit code. This connects his phone through the PBX

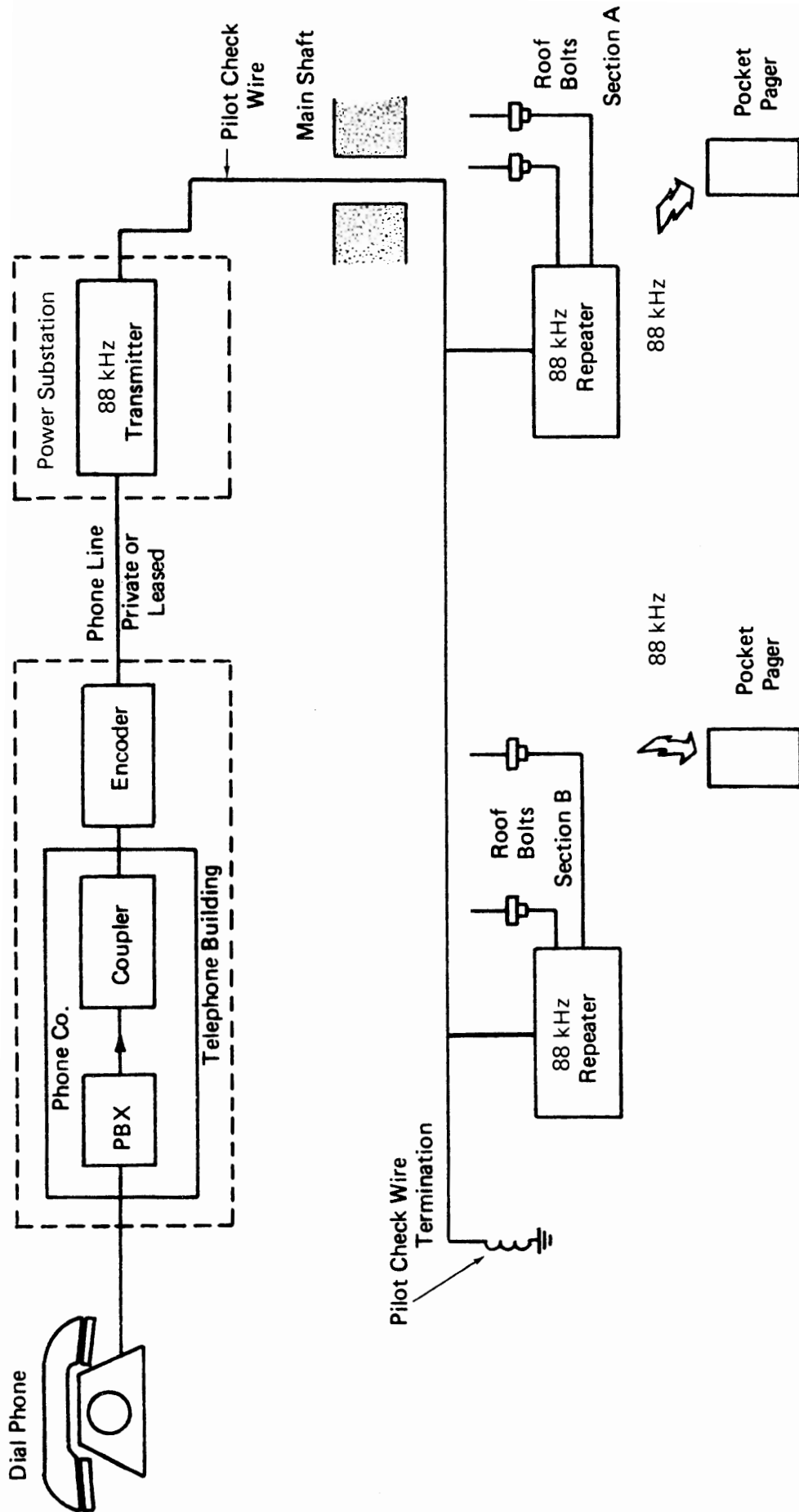


FIGURE 6 WHOLE MINE PAGING SYSTEM

to a Reach encoder which translates his dialed code to the corresponding Reach receiver's code. The signal generated by the encoder is transferred through a private line to a 20 watt 88 kHz transmitter located in the power substation. The 88-kHz transmitter output voltage is connected between the pilot check wire and ground of the power cable that runs down into the mine. In the mine the 88-kHz signal is taken from the pilot check wire and fed through a 20 watt 88-kHz repeater. The output of this repeater is connected to a pair of roof bolts, and the pocket pagers worn by key personnel in the mine respond to their unique pocket-page code. The person calling the page has an opportunity for 10 seconds of message which can be received by the person carrying the pocket pager. In general, it is intended that the person being paged go to the nearest phone in the mine and respond to the request for communication. Figure 6 illustrates two 88-kHz transmitters used to cover two working sections. This number can be expanded to cover each of the working sections in a mine. The principal of operation is the same.

Figure 7 illustrates the installation of the Reach encoder, and Figure 8 shows the 88 kHz transmitter in the mine office. The pilot wire termination is shown in Figure 9, and the underground 88 kHz repeater as shown in Figure 4. Figure 10 illustrates the way in which the pocket pager can be worn.

- FIGURE 7. - Reach Encoder Installation.
- FIGURE 8. - 88-kHz Transmitter in Mine Office.
- FIGURE 9. - Pilot Wire Termination.
- FIGURE 10. - Miner Wearing Pocket Pager.

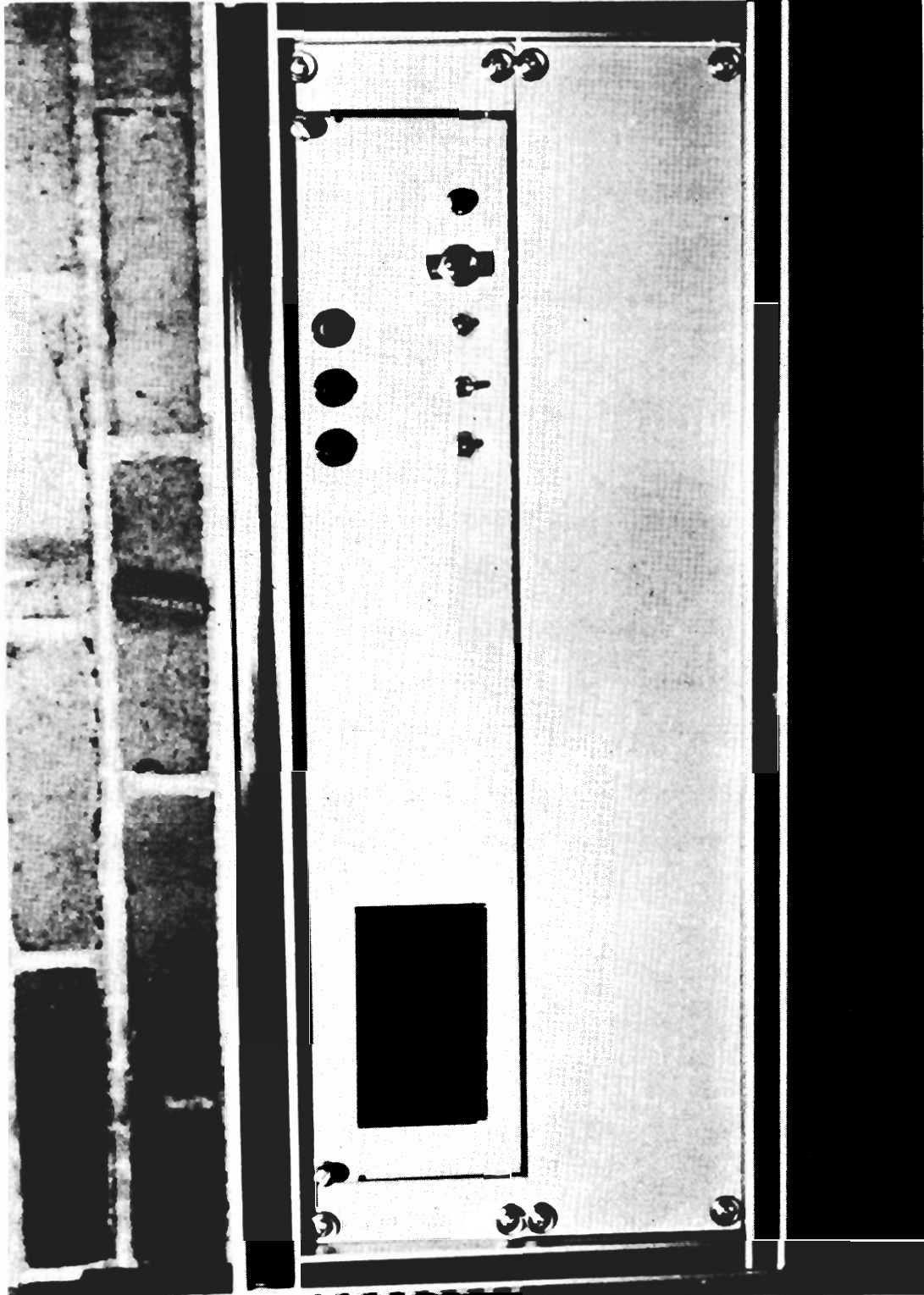


FIGURE 7 REACH ENCODER INSTALLATION

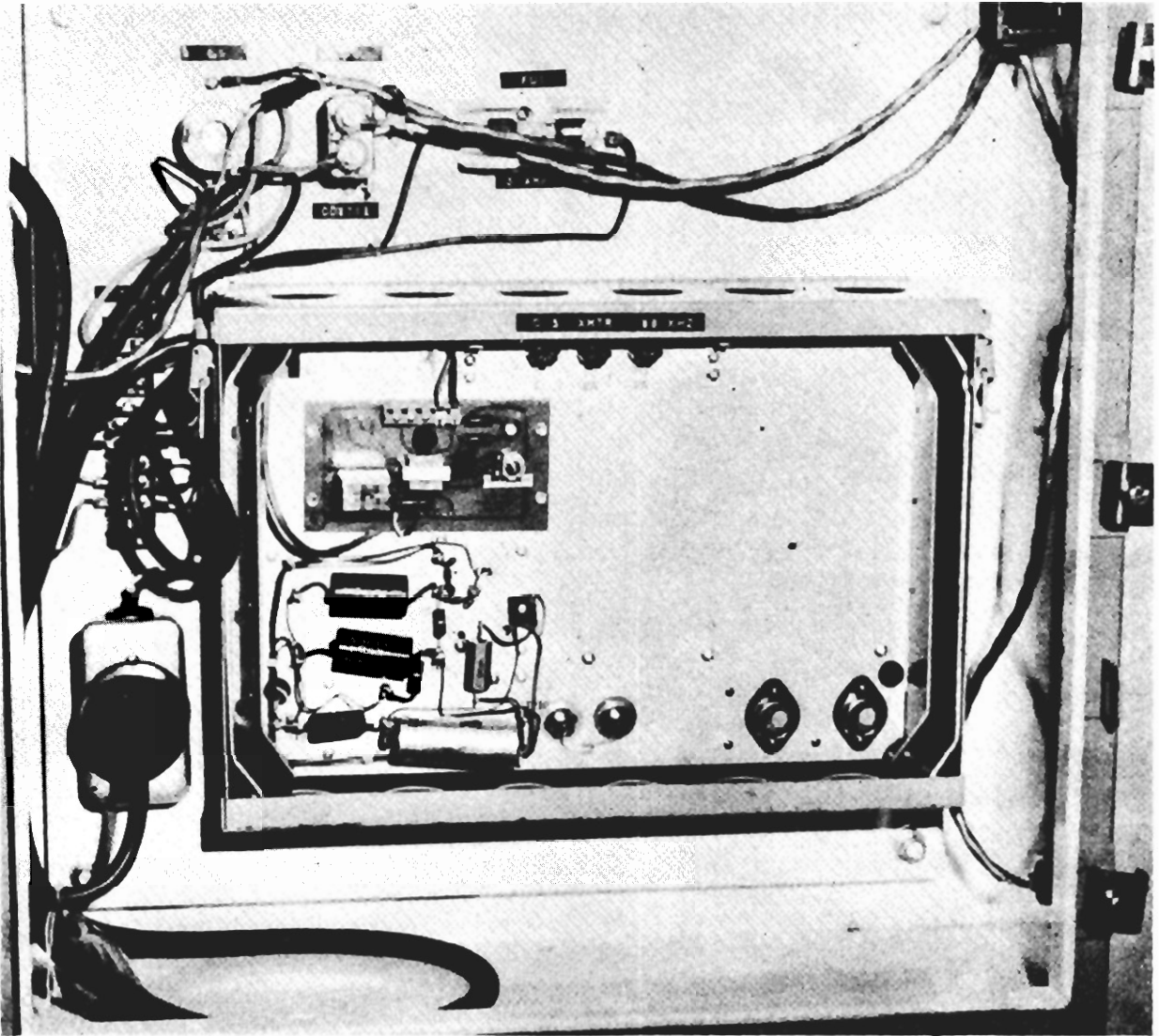


FIGURE 8 88-kHz TRANSMITTER IN MINE OFFICE

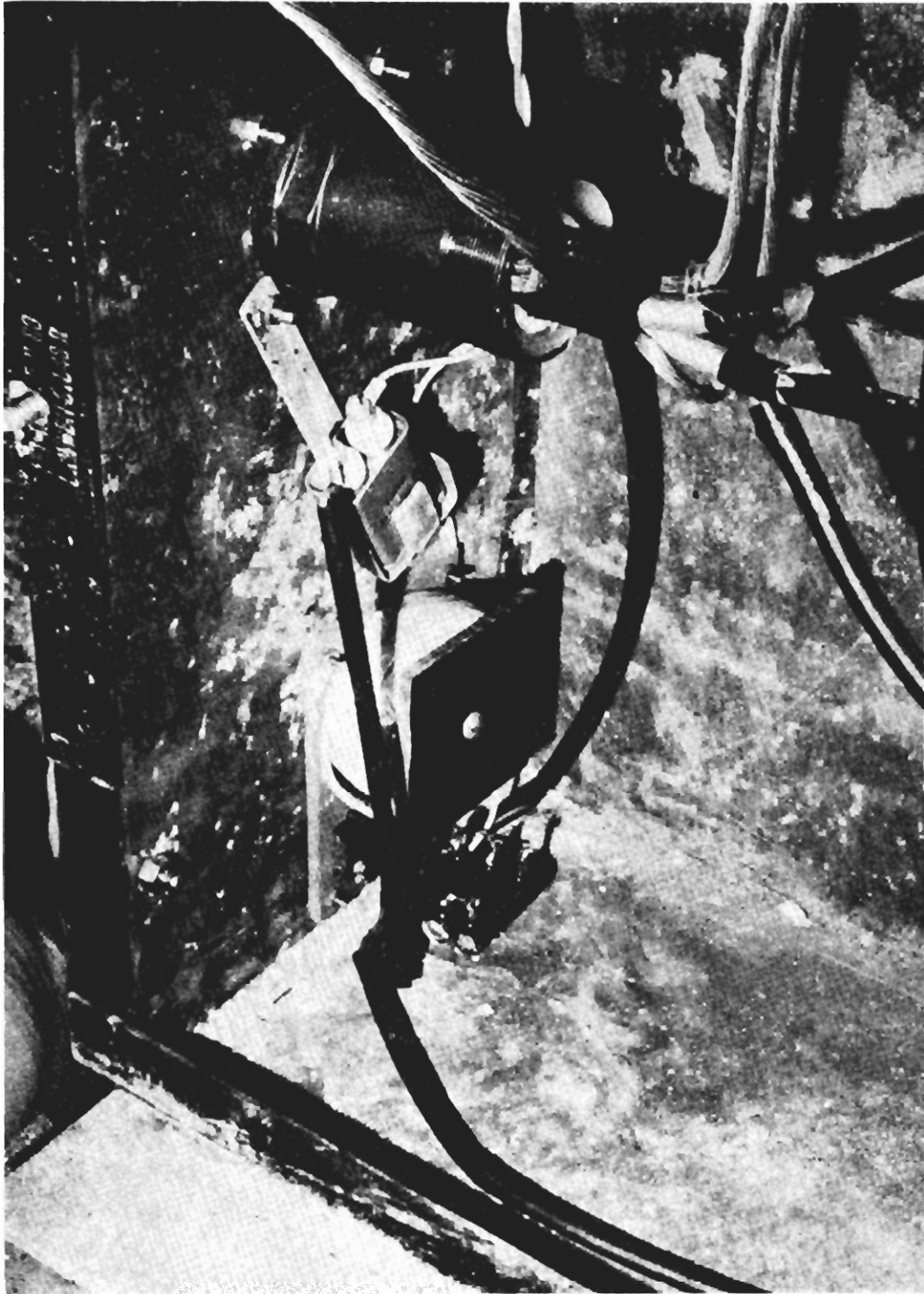


FIGURE 9 PILOT WIRE TERMINATION

8.18



FIGURE 10 MINER WEARING POCKET PAGER

8.19

There is a second means of employing paging at carrier frequencies inside the mine. The paging transmitter can be connected to the mine telephone wires, connecting the signal between both wires and ground. The phone wires and ground then become the transmission line for the carrier frequency mine paging system. Once again, repeaters feeding roof bolts can be added in the mine working section area to extend the coverage away from the transmission lines.

The 88-kHz system described above for whole-mine paging has many similarities with the trolley wire carrier communication systems used to dispatch dc haulage vehicles. As such, paging signals placed on the trolley wire can also be extended into the section via the cables of dc face machines connected to the trolley wire power system. Hence, in the vicinity of a trolley wire or trailing cables, a miner with a pocket pager will be able to pick up the page signals via the magnetic fields in the vicinity of these cables. Such an application is illustrated in Figure 11.

FIGURE 11. - Paging on Trailing Cable.

CALL ALERT PAGING

A special form of paging is commonly called "call alert." It differs from the pocket paging system in that it produces a selective call alert signal that notifies an individual when the mine paging telephone is being used to page him. This system is not capable of as wide an area of coverage as the above roof-bolt paging system; however,

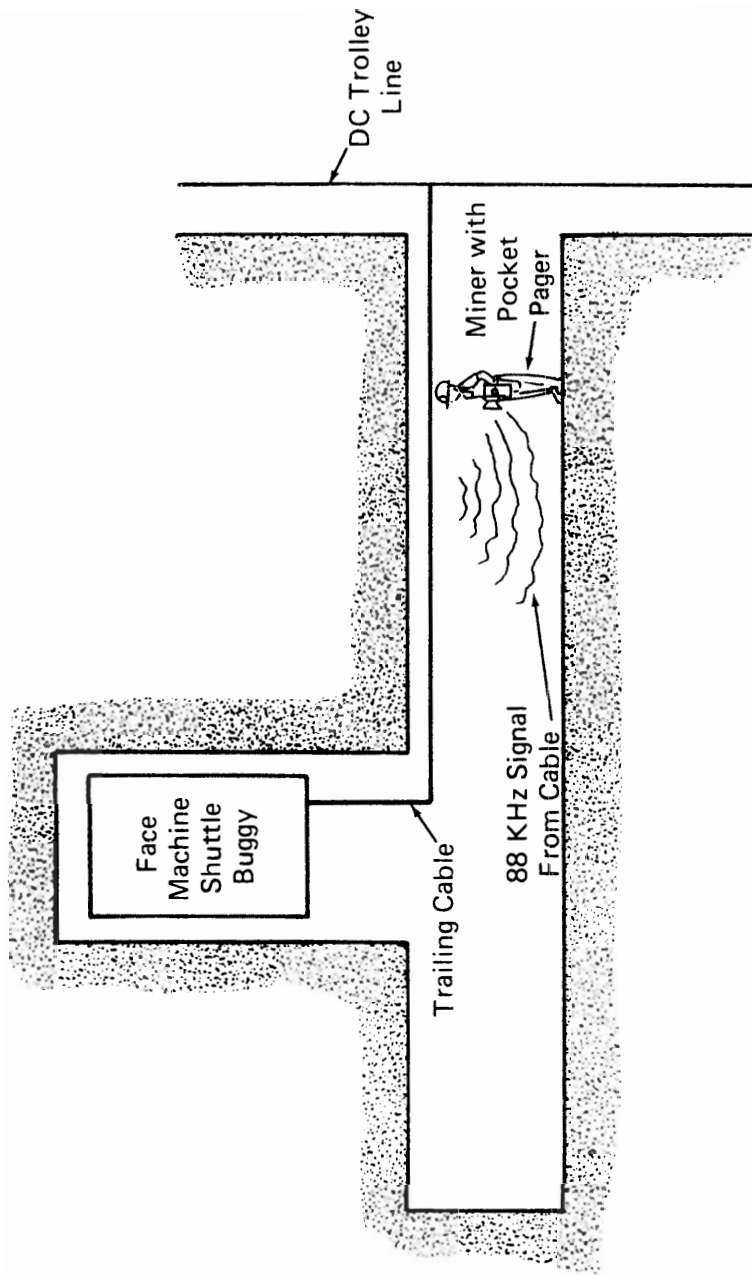


FIGURE 11 PAGING ON TRAILING CABLE

it is very effective in the working section. Once again additional equipment was added to the existing mine communications system. This time the equipment was added to the mine telephone line. A simple transmitter was added in the mine foreman's office and a receiver and call alert transmitter were added in the mine section. The loop antenna of the call alert transmitter was wrapped around a pillar.

In order to receive a call alert, the individual carries a pocket alert receiver. The receiver has a blinking light to indicate a call. From the surface, a non-audible tone is sent over the telephone wires and is received by a selective filter, which in turn energizes the call alert transmitter on the section being paged. Instead of paging over the mine pager telephone system, the paging is personalized to those section individuals carrying the call alert receivers. When the pocket receiver indicates a call alert, the individual walks to the mine pager phone on the section and replies to the page call. This system was developed from work performed in the Bureau of Mines program on electromagnetic detection of trapped miners.

There is an additional benefit to this system. The signal being transmitted on the section is a low-frequency signal that also penetrates the overburden. It has been possible to receive such signals on the surface some 1000 feet above the mine section. Miners on the section can use this transmitter for emergency signaling to the surface. Conversely, the miners can also use the call alert receiver to receive similar operational or emergency transmissions from a surface transmitter.

Principle of Operation

Figure 12 illustrates a call alert transmitter antenna and its

FIGURE 12. - Call Alert Antenna Illustrating Magnetic Field.

associated magnetic field. The current flowing in the loop produces a magnetic field which links this loop with a small pick up loop in a call alert receiver carried by a person. The operational range of this system is essentially the distance at which the received signals have become small enough for the background noise to interfere with their reception.

Expected Coverage

Once again, an experiment was done in the Bruceton Experimental mine to determine the efficacy of this system in providing paging coverage throughout a working section. A loop antenna was placed around a coal pillar and driven with a transmitter operating at a frequency of 3030 Hz, and a calibrated receiver tuned to this frequency was carried through the mine to determine the signal strength received at various parts of the mine. The results of these measurements are shown in Figure 13 which illustrates the extent of the call alert coverage. These cover-

FIGURE 13. - Call Alert Coverage.

ages are for a 5-Hz bandwidth receiver. Three contours are shown. The first is for the background noise level found at the Bruceton mine, which we call low noise. It is seen that the coverage provided at a

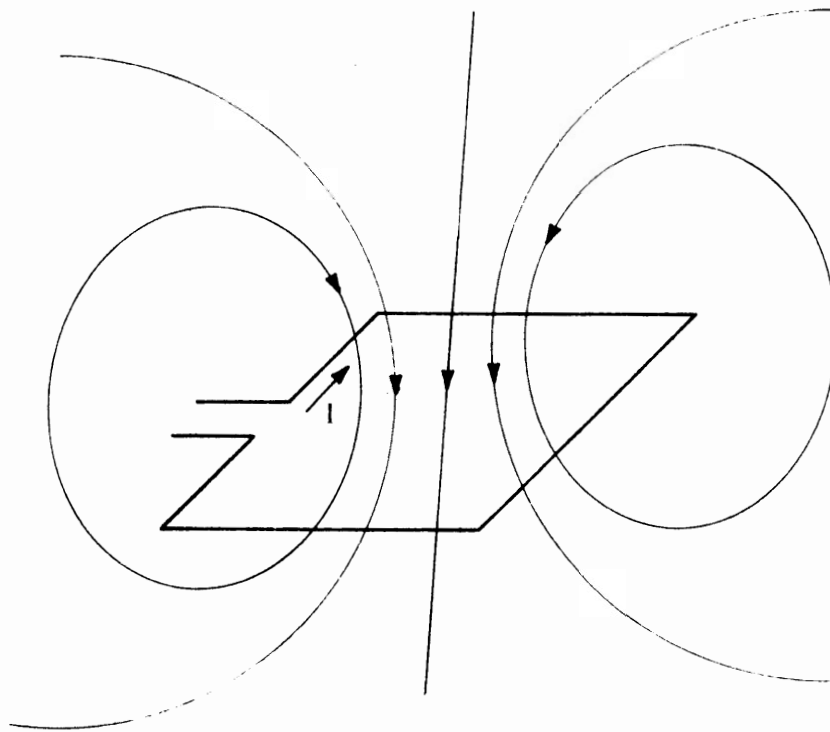


FIGURE 12 CALL ALERT ANTENNA ILLUSTRATING MAGNETIC FIELD

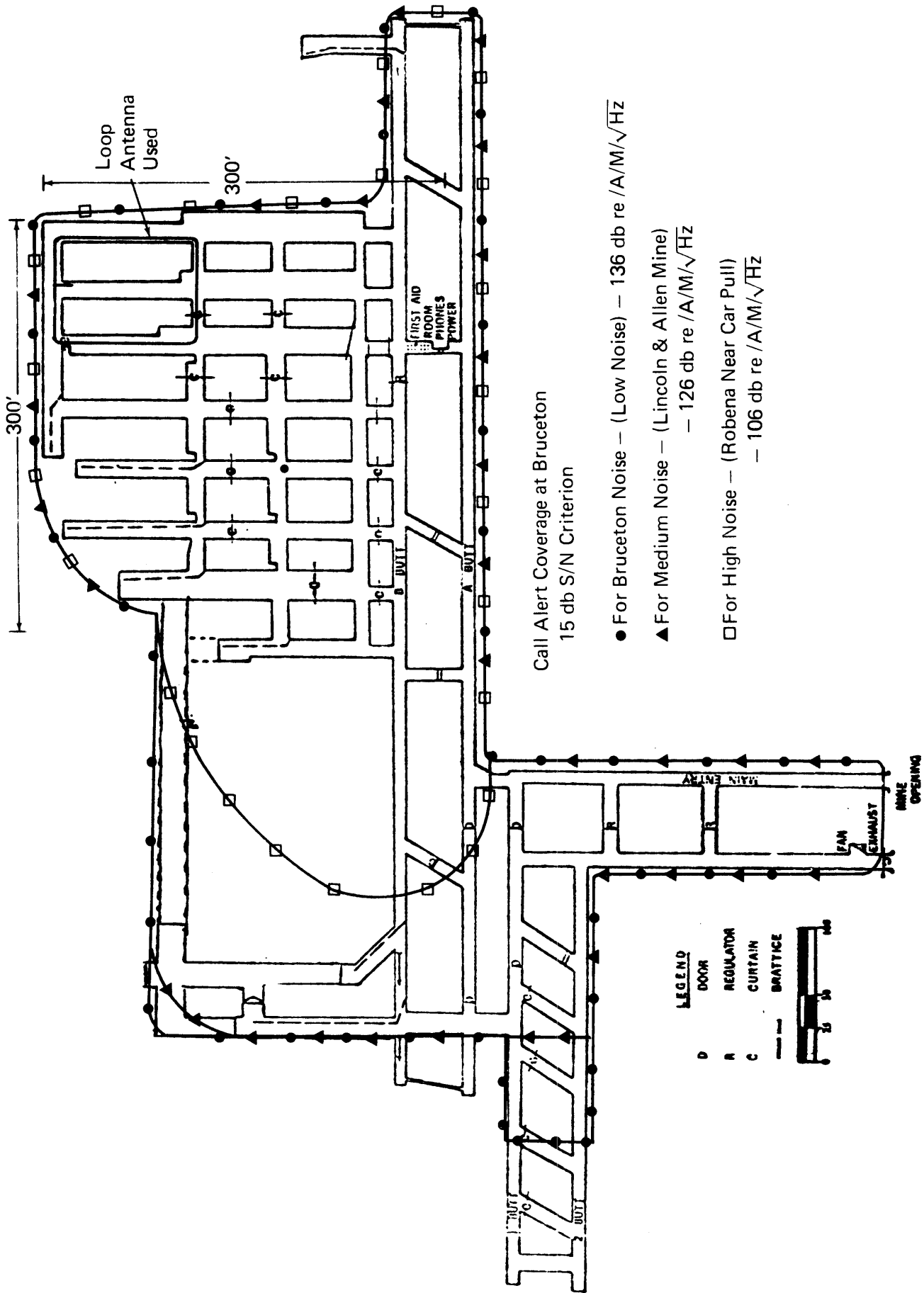


FIGURE 13 CALL ALERT COVERAGE

15-db signal-to-noise ratio extends through most of the mine area, excluding the far extreme left hand corner. Measured noise from operating mines has been used to determine the contours of coverage that would result were such noise levels present in the Bruceton mine. In the medium noise case, a small region of the above coverage is eliminated, while in the high-noise case, a further shrinkage of coverage is observed. The high-noise case represents noise levels measured by NBS at an operating mine near a car pull, and has been identified as the maximum noise condition. Figure 14 shows a photograph of the call alert transmitter and Figure 15 shows a photograph of the call alert receiver. Much like the roof bolt system, coverage over a typical working section can be expected with appropriate positioning of the transmitting loop.

FIGURE 14. - Call Alert Transmitter.

FIGURE 15. - Call Alert Receiver Worn by Miner.

System Description

The block diagram of Figure 16 illustrates the entire system configuration. A keying transmitter is located in the mine office. To initiate a

FIGURE 16. - Call Alert Paging System.

page, an individual pushes the "press to page" button on this transmitter. This action causes a 19-kHz carrier (other selected inaudible tones can also be used) to be impressed on the mine phone line. This tone enters the mine on the phone line. The keying receiver, attached to the phone



FIGURE 14 CALL ALERT TRANSMITTER



FIGURE 15 CALL ALERT RECEIVER WORN BY MINER

8.28

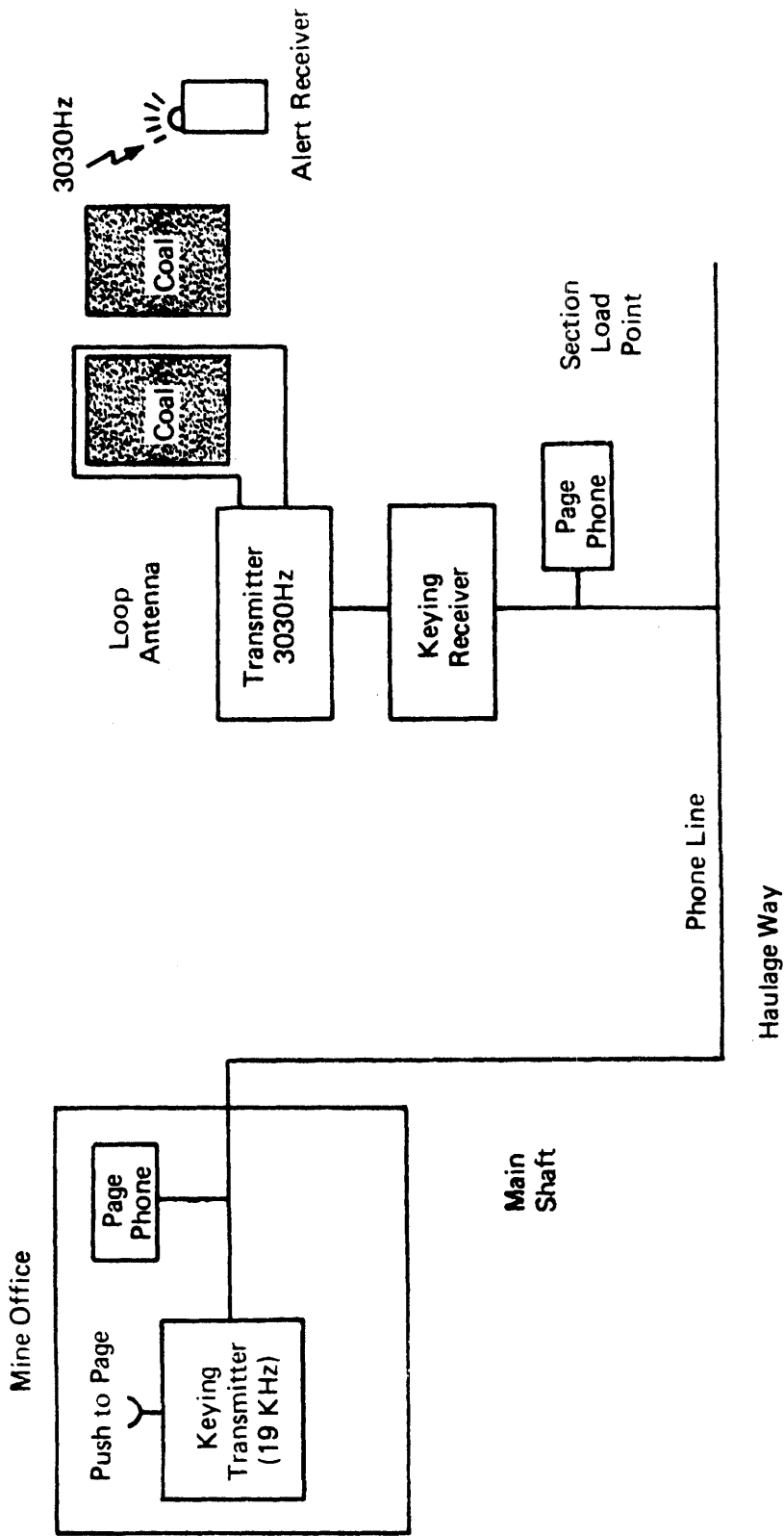


FIGURE 16 CALL ALERT PAGING SYSTEM

line located at a keypoint in a section, responds to this tone. These two units are illustrated in Figure 17. As long as the tone is present,

FIGURE 17. - Keying Transmitter and
Keying Receiver (Control Unit).

the keying receiver connects operating power to the call alert transmitter connected to the pillar mounted loop. In the present system this call alert transmitter drives a 3030-Hz signal current into the loop antenna of the system, thereby producing a 3030-Hz signal that penetrates to all regions of the section. A pocket-sized call alert receiver incorporating a small pick-up loop is carried by a person roving through the section. This receiver responds to the presence of the 3030-Hz signal by flashing a light on the receiver or by generating an audio alert signal. The person paged is thus notified to call the mine office.

A word of caution: Call alert systems use carrier signals over the telephone wires. A preliminary examination of several of the mine pager telephones indicates that these phones are not fully compatible with the normal range of telephone grade carriers. We are now investigating this problem and anticipate that a simple add-on device (applique) can be made for installation on existing mine pager phones to make them compatible with carrier applications. At this time, it is possible that some carrier frequency systems will require excessive amounts of power if utilized on present mine telephone installations.

CONCLUDING REMARKS

The emphasis of our paging efforts has been placed on the extension of existing mine communications to improve their utility under operational and emergency conditions. Primarily we have been concerned with extending the page message from the equipment that receives the page to the

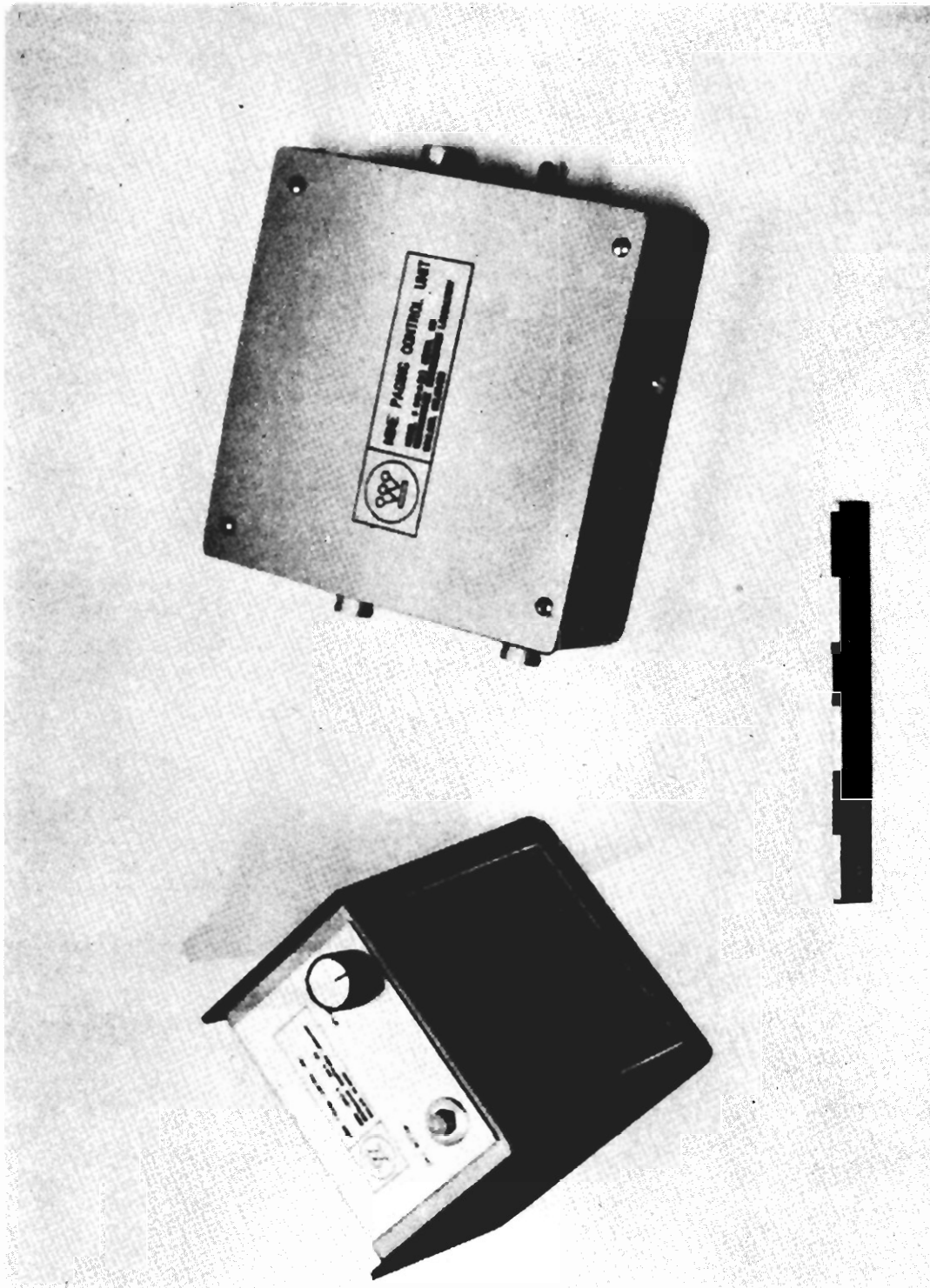


FIGURE 17 KEYING TRANSMITTER AND KEYING RECEIVER (Control Unit)

person who is being paged. Paging can also be added to wireless radio communication systems; however, there are very few mines currently using wireless radio. The objective in paging is to alert a person that he is wanted on the telephone. The person replying to the page will generally not reply over the same channel by which he was paged. The paging system and the call alert system discussed here meet different needs. The general features of these two systems are summarized in Table 1.

TABLE 1. - Roving miner paging

	Roof bolt system	Call alert system
Coverage	Part or whole mine	By section
Voice page	Yes	No
Selectivity	To individual	To section
Emergency use	Not practical	Yes
Equipment availability	Current	60 Days

C. TWO-WAY COMMUNICATIONS WITH ROVING MINERS

by

Robert L. Lagace¹ and Howard E. Parkinson²

ABSTRACT

UHF wireless and guided wireless radio systems are operational in the U.S. Bureau of Mines Safety Research Mine in Bruceston, Pa. The systems satisfy the need for instant personal two-way communications between key individuals roving in working sections and haulage ways, and between these individuals and the surface. The individuals are equipped with portable handy talkie radios that are Bureau-approved for operation in a gassy mine. The Bureau's systems operate at 420 MHz, a frequency allocated to government users. Systems belonging to industrial users such as mines can utilize the 450-470 MHz UHF band allocated to industrial land mobile applications. The UHF band is more effective than the VHF band for unaided propagation in the sections and haulage ways of mines.

The UHF wireless radio system does not need any special guiding cables, and is particularly attractive for mine section applications, as well as haulage ways. The UHF guided wireless radio system is based on

¹ Arthur D. Little, Inc., Cambridge, Mass.

² Supervisory Electrical Research Engineer, Industrial Hazards and Communications, Pittsburgh Mining and Safety Research Center, Bureau of Mines, U.S. Department of the Interior, Pittsburgh, Pa.

the use of a special radiating coaxial cable installed along main entries, and is suitable for haulage way applications. This paper treats the principles of operation, expected communication ranges, and the key features and limitations of both systems.

INTRODUCTION

Need for Two-Way Communications with Roving Miners

Historically, communication equipment for underground mine use has been based on "wired" systems, namely, the loudspeaking mine telephone system and the trolley wire carrier phone system. The mine telephone system includes both magneto phones and loudspeaking telephones, while the trolley wire carrier phone system utilizes carrier current transmitters and receivers. In both cases all the transmitting and receiving equipment is "hard wired" to the telephone line or to the trolley wire, respectively. As such, this equipment is not portable. Therefore, it is inadequate for paging or communicating with key individuals, such as foremen and maintenance men, when they are not in the immediate vicinity of the communication equipment.

The roving miner paging systems recently developed by the Bureau of Mines and discussed in a companion seminar paper, meet the need to deliver one-way paging messages and call alerts to key individuals on-the-move in the mine. These are messages or alerts that the paged individual must either act upon, or acknowledge via another communications channel in the mine. However, situations also arise in which an

instantaneous and continuing response from key roving miners is either essential or extremely desirable from an operational or safety point of view. The ability to reach and talk with an individual where he happens to be, and not only at a limited number of fixed stations, is particularly beneficial when:

- downtime can be reduced by permitting individuals working on machinery to communicate with surface supervisors without leaving the machinery; or
- the message is urgent and the individual is on-the-move underground.

Two-way wireless and guided wireless radio systems recently investigated by the Bureau can provide this personalized instantaneous communication to individuals over important parts of the mine.

Two-Way Wireless Radio in Mines

The thrust of our two-way wireless radio communication work has been to extend two-way communications to key miners roving within the section and in the haulage way. The principal objective has been to find ways in which commercially available, portable radio equipment can be adapted for practical use in operational coal mines.

Electromagnetic waves at radio frequencies are not capable of penetrating the overburdens of typical mines because of the severe attenuation suffered in the overburden by the waves at these frequencies. To utilize radio waves in mine entries and cross-cuts, the radio

signal sources must be brought into the mines and to the areas of interest, either directly or via guiding cables or wires.

The operating frequency is a key factor that significantly influences the communication range of any wireless radio system in mines. American coal mining methods require area coverage, as opposed to the linear haulage way coverage that is typically needed for European longwall mining. By area coverage we mean communications throughout a working section that may typically encompass an area 600 feet x 600 feet, and communications down cross-cuts to several hundred feet away from the main haulage ways.

We have found that frequencies in the UHF band offer the best area coverage for completely wireless two-way voice communications between portable handy talkie radios. This we have determined from theoretical considerations backed up by in-mine experiments. Two-way wireless communication ranges between hand-held units in mine entries are limited to approximately tens of feet at citizens' band frequencies near 30 MHz; are extended to several hundreds of feet at VHF band frequencies around 150 MHz; and are further extended to over 1500 feet for UHF band frequencies around 450 MHz. These ranges apply to straight line communications along an entry, and are reduced if corners are present in the transmission path. In addition to offering the greatest promise for extending two-way communications to roving individuals, the 450 MHz UHF frequency band is presently the upper limit for commercially available portable radio transceivers. This frequency band has also been receiving much publicity and interest in the underground mining industry.

Two specific UHF radio communication systems are treated in this paper. The first is truly wireless and particularly attractive for section applications, so it has been named UHF wireless section radio. The second makes use of a special coaxial cable for guiding and radiating UHF radio waves along mine entries, so it has been named UHF guided wireless radio.

UHF WIRELESS SECTION RADIO SYSTEM

Two-way wireless section radio systems can provide communications between key individuals who may be working at different locations within a section, and between these individuals and the surface. These systems can also be applied to haulage way communications. Figure 1 gives an overall view of such a system for a section application. It is described in detail under System Description, after discussion of the system's principles of operation and expected communications coverage.

Figure 1. - Two Way Wireless Section Radio System

Principles of Operation

Figure 2 depicts in schematic form a UHF radio wave propagating down a coal mine entry (tunnel), without the assistance of any metallic guiding wires or cables. At VHF/UHF frequencies, the entries themselves behave like "leaky" waveguides, guiding the signal energy along the length of the entry, while also losing part of the energy to the

TWO-WAY WIRELESS SECTION RADIO SYSTEM

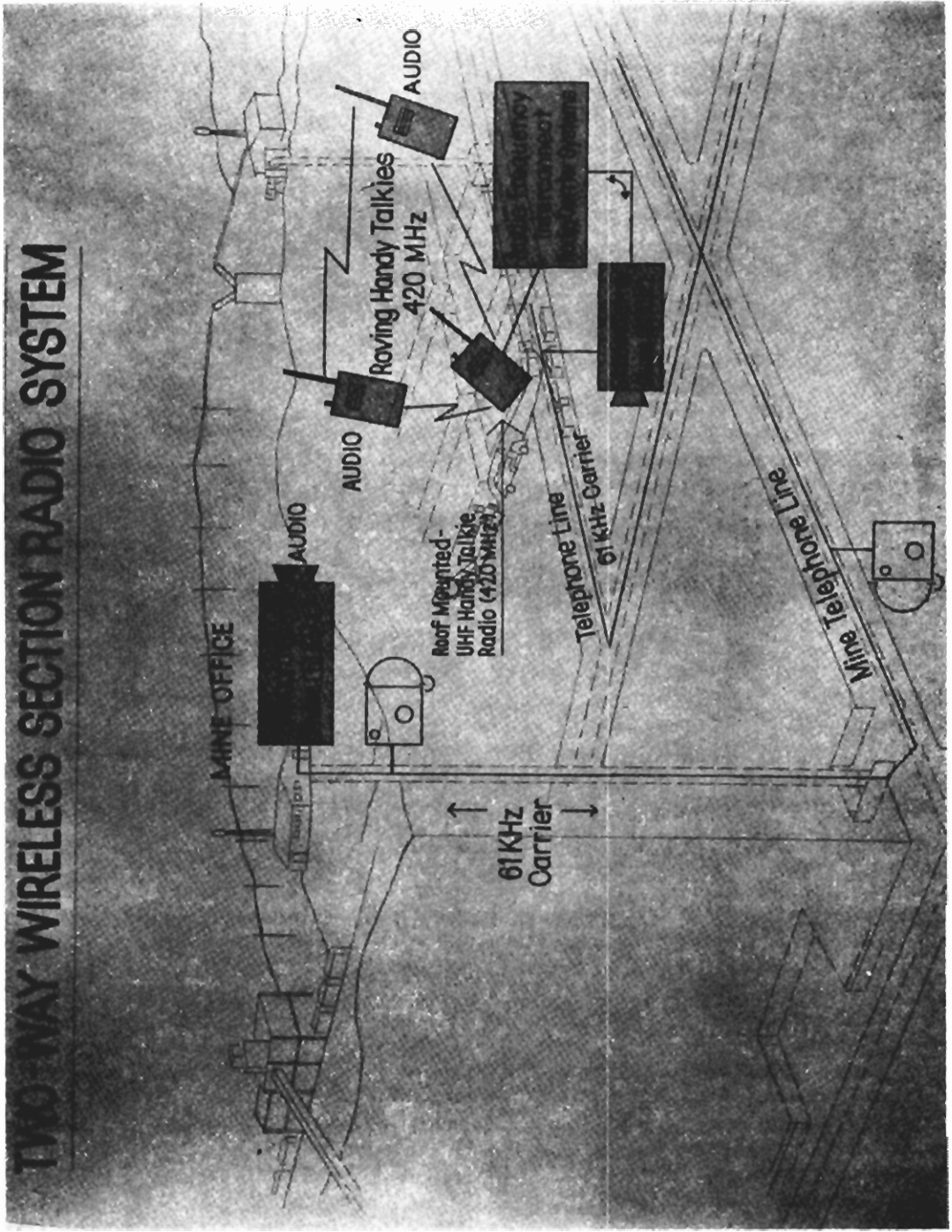


FIGURE 1 TWO-WAY WIRELESS SECTION RADIO SYSTEM

surrounding medium. By analogy, the roof, floor, and walls of a mine entry can be considered as imperfect mirrors and the radio waves as light beams. As the light beam, or radio wave, travels down the mine entry, bouncing off the walls, roof and floor, part of its energy is reflected at each bounce and therefore retained in the entry, while part of its energy is transmitted into the coal or rock by refraction and therefore lost.

Figure 2. - UHF Wireless Radio in Coal Mines.
Principle of Operation.

Figure 3 illustrates how the signal attenuation loss for mine entries varies with operating frequency for the dominant propagating mode. This loss represents the fractional decrease in strength, expressed in decibels (dB), suffered by the signal for each 100 feet it propagates down the entry. The curves in Figure 3 are based on data from propagation experiments performed in an operating high-coal mine, and on values calculated from theoretical equations. As shown, both theory and experiment indicate that: in high-coal entries, wireless radio signals are attenuated severely below the UHF frequency range, experience a broad favorable minimum in attenuation between 500 MHz and 2,500 MHz in the UHF band, and finally suffer a gradual increase in attenuation as the frequency is increased beyond the UHF frequency band. In low-coal the attenuation loss is shown to be more severe, particularly below 1,000 MHz. This low-coal behavior has only been partially confirmed by the routine use of 420 MHz handy talkies during field trips to mines.

Figure 3. - UHF Wireless Radio Signal Attenuation Loss
in Coal Mine Entries

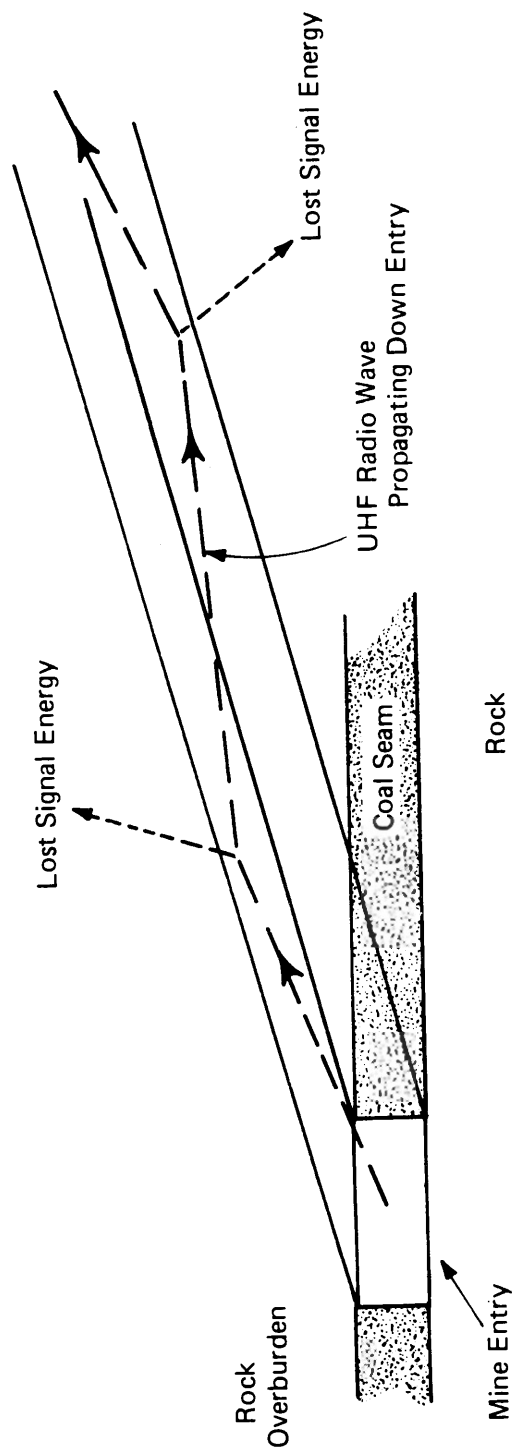


FIGURE 2 UHF WIRELESS RADIO IN COAL MINES -- PRINCIPLE OF OPERATION

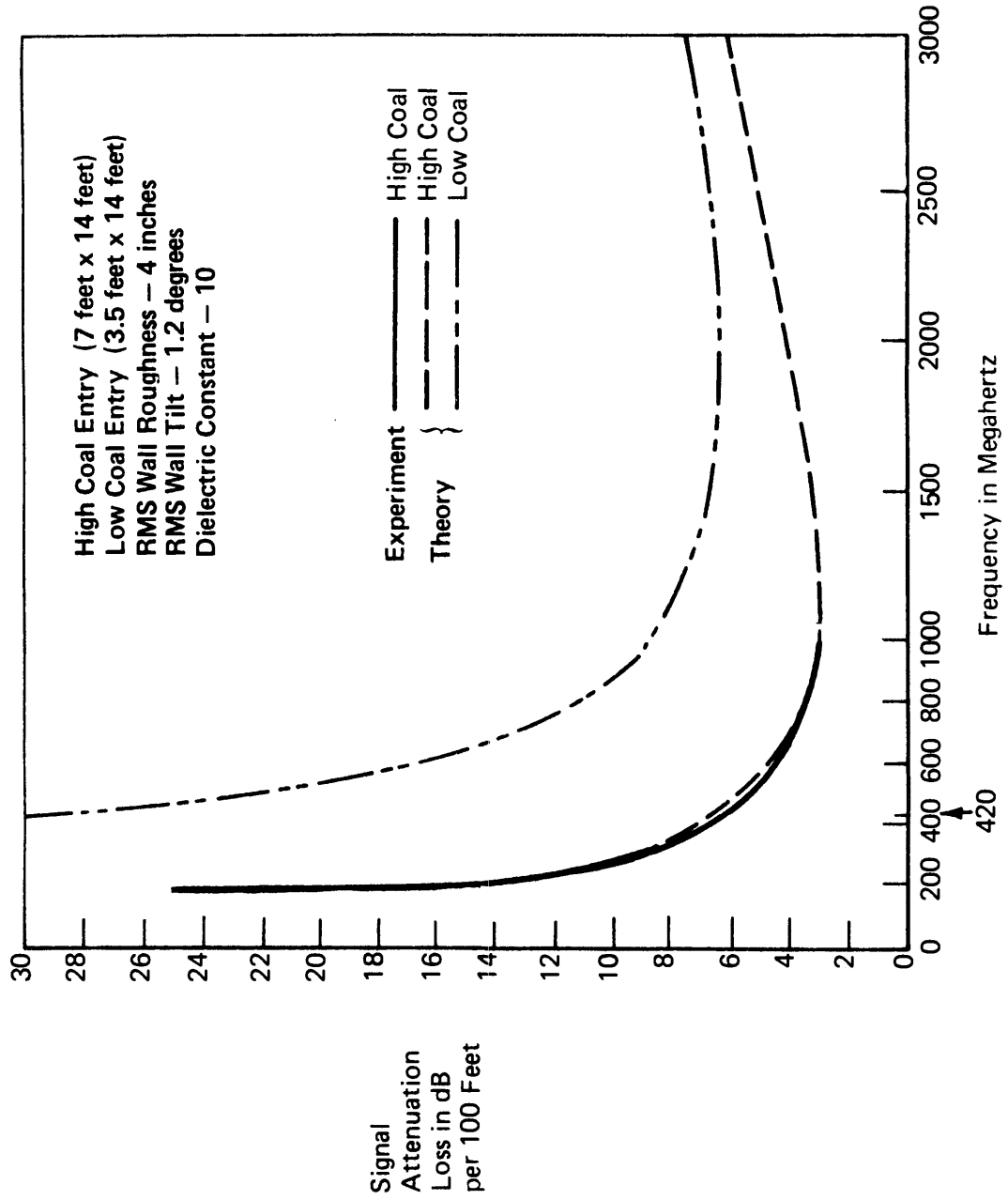


FIGURE 3 UHF WIRELESS RADIO SIGNAL ATTENUATION LOSS IN COAL MINE ENTRIES

The other major frequency dependent losses are antenna coupling loss and corner loss. When they are added to the attenuation loss, the appearance of an optimum operating frequency band becomes more pronounced. In high-coal, the optimum band is 400-to-1000 MHz. Within this band, the best frequency for a particular application will depend on the desired communication distance and whether the signal must travel around a corner to reach the receiver. For example, operating frequencies near 400 MHz are favored for transmission paths about 500 feet long that include one corner. Such paths are typical for section applications. Frequencies near 1000 MHz are favored for long straight line transmission paths along haulage ways.

The Bureau has tested portable mobile radio equipment up to the present frequency limit of equipment availability, the 450-MHz band, the band which also offers the most favorable performance for section applications in high-coal. Allocation of a new band of frequencies around 960 MHz for land mobile industrial applications is presently under consideration by the FCC. However, portable and fixed station 960 MHz equipment for haulage way applications will still not be commercially available for several years. Therefore our present investigations and range predictions were concentrated on the 450 MHz band.

Expected Coverage

Communication can be maintained between two separated individuals or stations until the separation distance increases to a point where the signal strength is not sufficient to overcome the background electrical noise. At UHF frequencies, measurements have shown that the levels of

this background noise will be governed by the intrinsic electrical noise of the UHF receivers rather than by externally generated electrical noise in the mine. The wireless radio coverage of a typical section in high-coal has been estimated for Motorola HT220 FM handy talkie units operating at a frequency of 420 MHz. These portable units have a transmitter power of two watts and receiver sensitivity of 0.5 microvolt for 20 dB of quieting.

Since communication on a working section requires coverage down cross-cuts, one must add to the straight line attenuation the loss incurred by the signal in going around at least one 90° corner. At 420 MHz, theory and experiment support the use of a corner loss of about 58 dB for the dominant propagating mode. To these losses must be added a total antenna coupling loss of about 46 dB to account for the insertion, polarization, and efficiency losses expected for two portable handy talkies. A nominal signal fade margin of 12 dB should also be included. The above values lead to the conservative section coverage prediction shown in Figure 4.

Figure 4. - Predicted UHF Wireless Radio Coverage

Figure 4 illustrates the coverage expected in a high-coal mine between a centrally located miner with a handy talkie unit and a second miner roving throughout the section with another unit. Miner-to-miner separation of more than half a section is possible, unaided by any transmission lines or other guiding cables. This separation can be doubled to cover the whole section by placing a repeater unit at the central location in the section.

Frequency — 420 MHz

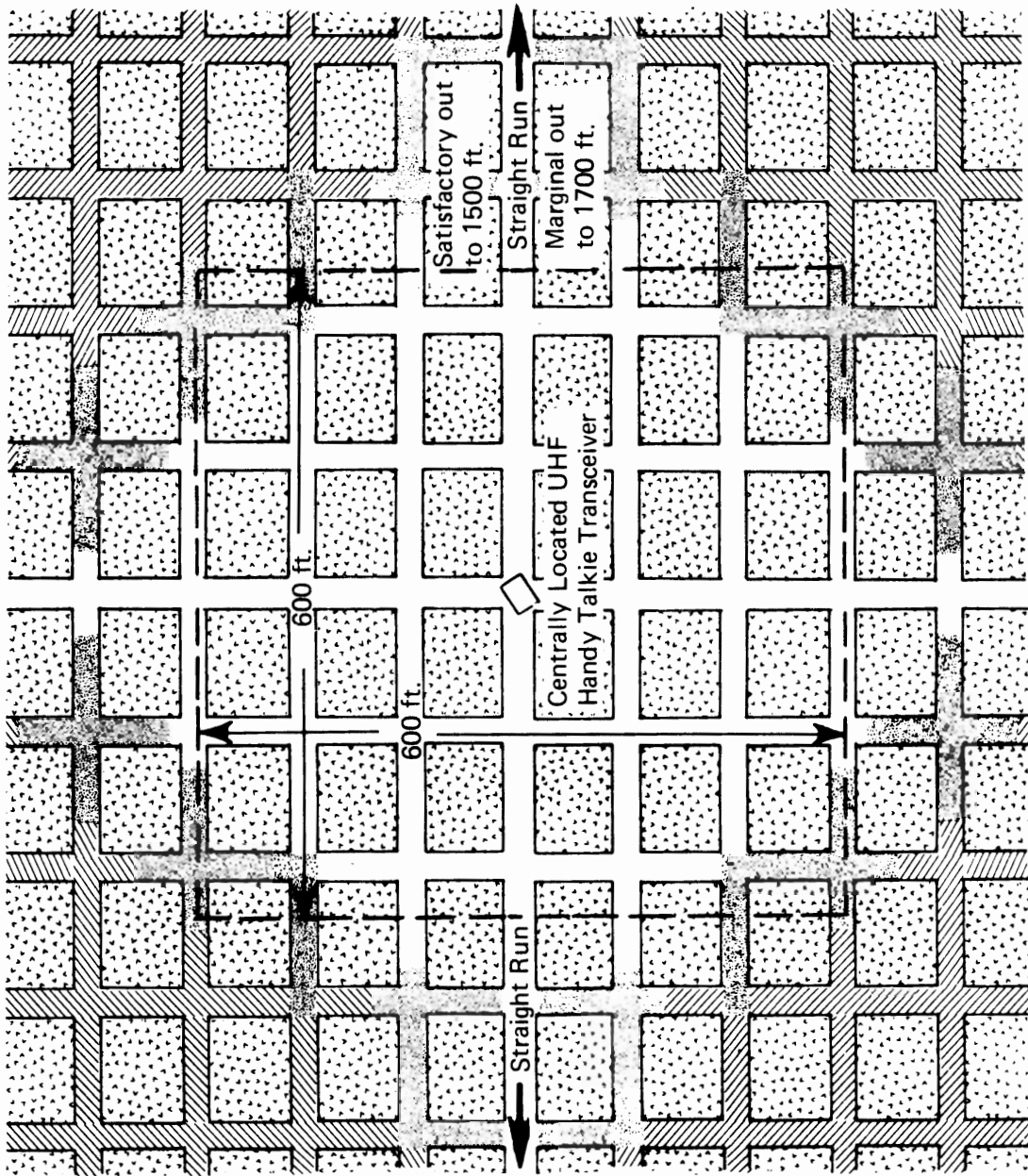


FIGURE 4 PREDICTED UHF WIRELESS RADIO COVERAGE

Note that when the signal must go around only one corner, satisfactory communication can be expected over a linear distance of approximately 500 feet down an entry and cross-cut. When no corners are encountered, as in a haulage way transmission path, satisfactory straight line communication can be expected over distances in excess of 1500 feet. These range limits can usually be somewhat extended if the handy talkies are rotated into the horizontal plane and pointed across the entry, thereby taking full advantage of the dominant horizontal field component. Practical ways to further extend section coverage, by reducing the relatively high corner loss, are presently under investigation.

Figure 5 represents a coverage diagram obtained for a portion of the Bureau's Safety Research mine at Bruceton. The coverage experienced in the Safety Research mine supports the coverage predictions of Figure 4. In Figure 5 the transmitter is located in the upper right-hand corner, and the coverage represents roughly one quadrant of a working section as indicated by the dimensions. The other three quadrants will experience the same coverage. Note that when the signal has to go around one corner, the coverage is as predicted, but that two corners produce a quick transition to unsatisfactory performance. The coverage to the left of Figure 5 does not extend beyond 200 feet because of the absence of a connecting cross-cut. Also depicted in Figure 5 are the main elements of the wireless section radio system installed in the Safety Research mine. This system will be described in the next part of this paper.

Figure 5. - UHF Two-Way Wireless Section Radio Coverage
In the Safety Research Mine

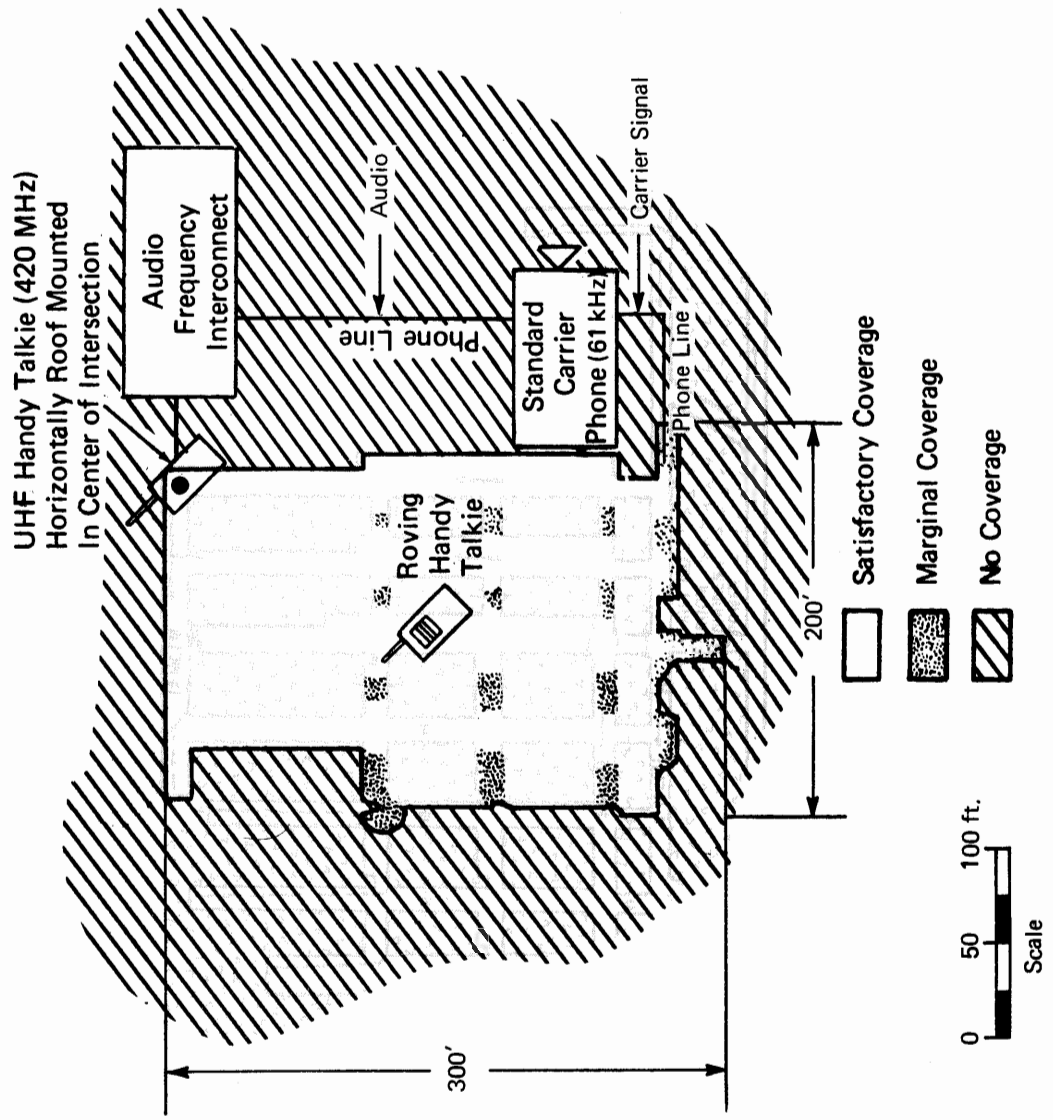


FIGURE 5 UHF TWO-WAY WIRELESS SECTION RADIO COVERAGE IN THE SAFETY RESEARCH MINE

System Description

An overall block diagram of a wireless section radio system is shown in Figure 6. Roving miner-to-miner direct wireless communication within the section is obtained by using channel two on the portable handy talkie units. In this direct mode of operation, the portable units transmit and receive on channel two. The system also provides roving miner communication with the surface on this same channel. This is accomplished by the use of a special interconnect unit which is roof-mounted with another handy talkie in an intersection at a centrally located position in the section. This radio-to-carrier system interconnect unit couples the audio frequency portion of the roof-mounted UHF handy talkie to the audio frequency portion of a 61 kHz standard miner carrier phone that is attached to the mine telephone line. In the mine office at the other end of the mine telephone line is a corresponding carrier phone unit which completes the mine-to-surface communication link. A conversation can be initiated from either the mine office or the roving miner on the section by simply using the mine office carrier phone or the portable handy talkies in their standard modes of operation. The system described provides an instantaneous direct private line to key roving miners on a section, even when the mine telephone line is busy with normal audio frequency communication traffic.

Figure 6. - Two-Way Wireless Section Radio System Block Diagram

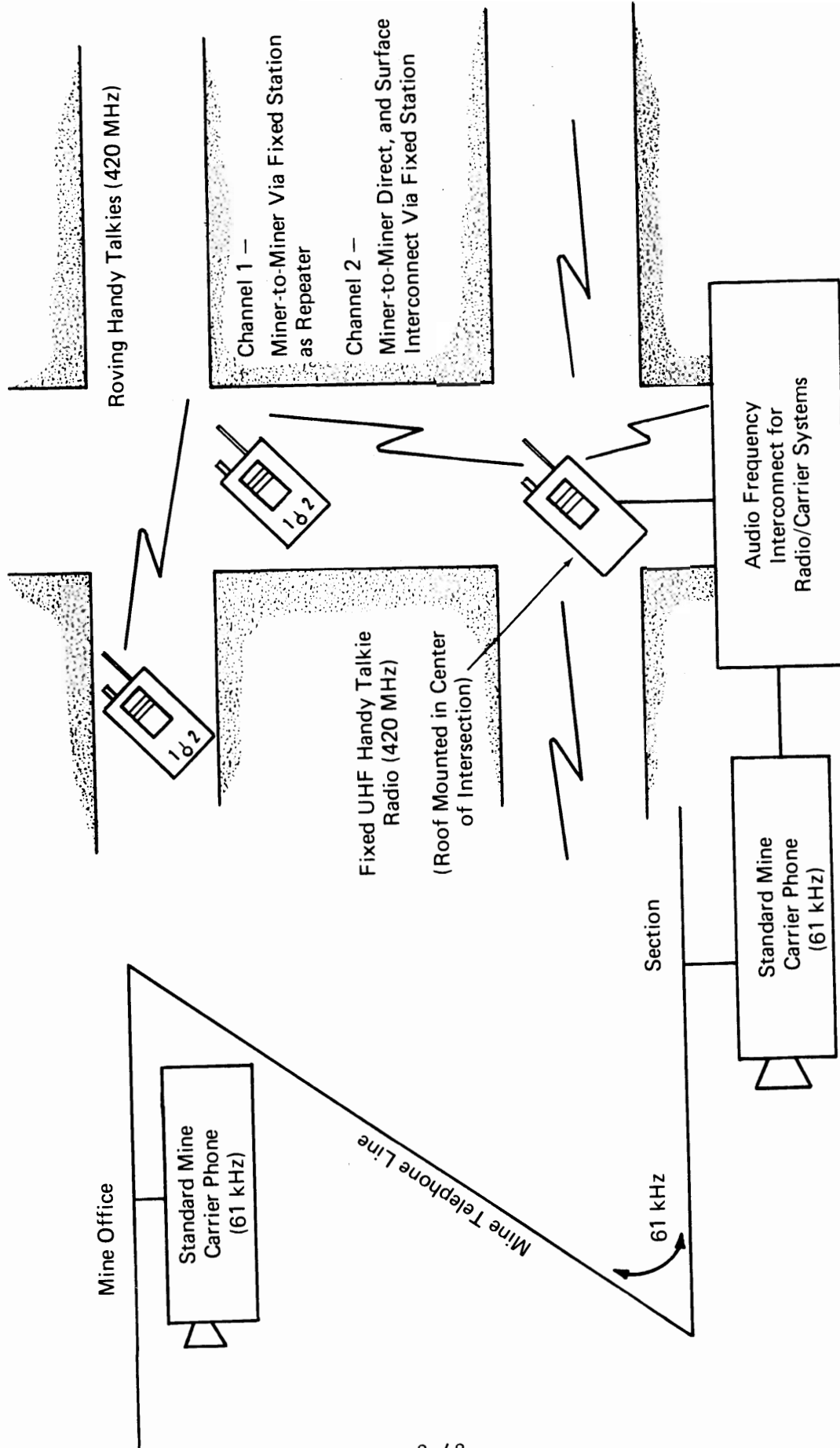


FIGURE 6 TWO-WAY WIRELESS SECTION RADIO SYSTEM BLOCK DIAGRAM

As stated in the coverage discussion, the roving miner-to-miner communication range can be doubled, thereby extending roving miner coverage to the whole section by using a roof-mounted repeater at the central location. To operate in the repeater mode, miners would switch to channel one. In this repeater mode of operation, the portable units transmit on channel one but still receive on channel two. This allows a centrally located repeater station to pick up the channel one transmissions of the miners and rebroadcast them on channel two for subsequent reception by the other handy talkies, thereby doubling the miner-to-miner range of the system.

Another benefit is obtained when in the repeater mode. Namely, roving miner-to-miner communications traffic will not clutter the section-to-surface interconnect channel, but messages from the surface will still be receivable by the roving miners.

Figure 7 shows a Motorola HT220 intrinsically safe handy talkie unit attached to a miner's belt. Operation can be via a push-to-talk switch and speaker-microphone that is an integral part of the handy talkie unit. Alternatively, the switch and speaker-microphone can be in the form of a hand-held accessory as shown in Figure 7. This accessory can be conveniently clipped to a pocket or lapel. Operation is also possible by means of a bone conductance microphone and ear speakers attached to the miner's hardhat as shown in Figure 8. The bone conductance microphone is situated in the middle of the hardhat webbing so that it can pick up the skull vibrations created when a person speaks. The ear speakers are put

close enough to the ears to hear the received audio while still leaving the ears open to the normal sounds in the mine. This hardhat unit can be operated by a belt-mounted push button as shown in Figure 8, or by means of a voice-operated switch which keys the transmitter on whenever the person speaks. This allows completely hands-free operation. Figure 9 depicts a handy talkie unit installed in a roof-mounted radio-to-carrier surface interconnect unit fabricated by Collins Radio Co. This station is typically mounted horizontally at a 45-degree angle in an intersection centrally located in the section. The cabling on the left goes to a standard mine carrier phone attached to the mine telephone line.

Figure 7. - Miner Using Intrinsically Safe Handy Talkie Unit

Figure 8. - Handy Talkie Operation Using Hardhat with Ear
Speakers and Bond Conductance Microphone

Figure 9. - Roof-Mounted Radio-to-Carrier Surface Interconnect
Unit and Handy Talkie Unit

The basic system depicted in Figure 6 can be used in a variety of ways and circumstances. It can be used to extend two-way communications between key roving miners within a section, and between these miners and the surface. The system can be used to communicate with roving miners along any haulage way having a mine telephone line by placing interconnect and repeater stations similar to those for sections at approximately 0.6 mile intervals along the haulage way. The system with the surface interconnect also lends itself to installation and use as a temporary surface-to-roving miner communication link during maintenance or rescue operations. Finally, this particular system can be modified for use with less expensive pocket pagers, instead of handy talkies to provide a more limited call alert or paging mode of operation.



FIGURE 7 MINER USING INTRINSICALLY SAFE HANDY TALKIE UNIT

8.51



FIGURE 8 HANDY TALKIE OPERATION USING HARDHAT WITH
EAR SPEAKERS AND BONE CONDUCTANCE MICROPHONE

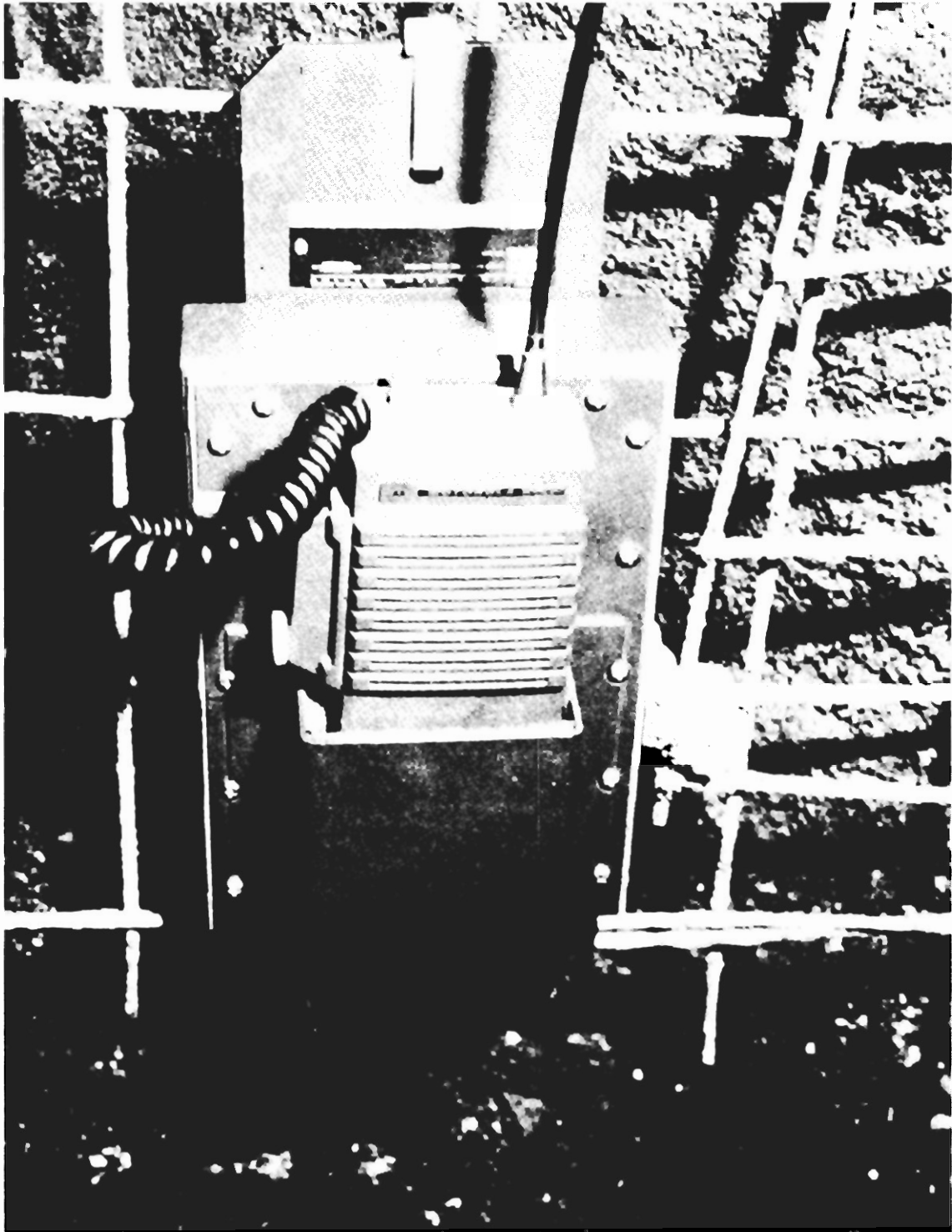


FIGURE 9 ROOF-MOUNTED RADIO-TO-CARRIER SURFACE
INTERCONNECT UNIT AND HANDY TALKIE UNIT

8.53

UHF GUIDED WIRELESS RADIO SYSTEM

The second UHF radio system treated in this paper is the guided wireless radio system. This system can provide communications between key individuals who may be roving at different locations along or near haulage ways, and between these same individuals and the surface. As in the wireless section radio application, the key roving individuals carry portable handy talkie radio transceivers. However, unlike wireless section radio, guided wireless radio uses a special cable to pick up, transport (guide), and radiate the radio frequency energy along haulage ways and main entries to communicate with the portable handy talkies. Figure 10 gives an overall conceptual view of a roving miner two-way haulage way communication system based on the guided wireless radio concept at UHF frequencies. As illustrated, such a system operating at UHF requires that a special cable (Radiax ^{T.M.} in this case) and auxiliary lines be hung along the walls of the haulage ways and selected section entries, together with periodically spaced repeater or base stations. The system will be described in detail under System Description.

Figure 10. - Guided Wireless Radio System

The UHF Radiax cable system was investigated because it has been receiving increased publicity and attention by the equipment suppliers and mine operators, and because of the favorable propagation characteristics at UHF for the area coverage desired in American coal mines. However, our investigations indicate that the desired area coverage is not achievable in an economical manner with Radiax cable. Furthermore,

much lower frequencies can be effectively used with more economical guiding cables if the desired communications can be restricted primarily to the haulage ways as in Europe.

Principles of Operation

Figure 11 depicts in schematic form a cross-section view of a coaxial cable and the lateral variation of its associated fields. In such cables the bulk of the radio frequency electromagnetic energy is transported down the cable between the center conductor and the shield. However, the shields of most practical cables do not provide perfect containment of the internal electromagnetic fields nor isolation from external fields. As shown, a small fraction of the cable's internal field is usually coupled to the external space. External fields are coupled into the cable in a similar manner. The existence of this weak coupling between internal and external fields forms the basis for several guided wireless systems for communicating with roving miners. Cables which transport most of the signal energy inside the cable have an added advantage; namely, performance is essentially not affected by normal accumulations of dirt and moisture, nor by installing the cable directly against the rib of a haulage way.

Figure 11. - Guided Wireless Radio with Coaxial Cable,
Principle of Operation

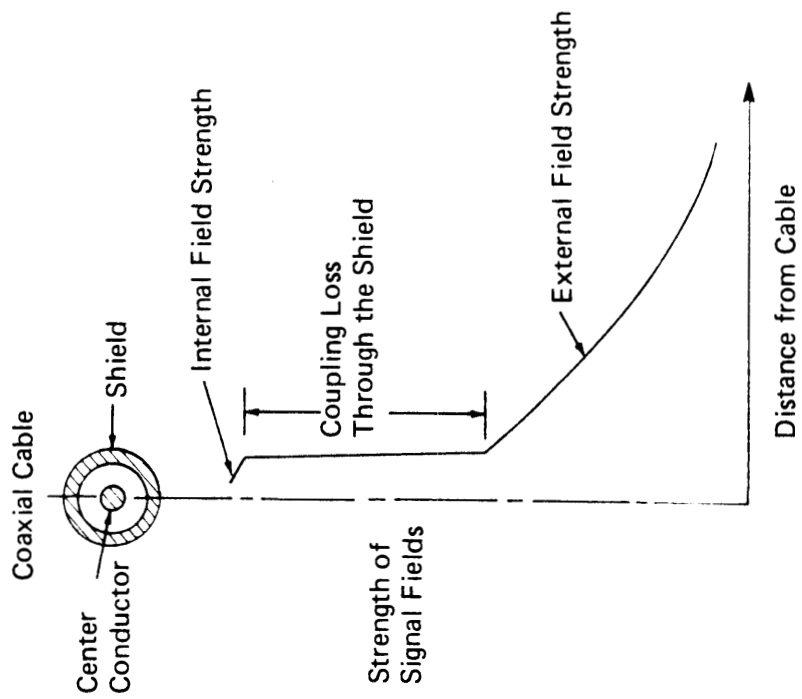


FIGURE 11 GUIDED WIRELESS RADIO WITH COAXIAL CABLE, PRINCIPLE OF OPERATION

As shown in Figure 11, the fields coupled to the external space will continue to decrease in strength with increasing distance from the cable. In addition, the internal and external fields will be attenuated, primarily because of the cable's resistance, as they travel along the cable to and from the fixed and portable communication stations. The amount of coupling loss and longitudinal attenuation loss experienced depends on the material and construction of the cable and on the operating frequency.

The UHF guided wireless system treated in this seminar is one based on the use of special semi-flexible RX4-1 Radiax coaxial cable of 1/2-inch diameter and 50 ohm characteristic impedance. The cable has a solid copper shield in which holes have been machined to increase the amount of coupling to the external space, as opposed to the braided-type shield used in conventional flexible cables for lower frequency applications. A cut-away view of the Radiax cable is shown in Figure 12. Its cost is more than ten times that of conventional braided cable used for cable television home installations. According to the cable manufacturer, Andrew Corporation, a lateral coupling loss of 85 ± 10 dB is experienced when the external signal strength is measured at a distance of 20 feet from RX4-1 Radiax cable. This loss includes the shield coupling loss and the radial spreading loss for this distance and applies for both incoming and outgoing signals. The longitudinal attenuation loss is 2.1 dB/100 feet.

Figure 12. - Radiax Coaxial Cable, Cut-a-Way View

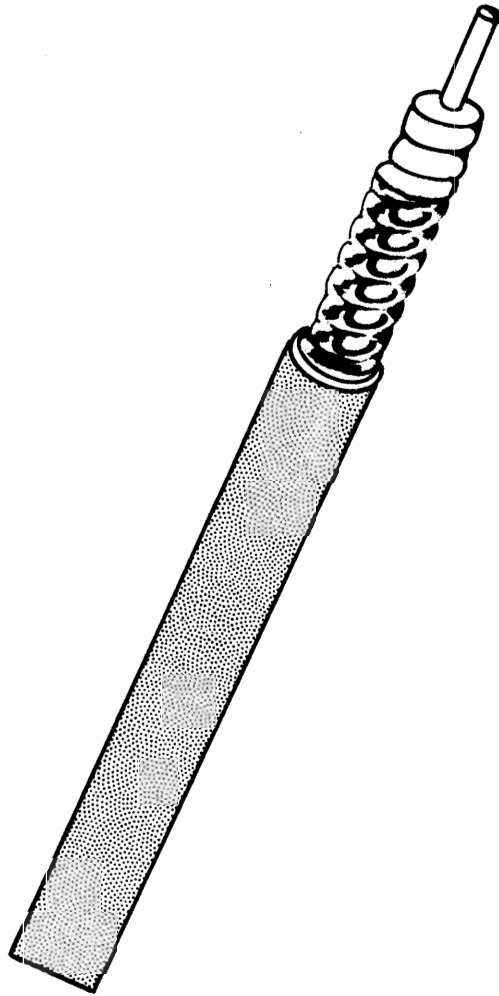


FIGURE 12 RADIAX COAXIAL CABLE, CUT-AWAY VIEW

Figure 13 is a sketch illustrating how signals both in the cable and in the haulage way decrease in strength as the distance along the cable from a repeater station is increased. Signal voltages and external fields are reduced in strength by a factor of 10⁻¹ (20 dB) for every 950 feet of cable traveled, due to the 2.1 dB/100 ft longitudinal attenuation rate. Figure 13 depicts the decrease in signal strength for transmissions by the repeater. A similar signal strength decrease occurs for transmissions from a handy talkie, but with the signal strength now being largest at the handy talkie location and decreasing as the signal travels in the cable towards the repeater.

Figure 13. - Two-Way Communication Range for Radiax Guided
Wireless Radio System

In spite of the holes, the coupling loss imposed by the shield is still high and requires the use of repeaters (to amplify and retransmit incoming signals) to allow communication via this cable between roving miners carrying portable handy talkie radios. The spacing of these repeaters along the cable (base stations if only a surface-to-mine channel is desired) will be governed primarily by the lateral range desired from the cable, the longitudinal attenuation rate of the cable, and the transmitter power of the portable units. Since the transmitter power available for portable units is generally lower than that available for fixed repeater or base stations, the portable units set the coverage limits for two-way communications.

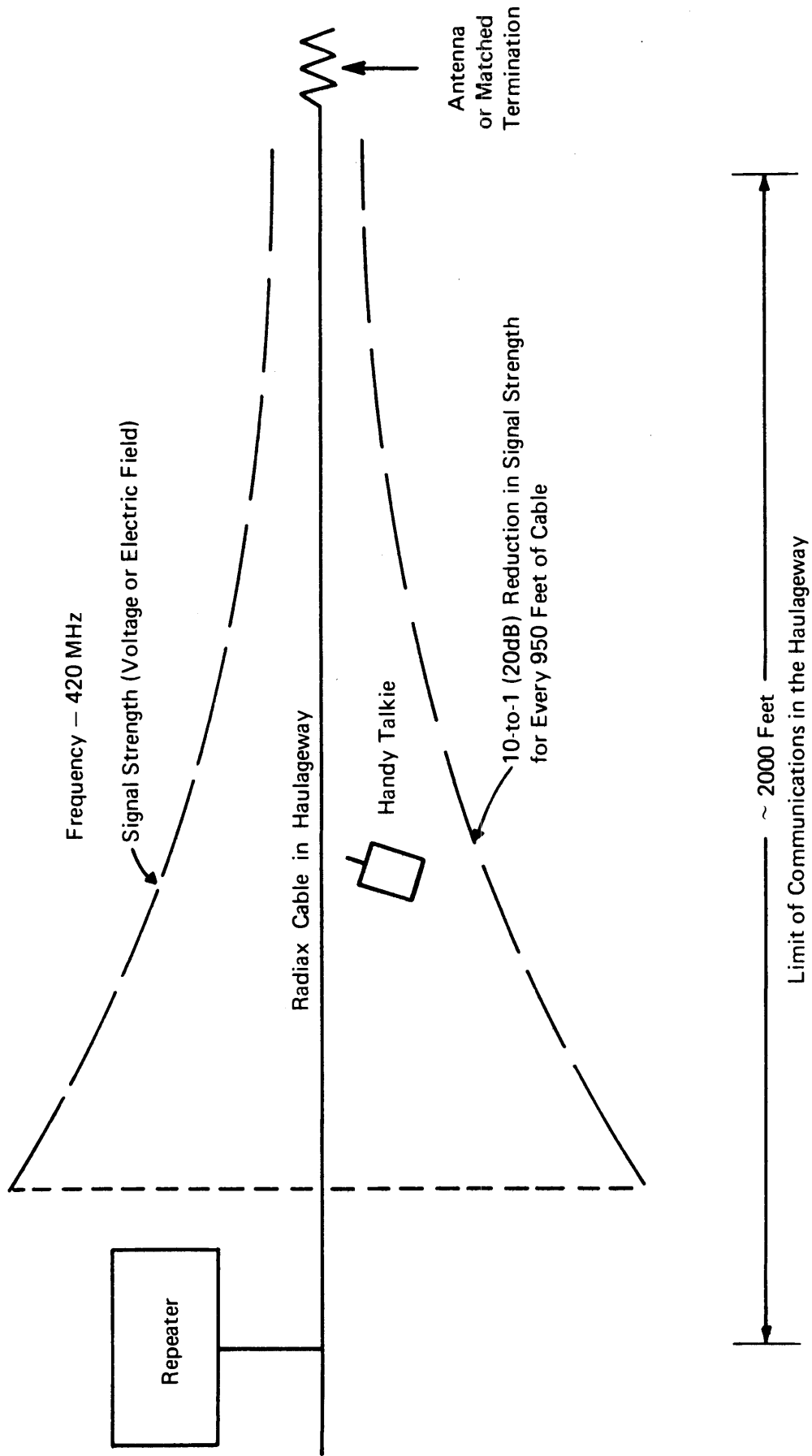


FIGURE 13 TWO-WAY COMMUNICATION RANGE FOR RADIAX GUIDED WIRELESS RADIO SYSTEM

Expected Coverage

The two-way coverage obtainable with a guided wireless radio system has been estimated for a haulage way installation consisting of the Andrew RX4-1 Radiax coaxial cable, two-watt base stations and repeaters, and the same Motorola HT220 two-watt handy talkies used for the wireless section radio system. As in the case of wireless section radio, communication range will be limited by intrinsic receiver noise as opposed to external electrical noise. The coverage estimates are based on lateral coupling loss and longitudinal attenuation data supplied by the cable manufacturer, preliminary experimental data obtained for the Radiax installation in the Bureau's Safety Research mine, and some of the theoretical and experimental results discussed under wireless section radio. Of particular interest are the ranges expected along haulage ways and down entries crossing haulage ways.

When an entry crossing the haulage way is close to a repeater station, two-way lateral coverage should be possible to handy talkie radios located 300-to-500 feet down the cross entry. Figure 14 illustrates the expected signal behavior and coverage down such a cross entry. Once the UHF signal field becomes well established in the cross entry, its propagation down the entry and around subsequent corners will be governed by the same principles and attenuation rates discussed under wireless section radio.

Figure 14. - Guided Wireless Radio System, Propagation
Down Cross-Cuts Off Haulage Ways

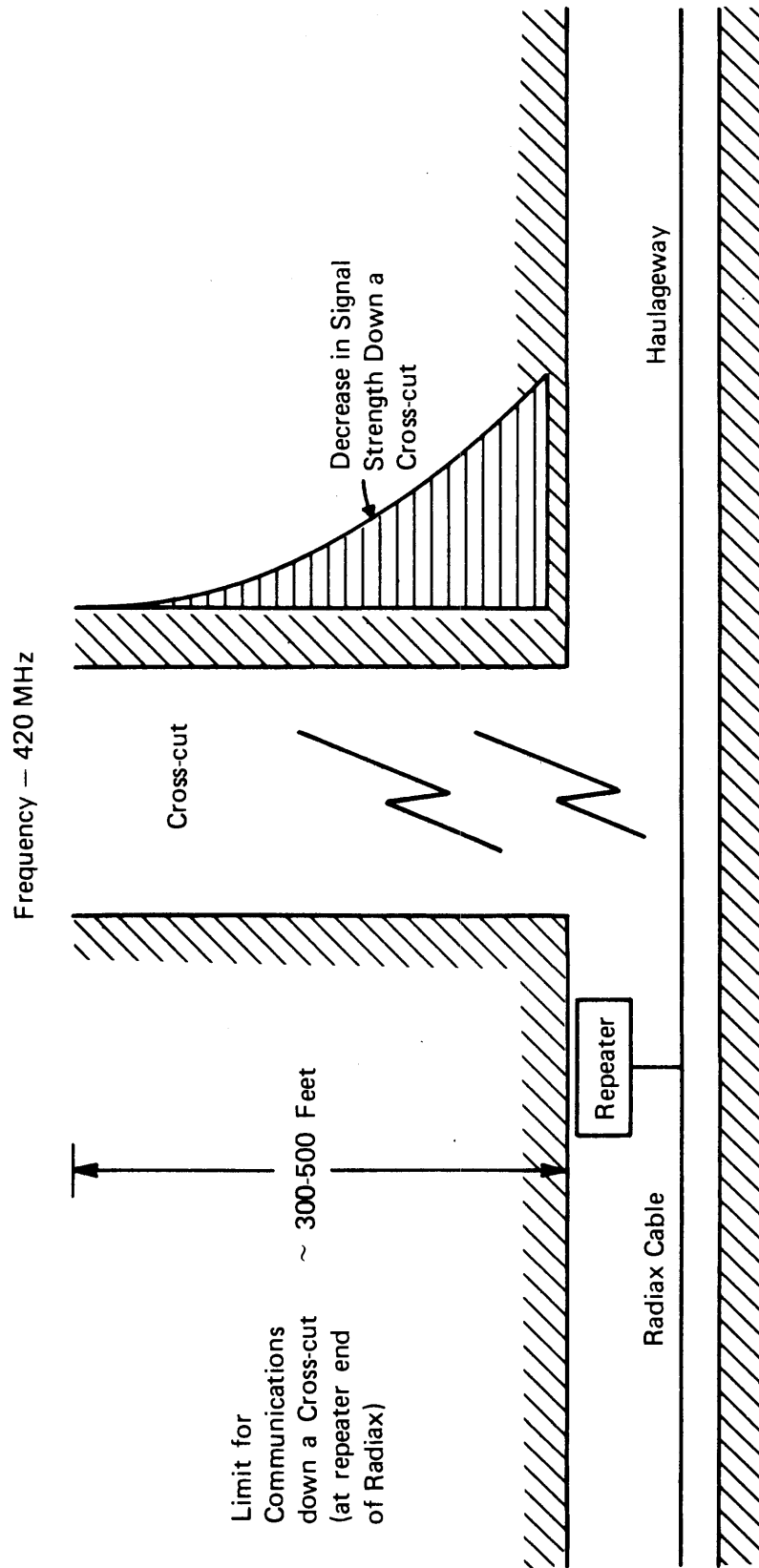


FIGURE 14 GUIDED WIRELESS RADIO SYSTEM, PROPAGATION DOWN CROSS-CUTS OFF HAULAGEWAYS

As the distance between the cross entry and the haulage way repeater station becomes larger, the signal available at the mouth of the entry will become weaker, so the lateral coverage down the cross entry will be correspondingly reduced. Eventually the two-way coverage will be restricted to the confines of the haulage way cross-section. The manufacturers of the cable and portable handy talkies, Andrew and Motorola respectively, have found that coverage becomes confined to the haulage way at a distance of approximately 2,000 feet down the cable from the repeater station as indicated in Figure 13 above. This 2,000-foot distance limit dictates that a UHF Radiax cable system, if designed to give two-way coverage primarily in the haulage way, will require a repeater placed at the center of each 4,000-foot run of cable. If coverage is also desired down cross entries, the spacing between the repeaters will have to be reduced to meet the minimum two-way lateral coverage required in the cross entry located midway between repeater stations.

In sum, the UHF Radiax-based guided wireless system does provide some lateral two-way coverage down entries crossing haulage ways, but this lateral coverage does not remain constant or large over a substantial length of a cable run. This decreases the attractiveness of the Radiax system from the standpoints of cost and practicality for providing area coverage in a U.S. mine environment. If, on the other hand, the coverage requirement can be limited to the haulage way, this requirement can be more economically satisfied in a practical manner by using much lower frequencies together with less expensive coaxial cables, the mine power cables, or the trolley wire/track transmission line.

System Description

Figure 15 is a block diagram of a basic UHF guided wireless radio system using Radiax cable. It represents the kind of equipment needed for a UHF haulage way application. The system also has a branch-off and associated antenna termination to allow communication with roving miners on a section. Communications from the surface to a roving miner are established by means of audio and control lines that go from the control console on the surface to repeaters (or base stations) at fixed locations in the haulage way. The transmitters of these fixed stations send UHF radio signals down the Radiax cable to roving miners equipped with portable handy talkies. These handy talkies pick up a portion of the signal energy coupled into the haulage way by the holes in the shield of the cable. Conversely, radio transmissions from the roving miners are picked up via the holes in the cable and carried inside the cable to a repeater or base station, where the audio output is sent via the audio and control lines to the control console on the surface.

Figure 15. - A UHF Guided Wireless Radio System
Using Radiax Cable

If only roving miner-to-surface communication is required, base stations instead of repeaters can be used, with only a single frequency (channel two) for transmit and receive being required for both the base stations and portable units. If roving miner-to-roving miner communication is required, in addition to communication with the surface, repeater stations that receive, amplify, and retransmit signals from the

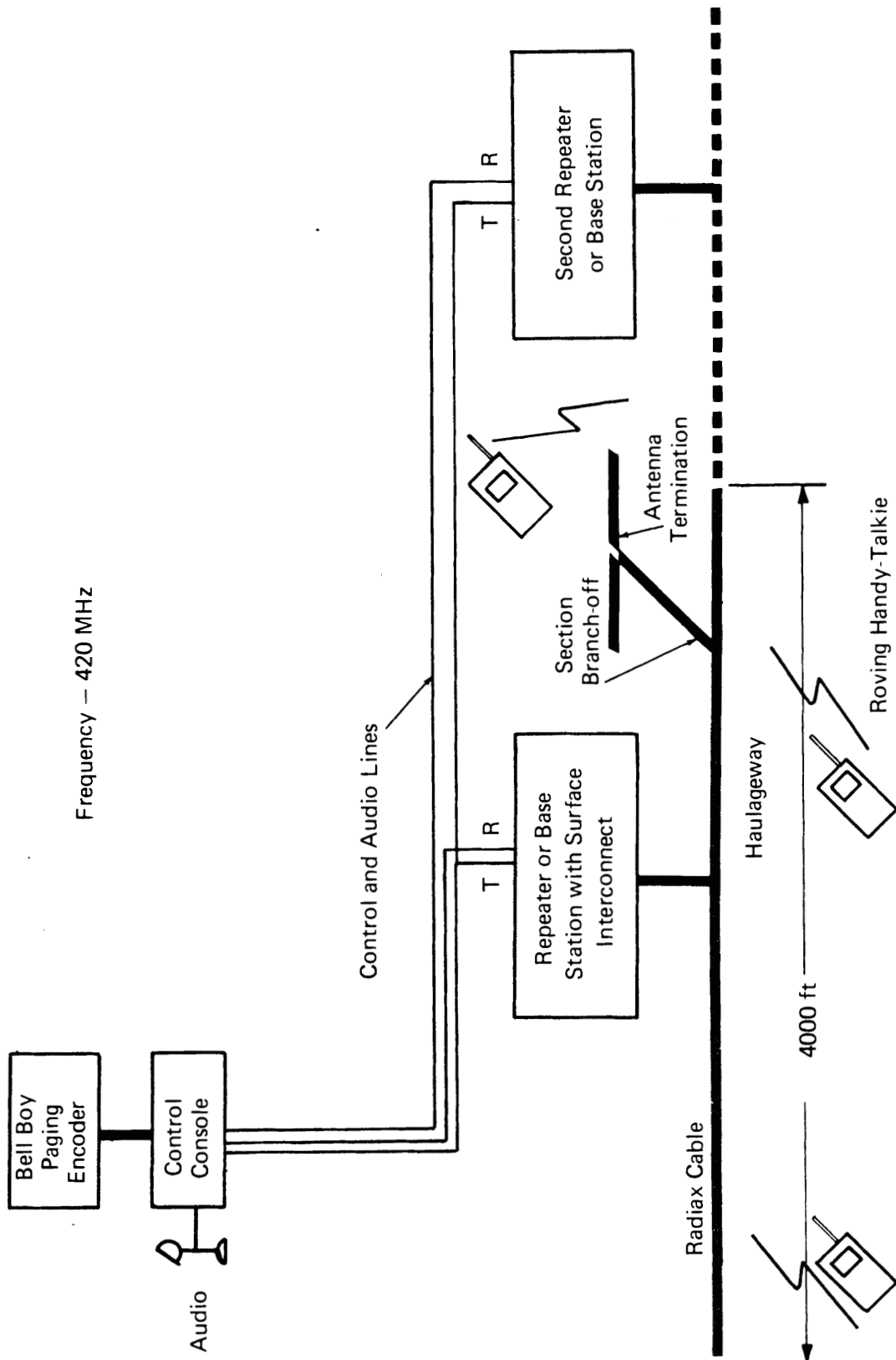


FIGURE 15 A UHF GUIDED WIRELESS RADIO SYSTEM USING RADIAX CABLE

portables must be used, together with two frequencies. (In this case, channels one and two will be needed for transmit and receive by the portables, respectively, and vice versa for the repeater stations.) Adequate two-way coverage in the haulage way is obtained by spacing the repeaters or base stations 4000 feet apart.

As shown in Figure 15, each fixed station has an independent audio line for relaying received messages to the surface. However, a common audio line is used to activate all fixed stations along the haulage way for transmitting messages from the surface. This allows the surface to cover the entire haulage way with a single transmission, and to receive noninterfering replies from miners located along different 4000-foot sections of the cable. To provide roving miner-to-roving miner communication between miners located along different 4000-foot sections of cable, additional audio and control lines must be run between each of the repeater stations, to allow each message from a portable to be automatically retransmitted by all repeater stations along the haulage way.

Figure 16 depicts a UHF guided wireless radio Radiax cable system installed in the Bureau's Safety Research mine. The dimensions of this small mine approach those of a 600 ft. x 600 ft. mine section, so the cable layout is somewhat representative for a section application without an antenna termination. A two frequency 12-watt Motorola repeater station located outside the mine is used for miner-to-miner and miner-to-surface communications. A single frequency 40-watt Motorola base station located in the mine is used as an alternative miner-to-surface communication path. The system is also equipped with a paging encoder as indicated

in Figure 15. This encoder provides a more limited call alert or paging mode of operation with less expensive pocket pagers instead of handy talkies.

Figure 16. - UHF 420 MHz Guided Wireless Radio System
Installed in the Safety Research Mine

Figure 17 shows the system control console which would normally be located on the surface. Figure 18 is a photograph of the two-frequency 12-watt repeater station, while Figure 19 shows the 40-watt base station and special power supply unit. The 2-watt handy talkies are the same ones discussed under wireless section radio and are shown in Figure 7.

Figure 17. - System Control Console

Figure 18. - Two-Frequency 12-Watt Repeater Station

Figure 19. - Single Frequency 40-Watt Base Station
and Special Power Supply Unit

The installation shown in Figure 16 did not meet our performance expectations despite the use of approximately 2,000 feet of Radiax cable. Complete two-way coverage of the mine was not obtained. The worst areas were largely located in the left half of the mine, particularly in the vertical cross-cut with the 45-degree corner on the map in Figure 16, but pockets of weak performance were also present in other parts of the mine. Means of improving this performance by the addition of antenna terminations at selected locations are currently under investigation.

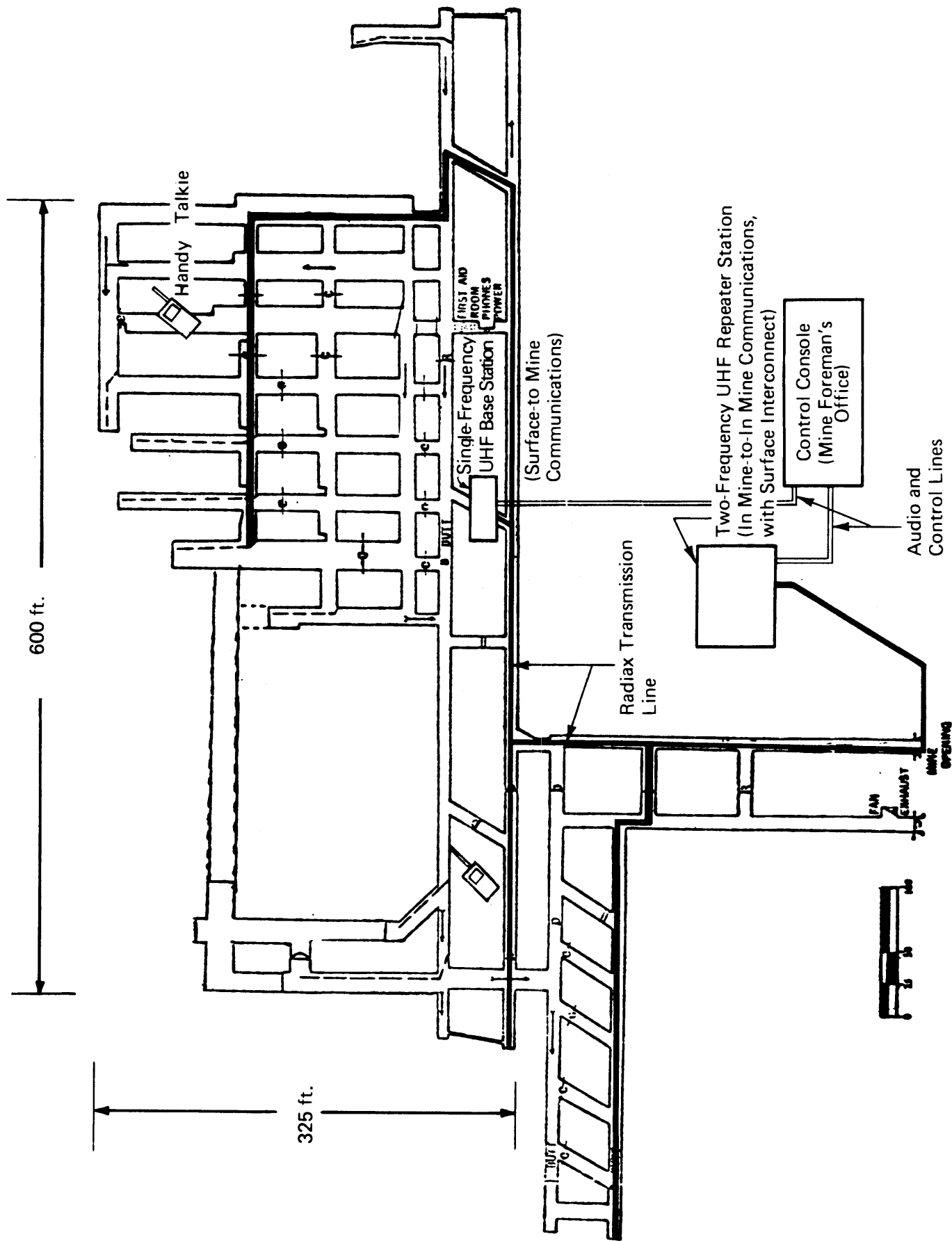


FIGURE 16 UHF 420 MHz GUIDED WIRELESS RADIO SYSTEM INSTALLED IN THE SAFETY RESEARCH MINE



FIGURE 17 SYSTEM CONTROL CONSOLE



FIGURE 18 TWO-FREQUENCY 12-WATT REPEATER STATION

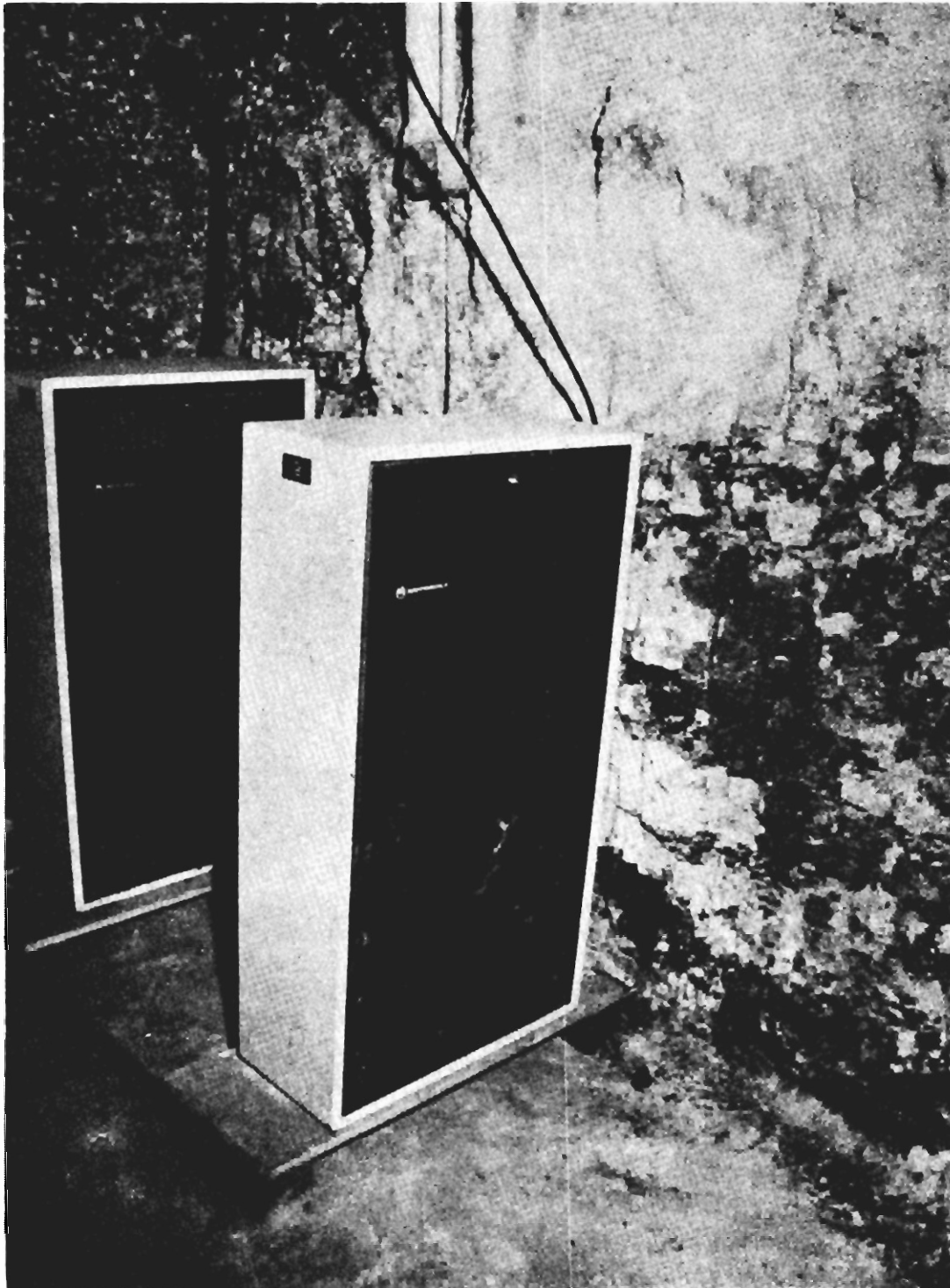


FIGURE 19 SINGLE FREQUENCY 40-WATT BASE STATION
AND SPECIAL POWER SUPPLY UNIT
8.72

UHF OVERLAND LOOPBACK

The Bureau has also investigated means of looping underground communication channels back to their points of origin on the surface. An example of a typical overland radio loopback channel is shown as part of Figure 10. In this illustration it is used to loopback a Radiax guided wireless radio communications channel. As shown in Figure 10 the audio output of an in-mine fixed station is brought, via audio and control lines in a power borehole or ventilation shaft, to a surface loopback station consisting of a 12-watt, six-channel UHF transmitter/receiver and associated antenna. Figure 20 is a photograph of such a surface loopback station located near a borehole. The UHF radio loopback system can also loopback the outputs of the underground mine phone and carrier phone communication channels, and those of mine environment monitoring channels. This is done by running independent sets of wires up the same borehole to the UHF loopback station on the surface and occupying more of its UHF channels. On the surface, all messages are transmitted overland to a similar transmit/receive station located near the mine foreman's office, and subsequently to appropriate monitoring or control stations.

Figure 20. - Surface Transmitter/Receiver/Antenna Station
for Overland Radio Loopback

By placing the surface stations at strategic locations, the mine phone line, trolley wire, and environment monitoring channels as well as wireless and guided wireless channels can be looped back together. In this manner every transmission that goes into the mine via a primary route can be sent out again via the overland loopback. If a break should occur in any

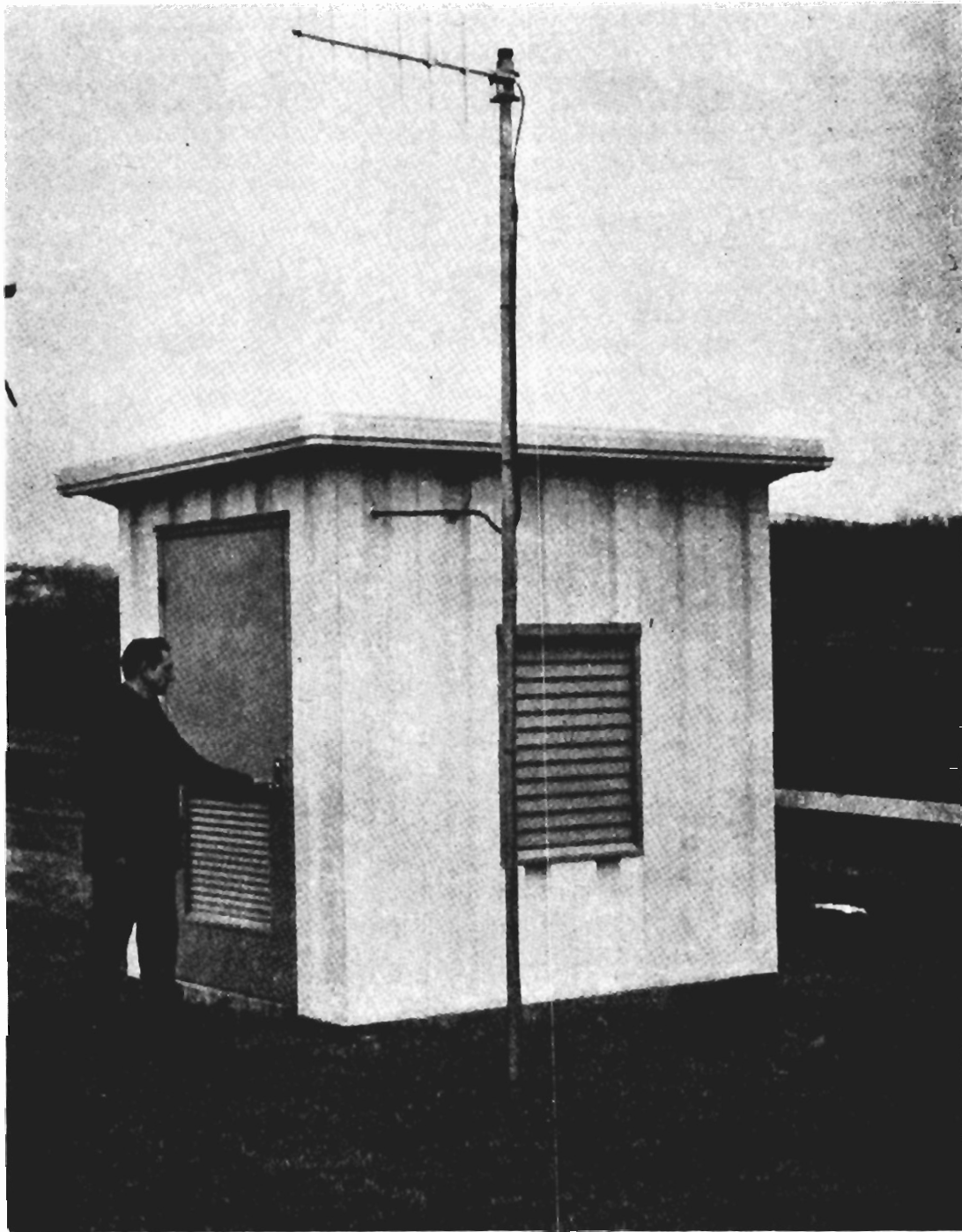


FIGURE 20 SURFACE TRANSMITTER/RECEIVER/ANTENNA
STATION FOR OVERLAND RADIO LOOPBACK

one of the communication channels and a miner in by the break cannot be reached by the primary route, the loopback route can be used to reach him. Surface power lines and telephone lines are also suitable for looping back in-mine communication channels.

CONCLUDING REMARKS

The general features of the methods discussed in this paper for establishing two-way wireless and guided wireless radio communications between underground roving miners at UHF are summarized in Table 1.

Table 1. - UHF Radio In Mines for Roving Miner-to-Miner Communications

<u>Method</u>	<u>Units of Coverage</u>	<u>Equipment (per unit of coverage)</u>
Direct Wireless	Half Section, or 0.3 Mile of Haulage Way	Handy Talkies
Wireless Via Repeater	Whole Section, or 0.6 Mile of Haulage Way	Handy Talkies, Plus Central Low-Power Repeater
Guided Wireless Via Repeater and Radiax Cable	Whole Section, or 0.8 Mile of Haulage Way	Handy Talkies, Plus Central High-Power Standard Repeater, Plus Radiax Cable Along Haulage Way or Distrib- uted in Section

Furthermore, roving miner communications can be established with the surface, and between separate coverage units along haulage ways or different sections, by adding interconnect equipment appropriate to each method. The wireless-via-repeater method can use a radio-to-carrier

interconnect to the existing mine phone line at each repeater location, together with a standard carrier phone at the surface end of the mine phone line. The guided wireless method can use interconnect equipment similar to that for the wireless method, or install a set of audio and control lines connecting all the repeater stations with each other and with a surface console station. The latter approach is the current practice for Radiax-based guided wireless systems.

In sum, our investigations reveal that UHF wireless section radio is more effective, practical and economical than Radiax-based UHF guided wireless radio for both section and haulage way roving miner applications. Wireless section radio also provides superior flexibility for establishing two-way communications at locations that may temporarily require wireless coverage because of an emergency or maintenance problem. For strictly haulage way applications, much lower frequencies and lower cost transmission lines appear to offer other advantages, and are presently being investigated.

II. THROUGH-THE-EARTH ELECTROMAGNETICS WORKSHOP

A. INTRODUCTION

During the summer of 1973, ADL provided technical and support assistance to PMSRC related to a Bureau-sponsored Through-the-Earth Electromagnetics Workshop at the Colorado School of Mines. This workshop brought together people currently doing research and development relating to the design of electromagnetic systems for communicating with, and/or locating, sub-surface miners. The objective of this workshop was to present and discuss the latest results of the work of these investigators; to summarize the present status of developments related to this work; and to recommend short- and long-term research and development efforts needed to advance the state-of-the-art and further the development of practical electromagnetic mine communication and location systems.

ADL's assistance included: technical planning and supporting services related to the Bureau's participation in the workshop; active participation of ADL staff during the workshop, both in the presentation of a Bureau-sponsored paper entitled, "Theory of the Propagation of UHF Radio Waves in Coal Mine Tunnels", and as Chairmen of two Working Groups on "Uplink and Downlink Communications" and "Operational Communications"; reviewing of papers submitted for the Workshop Proceedings; and preparation of two reports summarizing the present status and recommendations regarding the research and development areas treated by the above Working Groups.

The UHF Theory summary paper and the two Working Group summary reports mentioned above will appear in the Proceedings of the Workshop,* and have been included in the following sections of this Part for convenient reference.

* These Proceedings are to be published as part of the Colorado School of Mines Final Report to the Bureau of Mines on Grant G133023.

**B. THEORY OF THE PROPAGATION OF UHF RADIO WAVES
IN COAL MINE TUNNELS**

by

**Alfred G. Emslie,¹
Robert L. Lagace,² and Peter F. Strong²**

ABSTRACT

This paper is concerned with the theoretical study of UHF radio communication in coal mines, with particular reference to the rate of loss of signal strength along a tunnel, and from one tunnel to another around a corner. Of prime interest are the nature of the propagation mechanism and the prediction of the radio frequency that propagates with the smallest loss. Our theoretical results are compared with measurements made by Collins Radio Co. This work was conducted as part of the Pittsburgh Mining and Safety Research Center's investigation of new ways to reach and extend two-way communications to the key individuals that are highly mobile within the sections and haulage ways of coal mines.

INTRODUCTION

At frequencies in the range of 200-4,000 MHz the rock and coal bounding a coal mine tunnel act as relatively low loss dielectrics with dielectric constants in the range 5-10. Under these conditions a reasonable hypothesis is that transmission takes the form of waveguide propagation in a tunnel, since the wavelengths of the UHF waves are smaller than the tunnel dimensions. An electromagnetic wave traveling along a rectangular tunnel in a dielectric medium can propagate in any one of a number of allowed waveguide modes. All of these modes are "lossy modes" owing to the fact that any part of the wave that impinges on a wall of the tunnel is partially refracted into the surrounding dielectric and partially reflected back into the waveguide. The refracted part propagates away from the waveguide and represents a power loss. This type of waveguide mode differs from the light-pipe modes in glass fibers in which total internal reflection occurs at the wall of the fiber, with zero power loss if the fiber and the matrix in which it is embedded are both lossless. It is to be noted that the attenuation rates of the waveguide modes studied in this paper depend almost entirely on refraction loss, both for the dominant mode and higher modes excited by scattering, rather than on ohmic loss. The effect of ohmic loss due to the small conductivity of the surrounding material is found to be negligible at the frequencies of interest here, and will not be further discussed.

The views and conclusions contained in this document are those of the authors and should not be interpreted as necessarily representing the official policies of the Interior Department's Bureau of Mines or the U.S. Government. This paper was prepared under USBM Contract No. H0122026.

1. Consultant: Formerly with Arthur D. Little, Inc. (Retired)
2. Arthur D. Little, Inc., Cambridge, Massachusetts.

The study reported here is concerned with tunnels of rectangular cross section and the theory includes the case where the dielectric constant of the material on the side walls of the tunnel is different from that on top and bottom walls. The work extends the earlier theoretical work by Marcatili and Schmeltzer⁽¹⁾ and by Glaser⁽²⁾ which applies to waveguides of circular and parallel-plate geometry in a medium of uniform dielectric constant.

In this paper we present the main features of the propagation of UHF waves in tunnels. Details of the derivations are contained in Arthur D. Little, Inc. reports.⁽³⁾

THE FUNDAMENTAL (1,1) WAVEGUIDE MODES

The propagation modes with the lowest attenuation rates in a rectangular tunnel in a dielectric medium are the two (1,1) modes which have the electric field \vec{E} polarized predominantly in the horizontal and vertical directions, respectively. We will refer to these two modes as the E_h and E_v modes.

The main field components of the E_h mode in the tunnel are

$$E_x = E_0 \cos k_x x \cos k_y y e^{-ik_z z} \quad (1)$$

$$H_y = (k_z / \omega \mu_0) E_0 \cos k_x x \cos k_y y e^{-ik_z z} \quad (2)$$

where the symbols have their customary meaning. The coordinate system is centered in the tunnel with x horizontal, y vertical, and z along the tunnel. In addition to these transverse field components there are small longitudinal components E_z and H_z and a small transverse component H_x . For the frequencies of interest here k_x and k_y are small compared with k_z which means that the wave propagation is mostly in the z -direction. From a geometrical optics point of view, the ray makes small grazing angles with the tunnel walls.

In the dielectric surrounding the tunnel the wave solution has the form of progressive waves in the transverse as well as the longitudinal directions. The propagation constant k_z for the (1,1) mode is an eigenvalue determined by the boundary conditions of continuity of the tangential components of \vec{E} and \vec{H} at the walls of the tunnel. Owing to the simple form of the wave given by (1) and (2) these conditions can be satisfied only approximately. However, a good approximation to k_z is obtained. The imaginary part of k_z , which arises owing to the leaky nature of the mode, gives the attenuation rate of the wave. The loss L_{E_h} in dB for the (1,1) E_h mode is given by

$$L_{E_h} = 4.343 \lambda^2 z \left(\frac{K_1}{d_1^3 \sqrt{K_1 - 1}} + \frac{1}{d_2^3 \sqrt{K_2 - 1}} \right) \quad (3)$$

where K_1 is the dielectric constant of the side walls and K_2 of the roof and floor of the tunnel. The corresponding result for the (1,1) E_v mode is

$$L_{E_v} = 4.343 \lambda^2 z \left(\frac{1}{d_1^3 \sqrt{K_1 - 1}} + \frac{K_2}{d_2^3 \sqrt{K_2 - 1}} \right) \quad (4)$$

These results are valid if the wavelength λ is small compared with the tunnel dimensions d_1 and d_2 . The same formulas are also obtained if one adds the attenuations for horizontal and vertical slot waveguides with dimensions d_2 and d_1 , and dielectric constants K_2 and K_1 , respectively. The losses calculated by (3) and (4) also agree closely with those calculated by a ray approach.

Figure 1 shows loss rates in dB/100 ft as functions of frequency calculated by (3) and (4) for the (1,1) E_h and E_v modes in a tunnel of width 14 ft and height 7 ft, representative of a haulage way in a seam of high coal, and for $K_1 = K_2 = 10$, corresponding to coal on all the walls of the tunnel. It is seen that the loss rate is much greater for the E_v mode. Figure 2 shows the calculated E_h loss rate for a tunnel of half the height. The higher loss rate in the low coal tunnel is due to the effect of the d_2^3 term in (3).

Two experimental values obtained by Collins Radio Co.⁽⁴⁾ for horizontal-horizontal antenna orientations are also shown in Figure 1. These values agree well with theory for the E_h mode for 415 MHz, but not so well for 1000 MHz. The departure suggests that some additional loss mechanism sets in at higher frequencies.

It is also significant that the experimental values of the loss rates for all three orientation arrangements of the transmitting and receiving dipole antennas, namely, horizontal-horizontal, vertical-horizontal, and vertical-vertical, are surprisingly close to each other. The independence of loss rate with respect to polarization is not predicted by the theory discussed so far, as seen in Figure 1 for the E_h and E_v modes. Indeed, the theory predicts no transmission at all for the VH antenna arrangement.

PROPAGATION MODEL

The higher observed loss rate at the higher frequencies relative to the calculated E_h mode values, and the independence of the loss rate on antenna orientation can both be accounted for if one allows for scattering of the dominant (1,1) E_h mode by roughness and tilt of the tunnel walls. The scattered radiation goes into many higher modes and can be regarded as a diffuse radiation component that accompanies the E_h mode. The diffuse component is in dynamical equilibrium with the E_h mode in the sense that its rate of generation by scattering of the E_h mode is balanced by its rate of loss by refraction into the surrounding dielectric. Since the diffuse component consists of contributions from the (1,1) E_v mode and many higher order waveguide modes, all of which have much higher refractive loss rates than the fundamental E_h mode, the dynamical balance point is such that the level of the diffuse component is many dB below that of the E_h mode at any point in the tunnel.

Our propagation model, comprising the (1,1) E_h mode plus an equilibrium diffuse component, explains the discrepancy between theory and experiment in Figure 1, since the loss due to scattering

of the E_h mode is greater at 1000 MHz than at 415 MHz owing to the larger effect of wall tilt at the higher frequency. The model accounts for the independence of loss rate on antenna orientation, since the loss rate is always that of the E_h mode, except for initial and final transition regions, no matter what the orientations of the two antennas may be. The transition regions, however, cause different insertion losses for the different antenna orientations.

Further strong support for the theoretical model is provided by the discovery by Collins Radio Co. that a large loss in signal strength occurs when the receiving antenna is moved around a corner into a cross tunnel; and that the signal strength around the corner is independent of receiving antenna orientation. This is exactly what our model predicts since the well collimated E_h mode in the main tunnel couples very weakly into the cross tunnel, whereas the uncollimated diffuse component couples quite efficiently. Since the diffuse radiation component is likely to be almost unpolarized, the observed independence of signal strength on receiving antenna orientation is understandable.

Another experimental result is that the initial attenuation rate in the cross tunnel is much higher than the rate in the main tunnel. This is also in accord with the model since the diffuse radiation component has a much larger loss rate than the E_h mode owing to its steeper angles of incidence on the tunnel walls.

THE DIFFUSE RADIATION COMPONENT

Scattering of the (1,1) E_h mode into other modes to generate the diffuse component occurs by two mechanisms: wall roughness and wall tilt.

Roughness is here regarded as local variations in the level of the surface relative to the mean level of the surface of a wall. For the case of a Gaussian distribution of the surface level, defined by a root mean square roughness h , the loss in dB by the E_h mode is given by the formula

$$L_{\text{roughness}} = 4.343 \pi^2 h^2 \lambda (1/d_1^4 + 1/d_2^4) z. \quad (5)$$

This is also the gain by the diffuse component due to roughness.

Long range tilt of the tunnel walls relative to the mean planes which define the dimensions d_1 and d_2 of the tunnel causes radiation in the E_h mode to be deflected away from the directions defined by the phase condition for the mode. One can calculate the average coupling factor of such deflected radiation back into the E_h mode and thereby find the loss rate due to tilt. The result in dB is

$$L_{\text{tilt}} = 4.343 \pi^2 \theta^2 z/\lambda \quad (6)$$

where θ is the root mean square tilt. Eq. (6) also gives the rate at which the diffuse component gains power from the E_h mode as a result of the tilt.

It is noted from (5) and (6) that roughness is most important at low frequencies while tilt is most important at high frequencies.

Figure 3 shows the effect on the (1,1) E_h mode propagation of adding the loss rates due to roughness and tilt to the direct refraction loss given in Figure 1. The curves are calculated for a root mean square roughness of 4 inches and for various assumed values of θ . It is seen that a value $\theta = 1^\circ$ gives good agreement with the experimental values of Collins Radio Co. The effect of tilt is much greater than that of roughness in the frequency range of interest.

Having determined the value of θ , for the assumed value of h , we can now find the intensity ratio of the diffuse component to the E_h mode from the equilibrium balance equation

$$I_{d, \text{ main}} / I_{h, \text{ main}} = L_{hd} / L_d \quad (7)$$

where L_{hd} is the loss rate from the E_h mode into the diffuse component, and L_d is the loss rate of the diffuse component by refraction. To estimate L_d approximately, we take the loss rate to be that of an "average ray" of the diffuse component having direction cosines $(1/\sqrt{3}, 1/\sqrt{3}, 1/\sqrt{3})$. Then

$$L_d = 10 (z/d_1 + z/d_2) \log_{10} 1/R \quad (8)$$

where R , the Fresnel reflectance of the average ray for $K_1 = K_2 = 10$, has the value 0.28. Then for $d_1 = 14$ ft, $d_2 = 7$ ft, $z = 100$ ft, we find that $L_d = 119$ dB/100 ft. This value has to be corrected for the loss of diffuse radiation into cross tunnels which we assume have the same dimensions as the main tunnel and occur every 75 ft. From relative area considerations we find that this loss is 2 dB/100 ft. The corrected value is therefore

$$L_d = 121 \text{ dB/100 ft.} \quad (9)$$

which is independent of frequency.

The loss rate L_{hd} is shown in Table I as a function of frequency for the 14 ft x 7 ft tunnel. The values are the sum of the roughness and tilt losses calculated by (5) and (6) for $h = 4$ inches rms and $\theta = 1^\circ$ rms. The diffuse component level relative to the E_h mode, calculated by (7), is given in the fourth column of Table I. The diffuse component is larger at high frequencies owing to the increased scattering of the E_h mode by wall tilt.

PROPAGATION AROUND A CORNER

From solid angle considerations one finds that the fraction of the diffuse component in the main tunnel that enters the 14 ft x 7 ft aperture of a cross tunnel is 15% or -8.2 dB. The diffuse level just inside the aperture of the cross tunnel, relative to the E_h mode level in the main tunnel is therefore obtained by subtracting 8.2 dB from the values in column 4 of Table I. The results are shown in column 5 of the table. A dipole antenna with either horizontal or vertical orientation

placed at this point responds to one half of the diffuse radiation, and therefore gives a signal that is 3 dB less than the values in column 5 of Table I, relative to a horizontal antenna in the main tunnel.

If a horizontal antenna is moved down the cross tunnel the loss rate is initially 119 dB/100 ft (the value calculated above without correction for tunnels branching from the cross tunnel). Ultimately, however, the loss rate becomes that of the E_h mode excited in the cross tunnel by the diffuse radiation in the main tunnel. We determine the E_h level at the beginning of the cross tunnel by calculating the fraction of the diffuse radiation leaving the exit aperture of the main tunnel which lies within the solid angle of acceptance of the E_h mode in the cross tunnel. The result is

$$I_{h, \text{cross}}/I_{d, \text{main}} = \lambda^3 / 16 \pi d_1^2 d_2 \quad (10)$$

This ratio, in dB, is given in column 2 of Table II.

Column 3 of Table II is the E_h level at the beginning of the cross tunnel relative to the E_h level in the main tunnel found by adding column 2 of Table II and column 4 of Table I. We find the corresponding ratio at 100 ft down the cross tunnel by adding the E_h propagation loss rates given in Figure 3 for $\theta = 1^\circ$. The results are shown in the last column of Table II.

The foregoing theoretical results for the diffuse and E_h components in the cross tunnel allow us to plot straight lines showing the initial and final trends in signal level in the cross tunnel. These asymptotic lines are shown in Figures 4 and 5 for 415 MHz and 1000 MHz, in comparison with the cross tunnel measurements of Collins Radio Co. The agreement both in absolute level and distance dependence gives good support to the theoretical model.

EFFECT OF ANTENNA ORIENTATION

The theoretical model also allows us to predict the effect of antenna orientation when the transmitting and receiving antennas are far enough apart so that dynamical equilibrium between the E_h mode and the diffuse component is established. We start with both antennas horizontal (HH configuration) and consider this as the 0 dB reference. Then if the receiving antenna is rotated to the vertical (HV configuration) this antenna is now orthogonal to the E_h mode, and therefore responds only to one half of the diffuse component, so that the loss is 3 dB more than the values in Table I, column 4. The result is shown in Table III column 2. Now, by the principle of reciprocity, the transmission for VH is the same as for HV as shown in column 3 of Table III. We now rotate the receiving antenna to get the configuration VV. Again we incur an additional transmission loss of 3 dB more than the values in Table I, column 4. The VV values are shown in Table III, column 4.

ANTENNA INSERTION LOSS

Dipole or whip antennas are the most convenient for portable radio communications between individuals. However, a considerable loss of signal power occurs at both the transmitter and receiver when simple dipole antennas are used because of the inefficient coupling of these antennas to the waveguide mode. The insertion loss of each dipole antenna can be calculated by a standard

microwave circuit technique for computing the amount of power coupled into a waveguide mode by a probe, whereby the dipole antenna is represented as a surface current filament having a sinusoidal current distribution along its length. The result is

$$C = \lambda^2 Z_0 / \pi^2 d_1 d_2 R_r. \quad (11)$$

Z_0 is the characteristic impedance of the E_h (1,1) mode and R_r is the radiation resistance of the antenna, which are approximately 377 and 73 ohms, respectively, provided that λ is small compared with d_1 and d_2 .

Formula (11) applies to antennas placed at the center of the tunnel and gives the results shown in Table IV, where the insertion loss L_i in dB is equal to $-10 \log_{10} C$. It is seen that the insertion loss decreases rapidly with increasing wavelength, as one would expect, since the antenna size occupies a larger fraction of the width of the waveguide. The overall insertion loss, for both antennas, is twice the value given in the table. A considerable reduction in loss would result if high gain antenna systems were used.

OVERALL LOSS IN A STRAIGHT TUNNEL

The overall loss in signal strength in a straight tunnel is the sum of the propagation loss and the insertion losses of the transmitting and receiving antennas. Table V lists the component loss rates for the (1,1) E_h mode due to direct refraction, roughness, and tilt; the total propagation loss rate; the insertion loss for two half-wave antennas; and the overall loss for five different distances. The overall loss for the HH orientation is also shown in Figure 6, where it is seen that the optimum frequency for minimum overall loss is in the range 500-1000 MHz, depending on the desired communication distance.

It is also of interest to combine the results in Table V with those in Table III to obtain the overall loss versus distance for the HH, HV (or VH), and VV antenna orientations. In order to compare the theoretical values with the experimental data of Collins Radio Co., which are expressed with reference to isotropic antennas, we add 4.3 dB to the overall loss calculated for half-wave dipoles. The theoretical results for the three different antenna orientations for frequencies of 415 MHz and 1,000 MHz are compared with the experimental data in Figures 7 and 8. It is seen that the theory agrees quite well with the general trend of the data.

OVERALL LOSS ALONG A PATH WITH ONE CORNER

Table VI gives the overall E_h mode loss for a path from one tunnel to another, including the corner loss involved in re-establishing the E_h mode in the second tunnel. The loss is the sum of the corner loss, given in column 3 of Table II and repeated in Table VI, and the straight tunnel loss given in Table V for various total distances. The results in Table VI are for the case of half-wave dipole transmitting and receiving antennas and are valid when neither antenna is within about 100 ft of the corner. The overall loss is less than the values in Table VI if the receiving antenna is within this distance, owing to the presence of the rapidly attenuating diffuse component that passes

around the corner. From the principle of reciprocity, the same is true if the transmitting antenna is within 100 ft of the corner.

The results indicate that the optimum frequency lies in the range 400-1,000 MHz. However, if one installs horizontal half-wave resonant scattering dipoles with 45° azimuth in the important tunnel intersections, in order to guide the E_h mode around the corner, the optimum may shift to somewhat lower frequencies since a greater fraction of the incident E_h wave will be deflected by the longer low-frequency dipoles.

CONCLUSIONS

The kind of propagation model developed in this paper, involving the (1,1) E_h waveguide mode accompanied by a diffuse component in dynamical equilibrium with it, seems to be necessary to account for the many effects observed in the measurements of Collins Radio Company: the exponential decay of the wave; the marked polarization effects in a straight tunnel; the independence of decay rate on antenna orientation; the absence of polarization at the beginning of a cross tunnel; the two-slope decay characteristic in a cross tunnel; and overall frequency dependence. All of these effects are moderately well accounted for by the theoretical model. However, considerable refinement of the theory could be made by removing some of the present oversimplifications, such as: the assumption of perfectly diffuse scattering both in the main tunnel and immediately around a corner in a cross tunnel; the use of the "average ray" approximation; and the description of the propagation around a corner in terms of two asymptotes only.

The last item particularly deserves more attention since we have not included the conversion of the diffuse component in the transition region near the beginning of the cross tunnel into the E_h mode. For this reason we think that the good fit of the theory to the experimental data in Figures 4 and 5 may be somewhat fortuitous. More data at greater distances down a cross tunnel would be very desirable to settle this question. Data covering a wider frequency range in both main and cross tunnels would also allow a more stringent test of the theory.

REFERENCES

1. E. A. J. Marcatili and R. A. Schmeltzer, "Hollow Metallic and Dielectric Waveguides for Long Distance Optical Transmission and Lasers," The Bell System Technical Journal, Vol. 43, 1783, 1964.
2. J. I. Glaser, "Attenuation and Guidance of Modes in Hollow Dielectric Waveguides," IEEE Transactions on Microwave Theory and Techniques, March 1969, p. 173; and M.I.T. Ph.D. Thesis, "Low-Loss Waves in Hollow Dielectric Tubes," February 1967.
3. Arthur D. Little, Inc., reports to U.S. Department of the Interior, Bureau of Mines, Pittsburgh, Pa.
4. Collins Radio Company, "Coal Mine Communications Field Test Report," December 29, 1972 prepared for U.S. Department of the Interior, Bureau of Mines, Pittsburgh, Pa.

FIGURE 1
REFRACTION LOSS FOR E_h AND E_v MODES
IN HIGH COAL

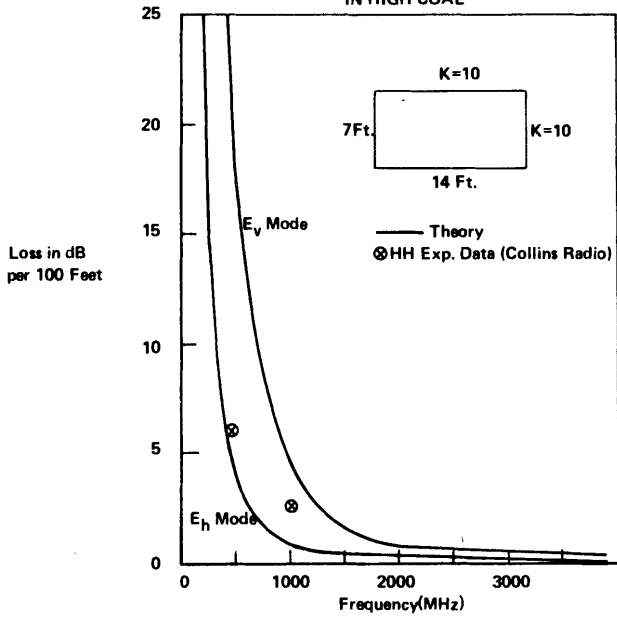


FIGURE 3
RESULTANT PROPAGATION LOSS FOR E_h MODE IN HIGH COAL
(Refraction, Wall Roughness and Tilt)

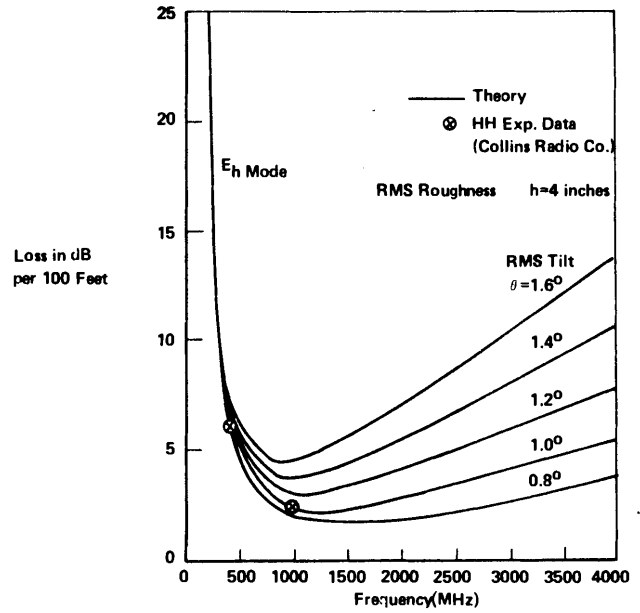


FIGURE 2
REFRACTION LOSS FOR E_h MODE IN LOW COAL

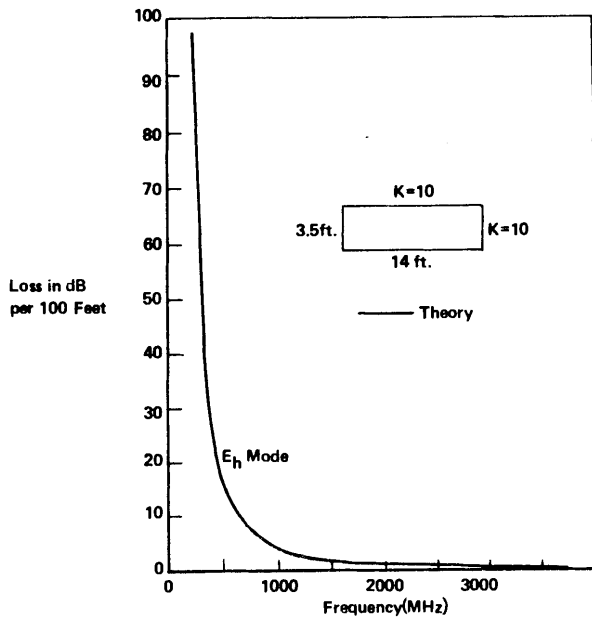


FIGURE 4
CORNER LOSS IN HIGH COAL

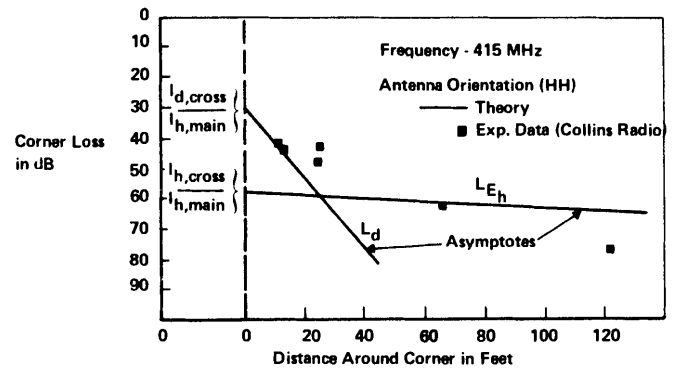


FIGURE 5
CORNER LOSS IN HIGH COAL

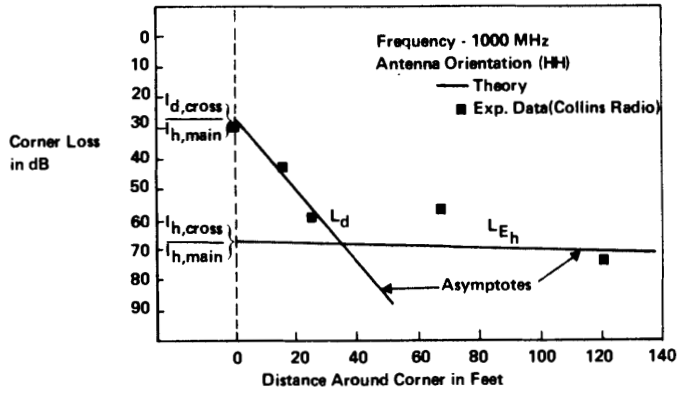


FIGURE 6
TOTAL LOSS FOR VARIOUS DISTANCES ALONG A STRAIGHT TUNNEL

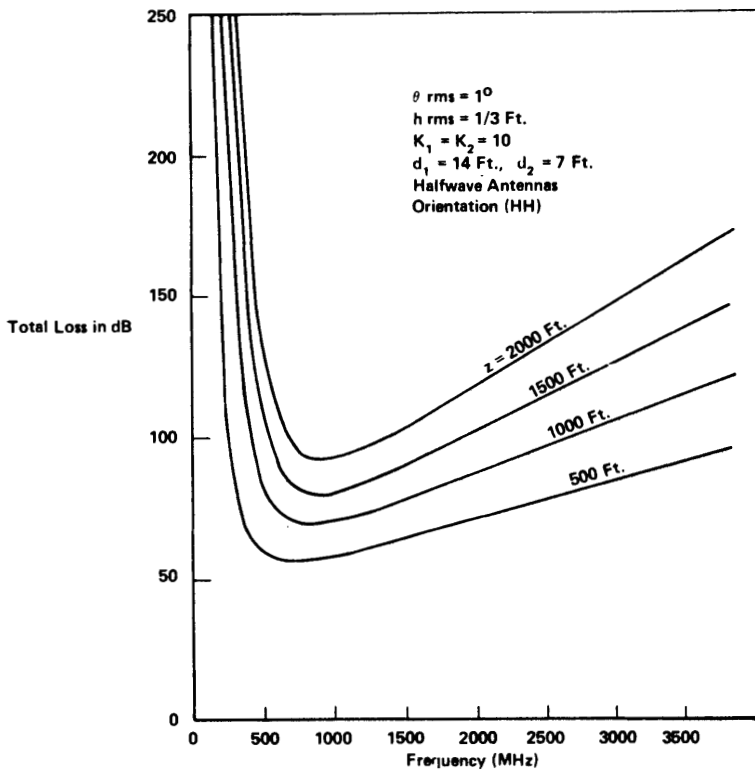


FIGURE 7
OVERALL LOSS IN A STRAIGHT TUNNEL IN HIGH COAL
(For Isotropic Antennas)

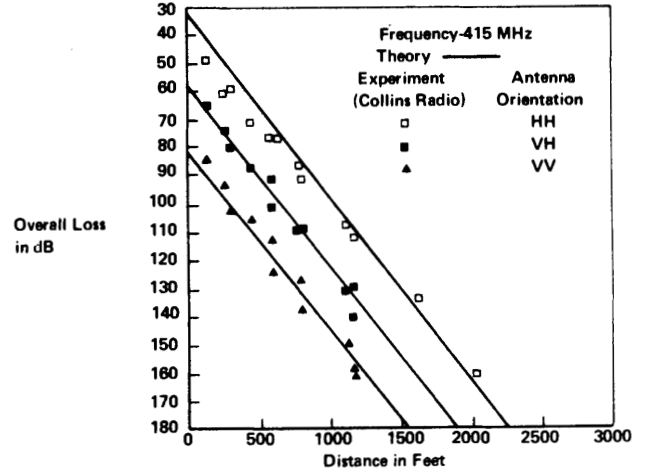


FIGURE 8
OVERALL LOSS IN A STRAIGHT TUNNEL IN HIGH COAL
(For Isotropic Antennas)

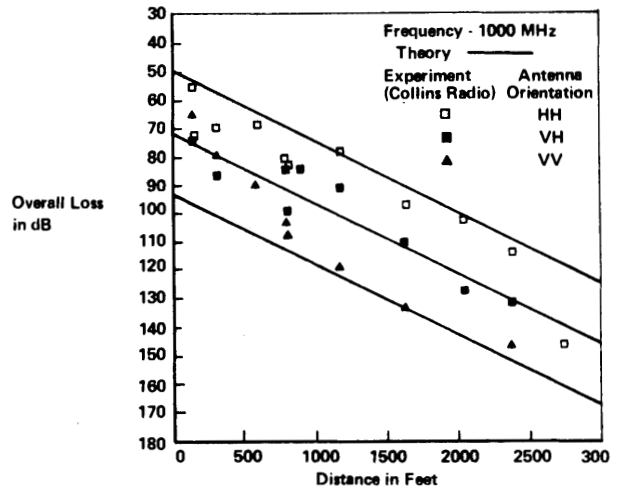


TABLE I

DIFFUSE RADIATION COMPONENT IN MAIN TUNNEL AND AT BEGINNING OF CROSS TUNNEL

f (MHz)	λ (Ft.)	L_{hd} (dB/100 ft.)	$\frac{I_{d, main}}{I_{h, main}}$ (dB)	$\frac{I_{d, cross}}{I_{h, main}}$ (dB)
4,000	.245	5.4	-13.5	-21.7
3,000	.327	4.1	-14.7	-22.9
2,000	.49	2.8	-16.4	-24.6
1,000	.98	1.5	-19.0	-27.2
415	2.37	1.1	-20.6	-28.8
200	4.92	1.3	-19.7	-27.9

TABLE II

EXCITATION OF E_h MODE IN CROSS TUNNEL BY DIFFUSE COMPONENT IN MAIN TUNNEL

f (MHz)	$\frac{I_{h, cross}}{I_{d, main}}$ (dB)	$\frac{I_{h, cross}}{I_{h, main}}$ (dB)	$\frac{I_{h, cross}}{I_{h, main}} / 0$ (dB)	$\frac{I_{h, cross}}{I_{h, main}} / 100'$ (dB)
4,000	-66.7	-80.2	-85.6	85.6
3,000	-62.9	-77.6	-81.8	81.8
2,000	-57.7	-74.1	-77.1	77.1
1,000	-48.6	-67.6	-70.1	70.1
415	-37.1	-57.7	-64.1	64.1
200	-27.6	-47.3	-71.6	71.6

TABLE III

EFFECT OF ANTENNA ORIENTATION

f (MHz)	HH (dB)	HV (dB)	VH (dB)	VV (dB)
1000	0	-22.0	-22.0	-44.0
415	0	-23.6	-23.6	-47.2
200	0	-22.7	-22.7	-45.4

TABLE IV
INSERTION LOSS (L_i)
(For a Half-Wave Antenna)

F (MHz)	λ (Feet)	L_i (dB)
4000	0.245	35.0
3000	0.327	32.4
2000	0.49	28.9
1000	0.98	22.9
415	2.37	15.2
200	4.92	8.9

TABLE V

CALCULATION OF OVERALL LOSS FOR E_h MODE WITH TWO HALF WAVE DIPOLE ANTENNAS

($h = 7/3$ Ft. $\theta = 10^\circ$, $K_1 = K_2 = 10$, $d_1 = 14$ Ft., $d_2 = 7$ Ft.)

f (MHz)	$L_{refraction}$ (dB/100')	$L_{roughness}$ (dB/100')	L_{tilt} (dB/100')	$L_{propagation}$ (dB/100')	$L_{insertion}$ (dB)	$L_{overall}$ (dB)				
						100'	500'	1000'	1500'	2000'
4000	.06	.05	5.33	5.44	69.90	75	97	124	152	179
3000	.10	.07	3.99	4.16	64.88	69	86	107	127	148
2000	.23	.10	2.66	2.99	57.86	61	73	88	103	118
1000	.91	.21	1.33	2.45	45.82	48	58	70	81	93
415	5.34	.50	0.55	6.39	30.48	37	62	94	126	158
200	23.00	1.04	0.27	24.31	17.80	42	139	261	383	504
100	92.00	2.08	0.14	94.20	5.80	100	477	948	1419	1890

TABLE VI

OVERALL LOSS ALONG A PATH INCLUDING ONE CORNER E_h MODE WITH HALF WAVE DIPOLE ANTENNAS

f (MHz)	E_h Loss per Corner (dB)	Overall Loss (dB)			
		500'	1000'	1500'	2000'
4000	80.2	177	205	232	259
3000	77.6	163	184	205	226
2000	74.1	147	162	177	192
1000	67.6	126	138	148	161
415	57.7	120	152	184	216
200	47.3	187	308	430	551

C. SUMMARY REPORT OF
UPLINK AND DOWNLINK COMMUNICATIONS
WORKING GROUP

THROUGH-THE-EARTH ELECTROMAGNETICS WORKSHOP
Golden, Colorado
August, 1973

GROUP CHAIRMAN
ROBERT L. LAGACE
ARTHUR D. LITTLE, INC.

OUTLINE

OVERVIEW

BRIEF DESCRIPTION OF THE FOUR PROMISING SYSTEMS

- Uplink-Data
- Downlink-Voice
- Sidelink-Call Alert Coded Page
- Sidelink-Roof Bolt Voice Page

PRESENT STATUS AND RECOMMENDED FUTURE WORK

Uplink Data System

1. Overview
 - a. Nominal Mines
 - b. Deep Mines
 - c. Equipment
2. The Channel-Transmission Loss
 - a. Loops
 - b. Parasitic Structures
 - c. Grounded Wires
3. The Channel-Noise
 - a. Past Data
 - b. NBS Mine Noise Measurements
 - c. Whistler and Geomagnetic Data
 - d. Data Utilization
4. The Source-Message, Coding, Modulation, Operating Frequency
5. The Receiver-Sensor, Demodulation/Decoding, Special Processing

Downlink Voice System

1. Overview
 - a. Experience to Date
 - b. Future Developments
 - c. Deep Mines
2. The Channel-Transmission Loss
 - a. Long Wire Antennas
 - b. Parasitic Structures
3. The Channel-Noise
4. The Source-Message, Coding, Modulation, Operating Frequency
5. The Receiver-Sensor, Demodulation/Decoding, Special Processing
 - a. Downlink
 - b. Uplink

Sidelink Call Alert Coded Page System

1. Overview
2. The Channel-Transmission Loss
 - a. Loops
 - b. Parasitic Structures
 - c. Roof Bolts
3. The Channel-Noise
- 4,5. The Source and Receiver

Sidelink Roof Bolt Voice Page System

1. Overview
2. The Channel-Transmission Loss
 - a. Finite Wire Antenna Terminated by Roof Bolts
 - b. Parasitic Structures
3. The Channel-Noise
- 4,5. The Source and Receiver

OVERVIEW

The attention of this group was focussed on four through-the-earth communication systems that are presently of high interest to the U.S. Bureau of Mines; four systems for providing operational/emergency communications on the working sections of coal mines, indeed up to the very face of the section. The systems are: uplink-data, downlink-voice, sidelink-call alert coded page, sidelink-roof bolt voice page. Each of these systems makes use of the mine overburden as the signal transmission medium, as opposed to the guiding wires, cables, and tunnels treated by the operational communications working group. Each of these systems satisfies one or more of the Bureau's objectives for mine communications systems; namely

- reliable links for monitoring the mine environment under both operational and emergency conditions.
- reliable links for communicating with miners during emergencies.
- special links for increasing the efficiency of day-to-day operations of the mine.

Each of these systems has been successfully demonstrated on a limited experimental basis, and prototypes of all these systems are installed and operating in the USBM experimental mine in Bruceton, Pa. Each of these systems must now be optimized regarding its performance, and engineered for practical routine application to the working sections of actual operating coal mines, particularly those of the room and pillar type.

This optimization and engineering must take place subject to the principal constraints listed by Howard E. Parkinson in his Workshop paper entitled, "Objectives and Constraints of Through-the-Earth Electromagnetic Communications Systems" and enumerated below.

- Depth of Mine Overburden
- Overburden Conductivity
- Electromagnetic Noise In and Above Mines
- Limited In-Mine Electrical Energy (Stationary or Man Carried) During an Emergency
- Intrinsic Safety for In-Mine Equipment
- Practical and Rugged Equipment for Use Under Both Operational/ Emergency Conditions
- Severe Weight Limitations for Man Carried Equipment
- Reasonably Low Costs Especially for Man Carried Equipment

Part II of this paper provides a brief description of each system, while Part III summarizes the present status of developments related to these systems and some recommendations for future work needed to advance these systems to the practical application stage.

BRIEF DESCRIPTION OF THE FOUR PROMISING SYSTEMS

Uplink-Data

This is a vertical through-the-earth narrow band data channel for monitoring important parameters of the mine environment under operational and emergency conditions, and for receiving coded messages or replies from miners during an emergency. Operating ranges compatible with 1,000 foot deep mines with $\sigma = 10^{-2}$ mho/m overburden are required. The in-mine transmitter would be located at a key place on the section, such as the loading point, where the present mine pager phone is also terminated. The surface receiver would have to be located in the vicinity of the point directly above the in-mine transmitter, primarily because of the inherent power limitations imposed on an in-mine transmitter during an emergency. This location requirement for the surface receiver may pose a difficulty for some mines with regard to surface access rights over advancing sections, and therefore may restrain such uplink communications to emergency situations during which mobile equipment can be temporarily installed over the known location of the in-mine transmitter. During normal mine operations, the mine environmental data could be monitored by means of a carrier channel over the mine pager phone line.

The limited in-mine transmitter power available during an emergency and the electromagnetic noise levels present on the surface have led to the conclusion that uplink transmission of baseband voice is not a practical goal. Therefore it has been deleted as a requirement until practical, voice bandwidth compression techniques or other types of signal processing become available to change this conclusion.

Downlink-Voice

This is a vertical through-the-earth voice channel for transmitting messages, during a mine emergency, to miners carrying a small emergency voice receiver, preferably built into their helmets. As in the case of the uplink receiver, difficulties regarding surface access rights over advancing sections may require a mobile surface transmitter installation that is temporarily installed only during emergencies. However, since the transmitter power available on the surface is much greater than that underground during an emergency, the downlink allows greater operational flexibility in communicating with moving miners, and may reduce the surface access rights problem somewhat, because of the potentially greater coverage area of each surface transmitter. As in the uplink case, operating ranges compatible with 1,000 foot deep mines with $\sigma = 10^{-2}$ mho/m overburden are required.

Sidelink-Call Alert Coded Page

This is a horizontal through-the-earth narrow band channel for transmitting a call alert paging signal to key individuals roving on a working section during normal mine operations, to notify them that they are wanted on the mine pager phone. The transmitter, activated by a signal sent over the mine phone line, would be somewhat centrally located near the section loading point as in the uplink system, and conceivably could be integrated with the uplink equipment if desired. The receivers would be carried by the miner, preferably in his helmet as in the case of the emergency voice receiver for the downlink system. In fact the Bureau's present desire is to have this emergency voice receiver serve a dual role, for key supervisory and maintenance people, by also operating as a

narrowband call alert receiver under normal operating conditions. Such a call alert system would extend mine phone paging to roving individuals right up to the working face, thereby increasing both safety and operational efficiency. This would require operating ranges on the order of 400 to 800 feet in overburdens of $\sigma = 10^{-2}$ mho/m in order to cover a typical 600 by 600 foot section, depending on the location of the transmitter.

Sidelink-Roof Bolt Voice Page

This is a horizontal through-the-earth voice channel for transmitting a more comprehensive voice message or page, as opposed to a simple call alert, to key individuals roving on a working section during normal operating conditions. As in the call alert system the transmitter could also be located at the section loading point, thereby requiring the same operating range as the call alert system. However it most likely would not share equipment with an uplink system as a call alert system might. Being a voice bandwidth system for use under operational conditions when electromagnetic noise levels are high, particularly in the audio band, a significantly higher operating frequency than that possible for a narrowband call alert or uplink system is favored. The receiver for the roof bolt paging system is presently conceived as a pocket-sized unit, but other packages such as a helmet mounted unit are not excluded.

PRESENT STATUS AND RECOMMENDED FUTURE WORK

To arrive at a design that is at least acceptable, if not optimum, regarding performance and practicality for any of the above communication systems, one usually must first determine how each of the major elements comprising the system influence its performance, and then use them so as to get the desired results. An often indispensable aid to this process, particularly when design information for one or more of the major system elements is missing, is to put together a breadboard system based on existing related hardware and try it out. Several of the above through-the-earth systems have evolved, with beneficial results, from the latter approach. Concurrently, some of the previously missing design information on transmission loss and noise has been accumulated. Therefore, it will now be possible to better optimize each of these systems by quantitative analysis and comparison of alternative designs.

No papers evaluating or describing any of the above through-the-earth systems were presented during the Workshop. However, several papers treating two major system elements, channel transmission loss and noise, were given. These and some past work by the attendees of this working group provided the basis for the group's findings and recommendations. We grouped the system elements as follows:

- The Source: its message, modulation or coding, transmitter, and operating frequency.
- The Channel: its transmission loss for each antenna type, and its noise characteristics.
- The Receiver: its pick up sensor, demodulation/decoding, and special processing for signal to noise improvement.

These elements were then discussed in the context of each of the four systems to the level of detail that was possible under the circumstances. The order of treatment for each system will be Channel, Source, and Receiver, which mainly reflects the emphasis of this Workshop's charter and papers. Progress made to date in the Channel area should now allow more emphasis to be placed on overall system design and analysis, thereby calling greater attention to the Source and Receiver areas.

In the discussions below, that for the uplink system is somewhat longer than the others, because certain elements that have common application to several of the systems are first introduced in the uplink treatment.

Uplink Data System

This section treats the principal narrowband data uplink application. The more difficult, less practical uplink voice application is treated briefly in the downlink voice section.

1. Overview

To date the combination of overburden transmission loss and available surface noise data have identified the frequency band below 5 kHz as the most favorable for practical narrow band uplink data systems intended for coal mines with overburden depths of up to 1,000 feet and conductivity of $\sigma = 10^{-2}$ mho/m. Though shallower mines allow a somewhat higher frequency limit, and more conductive ($\sigma = 10^{-1}$ mho/m) or deeper mine overburdens demand a significantly lower frequency limit, the under 5 kHz limit should cover most coal mine situations.

a. Nominal Mines

Signal to noise analyses performed by Westinghouse Georesearch Laboratory (WGL) support this under 5 kHz conclusion for 10^{-2} mho/m overburdens, while also identifying the frequency band between 500 Hz-to-3 kHz as a distinctly optimum one for narrowband systems. The WGL analyses were based on Wait/WGL transmission loss curves for loop transmitters and broadband atmospheric noise data (under 10 kHz) taken by WGL in Colorado. Signal to noise analyses performed by Arthur D. Little, Inc. (ADL) reach a similar under 5 kHz overall conclusion, but do not reveal the presence of an optimum frequency band as distinct as the one by WGL. The ADL analyses were based on the same transmission loss curves of Wait/WGL, but different broadband noise data, namely surface atmospheric noise data (under 300 Hz) taken by MIT Lincoln Laboratory (LL) in Florida and early WGL and National Bureau of Standards (NBS) surface noise data (under 10 kHz) taken over four Western coal mines. The differences in the results of the two analyses, regarding the presence or absence of a clearly optimum frequency band between 500-3000 Hz for $\sigma = 10^{-2}$ mho/m overburdens (based on broadband noise levels) should be easily resolved when the large amount of noise data recently taken over coal mines by NBS soon becomes available. However, WGL and NBS field experiences have revealed a potentially more serious noise problem that may tend to favor use of frequencies between 1-5 kHz over coal mines, namely the extremely strong harmonics of 60 Hz and 360 Hz caused by the mine power conversion equipment, harmonic levels that are high enough in some cases to interfere with even narrowband systems operating between the harmonics.

b. Deep Mines

For mines with overburdens deeper than 1,000 feet (such as hardrock mines) or conductivities greater than 10^{-2} mho/m, it is generally agreed that operating frequencies will definitely be forced downward to perhaps 500 Hz or 100 Hz. In some extremely deep hardrock mines that approach 10,000 feet, lower frequencies yet may be needed if direct transmission to the surface is required. The favorable downlink signal transmission test results to depths of 11,000 feet achieved with under 100 watts by Sandia Laboratories, using Develco, Inc. equipment at frequencies below 20 Hz, should be carefully evaluated and exploited if such depths become important to the Bureau. However, it should be kept in mind that such a downlink transmission test has the advantages of power and large antenna size on the surface, and a relatively noise free underground receiver, which is the converse of the mine uplink problem.

c. Equipment

An experimental prototype uplink data monitoring system has been built by WGL for the Bureau. It operates at designated frequencies between 3-5 kHz, utilizes PCM/FSK modulation, a loop transmitter antenna, and is presently installed in the Bureau's experimental mine in Bruceton, Pa. Similar experimental equipment that illustrates the feasibility of uplink data transmission, even with limited available power, has also been built by WGL for miner location applications. An example is the keyed CW electromagnetic transmitter for miner location which utilizes a one turn, 360 foot periphery loop and the miner's 4-volt cap lamp battery to generate a magnetic moment of about 2,000 ampere-meters² at 2 kHz. Detection ranges in excess of 1,000 feet have been obtained at several mine sites using this and similar units, as reported during this Workshop. It should be noted that the approximately 80 foot overburden at the USBM experimental mine is not considered by the Bureau as being typical of that found over operating mines.

A multichannel uplink data system of practical design suited for installation and test in an operating coal mine with up to 1,000 feet of overburden will soon be needed. The basic monitoring requirements of the in-mine station are now being formulated, so that an overall uplink data communication system can then be designed and optimized for the operating conditions of this mine.

2. The Channel-Transmission Loss

a. Loops

Uplink communications to date have primarily utilized loop source antennas of vertically oriented magnetic moment. These have consisted typically of one turn loops (up to 500 foot periphery) wrapped around one or two coal pillars; and less frequently a smaller one turn loop (up to 100 foot periphery) placed in an entry. Such loops have been preferred over long wire antennas for in-mine installations because of their lower input resistance, fixed impedance characteristics over time, and convenience of installation and maintenance in the adverse mine environment. The primarily vertical magnetic fields produced by vertical axis loops can also offer a signal to noise advantage on the surface in some cases, depending on the sources of the noise, i.e. natural or man-made.

The theoretical results of Wait and ITS, regarding the field strengths expected on the surface from infinitesimal loops of moment NIA placed in homogeneous and layered conducting overburdens, are well established and have been found to be in good agreement with experimental data obtained by WGL and Colorado School of Mines (CSM) at several mine sites. For the large overburden depths of interest and sizes of corresponding loops required, the simplifying infinitesimal loop assumptions apply. Furthermore it has been shown by Wait and ITS that typical conducting obstacles, such as pipes, and inhomogeneities found in the transmission path to the surface should produce only small effects on the resultant magnetic field seen at the surface for the under 5 kHz band of interest. WGL and ITS have also shown that the effects of surface topography on the resultant surface field are also small. Consequently these effects can largely be ignored for communications applications, as opposed to location applications where some of the effects can take on greater importance in some cases.

Therefore it was concluded that no new theoretical derivations were required on uplink transmission loss for loop transmitters; but that appropriate curves, tables, nomographs, etc., based on the available theoretical results should be prepared, as an aid to uplink systems designers who desire to apply the theory to typical mine overburdens. Included in these design aids should be curves that show the additional amount of signal loss suffered as the horizontal displacement between surface and in-mine loops is increased. This will help determine the surface coverage obtainable from a single in-mine loop.

b. Parasitic Structures

All of the above results apply for cases in which no large closed loops of wire, cable, or steel roof mesh are close enough to the finite, relatively large, in-mine transmitter loops to allow significant currents to be induced in these parasitic structures, which in turn might reduce the effective strength or field of the transmit loops. The likelihood of encountering parasitic structures on working sections is high, but the degree to which they could adversely affect system performance, has not been ascertained. Since this may be a potential problem to both the uplink data system and the call alert page system to be discussed below, the practical influence of such structures needs to be assessed. However, until that is done, uplink or call alert system transmit loops should be installed away from such structures as steel roof mesh, trolley lines, and probably power cables, since the effects of their presence will decrease with increasing separation.

c. Grounded Wires

Lastly, should there be a renewed interest in comparing the performance of a loop source uplink system with that for a grounded finite straight wire source that utilizes a wire terminated by a roof bolt ground rod at each end, ITS has derived expressions and curves for the magnetic field produced on the surface by such a buried finite wire source. The results apply to the case of the wire inclined at an arbitrary tilt angle to the horizontal in a homogeneous overburden. They show that small tilt angles made by the wire with a flat or hilly surface do not influence the magnitude of the surface field.

3. The Channel-Noise

a. Past Data

Up until this year very little good noise data pertinent to coal mine environments, underground or on the surface, were available for making comprehensive systems analyses or optimizing uplink or downlink system designs. With respect to noise levels on the surface, the ELF noise measurements made by Lincoln Laboratory for the Navy were the most useful below 300 Hz, even though not taken over coal mines, but in Florida and other parts of the world. Between 300 Hz and 5 kHz the surface noise data were even more sparse, consisting of limited atmospheric noise measurements taken by WGL in Colorado, and limited noise measurements conducted by NBS and WGL at a few coal mines.

These surface data were not considered adequate, because it was suspected that the predominant sources of both broadband and discrete frequency noise on the surface over coal mines would be man-made, since mines were such large power consumers and/or located near industrialized areas. Though broadband atmospheric noise would probably play an important role, broadband noise levels produced on the surface by the mine equipment, and by poorly maintained rural high voltage power lines, were viewed as having a potentially greater influence at a local mine site, except in the case of local thunderstorms. More importantly, even less data were available on the in-mine noise environment for the design of downlink and in-mine systems.

b. NBS Mine Noise Measurements

Therefore, during this past year, NBS conducted a major noise measurement effort for the Bureau of Mines in an attempt to characterize in a practical manner the electromagnetic noise environment in and above several "representative" coal mines. Data has been taken at a 600 volt all DC coal mine; a coal mine with 300 VDC rail haulage and shuttle cars, and AC face machinery and belt haulage; a 300 volt DC longwall mine with AC haulage; and a hardrock AC mine with diesel haulage. The measurements encompass operating and quiet conditions for different machines, locations, power centers and boreholes, in working sections, haulageways and on the surface. Some of these noise data have already been processed and made available, with the remainder to become available within the next six months.

In-mine measurements have included wideband recordings from 100 Hz to 300 kHz of three magnetic field components, and of voltages on telephone lines, trolley lines, and roof bolts; from which noise power spectra are being generated. In addition, narrowband (2 kHz) spot frequency recordings were made at eight frequencies covering the 10 kHz to 32 MHz band, of three magnetic field components; from which noise amplitude probability distributions (APD's) are being generated. On the surface, only the components of magnetic field are required, but over a more restricted frequency range, because of the lower frequencies required for uplink systems. The surface wideband recordings for generating spectra cover 100 Hz to 10 kHz, while the narrowband spot frequency recordings for generating APD's cover four frequencies in the 10 kHz to 150 kHz band.

The preliminary results now available from these NBS noise measurements indicate that high levels of discrete frequency noise at harmonics of 60 Hz and 360 Hz predominate over broadband spectrum levels below about 10 kHz, both in

the mine and on the surface, with the broadband noise predominating above about 15 kHz, and the levels of both noise types decreasing with increasing frequency. Furthermore, the discrete frequency surface noise levels are highly correlated with in-mine levels below about 7 kHz, the degree of correlation falling off rapidly above 7 kHz. Noise levels also have a strong dependence on distance from power cables, and can vary over dynamic ranges in excess of 60 dB.

c. Whistler and Geomagnetic Data

A representative from Develco, Inc. stated that "mountains" of atmospheric noise data had been taken some years ago in the 1-30 kHz frequency band by Stanford Research Institute with regard to its whistler work. Though some of this data might possibly be useful for the under 5 kHz band of interest, he was also of the opinion that the data had not been analyzed in a form convenient to the uplink application, and that in any case, access to and subsequent understanding of this old data might involve much more difficulty than any potential benefits would justify.

A representative from University of Alberta claimed the presence of a minimum in the geomagnetic noise spectrum between 0.2-8 Hz, with 5 Hz perhaps being the most favorable frequency. Though there was some uncertainty regarding the level of this noise minimum among the Workshop participants, this claim should be checked out, since it might be worth considering for very deep mines. A book by Campbell and Matsushita was given as a reference.

d. Data Utilization

It was concluded that the NBS noise data taken to date at six coal mines and one hard rock mine, together with the planned NBS measurements at an all AC coal mine and another hard rock mine, when added to past atmospheric noise data taken below 10 kHz, should provide a substantial data base from which the design and optimization of mine communications systems can proceed in an orderly manner. Therefore, it was concluded that no new noise measurements over and above that already planned by NBS were required at this time.

In the under 5 kHz frequency band presently of interest to uplink data systems noise, power spectra and dubs of selected NBS tape recordings of the surface noise will be made available to system designers. Surface data up to 10 kHz will also be available if needed. The uplink system designers will need data on the levels of both discrete frequency and broadband noise components: broadband spectrum levels (and amplitude statistics if possible) for optimizing the coding, modulation, and receiver processing for narrowband data uplink; and discrete component levels for estimating likely levels of out-of-band interference, and ways to combat them by choice of operating frequencies and/or receiver signal processing techniques.

To better estimate these noise levels, particularly the broadband noise levels between discrete harmonic components, it was recommended that NBS provide expanded frequency scale spectra, covering only the 0-5 kHz band per spectrum plot, as opposed to the more compressed plots presently being prepared. Spectra for vertical and horizontal magnetic field components on the surface under both operational and "quieter" emergency conditions will be required. Note: these 0-5 kHz expanded spectra will be required not only for

the surface noise data, but also for the underground data for use in the design of call-alert and baseband-voice-downlink communications for mine sections. Though not discussed in the working group, amplitude statistics for the broadband levels between harmonics may also be required.

For deep mine applications that may require operating frequencies in the vicinity of 100 Hz and below, the present NBS mine noise data down to 100 Hz and the LL atmospheric noise data down to about 3 Hz may be adequate for designing such systems. The need for additional noise measurements at these low frequencies should be carefully evaluated and justified before embarking on such a measurement program, because of the increased measurement difficulties encountered at these frequencies.

4. The Source - Message, Coding, Modulation, Operating Frequency.

The group agreed that firm conclusions regarding preferred techniques for coding, modulation, and operating frequency for a data uplink were premature, and could only be reached after a detailed overall systems analysis. Such an analysis would need to consider such things as the actual data message requirements, the bandwidth and power available, the transmission loss, characteristics of the noise, etc. Though the frequency band between 1-5 kHz is currently favored, based on past noise data, even this should be re-evaluated in the light of the new and more comprehensive NBS mine noise data.

The present WGL transmitters used for miner location utilize a CW signal that is simply keyed on and off with a ten to one duty cycle, to keep it simple, conserve cap lamp battery life, and to help distinguish it from adjacent power line harmonics. Operating frequencies are located between the harmonics of 60 Hz in the 1-3 kHz band. The present WGL uplink data system installed in the Bureau's experimental mine utilizes PCM/FSK to transmit the monitored data, and operates at select channel frequencies in the 3400 to 4500 Hz band, also placed between 60 Hz harmonics. The location transmitter is described in a Workshop paper, whereas the present experimental uplink data system is described in WGL reports. The specific results obtained with these systems should be reviewed as an aid to future designs.

As mentioned earlier, the data requirements and subsequent systems design have not yet been formulated for the uplink data system that will soon be developed for installation in an operating mine. This system design should benefit from the additional noise data and field experience now available.

5. The Receiver - Sensor, Demodulation/Decoding, Special Processing

As for the source, firm overall conclusions could not be reached, but several suggestions were made. An electrostatically shielded and balanced air core loop was recommended as a sensor. Notch filters were suggested to reduce interference from strong harmonics adjacent to the channel frequency.

The present WGL location receiver utilizes several stages of bandpass filtering to obtain a resultant bandwidth of 6 Hz. Notches as described above apparently have not yet been required at the mine sites visited to date. The present WGL uplink data system utilizes a phase-locked-loop FSK detector prior to decoding. Neither system was discussed.

Lastly, MIT Lincoln Laboratory (LL) has done extensive signal design and non-linear receiver processing work aimed at optimizing ELF secure narrow-band data communications (for the Navy Sanguine program) in the face of highly impulsive ELF atmospheric noise, and occasional discrete power line components. Reductions in required signal power of 10-20 dB have been reported, depending on the level of man-made discrete frequency interference, which apparently makes the techniques less effective. LL has been cooperative in the past by making its noise data and instrumentation information available to the Bureau and its contractors; and by recently offering suggestions regarding computer simulation of receiver design configurations for testing performance in the presence of environmental noise. This work should be reviewed to see if it can be applied to the mine problem in a practical and economic manner, particularly in those cases where transmitter power is at a premium and the noise environment severe. This work has recently been reported in the open literature, and more extensively in LL Technical Reports which are available from LL.

Downlink Voice System

1. Overview

a. Experience to Date

The objective of a downlink emergency voice system is to provide coverage of as large an area as possible to mobile miners during an emergency, in mines with nominal overburden characteristics of conductivity $\sigma = 10^{-2}$ mho/m and depths to 1,000 feet; and to do this with as few antennas on the surface as possible within practical limits. This being the case, the overburden transmission loss, the "quiet-mine" noise data available to date, and the greater space and power available on the surface, have favored direct transmission of 500-3,000 Hz baseband voice signals by means of grounded long wire antennas on the surface. Under relatively "quiet" emergency conditions, the present system designed by WGL with a transmitter capacity of 200 watts, has successfully transmitted intelligible voice messages to miners carrying simple manpack receivers to depths of about 1,000 feet. Mine overburdens of low conductivity will of course extend this usable range, while deeper or more conductive overburdens will quickly deteriorate performance or require significantly more power.

The success experienced under emergency conditions led to speculation that such a downlink voice system could have some beneficial operational applications as well, if the surface transmitter power and manpack receiver processing demands did not become excessive. However system performance was discovered to be even more dramatically affected by the in-mine operational noise environment than by the depth and conductivity. Namely, the noise levels severely deteriorated message intelligibility and usable range, demanding greatly increased power to maintain performance. This behavior is predicted by system analyses by both ADL and WGL, using early NBS and WGL in-mine noise data, and has been confirmed several times in operating mines by WGL. The deterioration occurs mainly because of the high levels of 60 Hz and 360 Hz harmonics produced by the mine machinery and DC power conversion equipment, and less often by the broadband impulsive noise near arcing trolleys, levels that can vary over a dynamic range in excess of 60 dB depending on location and machinery operating cycles. By applying simple corrective measures such as varying the orientation of the manpack receiver antenna for minimum noise pickup, which can be an operational incon-

venience, and by severely attenuating the large 360 Hz harmonic component by filtering in the manpack receiver, WGL was able to obtain some improvement in performance; but not enough to make it a dependable and practical system under mine operational conditions.

b. Future Developments

The above experience under operational conditions, when combined with the problems associated with gaining surface access rights over advancing coal mine sections (for the installation of long wire antennas, perhaps several thousand feet in length, or smaller loops, which have to be moved more often) make it very unlikely that the permanent surface installations required for operational applications will be a practical possibility in the near future. Thus in the near term, downlink voice will remain an emergency condition mobile system; thereby keeping the communication problem closer to the one originally treated by WGL, but with some added features.

The emphasis for future efforts on this system should probably be in the development of a reliable, compact, dual purpose receiver to be carried by a miner, preferably integrated into his helmet and operated from the cap lamp battery, as described by H. Parkinson in his paper. It will function as a downlink baseband voice receiver under emergency conditions, and as a call alert page receiver under operational conditions for key mining personnel, as mentioned in Section II. Though the present surface transmitter is apparently adequate to handle several emergency conditions, it too will probably need to be redesigned and optimized: for truly mobile utilization in the sense of being easily transportable by backpack or helicopter to the desired spots above the mine; for compatibility with the new dual purpose miner carried receivers to be developed; and for the mine emergency noise conditions likely to be prevailing. Since the downlink voice transmitter will have to be transported to and installed at selected locations above the mine after an emergency has occurred, the mine or section of interest will most likely be in a nearly power-down noise condition with only essential, lower-powered, electrical equipment such as pumps, fans, etc. in operation.

c. Deep Mines

The above applies to the nominal coal mine conditions specified. The deep hardrock mine situation is a vastly more difficult one as described in the uplink section, requiring frequencies down to 500 Hz and possibly 100 Hz and below even for narrowband data applications. Therefore, unless practical and economical techniques for dramatically compressing the bandwidth required for intelligible voice transmission become available, downlink voice to deep mines on the order of 10,000 feet will not be practically feasible under any noise conditions.

2. The Channel-Transmission Loss

a. Long Wire Antennas

Downlink communications to date have primarily utilized grounded, horizontal long wire source antennas on the surface, which reportedly give good coverage in the mine to a strip of width about equal to the depth of the mine under the wire, and sometimes wider, depending on the depth and available transmitter power. Antenna lengths have typically ranged from a low of about 1,500 feet up to greater than a mile, WGL field experience indicating that a length greater than about three times the mine depth being adequate to assume infinitely long wire behavior for the transmission loss. In the mine, the wire's magnetic field is primarily horizontal, with a gradually increasing vertical component as one moves away from the wire in a perpendicular direction; as opposed to the field of a surface loop which has primarily a vertical component. In those cases where the position of the miner or communication station is relatively well known and fixed, a large one turn loop, like that for the uplink, placed over the miner's position can offer a performance advantage as well as one of convenience, depending on the orientation of the miner's receive loop and the direction of the maximum noise component in the mine.

Grounding of the long-wire antenna has been accomplished by means of four or more ground rods at each end of the wire, with special care being taken to ensure good connections by the use of mud and copious amounts of rock salt. In this manner, total resistance values between about 50 and 100 ohms can be achieved for the long wire antenna; however, maintaining these values over long periods of time can sometimes be a problem.

To establish values of average overburden conductivity for estimating system operating ranges at different mine sites, the well established dipole-dipole measurement technique has been used extensively, and found to give results that agree reasonably well with system test results in most cases over coal mines.

The theoretical results of Wait and ITS, regarding the magnetic fields expected underground from infinitely long, insulated wire sources, placed on the surface of homogeneous and layered conducting overburdens, are well established and have been found to be generally in good agreement with experimental data obtained by WGL and CSM at several mine sites. Similar results have been obtained for surface loops. However WGL field experiences have also revealed a somewhat greater tendency for occasional experimental deviations, from predicted field strength values for the long wire antennas. A possible cause cited for this behavior was the presence of long conductors such as power cables, trolley wires, or rails in the mine, or large inhomogenieties in the overburden. This bears some further investigation.

A constant current assumption is used throughout these derivations. This has been shown to be valid for the frequencies of interest provided the conductors are insulated, which they are in practical applications of interest. The Navy experience in particular, with the huge Sanguine transmit antenna, provides good testimony to the validity of this constant current assumption.

ITS and Wait have also derived expressions and curves for the underground magnetic and electric fields produced by finite, grounded, insulated wire antennas on the surface of a homogeneous, unlayered half space, and for the converse situation of the surface fields from buried finite grounded wires. These cases are more closely related to actual field installations. Both analyses reveal that a finite grounded wire can be treated as an infinitesimal dipole when the observation distance, or depth, is more than about twice the cable length; and treated as an infinitely long wire when the observation distance is less than about one quarter of the cable length, this latter behavior having been experimentally observed at several mines by WGL. In between these depths neither approximation is good, the exact curves or analytical formulation being required. Examination of these curves also indicates only slight departure from infinitely long wire field values for distances up to half the length of the wire, and a reduction from infinite wire field values of only about 3 to 6 dB up to distances, or depths, equal to the length of the wire. The degree to which this behavior changes as the observation point moves toward and beyond the end of the wire was not discussed, but should be obtainable from the analysis. These results will be quite useful for determining minimum practical lengths for surface and underground antenna installations, and as a means for understanding observed experimental behavior.

It was concluded that no new theoretical derivations were needed for loops or infinitely long wire sources on the surface for downlink transmission loss, but as in the uplink case, appropriate practical curves, tables, nomographs, etc. be prepared based on the above results for homogeneous and layered overburdens. Similar curves, nomographs, etc. are needed of the magnetic and electric fields for the finite wire cases treated by ITS. As in the uplink case, curves should be included that depict the increase in signal loss with horizontal in-mine movement away from the long wire, finite wire, and loop positions on the surface, in order to determine in-mine coverage areas.

The effects of a layered overburden on the fields of finite grounded wires have not been treated yet. If it is concluded that layering is likely to influence the downlink field behavior in a significant manner, this case should also be treated by analysis and corresponding practical application curves produced. A summary assessment of the importance of layering to the fields produced by the other sources would also be desirable. Lastly, new and better ways of quickly making good, and long lasting, ground terminations in different ground covers should receive some attention.

b. Parasitic Structures

Long wire and loop antennas deployed on the surface are not as likely as in-mine installations to encounter parasitic structures in their immediate vicinity, unless they have to be deployed in and across the streets of a town, or perhaps directly over a gas pipe or under power lines in rural areas. In the first case the complexity of the parasitic structure configuration will probably defy analytical treatment, and what is perhaps more needed is a practical strategy for choice of antenna type and its deployment, based on present knowledge. In the second instance, Wait and ITS have examined cases of long wire sources parallel to buried conducting non-insulated cylinders.

These results should be examined for their potential application to the gas pipe structure. However, since the effects of such structures generally decrease with increasing distance and orientation angle, perhaps a practical solution to this potential problem is again a deployment strategy for minimum effect, when the presence of this conductor is known and flexibility in antenna deployment is available.

In the section and haulage ways at the receiving end of the downlink, metal structures in the vicinity of the man-carried receiving antennas may play a more important role in altering or providing a shielding effect to underground fields, and, may account for some of the lower than predicted levels experienced by WGL in a few instances. Prime suspects for these infrequently reported anomalies could be closed loops made by two or more vehicle trolley poles across the trolley-track transmission line, say in the vicinity of the section loading point, or steel mesh used for roof support in the entries of some mines. The effects of these structures should be estimated using approximate methods, to see if they, as opposed to large unknown conducting anomalies in the overburden, could account for the significantly reduced horizontal field strength levels observed.

3. The Channel-Noise

As concluded during the workshop and discussed in the downlink overview section, it can be assumed for the purpose of system design and optimization that the mine or mine sections will be in a non-operational, power-down, condition during the operation of the downlink emergency voice system. All major mining and haulage equipment will be turned off, only minor equipment such as pumps, fans, etc., may be left on.

The in-mine wideband noise recordings made by NBS should provide a more than adequate data base from which to optimize the design of the downlink baseband voice system. Expanded frequency-scale power spectra covering the 0-5 kHz band, and depicting discrete frequency and broadband noise levels of both horizontal and vertical components of the magnetic field intensity will be needed. Dubs of selected noise tape recordings are also desired for testing receiver processing techniques and overall system performance in the laboratory. Of particular interest will be data during quiet times and locations on the sections and haulageways, that characterize the emergency power down conditions. Consultation with Bureau of Mines and NBS staff will no doubt be helpful if not necessary in the selection of measurement conditions and data that typify this condition.

4. The Source-Message, Coding, Modulation, Operating Frequency

The source topic was given only brief treatment by the group. It was noted that performance calculations by ADL using early NBS and WGL mine noise data indicate that intelligible downlink baseband voice reception is possible to 1,000 feet in 10^{-2} mho/m overburdens, with under 50 watts of average power under low noise mine conditions. This kind of performance is supported by WGL experience in the field. Indeed, even as little as 5 watts may be required under some highly favorable non-operational conditions. (These reasonable average power requirements can climb to prohibitive levels above 10 kilowatts under operational conditions in DC mines.)

The emphasis for the downlink voice system has remained on the direct transmission of baseband voice signals through-the-earth, particularly under the relatively favorable emergency power-down noise condition. Under this condition, the high-level harmonics of 60 Hz, and particularly those of 360 Hz, will be greatly reduced. Updated performance and overall systems analysis calculations based on the more comprehensive mine noise data recently taken by NBS will help to verify (or deny) the desirability of this frequency band of operation, and better establish the required power levels. These noise data should also help identify transmitter signal conditioning techniques and receiver signal and/or noise processing techniques that can be used to reduce the power, size, and weight required for the mobile, emergency surface transmitter.

The use of pre-emphasized and/or clipped speech upon transmission were suggested for consideration as ways to reduce the peak power requirements of the transmitter, while sacrificing only little intelligibility for the same average speech power transmitted. Means of significantly reducing the bandwidth needed (by more than an order of magnitude) to transmit voice intelligibly have been claimed in the literature. Since such reductions would correspondingly reduce transmitter power, these reported methods should also be investigated.

An alternative method for improving mine communications was also recommended by the group as perhaps a long-term goal for the mining equipment suppliers. Namely, the effective suppression of electrical noise at its source in the equipment whenever practically possible, by means of improved designs and/or addition of special noise suppression equipment.

5. The Receiver-Sensor, Demodulation/Decoding, Special Processing

a. Downlink

As for the source, only brief consideration was given to this topic. A helmet mounted loop antenna design is desired, together with a similarly mounted compact dual-purpose receiver, as mentioned in the system description section. The call-alert function of the receiver will be discussed later.

Use of notch filtering to reduce the interfering effects of high-level harmonics of 60 Hz and 360 Hz, thereby reducing required transmitter power, was the principal suggestion. Such filters have been successfully applied in France, and reference material on these applications will be forwarded to the Bureau of Mines by representatives of the University of Lille. Dramatic improvements in voice reception in the face of harmonic interference have also been demonstrated by ADL in the laboratory, with a breadboard design of a simple electronic commutator-type filter that is particularly suited to rejecting harmonic signals. The French and ADL reported results should be reviewed, together with other reported notch filter work. They should be reviewed for their effectiveness against the mine emergency condition harmonic interference; and for their practical application to a compact helmet mounted receiver, should the measured harmonic levels warrant the use of notch filtering under emergency power-down conditions. In regard to this latter point, it may be necessary to evaluate the effect of pure or complex "tones" of noise,

such as those created by harmonics of 60 Hz and 360 Hz, on the intelligibility of received speech. The effect of direct audio noise in the mine environment (which will probably be low under emergency conditions) should also receive brief consideration along with that of the overall speech sound level to be delivered to the miner.

b. Uplink

Performance calculations, similar to those for the downlink discussed above have also been performed by ADL for a baseband voice uplink using a multiturn 100-foot periphery loop transmit antenna instead of a long wire. The results indicate that, except under the most favorable conditions of depth (300 feet) and the quietest of surface noise conditions, the levels of transmitter power, voltage, and current required are well in excess of those demanded by intrinsic safety, long operating life, and practical size and weight for an in-mine emergency unit. These uplink transmitter requirements for voice should be reconfirmed, along with those for the downlink voice system, in light of the more comprehensive NBS mine noise data now available and the larger in-mine loop antennas being considered. However, it appears that an uplink voice system that can operate from available emergency power will continue to remain impractical until an economic and practical way is found to significantly reduce the bandwidth required to transmit intelligible speech.

Sidelink Call Alert Coded Page System

1. Overview

The call alert system is a recent by-product of the success experienced with the experimental electromagnetic CW transmitter developed by WGL for locating miners trapped beneath overburdens of 10^{-2} mho/m conductivity to depths of 1,000 feet. As mentioned previously, the location transmitter is intrinsically safe, operates from a miner's 4-volt cap lamp battery into a one-turn loop placed in an entry or wrapped around a coal pillar, and generates a periodically interrupted CW signal in the 1-3 kHz band. This signal is detectable on the surface above the miner and is suitable for locating the miner's horizontal position. The development of this location transmitter has now progressed to where an improved preproduction prototype unit is being manufactured by Collins Radio Co. in limited quantities for testing in some operating mines.

Since the horizontal ranges desired for the call alert system described in section II are commensurate with the vertical ranges obtained for miner location, the Bureau is presently giving high priority to the development of a call alert page system centered around an adapted version of the WGL location transmitter. As presently conceived, this paging transmitter will be activated by means of a carrier signal sent over the mine phone line from the surface to the desired section. The call alert transmitter will be connected to a loop wrapped around a coal pillar, perhaps at the section loading point, and will transmit a single frequency tone (perhaps simply coded) to a compact, dual-purpose, helmet-mounted receiver worn by the individual being paged to the section's mine phone. Under low noise emergency conditions, this receiver will

be operable in a baseband voice mode for downlink message reception. Under high noise operational conditions, it will operate in a narrowband call alert mode, receiving a prearranged CW paging signal spaced between the strong 60 Hz harmonics usually present under these conditions.

A first generation experimental call alert system has been built from existing hardware by WGL, and installed in the Bureau's experimental mine to demonstrate concept feasibility in a non-operational environment. Though the operating frequencies of the present experimental unit are in the 1-3 kHz band, to take advantage of the frequencies available with the present location transmitter, an overall system analysis for an operational noise environment may reveal a more effective operating frequency.

Overall system requirements are presently being formulated by the Bureau. These will form the basis for subsequent systems analysis and optimization of designs that can be converted into practical, intrinsically-safe hardware for day-to-day use in operating mines.

2. The Channel-Transmission Loss

a. Loops

In-mine call alert paging is a sidelink application utilizing two essentially coplanar loops, while miner location is an uplink application utilizing two essentially coaxial loops. Examination of Wait's theoretical coupling curves for infinitesimal loops buried in homogeneous overburdens reveals that the operating range for a horizontal coplanar geometry is reduced by only about 20% over the range for a vertical coaxial geometry, for ranges in the vicinity of three skin depths. This operating range is reduced even less at greater distances. Vertical ranges in excess of 1,000 feet have been obtained with the location transmitter. At 2 kHz (the center of the 1-3 kHz operating band of the location transmitter), the three skin depth range is 1,100 feet, which gives rise to a potential sidelink operating range of 900 feet. This 900 foot range is in excess of the 400 to 800 foot range needed for call alert coverage of the typical 600 by 600 foot section mentioned in section II. The above range conclusions are, of course, based on equal noise conditions for each case. Since the noise environment will likely be more severe for the in-mine, operational, call alert application, its effect on operating range and transmitter/receiver design has to be determined.

At the under 5 kHz frequencies of present interest for the call alert system, the theoretical work of Wait/ITS has shown that the effects of layering (such as that found above and below coal seams) and air-filled cavities (such as tunnels in coal seams) should not be significant for loops, and therefore can largely be ignored for communications applications. Similarly, the infinitesimal loop theoretical results should be adequate for making performance predictions, particularly at the desired range limits, for mine sections free of parasitic influences. At ranges close to the loop installation, the infinitesimal loop results will tend to overestimate signal strengths somewhat. This discrepancy will become important primarily when treating potential coupling to nearby parasitic structures, as discussed below. Therefore, curves, tables, nomographs should be prepared for the vertical magnetic

field component in the plane of the transmit loop, based on the available theoretical results for coplanar infinitesimal loops. These can be used temporarily for making preliminary performance predictions until more information is forthcoming on the effects of the conductors prevalent in mine sections.

b. Parasitic Structures

Mine sections typically contain many conductors, such as trolley wires and rails, fixed and trailing power cables, roof bolts, and sometimes steel roof-supported mesh, that can affect the strength and orientation of magnetic fields. Therefore, a series of limited signal strength measurements should be conducted in operational mine sections, and in other mine locations that are relatively conductor-free. These simple experiments are needed; to verify whether the homogeneous-overburden coplanar loop results can be applied with confidence to operational sections, and to formulate practical design guides for operational sections. Preliminary results from field measurements taken by ADL in the Bureau's experimental mine indicate that significant departures from the theoretical results can in fact occur.

In parallel with the above field measurements, corresponding theoretical analyses are needed to predict the degree to which the direction and strength of the magnetic fields produced in the tunnels, by finite loops wrapped around coal pillars, will be affected by the above mentioned conductors in working sections of the mines. Of particular interest will be the effects caused by trailing and fixed power cables, roof bolts, and trolley wire/rail structures, which appear manageable analytically. The potential problems caused by heavy metal mesh occasionally used for roof support were acknowledged, but assigned a lower priority for analytical treatment, because of the infrequent use of this mesh and perceived analytical difficulties.

ITS has done some investigation of the currents induced in a thin, infinitely long, cylindrical conductor by a nearby infinitesimal loop transmitter. This work reportedly is easily extendable; to include the effects of the magnetic field produced by this induced current, and to include the effects produced by a finite loop source. The utility of this approach should be investigated, and pursued if found applicable.

ITS has also examined the influence of buried spherical and prolate spheroidal conducting objects on the fields produced by infinitesimal loop sources. Though originally done in connection with the miner location problem, the results can be applied to the call alert application, to estimate the likely field effects produced by machinery and shuttle cars. For the frequencies, sizes, geometries, and distances of interest, these objects will not significantly alter the magnitude of the fields, but mainly their direction somewhat in the immediate vicinity of the objects. No further investigations of this area were recommended.

c. Roof Bolts

If a finite wire terminated by roof bolts is shown to be a favorable transmit antenna for the roof bolt paging system, a suggestion was made that it also be considered for use in the call alert system.

3. The Channel-Noise

Since this is a narrowband operational system for mine sections, the in-mine wideband noise recordings made by NBS should provide an adequate data base. Of particular interest will be expanded frequency-scale power spectra showing levels of discrete and broadband noise covering the 0-5 kHz band; and representing data taken primarily on working sections in the vicinity of face machinery and power cables and conversion equipment, under representative operating conditions. Vertical field components of the noise will be most important for this application. Dubs of select recordings will also be desirable as mentioned previously. Although frequencies below 5 kHz are presently favored, data can and should be examined above 5 kHz for this system.

4,5. The Source and Receiver

Only little attention was devoted to this topic, with the group agreeing that a definition of system requirements and an overall system analysis were needed to identify the most favorable and practical system design approaches. However, a few brief comments were made.

The transmitted call alert signal could be a single tone, keyed on and off with a fixed duty cycle, as in the present experimental unit. For a single page signal per section, the simple, single tone system now used in the experimental unit could be adequate. For several pages addressable to different individuals per section, some means of coding the single tone, or use of multiple tones would be needed. The most favorable coding method from practical and noise immunity standpoints needs to be determined.

On the receiving end, it was noted that notch filters may be needed to minimize interference from 60 Hz harmonics adjacent to the signal frequency. The most practical and effective noise processing techniques suited to a compact, helmet-mounted receiver need to be determined.

As mentioned in section II, this system could conceivably share equipment with an uplink data station also located on the mine section.

Sidelink Roof Bolt Voice Page System

1. Overview

The roof bolt voice paging system is a system conceived and recently developed by the Bureau for transmitting voice messages to key individuals carrying small pocket pagers on working sections under operational conditions. A prototype, using readily available commercial equipment, is presently installed in the Bureau's experimental mine to demonstrate its feasibility in a non-operational environment. The system concept developed as a result of some successful in-mine experiments performed by the Pittsburgh Mining and Safety Research Center; whereby a 20-watt trolley phone 88 kHz FM transmitter was connected to two roof bolts approximately 50 to 100 feet apart in an operating mine, and its voice transmission then received at distances up to about 600 feet away with a small pocket pager utilizing a ferrite loop stick antenna.

Limited field experience to date indicates that operating ranges commensurate with the 400 to 600 feet required to provide section coverage may be achievable, under operational conditions, with an operating frequency in the vicinity of 100 kHz. At this point in time a more quantitative understanding of the transmission loss and what affects it is needed; in order to determine the most favorable operating frequency, to develop practical guidelines for tailoring installations and estimating performance in different mines, and to eventually develop an improved system.

2. The Channel-Transmission Loss

a. Finite Wire Antennas Terminated by Roof Bolts

The finite wire antenna in this case is an insulated wire that runs along the roof of a tunnel and is terminated at each end by attachment to a roof bolt. Field experience to date has found the total termination impedance for such roof bolt pairs, separated by 50 to 200 feet, to fall in the range of 120 to 50 ohms resistive. Theoretical curves and supporting experimental data are needed, to adequately describe the behavior of the magnetic fields produced in the tunnels throughout a section in which such a finite wire transmitter is located.

The theoretical work of Wait and ITS on finite wire antennas buried in homogeneous overburdens, described in sections IIA2c and IIB2a, should be particularly useful in this regard and for estimating system coverage areas in mine sections. Though the present results are for the electric and magnetic fields produced on the surface from such buried antennas, ITS maintains that the desired field strengths in the coal seam tunnels can be easily obtained from its present buried-finite-wire analysis. This case of interest corresponds to receiver locations below, but in the immediate vicinity of, the plane of the finite wire.

Frequencies presently being investigated for this voice page application range from 10 kHz to 300 kHz, with present experimental systems operating around 100 kHz. Although the frequencies in the upper part of this band are higher than originally anticipated for buried finite wire applications, ITS believes that its present analysis should apply.

Therefore, it was concluded that the ITS theoretical analysis of the fields from buried finite wires should be used to determine the desired magnetic fields in the coal seam, in the 1-300 kHz band; and to prepare appropriate practical curves, tables, etc. for use by system designers. In addition, since the overburden is usually layered above and below coal seams, and since layers of varying conductivity can potentially influence the fields from finite wire antennas more than those from finite loops, a theoretical analysis to determine the effects of a simple, representative, layered model should be performed.

The non-conducting volumes created by the grid of tunnels in the coal seam were considered too difficult for exact analytical treatment at this stage; and in fact may not create significant effects on the magnetic fields in the tunnels, because the tunnels are relatively narrow and the currents can still flow without much alteration through the wider coal pillars.

Collins Radio and Spectra Associates are also reported to have performed theoretical analyses of the fields from buried wires, for the infinitely long and infinitesimally small cases. This work should also be reviewed, compared with the ITS results, and utilized if applicable.

Collins Radio has also conducted some limited measurements of the magnetic fields produced by 52 feet long, finite wire roof bolt antennas in an operating mine. Three field components were measured at three distances between 300 and 700 feet away from the finite wire, in both the broadside and axial directions, and at five frequencies in the 1-50 kHz band. Though these measurements do not fully characterize the expected transmission loss behavior, the data serve as a good starting point for comparisons with theory and establishing practical design guidelines. More measurements are needed, covering a greater range of distance, frequency, and roof bolt spacing, and particularly in mine working sections.

b. Parasitic Structures

As in the case of the call alert system, a roof bolt system installed in a working section can be expected to encounter many conducting parasitic structures that may alter the directions and magnitudes of the signal magnetic fields. These effects may even be magnified for finite wire systems operating at the higher frequencies anticipated. Indeed, some limited field measurements taken at 88 kHz by ADL, for a roof bolt antenna installation in the Bureau's experimental mine, indicate an extremely high variability in the levels of the measured vertical field component at comparable ranges from the roof bolt antenna. Therefore, and for the same reasons given for the call alert system, a similar experimental and theoretical effort is recommended to resolve the issues concerning the effects of parasitic conducting structures found in representative working sections of operating mines.

3. The Channel-Noise

Since the roof bolt system is a voice paging system for use under operational conditions, its operating frequency will most likely be above about 10 kHz, where the operational noise levels decrease to more tolerable levels. Present consideration is being focussed on the 10 kHz to 300 kHz band. The present experimental system operates at 88 and 100 kHz, but since these frequencies are already utilized by mine trolley wire carrier systems, alternative non-interfering frequencies are also desirable.

As for the other systems, the recently obtained NBS in-mine noise data should serve as a more than adequate data base for systems analysis and optimization in the 10 kHz to 300 kHz band. From the wideband tape recordings, power spectra for horizontal and vertical magnetic field components will be available, depicting discrete and broadband noise levels over the frequency range from 0-100 kHz and 0-300 kHz. In addition, noise amplitude probability distributions and rms levels will be available from the narrowband (2 kHz) spot frequency noise recordings, at eight frequencies over the 10 kHz to 32 MHz band, four of which fall below 300 kHz. Appropriate dubs of selected tape recordings for both types of noise measurement

should also be available. Detailed reports documenting these measurements and data will soon be published by NBS.

4,5. The Source and Receiver

The present experimental system is designed around a commercially available 20 watt, mine trolley wire phone transmitter that employs conventional FM modulation and an industrial pocket pager FM receiver that operate at a carrier frequency of either 88 or 100 kHz. Lack of time prevented discussion of the overall system by the group, but it was concluded that the degree to which this system can or should be optimized or otherwise improved with regard to performance, practicality, intrinsic safety, etc. will eventually be determined by the system requirements and a subsequent system analysis.

D. SUMMARY REPORT OF
OPERATIONAL COMMUNICATIONS
WORKING GROUP

THROUGH-THE-EARTH ELECTROMAGNETICS WORKSHOP

Golden, Colorado

August, 1973

GROUP CHAIRMAN

MARTYN F. ROETTER
ARTHUR D. LITTLE, INC.

OUTLINE

SUMMARY

- Short-Term Projects
- Longer-Term Projects

OPERATIONAL COMMUNICATIONS FUNCTIONS

ENVIRONMENTAL CONSTRAINTS

OPERATIONAL COMMUNICATIONS SYSTEMS

UHF Radio (U.S.)

1. State-of-the-Art
2. Future Development Programs
 - a. Short-Term
 - b. Long-Term

Leaky Coaxial Cable Communication Systems (Europe)

1. State-of-the-Art
 - a. INIEX/Delogne System (Belgium) Employing Regularly Spaced Radiating Devices
 - b. Coaxial Cable with High Surface Transfer Impedance -- Specially Designed "Leaky" Braid Outer Conductor (France)
 - c. Coaxial Cable with Repeaters (U.K.)
2. Future Development Programs
 - a. Short-Term
 - b. Long-Term

Simple Wire Systems (Europe)

1. Wire Pairs
2. Single Wire

Low Frequency Radio in a Hoist Shaft (U.S.)

1. State-of-the-Art
2. Future Development Programs
 - a. Short-Term

SUMMARY

The work of the operational communication systems' group dealt with a range of communication needs and functions within mines, primarily along haulageways, to and within sections up to the working face itself, and in mine shafts. A mixture of communication techniques and hardware is needed to satisfy this variety of communication needs within the differing environments encountered in U.S. mines. Substantial progress, both experimental and theoretical, has been made in recent years towards developing alternative communication systems suitable for use in mines which are based on "guided" waves, including wire-less (waveguide-like propagation in mine tunnels) and wire-based systems (leaky coaxial cables or wires). Major priorities identified for further work needed to confirm (or deny) the applicability, and refine the operational specifications of promising communication systems for mine use include:

Short-Term Projects

- Cost/performance analyses of promising leaky coaxial cable and UHF radio communication systems which require further data from:
 - Experimental investigation under U.S. mine conditions of the performance of potentially applicable leaky coaxial cable communication systems developed in Europe (France, Belgium, and the U.K).
 - Cost estimates on these coaxial cable communication systems.
 - Measurements of UHF radio propagation in low-coal mines.
 - Investigation of the influence of obstacles (e.g. shuttle cars and section machinery) in the entries on UHF radio propagation in mines.
- Investigation of the problems of transmitter and receiver coupling and termination matching associated with the two-way propagation of low frequency radio waves in hoist shafts.

Longer-Term Projects

i.e. of lesser urgency or where less information is currently available.

- Investigation of techniques for coupling UHF radio to leaky coaxial cable communication systems.
- Delineation of the role of, and needed interfaces for, operational communication capability related to emergency, paging and monitoring functions.

OPERATIONAL COMMUNICATIONS FUNCTIONS

The communication functions under discussion in this report are primarily:

- Two-way communication along main haulageways up to 4-5 miles long, to vehicles and to maintenance personnel.
- Two-way communication in sections up to working faces; all entries near the working face should be covered, but possibly only a limited proportion of those at or near main haulageways. Communication with roving personnel at up to 3,000 feet away from main haulageways must be established. More than one kind of working face must be dealt with, i.e. room and pillar (predominant in the U.S.) and longwall.
- Two-way communication in mine hoist shafts (on the order of 10,000 feet long).

Two distinctive categories of communication are involved, the first depending upon a base station, and the other dealing with direct mobile-to-mobile communication.

Although not discussed in detail, it is recognized that the communication systems designed to fulfil these purposes may interface with other communication systems such as trolley phone, as well as play a role in assuring some emergency, paging (call alert), and one-way monitoring communication functions.

ENVIRONMENTAL CONSTRAINTS

The primary constraints recognized as affecting the communication systems under consideration are:

- Daily utility of equipment
- Intrinsic safety
- Ruggedness and resistance to harsh mine environment
- Available power
- Weight and size limitations
- Cost limitations

The electromagnetic noise environment at the frequencies typically proposed or employed (a few MHz up to 1 GHz) appears not to be a significant factor in determining communication system performance. A possible exception to this rule or slightly less clear-cut situation may prevail in the case of low frequency (LF) radio propagation proposed for communication in mine shafts (at frequencies of a few tens of kilohertz).

OPERATIONAL COMMUNICATIONS SYSTEMS

Several alternative communication systems are in principle technically capable of satisfying the communication needs just described. A tentative conclusion in the light of our present state of knowledge is that communication along haulageways may be efficiently provided by one or more of the proposed leaky coaxial cable systems discussed later. However, leaky coaxial cable systems seem incapable of providing communications capability at more than 10 to 20 meters lateral distance from the cable. Thus in order to provide wide area communications coverage within the network of tunnels in a coal mine section, it would be necessary to string cables along most of them. The cost and practical obstacles to stringing all this cable in a continually changing section geography favor the application of UHF radio for wide area communications within a section. There is both theoretical and experimental evidence to indicate that UHF radio is capable of providing this function.

Coaxial cable, radio, and low frequency TEM radio wave transmission in the shaft are all potential candidates for providing communication in a mine shaft. No single one of these communication techniques has yet been identified as being especially advantageous in this application.

The communication techniques discussed fall under the general description of "guided" waves and comprise:

- Wire-less (UHF frequencies)

- Wire-based
 - Coaxial cable with periodic radiative structures (INIEX/Delogne)
 - Coaxial cable with high surface transfer impedance (braid outer conductor)
 - Coaxial cable with repeaters
 - Wire pairs
 - Single wire (including LF radio propagation in mine hoist shafts)

It is also recognized that power-line carrier communication techniques are potentially attractive for some of the communication applications under consideration; it is worthwhile to investigate power line carrier systems further, however, no serious evaluation of them was made in this workshop. Power line carrier systems are already used along the trolleyway in some mines.

In the following, promising communication systems are identified and their current state of development described. Problems and areas where additional data or further theoretical understanding are needed are listed, and priorities for future development work are suggested.

UHF Radio (U.S.)

1. State-of-the-Art

Marked progress has recently been made in understanding the characteristics and capabilities of UHF radio wave propagation along coal mine tunnels. Measurements taken in mines by Collins Radio indicate that effective communication can be provided throughout most of a typical U.S. coal mine section by UHF radio. A theoretical analysis carried out by Arthur D. Little, Inc. (ADL) staff based upon the hypothesis of waveguide propagation is in agreement with the Collins measurements in several important respects. The theoretical model is believed to reflect the basic structure of UHF radio wave propagation in coal mine tunnels, although it is presently not intended to give accurate signal loss estimates around corners when either the transmitter or receiver is near the corner (less than 50-100 feet). In those cases the model's loss asymptotes will over estimate the loss.

During the workshop an apparent violation of the reciprocity theorem was discovered in an application of the ADL theory to extend Collins Radio's data for a determination of the extent of coverage provided by UHF communication within a section. This apparent violation is believed to result from an application of the ADL model in a region where it is invalid, namely in the corner loss situation just mentioned. The reciprocity theorem must be respected, and a refinement of the model is needed to predict transmission loss around a corner when either the transmitter or receiver is nearby the corner. Collins Radio has re-evaluated the section coverage predicted for UHF radio which can be deduced from their data and extrapolated by the ADL theory, assuming the reciprocity theorem holds. The results of this computation are attached; they are very encouraging.

Leaky coaxial cable communication systems operating between 2-20 MHz appear incapable of providing communication along cross-cuts in which they are not strung, and hence appear both costly and unlikely of implementation for communication in the grid of many tunnels which constitute a section. UHF radio is likely to be more effective in this situation of areal rather than essentially linear or tubular communication coverage. In summary,

both theoretical and experimental results obtained to date warrant further development of UHF radio techniques for providing practical communications in coal mine sections.

2. Future Development Programs

(a) Short-Term

No measurements have yet been taken of UHF radio wave propagation in low-coal mines* which constitute a significant fraction of U.S. coal mining activity. These measurements are needed to determine if the different geometry of low-coal as against high-coal mine tunnels permits practical communication of UHF.

Additionally information is needed on the influence of obstacles in entries and tunnels on UHF radio wave propagation. In a coal mine "obstacles" such as section machinery and shuttle cars are inherently present. Some of these obstacles can block the major portion of an entry and may wipe out effective communication to various areas of the mine section as they move around. Multipath propagation effects may help in overcoming this problem; at any rate, data are urgently needed.

Less urgently, it would be revealing to obtain UHF propagation data of higher frequencies (above 1 GHz) where critical tests of the ADL theory, including the selection of the optimum operating frequency, would be possible. In practical terms these measurements are not, as already mentioned, of the highest urgency, as the use of a frequency above 1 GHz for mobile UHF radio is improbable since it would entail significantly more expensive (because non-standard equipment). Standard UHF frequencies for mobile communication are in the 450 MHz band, and the 960 MHz band soon to be opened by the FCC. It may additionally be noted that the FCC may not in any case approve non-standard UHF frequencies for underground mobile communication, even though in principle, use of non-standard frequencies is acceptable for underground use as long as no leakage to the surface occurs. The basis for this attitude may be explained by the ease with which mobile, as against fixed communications gear, may be taken out of the mine for personal use.

*However, the reduced range performance of 420 MHz portable handy talkies recently encountered by Bureau of Standards staff during a noise measurement field trip to a low coal mine appears to partially confirm the significantly higher propagation loss predicted for coal mines by the theory.

The Bureau of Mines should also delineate clearly the alternatives and practical considerations associated with the placing of the UHF transmitter (and possibly repeaters) to provide the best communication coverage within a section, taking account of its continually changing features.

(b) Long-Term

A future scenario may be envisaged in which a leaky coaxial cable communication system is in use along mine haulageways, whereas UHF radio provides communication up to working faces. In this situation the effective exploitation of all the advantages of these two communication techniques would be enhanced by the ability to couple them together. The techniques, costs, and performance of methods practicable to accomplish this coupling should be investigated.

Leaky Coaxial Cable Communication Systems (Europe)

1. State-of-the-Art

Three major classes of coaxial cable communication systems designed for use in mines have been reported as being in various stages of development in Europe.

(a) INIEX/Delogne system (Belgium) employing regularly spaced radiating devices

Much experimental and theoretical investigation of this system has been performed including trials at the Bruceton, Pa. experimental mine of the USBM. The optimum operational frequency is believed to fall in the range of 2-20 MHz. Prototype installations are on order in Belgium, at a price of about \$2500/km. Firm production sales prices are not yet available. The INIEX/Delogne scheme appears potentially suitable for application in U.S. mines, although several uncertainties regarding performance/cost trade-offs in typical U.S. mine environments still have to be resolved, as discussed below. These uncertainties are connected in particular with the restraint in U.S. mines, in contrast to Europe, of having to install the cable close to the rib with consequent increases in attenuation, over a more central location in the tunnel, and with the influences on performance of dirt and water on the cable and on the radiative devices.

(b) Coaxial cable with high surface transfer impedance -- specially designed "leaky" braid outer conductor (France)

Theoretical investigations carried out at the University of Lille in France indicate that effective communication along several miles of mine haulageway may be achieved by use of a coaxial cable whose braid outer conductor is designed for "optimum" leakage of radiation. Experimental investigations of this scheme in a French mine are planned to be carried out in a few months' time. The optimum operational frequency is believed to be between 5-10 MHz.

Similar uncertainties exist with regard to the effects of dirt, water, and proximity to the walls of the tunnel on the performance of the proposed French scheme in U.S. mine environments, as were mentioned in the context of the Belgian cable system.

(c) Coaxial Cable with Repeaters (U.K.)

It has been reported that coaxial cable communication systems incorporating repeaters are being tested experimentally in the U.K. At this workshop little information on the cost and performance of this system was available. Additional uncertainties in the performance and cost evaluation of this system are introduced by questions associated with the reliability and maintainability of the repeaters that can realistically be expected in a mine environment.

2. Future Development Programs

(a) Short-Term

Progress achieved in Europe in the development of the coaxial cable communication systems mentioned above should be carefully and continually monitored and evaluated. In particular, cost estimates and further operating performance data should be obtained as soon as possible.

Nevertheless, European results, while valuable and to date encouraging, cannot be directly applied to the different environment of U.S. mines. In particular it appears impossible to install communication cables in U.S. mines in the locations recommended by European researchers. Specifically cables will have to be installed close to the ribs or walls of tunnels. Accordingly different attenuation rates, and correspondingly different optimum operating frequencies or trade-offs between the rate of "leakage" of power and total communication system length may prevail than in the European situation. Experimental investigations in U.S. mines with the proposed European coaxial cable systems are required before their applicability in this country can be definitively confirmed or denied, and if confirmed, operational specifications written (frequency, design of radiative structure or "leaky" outer conductor, and so forth).

(b) Long-Term

As was discussed in the section on UHF radio, techniques for coupling coaxial cable systems to UHF radio communication should be investigated.

Simple Wire Systems (Europe)

1. Wire Pairs

The technical feasibility of communication via waves propagated along wire pairs is well established, and the coupling between and characteristics of the unbalanced and balanced modes of propagation are well understood. However the sensitivity and lack of resistance of simple wire pairs to the deleterious effects of the mine environment (dirt, water, rough handling) tend to rule them out as practical implementations of in-mine communication systems.

2. Single Wire

A single wire communication system is impractical as a solution to a mines' operational communication needs along haulageways or in sections, although a similar type of communication system operating in the low frequency (LF) range holds promise for use in mine shafts.

Low Frequency Radio in a Hoist Shaft (U.S.)

1. State-of-the-Art

Theoretical investigations at ADL have analyzed the propagation of LF radio waves in deep (10,000 feet) hoist shafts in which the hoist cable is the only metal conductor present. Propagation losses of approximately 2dB over 10,000 feet at frequencies near 50 kHz have been computed. This is a very encouraging result.

2. Future Development Programs

(a) Short-Term

Two difficulties with respect to LF propagation in hoist shafts have been identified. Firstly, the large penetration of the wave into the rock outer conductor may present a problem with regard to coupling the transmitter or receiver to the transmission line with a minimum of insertion loss. The amount of the insertion loss that can be tolerated has not yet been specified; it may be quite large, in view of the remarkably low transmission losses calculated. The coupling problem merits attention to determine, for example, how closely to the theoretical distribution of the vertical component of current density, in the fundamental propagation mode, should the actual driving current be distributed.

Secondly, in order to minimize reflections, both ends of the hoist cable-shaft transmission system must be terminated in approximately the characteristic impedance of the transmission line. Further work is needed to resolve the question of how, how well, and how expensively matching terminations may be provided.

Dark Regions Indicate Areas
Not Covered by UHF Radio
(Ignore Diagonal Lines)



FIGURE 1 PREDICTED COVERAGE OF MINE SECTION BY UHF RADIO FOR TWO ASSUMED SITUATIONS

Source: Collins Radio Co.

PART NINE

ADDITIONAL TECHNICAL SUPPORT AND CONSULTING
SERVICES RELATED TO MINE COMMUNICATIONS AND
MINER LOCATION

PART NINE

ADDITIONAL TECHNICAL SUPPORT AND CONSULTING
SERVICES RELATED TO MINE COMMUNICATIONS AND
MINER LOCATION

TABLE OF CONTENTS

	<u>Page</u>
List of Tables	9.iv
List of Figures	9.v
INTRODUCTION	9.1
I. SHORT-TERM ASSIGNMENTS	9.1
II. USER REQUIREMENTS AND THE DESIGN OF MINE COMMUNICATION SYSTEMS	9.3
A. INTRODUCTION	9.3
B. ACQUISITION OF KEY USER REQUIREMENT DATA AND INFORMATION	9.4
C. ANALYSIS OF DATA AND FORMULATION OF TRAFFIC AND PERFORMANCE REQUIREMENTS	9.5
D. SYNTHESIS OF CANDIDATE SYSTEMS	9.6
E. HARDWARE SPECIFICATION	9.6
F. CONCLUDING REMARKS	9.6
ADDENDUM	9.7

PART NINE

ADDITIONAL TECHNICAL SUPPORT AND CONSULTING
SERVICES RELATED TO MINE COMMUNICATIONS AND
MINER LOCATION

TABLE OF CONTENTS
(Continued)

	<u>Page</u>
III. ON MODELS, DISPLACEMENT CURRENTS AND CONDUCTION CURRENTS	9.9
A. BACKGROUND	9.9
B. FIELD EQUATIONS IN NORMALIZED FORM	9.9
C. SCALING CONSIDERATIONS	9.12
D. CONCLUSIONS	9.19
APPENDIX A - HIGH CONDUCTANCE ELECTROLYTES FOR SEA WATER/AIR INTERFACE MODELS	9.20
APPENDIX B - ESTIMATES OF APPROXIMATION ERRORS WHEN DISPLACEMENT OR CONDUCTION CURRENTS ARE NEGLECTED	9.24
APPENDIX C - TRIP TO HARVARD UNIVERSITY FOR DISCUSSIONS ON MODELS	9.31
IV. PERMANENT MAGNETS AS SIGNAL SOURCES FOR TRAPPED MINER LOCATION AND COMMUNICATION	9.34
A. ROTATING BAR MAGNETS	9.34
B. MAGNETIC FIELD GRADIENT DETECTION	9.36
C. CONCLUDING REMARKS	9.37
V. PRELIMINARY FEASIBILITY EXPERIMENT FOR A MINE WIRELESS ALARM SYSTEM	9.38
A. INTRODUCTION	9.38
B. EQUIPMENT	9.38
C. EXPERIMENT	9.42
D. CONCLUDING REMARKS	9.47

PART NINE

ADDITIONAL TECHNICAL SUPPORT AND CONSULTING
SERVICES RELATED TO MINE COMMUNICATIONS AND
MINER LOCATION

LIST OF TABLES

<u>Table No.</u>	<u>Title</u>	<u>Page</u>
A1	Bibliography of Recent Conductance Measurements in Concentrated Aqueous Solutions	9.21
A2	Specific Conductances of Several Salts	9.22
A3	Maximum Conductance Solutions of H ₂ SO ₄	9.23
A4	Conductance of KOH Solutions at 18°C	9.23
1	Field Strengths and Gradients for Samarium Cobalt Bar-Type Magnets	9.34
2	Ranges at Which Signal and Noise Fields are Equal (for Bar Magnet Signals and Geomagnetic Noise)	9.35

PART NINE

ADDITIONAL TECHNICAL SUPPORT AND CONSULTING
SERVICES RELATED TO MINE COMMUNICATIONS AND
MINER LOCATION

LIST OF FIGURES

<u>Figure No.</u>	<u>Title</u>	<u>Page</u>
	<u>Chapter V</u>	
1	Block Diagram of Equipment for Preliminary Feasibility Experiment	9.39
2	Seismic Sine Wave Force Generator	9.41
3	Simplified CCS-3A and B Functional Diagram	9.41
4	Experiment Geometries	9.43
5	Signal and Noise for Trailer Test	9.45
6	Signal and Noise for Telephone Pole Test	9.46

PART NINE

ADDITIONAL TECHNICAL SUPPORT AND CONSULTING SERVICES RELATED TO MINE COMMUNICATIONS AND MINER LOCATION

INTRODUCTION

Over and above the technical support and consulting work described in the preceding Parts of this Volume, ADL staff also provided a wide range of additional technical assistance to the Bureau on an ad hoc basis over the course of the contract, and particularly in 1973. Some of these assignments were on tasks that temporarily assumed a high priority at PMSRC, requiring a fast response, while others were more suited to conventional schedules but on communication and location topics less directly related to those in the preceding Parts. Chapter I briefly describes some of the diverse short-term assignments while Chapters II through V treat assignments on the other topics.

I. SHORT-TERM ASSIGNMENTS

A sampling of short-term, fast-response assignments undertaken on mine communications and miner location for PMSRC during 1973 are given below. These assignments included technical reviews, discussions and recommendations related to the theory, experimental data, designs, and hardware implementation of experimental CW and pulse miner location EM transmitters; preparation of technical performance specifications for a miniaturized preproduction prototype CW electromagnetic location transmitter; review of specifications for a seismic signal detection experimental study; participation in technical discussions and experiments with PMSRC and equipment suppliers regarding the UHF radio/radiacable communications installation in the Bruceton mine; participation in an informal conference to discuss mine communication and monitoring needs and preferences with representatives of the Bureau, mine operators, and equipment manufacturers; participation in technical discussions with representatives of a U.S. mine operator and CERCHAR* concerning the characterization of faults on trolley lines and means of improving their rapid detection;** recommendation of simple signal, noise, and ground fault measurements on mine phone lines; review of an inexpensive automatic telephone dialer; preliminary discussions regarding the feasibility of adapting and assembling a collection of available telephone industry carrier equipment for installation and test in an operating coal mine; evaluation of a proposed call alert mine paging system; review of hardware designs and future experiments for a mine communication sled; design critique of a proposed six-channel narrow-band FM voice modem for carrier communication on the mine phone line; preparation of technical performance

* Laboratoire Du Centre D'Etudes Et Recherches Des Charbonnages De France.

** ADL has since undertaken Contract H0242004 to evaluate the feasibility of a new trolley fault detection concept which is based on measuring the difference in current between that drawn by a locomotive, and/or other legitimate loads, and the current supplied at trolley feed points.

and interface specifications for a hoist shaft radio communication system for deep shafts; review of hoist shaft attenuation loss analyses and measurements conducted in hoist shafts; participation in design review meetings for improved experimental and preproduction prototype CW location transmitters; review of a specific patented voice bandwidth compression technique; and a preliminary investigation and recommendations regarding the feasibility of a slowed-down-speech bandwidth-compression method for emergency through-the-earth voice communications. These short-term assignments usually concluded with verbal reports or short informal reports or memoranda submitted to PMSRC. The following Chapters treat in a more comprehensive manner the other mine communication and miner location assignments mentioned in the Introduction to this Part.

II. USER REQUIREMENTS AND THE DESIGN OF MINE COMMUNICATION SYSTEMS

A. INTRODUCTION

During the course of our work early in 1973, PMSRC asked us to briefly outline a program for identifying mine communications needs and traffic requirements for the purpose of designing totally integrated mine communication systems.* Such systems would tie together the two major communication areas; the first at the surface which is a communication network tying together management, shops, stores, underground production facilities, and dispatch; and the second which is an underground communication network tying together shops, sections and working faces, haulage way vehicles, and key miners on-the-move. The two principal objectives of such integrated mine communications systems are

- (1) to provide increased safety for the miners, and
- (2) to provide increased productivity of the mining operations.

This Chapter sets forth some of the basic principles and steps commonly used in designing communications systems. Good communication system design generally starts with identification of user requirements, progresses to synthesis and comparative analysis of candidate systems, and then to the hardware specification and detailed design stage. While in many cases a communication system may be limited by equipment capabilities, nevertheless true user requirements should be identified, even if some of them turn out to be difficult to satisfy.

The key to the specification of any communications systems is the establishment of the user requirements, that is a determination of the generic needs of all users of the communications system. There are several aspects that are essential to the study of user requirements. One is a determination of the total traffic that is generated from all users in the system. This traffic can be quantified not only in terms of total traffic, but also its time dependent aspects, so that busy hour traffic loads can be determined for specifying the total number of channels required. In addition to traffic and its time dependence, the actual terminals (nodes) for the messages communicated in the system should be clearly identified. In situations such as coal mines where current communication facilities exist, one cannot assume that the true message terminals of the system correspond exactly to those that currently exist. In fact it may be that the current communication system is inhibiting the actual communication function by restricting the number of terminals in the system.

For example, in some mines the dispatcher's office is the message terminal point on the surface. However, in many cases a message is not meant ultimately for the dispatcher, but is in effect relayed to some other surface facility and personnel. Therefore, a channel to carry that message should not necessarily terminate at the dispatcher.

* Collins Radio Co. is now conducting such a user requirements program for the Bureau under Contract H0232056.

To determine the necessary terminals in a communication system, and in addition the amount of traffic, an analysis of the content of the actual messages transmitted in the system should be performed. This will identify the ultimate destination of the messages, whether or not they are being relayed through one of the users in the system who is located at a present terminal, and the average length of the messages. The average message length and the total number of messages gives in effect the total traffic handling capacity required. A brief study program has been outlined below to obtain these data and identify the basic elements and operational capabilities of a system that would satisfy mine communication requirements from both voice and data standpoints.

A short user requirements study should be performed taking a selected number of mines, perhaps four, and analyzing their present communications as outlined below.

B. ACQUISITION OF KEY USER REQUIREMENT DATA AND INFORMATION

1. A key ingredient of a user requirements study is the monitoring of a mine's communications system for a period of one day. This could be accomplished with the aid of a tape recorder(s) bridged across the current communication system. Pertinent information derivable from these recordings would include:
 - a. total number of messages during the total working shift.
 - b. density of messages per unit time; this will be used to determine peak traffic requirements.
 - c. an analysis of the average length of messages by recording the start and end times of all messages during the day.
 - d. an analysis of the content of the messages, whereby one can determine the types of messages, the sources and ultimate recipients of the messages, and whether these sources and recipients are at present terminals (nodes) in the communication system or at some other locations in the mine.
2. In addition to tape recorder data gathering, key operating personnel at the mines should be interviewed to help determine:
 - a. their specific underground and surface communication needs;
 - b. their evaluation of the present methods of mine communication;
 - c. their suggestions of better methods of mine communication;
 - d. their opinion as to whether some messages now transmitted by voice communications could be sent automatically in a formatted manner, so that current voice communication traffic could be reduced.

3. Additional interviews with key operating personnel should be conducted to determine similar needs with regard to monitoring of mine environmental parameters and production. Respondents should be asked to identify:
 - a. what mine operations require monitoring at present, which new operations in the mine would be useful to monitor in the future, and what kind of monitoring system would be useful.
 - b. what parameters of specific mine operations should be monitored, the total number of monitoring stations and their locations, what parameter values would be meaningful, and whether any of the monitoring could be done periodically as opposed to continuously, or on an exception basis, whereby a signal would be sent only if a value fell outside prescribed limits.
 - c. what present voice messages sent on the communications system could be advantageously formatted for coded delivery via a monitoring system.

C. ANALYSIS OF DATA AND FORMULATION OF TRAFFIC AND PERFORMANCE REQUIREMENTS

The information and data obtained from the above interviews and tape recordings should then be analyzed to determine:

- a. the current and future communications traffic and the required number of channels to support this traffic.
- b. the message terminal (node) points for the communication channels determined in a. above.
- c. the need for private communication channels and their terminal points.
- d. some estimate of the actual transmission performance specifications required for the mine communication system.*
- e. what key elements in the mine should be monitored.
- f. the number of channels required to support monitoring traffic.
- g. the required terminal points in the monitoring system.

* ADL is conducting investigations for the Bureau related to the future development of guidelines, standards and practices for mine communications under Contract H0133038.

D. SYNTHESIS OF CANDIDATE SYSTEMS

Once the analysis in C. has been completed and a review made of all the data and documentation obtained under B. and C. above, several candidate systems could then be synthesized to meet the needs and requirements, thereby identifying the terminal points, the channels required, the operating features of those channels, and suggested methods of multiplexing additional voice and/or monitoring channels onto the system. This will require some iteration and a comparative analysis of the candidate systems. During this process, there will be a substantial amount of interaction between the system synthesis and user requirement tasks so that performance and cost tradeoffs can be made between the two. From this analysis, a practical and economically sound system(s) tailored for use in mines can then be determined.

In this process, answers should be found to several important questions related to improving the efficiency and safety of mine operations, such as: is a PABX really needed to support current and future mine communications?; is dial switching really necessary for point-to-point communication in the mine?; what system configurations are best suited for reliable mine communications?; what features should each terminal unit in the mine have to support the user requirements?; is direct two-way communications to the face required on a real-time basis?; which monitored parameters contribute most to increased production and which to increased safety?; and what are the future trends in mine communication and monitoring?

E. HARDWARE SPECIFICATION

Given well-documented user requirements and several candidate communication systems, hardware can then be specified and evaluated to implement specific systems. Determinations can then be made whether the channels should be voice, data, or radio channels, or other means of communication; whether they should be one-way (simplex) or two-way, and whether the terminals should be at fixed locations or mobile. This hardware specification stage will also interact strongly with the first two activities; user requirements and systems synthesis. Indeed, in many cases the trade-offs and the compromises to be made in implementing a communication system in hardware can be substantial in order to obtain a practical working system that meets specific needs.

F. CONCLUDING REMARKS

The program outlined above should go a long way towards helping establish some specific designs for integrated mine communications systems. The following Addendum lists in outline form, several key areas that should receive attention in the user requirements and traffic study. This list, which is not meant to be complete, should be used in conjunction with the items listed under A and B above as a starting point for the detailed design of integrated communications systems tailored specifically for mine applications.

ADDENDUM

USER REQUIREMENTS AND TRAFFIC STUDY PRELIMINARY LIST OF ITEMS TO BE CONSIDERED

I. Message

- | | |
|----------------------------|-------------------|
| A. Type | B. Content |
| 1. Voice | 1. Public |
| 2. Data | 2. Private |
| 3. Destination | 3. Routine |
| a. To a person | 4. Administrative |
| b. To a group | 5. Operational |
| c. To an area | 6. Status |
| d. To a machine | 7. Priority |
| e. Acknowledgment required | 8. Emergency |
| 4. Message life | |

II. Environment

- A. Normal operations
- B. Peak conditions
- C. Emergency conditions
- D. Surface or Sub-surface

III. Terminals

Identify all terminal points (sources and recipients for all messages).

- A. Surface network which includes:
 - 1. Shop-stores
 - 2. Production and DispatchCheck on need for other terminal points in surface facilities.
Also ability to talk over switched network or radio.
- B. Subsurface network may include:
 - 1. Shops
 - 2. Haulage system
 - 3. Sections, including working face area
- C. Mobile Terminals
 - 1. On haulage vehicles
 - 2. Personnel terminals (on Foreman & other supervisory personnel)
- D. Fixed Terminals
 - 1. Wall phones
 - 2. Wall loudspeakers
 - 3. Visual/audible displays
- E. Environmental Terminals
 - 1. Methane detectors
 - 2. Temperature, Air Flow, Smoke, CO, etc.
 - 3. Vehicle location and control sensors

IV. Channels

- A. Type (communication facilities - wires, radio, etc.)
 - 1. Private with key actuation

2. Public with party line features
3. Public address
4. Dedicated for data
- B. Physical - Determine best routing of communications facilities.
 1. For ease of installation and maintenance
 2. Integrity during emergency
 3. Possible loop systems
- C. Grade of Service
 1. Voice grade
 2. Data grade
 3. CCITT or AT&T standards (quality)
 4. Noise environment at terminals

V. Traffic

- A. Volume
 1. How much and how often
 2. Peak hourly traffic, e.g., around a shift change
- B. Timing
 1. Hourly and/or seasonal variations
 2. Tolerable message delay (queue)

III. ON MODELS, DISPLACEMENT CURRENTS AND CONDUCTION CURRENTS

The theoretical work on through-the-earth communications and miner location by electromagnetic methods has created an interest in the size of the errors introduced by neglecting displacement currents relative to conduction currents and also in the subject of scale modeling with regard to mine overburden/air interface applications. Since we had to address these subjects on a past government project in 1968, with regard to a sea-water/air interface scale-modeling application, we have appropriately edited some of our past memoranda treating these subjects, and included them in this Chapter as a ready reference. The results can be applied to the miner location and communication work by substitution of the appropriate overburden parameter values into the equations.

A. BACKGROUND

Questions have arisen about the size of the errors that may be incurred should "non-ideal" scale models be used. To answer these questions, we have taken a look at the potential utility of models with respect to applications involving conducting objects straddling the air/sea water interface. We looked at each of the media separately with the purpose of identifying those combinations of conditions that might allow the use of single and mixed media models with an acceptably small resultant error.

B. FIELD EQUATIONS IN NORMALIZED FORM

Consider the curl Maxwell field equations in linear, uniform, isotropic media

$$\nabla \times \bar{E} = -\mu \frac{\partial \bar{H}}{\partial t} \quad \nabla \times \bar{H} = \epsilon \frac{\partial \bar{E}}{\partial t} + \sigma \bar{E} + \bar{J}_s \quad (1a,b)*$$

where \bar{J}_s is an independent source current density. For sinusoidal excitation, (1a,b) reduces to

$$\nabla \times \bar{E} = -j\omega\mu\bar{H} \quad \nabla \times \bar{H} = (\sigma + j\omega\epsilon) \bar{E} + \bar{J}_s$$

(2a,b)

These Equations (2a,b) can be further combined by taking the curl of one of them and substituting the other into the result. Taking the curl of (2b) for the magnetic field

* References to Figures, Tables, and Equations apply to those in this Chapter unless otherwise noted.

$$\nabla \times \nabla \times \bar{H} = (\sigma + j\omega\epsilon) \nabla \times \bar{E} + \nabla \times \bar{J}_s \quad (3)$$

Since $\nabla \times \nabla \times \bar{H} = \nabla (\nabla \cdot \bar{H}) - \nabla^2 \bar{H}$, (4a,b)

$$\nabla \cdot \bar{H} = 0$$

and $\nabla \times \bar{E} = -j\omega\mu\bar{H}$, (2a)

Equation (3) reduces to

$$\nabla^2 \bar{H} = j\omega\mu (\sigma + j\omega\epsilon) \bar{H} - (\nabla \times \bar{J}_s)$$

(5)

which is the vector Helmholtz wave equation for \bar{H} . Similarly for the electric field:

$$\nabla \times \nabla \times \bar{E} = -j\omega\mu (\nabla \times \bar{H}). \quad (6)$$

Since $\nabla \times \nabla \times \bar{E} = \nabla (\nabla \cdot \bar{E}) - \nabla^2 \bar{E}$, (7a,b)

$\nabla \cdot \bar{E} = 0$ in charge-free, uniform, isotropic media, and

$$\nabla \times \bar{H} = (\sigma + j\omega\epsilon) \bar{E} + \bar{J}_s \quad (2b)$$

Equation (6) reduces to:

$$\nabla^2 \bar{E} = j\omega\mu (\sigma + j\omega\epsilon) \bar{E} - j\omega\mu \bar{J}_s$$

(8)

the vector Helmholtz equation for \bar{E} .

These equations can also be rewritten in dimensionless form by using

$$\bar{E} = e\bar{E}', \quad \bar{H} = h\bar{H}', \quad \bar{J}_s = j_s\bar{J}'_s \quad (9)$$

$$\text{length} = \ell = \ell_o L, \quad \text{frequency} = \omega = \omega_o \Omega \quad (10a,b)$$

$$\bar{E}' = \frac{\bar{E}}{e}, \quad \bar{H}' = \frac{\bar{H}}{h}, \quad L = \frac{\ell}{\ell_o}, \quad \Omega = \frac{\omega}{\omega_o}, \quad \bar{J}'_s = \frac{\bar{J}_s}{j_s}, \quad \text{and } \nabla_L \quad (11a,b,c,d,e)$$

represent the dimensionless fields and other quantities simply normalized to some characteristic value or dimension of the problem. For example, L is a dimensionless length where ℓ_o may represent a full-scale characteristic dimension of a typical object, Ω is a dimensionless frequency where ω_o may represent the full-scale center frequency of excitation, and ∇_L is the normalized del operator. We now can substitute the above expressions (11) into the curl and wave equations to get

$$\nabla_L \times \bar{E}' = -j\ell_o\omega_o\mu \left(\frac{h}{e}\right) \Omega\bar{H}' \quad (12)$$

$$\nabla_L \times \bar{H}' = \ell_o(\sigma + j\epsilon\omega_o\Omega) \left(\frac{e}{h}\right) \bar{E}' + \ell_o\left(\frac{j_s}{h}\right)\bar{J}'_s \quad (13)$$

$$\nabla_L^2 \bar{H}' = j\ell_o^2\mu\omega_o\Omega(\sigma + j\epsilon\omega_o\Omega) \bar{H}' - \ell_o\left(\frac{j_s}{h}\right)(\nabla_L \times \bar{J}'_s) \quad (14)$$

$$\nabla_L^2 \bar{E}' = j\ell_o^2\mu\omega_o\Omega(\sigma + j\epsilon\omega_o\Omega) \bar{E}' - j\ell_o^2\mu\omega_o\left(\frac{j_s}{e}\right)\Omega\bar{J}'_s \quad (15)$$

These are the pertinent field equations expressed in a general normalized form that can be used conveniently to discuss scaling considerations.

C. SCALING CONSIDERATIONS⁽¹⁾

For emphasizing the relative importance between conduction and displacement currents in a particular medium, it is useful to express the equations in terms of the ratios $\frac{\omega\epsilon}{\sigma}$ or $\frac{\sigma}{\omega\epsilon}$ depending on whether the medium is predominantly conducting or not respectively

1. Conducting Media

To emphasize the relative importance of displacement to conduction currents ($\frac{\omega\epsilon}{\sigma}$) in primarily conducting media, Equations (13) and (14) can be rewritten in the convenient form below.

$$\nabla_L^2 \bar{H}' = j\lambda_o^2 \mu \sigma \omega_o \Omega \left(1 + j \frac{\epsilon \omega_o}{\sigma} \Omega\right) \bar{H}' - \lambda_o \left(\frac{j_s}{h}\right) (\nabla_L \times \bar{J}'_s) \quad (16)$$

and

$$\nabla_L^2 \bar{E}' = j\lambda_o^2 \mu \sigma \omega_o \Omega \left(1 + \frac{j\epsilon \omega_o}{\sigma} \Omega\right) \bar{E}' - j\lambda_o^2 \omega_o \mu \left(\frac{j_s}{e}\right) \Omega \bar{J}'_s \quad (17)$$

Examination of Equations 16 and 17 reveals that the normalized solutions will remain unchanged so long as the terms

$$\lambda_o^2 \omega_o \mu \sigma = C_1, \quad \frac{\epsilon \omega_o}{\sigma} = C_2, \quad \lambda_o \left(\frac{j_s}{h}\right) = C_3, \quad \text{and} \quad \lambda_o^2 \omega_o \mu \left(\frac{j_s}{e}\right) = C_4 \quad (18a,b,c,d)$$

remain constant with any change in dimensions, frequency or material constants. Substituting for these constants in the electric and magnetic field Equations (16) and (17) we get

$$\nabla_L^2 \bar{H}' = jC_1 \Omega (1 + jC_2 \Omega) \bar{H}' - C_3 (\nabla \times \bar{J}'_s) \quad (19a)$$

and

$$\nabla_L^2 \bar{E}' = jC_1 \Omega (1 + jC_2 \Omega) \bar{E}' - jC_4 \Omega \bar{J}'_s \quad (19b)$$

(1) Similar treatments can be found in the book "Antenna Theory" by Schelkunoff and Friis, and in the Proc. IRE Nov. 1948, "Theory of Models of Electromagnetic Systems" by George Sinclair.

The requirement that all four of these terms remain constant during any scaling operations led to the scaling restrictions on material properties discussed in a previous ADL memo on models. These restrictions become particularly severe in view of scarcity of magnetic liquids, and the difficulty of obtaining high-conductivity liquids that are not also extremely corrosive. A brief summary of the nature of high conductivity liquids has been included as Appendix A for a ready reference. However let us now re-examine the restrictions imposed by modeling when the accuracy requirements are relaxed a little allowing certain terms in the wave equation to be neglected.

In conducting media when the conduction current is much larger than the displacement current, the constant C_2 can become negligible compared to unity. If the normalized frequency multiplier Ω also does not deviate enough from unity to make the factor $C_2\Omega$ appreciable compared to one, then the factor $C_2\Omega$ can be ignored for scaling considerations involving conducting media completely surrounded by conducting boundaries.

In metals $C_2\Omega$ will always be negligible for any practical frequencies of interest. However, in normal sea water

$$C_2 \Omega = \omega \epsilon / \sigma = \omega_0 \Omega \epsilon / \sigma = f(\text{in kc}) \times 1.1 \times 10^{-6} \quad (19)$$

for $\epsilon = 81\epsilon_0$, $\sigma = 4$ mho/m. Therefore, $C_2\Omega$ will satisfy an arbitrary smallness criterion of less than 0.001 only when the upper limit of the signal frequency band does not exceed 900 kc.

$$f_0 \text{ max} \leq 900 \text{ kc (sea water)*} \quad (20)$$

Since the maximum frequency-spread-factor expected about the signal center frequency is 10, the center frequency should not exceed 90 kc for $C_2\Omega$ to remain less than 0.001. When the center frequency remains below 90 kc, the equations can then be written to good approximation as

* For coal mine overburdens with representative values of $\epsilon = 5\epsilon_0$ and $\sigma = 10^{-2}$ mho/m, the smallness criterion of $\frac{\omega \epsilon}{\sigma} \leq 0.001$ will not be exceeded if the frequency $f_0 \text{ max}$, does not exceed 37 kc (kHz).

$$\nabla_L^2 \bar{H}' = jC_1 \Omega \bar{H}' - C_3 (\nabla_L \times J'_s) \quad (21a,b)$$

$$\nabla_L^2 \bar{E}' = jC_1 \Omega \bar{E}' - jC_4 \Omega \bar{J}'_s$$

where

$$C_1 = \ell_o^2 \omega_o \mu \sigma, \quad C_3 = \ell_o \left(\frac{j_s}{h} \right), \quad \text{and} \quad C_4 = \ell_o^2 \omega_o \mu \left(\frac{j_s}{e} \right) \cdot \quad (22,a,b,c)$$

Since our interest is in the magnetic field,* let us now look at the modeling restrictions imposed if both the form and the absolute value of the magnetic field is to be preserved in a scale model without changing the σ and μ properties of a conducting medium such as sea water. To scale the size ℓ_o by a factor of $1/S$, then requires the frequency ω_o to be scaled by the factor S^2 and the current density j_s to be scaled by the factor S . The S^2 scaling of ω_o corresponds to a scaling factor $1/S$ with respect to wavelength since wavelength in a conducting medium is given by $\lambda_c = 2\pi \sqrt{\frac{2}{\omega \mu \sigma}}$. (The S scaling of current density j_s corresponds to a $1/S$ scaling of current i_s since $j_s = \frac{i_s}{\text{area}}$.)

However, by neglecting C_2 and using the above scaling procedure in order to keep the magnetic field the same in the model, we have sacrificed an exact scaling in the electric field since the C_4 term in Equations (21b) does not remain constant but gets scaled by a factor S . Examination of Equation (14) shows the direct effect of this on the electric field; namely the electric field e in the model will be scaled by an unwanted factor S . Consequently electric fields measured in such models of conducting media must be multiplied by a factor $1/S$ to obtain full-scale values, a small inconvenience in our intended applications.

In the intended application, the full-scale highest frequency should not have to exceed a value of about 5 kc, based on attenuation and detection considerations. Using the factor-of-10 variation from center frequency criterion, the reference center frequency is then set to 500 cps. The maximum allowable scaling factor satisfying the above conditions can then be found by forming the ratio

* This is also true in the miner location application since the miner's signal source is a current-fed loop of wire.

$$S^2 = f_{\text{omax}} / f_{\text{oref}} \left[\begin{array}{l} \\ \text{cent. freq.} \end{array} \right] = \frac{90,000}{500} = 180, \quad (23)$$

resulting in a scaling factor of

$$S \leq 13, 1/S \geq \frac{1}{13} \bullet \quad (24)$$

A 10 to 1 scaling looks promising, but a scaling factor on the order of 20 to 1 is a more practical and convenient goal. Such a scale factor would require an f_{omax} of 2 megacycles, thereby increasing the $\omega\epsilon/\sigma$ term to 0.002. Though this is still not a large quantity, estimates were made of the errors introduced when values of $\omega\epsilon/\sigma$ up to 0.01 are neglected in the wave equations.

A brief analysis for both high and low loss media has been included in Appendix B at the end of this memo for ready reference. Though far from a definitive treatment of the matter, it indicates that errors will be inconsequential in most low-loss dielectric media, and certainly tolerable, (on the order of 5%) if not inconsequential, in conducting media even when values of $\omega\epsilon/\sigma$ as high as 0.01 are neglected.* Therefore, the arbitrary smallness criterion of 0.001-0.002 chosen for neglecting $\omega\epsilon/\sigma$ should give a more than adequate error margin.

2. Low-Loss Dielectric Media

If the problem involves the presence of non-conducting or poorly conducting media also, then the Maxwell equations in these media must also be satisfied simultaneously for the desired scale factors. When the conduction current can be considered small compared to displacement currents in a medium ($\sigma/\omega\epsilon \ll 1$), Equations (14) and (15) can be rewritten in the form

* A value of $\frac{\omega\epsilon}{\sigma} \leq 0.01$ gives an $f_{\text{omax}}=370$ kc for the previously stated mine overburden parameter values. This maximum frequency translates into a maximum dimensional scale factor of 11 for modeling the overburden without an air interface, for a full-scale 3 kc application, when changing only the operating frequency and physical size but not the overburden material electrical characteristics for the model.

$$\nabla_L^2 \bar{H}' = -\left(1 - \frac{j\sigma}{\omega_0 \epsilon \Omega}\right) \ell_0^2 \omega_0^2 \epsilon \mu \Omega^2 \bar{H}' - \ell_0 \left(\frac{j\mathbf{s}}{h}\right) (\nabla_L \times \bar{J}'_s) \quad (25a,b)$$

$$\nabla_L^2 \bar{E}' = \left(1 - \frac{j\sigma}{\omega_0 \epsilon \Omega}\right) \ell_0^2 \omega_0^2 \epsilon \mu \Omega^2 \bar{E}' - j \ell_0^2 \mu \omega_0 \left(\frac{j\mathbf{s}}{e}\right) \Omega \bar{J}'_s$$

where

$$C_3 = \ell_0 \left(\frac{j\mathbf{s}}{h}\right), \quad C_4 = \ell_0^2 \mu \omega_0 \left(\frac{j\mathbf{s}}{e}\right), \quad C_5 = \frac{\sigma}{\omega_0 \epsilon} \text{ and } C_6 = \ell_0^2 \omega_0^2 \epsilon \mu, \quad (26a,b,c,d)$$

so that

$$\nabla_L^2 \bar{H}' = -\left(1 - j \frac{C_5}{\Omega}\right) C_6 \Omega^2 \bar{H}' - C_3 (\nabla_L \times \bar{J}'_s) \quad (27)$$

$$\nabla_L^2 \bar{E}' = -\left(1 - j \frac{C_5}{\Omega}\right) C_6 \Omega^2 \bar{E}' - j C_4 \Omega \bar{J}'_s \quad (28)$$

In a vacuum, $\sigma = 0$, so that C_5 becomes identically zero, and independent of frequency and scaling considerations. In most dielectrics, σ will still be small but perhaps not always small enough for $\frac{\sigma}{\omega_0 \epsilon \Omega}$ to also satisfy an arbitrary smallness criterion of 0.001 for all frequencies of interest. In our applications the most important dielectric will be the air above the water surface interface; and we will use the arbitrary small value of $\sigma = 10^{-15}$ mho/m which assumes a loss tangent $\tan \delta = 10^{-6}$ (ratio of conduction to displacement current in air) at 1 kc. Then C_5/Ω becomes

$$\frac{C_5}{\Omega} = \tan \delta = \frac{\sigma}{\omega_0 \Omega \epsilon} = \frac{1.8 \times 10^{-8}}{f \text{ (in kc)}}, \quad (29)$$

and C_5/Ω will satisfy the smallness criterion of less than 0.001 so long as the lower limit of the signal frequency band does not go below 0.02 cps thereby confining the center frequency to remain above 0.2 cps for a 10 to 1 bandspread signal. Since we desire reduced-size models requiring increases in frequency, and minimum full-scale frequencies are expected to be above 50 cps, C_5/Ω will always be negligible for air. If other dielectrics are required in a model they must be subjected to the (C_5/Ω) smallness test before they can be used with confidence. When the C_5/Ω term can be neglected, Equations (27) and (28) reduce to:

$$\nabla_L^2 \bar{H}' = -C_6 \Omega^2 \bar{H}' - C_3 (\nabla \times \bar{J}'_s) \quad (31a,b)$$

$$\nabla_L^2 \bar{E}' = -C_6 \Omega^2 \bar{E}' - jC_4 \Omega \bar{J}'_s$$

where

$$C_6 = \ell_0^2 \omega_0^2 \epsilon \mu, \quad C_3 = \ell_0 \left(\frac{j_s}{h} \right) \text{ and } C_4 = \ell_0^2 \mu \omega_0 \left(\frac{j_s}{e} \right) \quad (32a,b,c)$$

Again our interests are mainly with the magnetic field. Therefore, we find that to scale the size ℓ_0 by a factor $1/S$ without changing the ϵ and μ properties of an air medium, and while preserving the form and magnitude of the H-field in the models, we must scale the frequency ω_0 by a factor S (again corresponding to a scaling of the wavelength by a factor $1/S$ as in the conducting case), and we must scale the current density j_s again by a factor S as in the conducting case. However, unlike the conducting case, the form and magnitude of the electric field does not get sacrificed in the model, since C_4 also remains constant in lossless media when both ω_0 and j_s are scaled linearly. This is the well-known and commonly used scaling procedure for lossless media.

3. Mixed Media

The modeling of geometries involving only good-conducting or non-conducting materials is relatively straightforward. Each can be simply accomplished without the need to change material properties in the model by scaling the frequency according to the first or second power of the inverse of the dimensional scaling factor ($1/S$) for non-conducting or conducting media respectively. On the other hand, problems involving both types of media can pose serious modeling difficulties, since these cases will usually require important, but unattainable, changes in material properties

to produce the proper model. Such is the case for our application involving a finite metal object straddling an infinite interface between air and sea water, and a source located beneath the interface in the sea water. In this problem, the constants $C_{1W} = \lambda_0^2 \omega_0 \mu_W \sigma_W$ for sea water and $C_{6A} = \lambda_0^2 \omega_0^2 \epsilon_A \mu_A$ for air are the critical ones that impose conflicting scaling requirements. $C_{1M} = \lambda_0^2 \omega_0 \mu_M \sigma_M$ for the object will not pose a significant modeling problem in the intended application since $\sigma_M \gg \sigma_W$.

To satisfy the air requirement C_6 without changing the air's material constants simply requires an S scaling of frequency for an 1/S scaling of dimensions. Since the frequency is common to both media, the product $\mu_W \sigma_W$ must also be scaled by S^* to maintain C_1 constant in the model's "sea water" medium.

For a 1/20 scale model ($S = 20$), $\mu_W \sigma_W$ must be increased by a factor of 20. If not, the model will correspond to a full-scale case in fresh water, which will be of questionable value. Use of a magnetic solid or powder such as ferrite for the "sea water" in the model is most unattractive from a practical standpoint, as is a solid or powdered metal mixture to increase the $\mu_W \sigma_W$ product. On the other hand, liquids with adequate natural magnetic and/or conducting properties are either not available or hazardous for use in models. Another alternative might be to suspend small magnetic particles in sea water itself. But the difficulties involved with mechanical stirrers etc. required to maintain the uniformity and required density of particles throughout the model tank also make this alternative impractical and unattractive for the intended application.

Since an adequate substitute for sea water is not practical,** another modeling approach consists in satisfying the sea water requirement C_1 by simply scaling frequency by S^2 for a 1/S scaling of dimensions. This will in turn require that the product $\epsilon_A \mu_A$ of air must be reduced by the factor $1/S^2$ to maintain C_6 constant in the model. Since $\epsilon_A \mu_A$ is already identical to free space, the above reduction condition cannot be satisfied.

For a 1/20 scale model ($S = 20$) the required reduction in $\epsilon_0 \mu_0$ is (1/400). Therefore, if the need for this reduction was ignored and air was still used in a 20 to 1 scale model, then the air above the water interface in such a model will appear to have the properties of a material with an $\epsilon \mu$ product 400 times that of air.* As such, this apparent increase in $\epsilon \mu$ will affect the fields in both media by introducing a modified, boundary discontinuity condition, in addition to changing the material values in the constituent relations between the fields.

* These results would also apply to a similarly scaled model with a mine overburden/air interface.

** In a mine overburden/air interface application it may be practical to obtain model "overburden" materials of sufficiently increased conductivity over the full scale value of 10^{-2} mho/m to satisfy the mixed media scaling conditions.

If we think of this change in $\epsilon\mu$ to be manifested solely in a 400-fold increase in the effective μ of the air medium for a 20 to 1 scale model, we would expect the magnetic field lines in the model to be more attracted to the surface (increased strength of components normal to the surface) than in the full-scale case. In other words, in the absence of a metal (perfectly conducting) object, the air boundary would tend to appear like a non-conducting but moderately magnetic surface in the reduced-scale model. As such the perturbations introduced by the presence of a metal object may be more pronounced in such a reduced-scale model than its corresponding effect in the full-scale model. In fact, the probable differences in the character of the field behavior can create a more severe problem than the neglecting of a small term in the wave equation for a single-medium problem, thereby making it too risky to proceed with such modeling without firmer assurances of utility. In summary, mixed-media modeling alternatives for the full-scale materials required by the application of interest are either highly impractical or of questionable validity; (as confirmed by subsequent visit with K. Izuka of Harvard University and reported in Appendix C).

D. CONCLUSIONS

On the basis of the above findings there appears to be no question that scale modeling is feasible for models that involve only good conducting materials, and that 20 to 1 dimensional scaling factors can be easily achieved for the frequencies of interest without appreciable errors, by simply scaling frequency by the square of the inverse of the dimensional scale factor. This case will apply for conducting objects completely submerged in sea water and far from the surface, provided non-conducting objects either are not present or whose properties are scaled as described in Section G.3.

For reduced-scale models in mixed (conducting and non-conducting) media particularly when a conducting object is located near the interface between two media, sizable errors can be introduced if the scaling conditions proper to each medium are not followed. In a sea water/air application requiring a size reduction on the order of 20 to 1, it becomes impractical or impossible to change the material properties as required to satisfy these scaling conditions.* Consequently additional investment of time and effort in the pursuit of sea water/air mixed media modeling is not warranted.

* As stated in the ** footnote on the previous page, in mine overburden/air interface applications it may be more practical to satisfy these conditions. Indeed, for the 100-to-1 or greater scaling factors that may be required to obtain practically-sized models for 1000-foot full-scale overburdens, sea water may prove to be a suitable material for the overburden in the model. In any case, careful consideration and proper precautions must be taken before embarking on all mixed-media modeling enterprises, to ensure not only that significant errors will not be incurred but also that the expected results will justify the effort and expense required.

APPENDIX A

HIGH CONDUCTANCE ELECTROLYTES FOR SEA WATER/AIR INTERFACE MODELS

1. Overview

The requirement is for electrolytes having conductances of 0.4 mho/cm (40 mho/meter), as a minimum. Only the following kinds of electrolyte might come up to this exactingly high requirement.

- 1) Aqueous solutions of salts,
- 2) Aqueous solutions of acids and alkalis,
- 3) Fused salt systems,
- 4) Metal-ammonia solutions

Practicality eliminates the last two possibilities. An examination of the data available for the first two categories suggests that only strong acid or alkali aqueous solutions are likely to be adequate, but these present a safety hazard for the concentrations needed.

2. Salt Solutions

Recent, accurate data on concentrated aqueous solutions are few in number; Table One contains a list of salts and references to conductance data. It is a general rule that 1:1 electrolytes have the largest specific conductivities of all the kinds of electrolytes. Of these, the salts with the largest cations have the greatest conductivities. Cost considerations eliminate all but sodium, potassium and ammonia salts. Table Two gives values of specific conductance for some common salts of these cations. Evidently only 5.0 molar NH_4Cl and 8.0 molar NH_4NO_3 could provide the conductances required. These solutions are very strong, only marginally equal to the task, and may be excessively corrosive.

Substitution of an organic amine, such as methylamine, for ammonia, might marginally increase conductance. This is not certain, above a certain size of cation conductance values begin to fall, and solubilities also are different.

3. Acid and Alkali Solutions

The greater conductivity of these solutions arises from the conduction of hydrogen and hydroxyl ions through hydrogen bond transitions. Tables Three and Four show that H_2SO_4 and KOH solutions containing between 25 and 35% of the electrolyte have high conductances. However, the acid solution is highly corrosive to most metals and both solutions can effect considerable damage to human body tissue. In addition since the mechanism of conduction in an acid is drastically different to that in a salt solution, (see Chemical Oceanography, Academic Press, 1965) this raises all manner of other doubts. The same remarks apply to using alkali solutions.

Table A1

Bibliography of Recent Conductance Measurements in Concentrated Aqueous Solutions

Solute	Max. conc. mole/l.	Temp. °C	Ref.	Solute	Max. conc. mole/l.	Temp. °C	Ref.
HCl	9-12	5-65	1	KBr	3.75	0, 25	6*
LiClO ₃	19	25	2*	KI	6	25, 50	6
LiClO ₄	23-11†	131-8	2*	KH ₂ PO ₄	1.9	25	8
LiNO ₃	13-6	25	3*	NH ₄ Cl	5	25	10
LiNO ₃	14-†	110	3*	NH ₄ NO ₃	8	25	10
NaCl	5	25	5	NH ₄ NO ₃	11	25, 35	11*
NaCl	5	50	6	NH ₄ NO ₃	15	95	16*
NaI	10	0, 30, 50	7*	NH ₄ NO ₃	18-0†	180	12*
NaClO ₃	10	0, 30, 50	7*	AgNO ₃	8	25, 35	11*
NaCNS	10	0, 30, 50	7*	AgNO ₃	14	95	16*
Na ₂ HPO ₄	3-9	25	8	AgNO ₃	23-19†	221.7	12*
KCl	4	25	5	H ₂ SO ₄	18	50, 75	13*
LiNO ₃ in EtOH and EtOH-H ₂ O	3-11	25	4*	H ₂ SO ₄	18	25-155	14
H ₃ PO ₄				18	25	8*	
				K ₃ Fe(CN) ₆	1	25	15
				K ₄ Fe(CN) ₆	0.7	25	15
				MgSO ₄	2.9	25	15
				HCOOK	6.5	50.5	17*
				HCOOS	10	50.5	17*

* These papers include viscosity data. † Fused salt.

For work at lower concentrations, see references to Table 1; for extensive earlier work, usually of lower accuracy, see *Int. crit. Tab.*, Vol. VI, pp. 230-256.

- 1 OWEN, B. B. and SWEETON, F. H., *J. Amer. chem. Soc.*, 63 (1941) 2811
- 2 CAMPBELL, A. N. and PATTERSON, W. G., *Canad. J. Chem.*, 36 (1958) 1004
- 3 CAMPBELL, A. N., DEBUS, G. H. and KARTZMARK, E. M., *ibid.*, 33 (1955) 1503
- 4 CAMPBELL, A. N., DEBUS, G. H. and KARTZMARK, E. M., *ibid.*, 34 (1956) 1222
- 5 CHAMBERS, J. F., STOKES, J. M. and STOKES, R. H., *J. phys. Chem.*, 60 (1956) 985
- 6 CHAMBERS, J. F., *ibid.*, 62 (1958) 1136
- 7 MILLER, M. L., *ibid.*, 60 (1956) 189
- 8 MASON, C. M. and CULVERN, J. B., *J. Amer. chem. Soc.*, 71 (1949) 2387
- 9 JONES, G. and BICKFORD, C. E., *ibid.*, 56 (1934) 602
- 10 WISHAW, B. F. and STOKES, R. H., *ibid.*, 76 (1954) 2065
- 11 CAMPBELL, A. N. and KARTZMARK, E. M., *Canad. J. Res.*, 23B (1950) 43;
CAMPBELL, A. N., GRAY, A. P. and KARTZMARK, E. M., *Canad. J. Chem.*,
31 (1953) 617
- 12 CAMPBELL, A. N., KARTZMARK, E. M., BEDNAS, M. E. and HERRON, J. T.,
ibid., 32 (1954) 1051
- 13 CAMPBELL, A. N., KARTZMARK, E. M., BISSET, D. and BEDNAS, M. E., *ibid.*, 31
(1953) 303
- 14 ROUGHTON, J. E., *J. appl. Chem.*, 1 (1951) S141
- 15 CALVERT, R., CORNELIUS, J. A., GRIFFITHS, V. S. and STOCK, D. I., *J. phys.
Chem.*, 62 (1958) 47
- 16 CAMPBELL, A. N., KARTZMARK, E. M., *Can. J. Chem.*, 30 (1952) 128
- 17 RICE, M. J. and KRAUS, C. A., *Proc. Nat. Acad. Sci. (U.S.A.)*, 39 (1953) 802

Source: Chemical Oceanography, Academic Press, 1965

Table A2Specific Conductances of Several Salts

mho/cm at 25°C

<u>Conc.</u> m/l	<u>NaCl</u>	<u>KCL</u>	<u>NH₄Cl</u>	<u>NH₄NO₃</u>
1.0	0.085	0.111	0.111	0.101
2.0	0.150	0.210	0.210	0.184
3.0	0.196	0.298	0.300	0.256
4.0	0.229	0.374	0.380	0.305
5.0	0.247		0.440	0.347
6.0				0.375
7.0				0.396
8.0				0.456

Table A3Maximum Conductance Solutions of H₂SO₄

Temp. °C		30	25	20	10	0
Spec. Conductance	mho/cm	0.886	0.824	0.763	0.641	0.518
Spec. Resistance	ohm. cm	1.129	1.213	1.310	1.562	1.928
Composition	%	31.5	31.1	30.6	29.8	28.8

Table A4Conductance of KOH Solutions at 18°C

Composition	%	10	20	25	30	35	45
Spec. Conductance	mho/cm	0.313	0.500	0.537	0.543	0.510	0.390
Spec Resistance	ohm.cm	3.2	2.0	1.80	1.84	1.96	2.56

APPENDIX B
 ESTIMATES OF APPROXIMATION ERRORS
 WHEN DISPLACEMENT OR CONDUCTION
 CURRENTS ARE NEGLECTED

This Appendix presents a closer look at the type and magnitude of errors introduced by neglecting the terms $\frac{\omega\epsilon}{\sigma}$ or $\frac{\sigma}{\omega\epsilon}$ in the wave equation, for good and poorly conducting media respectively. Assuming harmonic time variation $e^{j\omega t}$ as before, the wave equations in a source free medium maybe written as

$$(\nabla^2 + \omega^2\epsilon\mu - j\omega\mu\sigma) \begin{Bmatrix} E \\ H \end{Bmatrix} = (\nabla^2 + K^2) \begin{Bmatrix} E \\ H \end{Bmatrix} = 0 \quad (B1)$$

where

$$K^2 = \omega^2\epsilon\mu - j\omega\mu\sigma \quad (B2)$$

In order to emphasize the leading term in the two approximations, let us denote for the low loss - high frequency case

$$K_o^2 = \omega^2\epsilon\mu \left(1 - j \frac{\sigma}{\omega\epsilon} \right) \quad \text{where } \frac{\sigma}{\omega\epsilon} \ll 1 \quad (B3)$$

$$K_o = \omega\sqrt{\epsilon\mu} \left(1 - j \frac{\sigma}{\omega\epsilon} \right)^{\frac{1}{2}} \quad (B4)$$

and for conductive media

$$K_c^2 = -j\omega\mu\sigma \left(1 + j \frac{\omega\epsilon}{\sigma} \right) \quad \text{where } \frac{\omega\epsilon}{\sigma} \ll 1 \quad (B5)$$

and

$$K_c = (1-j) \sqrt{\frac{\omega \mu \sigma}{2}} \left(1 + j \frac{\omega \epsilon}{\sigma} \right)^{\frac{1}{2}} = \frac{1-j}{\delta} \left(1 + j \frac{\omega \epsilon}{\sigma} \right)^{\frac{1}{2}} \quad (B6)$$

In Equations (B4) and (B6) the term $\sqrt{1 \pm j\Delta}$ has been separated out for examination, where Δ is given alternatively as $\frac{\omega \epsilon}{\sigma}$ and $\frac{\sigma}{\omega \epsilon}$ for good or poorly conducting media respectively. It is of interest to find the variation of the above square-rooted quantity as a function of Δ .

$$\begin{array}{l} \text{Good} \\ \text{Conducting:} \end{array} \quad \sqrt{1+j\Delta} = \pm \left[\left(\frac{\sqrt{1+\Delta^2} + 1}{2} \right)^{\frac{1}{2}} + j \left(\frac{\sqrt{1+\Delta^2} - 1}{2} \right)^{\frac{1}{2}} \right] \quad (B7)$$

$$\begin{array}{l} \text{Poorly} \\ \text{Conducting:} \end{array} \quad \sqrt{1-j\Delta} = \pm \left[\left(\frac{\sqrt{1+\Delta^2} + 1}{2} \right)^{\frac{1}{2}} - j \left(\frac{\sqrt{1+\Delta^2} - 1}{2} \right)^{\frac{1}{2}} \right] \quad (B8)$$

Since $\Delta \ll 1$ Equations (B7) and (B8) can be approximated by neglecting higher order terms. Thus:

$$\sqrt{1+j\Delta} \approx \pm \left[\left(1 + \frac{\Delta^2}{8} \right) + j \frac{\Delta}{2} \right] \quad (B9)$$

$$\sqrt{1-j\Delta} \approx \pm \left[\left(1 + \frac{\Delta^2}{8} \right) - j \frac{\Delta}{2} \right] \quad (B10)$$

Neglecting higher than second order terms in Δ the magnitude of the complex quantities in Equations (B9) and (B10) become

$$|\sqrt{1 \pm j\Delta}| \approx \sqrt{1 + \frac{\Delta^2}{2} + \frac{\Delta^4}{64}} \approx 1 + \left(\frac{\Delta}{2}\right)^2. \quad (\text{B11})$$

So Equations (B4) and (B6) can be rewritten as:

$$|K_o| = \left| \omega\sqrt{\epsilon\mu} \left(1 - j\frac{\sigma}{\omega\epsilon}\right)^{\frac{1}{2}} \right| \approx \omega\sqrt{\epsilon\mu} \left(1 + \left(\frac{\sigma}{2\omega\epsilon}\right)^2\right) \quad \text{for low loss media} \quad (\text{B12})$$

$$|K_c| = \left| \left(\frac{1-j}{\delta}\right) \left(1 + j\frac{\omega\epsilon}{\sigma}\right)^{\frac{1}{2}} \right| \approx \sqrt{\omega\mu\sigma} \left(1 + \left(\frac{\omega\epsilon}{2\sigma}\right)^2\right) \quad \text{for lossy media.} \quad (\text{B13})$$

There is also a corresponding phase angle change in the K vector due to the presence of the however small, but not negligible, Δ .

What can then be said about the error one makes when neglecting either the conduction or displacement part of the total current? Consider the poorly conducting case first. Judging from Equation (B10) for nearly lossless media (air), a first order attenuation term, and a second order term in the propagation constant that reduces the wavelength in the medium, are being neglected when conduction currents are ignored. Using Cartesian coordinates in the example, the elementary solution of Equation (B1) takes the following form:

$$\begin{aligned}
 \left. \begin{array}{l} E \\ H \end{array} \right\} & e^{-j\bar{K}_o \bar{r}} = e^{-j\omega\sqrt{\epsilon\mu} \cdot \sqrt{1-j\Delta} \cdot \bar{r}} \approx e^{-j\omega\sqrt{\epsilon\mu} \left[\left(1 + \frac{\Delta^2}{8}\right) - j\frac{\Delta}{2} \right] \cdot \bar{r}} \\
 & = e^{-j\omega\sqrt{\epsilon\mu} \cdot \bar{r}} \cdot \left[e^{-\frac{\Delta\omega\sqrt{\epsilon\mu}}{2} \cdot \bar{r}} \cdot e^{-j\frac{\Delta^2\omega\sqrt{\epsilon\mu}}{8} \cdot \bar{r}} \right] \\
 & = e^{-j\bar{K}_o \bar{r}} \cdot \left[e^{-\frac{1}{\delta K_o} \cdot \frac{\bar{r}}{\delta}} \cdot e^{-j\frac{1}{2} \left(\frac{1}{\delta K_o}\right)^3 \cdot \frac{\bar{r}}{\delta}} \right]
 \end{aligned} \tag{B14}$$

where the expression in the square bracket is the quantity being neglected and where the factor $\left(\frac{1}{\delta K_o}\right)$ is the ratio of wavelengths $\frac{\lambda_o}{\lambda_c}$ in a slightly lossy medium where $\left(\lambda_o = \frac{2\pi}{K_o} = \frac{1}{f\sqrt{\epsilon\mu}} \text{ and } \lambda_c = 2\pi\delta \sqrt{\frac{2}{\mu\sigma\omega}}\right)$. λ_o in the case of no conduction current present, and λ_c in the case of only conduction current present. According to Equation (B14) the small attenuation that would be neglected is specified by the large skindepth of air, and even that is further reduced by being multiplied by a factor which is proportional to the square root of ratio of conduction to displacement current which is a small quantity (10^{-3} to 10^{-6} depending on what conductivity one associates with air). The imaginary component of the exponent in the square bracket in Equation (B14) is an even smaller, truly second order quantity which, even if assuming $\Delta = \frac{\sigma}{\omega\epsilon} = 10^{-3}$ (very unlikely in air), would cause a perturbation in the propagation constant (wavelength) of

approximately one ten millionth of the original value. Certainly practical measurements couldn't be performed to show up this kind of inaccuracy of error.

Let us now consider the good conducting case. A more interesting part of this investigation on error is concerned with the sea water medium; since this is a medium that is not as good a conductor, as the air is a good dielectric, the approximations can be expected to give larger errors. Therefore, we are interested in finding the frequency regime defined by the upper limit which the $\frac{\omega\epsilon}{\sigma}$ ($\ll 1$) value may take, but shouldn't exceed in order that errors introduced by neglecting the $\frac{\omega\epsilon}{\sigma}$ term will not be excessive. If $\frac{\omega\epsilon}{\sigma}$ is infinitesimally small, then it can be neglected without worrying about the after effects. In this case, from Equation (B6) the propagation constant is given by:

$$K_c = (1 - j) \sqrt{\frac{\omega\mu\sigma}{2}} \quad (B15)$$

Therefore in Cartesian coordinates the elementary solution may take the form:

$$e^{-j\bar{K}_c \bar{r}} = e^{-\frac{\bar{r}}{\delta}} \cdot e^{-j \frac{\bar{r}}{\delta}} \quad (B16)$$

There is both an attenuation and propagation term. The wavelength of propagation in this lossy medium, is given by

$$\lambda_c = 2\pi\delta = 2\pi \sqrt{\frac{2}{\mu\sigma\omega}} \quad (B17)$$

where δ is the skindepth in the medium. The added term in Equation (B6) means added terms in Equation (B16) that we can easily express with the help of Equation (B9). Using Cartesian coordinates again the solution to Equation (B1) takes the following form: (assuming now, that $\Delta = \frac{\omega\epsilon}{\sigma} \ll 1$)

$$\begin{aligned} \frac{E}{H} &\propto e^{-jK_c \bar{r}} = e^{-(1+j) \frac{\bar{r}}{\delta} \sqrt{1+j\Delta}} \approx e^{-(1+j) \frac{\bar{r}}{\delta} \left[\left(1 + \frac{\Delta^2}{8} \right) + j\frac{\Delta}{2} \right]} \\ &= e^{-\frac{\bar{r}}{\delta}} \cdot e^{-j\frac{\bar{r}}{\delta} \left[e^{\left(\frac{\Delta}{2} - \frac{\Delta^2}{8} \right) \frac{\bar{r}}{\delta}} \cdot e^{-j \left(\frac{\Delta}{2} + \frac{\Delta^2}{8} \right) \frac{\bar{r}}{\delta}} \right]} \end{aligned} \quad (B18)$$

Now, unlike in Equation (B14) for air, both the attenuating and propagating terms have linear and second order terms in $\Delta (= \frac{\omega\epsilon}{\sigma})$ in the exponent of the solution. The leading (linear) terms in Δ are the important ones, since $\frac{\omega\epsilon}{\sigma} \ll 1$.

The limit on the maximum value of Δ that can be neglected will be determined mostly by what accuracies can be expected from the experiments performed in the model environment. In practice, experimental difficulties in underwater measurements, and the perturbing effects of supports, leads and cables will, in most cases, make a 5% experimental error quite acceptable. Now a maximum value of $\Delta=10^{-2}$ will generally bring a 0.5% error in both the real and imaginary parts of the exponent of the field solution as depicted by the $\frac{\Delta}{2}$ linear correction terms in Equation (B18). Since the measurements will be conducted well within about ten skindepths (10δ in the medium) of the source, the 0.5% error in the real part of the exponent will produce an amplitude error of less than 5% in the field attenuation factor. A similar 0.5% error in the imaginary part of the exponent (the

argument of a trigonometric or Bessel function) will in turn, produce a shift in the position of an instantaneous null location by less than 1% of a wavelength at the same 10δ distance away from the source.

In theory at least any field configuration, including sources, can be given by a linear combination of homogeneous and inhomogeneous plane waves. Sometimes it is more convenient (especially in an angularly symmetric case such as a loop in a half space, with its plane parallel to the interface) to use cylindrical coordinates and Bessel functions instead of the Cartesian coordinates and trigonometric functions, which we have used to demonstrate the effect of perturbation by the minority current. A similar treatment of errors can also be carried through in cylindrical coordinates (or in spherical coordinates for that matter). However, in view of the extremely favorable results obtained for the elementary solutions in Cartesian coordinates for values of $\frac{\omega \epsilon}{\sigma}$ up to 0.01, and the general similarities in the nature of the resultant fields in all three coordinate systems, the arbitrary 0.002 upper limit for $\frac{\omega \epsilon}{\sigma}$ imposed in the body of this memo should be more than adequate to cover the small differences that may occur in a single media problem.

APPENDIX C

TRIP TO HARVARD UNIVERSITY*

FOR DISCUSSIONS ON MODELS

ADL and client staff visited Dr. Kiego Izuka, a professor at Harvard University working with electromagnetic modeling, in order to get a more practical flavor of the precautions, pitfalls, advantages, and hardware involved in the utilization of models.

The first half of the visit was spent discussing modeling problems when dealing with mixed media, in particular, environments which include a sea water-air interface. The second half of the visit was spent discussing and observing Dr. Izuka's facility for modeling propagation in media where the conductivity does not remain constant but varies in some prescribed manner with distance.

1. Modeling Problems with Mixed Media

Discussion of the sea water-air modeling problems divided naturally into three areas. The first dealt with single medium problems consisting of either dielectric or conducting media. General agreement was reached on the matter of which terms in the wave equation could be neglected for each media. Namely, the displacement current term in conducting media, and the conduction current term in low-loss dielectric media.

Discussion continued on the subject of whether neglecting to model the air medium properly in a scale model involving a sea water-air interface would make much of a difference. To try to get a handle on and illustrate this point, Dr. Izuka presented two cases. The first involved a model configuration involving two different dielectric media, separated by an infinite interface as in the air-sea water problem. It was clear in this case, that if a 100 to 1 change in the upper dielectric constant was neglected, the effects on the field in the two regions would be startling, and certainly could not be neglected. If such a case were now extended to one in which the lower dielectric medium was gradually made more and more lossy, the effects of neglecting a 100 to 1 change dielectric constant in the upper medium would still exist, but would gradually become less important. However, the conclusion reached at the meeting was that it was not obvious that such a 100 to 1 change in dielectric constant in the upper medium could be ignored as negligible for a conducting medium such as sea water whose conductivity was only a moderately large one. Secondly, Dr. Izuka did not know of any simple way to estimate the magnitude of the error involved should a factor on the order of 100 to 1 in dielectric constant be neglected in a modeling situation. However, the one precise way of obtaining this error information would

* During a previous government project in 1968.

be to derive analytical expressions for the fields expected in both media at the locations of interest, and then to simply evaluate these expressions for both values of dielectric constant (1 to 1, and 100 to 1 change). Comparison of the answers for these two situations would give the answer of how much difference it makes to ignore the scaling of dielectric constant. Unfortunately the dilemma at the present time is that such an expression is not readily available to us for substituting these values of dielectric constant and evaluating the effects on the field within the spacial regimes of the source that are important to our application. However, Dr. Izuka did say that particularly in cases involving more complicated geometries in which the distances from the source to the metal object to the surface interface and the dimensions of the metal object are all comparable to each other and the wavelength, then there was extremely high probability of incurring significant errors in field behavior if the properties of the materials in question were not scaled properly in the model. This unfortunately, he has seen happen so many times with experimenters wishing to get quick results, and finally winding up with meaningless results as a result of their haste and lack of foresight.

(Dr. Izuka also brought up a curious point in dealing with modeling problems with infinite interfaces, namely that there may be cases in which it is also necessary to scale the material properties of even lossless media when attempting to scale the problem. Apparently considerations such as these become important when the configuration is an unbounded one involving infinite interfaces, however, this point was not made entirely clear.) The upshot of this talk was one of extreme caution in modeling; either model precisely as dictated by the equations or be extremely sure before hand, that your approximations will indeed result in small errors.

2. Dr. Izuka's Modeling Facility

The second half of the visit we spent looking at Dr. Izuka's modeling facility. Since Dr. Izuka is interested in examining propagation phenomena in media whose conductivity is a function of position, his problems are slightly different than the ones in which we are interested. In particular his problems apply directly to propagation within the earth's mantle in which typically the conductivity of the earth will decrease quite rapidly between zero and 5 kilometers beneath the surface, maintain a minimum value to an approximate depth of 15 kilometers and then gradually increase again to about the σ value near the surface at depths on the order of perhaps 30 kilometers beneath the surface of the earth. These changes in conductivity with depth occur initially because increasing pressure tends to squeeze all moisture out of the materials thereby creating a minimum in conductivity. However, the trend in conductivity reverses itself again because of the increase in temperature as one descends further into the earth's crust. This increases the conductivity again, thereby forming a type of wave guide structure in which waves can propagate in a guided manner.

To model this situation Dr. Izuka has had to construct a fairly elaborate modeling procedure. Since he's working at UHF frequencies his structure is on the order of 15 by 15 feet square by 3 feet in height. The most critical part of his problem was to find a way to vary the conductivity of his medium in ways similar to that in the earth's mantle. He accomplishes this by using a solution of Agar-Agar (a bacterial substance) dissolved in water, which when allowed to cure, becomes a gelatinous substance. The desired conductivity profiles can now be obtained in this substance by allowing aqueous solutions of various salinities diffuse themselves as a function of time through this Agar-Agar gelatine. Diffusion times to obtain the proper conductivity profiles can take on the order of weeks. So to obtain the proper profile the salt water is allowed to diffuse the proper number of days or weeks into the Agar-Agar until the desired profile is obtained. Repeatability in reproducing a given conductivity profile is extremely difficult or nearly impossible. But this is not of great concern to Dr. Izuka since his interest is principally in profiles of the general shape that he can produce and not necessarily in specific precisely controlled profiles. He has found his techniques to be quite successful in obtaining the proper modeling conditions of interest to him and is now modifying his setup to make measurements more convenient. Discussion of his facility also centered around several precautions that he has to take to get reliable results. (Using absorbers and staying away from edges, brushing air bubbles from surface, watertight probes, etc.) His facility was impressive even though it had no direct application to our problem.

3. Conclusions

In summary, the conclusions reached during the meeting with Dr. Izuka confirmed those in the body of this memorandum. Namely, that significant errors can be incurred by not modeling the material parameters properly in a mixed media scaling problem; there is no simple way to estimate the magnitude of these errors, particularly in cases involving complicated geometries as expected in the intended application; consequently one could never be confident of the validity of the results obtained from such inexact models involving mixed media. Since people who have attempted to disregard these facts in the past have suffered for their lack of wisdom and foresight, ADL's position on the matter is that the pursuit of experiments with inexact mixed media models is unwise, risky and unjustified.

IV. PERMANENT MAGNETS AS SIGNAL SOURCES FOR TRAPPED MINER
LOCATION AND COMMUNICATION

During the initial phase of our work, the potential utility of permanent magnets for the location of and communication with trapped miners was briefly examined. Consideration was given to the detection of not only the magnetic field itself but also the field gradient.

A. ROTATING BAR MAGNETS

In principle, a miner location or communication system could be built based upon the detection of the field of a rotating bar magnet. At any point in space, this field will oscillate in value as the relative orientation of the magnet changes during rotation, say, under manual power.

The amplitude of the radial component of this field oscillation may be written as

$$H_o = \frac{M}{2\pi r^3} \quad (1)$$

where r is the range in meters, and M the magnetic moment in ampere-meters². Taking a magnet with uniform residual induction B_r , the magnetic moment is given by

$$M = \frac{B_r V}{\mu_o}, \quad \text{V being the volume of the magnet, and} \quad (2)$$

μ_o being the permeability of free space.

The following table provides an idea of typical field strengths and gradients that will be produced in such a scheme by a bar-type magnet about 16 inches long made out of samarium cobalt, presently the best but most expensive permanent magnet material. All fields are expressed in rationalized MKS units.

Table 1
FIELD STRENGTHS AND GRADIENTS FOR SAMARIUM COBALT BAR-TYPE MAGNETS

Magnet Source Residual Induction B_r , (weber/m ²)	Magnet's Vol m ³	Magnetic moment amp-m ²	Magnet's Wt. lbs.	Range r, ft.	Magnet Field H_o , a/m	Magnet Field Gradient $\frac{dH_o}{dr}$, a/m/m
0.7	10 ⁻³	555	15	2500	2.2x10 ⁻⁷	9.1x10 ⁻¹⁰
0.7	10 ⁻³	555	15	1000	3.4x10 ⁻⁶	3.4x10 ⁻⁸
0.7	10 ⁻²	5555	150	2500	2.2x10 ⁻⁶	9.1x10 ⁻⁸
0.7	10 ⁻²	5555	150	1000	3.4x10 ⁻⁵	3.4x10 ⁻⁷

For a magnet of barium ferrite, $B_r = 0.3$ weber/m², but a saving of 3 to 1 in weight and 100 to 1 in material cost can be realized over a samarium cobalt magnet.

Magnet rotation rates on the order of 1-3 Hz are reasonable, with 10 Hz perhaps a practical upper limit. In this frequency range the detection of the resultant field is likely to be geomagnetically noise limited. This noise owes its origin to atmospheric and ionospheric phenomena. It has amplitudes typically in the range of 10^{-6} a/m- 10^{-4} a/m; but can rise to levels greater than 10^{-3} a/m at frequencies below 1 Hz, and fall to levels below 10^{-6} a/m above 10 Hz. The noise is typically normalized to a bandwidth of 1 Hz above 1 Hz, but, below 1 Hz it is referred to octave frequency intervals starting, for example, from 0.01 Hz.

An idea of this noise limitation may be obtained on the assumption, admittedly very approximate, that the geomagnetic noise arises from a magnetic dipole at a range, R, far away from the magnet signal source.* The following table shows the ranges from a magnetic source at which the field and field gradient of the geomagnetic noise in a 1 Hz bandwidth are equal to those of the 150 lb, 10^{-2} m³ permanent magnet of Table 1. Two different rotation frequencies were chosen, one between 1 - 3 Hz and another around 10 Hz. Three representative values of the noise field at the point of observation have been taken. However, for the sake of computing gradients, in all cases the source of the geomagnetic noise has been assumed to be at two different distances from the point of observation, in order to determine the potential performance of gradient detection schemes versus field detection schemes.

Table 2

RANGES AT WHICH SIGNAL AND NOISE FIELDS AND GRADIENTS ARE EQUAL
(FOR BAR MAGNET SIGNALS AND GEOMAGNETIC NOISE)

Distance from Geomagnetic Noise Source R, Miles	Field		Field Gradient	
	Noise Field H_n , a/m	Distance from Permanent Mag- net Source (3) r_d , ft.	Noise Field Gradient dH_n/dR , a/m/m	Distance from Permanent Mag- net Source (3) r_d^1 , ft.
625	(1) 8×10^{-7}	3900	(1) 2.4×10^{-12}	21500
625	(2) { 8×10^{-6} 8×10^{-5}	1800	(2) { 2.4×10^{-11} 2.4×10^{-10}	12000
625		830		6700
100	(1) 8×10^{-7}	3900	(1) 1.5×10^{-11}	13400
100	(2) { 8×10^{-6} 8×10^{-5}	1800	(2) { 1.5×10^{-10} 1.5×10^{-9}	7500
100		830		4200

(1) For an assumed noise source frequency around 10 Hz.

(2) For two different assumed noise source strengths in the 1-3 Hz frequency band.

* This analysis cannot be expected to hold in the presence of strong, local thunderstorm activity.

- (3) Distance from samarium cobalt magnet source where field or field gradient is equal to that of noise source.

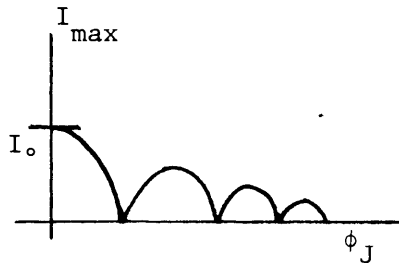
These tables indicate that permanent magnets can offer magnetic moments and detection ranges that compare favorably with those obtainable from current-fed loops and field detection systems. They also indicate there is a potential advantage to be gained in using a detection scheme based on the field gradient (r_{d}^i) rather than on the field itself (r_{d}), by making use of the fact that geomagnetic noise sources are frequently a great distance away, except in the case of very local thunderstorm activity. Geomagnetic gradient noise measurements are required to verify this assumption, which underlies the interest in gradiometers. In what follows, a brief outline of the principles behind a gradient detection system is presented.

B. MAGNETIC FIELD GRADIENT DETECTION

In recent years new types of magnetometers with sensitivities three to five orders of magnitude better than present devices have been proposed and demonstrated in the laboratory, and in certain well controlled applications, e.g., medical. These devices make use of the properties of superconducting thin films. Particularly attractive are magnetometers of the Josephson type. Their operation depends upon the observation that as the magnetic field to which a superconductor-barrier-superconductor structure -- a so-called Josephson -- is steadily increased, the maximum value of the current which can be driven through the structure, without developing a voltage there, first drops to zero and then rises to a peak value less than the peak when in zero field; it then once more falls to zero and again rises to a still lower peak, and so forth.

If the total flux within the junction is ϕ_J , and the flux quantum is denoted by ϕ_0 , then

$$I_{\text{max}} = I_0 \cdot \frac{\sin(\pi \phi_J / \phi_0)}{\pi \phi_J / \phi_0} \quad (3)$$



where I_0 is the maximum current through the junction in zero field.

The barrier may be a point contact of one superconductor upon the other, or a constriction in a superconducting ring. By applying a time dependent flux or current to a "weak link" such as a constriction, the critical current value through the weak link may be periodically exceeded driving the weak link out of the zero-voltage condition. Hence, an AC voltage will be produced across the weak link which varies periodically at the same rate, and whose amplitude depends on the background DC magnetic field present. In practice a feedback scheme is employed to maintain the flux through the loop (or the current through the weak link) constant, and the control signal is the instrumental output.

Josephson magnetometers are sufficiently small (a few cubic millimeters) that it appears feasible to construct a differential (gradiometer) system with linear dimensions of the order of a foot. Essentially, 2 superconducting coils are connected in series opposition, with a weak link in the circuit so that the system is sensitive only to differences in the flux across the 2 coils. Provided the coils are identical (and this restriction in practice places a limit on the attainable sensitivity), this translates into a measurement of the difference in magnetic field strengths at the position of the 2 coils and, hence, to a measurement of the magnetic field gradient.

It seems possible that systems such as the one just outlined would have field gradient sensitivities in the range of 10^{-8} - 10^{-9} (amps/meter)/meter. However, there are still several major engineering difficulties to be overcome as well as some uncertainties in the nature of the noise environment to which gradiometers will be exposed. Hence, some years of effort will be required for progress from the lab to the field instrument stage. The above values for the sensitivity attainable in principle have been arrived at as a result of considering inherent limitations imposed by such factors as constructional tolerances and thermal fluctuations.

C. CONCLUDING REMARKS

It will be noted that the above Josephson-type gradiometer sensitivities are not good enough for detecting signal field gradients equal to those of the noise displayed in Table 2. Hence, the corresponding detection ranges will be reduced to anywhere from 80% to 30% of the values for r_d^1 quoted there, but may still remain about twice as large as the detection ranges r_d for the fields themselves. In view of the current development status of these gradiometers and the engineering difficulties that remain, the Josephson gradiometer system is not worth pursuing further at this time for Bureau of Mines communication and location applications.

However, the technique of using a rotating bar magnet as an underground emergency source for EM location may be worth a bit more consideration, especially if the lighter and lower cost barium ferrite material could be used. Then a 16-inch long 2-inch-square bar magnet with a magnetic moment of about 250 amp-m² would weigh only about 5 lbs. If this bar also had a hole through it midway between the end points, it could then be mounted by a trapped miner to a convenient entry wall, like say a propeller or pinwheel, by simply passing a spike through the hole in the magnet and driving the spike into the wall with a hammer. The magnet could then be easily rotated manually like a propeller by spinning it or cranking it around. Such a simple and rudimentary scheme appears to be worth a closer examination, particularly since it requires no electrical power.

V. PRELIMINARY FEASIBILITY EXPERIMENT FOR A MINE WIRELESS ALARM SYSTEM

A. INTRODUCTION

One Bureau of Mines approach for providing an effective and low cost wireless alarm system to alert mine surface personnel of mine emergency situations and locations, is one utilizing manually-actuated, addressable, wireless fireboxes located at strategic locations in a mine. These fireboxes would be actuated by miners at the scene, or while fleeing the scene, in much the same manner as surface community fire alarm boxes. These boxes could also serve as miner location devices; marking an escape route followed by miners who actuated the boxes as they passed them, and indicating the resting places of trapped miners or the continued existence of life at a location if the boxes were capable of being reactivated and reused.

A potentially attractive candidate for such a firebox system is a simple sinusoidal seismic force generator, similar to a small portable unit developed for the Limited Warfare Lab (LWL) several years ago, if used with geophones and a narrowband waveform analyzer on the surface.

This approach appeared particularly attractive because of the inherent simplicity of the generator and the detection advantages offered, in the presence of background seismic noise, by the sinusoidal force (and corresponding displacement) signal produced by the generator. A call to the LWL investigators revealed that little documentation existed regarding LWL tests with the device. The principal investigators could only remember that: detection ranges of 300-400 yards were obtained by using the generator with the narrowband receiver and that background seismic noise was generally the limitation to performance.

Reliable experimental data was indeed not available for the force generator and its possible detection range, so a simple crude experiment was defined and performed to see if the approach was worth pursuing further. The results obtained were positive enough for us to recommend that another simple but more refined experiment was worth doing, in a controlled mine environment such as the Bruceton Safety Research mine, to see if further investigation is warranted.

B. EQUIPMENT

The equipment used for the experiment is shown in block diagram form in Figure 1 and described below.

- (1) force generator,
- (2) sensor and associated amplifiers and filters, and
- (3) minicomputer narrowband waveform analyzer.

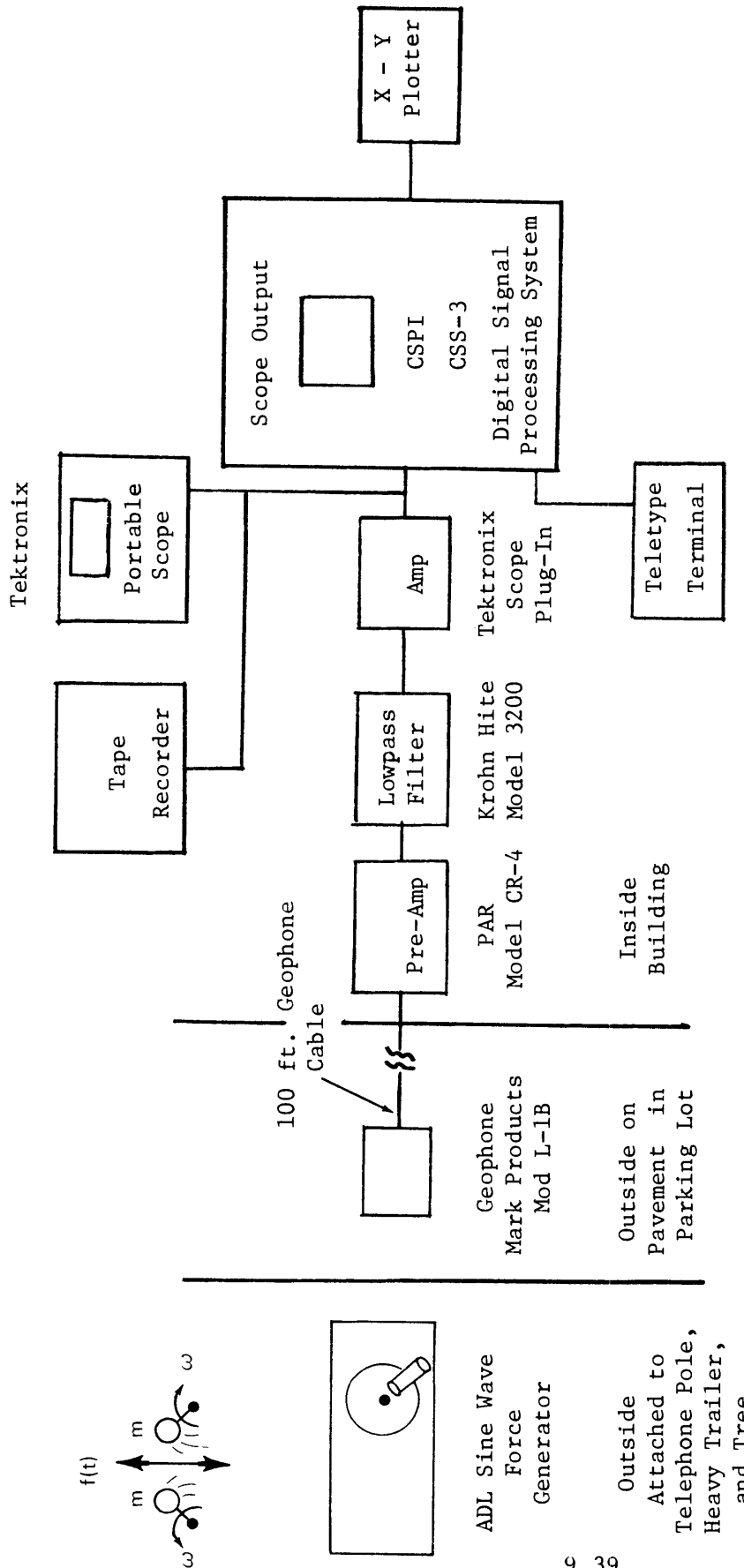


FIGURE 1 BLOCK DIAGRAM OF EQUIPMENT FOR PRELIMINARY FEASIBILITY EXPERIMENT

A sinusoidal force generator similar to the LWL unit was obtained, on loan, from a local ADL client for whom we had fabricated such a unit some time ago for another application. A photograph of the force generator is shown in Figure 2. This generator produces a vertical sine wave of force by counter rotation of two unbalanced loads (1 lb. weights) attached to two shafts. Rotation of the shafts is by a geared-up hand crank. The force produces sinusoidal seismic waves in the ground, which are in-turn sensed by a geophone and detected in the presence of noise after narrowband analysis or filtering.

The vertical force waveform produced by this generator is given by $f(t) = 2m\omega^2 r \sin \omega t$, where m is the mass of each weight, ω is the angular rotation frequency and r is the radius of the effective center of each weight from the axis of its shaft. This unit produces approximately 140 lbs of peak force (280 lbs. peak-to-peak) when the weights are rotating at a 20 Hz rate.

This particular generator can be used most simply by firmly securing it to a tree, firmly planted pole, or vertical member, by means of the attached belt and tension adjustment screws. Tension must be sufficient to prevent slippage up and down during operation. The generator is operated by turning the handcrank slowly at first, and then increasing the speed to that corresponding to the desired frequency. The speed is then maintained by observing the speed indicator, a crude vibrating reed temporarily attached to the generator for this experiment. Operating frequencies in the vicinity of 20 Hz were desired for this experiment.

The sensor was a Mark Products, Inc., Model L-1B geophone with 550 ohm output impedance. The geophone was connected to the amplifiers and filters via approximately 100 feet of geophone cable. The preamplifier was a Princeton Applied Research (PAR) Model CR-4 with adjustable upper and lower cut-off frequencies. The filter was a Krohn-Hite Model 3200 lowpass filter with a 24dB/octave roll-off rate (the lowpass cut-off was set to 40Hz). A Tektronix scope plug-in unit was also used as an amplifier to get additional gain, because the PAR unit did not provide an output voltage large enough to efficiently drive the A/D converter of the signal processing and analysis equipment.

The narrowband waveform analyzer used was a Computer Signal Processors, Inc. (CSPI) CSS-3 digital signal processing system like that purchased for the Bureau of Mines CMRSS seismic location subsystem. It is shown in block diagram form in Figure 3. The CSS-3 consists of a Varian 6200 minicomputer and an extensive signal processing software package; a minimum of 8192 words of core memory; a 12-bit A/D converter and two 12-bit D/A converters; a CRT display, display cursor and axis generator; an X-Y plotter interface; and a teletypewriter with paper tape reader and punch. The CSS-3 system was used for this experiment because: it could provide the flexible, real-time, high-resolution spectrum analysis desired to detect a sinusoidal seismic signal in the midst of high seismic background noise; the Bureau of Mines presently has two of these CSS-3 systems in its inventory; and CSPI which is conveniently located in the Boston area was most cooperative in providing a demonstration of the CSS-3 by making it a part of this experiment performed at their plant in Burlington, Mass.

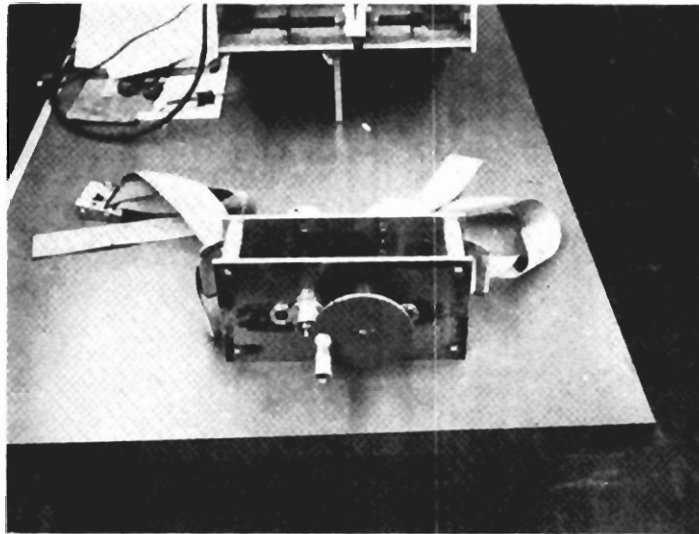


FIGURE 2 SEISMIC SINE WAVE FORCE GENERATOR

Weight — 200 lbs.

Dimensions — Height 48.5", Width 22", Depth 26.5"

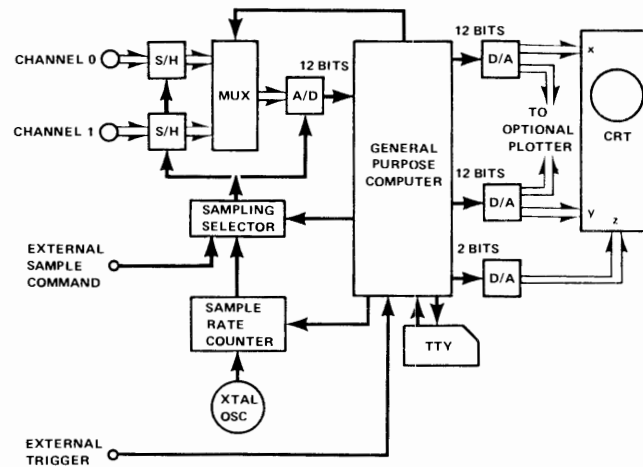


FIGURE 3 SIMPLIFIED CCS-3A AND B FUNCTIONAL DIAGRAM

A Tektronix portable scope and tape recorder were used to monitor the received signals and background noise, the tape recorder being used to playback some of the more interesting waveforms through the CSS-3 for additional analysis using different resolutions or other analysis parameters.

C. EXPERIMENT

The experiment was performed late in the afternoon of 8 May 1972 by R. Lagace and R. Spencer of ADL and M. Schrage and J. Ferguson of CSPI at the CSPI plant in intermittent light rain. It was a quickly conceived and executed preliminary experiment with a purposely limited objective: to obtain an answer to the question, "Is it possible to sense and detect over moderate distances a sinusoidal seismic signal generated by the small ADL force generator in the midst of background seismic noise, by using a geophone and the CSS-3 and its high-resolution Fast Fourier Transform (FFT) real-time spectrum analysis software?"

The spectrum analysis software is similar to that recently used by NBS on a large computer and by WGL on the CSS-3 to analyze EM noise waveforms in and above coal mines. In particular, we began with the Basic CSS-3 Fourier Transform Function, which is equivalent to 512 constant bandwidth filters covering the range from DC to a desired upper frequency (50 Hz in our experiment); but quickly changed to the Zoom Fourier Transform Function which places all the 512 narrowband filters in a band about the specific frequencies of interest, thereby providing greatly increased resolution in the Zoom frequency band. For this experiment, a 10-12 Hz band centered around the nominal generator frequency of 20 Hz was chosen. Analysis bandwidths (or resolutions) of 0.1 Hz and 0.2 Hz were found to be the most practical with respect to the highest resolution consistent with good detectability of a sine wave signal from a source whose frequency could not be precisely controlled under the manual operating conditions. During these limited tests, several analysis parameters were varied in an attempt to find those most favorable to the prevailing signal and noise conditions. Values of 1/4 and 1/8 for the Zoom factor, and values of 1/2 and 1/4 for the exponential weighting factor for averaging gave the most useful results.

Signal detection experiments were performed with the force generator attached to three different objects in or adjacent to the CSPI parking lot; a telephone pole, a tree, and an unhitched trailer. The appropriate location of the objects and corresponding geophone locations are shown in the sketch of Figure 4. No attempt was made to bury the geophone or otherwise provide better coupling to the ground.

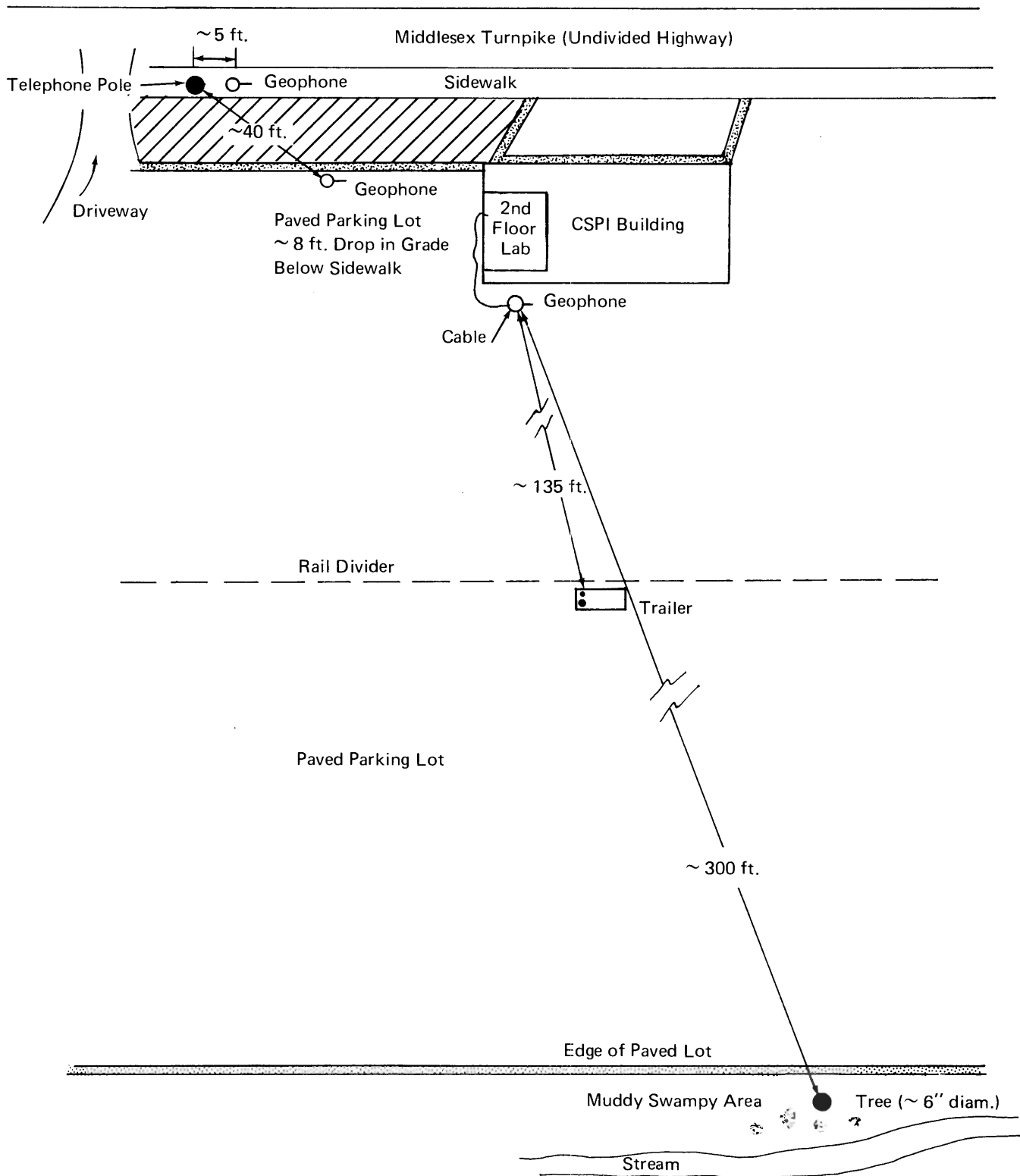


FIGURE 4 EXPERIMENT GEOMETRIES

When signalled by the lab team, the force generator operator cranked the generator at as constant a speed as he could maintain for about one or two minute intervals. The lab team in turn processed the incoming signal and noise on the CSS-3 in real-time to produce high-resolution signal spectrum plots, while also recording the waveforms on magnetic tape for later reprocessing and analysis if desired. The seismic background noise was also analyzed and plotted either just before or just after the signal was turned on and off respectively. The waveform magnitude (or "voltage") spectrum output was displayed on the CRT on the front of the CSS-3 cabinet and plotted on the associated X-Y plotter, both on linear scales as opposed to dB scales. To obtain the signal power spectrum, the plotted values must be squared.

As a result of the preliminary nature of this experiment, no attempt was made to calibrate the equipment, and though an initial attempt was made to record all equipment gain settings and adjustments, the number of spur-of-the-moment changes made in trying to optimize performance during this short experiment proved to be too burdensome to record completely. Therefore the vertical scales of the spectra are not calibrated or in absolute units and may differ from Figure to Figure. However since the experiment conditions were kept the same for the signal-plus-noise and noise-alone runs of each test, these curves in each Figure can be compared directly with each other.

1. The Trailer Test

The 135 ft. trailer test was the most successful one of the afternoon, producing a positive, extremely well-defined detection and identification of the force generator signal, with a voltage signal-to-noise ratio in excess of 8 to 1, as depicted in the X-Y plot of Figure 5. This success was attributed to the firm attachment of the generator to the trailer, the good coupling provided by the trailer to the pavement on which the geophone was also resting and well-controlled generator rotation frequency.

2. The Telephone Pole Test

The other tests were not so dramatically successful, because of poor coupling of the generator to the medium in the case of the tree in the swamp and the telephone pole in the sidewalk, and poor frequency control in almost all cases. Figure 6 is an X-Y plot for the telephone pole test, a trial run to test the equipment. The force generator was strapped to the telephone pole and the geophone placed above five feet away on the sidewalk. The Zoom FFT was not used in this first run, but only the Basic Fourier Transform Function. So the frequency scale is not centered around the generator frequency but runs from 0 to 50 Hz, and a wider analysis bandwidth of 0.6 Hz is used. In spite of a somewhat insecure pole attachment and a high background noise environment being so close to the road, the X-Y plot revealed a voltage signal-to-noise ratio greater than 7 to 1 for the 0.6 Hz bandwidth, which would increase to a ratio greater than 12 to 1 if the 0.2 Hz bandwidth had been used.

Seismic Force Generator Attached to Trailer Support
 Distance to Geophone ~ 135 ft.

Real Time Spectrum Analysis with FFT on CSPI - CSS - 3
 in Zoom Mode Around Signal Freq.

Analysis Bandwidth ~ 0.2 Hz
 Sampling Rate - 200 Hz, #Samples 128
 Zoom Factor - 1/8
 Exponential Weighting with Factor of 1/4

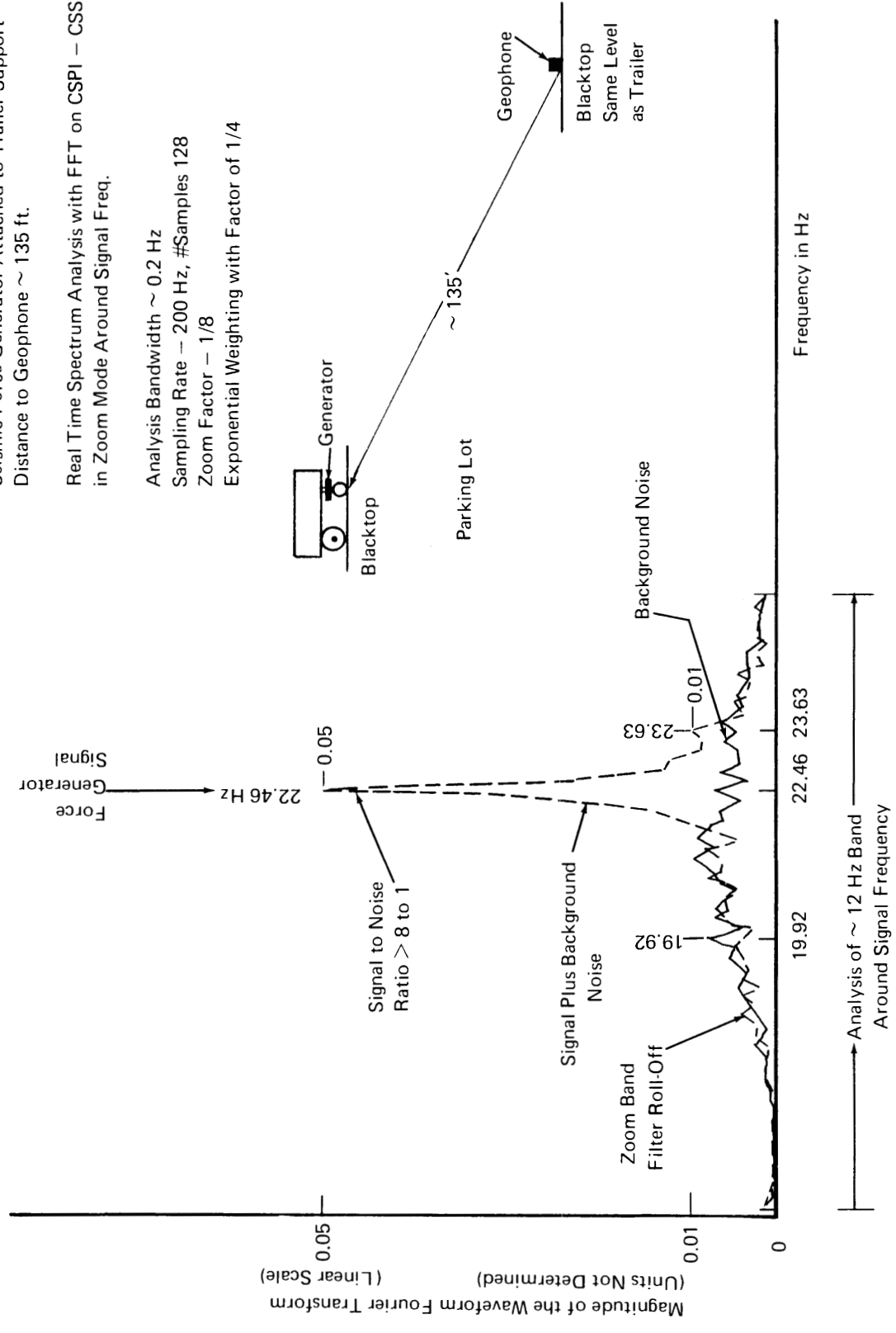


FIGURE 5 SIGNAL AND NOISE FOR TRAILER TEST

Seismic Force Generator Attached to Telephone Pole —
Distance to Geophone on Sidewalk ~ 5 ft.

Real Time Spectrum Analysis with Basic FFT Routine
on CSPI — CSS — 3

Analysis Bandwidth ~ 0.6Hz

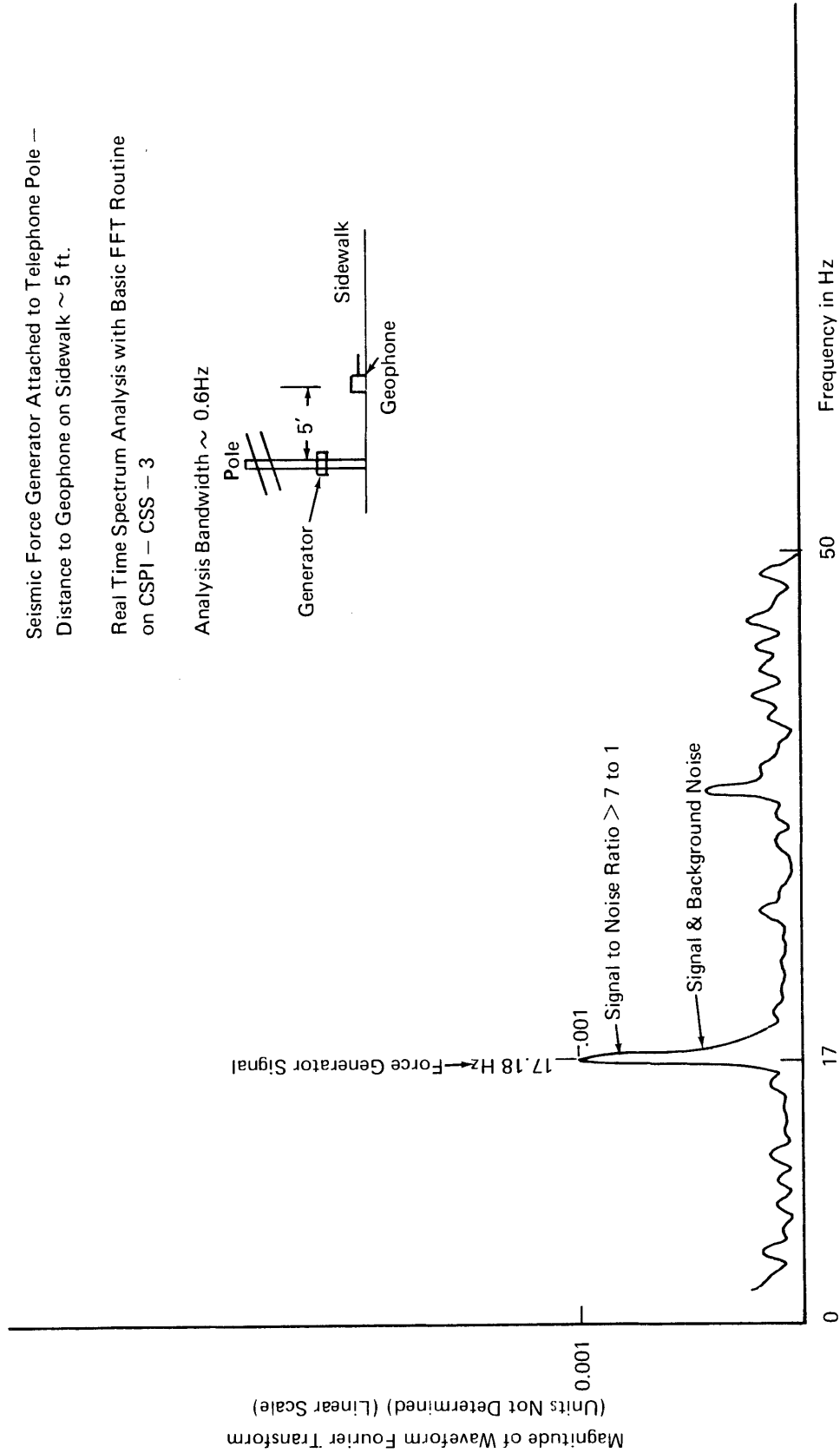
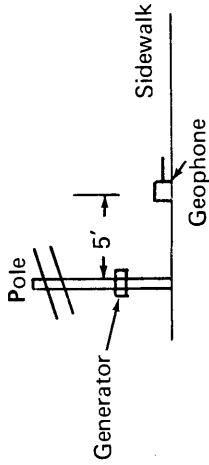


FIGURE 6 SIGNAL AND NOISE FOR TELEPHONE POLE TEST

Two more runs were made with the generator strapped to the telephone pole, but with the geophone placed about 40 feet away on the pavement of the parking lot which is approximately 8 feet below the level of the sidewalk, as shown in Figure 4. A voltage signal-to-noise ratio of better than 3/1 in a 0.2 Hz analysis bandwidth was observed despite the fact that frequency control was poor.

3. The Tree Test

The tree in the swampy ground test was the last, and the least successful or conclusive one, primarily, we believe, because of the poor coupling to the medium provided by the swampy ground. The force generator was attached to a tree about 10 feet beyond the parking lot pavement, and approximately 300 feet from the geophone location used for the previous trailer 135 foot experiment.

D. CONCLUDING REMARKS

On the whole, this preliminary experiment with a small, low power sine wave force generator and the CSS-3 processor, has yielded extremely encouraging results regarding the potential utility of such a system as an emergency wireless alarm system for coal mines. If the 135-foot trailer test results shown in Figure 5 are indicative of the kind of performance one can expect when such a force generator is well-coupled to the medium and its frequency adequately controlled, then the prognosis looks good. We believe that these initial results are favorable enough to justify another simple but more refined experiment, but this time in a controlled benign mine environment such as the Bruceton Safety Research mine* to see if a more comprehensive investigation is warranted. Consideration should also be given to performing such an experiment with a new version of the generator, which will fit into a package of about the same size, but be capable of providing a 1000 lb. peak-to-peak force at 20 Hz, thereby increasing its range of detection. Such a unit could be easily and quickly built with improved frequency control, and more flexible ways of attaching it to structures found in mines.

* As a preliminary to an experimental test program in an appropriate mine, J. Powell of PMSRC and R. Spencer of ADL conducted some brief experiments at the Bruceton Safety Research mine using the hand operated force generator. These tests were done on July 12 and 13, 1972. The geophones (Geospace GS-11D), preamplifiers, filters and visicorder of the Bureau's CMRSS rescue system were used in the experiments. Although success was experienced on the surface at ranges near 40 feet, in-mine experiments with geophone-source ranges from 200 feet to 15 feet showed no clearly distinguishable results. Relatively wide receiver bandwidths of 5 to 20 Hz were used in these experiments and there were questions of geophone and preamplifier integrity. Further work, as discussed above, is needed to establish the capabilities of such a force generator system for "firebox" applications.

BIBLIOGRAPHIC DATA SHEET	1. Report No. ADL-C-73912-VOL. I	2.	3. Recipient's Accession No.
	4. Title and Subtitle SURVEY OF ELECTROMAGNETIC AND SEISMIC NOISE RELATED TO MINE RESCUE COMMUNICATIONS. VOL. I. Emergency and Operational Mine Communications.		5. Report Date (Preparation) January, 1974
7. Author(s) Robert L. Lagace, Alfred G. Emslie, Martyn F. Roetter, Richard H. Spencer, et al.		8. Performing Organization Rept. No.	
9. Performing Organization Name and Address Little (Arthur D.), Inc. 25 Acorn Park Cambridge, Massachusetts 02140		10. Project/Task/Work Unit No.	11. Contract/Grant No. USBM-HO122026
12. Sponsoring Organization Name and Address U.S. Department of the Interior, Bureau of Mines, Pittsburgh Mining and Safety Research Center, 4800 Forbes Avenue, Pittsburgh, Pennsylvania 15213		13. Type of Report & Period Covered FINAL Aug. 1971 - Dec. 1973	
14.			
15. Supplementary Notes Initiated under the Coal Mine Health and Safety Research Program.			
16. Abstracts Volume I of this report deals with theoretical, experimental, and practical implementation aspects of the U.S. Bureau of Mines programs related to present and planned, emergency and operational, mine communications and miner location systems for underground coal mines. Investigations, evaluations, experiments, and analyses for these programs were made; breadboard and prototype hardware was developed; and assistance given in the formulation and presentation of technology transfer seminars on mine communications. Major subject areas treated in this volume are: electromagnetic noise and its measurement for mine environments, electromagnetic through-the-earth emergency and operational mine communications and miner location systems; signal propagation characteristics for wireless and guided-wireless radio waves in coal mine tunnels, and for mine hoist shaft and trolley wire communications; a mine pager phone-to-public telephone interconnect; paging and two-way communications with roving miners; technology transfer seminars and a through-the-earth state-of-the-art workshop on electromagnetic mine communications; and selected topics related to the above major areas.			
17. Key Words and Document Analysis. 17a. Descriptors			
Mines-Communications Mines-Coal Coal Mines Rescue Operations-Mines Through-the-Earth Communications-Electromagnetic Tunnel Communications Mobile Communications		Miner Location Electromagnetic Location Electromagnetic Noise Electromagnetic Wave Propagation Technology Transfer	
17b. Identifiers/Open-Ended Terms			
17c. COSATI Field/Group			
18. Availability Statement		19. Security Class (This Report) UNCLASSIFIED	21. No. of Pages 514
		20. Security Class (This Page) UNCLASSIFIED	22. Price



CAMBRIDGE,
MASSACHUSETTS

NEW YORK
SAN FRANCISCO
WASHINGTON
ATHENS
BRUSSELS
CARACAS
LONDON
MEXICO CITY
PARIS
RIO DE JANEIRO
TORONTO
WIESBADEN